

# Insights in nanobiotechnology: Novel developments, current challenges, and future perspectives 2022/2023

**Edited by**

Gianni Ciofani and Marco P. Monopoli

**Published in**

Frontiers in Bioengineering and Biotechnology



## FRONTIERS EBOOK COPYRIGHT STATEMENT

The copyright in the text of individual articles in this ebook is the property of their respective authors or their respective institutions or funders. The copyright in graphics and images within each article may be subject to copyright of other parties. In both cases this is subject to a license granted to Frontiers.

The compilation of articles constituting this ebook is the property of Frontiers.

Each article within this ebook, and the ebook itself, are published under the most recent version of the Creative Commons CC-BY licence. The version current at the date of publication of this ebook is CC-BY 4.0. If the CC-BY licence is updated, the licence granted by Frontiers is automatically updated to the new version.

When exercising any right under the CC-BY licence, Frontiers must be attributed as the original publisher of the article or ebook, as applicable.

Authors have the responsibility of ensuring that any graphics or other materials which are the property of others may be included in the CC-BY licence, but this should be checked before relying on the CC-BY licence to reproduce those materials. Any copyright notices relating to those materials must be complied with.

Copyright and source acknowledgement notices may not be removed and must be displayed in any copy, derivative work or partial copy which includes the elements in question.

All copyright, and all rights therein, are protected by national and international copyright laws. The above represents a summary only. For further information please read Frontiers' Conditions for Website Use and Copyright Statement, and the applicable CC-BY licence.

ISSN 1664-8714  
ISBN 978-2-8325-4006-0  
DOI 10.3389/978-2-8325-4006-0

## About Frontiers

Frontiers is more than just an open access publisher of scholarly articles: it is a pioneering approach to the world of academia, radically improving the way scholarly research is managed. The grand vision of Frontiers is a world where all people have an equal opportunity to seek, share and generate knowledge. Frontiers provides immediate and permanent online open access to all its publications, but this alone is not enough to realize our grand goals.

## Frontiers journal series

The Frontiers journal series is a multi-tier and interdisciplinary set of open-access, online journals, promising a paradigm shift from the current review, selection and dissemination processes in academic publishing. All Frontiers journals are driven by researchers for researchers; therefore, they constitute a service to the scholarly community. At the same time, the *Frontiers journal series* operates on a revolutionary invention, the tiered publishing system, initially addressing specific communities of scholars, and gradually climbing up to broader public understanding, thus serving the interests of the lay society, too.

## Dedication to quality

Each Frontiers article is a landmark of the highest quality, thanks to genuinely collaborative interactions between authors and review editors, who include some of the world's best academicians. Research must be certified by peers before entering a stream of knowledge that may eventually reach the public - and shape society; therefore, Frontiers only applies the most rigorous and unbiased reviews. Frontiers revolutionizes research publishing by freely delivering the most outstanding research, evaluated with no bias from both the academic and social point of view. By applying the most advanced information technologies, Frontiers is catapulting scholarly publishing into a new generation.

## What are Frontiers Research Topics?

Frontiers Research Topics are very popular trademarks of the *Frontiers journals series*: they are collections of at least ten articles, all centered on a particular subject. With their unique mix of varied contributions from Original Research to Review Articles, Frontiers Research Topics unify the most influential researchers, the latest key findings and historical advances in a hot research area.

Find out more on how to host your own Frontiers Research Topic or contribute to one as an author by contacting the Frontiers editorial office: [frontiersin.org/about/contact](https://frontiersin.org/about/contact)

# Insights in nanobiotechnology 2022/2023: Novel developments, current challenges, and future perspectives

## Topic editors

Gianni Ciofani — Italian Institute of Technology (IIT), Italy

Marco P. Monopoli — Royal College of Surgeons in Ireland, Ireland

## Citation

Ciofani, G., Monopoli, M. P., eds. (2023). *Insights in nanobiotechnology 2022/2023: Novel developments, current challenges, and future perspectives*. Lausanne: Frontiers Media SA. doi: 10.3389/978-2-8325-4006-0

*Dr. Ciofani is a shareholder of Kidaria Bioscience SRL, but declares no competing interests related to the article collection*

# Table of contents

04	<b>Editorial: Insights in nanobiotechnology 2022/2023: novel developments, current challenges, and future perspectives</b> Gianni Ciofani and Marco P. Monopoli
06	<b>An Opinion on How Nanobiotechnology is Assisting Humankind to Overcome the Coronavirus Disease 2019</b> Tania Limongi and Francesca Susa
11	<b>Forging the Frontiers of Image-Guided Neurosurgery—The Emerging Uses of Theranostics in Neurosurgical Oncology</b> Fred C. Lam, Uyanga Tsedev, Ekkehard M. Kasper and Angela M. Belcher
20	<b>Emerging applications of nanotechnology in context to immunology: A comprehensive review</b> Hifsa Mobeen, Muhammad Safdar, Asma Fatima, Samia Afzal, Hassan Zaman and Zuhair Mehdi
40	<b>Whole transcriptomic analysis of mesenchymal stem cells cultured in Nichoid micro-scaffolds</b> Carolina Testa, Stefania Oliveto, Emanuela Jacchetti, Francesca Donnalaja, Chiara Martinelli, Pietro Pinoli, Roberto Osellame, Giulio Cerullo, Stefano Ceri, Stefano Biffo and Manuela T. Raimondi
54	<b>A novel approach for large-scale manufacturing of small extracellular vesicles from bone marrow-derived mesenchymal stromal cells using a hollow fiber bioreactor</b> Viktoria Jakl, Melanie Ehmele, Martina Winkelmann, Simon Ehrenberg, Tim Eiseler, Benedikt Friemert, Markus Thomas Rojewski and Hubert Schrezenmeier
72	<b>Intracellular delivery of therapeutic proteins. New advancements and future directions</b> Ilaria Porello and Francesco Cellesi
80	<b>Effects of citrate-stabilized gold and silver nanoparticles on some safety parameters of <i>Porphyridium cruentum</i> biomass</b> Ludmila Rudi, Liliana Cepoi, Tatiana Chiriac, Vera Miscu, Ana Valuta and Svetlana Djur
93	<b>Evaluation of a static mixer as a new microfluidic method for liposome formulation</b> Aoba Ota, Ayaka Mochizuki, Keitaro Sou and Shinji Takeoka
106	<b>Engineering global and local signal generators for probing temporal and spatial cellular signaling dynamics</b> Haowen Yang and Jurjen Tel
121	<b>Advances in dendritic cell targeting nano-delivery systems for induction of immune tolerance</b> Guojiao Lin, Jialiang Wang, Yong-Guang Yang, Yuning Zhang and Tianmeng Sun





## OPEN ACCESS

EDITED AND REVIEWED BY  
Hung-Yin Lin,  
National University of Kaohsiung, Taiwan

\*CORRESPONDENCE  
Gianni Ciofani,  
✉ [gianni.ciofani@iit.it](mailto:gianni.ciofani@iit.it)

RECEIVED 01 November 2023  
ACCEPTED 06 November 2023  
PUBLISHED 10 November 2023

CITATION  
Ciofani G and Monopoli MP (2023),  
Editorial: Insights in nanobiotechnology  
2022/2023: novel developments, current  
challenges, and future perspectives.  
*Front. Bioeng. Biotechnol.* 11:1331760.  
doi: 10.3389/fbioe.2023.1331760

COPYRIGHT  
© 2023 Ciofani and Monopoli. This is an  
open-access article distributed under the  
terms of the [Creative Commons  
Attribution License \(CC BY\)](https://creativecommons.org/licenses/by/4.0/). The use,  
distribution or reproduction in other  
forums is permitted, provided the original  
author(s) and the copyright owner(s) are  
credited and that the original publication  
in this journal is cited, in accordance with  
accepted academic practice. No use,  
distribution or reproduction is permitted  
which does not comply with these terms.

# Editorial: Insights in nanobiotechnology 2022/2023: novel developments, current challenges, and future perspectives

Gianni Ciofani<sup>1\*</sup> and Marco P. Monopoli<sup>2</sup>

<sup>1</sup>Istituto Italiano di Tecnologia, Smart Bio-Interfaces, Pontedera, Italy, <sup>2</sup>RCSI University of Medicine and Health Studies, Chemistry Department, Dublin, Ireland

## KEYWORDS

stem cells, liposomes, extracellular vesicles (EVs), nanoparticles, immunology, pandemic (COVID-19), neurosurgery

## Editorial on the Research Topic

*Insights in nanobiotechnology 2022/2023: novel developments, current challenges, and future perspectives*

The Research Topic “*Insights in nanobiotechnology 2022/2023: novel developments, current challenges, and future perspectives*” is an annual Research Topic featuring peer reviewed reviews, opinion papers, and research articles that looks to explore new insights, novel developments, current challenges, latest discoveries, recent advances, and future perspectives in the field of Nanobiotechnology. Among the 10 peer reviewed manuscripts published in the framework of this Research Topic, we have four Original Researches, three Reviews, one Mini-Review, and two Opinions.

Testa et al. report on a whole transcriptomic analysis of stem cells cultured on microfabricated scaffolds, named “Nichoids”, showing as stemness is preserved with respect to traditional 2D cultures, highlighting the important implication this culture approach owns for different applications in biomedicine.

Moving to the fields of nanoparticles for theranostic applications, Ota et al. present an innovative strategy for liposome preparation, comparing its performance, in terms of encapsulation efficiency, drug loading, lamellarity, and user-friendliness with a commonly used microfluidic device.

Jakl et al. show a novel approach for large-scale manufacturing of small extracellular vesicles (EVs) from bone marrow-derived mesenchymal stromal cells. EVs are membrane-surrounded nanostructures secreted ubiquitously by cells, i.e., “cellular nanoparticles” mediating communication among cells and containing hundreds of molecules, including miRNA, proteins, DNA, and lipids. These molecules work synergistically to activate multiple cells, and thus EV-based therapy is considered as the next-generation of stem cell therapy.

The last Original Research, from Rudi et al. is instead focused on the effects citrate-stabilized gold and silver nanoparticles on cultures of microalgae. These nanomaterials resulted to be a stress factor for red microalga *Porphyridium cruentum*, causing significant changes in both biotechnological and biomass safety parameters, and leading to an enhanced lipid accumulation and reduced malondialdehyde values in the biomass.

Coming to reviews, [Mobeen et al.](#) depict an overview of the emerging role of nanotechnology in immunology, highlighting novel theranostic immunological applications of nanomedicine. [Yang and Tel](#), instead, presents recent advancements in global and local signal generators, highlighting their applications in studying temporal and spatial cellular signalling activity.

The third Review in this Research Topic, from [Lin et al.](#), highlights how nanoplateforms can be tailored for targeted delivery to dendritic cells, thus inducing immune tolerance: this approach envisions great perspectives in the treatment of autoimmune diseases, organ transplantation, and allergic diseases.

In the mini-review of [Porello and Cellesi](#), the authors provide a nice overview of the state-of-the-art methods for intracellular protein delivery to mammalian cells, highlighting current challenges, new developments, and future research opportunities.

The Opinion paper of [Limongi and Susa](#) is focused on one of the major recent challenge faced by the humankind, *i.e.*, the COVID-19 pandemic. The Authors focused their attention on how much nanobiotechnology contributed and still is contributing to the development of safe and efficient solutions to prevent, diagnose, and treat COVID-19, and any similar infection or pathology.

[Lam et al.](#) describes important translational issues in Nanobiotechnology that can be used as theranostics in neurosurgical oncology, highlighting recent advancements in the application of nanoplateforms for fluorescence image-guided brain tumor resection and treatment.

Concluding, we hope this Research Topic could have provided useful cues and insights to the Readers, shedding lights on the most recent development in the application of nanotechnology to biology and human healthcare.

## Author contributions

GC: Conceptualization, Writing–original draft. MM: Writing–review and editing.

## Funding

The author(s) declare that no financial support was received for the research, authorship, and/or publication of this article.

## Conflict of interest

The authors declare that the research was conducted in the absence of any commercial or financial relationships that could be construed as a potential conflict of interest.

The author(s) declared that they were an editorial board member of Frontiers, at the time of submission. This had no impact on the peer review process and the final decision.

## Publisher's note

All claims expressed in this article are solely those of the authors and do not necessarily represent those of their affiliated organizations, or those of the publisher, the editors and the reviewers. Any product that may be evaluated in this article, or claim that may be made by its manufacturer, is not guaranteed or endorsed by the publisher.



# An Opinion on How Nanobiotechnology is Assisting Humankind to Overcome the Coronavirus Disease 2019

Tania Limongi\* and Francesca Susa

Department of Applied Science and Technology, Politecnico di Torino, Turin, Italy

**Keywords:** COVID-19, SARS-CoV-2, nanobiotechnology, health emergencies, prevention, diagnostics, treatments, patents

## INTRODUCTION

Analyzing results from a PubMed search done at the end of March 2022, more than 550,000 scientific publications relating to “Biotechnology” have been published. At the same time, if searching for “Nanobiotechnology,” it can be seen that more than 7,100 publications have been written in the last 20 years, with an ever-increasing annual publication rate. Nanobiotechnology, a relatively young branch of knowledge, is the crossing point between bio and nano technology, and comprises a wide range of nanotechnological applications in the life sciences field. In the last 2 years, just one hundred years after the last Pandemic Flu, humanity has sadly been hit by one of the worst infectious disease emergences of modern times. We believe that only in conjunction with this terrible health crisis have the real power of what are commonly recognized as Nanobiotechnologies been realized. Since the onset of the pandemic, these technologies have been the subject of heated discussions for scientists, clinicians, journalists, politicians, and ordinary people. For instance, next to the most accredited zoonotic transfer origin of SARS-CoV-2 (Andersen et al., 2020), it was even speculated (Casadevall et al., 2021) to have a nanobiotechnological origin in one of the biosafety level-4 biological laboratories of the Wuhan Institute of Virology.

Although there is still no way to reach unquestionable conclusions on the origins of this pandemic, allowing us to establish how much was due to chance, nature, or to the fast development of human technologies, in this opinion we will prove how much nanobiotechnology is doing in assisting the whole scientific community in quickly and effectively resolving this global health crisis. We want to highlight how much nanobiotechnology is contributing in such a short time with nanomaterials and technology to the development of safe and efficient solutions to prevent, diagnose, and treat COVID-19 and any infections of the same nature.

## WHY AND HOW TO USE “NANO” TO ASSIST “BIO”

For at least a couple of decades, technology and nanoscience have demonstrated an important role in the design of effective solutions for biomedical applications, offering new methods and materials. Due to their dimensions ranging from a few to hundreds of nanometers, nanomaterials, whether of biological, inorganic, or synthetic origin, demonstrate exclusive performances (Xiao et al., 2022) as core elements or components of a wide range of nanotechnological solutions to various kinds of diseases.

Nanobioengineered solutions, including nanomaterials and nanovehicles, are ever more frequently used for medical microbiology, tissue repair and regeneration, drug delivery, diagnosis, and treatment of inflammatory and cancer diseases (Susa et al., 2019; Contera et al., 2020). Furthermore, a wide range of micro and nanofabrication processes allows the design and

## OPEN ACCESS

### Edited by:

Gianni Ciofani,  
Italian Institute of Technology (IIT), Italy

### Reviewed by:

Fernando Soto,  
Stanford University, United States  
Flavia Vitale,  
University of Pennsylvania,  
United States

### \*Correspondence:

Tania Limongi  
tania.limongi@polito.it

### Specialty section:

This article was submitted to  
Nanobiotechnology,  
a section of the journal  
Frontiers in Bioengineering and  
Biotechnology

**Received:** 08 April 2022

**Accepted:** 10 May 2022

**Published:** 13 June 2022

### Citation:

Limongi T and Susa F (2022) An  
Opinion on How Nanobiotechnology is  
Assisting Humankind to Overcome the  
Coronavirus Disease 2019.  
Front. Bioeng. Biotechnol. 10:916165.  
doi: 10.3389/fbioe.2022.916165

fabrication of highly sensitive sensors and transistor-based biosensors able to detect and analyze multicomponent mixtures from human samples for early diagnosis or real-time continuous monitoring (Coluccio et al., 2015; Nagamine and Tokito, 2021; Park et al., 2021; Sung et al., 2021; Finnegan et al., 2022; Kaloumenou et al., 2022).

The impact of the use of nanotechnologies and of their related and waste products must be assessed based on both people and the environment. In agreement with most of our colleagues, we believe that nanobiotechnology-based solutions deserve special administrative rules (Osman, 2019; Allan et al., 2021; Carlander and Skentelbery, 2021). Although regulatory organizations, such as the Global Coalition for Regulatory Science Research, the European Commission's Joint Research Centre, the United States Environmental Protection Agency and the U.S. Food and Drug Administration, have begun to regulate the potential problems arising from the use of nanotechnologies, there is still an urgent need to define universally shared toxicity standards and updated regulatory guidelines (Subhan and Subhan, 2022).

## **HAS THE NANOTECHNOLOGICAL CONTRIBUTION MADE A DIFFERENCE IN THE FIGHT AGAINST COVID-19 COMPARED TO OTHER EPIDEMICS?**

Among the various pathologies, infectious ones involve a very high incidence rate and, obviously, actions against these diseases, such as human immunodeficiency virus, malaria, and tuberculosis, are particularly challenging, considering their unending spread and high mortality rate (Kirtane et al., 2021).

More than 2 years ago, humanity was confronted by the SARS-CoV-2 virus that caused COVID-19 disease. There is no question that this tragic event has radically changed the lives of billions of people, since it rapidly spread everywhere, leading to the closure of public and private facilities, filling hospitals, and shutting down worldwide economies and social activities. Professionals from different backgrounds joined forces to try to stem this pandemic with all the losses in human and socio-economic life that it entailed. The massive investigation effort made for COVID-19 prevention, diagnosis, and treatment started 2 years ago, is still ongoing, and should be recognized as a prodigious success since it is substantially contributing to this pandemic disease becoming endemic.

Many solutions, such as vaccine production and medication repurposing, have been adopted and, among the various strategies used, nanotechnology undoubtedly has provided better solutions in the implementation of valid preventive and diagnostic actions, such as through the design of faster and more effective treatments (Weiss et al., 2020).

A very recent (March 2022) query, done in the Web of Science Core Collection, for the string "COVID-19 nanotechnology" provided more than 400 papers published between 2020 and 2022. By refining the search, adding respectively the words "prevention," "diagnostics," and "treatments," we noticed that about 10% concern prevention application, 40% diagnostics, and 50% treatments. This bibliographic research had clearly shown how,

in just 2 years, a remarkable variety of nanotechnological approaches assisted scientific and medical communities in developing nanomaterials for the implementation of disinfection systems, molecular or antigenic diagnosis kits, antiviral drugs, and nanoarchitected vaccines (Ruiz-Hitzky et al., 2020).

## **HAVE PATENTS, DURING THE COVID-19 EMERGENCY, PROMOTED DISCLOSURE OF INVENTIONS, REDUCING DUPLICATION OF RESEARCH, COSTS OF RESEARCH, AND BARGAINING?**

Given the exceptional number of scientific publications produced on the just introduced topic by colleagues in these pandemic years, in this opinion article for the Nanobiotechnology section of the journal *Frontiers in Bioengineering and Biotechnology*, we focused on one of the most important engineering and technological aspects of the discussion, patents.

One of the first works on this aspect of the pandemic is the one in which Ruiz-Hitzky and others provided an indication on patented work related to nanotechnology applied to coronaviruses (Ruiz-Hitzky et al., 2020). They carried out a systematic search on the distribution of patents dealing with SARS-CoV viruses (comprising SARS-CoV and SARS-CoV-2) by using the "coronavirus and nano" topics to refine the query in the ESPACENET patent website. Since their article was published in September 2020 and their ESPACENET database query focused generically on the terms "coronavirus and nano," on April 2022, we did a new search on both VaxPal and ESPACENET websites, looking for patents related to the applications of nanobiotechnologies for COVID-19 prevention, vaccines, diagnosis, and treatments. The results confirmed that, in all the application areas of our interest such as prevention, diagnostic, and therapeutic, nanotechnologies have given and are greatly assisting in the successful management of a sudden and unexpected global emergency like the COVID-19 pandemic. More in detail, as summarized in **Table 1**, considering the 45 resulting patents, four refer to prevention, 20 to vaccines development, 14 to diagnostics, and seven to therapeutic applications. Most of them were filed by companies and academic institutes (18 and 16 patents, respectively), eight by private organizations, and three by governmental entities.

## **CAN A FLUID AND TRANSVERSAL NETWORK BETWEEN DIFFERENT SKILLS FAVOR A FASTER AND MORE EFFECTIVE MANAGEMENT OF HEALTH EMERGENCIES SUCH AS THE ONE WE HAVE BEEN SUFFERING WORLDWIDE IN RECENT YEARS?**

In this opinion piece we tried to highlight how, in nanobiotechnology, the intercommunication of skills has allowed technology to design and apply nanoscale solutions

**TABLE 1 |** Patents related to the applications of nanobiotechnologies for COVID-19 prevention, vaccines, diagnosis, and treatments. Data from Tavares et al. (2022) and from a query on VaxPal and ESPACENET websites carried out on April 2022.

Application	Nanotechnology	Product	Patent number	Producer
Prevention	Porous structure Nanoparticles	Filtration article for personal protective equipment Compositions and methods for reducing the transmissivity of illnesses using an oral delivery system	US2021331107A1 US2022080020A1	Company: Ion Defense Tech LLC Private : Montagnier Luc and Lorenzen Lee H
	Lipid nanoparticles	Topical application of povidone-iodine on mucous membranes	WO2020232515	Private: Firebrick Pharma PTY LTD
Vaccine	Silver nanoparticles	Nanosilver spray	CN111466407	Private: Dong Nan
	Lipid nanoparticles	mRNA-1273	US10898574B2	Company: ModernaTX
		Tozinameran (BNT162b2)	WO2017075531A1	Company: Pfizer-BioNTech: Acuitas
		Zorecimeran (CVnCoV)	WO2021123332A1	Company: CureVac
		ARCoV	CN111333704A	Company -Government: Academy of Military Science, Walvax Biotechnology, Suzhou Abogen Biosciences
		LNP-nCoVsaRNA Vaccine	WO2021212101A1 KR2020118386	Academic: Imperial College of London Private: Lee Ho Jun
			CN112662695	Academic: Institute Medical Biology CAMS
			IN202021024459	Private: Lohagaonkar Kunal Sambhaji, Lohagaonkar Manisha Kunal
			CN111218458	Company: Zhuhai Lifanda Biotechnology CO LTD
			CN112300251	Academic: Sichuan University
	Proteo-lipid vehicle Nanoparticles	Covigenix VAX-001 NVX-CoV2373 Nano-vaccine Vaccine	US2019367566A1 WO2021154812A1 CN111607002 CN112480217	Company: Entos Pharmaceuticals Company: Novavax Academic: Sun Yat Sen University Company: Guangzhou Ribobio CO LTD, Agena Biopharmaceutical CO LTD
	Ferritin nanoparticles	SpFN	WO2021178971A1	Government: Walter Reed Army Institute of Research
Diagnostics	Gold nanoparticles	Vaccine	RO134811A0	Academic: Institutul Nat De Cercetare Dezvoltare Pentru Fizica Tehnica IFT Iasi
	Aluminum nanoparticles	Vaccine	CN111939253	Company: Hefei Novel Gene Tech Service CO LTD
	Self-assembling nanoparticles	Vaccine	US20210139543 CN111991556	Private: Scripps Research Institute Academic: Sun Yat Sen University, Sun Yat Sen University Cancer Center Sun Yat Sen University Affiliated Cancer Hospital
	Coronavirus subunit nanoparticles	Nano-vaccine	CN111603556	Academic: Sun Yat Sen University
	Electrodes and hydrophobic substrate	Sensor and Method for Detecting Target Molecules	US2021255172A1	Academic: Southern Methodist University
	Acoustic sensor	Methods for identifying infectious disease	WO2021221925A1	Company: Aviana molecular Tech LLC
	Carbon-based biosensor	Multiplex biosensor for rapid point-of-care diagnostics	WO2021231948A1	Company: Hememics Biotechnologies Inc
	Fluorescent probe-based biosensor	Fluorescent probe based biosensor and assay for the detection of SARS-CoV-2	US10962529B1	Academic: King Abdulaziz university
	Gold/Silver nanoparticles-aptamer	Optical fiber sensor	CN112730340	Academic: Northwestern University
	Colloidal gold	Immunochromatographic test	CN112485436	Academic: Guilin Electronic Tech University
	Gold nanoparticles	SARS-CoV-2 affinity polypeptide	CN112375754	Academic: Tsinghua University
		Nano plasma resonance	CN111812321	Company: Liangzhun Shanghai Medical Apparatus CO LTD
Treatment		Test kit	CN105018644	Government: Jiangsu Provincial Center For Disease Prevention And Control
	Gold magnetic nanoparticles	Nucleic acid detection method	CN112375812	Company: Xian Goldmag Nanobiotech CO LTD
	Magnetic nanoparticles	Anti-SARS-CoV-2 nucleocapsid protein Ig	CN112239501	Company: Dongguan Pengzhi Biotechnology CO LTD
		Test kit	CN112079906	Private:Zhang Ying
	Silver nanoparticles	Silver-complexed therapeutic neutralizing antibody	CN111471105	Academic: Guangxi Medical University
	Oleic acid-modified zinc sulfide nanoparticles	Detection device	CN111579792	Private: Yang Xiaojun
	Lipid nanoparticles	Nanoparticle Depot For Controlled And Sustained Gene Delivery	US2021330597A1	Academic: New Jersey institute technology
		Anti SARS-CoV-2 drugs	CN112472791	Academic: Fudan University

(Continued on following page)



**TABLE 1 |** (Continued) Patents related to the applications of nanobiotechnologies for COVID-19 prevention, vaccines, diagnosis, and treatments. Data from Tavares et al. (2022) and from a query on VaxPal and ESPACENET websites carried out on April 2022.

Application	Nanotechnology	Product	Patent number	Producer
	Collagen and metal nanoparticles	Collagen as a delivery tool for metal-based anti-viral agents	WO2021229577A1	Company: Collplant LTD
	Chitosan-based nanoparticles	Novochizol	WO2021160667A1	Company: Bosti Trading LTD
	Magnetic nanoparticles	Nano-antibody	CN112500480	Company: Shanghai Novamab Biopharmaceuticals CO LTD
	Polymeric nanoparticles	Alveolar macrophage-like multifunctional nanoparticles	CN112438960	Academic: The Fifth Affiliated Hospital Sun Yat Sen University
	Nanoparticles	gRNA targeting SARS-CoV-2	CN112143731	Company: Guangzhou Reforgene Biological Tech CO LTD

for biological applications. Coronavirus prevention, recognition, and handling technologies represent the central weaponries in the fight against Covid diseases. Patent worldwide status mirrors the innovation's grade in the nanobiotechnological field. According to our opinion, in addition to what has already been designed and implemented, the most ambitious objectives will certainly be achieved with the development of integrated hybrid systems. Recent progresses in nanoscience, smart materials, wireless expertise, and wearable integrated circuit technology allowed Collins and others to engineer a face mask capable of both functioning as an individual protection device and, at the same time, sensing possible viral particles in the wearer's breath (Nguyen et al., 2021).

We believe that, in the wake of what is already in progress in the nanobiotechnological field with the development of advanced lab on chip and smart nanofeatured devices, it will be possible to develop solutions capable of quickly giving reliable and reproducible results even in personalized medicine, both in diagnostics and in therapy.

We would like to give our opinion on how it could be possible to integrate, on a single microchip, some nano-technologies, nano-features, and nanosystems including thin films and 3D printing for fluidics, separations as molecular and cellular sorting, nucleic acids sequencing, manipulation and genomics, proteomics, or metabolomics for targeted analysis.

Referring to infectious diseases, such as COVID-19, through a simple prick on a finger, using a nanofeatured chip, it could be possible to carry out both the diagnosis and the eventually related post-exposure prophylaxis since testing the presence of the viral

RNA or protein simultaneously and estimating how long before the infection started, some therapies, like the one based on monoclonal antibodies, which are efficient only if started before the recommended terms (Taylor et al., 2021), can be administered.

To conclude, although much progress has been made in biotechnological development towards the nanotechnological approach, much still needs to be done in regards to the safety, regulatory, and policy perspective. In our opinion, this could be done by trying to fill the lack of global standardization in the application of robust methods and in the characterization of reference materials through the combination of the needs of consumers/patients and of the skills of scientists, clinics, engineers, jurists, standardization bodies, and companies.

## AUTHOR CONTRIBUTIONS

TL: conceptualization, hypothesis, discussion, writing, and revision. FS: discussion, writing. All authors contributed to the article and approved the submitted version.

## FUNDING

This work was supported by the starting grant of the Politecnico of Torino to new fixed term researchers in strategic research fields and by the Frontiers Fee Support program.

## REFERENCES

- Allan, J., Belz, S., Hoeveler, A., Hugas, M., Okuda, H., Patri, A., et al. (2021). Regulatory Landscape of Nanotechnology and Nanoplastics from a Global Perspective. *Regul. Toxicol. Pharmacol.* 122, 104885. doi:10.1016/j.yrtph.2021.104885
- Andersen, K. G., Rambaut, A., Lipkin, W. I., Holmes, E. C., and Garry, R. F. (2020). The Proximal Origin of SARS-CoV-2. *Nat. Med.* 26 (4), 450–452. doi:10.1038/s41591-020-0820-9
- Carlander, D., and Skentelbery, C. (2021). "EU Regulations and Nanotechnology Innovation," in *Nanotoxicology in Humans and the Environment* (Springer), 229–248. doi:10.1007/978-3-030-79808-6\_8
- Casadevall, A., Weiss, S. R., and Imperiale, M. J. (2021). Can Science Help Resolve the Controversy on the Origins of the SARS-CoV-2 Pandemic? *mBio* 12 (4), e01948–01921. doi:10.1128/mBio.01948-21

- Coluccio, M. L., Gentile, F., Das, G., Nicastri, A., Perri, A. M., Candeloro, P., et al. (2015). Detection of Single Amino Acid Mutation in Human Breast Cancer by Disordered Plasmonic Self-Similar Chain. *Sci. Adv.* 1 (8), e1500487. doi:10.1126/sciadv.1500487
- Contera, S., Bernardino de la Serna, J., and Tetley, T. D. (2020). Biotechnology, Nanotechnology and Medicine. *Emerg. Top. Life Sci.* 4 (6), 551–554. doi:10.1042/etls20200350
- Finnegan, M., Duffy, E., and Morrin, A. (2022). The Determination of Skin Surface pH via the Skin Volatile Emission Using Wearable Colorimetric Sensors. *Sens. Bio-Sensing Res.* 35, 100473. doi:10.1016/j.sbsr.2022.100473
- Kaloumenou, M., Skotadis, E., Lagopati, N., Efstathopoulos, E., and Tsoukalas, D. (2022). Breath Analysis: A Promising Tool for Disease Diagnosis—The Role of Sensors. *Sensors* 22 (3), 1238. doi:10.3390/s22031238
- Kirtane, A. R., Verma, M., Karandikar, P., Furin, J., Langer, R., and Traverso, G. (2021). Nanotechnology Approaches for Global Infectious Diseases. *Nat. Nanotechnol.* 16 (4), 369–384. doi:10.1038/s41565-021-00866-8

- Nagamine, K., and Tokito, S. (2021). Organic-transistor-based Biosensors Interfaced with Human Skin for Non-invasive Perspiration Analysis. *Sensors Actuators B Chem.* 349, 130778. doi:10.1016/j.snb.2021.130778
- Nguyen, P. Q., Soenksen, L. R., Donghia, N. M., Angenent-Mari, N. M., de Puig, H., Huang, A., et al. (2021). Wearable Materials with Embedded Synthetic Biology Sensors for Biomolecule Detection. *Nat. Biotechnol.* 39 (11), 1366–1374. doi:10.1038/s41587-021-00950-3
- Osman, E. M. (2019). Environmental and Health Safety Considerations of Nanotechnology, Nano Safety. *Biomed. J. Sci. Tech. Res.* 19 (4), 14501–14515. doi:10.26717/bjstr.2019.19.003346
- Park, H., Park, W., and Lee, C. H. (2021). Electrochemically Active Materials and Wearable Biosensors for the *In Situ* Analysis of Body Fluids for Human Healthcare. *NPG Asia Mater* 13 (1), 23. doi:10.1038/s41427-020-00280-x
- Ruiz-Hitzky, E., Darder, M., Wicklein, B., Ruiz-Garcia, C., Martín-Sampedro, R., Del Real, G., et al. (2020). Nanotechnology Responses to COVID-19. *Adv. Healthc. Mater.* 9 (19), 2000979.
- Subhan, M. A., and Subhan, T. (2022). “Safety and Global Regulations for Application of Nanomaterials,” in *Chapter 5 - Safety and Global Regulations for Application of nanomaterials* *Nanomaterials Recycling*. Editors M. Rai and T. A. Nguyen (Elsevier), 83–107. doi:10.1016/b978-0-323-90982-2.00005-6
- Sung, W.-H., Tsao, Y.-T., Shen, C.-J., Tsai, C.-Y., and Cheng, C.-M. (2021). Small-volume Detection: Platform Developments for Clinically-Relevant Applications. *J. Nanobiotechnol* 19 (1), 114. doi:10.1186/s12951-021-00852-1
- Susa, F., Limongi, T., Dumontel, B., Vighetto, V., and Cauda, V. (2019). Engineered Extracellular Vesicles as a Reliable Tool in Cancer Nanomedicine. *Cancers* 11 (12), 1979. doi:10.3390/cancers11121979
- Tavares, J. L., Cavalcanti, I. D. L., Santos Magalhães, N. S., and Lira Nogueira, M. C. d. B. (2022). Nanotechnology and COVID-19: Quo Vadis? *J. Nanopart Res.* 24 (3), 62. doi:10.1007/s11051-022-05452-0
- Taylor, P. C., Adams, A. C., Hufford, M. M., de la Torre, I., Winthrop, K., and Gottlieb, R. L. (2021). Neutralizing Monoclonal Antibodies for Treatment of COVID-19. *Nat. Rev. Immunol.* 21 (6), 382–393. doi:10.1038/s41577-021-00542-x
- Weiss, C., Carriere, M., Fusco, L., Capua, I., Regla-Nava, J. A., Pasquali, M., et al. (2020). Toward Nanotechnology-Enabled Approaches against the COVID-19 Pandemic. *ACS Nano* 14 (6), 6383–6406. doi:10.1021/acsnano.0c03697
- Xiao, M.-F., Zeng, C., Li, S.-H., and Yuan, F.-L. (2022). Applications of Nanomaterials in COVID-19 Pandemic. *Rare Mater.* 41 (1), 1–13. doi:10.1007/s12598-021-01789-y

**Conflict of Interest:** The authors declare that the research was conducted in the absence of any commercial or financial relationships that could be construed as a potential conflict of interest.

**Publisher’s Note:** All claims expressed in this article are solely those of the authors and do not necessarily represent those of their affiliated organizations, or those of the publisher, the editors and the reviewers. Any product that may be evaluated in this article, or claim that may be made by its manufacturer, is not guaranteed or endorsed by the publisher.

Copyright © 2022 Limongi and Susa. This is an open-access article distributed under the terms of the Creative Commons Attribution License (CC BY). The use, distribution or reproduction in other forums is permitted, provided the original author(s) and the copyright owner(s) are credited and that the original publication in this journal is cited, in accordance with accepted academic practice. No use, distribution or reproduction is permitted which does not comply with these terms.





# Forging the Frontiers of Image-Guided Neurosurgery—The Emerging Uses of Theranostics in Neurosurgical Oncology

Fred C. Lam<sup>1,2,\*†</sup>, Uyanga Tsedev<sup>1,3†</sup>, Ekkehard M. Kasper<sup>2</sup> and Angela M. Belcher<sup>1,3</sup>

<sup>1</sup>The David H. Koch Institute for Integrative Cancer Research, Massachusetts Institute of Technology, Cambridge, MA, United States, <sup>2</sup>Division of Neurosurgery, Saint Elizabeth's Medical Center, Brighton, MA, United States, <sup>3</sup>Department of Biological Engineering, Massachusetts Institute of Technology, Cambridge, MA, United States

**Keywords:** theranostic, neurosurgery, fluorescence-guide surgery, nanotechnology, NIR imaging *in vivo*

## OPEN ACCESS

### Edited by:

Orit Shefi,  
Bar-Ilan University, Israel

### Reviewed by:

Carlotta Pucci,  
Italian Institute of Technology (IIT), Italy  
Shazia Bano,  
Harvard Medical School,  
United States

### \*Correspondence:

Fred C. Lam  
fredlam@mit.edu

<sup>†</sup>These authors have contributed  
equally to this work

### Specialty section:

This article was submitted to  
Nanobiotechnology,  
a section of the journal  
Frontiers in Bioengineering and  
Biotechnology

**Received:** 18 January 2022

**Accepted:** 31 May 2022

**Published:** 12 July 2022

### Citation:

Lam FC, Tsedev U, Kasper EM and  
Belcher AM (2022) Forging the  
Frontiers of Image-Guided  
Neurosurgery—The Emerging Uses of  
Theranostics in  
Neurosurgical Oncology.  
Front. Bioeng. Biotechnol. 10:857093.  
doi: 10.3389/fbioe.2022.857093

## INTRODUCTION

### A Brief History of Neurosurgical Oncology

Modern neurosurgical treatment of brain tumors involves maximal safe resection of tumorous tissue whilst preserving adjacent normal neurovascular anatomy in order to minimize the risk of neurological injury to the patient (Sunaert, 2006). A surgical series of 8 patients performed by renowned Johns Hopkins neurosurgeon Dr. Walter Edward Dandy, published in 1933, involved surgical removal of the right cerebral hemisphere with preservation of the right basal ganglia, in right-handed patients who presented with left-sided paralysis due to their right hemispheric tumors (Dandy, 1933). This pioneering report demonstrated the invasiveness of malignant brain tumors despite heroic surgical efforts, as patients inevitably succumbed to residual disease in the preserved basal ganglia, with invasion into the opposite hemisphere, emphasizing both the need for better visualization of tumor cells within the brain during surgery and the necessity for adjuvant chemotherapy and radiation therapy to treat residual tumor burden. Further pioneering work throughout the past century by other neurosurgical greats including: Drs. Harvey Cushing, William Halsted, Fedor Krause, Victor Horsley, Wilder Penfield, Gazi Yaşargil, Rolando Del Maestro, and others, paved the way for the advent of cortical brain mapping techniques, use of the operating microscope, and stereotactic surgery—all of which are now common tools in the neurosurgeon's armamentarium to enable safe surgical resection of brain tumors (exquisitely reviewed in "A History of Neuro-Oncology," by Dr. Rolando Del Maestro) (Del Maestro, 2006).

Further pioneering work published in 1916 by Dr. Dandy and his then senior neurosurgery resident, Dr. George J. Heuer, reported the localization of brain tumors in one hundred consecutive patients using x-ray roentgenography (Heuer and Dandy, 1916). This was followed by a series of studies by Dr. Dandy in which he injected air, and later, contrast agents, into the ventricular and lumbar subarachnoid spaces to diagnosis and localize brain and spinal tumors using x-rays (Dandy, 1918; Dandy, 1919). The herculean efforts of renowned neurologist Dr. Egas Antonio Ceatano de Moniz and neurosurgeon Dr. Pedro Almeida Lima in Lisbon, Portugal, in developing the technique of cerebral angiography for the localization and visualization of the blood supply of brain tumors, led to Dr. Lima's documentation of over 2000 angiograms in 1949, paving the way for the indispensable use of cerebral angiography in modern day neurosurgery for the diagnosis and treatment of brain tumors and the coiling of cerebral aneurysms (Moniz, 1927; Del Maestro, 2006).

## Intraoperative Image-Guided Technology in Neurosurgical Oncology

The use of intravenous fluorescein tagged with radioactive  $^{131}\text{I}$  iodine to differentiate tumor tissue from normal brain under ultraviolet (UV) light by Dr. George Eugene Moore in 1947 at the University of Minnesota was one of the first reports of exploiting the inherent leakiness of the blood-brain barrier (BBB) around brain tumors to allow for the extravasation of a radioactive fluorophore to enhance visualization of brain tumors. This landmark discovery paved the way for the introduction of radioactive nucleotides such as  $^{18}\text{F}$  fluorodeoxyglucose for use with computed tomography (CT) and positron emission tomography (PET) to localize metabolically active tumor cells in the brain. However, it was the advent of nuclear magnetic resonance (NMR) by Professors Felix Block from Stanford University and Edward Purcell from Harvard, for which they were awarded the Nobel Prize in Physics in 1952, that led to the introduction of magnetic resonance imaging (MRI) scanners, which has since revolutionized our ability to visualize with stunning resolution the neurovascular anatomy of the brain and spinal cord. Since then, adaptations such as functional MRI (fMRI) (Ogawa et al., 1990; Kwong et al., 1992) and diffusion tensor imaging (DTI) (O'Donnell and Westin, 2011; Alexander et al., 2007) have allowed for the neurosurgeon to superimpose multiple layers of imaging information on top of contrast agent enhanced MRI sequences to allow for rendering of the spatial characteristics of brain tumors in eloquent regions of the brain (using fMRI) with respect to neighboring neuronal fiber tracts (using DTI) to achieve maximal safe resection of brain tumors (Algethami et al., 2021).

Incorporating different image-guided technologies into the operative neurosurgical workflow varies depending on the modality that is used. Many neurosurgical centers now have access to portable neuronavigation systems such as the Medtronic StealthStation™ (Minneapolis, MN, United States) that occupy minimal footprint in the operating room and can overlay high resolution CT or MRI imaging with fMRI or DTI images to allow for fixed 3D mapping of intracranial lesions for presurgical planning (Algethami et al., 2021). The disadvantage of these fixed imaging systems is that they do not allow for real-time evaluation of intraoperative resection margins, unlike intraoperative MRI (iMRI), which currently provides the highest quality resolution of EoR and assessment of changes in the brain throughout the course of a tumor resection (Rogers et al., 2021). However, given the large footprint required to accommodate an MRI scanner, the need for specialized operating rooms with MRI compatible (non-ferromagnetic) instruments that are required to allow for positioning of the patient in and out of the scanner whilst providing adequate surgical access throughout the course of the operation, and the high costs associated with purchasing and installation of the MRI scanner and the MRI compatible instruments, the use of iMRI is currently limited to specialized neurosurgical centers that can afford this technology (Mislow et al., 2009; Chicoine et al., 2011).

Despite the improvements in preoperative imaging planning workflow, the surgeon is often times limited in their ability to differentiate tumor tissue from adjacent normal neuroanatomy under direct white light microscopy. This is particularly

challenging during resection of infiltrative tumors such as high-grade gliomas, the most common and aggressive primary brain tumor in adults. To overcome this limitation, fluorescence-guided surgery (FGS) using tumor-targeting fluorophores have steadily been introduced into the neurosurgeon's armamentarium (Vahrmeijer et al., 2013). The FDA-approved protoporphyrin IX prometabolite 5-aminolevulinic acid (5-ALA) has yielded promising results in increasing the EoR for high-grade gliomas (Stummer et al., 2006; Della Puppa et al., 2014a; Belloch et al., 2014), but has shown no clear benefit in lower-grade disease where tumor cells are less metabolically active, thereby decreasing the levels of intraoperative fluorescence to allow for maximal safe EoR (Mirza et al., 2022). Furthermore, the need to orally administer 5-ALA to the patient 2.5–3 h prior to induction of anesthesia followed by strict avoidance of direct exposure to sunlight or bright room lights for 24 h after 5-ALA administration due to increased skin photosensitivity (Tonn and Stummer, 2008) and the relative high cost of 5-ALA, have limited its widespread use. Alternatively, the FDA-approved fluorescent dye sodium fluorescein, which has been widely used and tested for safety in the field of ophthalmology, is inexpensive, can be administered intravenously at the time of surgery, and relies on the leakiness of the surrounding BBB to accumulate at the site of high grade brain tumors (Acerbi et al., 2014; Cavallo et al., 2018). Unlike 5-ALA, fluorescein does not depend on the metabolic activity of tumor cells and could lead to false-positive identification of non-tumorous cells surrounding the leaky BBB, however several studies comparing fluorescein-guided to white light resections have demonstrated a high level of accuracy in identification of tumor tissues (Kuroiwa et al., 1998; Kuroiwa et al., 1999; Acerbi et al., 2013; Acerbi et al., 2014). The much lower cost of fluorescein and its safety profile supported by the ophthalmologic literature have increased its prevalence for use in neurosurgical procedures (Kwiterovich et al., 1991; Kwan et al., 2006). Disadvantages of 5-ALA and sodium fluorescein are that while both fluorophores can clearly demarcate tumor boundaries, they lack depth of tissue penetration with laser excitation in their respective wavelengths and their signal can be masked by endogenous cellular autofluorescence (Acerbi et al., 2014; Mirza et al., 2022). More recently, the FDA-approved near-infrared fluorophore indocyanine green (ICG), traditionally used in angiography procedures, has gained popularity in FGS. Like fluorescein, ICG also accumulates at the tumor site through leaky BBB vasculature but has also been shown to achieve endocytosis inside tumor cells (Onda et al., 2016), whereas fluorescein does not, allowing for higher sensitivity of detection of tumor cells during surgery which correlates well with gadolinium contrast-enhancing tumor signal on preoperative MRI (Lee et al., 2016).

## Evidence for Using Intraoperative Imaging Technology to Maximize Extent of Resection to Improve Survival Outcomes in Neurosurgical Oncology

Successful outcomes in neurosurgical oncology is increasingly being defined by the EoR to achieve a gross total resection (GTR) or maximal safe cytoreduction (Rogers et al., 2021). Several

studies have reported the EoR as the single most significant variable for impacting survival in patients with newly diagnosed or recurrent high grade gliomas (HGG) (Lacroix et al., 2001; Sanai et al., 2011; Oppenlander et al., 2014). Similarly, a GTR or maximal safe EoR were associated with significantly longer progression free survival (PFS) and overall survival (OS) in patients with low grade gliomas compared to performing a biopsy alone (Roelz et al., 2016; Scherer et al., 2020).

Studies comparing across image-guided surgical modalities demonstrated that iMRI was superior over both 5-ALA FGS and conventional neuronavigation approaches in obtaining GTRs and led to prolonged survival (Knauth et al., 1999; Bohinski et al., 2001; Senft et al., 2011; Golub et al., 2020). A recent Cochrane Database network meta-analysis comparing image-guided technologies to maximize EoR for resection of gliomas yielded a paucity of high level evidence supporting the use of iMRI or 5-ALA in achieving maximal EoR with heavily biased results and inconclusive evidence regarding improvements in PFS and OS (Fountain et al., 2021). Furthermore, a brief cost benefit analysis suggested that image-guided surgery, iMRI, and 5-ALA FGS in particular, are associated with increased costs compared to conventional surgical resections, and therefore further research and randomized controlled trials will be needed in order to determine whether these modalities should be offered as standard of care for resection of brain tumors (Fountain et al., 2021). A more recent frequentist network meta-analysis was published identifying 23 studies with 2,643 patients comparing 5-ALA, sodium fluorescein, and iMRI, to no image guidance for the resection of HGGs (Naik et al., 2022). This study found that image guidance using iMRI, fluorescein, and 5-ALA led to greater rates of GTR, improved PFS, and OS compared to no image guidance. However, both meta-analyses confirmed that future studies are needed to assess superiority between modalities as well as other metrics including duration of surgery while using image guided techniques and cost.

One caveat that must be taken into consideration when interpreting the results of the aforementioned network meta-analysis is that the majority of studies using 5-ALA to maximize EoR were in patients with HGGs that were located in the supratentorial space (i.e. Frontal, parietal, occipital, and temporal lobes of the brain) (Stummer et al., 2006). These are regions of the brain that are relatively easy to access surgically, and patients can generally tolerate aggressive tumor tissue debulking without significant neurological sequelae. Thus, conventional neurosurgical approaches are more likely to yield EoR margins and outcomes that are comparable to image-guided approaches. However, lesions that are located in more sensitive regions of the brain (i.e. the brainstem, posterior fossa) may benefit from image-guided surgery in order to better appreciate tumor margins around brainstem nuclei and nerve fiber tracts that control essential neurological and life-sustaining functions while achieving maximal safe EoR (Della Puppa et al., 2014b; Della Puppa et al., 2015; Algethami et al., 2021). In fact, the importance of intraoperative visualization for maximal safe brain tumor resection has been recognized by the global neurosurgical oncology community, as evidenced by the inaugural 2021 conference on intraoperative visualization and the

connectome, organized by the prestigious Society for Neuro-Oncology ([https://www.soc-neuro-onc.org/WEB/WEB/Event\\_Content/Intraoperative\\_Visualization\\_and\\_the\\_Connectome.aspx](https://www.soc-neuro-onc.org/WEB/WEB/Event_Content/Intraoperative_Visualization_and_the_Connectome.aspx)).

## The Emerging Uses of Nanoscale Materials to Augment Fluorescence-Guided Neurosurgery

Forging the frontiers of image-guided neurosurgery is the emerging use of nanoscale materials for the detection and treatment of tumor cells in neurosurgical procedures. Nanoscale materials are self-assembling polymeric systems measuring less than 1,000 nm in their longest axis. These systems can be organic or inorganic in nature, and can be functionalized with targeting moieties to facilitate delivery across the BBB into the CNS with the ability to then deliver payload to specific cells of interest in the brain. Nanoparticles (NP) that have been developed for potential CNS applications typically have a maximal diameter of ~100 nm to facilitate trafficking across the tight junctions of the BBB. We previously developed a liposomal NP of ~100 nm in diameter that was functionalized with a fluorophore and transferrin to enable transferrin receptor-mediated transcytosis across the BBB to deliver dual combination therapies to glioma brain tumors in mice (Lam et al., 2018). Other researchers have developed mesoporous silica NPs, magnetic iron oxide NPs, gold NPs, copolymers, and carbon nanotubes, for delivery of cargo into the brain (a summary of these nanoplateforms with accompanying references are provided in **Table 1**). Functionalization of NPs with surface moieties such as transferrin, folate, cyclic RGD peptide, or angiopep-2, that enable trafficking across the BBB and targeting to tumor cells *in vivo* can improve specificity of delivery, although the effectiveness of receptor targeting of NPs in solid tumors has been recently questioned (Obaid, 2021 #233). We have provided a tabular summary of these NP formulations, specific targeting ligands and sequences, along with potential applications for use in neurosurgical oncology for ease of reference for our readers (**Table 1**).

The versatility of a single nanoscale delivery system to be multiplexed with detection and treatment capabilities defines it as a theranostic (d'Angelo et al., 2019). The ability of a theranostic to visualize tumor cells *in vivo* during surgery and track cellular biodistribution and treatment response throughout the course of adjuvant therapy, can allow for time and cost savings while adopting a personalized medicine approach to improve outcomes (d'Angelo et al., 2019; Mendes et al., 2018). For example, a fluorescent-labelled theranostic NP conjugated to a CD133 monoclonal antibody has recently been shown to enable NIR tracking of patient-derived glioma cancer stem cells in an orthotopic mouse model of glioma (Jing et al., 2016). Finally, a fluorescent-tagged monoclonal antibody targeting the epidermal growth factor receptor (EGFR), cetuximab-IRDye800, has recently been shown in a first-in-human trial demonstrating the ability to identify tumor tissue in glioma

**TABLE 1 |** Summary of different physicochemical and functional properties of nanoparticles with their potential clinical applications in neurosurgical oncology.

Types of nanoparticles	Liposomes/polymersomes Jiang et al. (2012), Zong et al. (2014), Shi et al. (2015) Iron oxide NP Alphandéry et al. (2015) Silica NP Wang et al. (2015) Gold NP Fan et al. (2014) Quantum dots Onoshima et al. (2015) Carbon nanotubes Wang et al. (2012), Ceppi et al. (2019) Bacteriophage Ghosh et al. (2012), Yi et al. (2012), Staquicini et al. (2020), Wang et al. (2021) Copolymers Ke et al. (2017)
BBB trafficking receptors, peptide sequences, and ligands	Mannose Du et al. (2014) Glucose Du et al. (2014) Lactate Pérez-Escuredo et al. (2016) Neutral amino acids Nawashiro et al. (2005), Kobayashi et al. (2008), Abbott et al. (2010), Geier et al. (2013) Cationic amino acids Barar et al. (2016) Anionic amino acids Smith (2000), Hawkins et al. (2006) Oligopeptides and polypeptides Butte et al. (2014), Dardevet et al. (2015) Transferrin Wang et al. (2009), Zhou et al. (2021) Folate Wang et al. (2009), Zhou et al. (2021) LRP1 Jiang et al. (2018)
Tumor targeting peptide sequences, ligands, and receptors	RGD Qin et al. (2011), Sharma et al. (2013), Zong et al. (2014), Liu et al. (2015), Shi et al. (2015), Wang et al. (2016), Joshi et al. (2017), Ke et al. (2017), Yao et al. (2017) NGR Sharma et al. (2017) CGKRK Sharma et al. (2017) Angiopep-2 Gao et al. (2014) Chlorotoxin Veisheh et al. (2009), Wang et al. (2020) HA Jiang et al. (2012) CD133 Jing et al. (2016) Folate Cho et al. (2019) Transferrin Dixit et al. (2015) LRP1 Jiang et al. (2018)
Potential clinical applications	Drug delivery to brain tumors d'Angelo et al. (2019), Dixit et al. (2015) Imaging of brain tumors Jing et al. (2016), Carr et al. (2018) Photo-thermal-acoustic therapy for brain tumors Golubewa et al. (2020) Anti-tumor gene therapy Staquicini et al. (2020) Fluorescence-guided tumor surgery Butte et al. (2014), Cho et al. (2018), Cho et al. (2019)

patients in real-time under NIR FGS with high correlations to pre-operative gadolinium-enhanced MR imaging and post-operative histopathological staining of tissue specimens (Miller et al., 2018), emphasizing the timeliness and importance of discussing novel brain tumor-targeting theranostic technologies that can potentially surpass the sole reliance of the heterogeneously leaky BBB around high grade tumors allowing for delivery of 5-ALA or ICG.

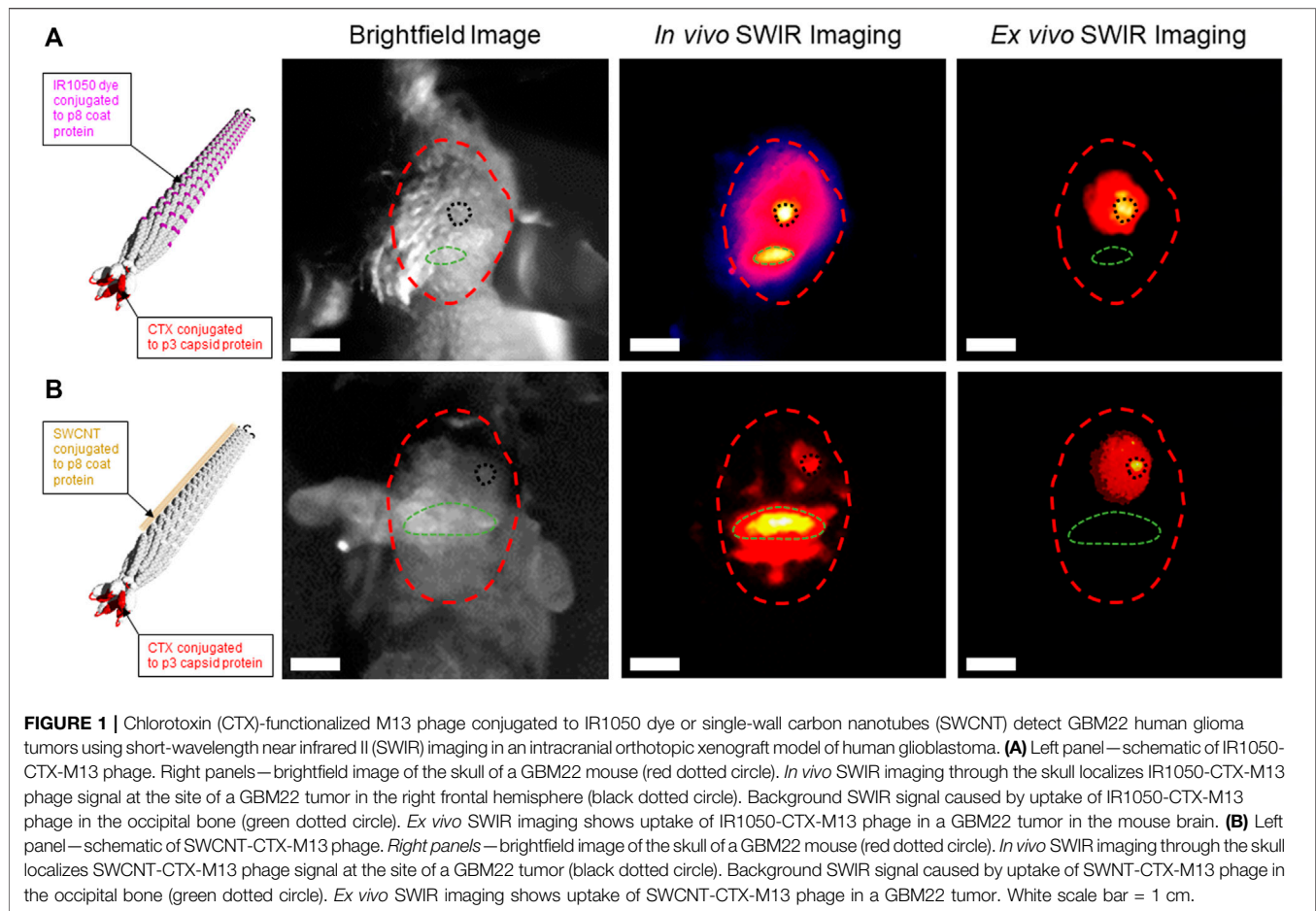
We previously leveraged the use of M13 bacteriophage (M13  $\phi$ )—highly specialized and modular nanoscale filamentous protein particles that can be genetically tuned for programmable assembly, chemically modified for surface functionalization of imaging, chemical, or antigenic moieties, for *in vivo* theranostic applications. These applications have included: Tumor-targeted imaging and drug delivery (Ghosh et al., 2012); Image-guided solid tumor resection (Yi et al., 2012; Ghosh et al., 2014); And high contrast short-wavelength infrared (SWIR) fluorescence imaging of vascular and lymphatic structures (Ceppi et al., 2019; Lin et al., 2019). In this mini review and opinion piece, we introduce proof-of-concept data demonstrating our ability to functionalize M13  $\phi$  for systemic delivery to detect glioma brain tumors using SWIR fluorescence

imaging in a patient-derived mouse model of glioma, demonstrating the potential for the use of M13  $\phi$  as a brain tumor theranostic.

## RESULTS

We previously published on our expertise to generate stable rod-like filamentous M13  $\phi$  with a narrow diameter of 5 nm and length of 900 nm that can be conjugated with various NIR fluorescent dyes or single-wall carbon nanotubes (SWCNT) to enable SWIR imaging of ovarian tumors and lymph nodes in a mouse model of ovarian cancer (Ghosh et al., 2012; Yi et al., 2012; Ghosh et al., 2014; Ceppi et al., 2019). We hypothesized that the extremely narrow diameter and high length-to-diameter aspect ratio of the M13  $\phi$  would allow it passage across the tight endothelial gap junctions of the BBB if functionalized with a known peptide moiety with proven ability to achieve endocytosis across the BBB with the ability to target glioma tumor cells in the brain following systemic delivery. Several such peptides have been identified including angiopep-2 (Liu et al., 2019), PepC7 (Li et al., 2012), and GL1 (Ho et al., 2010), amongst others, however, there





has only been one peptide to-date that has been FDA-approved for in-human use to assist in FGS of higher grade brain tumors—the 36 amino-acid peptide chlorotoxin (CTX), derived from the venom of the *Leiurus quinquestriatus* scorpion (Veisheh et al., 2009; Dardevet et al., 2015; Cohen-Inbar and Zaaroor, 2016). CTX peptide and CTX conjugates have demonstrated the ability to traverse the BBB and achieve binding to over 80% of tumor cells in an intracranial orthotopic model of glioma (Wang et al., 2020). To achieve functionalization of M13  $\phi$  with CTX, we cloned in the 108 base pair CTX gene sequence upstream of the phage p3 capping protein insertion site. We hypothesized that conjugation of CTX-M13  $\phi$  with either the NIR II IR1050 dye (**Figure 1A**, left panel, schematic) or SWCNT (**Figure 1B**, left panel, schematic) to the p8 coat proteins of M13  $\phi$  would allow detection of CTX-M13  $\phi$  at the site of patient-derived GBM22 brain tumors in an intracranial orthotopic xenograft murine model of GBM using SWIR imaging.

Brightfield images of the heads of GBM22 mice show their skulls outlined in red, their occipital bony prominence outlined in green, and the site of intracranial GBM22 tumor induction in the right posterior frontal lobe, outlined in black (**Figures 1A,B**, right panel, brightfield images). Twenty-four hours following tail vein injection of either IR1050-CTX-M13 or SWCNT-CTX-M13  $\phi$ , the heads of GBM22 mice were subjected to *in vivo* SWIR

imaging (**Figures 1A,B**, right panel, *In vivo* SWIR images, respectively). Results demonstrated IR1050-CTX-M13  $\phi$  or SWCNT-CTX-M13  $\phi$  signal localized to the right posterior frontal lobe region corresponding to the site of GBM22 tumor induction (**Figures 1A,B**, right panel, *In vivo* SWIR images, black dotted circles). Background uptake of IR1050-CTX-M13 or SWCNT-CTX-M13 phage was observed in the occipital bony protruberance of the mice (**Figures 1A,B**, right panel, *In vivo* SWIR images, green dotted circles, respectively). To further confirm the uptake of CTX-M13  $\phi$  at the site of GBM22 brain tumors, we removed the brains from the skulls of GBM22 mice and performed *ex vivo* SWIR imaging. *Ex vivo* SWIR imaging demonstrated focused IR1050-CTX-M13 or SWCNT-CTX-M13 signal at the site of GBM22 tumors (**Figures 1A,B**, right panel, *Ex vivo* SWIR images, black dotted circles, respectively). The elimination of signal from the bony region corresponding to the occipital bone during *ex vivo* SWIR imaging confirmed the nonspecific uptake of IR1050-CTX-M13  $\phi$  and SWCNT-CTX-M13  $\phi$  by the occipital bone (**Figures 1A,B**, right panel, *Ex vivo* SWIR images, green dotted circles) and the specificity of the CTX-M13  $\phi$  to detect GBM22 cells in the brain (**Figures 1A,B**, right panel, *Ex vivo* SWIR images, black dotted circles). Taken together, our preliminary data confirms the modular nature of M13  $\phi$  to be functionalized and conjugated for use in glioma

tumor detection using SWIR imaging with the potential for further development as a theranostic nanomaterial for the treatment of gliomas.

## DISCUSSION

Filamentous bacteriophage are highly stable and scalable nanoscale materials that have been characterized for their inert effects as a nano-carrier for the delivery of a range of vaccine-based therapies in humans (González-Mora et al., 2020; Margot et al., 2020; Chung et al., 2021). Like other filamentous bacteriophage systems, M13  $\phi$  is genetically tunable and can be manufactured at relative low costs with high uniformity across batches, making this nanoplatform an ideal candidate as a theranostic delivery system. Recent studies have demonstrated the ability of filamentous phage to achieve penetration into the CNS space through intranasal delivery or assisted by temporary disruption of the BBB through convection-enhanced delivery for the treatment of neurological diseases (Carrera et al., 2004; Wan et al., 2009; Dabrowska, 2019).

A recent study using a hybrid vector expressing an adeno-associated virus and a single-stranded M13 phage (AAVP) displaying a double-cyclic RGD4C motif ligand (which targets  $\alpha$  V integrin receptors expressed on the surface of tumor vascular endothelium) with the gene sequence for the cytotoxic protein tumor necrosis factor (RGD4C-AAVP-*TNF*), demonstrated tumor killing when systemically delivered over 3 consecutive doses in an intracranial orthotopic xenograft mouse model of U87MG human glioma (Staquicini et al., 2020). The same study also leveraged the RGD4C-AAVP construct to express *Herpes simplex* virus thymidine kinase (RGD4C-AAVP-*HSVtk*) in U87MG mice followed by treatment with ganciclovir as suicide gene therapy. Both the RGD4C-AAVP-*TNF* and RGD4C-AAVP-*HSVtk* constructs achieved the intended cytotoxic and theranostic effects, respectively, demonstrating the potential for using M13  $\phi$  as a theranostic for the treatment of human gliomas and potentially other brain tumors (Staquicini et al., 2020). Our preliminary data demonstrating the ability of IR1050-CTX-M13  $\phi$  and SWCNT-CTX-M13  $\phi$  to detect patient-derived GBM22 tumors in the brains of mice using SWIR imaging (Figures 1A,B, right panel, *Ex vivo* SWIR images), and our previously published studies using NIR II conjugated-M13  $\phi$  expressing tumor-targeting peptides to detect ovarian cancer tumors during real-time surgical resection in a mouse model of ovarian cancer (Yi et al., 2012; Ghosh et al., 2014), further enforces the potential of using M13  $\phi$  as a versatile theranostic platform for use in FGS and multimodal treatment of a wide range of tumors, including brain tumors. We are currently conducting further preclinical studies to better characterize the pharmacokinetics, pharmacodynamics, and safety of M13  $\phi$  in the CNS to assess the translational potential for use in human trials (Tsedeve et al., 2022).

The potential for tumor-targeting nanoscale materials to be used in the detection and treatment of a wide range of brain tumors can offer patients a personalized treatment path. In particular, the recent 2021 reclassification of CNS tumors into further molecular subtypes based on genetic modifiers and/or

diagnostic molecular pathological features (Louis et al., 2021), has uncovered limitations in using 5-ALA FGS for Gr III glial tumors (Mirza et al., 2022). This study compared outcomes in 69 patients with Gr III gliomas—39 patients had 5-ALA FGS and 30 patients had non-5-ALA FGS. Patients in the 5-ALA group had preoperative MR imaging that demonstrated some degree of contrast enhancement compared to those in the non-5-ALA group. The degree of intraoperative 5-ALA fluorescence directly correlated to the presence of contrast enhancement on preoperative imaging. Interestingly, the degree of intraoperative fluorescence was not associated with either 1p19q codeletion nor IDH mutational tumor status, however, significantly more patients with gliomas that had O-6-methylguanine-DNA methyltransferase methylation received 5-ALA FGS. There were no statistically significant differences in OS nor EoR between groups, but interestingly performance status was worse in the 5-ALA group in the immediate post-operative and 6-month follow-up periods. Patients in the 5-ALA group who had a GTR had significant improvements in OS compared to patients with subtotal resections (STR), however patients who had STRs in the non-5-ALA group had better performance scores at 6 months compared to patients with STRs in the 5-ALA group. This and other studies point towards a potential correlation between molecular subtyping with 5-ALA tumor fluorescence, and argues against the widespread use of 5-ALA FGS in these patients. Similarly, an elegant study by Obaid and colleagues using an NIR-II EGFR-targeting nanoliposome formulation to study the specificity of NP delivery to EGFR-expressing glioma cell lines *in vitro*, *in vivo*, and *ex vivo*, demonstrated that delivery of nanoliposomes to the tumor site did not correlate with EGFR expression in the three different glioma cell lines that were tested, underrepresenting the image-derived molecular specificity by up to 94.2% (Obaid et al., 2021). This suggests that the accumulation of functionalized nanoliposomes (which are the most commonly used types of NPs for clinical applications) at the sites of tumors may be more dependent on the enhanced permeability and retention properties of tumors rather than their specificity of molecular targeting—something that researchers should be aware of when using receptor-ligand biochemistry to improve a nanoparticle's delivery to the tissue site of interest to assist in FGS. Finally, the ability to tailor theranostics for patients who have subtypes of gliomas that do not respond well to FGS may offer an alternative personalized approach to treating this increasingly heterogeneous group of tumors.

## CONCLUSION

In conclusion, the increasing use of fluorescence image-guided tumor resection within the neurosurgical community opens an avenue for the introduction of innovative theranostic nanoplatforms that could further assist the tumor surgeon in achieving intraoperative detection and maximal EoR. Whilst future comparative studies are needed to definitively assess the ability of FGS to achieve better patient outcomes compared to the less costly, non-fluorescence-based navigated resection techniques, the potential for theranostics to be applied in a

more personalized fashion may lead to breakthroughs in treating complex and heterogeneous brain tumors such as gliomas in order to achieve better survival outcomes afforded by current standard of care treatment regimens, which have largely remained unchanged over the past several decades.

## REFERENCES

- Abbott, N. J., Patabendige, A. A. K., Dolman, D. E. M., Yusof, S. R., and Begley, D. J. (2010). Structure and Function of the Blood-Brain Barrier. *Neurobiol. Dis.* 37 (1), 13–25. doi:10.1016/j.nbd.2009.07.030
- Acerbi, F., Broggi, M., Eoli, M., Anghileri, E., Cuppini, L., Pollo, B., et al. (2013). Fluorescein-guided Surgery for Grade IV Gliomas with a Dedicated Filter on the Surgical Microscope: Preliminary Results in 12 Cases. *Acta Neurochir.* 155 (7), 1277–1286. doi:10.1007/s00701-013-1734-9
- Acerbi, F., Cavallo, C., Broggi, M., Cordella, R., Anghileri, E., Eoli, M., et al. (2014). Fluorescein-guided Surgery for Malignant Gliomas: A Review. *Neurosurg. Rev.* 37 (4), 547–557. doi:10.1007/s10143-014-0546-6
- Alexander, A. L., Lee, J. E., Lazar, M., and Field, A. S. (2007). Diffusion Tensor Imaging of the Brain. *Neurotherapeutics* 4 (3), 316–329. doi:10.1016/j.nurt.2007.05.011
- Algethami, H., Lam, F. C., Rojas, R., and Kasper, E. (2021). “Presurgical and Surgical Planning in Neurosurgical Oncology - A Case-Based Approach to Maximal Safe Surgical Resection in Neurosurgery,” in *IntechOpen*. doi:10.5772/intechopen.99155
- Alphandéry, E., Grand-Dewyse, P., Lefèvre, R., Mandawala, C., and Durand-Dubief, M. (2015). Cancer Therapy Using Nanoformulated Substances: Scientific, Regulatory and Financial Aspects. *Expert Rev. Anticancer Ther.* 15 (10), 1233–1255. doi:10.1586/14737140.2015.1086647
- Barar, J., Rafi, M. A., Pourseif, M. M., and Omid, Y. (2016). Blood-brain Barrier Transport Machineries and Targeted Therapy of Brain Diseases. *Bioimpacts* 6 (4), 225–248. doi:10.15171/bi.2016.30
- Belloch, J. P., Rovira, V., Llacer, J. L., Riesgo, P. A., and Cremades, A. (2014). Fluorescence-guided Surgery in High Grade Gliomas Using an Exoscope System. *Acta Neurochir.* 156 (4), 653–660. doi:10.1007/s00701-013-1976-6
- Bohinski, R. J., Kokkino, A. K., Warnick, R. E., Gaskill-Shipley, M. F., Kormos, D. W., Lukin, R. R., et al. (2001). Glioma Resection in a Shared-Resource Magnetic Resonance Operating Room after Optimal Image-Guided Frameless Stereotactic Resection. *Neurosurgery* 48 (4), 731–744. discussion 742–4. doi:10.1227/00006123-200104000-00007
- Butte, P. V., Mamelak, A., Parrish-Novak, J., Drazin, D., Shweikeh, F., Gangalum, P. R., et al. (2014). Near-infrared Imaging of Brain Tumors Using the Tumor Paint BLZ-100 to Achieve Near-Complete Resection of Brain Tumors. *Foc* 36 (2), E1. doi:10.3171/2013.11.focus13497
- Carr, J. A., Franke, D., Caram, J. R., Perkinson, C. F., Saif, M., Askoxylakis, V., et al. (2018). Shortwave Infrared Fluorescence Imaging with the Clinically Approved Near-Infrared Dye Indocyanine Green. *Proc. Natl. Acad. Sci. U.S.A.* 115 (17), 4465–4470. doi:10.1073/pnas.1718917115
- Carrera, M. R. A., Kaufmann, G. F., Mee, J. M., Meijler, M. M., Koob, G. F., and Janda, K. D. (2004). Treating Cocaine Addiction with Viruses. *Proc. Natl. Acad. Sci. U.S.A.* 101 (28), 10416–10421. doi:10.1073/pnas.0403795101
- Cavallo, C., De Laurentis, C., Vetrano, I. G., Falco, J., Broggi, M., Schiariti, M., et al. (2018). The Utilization of Fluorescein in Brain Tumor Surgery: A Systematic Review. *J. Neurosurg. Sci.* 62 (6), 690–703. doi:10.23736/S0390-5616.18.04480-6
- Ceppi, L., Bardhan, N. M., Na, Y., Siegel, A., Rajan, N., Fruscio, R., et al. (2019). Real-Time Single-Walled Carbon Nanotube-Based Fluorescence Imaging Improves Survival after Debulking Surgery in an Ovarian Cancer Model. *ACS Nano* 13 (5), 5356–5365. doi:10.1021/acsnano.8b09829
- Chicoine, M. R., Lim, C. C. H., Evans, J. A., Singla, A., Zipfel, G. J., Rich, K. M., et al. (2011). Implementation and Preliminary Clinical Experience with the Use of Ceiling Mounted Mobile High Field Intraoperative Magnetic Resonance Imaging between Two Operating Rooms. *Acta Neurochir. Suppl.* 109, 97–102. doi:10.1007/978-3-211-99651-5\_15
- Cho, S. S., Jeon, J., Buch, L., Nag, S., Nasrallah, M., Low, P. S., et al. (2018). Intraoperative Near-Infrared Imaging with Receptor-specific versus Passive Delivery of Fluorescent Agents in Pituitary Adenomas. *J. Neurosurg.* 131 (6), 1974–1984. doi:10.3171/2018.7.JNS181642
- Cho, S. S., Zeh, R., Pierce, J. T., Jeon, J., Nasrallah, M., Adappa, N. D., et al. (2019). Folate Receptor Near-Infrared Optical Imaging Provides Sensitive and Specific Intraoperative Visualization of Nonfunctional Pituitary Adenomas. *Onsurg* 16 (1), 59–70. doi:10.1093/ons/opy034
- Chung, J., Jung, Y., Hong, C., Kim, S., Moon, S., Kwak, E. A., et al. (2021). Filamentous Anti-influenza Agents Wrapping Around Viruses. *J. Colloid Interface Sci.* 583, 267–278. doi:10.1016/j.jcis.2020.09.012
- Cohen-Inbar, O., and Zaaroor, M. (2016). Glioblastoma Multiforme Targeted Therapy: The Chlorotoxin Story. *J. Clin. Neurosci.* 33, 52–58. doi:10.1016/j.jocn.2016.04.012
- d'Angelo, M., Castelli, V., Benedetti, E., Antonosante, A., Catanesi, M., Dominguez-Benot, R., et al. (2019). Theranostic Nanomedicine for Malignant Gliomas. *Front. Bioeng. Biotechnol.* 7, 325. doi:10.3389/fbioe.2019.00325
- Dabrowska, K. (2019). Phage Therapy: What Factors Shape Phage Pharmacokinetics and Bioavailability? Systematic and Critical Review. *Med. Res. Rev.* 39 (5), 2000–2025. doi:10.1002/med.21572
- Dandy, W. E. (1919). Fluoroscopy of the Cerebral Ventricles. *Johns Hopkins Hosp. Bull.* 30, 29–33. doi:10.1097/00007611-191908000-00051
- Dandy, W. E. (1933). Physiological Studies Following Extirpation of Right Cerebral Hemisphere in Man. *Bull. Johns Hopkins Hosp.* 33, 31–51.
- Dandy, W. E. (1918). Ventriculography Following the Injection of Air into the Cerebral Ventricles. *Ann. Surg.* 68, 5–11. doi:10.1097/00000658-191807000-00002
- Dardevet, L., Rani, D., Aziz, T., Bazin, I., Sabatier, J.-M., Fadl, M., et al. (2015). Chlorotoxin: A Helpful Natural Scorpion Peptide to Diagnose Glioma and Fight Tumor Invasion. *Toxins* 7 (4), 1079–1101. doi:10.3390/toxins7041079
- Del Maestro, R. F. (2006). *A History of Neuro-Oncology*. Montreal: DW Medical Consulting Inc.
- Della Puppa, A., Ciccarino, P., Lombardi, G., Rolma, G., Cecchin, D., and Rossetto, M. (2014). 5-Aminolevulinic Acid Fluorescence in High Grade Glioma Surgery: Surgical Outcome, Intraoperative Findings, and Fluorescence Patterns. *Biomed. Res. Int.* 2014, 232561. doi:10.1155/2014/232561
- Della Puppa, A., Gioffrè, G., Gardiman, M. P., Frasson, C., Cecchin, D., Scienza, R., et al. (2014). Intra-operative 5-aminolevulinic Acid (ALA)-induced Fluorescence of Medulloblastoma: Phenotypic Variability and CD133+ Expression According to Different Fluorescence Patterns. *Neurol. Sci.* 35 (1), 99–102. doi:10.1007/s10072-013-1597-0
- Della Puppa, A., Rustemi, O., Gioffrè, G., and Scienza, R. (2015). Approaching a Brainstem High-Grade Glioma (HGG) with the Assistance of 5-aminolevulinic Acid (5-ALA) Technology: A New Strategy for an Old Surgical Challenge. *Neurol. Sci.* 36 (5), 797–799. doi:10.1007/s10072-014-1901-7
- Dixit, S., Novak, T., Miller, K., Zhu, Y., Kenney, M. E., and Broome, A.-M. (2015). Transferrin Receptor-Targeted Theranostic Gold Nanoparticles for Photosensitizer Delivery in Brain Tumors. *Nanoscale* 7 (5), 1782–1790. doi:10.1039/c4nr04853a
- Du, D., Chang, N., Sun, S., Li, M., Yu, H., Liu, M., et al. (2014). The Role of Glucose Transporters in the Distribution of P-Aminophenyl- $\alpha$ -D-Mannopyranoside Modified Liposomes within Mice Brain. *J. Control. Release* 182, 99–110. doi:10.1016/j.jconrel.2014.03.006
- Fan, Z., Fu, P. P., Yu, H., and Ray, P. C. (2014). Theranostic Nanomedicine for Cancer Detection and Treatment. *J. Food Drug Analysis* 22 (1), 3–17. doi:10.1016/j.jfda.2014.01.001
- Fountain, D. M., Bryant, A., Barone, D. G., Waqar, M., Hart, M. G., Bulbeck, H., et al. (2021). Intraoperative Imaging Technology to Maximise Extent of

## AUTHOR CONTRIBUTIONS

FL and UT designed experiments, obtained SWIR *in vivo* imaging data, and wrote the manuscript. AB supervised the experiments and edited the manuscript.



- Resection for Glioma: A Network Meta-Analysis. *Cochrane Database Syst. Rev.* 1, CD013630. doi:10.1002/14651858.CD013630.pub2
- Gao, H., Zhang, S., Cao, S., Yang, Z., Pang, Z., and Jiang, X. (2014). Angiopep-2 and Activatable Cell-Penetrating Peptide Dual-Functionalized Nanoparticles for Systemic Glioma-Targeting Delivery. *Mol. Pharm.* 11 (8), 2755–2763. doi:10.1021/mp500113p
- Geier, E. G., Schlessinger, A., Fan, H., Gable, J. E., Irwin, J. J., Sali, A., et al. (2013). Structure-based Ligand Discovery for the Large-Neutral Amino Acid Transporter 1, LAT-1. *Proc. Natl. Acad. Sci. U.S.A.* 110 (14), 5480–5485. doi:10.1073/pnas.1218165110
- Ghosh, D., Bagley, A. F., Na, Y. J., Birrer, M. J., Bhatia, S. N., and Belcher, A. M. (2014). Deep, Noninvasive Imaging and Surgical Guidance of Submillimeter Tumors Using Targeted M13-Stabilized Single-Walled Carbon Nanotubes. *Proc. Natl. Acad. Sci. U.S.A.* 111 (38), 13948–13953. doi:10.1073/pnas.1400821111
- Ghosh, D., Kohli, A. G., Moser, F., Endy, D., and Belcher, A. M. (2012). Refactored M13 Bacteriophage as a Platform for Tumor Cell Imaging and Drug Delivery. *ACS Synth. Biol.* 1 (12), 576–582. doi:10.1021/sb300052u
- Golub, D., Hyde, J., Dogra, S., Nicholson, J., Kirkwood, K. A., Gohel, P., et al. (2020). Intraoperative MRI versus 5-ALA in High-Grade Glioma Resection: a Network Meta-Analysis. *J. Neurosurg.* 1–15. doi:10.3171/2019.12.JNS191203
- Golubewa, L., Timoshchenko, I., Romanov, O., Karpicz, R., Kulahava, T., Rutkauskas, D., et al. (2020). Single-walled Carbon Nanotubes as a Photo-Thermo-Acoustic Cancer Theranostic Agent: Theory and Proof of the Concept Experiment. *Sci. Rep.* 10 (1), 22174. doi:10.1038/s41598-020-79238-6
- González-Mora, A., Hernández-Pérez, J., Iqbal, H. M. N., Rito-Palomares, M., and Benavides, J. (2020). Bacteriophage-Based Vaccines: A Potent Approach for Antigen Delivery. *Vaccines (Basel)* 8 (3). doi:10.3390/vaccines8030504
- Hawkins, R. A., O'Kane, R. L., Simpson, I. A., and Viña, J. R. (2006). Structure of the Blood-Brain Barrier and its Role in the Transport of Amino Acids. *J. Nutr.* 136 (1 Suppl.), 218S–26S. doi:10.1093/jn/136.1.218S
- Heuer, G. J., and Dandy, W. E. (1916). Roentgenography in the Localization of Brain Tumor, Based upon a Series of One Hundred Consecutive Cases. *Johns Hopkins Bull.* 27, 1–32.
- Ho, I. A. W., Hui, K. M., and Lam, P. Y. P. (2010). Isolation of Peptide Ligands that Interact Specifically with Human Glioma Cells. *Peptides* 31 (4), 644–650. doi:10.1016/j.peptides.2009.12.020
- Jiang, T., Zhang, Z., Zhang, Y., Lv, H., Zhou, J., Li, C., et al. (2012). Dual-functional Liposomes Based on pH-Responsive Cell-Penetrating Peptide and Hyaluronic Acid for Tumor-Targeted Anticancer Drug Delivery. *Biomaterials* 33 (36), 9246–9258. doi:10.1016/j.biomaterials.2012.09.027
- Jiang, Y., Yang, W., Zhang, J., Meng, F., and Zhong, Z. (2018). Protein Toxin Chaperoned by LRP-1-Targeted Virus-Mimicking Vesicles Induces High-Efficiency Glioblastoma Therapy *In Vivo*. *Adv. Mater.* 30 (30), e1800316. doi:10.1002/adma.201800316
- Jing, H., Weidensteiner, C., Reichardt, W., Gaedicke, S., Zhu, X., Grosu, A.-L., et al. (2016). Imaging and Selective Elimination of Glioblastoma Stem Cells with Theranostic Near-Infrared-Labeled CD133-specific Antibodies. *Theranostics* 6 (6), 862–874. doi:10.7150/tno.12890
- Joshi, S., Cooke, J. R. N., Ellis, J. A., Emala, C. W., and Bruce, J. N. (2017). Targeting Brain Tumors by Intra-arterial Delivery of Cell-Penetrating Peptides: A Novel Approach for Primary and Metastatic Brain Malignancy. *J. Neurooncol* 135 (3), 497–506. doi:10.1007/s11060-017-2615-5
- Ke, W., Zha, Z., Mukerabigwi, J. F., Chen, W., Wang, Y., He, C., et al. (2017). Matrix Metalloproteinase-Responsive Multifunctional Peptide-Linked Amphiphilic Block Copolymers for Intelligent Systemic Anticancer Drug Delivery. *Bioconjugate Chem.* 28 (8), 2190–2198. doi:10.1021/acs.bioconjchem.7b00330
- Knauth, M., Wirtz, C. R., Tronnier, V. M., Aras, N., Kunze, S., and Sartor, K. (1999). Intraoperative MR Imaging Increases the Extent of Tumor Resection in Patients with High-Grade Gliomas. *AJNR Am. J. Neuroradiol.* 20 (9), 1642–1646.
- Kobayashi, K., Ohnishi, A., Promsuk, J., Shimizu, S., Kanai, Y., Shiokawa, Y., et al. (2008). Enhanced Tumor Growth Elicited by L-type Amino Acid Transporter 1 in Human Malignant Glioma Cells. *Neurosurgery* 62 (2), 493–504. discussion 503–4. doi:10.1227/01.neu.0000316018.51292.19
- Kuroiwa, T., Kajimoto, Y., and Ohta, T. (1999). Comparison between Operative Findings on Malignant Glioma by a Fluorescein Surgical Microscopy and Histological Findings. *Neurological Res.* 21 (1), 130–134. doi:10.1080/01616412.1999.11740909
- Kuroiwa, T., Kajimoto, Y., and Ohta, T. (1998). Development of a Fluorescein Operative Microscope for Use during Malignant Glioma Surgery. *Surg. Neurol.* 50 (1), 41–49. discussion 48–9. doi:10.1016/s0090-3019(98)00055-x
- Kwan, A. S., Barry, C., McAllister, I. L., and Constable, I. (2006). Fluorescein Angiography and Adverse Drug Reactions Revisited: the Lions Eye Experience. *Clin. Exp. Ophthalmol.* 34 (1), 33–38. doi:10.1111/j.1442-9071.2006.01136.x
- Kwiterovich, K. A., Maguire, M. G., Murphy, R. P., Schachar, A. P., Bressler, N. M., Bressler, S. B., et al. (1991). Frequency of Adverse Systemic Reactions after Fluorescein Angiography. *Ophthalmology* 98 (7), 1139–1142. doi:10.1016/s0161-6420(91)32165-1
- Kwong, K. K., Belliveau, J. W., Chesler, D. A., Goldberg, I. E., Weisskoff, R. M., Poncelet, B. P., et al. (1992). Dynamic Magnetic Resonance Imaging of Human Brain Activity during Primary Sensory Stimulation. *Proc. Natl. Acad. Sci. U.S.A.* 89 (12), 5675–5679. doi:10.1073/pnas.89.12.5675
- Lacroix, M., Abi-Said, D., Fournier, D. R., Gokaslan, Z. L., Shi, W., DeMonte, F., et al. (2001). A Multivariate Analysis of 416 Patients with Glioblastoma Multiforme: Prognosis, Extent of Resection, and Survival. *J. Neurosurg.* 95 (2), 190–198. doi:10.3171/jns.2001.95.2.0190
- Lam, F. C., Morton, S. W., Wyckoff, J., Vu Han, T.-L., Hwang, M. K., Maffa, A., et al. (2018). Enhanced Efficacy of Combined Temozolomide and Bromodomain Inhibitor Therapy for Gliomas Using Targeted Nanoparticles. *Nat. Commun.* 9 (1), 1991. doi:10.1038/s41467-018-04315-4
- Lee, J. Y. K., Thawani, J. P., Pierce, J., Zeh, R., Martinez-Lage, M., Chanin, M., et al. (2016). Intraoperative Near-Infrared Optical Imaging Can Localize Gadolinium-Enhancing Gliomas during Surgery. *Neurosurgery* 79 (6), 856–871. doi:10.1227/neu.00000000000001450
- Li, J., Zhang, Q., Pang, Z., Wang, Y., Liu, Q., Guo, L., et al. (2012). Identification of Peptide Sequences that Target to the Brain Using *In Vivo* Phage Display. *Amino Acids* 42 (6), 2373–2381. doi:10.1007/s00726-011-0979-y
- Lin, C.-W., Bachilo, S. M., Zheng, Y., Tsedev, U., Huang, S., Weisman, R. B., et al. (2019). Creating Fluorescent Quantum Defects in Carbon Nanotubes Using Hypochlorite and Light. *Nat. Commun.* 10 (1), 2874. doi:10.1038/s41467-019-10917-3
- Liu, C., Zhao, Z., Gao, H., Rostami, I., You, Q., Jia, X., et al. (2019). Enhanced Blood-Brain-Barrier Penetrability and Tumor-Targeting Efficiency by Peptide-Functionalized Poly(amidoamine) Dendrimer for the Therapy of Gliomas. *Nanotheranostics* 3 (4), 311–330. doi:10.7150/ntno.38954
- Liu, Y., Mei, L., Yu, Q., Zhang, Q., Gao, H., Zhang, Z., et al. (2015). Integrin  $\alpha v \beta 3$  Targeting Activity Study of Different Retro-Inverso Sequences of RGD and Their Potentiality in the Designing of Tumor Targeting Peptides. *Amino Acids* 47 (12), 2533–2539. doi:10.1007/s00726-015-2043-9
- Louis, D. N., Perry, A., Wesseling, P., Brat, D. J., Cree, I. A., Figarella-Branger, D., et al. (2021). The 2021 WHO Classification of Tumors of the Central Nervous System: A Summary. *Neuro Oncol.* 23 (8), 1231–1251. doi:10.1093/neuonc/noab106
- Margot, S., Saulnier, A., and Barban, V. (2020). Phages and Vaccination: towards New Opportunities? *Virol. (Montrouge)* 24 (1), 37–47. doi:10.1684/vir.2019.0794
- Mendes, M., Sousa, J. J., Pais, A., and Vitorino, C. (2018). Targeted Theranostic Nanoparticles for Brain Tumor Treatment. *Pharmaceutics* 10 (4). doi:10.3390/pharmaceutics10040181
- Miller, S. E., Tummers, W. S., Teraphongphom, N., van den Berg, N. S., Hasan, A., Ertsey, R. D., et al. (2018). First-in-human Intraoperative Near-Infrared Fluorescence Imaging of Glioblastoma Using Cetuximab-IRDye800. *J. Neurooncol* 139 (1), 135–143. doi:10.1007/s11060-018-2854-0
- Mirza, A. B., Jose Pedro, L., Ioannis, C., Timothy Martyn, B., Amisha, V., Qusai, A. B., et al. (2022). 5-Aminolevulinic Acid-Guided Resection in Grade III Tumors - A Comparative Cohort Study. *Oper. Neurosurg. Hagerst.* 22, 215–223. doi:10.1227/ons.0000000000000118
- Mislow, J. M. K., Golby, A. J., and Black, P. M. (2009). Origins of Intraoperative MRI. *Neurosurg. Clin. N. Am.* 20 (2), 137–146. doi:10.1016/j.nec.2009.04.002
- Moniz, E. (1927). L'Encephalographie arterielle son importance dans la localization des tumeurs cerebrales. *Rev. Neurol.* 2, 72–89.
- Naik, A., Smith, E. J., Barreau, A., Nyaeme, M., Cramer, S. W., Najafali, D., et al. (2022). Comparison of Fluorescein Sodium, 5-ALA, and Intraoperative MRI for Resection of High-Grade Gliomas: A Systematic Review and Network Meta-Analysis. *J. Clin. Neurosci.* 98, 240–247. doi:10.1016/j.jocn.2022.02.028

- Nawashiro, H., Otani, N., Uozumi, Y., Oigawa, H., Toyooka, T., Suzuki, T., et al. (2005). High Expression of L-type Amino Acid Transporter 1 in Infiltrating Glioma Cells. *Brain Tumor Pathol.* 22 (2), 89–91. doi:10.1007/s10014-005-0188-z
- O'Donnell, L. J., and Westin, C. F. (2011). An Introduction to Diffusion Tensor Image Analysis. *Neurosurg. Clin. N. Am.* 22, 185. doi:10.1016/j.nec.2010.12.004
- Obaid, G., Samkoe, K., Tichauer, K., Bano, S., Park, Y., Silber, Z., et al. (2021). Is Tumor Cell Specificity Distinct from Tumor Selectivity *In Vivo*? A Quantitative NIR Molecular Imaging Analysis of Nanoliposome Targeting. *Nano Res.* 14 (5), 1344–1354. doi:10.1007/s12274-020-3178-x
- Ogawa, S., Lee, T. M., Kay, A. R., and Tank, D. W. (1990). Brain Magnetic Resonance Imaging with Contrast Dependent on Blood Oxygenation. *Proc. Natl. Acad. Sci. U.S.A.* 87 (24), 9868–9872. doi:10.1073/pnas.87.24.9868
- Onda, N., Kimura, M., Yoshida, T., and Shibutani, M. (2016). Preferential Tumor Cellular Uptake and Retention of Indocyanine Green Forin Vivotumor Imaging. *Int. J. Cancer* 139 (3), 673–682. doi:10.1002/ijc.30102
- Onoshima, D., Yukawa, H., and Baba, Y. (2015). Multifunctional Quantum Dots-Based Cancer Diagnostics and Stem Cell Therapeutics for Regenerative Medicine. *Adv. Drug Deliv. Rev.* 95, 2–14. doi:10.1016/j.addr.2015.08.004
- Oppenlander, M. E., Wolf, A. B., Snyder, L. A., Bina, R., Wilson, J. R., Coons, S. W., et al. (2014). An Extent of Resection Threshold for Recurrent Glioblastoma and its Risk for Neurological Morbidity. *Jns* 120 (4), 846–853. doi:10.3171/2013.12.jns13184
- Pérez-Escuredo, J., Van Hée, V. F., Sboarina, M., Falces, J., Payen, V. L., Pellerin, L., et al. (2016). Monocarboxylate Transporters in the Brain and in Cancer. *Biochimica Biophysica Acta (BBA) - Mol. Cell Res.* 1863 (10), 2481–2497. doi:10.1016/j.bbamer.2016.03.013
- Qin, Y., Chen, H., Yuan, W., Kuai, R., Zhang, Q., Xie, F., et al. (2011). Liposome Formulated with TAT-Modified Cholesterol for Enhancing the Brain Delivery. *Int. J. Pharm.* 419 (1–2), 85–95. doi:10.1016/j.ijpharm.2011.07.021
- Roelz, R., Strohmaier, D., Jabbarli, R., Kraeutle, R., Egger, K., Coenen, V. A., et al. (2016). Residual Tumor Volume as Best Outcome Predictor in Low Grade Glioma - A Nine-Years Near-Randomized Survey of Surgery vs. Biopsy. *Sci. Rep.* 6, 32286. doi:10.1038/srep32286
- Rogers, C. M., Jones, P. S., and Weinberg, J. S. (2021). Intraoperative MRI for Brain Tumors. *J. Neurooncol* 151 (3), 479–490. doi:10.1007/s11060-020-03667-6
- Sanai, N., Polley, M.-Y., McDermott, M. W., Parsa, A. T., and Berger, M. S. (2011). An Extent of Resection Threshold for Newly Diagnosed Glioblastomas. *Jns* 115 (1), 3–8. doi:10.3171/2011.2.jns10998
- Scherer, M., Ahmeti, H., Roder, C., Gessler, F., Jungk, C., Pala, A., et al. (2020). Surgery for Diffuse WHO Grade II Gliomas: Volumetric Analysis of a Multicenter Retrospective Cohort from the German Study Group for Intraoperative Magnetic Resonance Imaging. *Neurosurg.* 86 (1), E64–E74. doi:10.1093/neuros/nyz397
- Senft, C., Bink, A., Franz, K., Vatter, H., Gasser, T., and Seifert, V. (2011). Intraoperative MRI Guidance and Extent of Resection in Glioma Surgery: a Randomised, Controlled Trial. *Lancet Oncol.* 12 (11), 997–1003. doi:10.1016/s1470-2045(11)70196-6
- Sharma, G., Modgil, A., Layek, B., Arora, K., Sun, C., Law, B., et al. (2013). Cell Penetrating Peptide Tethered Bi-ligand Liposomes for Delivery to Brain *In Vivo*: Biodistribution and Transfection. *J. Control. Release* 167 (1), 1–10. doi:10.1016/j.jconrel.2013.01.016
- Sharma, S., Mann, A. P., Mölder, T., Kotamraju, V. R., Mattrey, R., Teesalu, T., et al. (2017). Vascular Changes in Tumors Resistant to a Vascular Disrupting Nanoparticle Treatment. *J. Control. Release* 268, 49–56. doi:10.1016/j.jconrel.2017.10.006
- Shi, K., Long, Y., Xu, C., Wang, Y., Qiu, Y., Yu, Q., et al. (2015). Liposomes Combined an Integrin  $\alpha\beta 3$ -Specific Vector with pH-Responsive Cell-Penetrating Property for Highly Effective Antiglioma Therapy through the Blood-Brain Barrier. *ACS Appl. Mat. Interfaces* 7 (38), 21442–21454. doi:10.1021/acsami.5b06429
- Smith, Q. R. (2000). Transport of Glutamate and Other Amino Acids at the Blood-Brain Barrier. *J. Nutr.* 130 (4S Suppl. 1), 1016S–22S. doi:10.1093/jn/130.4.1016S
- Staquicini, F. I., Smith, T. L., Tang, F. H. F., Gelovani, J. G., Giordano, R. J., Libutti, S. K., et al. (2020). Targeted AAVP-Based Therapy in a Mouse Model of Human Glioblastoma: A Comparison of Cytotoxic versus Suicide Gene Delivery Strategies. *Cancer Gene Ther.* 27 (5), 301–310. doi:10.1038/s41417-019-0101-2
- Stummer, W., Pichlmeier, U., Meinel, T., Wiestler, O. D., Zanella, F., and Reulen, H.-J. (2006). Fluorescence-guided Surgery with 5-aminolevulinic Acid for Resection of Malignant Glioma: a Randomised Controlled Multicentre Phase III Trial. *Lancet Oncol.* 7 (5), 392–401. doi:10.1016/s1470-2045(06)70665-9
- Sunaert, S. (2006). Presurgical Planning for Tumor Resectioning. *J. Magn. Reson. Imaging* 23 (6), 887–905. doi:10.1002/jmri.20582
- Tonn, J. C., and Stummer, W. (2008). Fluorescence-guided Resection of Malignant Gliomas Using 5-aminolevulinic Acid: Practical Use, Risks, and Pitfalls. *Clin. Neurosurg.* 55, 20–26.
- Tsedev, U., Lin, C.-W., Hess, G. T., Sarkaria, J. N., Lam, F. C., and Belcher, A. M. (2022). Phage Particles of Controlled Length and Genome for In Vivo Targeted Glioblastoma Imaging and Therapeutic Delivery. *ACS Nano.* In press.
- Vahrmeijer, A. L., Hutteman, M., van der Vorst, J. R., van de Velde, C. J. H., and Frangioni, J. V. (2013). Image-guided Cancer Surgery Using Near-Infrared Fluorescence. *Nat. Rev. Clin. Oncol.* 10 (9), 507–518. doi:10.1038/nrclinonc.2013.123
- Veiseth, O., Gunn, J. W., Kievit, F. M., Sun, C., Fang, C., Lee, J. S., et al. (2009). Inhibition of Tumor-Cell Invasion with Chlorotoxin-Bound Superparamagnetic Nanoparticles. *Small* 5 (2), 256–264. doi:10.1002/sml.200800646
- Wan, X.-M., Chen, Y.-P., Xu, W.-R., Yang, W.-j., and Wen, L.-P. (2009). Identification of Nose-To-Brain Homing Peptide through Phage Display. *Peptides* 30 (2), 343–350. doi:10.1016/j.peptides.2008.09.026
- Wang, D., Starr, R., Chang, W. C., Aguilar, B., Alizadeh, D., Wright, S. L., et al. (2020). Chlorotoxin-directed CAR T Cells for Specific and Effective Targeting of Glioblastoma. *Sci. Transl. Med.* 12 (533). doi:10.1126/scitranslmed.aaw2672
- Wang, H., Liu, X., Wang, Y., Chen, Y., Jin, Q., and Ji, J. (2015). Doxorubicin Conjugated Phospholipid Prodrugs as Smart Nanomedicine Platforms for Cancer Therapy. *J. Mat. Chem. B* 3 (16), 3297–3305. doi:10.1039/c4tb01984a
- Wang, X., Wang, C., Cheng, L., Lee, S.-T., and Liu, Z. (2012). Noble Metal Coated Single-Walled Carbon Nanotubes for Applications in Surface Enhanced Raman Scattering Imaging and Photothermal Therapy. *J. Am. Chem. Soc.* 134 (17), 7414–7422. doi:10.1021/ja300140c
- Wang, Y.-Y., Lui, P. C., and Li, J. Y. (2009). Receptor-mediated Therapeutic Transport across the Blood-Brain Barrier. *Immunotherapy* 1 (6), 983–993. doi:10.2217/imt.09.75
- Wang, Y., Sheng, J., Chai, J., Zhu, C., Li, X., Yang, W., et al. (2021). Filamentous Bacteriophage-A Powerful Carrier for Glioma Therapy. *Front. Immunol.* 12, 729336. doi:10.3389/fimmu.2021.729336
- Wang, Y., Shi, K., Zhang, L., Hu, G., Wan, J., Tang, J., et al. (2016). Significantly Enhanced Tumor Cellular and Lysosomal Hydroxychloroquine Delivery by Smart Liposomes for Optimal Autophagy Inhibition and Improved Antitumor Efficiency with Liposomal Doxorubicin. *Autophagy* 12 (6), 949–962. doi:10.1080/15548627.2016.1162930
- Yao, J., Ma, Y., Zhang, W., Li, L., Zhang, Y., Zhang, L., et al. (2017). Design of New Acid-Activated Cell-Penetrating Peptides for Tumor Drug Delivery. *PeerJ* 5, e3429. doi:10.7717/peerj.3429
- Yi, H., Ghosh, D., Ham, M.-H., Qi, J., Barone, P. W., Strano, M. S., et al. (2012). M13 Phage-Functionalized Single-Walled Carbon Nanotubes as Nanoprobes for Second Near-Infrared Window Fluorescence Imaging of Targeted Tumors. *Nano Lett.* 12 (3), 1176–1183. doi:10.1021/nl2031663
- Zhou, X., Smith, Q. R., and Liu, X. (2021). Brain Penetrating Peptides and Peptide-Drug Conjugates to Overcome the Blood-Brain Barrier and Target CNS Diseases. *Wiley Interdiscip. Rev. Nanomed. Nanobiotechnol.* 13 (4), e1695. doi:10.1002/wnan.1695
- Zong, T., Mei, L., Gao, H., Cai, W., Zhu, P., Shi, K., et al. (2014). Synergistic Dual-Ligand Doxorubicin Liposomes Improve Targeting and Therapeutic Efficacy of Brain Glioma in Animals. *Mol. Pharm.* 11 (7), 2346–2357. doi:10.1021/mp500057n

**Conflict of Interest:** The authors declare that the research was conducted in the absence of any commercial or financial relationships that could be construed as a potential conflict of interest.

**Publisher's Note:** All claims expressed in this article are solely those of the authors and do not necessarily represent those of their affiliated organizations, or those of the publisher, the editors and the reviewers. Any product that may be evaluated in this article, or claim that may be made by its manufacturer, is not guaranteed or endorsed by the publisher.

Copyright © 2022 Lam, Tsedev, Kasper and Belcher. This is an open-access article distributed under the terms of the Creative Commons Attribution License (CC BY). The use, distribution or reproduction in other forums is permitted, provided the original author(s) and the copyright owner(s) are credited and that the original publication in this journal is cited, in accordance with accepted academic practice. No use, distribution or reproduction is permitted which does not comply with these terms.



## OPEN ACCESS

## EDITED BY

Mahmood Barani,  
Kerman University of Medical  
Sciences, Iran

## REVIEWED BY

Maryam Roostaei,  
Shahid Bahonar University of  
Kerman, Iran  
Narendra Pal Singh Chauhan,  
Bhupal Nobles University, India

## \*CORRESPONDENCE

Samia Afzal,  
samia.afzal@cemb.edu.pk

## SPECIALTY SECTION

This article was submitted to  
Nanobiotechnology,  
a section of the journal  
Frontiers in Bioengineering and  
Biotechnology

RECEIVED 23 August 2022

ACCEPTED 21 October 2022

PUBLISHED 14 November 2022

## CITATION

Mobeen H, Safdar M, Fatima A, Afzal S,  
Zaman H and Mehdi Z (2022), Emerging  
applications of nanotechnology in  
context to immunology: A  
comprehensive review.  
*Front. Bioeng. Biotechnol.* 10:1024871.  
doi: 10.3389/fbioe.2022.1024871

## COPYRIGHT

© 2022 Mobeen, Safdar, Fatima, Afzal,  
Zaman and Mehdi. This is an open-  
access article distributed under the  
terms of the [Creative Commons  
Attribution License \(CC BY\)](#). The use,  
distribution or reproduction in other  
forums is permitted, provided the  
original author(s) and the copyright  
owner(s) are credited and that the  
original publication in this journal is  
cited, in accordance with accepted  
academic practice. No use, distribution  
or reproduction is permitted which does  
not comply with these terms.

# Emerging applications of nanotechnology in context to immunology: A comprehensive review

Hifsa Mobeen<sup>1</sup>, Muhammad Safdar<sup>2</sup>, Asma Fatima<sup>3</sup>,  
Samia Afzal<sup>2\*</sup>, Hassan Zaman<sup>2</sup> and Zuhair Mehdi<sup>4</sup>

<sup>1</sup>Department of Allied Health Sciences, Superior University, Lahore, Pakistan, <sup>2</sup>Centre of Excellence in Molecular Biology, University of the Punjab, Lahore, Pakistan, <sup>3</sup>Pakistan Institute of Quality Control, Superior University, Lahore, Pakistan, <sup>4</sup>Centre for Applied Molecular Biology, University of the Punjab, Lahore, Pakistan

Numerous benefits of nanotechnology are available in many scientific domains. In this sense, nanoparticles serve as the fundamental foundation of nanotechnology. Recent developments in nanotechnology have demonstrated that nanoparticles have enormous promise for use in almost every field of life sciences. Nanoscience and nanotechnology use the distinctive characteristics of tiny nanoparticles (NPs) for various purposes in electronics, fabrics, cosmetics, biopharmaceutical industries, and medicines. The exclusive physical, chemical, and biological characteristics of nanoparticles prompt different immune responses in the body. Nanoparticles are believed to have strong potential for the development of advanced adjuvants, cytokines, vaccines, drugs, immunotherapies, and theranostic applications for the treatment of targeted bacterial, fungal, viral, and allergic diseases and removal of the tumor with minimal toxicity as compared to macro and microstructures. This review highlights the medical and non-medical applications with a detailed discussion on enhanced and targeted natural and acquired immunity against pathogens provoked by nanoparticles. The immunological aspects of the nanotechnology field are beyond the scope of this Review. However, we provide updated data that will explore novel theragnostic immunological applications of nanotechnology for better and immediate treatment.

## KEYWORDS

nanoscience, therapeutic nanoparticles, nano medicines, innate and adaptive immunity, nanomaterials nanoimmunostimulants

## 1 Introduction

### 1.1 The emergence of nanosciences and nanotechnology

Nanoscience has emerged as an imperative discipline in the recent decade and can be defined as the science of nanomaterials (Ashraf et al., 2021). The term “Nano” originates from a Greek word meaning “Dwarf” referring to a very small-sized object. It is also used as a prefix in science meaning 1 nm is equal to 1 millionth of mm or 1 billionth of m (Boholm, 2016). The word “nanoscience” can be traced back to the era of Greeks and Democritus when the matter was considered a serious riddled point of concern to be debated whether it is continuous or not, to be broken into smaller and shatterproof particles, which are now termed by scientists as atoms (Bayda et al., 2019). The distinguishing line between nanoscience and nanotechnology lies in the fact that nanoscience explains the size, structure, and physical and chemical properties of nanomaterials (Jeevanandam et al., 2018) while nanotechnology is the practical application of the nanoscience for assembly, manipulation (Komal, 2021), control, and manufacturing of nanoscale material. Nanotechnology is a catch-all phrase for materials and devices that operate at the nanoscale (Hulla et al., 2015) and is considered the frontier of the 21st century in modern research (Ahmed et al., 2020).

Nanotechnology has gained importance in the engineering and application of nanomaterials from the fact that physiochemical and biological properties of materials vary remarkably at nanoscale dimensions from their properties at the normal stage (solid phase). The main key feature for such behavior lies in small size and increased surface area at the nanoscale and following the laws of quantum mechanics instead of classical physics (Barkalina et al., 2014). One striking example of such behavior is the catalytic property of gold due to increased surface area to volume ratio at the nanoscale which is chemically inert at the normal scale (Asha and Narain, 2020). Nanotechnology has found its applications in a wide range of disciplines from industries, buildings, military, and agriculture, to the medical sector (Filipe and Ferreira, 2021).

In the last decade, biomedical application of nanotechnology in drug delivery, tissue engineering, and diagnostics purpose has increased greatly improving the efficacy of these technologies. The rapid expansion of nanotechnology in healthcare can be estimated by the fact that the number of medical-related patents has dramatically increased from 200 per year in 2000–10,000 per year in 2010 with an increasing rate day by day (Barkalina, Charalambous, Jones, & Coward, 2014). Nanotechnology can play a part in the inflection of the immune system thereby paving the way for new therapies for widespread diseases like HIV, cancer, and diabetes. Nanocarriers can exert specific effects on immune cells due to their characteristic physiochemical properties and unique composition (Dacoba et al., 2017).

### 1.2 The building blocks of nanotechnology

Nanomaterials (NMs) are basic entities in nanotechnology and can be explicated as materials that are formed using principles and methodology of nanotechnology with length and diameter in the size range of 1–1,000 nm and 1–100 nm respectively (Boverhof et al., 2015). Many types of nanomaterials can be engineered such as nanoparticles, nanospheres, nanocapsules, and nanotubes (Chang, 2019). Precisely designed and functional nanostructures like, nucleic acids, tiny cell structures, and proteins can also be found in nature (Behari, 2010). Nanoparticles (NPs) can be grouped into various categories depending on origin, shape, size, structure, and properties (physical, chemical, electronical, mechanical, optical, and quantum). There are many types of nanoparticles like polymeric NPs, magnetic NPs, nanosuspensions, and nanocrystals. They are characterized by unique properties due to their small size and high surface area-to-volume ratio. They play a very important role in commercial and domestic applications such as; catalysis, imaging, and medical and environmental applications (Khan et al., 2019).

Nanospheres can be described as microscopic structures with a regular form of a sphere. It is composed of a solid polymeric matrix without any polymeric shell. They are used to deliver bioactive substances in the deeper layers of skin with enhanced penetration ability (Frank et al., 2019). Nanocapsule is a polymeric capsule of nanoscale size. It is a membrane-walled structure known as a polymeric shell with an oil core, containing drugs in it at the nanoscale level. They play a vital role in the delivery of the drug by enhancing drug-loading efficiency due to encapsulated oil core, protecting and releasing an accurate dose of the drug to the target (Deng et al., 2020).

There are different criterion-based classifications of nanomaterials based on;

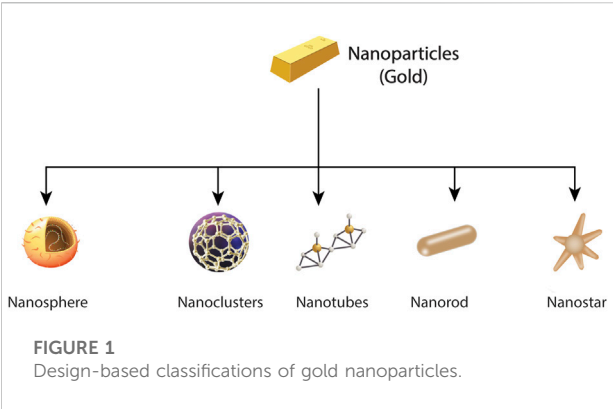
1. Source/Origin
2. Morphology
3. Dimensions
4. Phase of Matter
5. Material
6. Synthesis
7. Toxicity

## 2 Origin/source based-classification

Nanomaterials can be categorized into three main types natural, engineered/artificial, and incidental nanomaterials depending on the source.

Natural nanomaterials can be described as a material produced by biogeochemical processes naturally without any involvement of anthropogenic activity. Naturally occurring nanomaterials cover all the earth's spheres such as; the




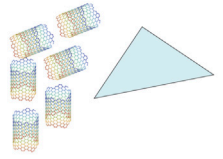
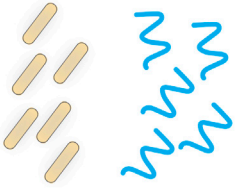
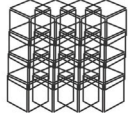


atmosphere (gasses), hydrosphere (oceans, lakes, and rivers), lithosphere (rocks), and biosphere (living organisms) (Hochella et al., 2015; Sharma et al., 2015).

Nanomaterials such as; nanoparticles and nanostructures can be seen in all simple (microorganisms) and complex living organisms (humans, animals, and plants). Advanced nanotechnology has contributed a lot to the understanding and utilization of organisms for beneficial biological and medical applications due to the presence of nanomaterials. Nanostructures are the keystone for life in the world. Animals, plants, and insects use nanomaterials for their survival and protection from harsh environments. Human beings contain nanostructures in the genetic material, bones, blood, and cartilage that maintain proper anatomy and physiology (Jeevanandam et al., 2018).

Engineered/artificial nanomaterials have been successfully designed and developed with desired properties and applications in different areas of interest by human beings. They synthesize them intentionally by using different physical, chemical, and biological techniques (Wagner et al., 2014). Anthropogenic activities such as; cooking and fuel exhaustion (Linak et al., 2000) welding, and smelting (Mandal and Ray Banerjee, 2020) are also playing a key role in the manufacturing of synthetic nanomaterials like carbon nanoparticles (De Volder et al., 2013) and Titanium dioxide nanoparticles (Weir et al., 2012) in cosmetic products and Sun blockers.

Incidental nanomaterials or waste particles come into existence accidentally and unintentionally due to direct or indirect anthropogenic activity. They are generated as a byproduct of industrial and natural processes such as; the emission of fuels from transport vehicles, welding, combustion processes, forest fires, Photochemical reactions, volcanic venting, and sloughing off of skin, hair, and leaves from animals and plants respectively. They are highly toxic and affect the quality of airways, waterways, and groundways. Anthropogenic activities are playing the least role in the production of atmospheric aerosols which is only about

Isotropic nanomaterials	Anisotropic nanomaterials
	
0 D	2 D
Spheres, Clusters	Nanofilms, Plates
Anisotropic nanomaterials	Anisotropic nanomaterials
	
1 D	3 D
Nanorods, Wires	Nanoparticles

**FIGURE 2**  
Dimension-based classification of nanoparticles.

10% of total aerosol as compared to naturally produced aerosols (Taylor, 2002).

### 3 Design-based classification

Nanomaterials can be seen in different forms like nanospheres, nanocages, nanoclusters nano reefs, nanotubes, nanorods, nanowires, nanostars, nanoshells, nano prisms, *etc.* For example, different shapes of gold nanoparticles (Landvik et al., 2018). Different shapes of gold nanoparticles are shown in Figure 1.

### 4 Dimension-based classification

The nanomaterials can be grouped into four types based on dimensions such as; bulk nanomaterials, nanoplates, nanotubes, and nanospheres with three, two, one, and zero dimensions respectively. This dimension-based classification depends on the movement of electrons along the dimension of the x, y, and z axis in nanoparticles as shown in Figure 2.

Bulk nanomaterials can be observed with three-dimensional (3D) structures in the nanoscale range. This class consists of diamonds, graphite, polycrystals, *etc.* The movement of electrons takes place along the x, y, and z-axis. They are widely used in

biomedical sciences as a catalyst. Nanoplates are thin layered structures with nanoscale sizes in which electrons move along the  $x$  and  $y$ -axis. Carbon-coated nanoplates and Graphene sheets are two-dimensional (2D) structures. They are considered building blocks of nanodevices (Jibowu, 2016).

The one-dimensional (1D), thin film-sized nanomaterials are found to be only one dimension at the nanoscale with a wide range of applications in chemistry, electronics, and pharmaceuticals (Gopi et al., 2016). Carbon nanotubes (CNTs), Gold nanowires, Nanoribbons, and nanorods are one-dimensional nanomaterials in which electrons move along the  $x$ -axis (Hangarter et al., 2010). Nanospheres are zero-dimensional nanostructures with all dimensions in the nanoscale range. They consist of quantum dots, Fullerenes, and Gold nanoparticles with the restricted movement of electrons in all directions (Pokropivny and Skorokhod, 2007; Lee et al., 2015).

## 5 The phase of matter based-classification

The four different types of nanomaterials based on the phase of matter are nanocomposites, nanofoams, nanoporous and nanocrystalline. Nanocomposites are solid forms of nanomaterials with at least one nanoscale dimension. They are playing role in pharmaceutical and therapeutic applications.

Nanofoams consist of two phases at the same time with at least one phase in the nanoscale dimension. They may be liquid or solid forms of nanomaterials filled with gases. Carbon nanofoams are used in magnetic resonance imaging by being injected into blood vessels to increase the quality of the image.

Nanoporous is a solid form of material with a porous structure with nanoscale dimension. They are used in drug delivery, gas purification, and energy storage devices. Nanocrystal is a polycrystalline material containing crystals with at least one nanoscale dimension ( $10^9$  m). They are used to treat wounds or burns as an antibacterial and anti-inflammatory agent (Landvik et al., 2018).

## 6 Material-based classification

Nanomaterials can be categorized into four types based on material such, Carbon-based nanomaterials, Inorganic-based Nanomaterials, Organic-based nanomaterials, and Composite-based nanomaterials.

Carbon-based nanomaterials: These nanomaterials are composed of carbon and are found in Fullerenes (C60), carbon nanotubes (CNTs), carbon nanofibers, and graphene. Different techniques are used to manufacture these materials such as; Laser ablation, Arc discharge, and chemical vapor deposition (CVD) (Patel et al., 2019). These carbon-based

nanomaterials have a wide range of applications in different fields of medicine and the environment as antimicrobial agents, and environmental sensors (Mauter and Elimelech, 2008).

Inorganic-based nanomaterials: These nanomaterials are highly stable as compared to organic-based nanomaterials with substances like metals, metal oxides, and meta salt. They can be manufactured into metals and metal oxides such as; Au or Ag NPs and TiO<sub>2</sub> and ZnO NPs respectively. They contain an inorganic central core with fluorescent, magnetic, electronic, and optical properties. These non-toxic and biologically compatible nanoparticles do not contain carbon. Different Inorganic-based nanomaterials such as; quantum dots (QDs), gold nanoparticles (AuNPs), silver nanoparticles (AgNPs), and carbon nanotubes (CNTs) have a broad range of applications (Collier et al., 2017).

Organic-based nanomaterials: These are two-dimensional nanosized materials showing unique physical and chemical properties due to their typical shape and size. The organic-based nanomaterials are ferritin, liposomes, micelles, peptide-based, and dendrimers. They are made of organic matter with noncovalent interactions for self-assembly (Khalid et al., 2020). These are non-toxic and Eco-friendly nanoparticles with variable morphology such as; hollow spheres (Liposomes) and nanocapsules with Temperature and light-sensitive properties (Tiwari et al., 2008). These polymeric nanoparticles are considered the ultimate choice for therapeutic drug delivery to combat disease (Mansha et al., 2017).

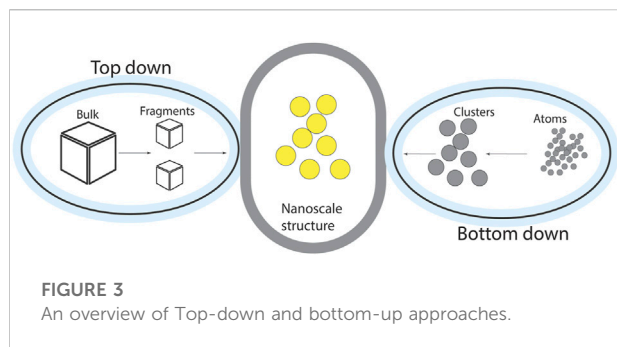
Composite-based nanomaterials: Composite-based nanomaterials consist of two or more components of a nanoscale range with specific physical and chemical properties such as; metalorganic frameworks. The composites are composed of different combinations of carbon-based, metal-based, and organic-based nanomaterials and any form of metal, ceramic, or polymer bulk materials. Their advanced functions and properties depend on the size, composition, and atomic order of aggregates. They are scientifically and technologically advanced materials and play a crucial role in different applications such as; efficient catalysts, metal-semiconductor junctions, modifiers of polymeric film for packaging, and optical sensors (Tanjina Hasnat, 2021).

### 6.1 Synthesis-based classification

The two broadly divided synthetic methods through which nanoparticles can be made for different purposes are; Top-down synthesis and Bottom-up synthesis.

### 6.2 Top-down synthesis

It is also known as a destructive method in which larger bulk materials are broken down into smaller molecules which are



ultimately converted into nanoparticles. This is intrinsically a simpler approach to designing structures with desired properties. The imperfection of surface structure, uncontrolled size, and structure of nanoparticles are serious issues faced by experts. In this technique, nanowires made by lithography are not smooth and possess structural defects on their surface. High-energy wet ball milling, electron beam lithography, atomic force manipulation, gas-phase condensation, aerosol spray, and etching are examples of this approach (Iravani, 2011). An overview of this approach is shown in Figure 3.

### 6.3 Bottom-up approach

The bottom-up approach is Eco-friendly and economical, which constructs material from the bottom with less production of waste. Sol-gel synthesis (Ramesh, 2013), colloidal precipitation, hydrothermal synthesis, electrodeposition, etc, are bottom-up techniques (Figure 3), used for nanostructures and nanomaterials preparation. The bottom-up approach is considered more ideal as compared to the Top-down

approach in the preparation of nanoparticles due to fewer defects and homogeneity.

### 6.4 Biological method

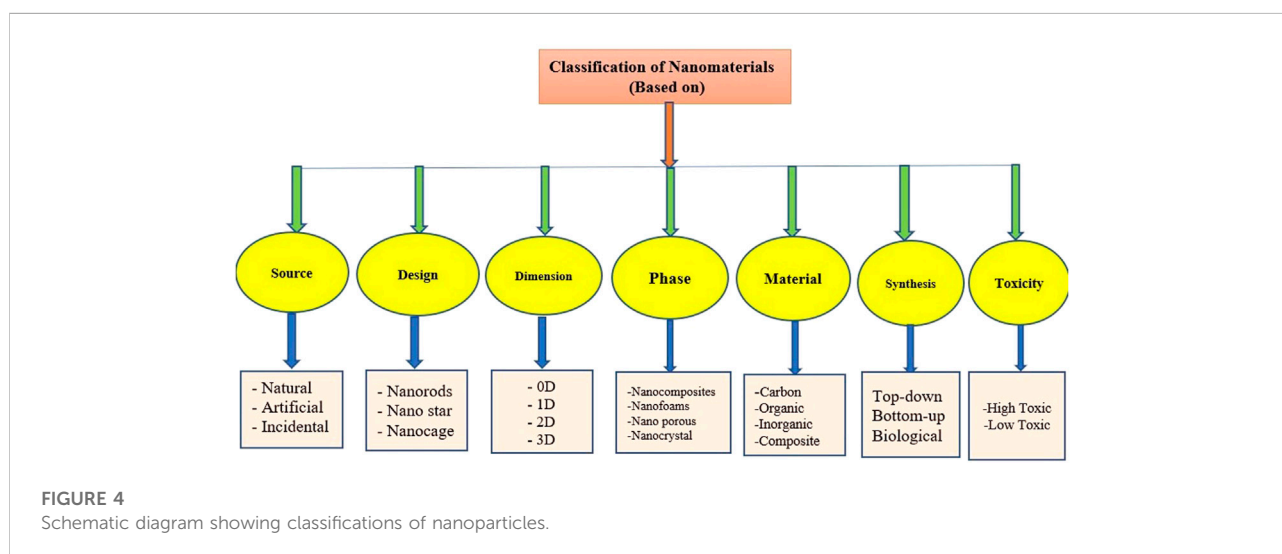
Biological sources including plant extract, fungi, and bacteria are used for the synthesis of nanoparticles. This method is more preferred, Eco-friendly, simple, and economical as compared to other physical and chemical methods (Iravani, 2014).

## 7 Toxicity-based classification

Nanomaterials are mostly used for beneficial purposes to facilitate human beings but they are also a factor in causing diseases by releasing toxic ions. They are categorized into three categories based on solubility and toxicity as shown in Figure 4. (I) Highly soluble nanoparticles affect the lungs and other viscera by releasing toxic ions such as; zinc oxide (ZnO). (II) Poorly soluble low-toxicity nanoparticles cause less toxicity as compared to highly soluble nanoparticles. They cause Fibrosis and cancer by the release of Titanium oxide (TiO). (III) Poorly soluble highly toxic nanoparticles cause Fibrosis and cancer by generating reactive oxygen species (ROS) such as; Nickel oxide (NiO) (Kuempel et al., 2012).

## 8 General applications

Nanotechnology has improved and revolutionized all fields of the world like healthcare, agriculture, military, aerospace, electronics, textile, sports, cosmetics, environmental preservation, and air purification.





## 8.1 Nanomedicine

Nanomedicine is the medical application of nanotechnology, playing a key role in diagnostic and therapeutic purposes efficiently and effectively. Nanopharmaceuticals utilize nanomaterials for target drug delivery, antibacterial activity, and as nano biosensors. These nanoparticles have several other applications in nanomedicine such as;

- Drugs are successfully targeted with optimal concentration and extended-release (ER) dosage for therapeutic purposes (Pradhan et al., 2021).
- Gene therapy with polymeric nanoparticles can be delivered to the desired target effectively and economically with low toxicity and protracted stability (Rai et al., 2019).
- Nanomaterials such as; nanoarrays, nanowires, and nanotubes are widely used for the prompt detection of biomarkers associated with various diseases with low sample consumption. It is considered an emerging, sensitive and successful technology for the detection of bacteria, viruses, and cancer cells at an early stage (Mocan et al., 2017).
- Some CuO NPs are used in the noninvasive methodology-based theranostic process because they possess a contrast-enhancing effect in Magnetic resonance imaging and ultrasound (Aresteanu et al., 2020; Zeng et al., 2020).

## 8.2 Nanoelectronics

Nanoelectronics is an advanced technology that is used to increase the potential of electronic devices and memory chips while reducing their weight, size, and power consumption.

- Electrodes manufactured from nanowires enable flat panel displays to be flexible and thinner.
- Nanolithography is used for the fabrication of chips.
- The transistors are made of nanowires, assembled on glass or thin films of flexible plastic.
- Magnetic Random Access Memory (MRAM) enabled by nanometer-scale magnetic tunnel junctions saves even encrypted data efficiently and effectively during a system shutdown or crash.
- Nanostructured polymer films such as; organic light-emitting diodes (OLEDs) are incorporated into the Display screens of TVs, laptop computers, and mobile phones which offer brighter and wider images with low power consumption (Subramanian and Lee, 2012).

## 8.3 Nanoagriculture

Nanotechnology has played a vital role in the agricultural industry with the development of nano-fertilizers, nano pesticides, and plant gene transformations to produce plants with desirable characteristics. With the increasing global population, it is necessary to make advancements in farming methods to generate higher yields with minimal waste production to meet the rising food demand by using nanotechnology techniques.

- Nano-fertilizers such as; Amorphous Calcium Phosphate (ACP) nanoparticles is economical and eco-friendly preparation used to increase crop yield (Carmona et al., 2021).
- Natural and synthetic resources are used to improve the quality and quantity of crops to meet the rising demands of food with an alarming and unchecked increase in the global population.
- Seed germination of tomato, wheat, and maize is positively stimulated with the application of multi-walled carbon nanotubes (MWCNTs) (Srivastava and Rao, 2014).
- The diagnostic and treatment purposes of different plant diseases have become possible now with the development of Nano sensors (Shang et al., 2019).

## 8.4 Nanotechnology in military

Nanoparticles found in the material of soldiers' uniforms make it more durable and protect soldiers from many dangers such as harsh environmental conditions and chemicals.

- Military Uniforms are manufactured with durable nonwoven light weight and breathable fabrics which possess different properties such as; water-repellent and heat resistance.
- Military equipment and weapons have become more advanced with the utilization of nanotechnology (Glenn, 2006).
- Other applications of nanotechnology in the military such as; Water and Bullet proof vests, Lifesaver bottles, Soldier smart cards, and Smart helmets are also helpful for soldiers in different ways.
- Wound dressings coated with nanoparticles allow the controlled release of drugs and growth factors for wound healing in the predetermined period.
- Chemical and biological nano sensors are used for the detection of harmful weapons (Ramsden, 2012).

## 8.5 Nano fabrics

Nanotechnology is widely used in the development of textiles with desired characteristics, such as durability, wrinkle-free, soft hand, water, heat, and stain repellence, and antimicrobial properties.

- Water, heat, and stain-repellent property of a fabric is due to nano-whiskers, which are added to the fabric to create a peach fuzz effect.
- Nano fabrics protect the wearer from the weather and ultraviolet rays by blocking their direct transmission to the skin through fabrics.
- Synthetic fibers such as nylon and polyester possess a charge after absorption of water but Cellulosic fibers do not carry any charge due to the presence of moisture content. Nano-sized titanium dioxide ( $\text{TiO}_2$ ) and zinc oxide (ZnO) whiskers impart anti-static properties to synthetic fibers.
- Nano-sized silver, titanium dioxide, and zinc oxide are used as antimicrobial agents in nano fabrics (Saleem and Zaidi, 2020).

## 8.6 Nanotechnology and cosmetics

Nanotechnology has contributed a lot to the protection of skin from ultraviolet rays and reversing the aging process at the cellular level through nanospheres, nano-emulsions, and nanoparticles. They alter the properties of cosmetic products including color, transparency, solubility, and chemical reactivity. Nanotechnology applications in cosmetics and skin care include:

- Zinc oxide and titanium dioxide appear transparent at the nanoscale rather than opaque, allowing their utilization in Sun blockers, foundations, and moisturizers (Bilal and Iqbal, 2020). Aluminum oxide nanoparticles used in foundations and face powders facilitate with “soft-focus” effect to conceal visible wrinkles. Carbon “fullerene”. Nanoparticles are also used in anti-aging creams and lotions. Therefore, the cosmetics industry has revolutionized itself by using nano-ingredients in the characterization of cosmetics (Singh and Nanda, 2012).
- Nano emulsions are synthesized by encapsulating nutrients in nanoparticles suspended in a liquid. They are found in Sun blockers, anti-wrinkle creams, foundations, face powders, soaps, shampoos, and conditioners (Özgün, 2013), which penetrate the skin deeply to deliver nutrients to the *epidermis* and *dermis* (Chevalier and Bolzinger, 2019).
- Nanogold is an antiaging, antioxidant, antibacterial, antifungal, and anti-inflammatory agent, which is used in cosmetic products to protect skin from free radicals (Yeh

et al., 2012). Nanogold exhibit various properties and shapes such as nanoshells, nanospheres, nanostars, nanocubes, nanorods, and nanoclusters which affect the resonance frequency of gold nanoparticles. The color of nanogold also changes from red—purple—blue—virtually black due to aggregation (Khan et al., 2014).

## 8.7 Nanobiotechnology

Nanobiotechnology has manufactured devices and systems at the nanoscale level to develop biological, diagnostic, and therapeutic assays to achieve targets in nanomedicine, molecular nanotechnology, food microbiology, and tissue engineering. Nanobiotechnology is used for various purposes such as;

- Nanofluidic biochips such as; lab-on-chip are used to perform biomedical analysis of liquids with very minute quantities and the detection of macromolecules such as DNA and proteins (Kovarik and Jacobson, 2009).
- Chip-based biosensors are also known as Point-of-care biosensors, which are used for the diagnosis of different infectious diseases and the detection of biomarkers precisely with a very small volume of samples (McRae et al., 2016).
- Solid-state nanopore sensors are tiny holes of proteins, which are used for direct and real-time analysis of DNA sequencing and RNA fragments at the single molecule level (Xue et al., 2020). Some carbon nanomaterials like carbon nanotubes, carbon nanofibrils, and graphite used in optoacoustic transducers improve their optoacoustic conversion efficiency and have laser damage threshold (Li et al., 2022).
- Nanomaterials are composed of nanoparticles (NPs) such as; magnetic NPs, AuNPs, AgNPs, silica NPs, quantum dots (QDs), polymeric micelles, liposomes, dendrimers, and fullerenes are used in biosensing, bioimaging, diagnostic, and therapeutic applications to facilitate healthcare industry economically (Nagamune, 2017).
- For efficient, highly-selective phosphate removal from wastewater, a new lanthanum carbonate-grafted ZSM-5 zeolite (LC-ZSM-5) was created (Yang et al., 2021).

## 8.8 Nano-oncology

Cancer is the second leading cause of death worldwide after cardiovascular diseases (CVS) (Luisa and Valentina, 2021). It is characterized by abnormal division of cells which even affects the normal healthy cells (Tran et al., 2017). Thus, it is necessary to develop an efficient technique for the early-stage diagnosis and treatment of cancer.

Nanoparticles (NPs) are widely used in anticancer therapy to deliver chemotherapeutic drugs to the target site (Dong et al., 2019; Zhang et al., 2019). The stealth properties of NPs can be improved by covering them with chemical or biological coatings, which ultimately reduce the formation of aggregates in the body fluids. The maximum delivery of chemotherapeutic agents specifically to the target site can be achieved through conjugation with targeting ligands (Limongi et al., 2019).

The increased permeability and retention effect (EPR) enable NPs to accumulate into cancers because they can cross the tumor vasculature easily and poor lymphatic drainage retains them to facilitate their therapeutic effect (Youn and Bae, 2018). A supramolecule is developed by grafting the epitopes of bioactive D-peptide onto the mini protein template. This functions as a p53 antagonist and possesses an advantageous pharmacological profile that includes endosome escape, intracellular reductive response, passive tumor targeting, and cell membrane penetration (Yan et al., 2020). An antitumor Benzofuro had been synthesized by using Nanopalladium as a catalyst. It showed promising results against T-24 and Hela cell lines (Wang et al., 2019).

Chemotherapeutic agents react strongly with abnormally dividing cells and inhibit the cell division process by interfering with DNA synthesis. These agents also damage normal healthy cells along with the treatment of cancer. Advanced nanotechnology-based therapeutic drug delivery system is more effective in treating cancerous cells with a chemotherapeutic agent with minimal effect on non-tumor healthy cells in the body by controlling their rate of release on the target site in specified time duration. The polymer (poly lactic-co-glycolic acid) (PLGA) is hydrophilic and used as a nanocarrier. It remains in the blood circulation longer enough without being used and removed by the liver metabolism (Jibowu, 2016).

## 8.9 Green nanotechnology

A branch of green technology that utilizes plant products for the protection of the environment by reducing greenhouse gases, pollution, and hazardous waste as well as by saving the ozone layer, water, energy, and non-renewable raw materials (Verma et al., 2019).

Green Nanotechnology has improved the environment in many ways by producing efficient and economical energy with generating less pollution but sometimes it may be undesirable when it affects the food web (Almeida et al., 2020).

- Solar cells have become more efficient, economical, and smaller in size with the advancement of nanotechnology. They use solar energy, which is a renewable resource (Banin et al., 2020).

- Nanotechnology has played a role in the treatment of groundwater, surface water, and wastewater by reverse osmosis and nanofiltration, contaminated by microorganisms, organic and inorganic solutes, and toxic metal ions, microorganisms (Jain et al., 2021).
- Nano remediation of soil and sediment with nanoparticles has reduced pollution in soil caused by industrial activities (Baragaño et al., 2020).
- Nanoparticles are efficiently playing a role in the removal of toxic materials from gases such as; CO and SO<sub>2</sub> (Guerra et al., 2018).
- Nanotechnology has been proven to be a beneficial tool in the cleaning up of oil spills in the aquatic system to save aquatic biodiversity by applying magnetic nanomaterials such as functionalized superparamagnetic iron oxide nanoparticles (SPIONs) and magnetic carbon nanotubes (CNTs). Nanowires are used to clean up oil spills by absorbing them up to twenty times their weight in hydrophobic liquids and rejecting water due to the coating of the being water-repellent (Singh et al., 2020).
- Nanotechnology has been considered a successful tool to improve the quality of air by using nanoparticles. They transform toxic gases (CO, NO, and hydrocarbons) of industrial factories into harmless ones by sensing, detecting, and remediating them (Mohamed, 2017).

## 8.10 Nanotechnology in immunology

Nanotechnology has been proven to be a promising approach for successful applications in the field of immunology with the production of nano vaccines, adjuvants, anticancer drugs, and immuno-modulatory cytokines to combat infectious and autoimmune diseases.

Nanoparticles possess the strong potential to stimulate immunity due to their unique properties. They act as adjuvants by protecting, stabilizing, and presenting foreign particles (antigens) to antigen-presenting cells (APC) like macrophages, dendritic cells, and B cells with controlled release of antigen in blood circulation and surrounding tissue for effective, prolonged, and strong immune response (Lenders et al., 2020).

The properties of nanoparticles can be a “double-edged sword,” as they exhibit immunotoxic and immunomodulatory functions. Metal-based nanoparticles have various effects on different cells such as;

- Interaction with cells possessing Toll-Like receptor signaling (TLR) and antigen presentation properties like macrophages and dendritic cells for the expression of proinflammatory cytokines and activation of T cells.

- Interact with innate immune cells like neutrophils, mast cells, and NK cells for activation and augmentation of innate immunity.
- Interaction with acquired immunity-related T and B cells to combat viral and bacterial infections (Luo et al., 2015).

### 8.10.1 Immunomodulation with nanoparticles

Layered defenses of increasing specificity protect us from infections. Physical barriers, skin, mucosal membrane of the mouth, respiratory, gastrointestinal, and urogenital tract limit the entry of microbes (bacteria, fungi, and parasites) and viruses which are non-specific innate immunity that provides an immediate response. These mucosal membranes are selectively permeable for nutrients, water, ions, and gases while limiting the entry of pathogens upon exposure (Nel et al., 2021).

The immune system has been divided into two major types: innate immunity and adaptive immunity. Innate immunity is the first line of the defense system, which depends on pattern recognition receptors (PRRs) to recognize conserved pathogen-associated molecular patterns found on pathogens (PAMPs). Therefore, innate immunity plays a key role in the early recognition and subsequent basic microbial eradication by phagocytes (macrophages and neutrophils) and their cytokines through inflammatory processes (Amarante-Mendes et al., 2018; Nickoloff, 2019).

When innate immunity fails to eradicate pathogens, adaptive immunity or specific immunity responds *via* humoral immunity and cell-mediated immunity but it starts after a lag time (Vincenzo et al., 2015). Antigen-presenting cells (APC) such as dendritic cells, macrophages, and B cells present antigens in association with class II MHC to CD4 helper T cells. Then CD4 cells respond to APC by producing cytokines while CD8 cells respond by apoptosis and cytokines (Gaudino and Kumar, 2019).

IFN-gamma produced by CD4 cells enhances the microbicidal activity of macrophages. CD4 cells produce IL-2 and enhance the cytotoxic action of CD8 cells. CD4 cells also help B cells in the production of antibodies by releasing IL-4 and IL-5 (Cruz-Adalia et al., 2017).

The immune system perceives nanoparticles as foreign substances and eradicates them from the body immediately. However, if these foreign nanoparticles are not considered a threat-causing factor, they are completely tolerated by the immune system without causing any harmful effects. Therefore, it is the point of concern to analyze the response of the body's immune system with the development of a novel nanoparticle for *in vivo* applications such as gene or drug delivery to minimize undesirable consequences (Muhammad et al., 2020).

Nanoparticles have been designed for safe and targeted drug delivery, vaccination, and tumor therapy without any immunological harmful consequences. Three major harmful consequences related to the immune system of the body must

be considered with the development of a novel nanoparticle for *in vivo* application.

- The first consequence is immunostimulant which is related to the destruction or rejection of nanoparticles with eradication from the body by the defensive immune system.
- The second is immunotoxicity, which could affect the functioning of the local and systemic immune system due to exposure to toxins and cause pathological problems.
- The third is immunocompatibility, in which the immune system could not be interfered with by any foreign object (Dobrovolskaia et al., 2016).

Several techniques can be used to load drugs with the nanoparticle for targeted and efficient drug delivery such as entrapped drug inside the nanoparticle (encapsulation), coated drug on the surface of the nanoparticle (coating), and chemically linked with the nanoparticle, which helps them to evade the phagocytic cells of the immune system. The unique properties of nanoparticles such as size, charge, hydrophobicity, and hydrophilicity direct nanoparticle-coated drug to the target safely (Dong et al., 2019).

Nanoparticles developed by encapsulation with polyethylene glycol (PEG) or PEGylation are widely used in targeted drug delivery and nanotechnology due to "stealth" properties and biocompatibility. PEGylation plays a vital role in drug delivery systems by evading or shielding them from recognition of the immune system (Suk et al., 2016). However, sometimes the immune system produces PEG-specific antibodies after the introduction of PEG-coated liposomes (Mohamed et al., 2019). Some important nanoparticles with their applications in immunotherapy are listed in Table 1.

### 8.10.2 Impact of nanoparticles on the stimulation of innate immunity

Innate immunity or natural immunity is the first line of defense of the body's immune system which response non-specifically and immediately to encounter pathogens with the activation of pre-existing defensive mechanisms including physical, anatomical, chemical, and biological barriers. The main components of natural immunity are;

- physical barriers including skin, mucous membranes, and mucus.
- Anatomical barriers consist of phagocytes (polymorphonuclear leukocytes, monocyte, macrophages, and dendritic cells), basophils, eosinophils, mast cells, and natural killer cells (NK).
- Phagocytic cell enzymes include lysozymes, elastase, and protease.
- Circulating plasma proteins comprise pathogen recognition receptors (PRRs). Mannose-binding lectins

TABLE 1 Nanoparticles uses in immunotherapy.

Nanoparticle type	Size (nm)	Applications	Target	References
ZnO NPs	30–150	Vaccine Carrier	TLRs	Sharma et al. (2019)
Polymeric NPs (PLGA)	100–200	Vaccine Carrier, adjuvant	DCs	Kim et al. (2018)
Exosome	40–100	Vaccine Carrier	T Cells	Romagnoli et al. (2015)
Liposome	100–160	Vaccine Carrier/Adjuvant	DCs/macrophage	Koshy et al. (2017)
Metal NPs (AuNPs)	20–80	Vaccine Carrier/Adjuvant	DCs	Almeida et al. (2014)
Metal NPs (IONPs)	20–80	Antibody carrier	DCs	Choi et al. (2015)
Polymeric NPs (Micellar)	25–50	Vaccine Carrier	DCs	Jeanbart et al. (2015)

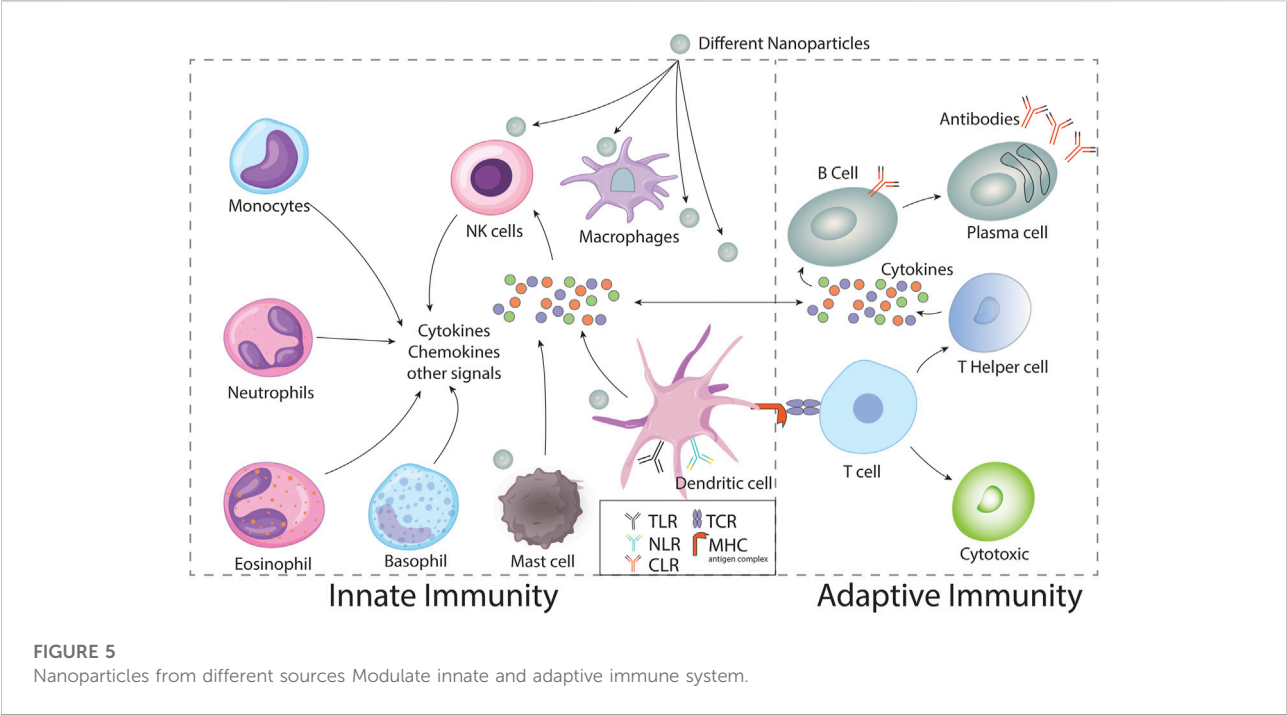


FIGURE 5 Nanoparticles from different sources Modulate innate and adaptive immune system.

(MBL), C-reactive proteins (CRP), and the complement system.

- Antimicrobial peptides such as; cathelicidin and defensins.
- Cell receptors like Toll-like receptors (TLR), Mannose receptors (MBL), and Dectins (Zhang et al., 2021).

In this review, we will first focus on the discussion of the enhanced stimulatory mechanism of cells related to innate immunity to resolve infections due to nanoparticle conjugation and then describe the impact of these nanoparticles on the cells of adaptive immunity with advanced specificity (Figure 5).

### 8.10.3 Role of nanoparticles in toll-like receptor signaling

Innate immunity depends on the recognition of pathogen-associated molecular pattern (PAMPs) by pattern recognition receptors (PRRs), which belongs to the family of toll-like receptors (TLRs). Toll gene controlling the dorso-ventricular polarization of embryo, originally discovered in *Drosophila*, was found to be playing role in immunity against fungal infections in the adult fly. Toll-like receptors found on the surface of the cell are TLR1, TLR2, TLR4, TLR5, TLR6, and TLR10 while TLR3, TLR7, TLR8, TLR9, TLR12, and TLR13 are located in intracellular vesicles such as endosomes and lysosomes (El-Zayat et al., 2019).



- The activations of the TLR signaling mechanism stimulate macrophage and natural killer (NK) cells associated with phagocytosis and cytotoxic activity respectively.
- They increase antigen presentation *via* upregulating the expression of major histocompatibility complex (MHC) and costimulatory molecules (CD80 and CD86) on antigen-presenting cells like dendritic cells, macrophages, and B-cells, leading to the activation of adaptive immunity.
- TLR agonists or nanoparticles are considered to be powerful adjuvants. TLR antagonists or inhibitors have been proven to be a therapeutic tool to treat septic shock and autoimmune diseases like systemic lupus erythematosus (SLE) and rheumatoid arthritis by downregulating the inflammatory responses (Gao et al., 2017).
- Nanoparticles like Titanium dioxide (TiO<sub>2</sub>) elicit an inflammatory response with the production of reactive oxygen species by increasing the expression of TLR7 on macrophages (Huang et al., 2017).
- ZnO nanoparticles possess anti-inflammatory and antimicrobial properties by the induction of MyD88-dependent proinflammatory cytokines through the signaling pathway of TLR (Moratin et al., 2021).

These advanced potential applications of nanoparticles may open novel and innovative directions for the synthesis and characterization of nanoparticle conjugates to meet advanced requirements in immunology.

#### 8.10.4 Immunostimulatory effect of nanoparticles on cytokine production

Cytokines are proteins that act as signaling molecules in mediating and regulating inflammatory protective mechanisms in innate and adaptive immunity. Inflammatory cytokines, such as IL-1, IL-6, and tumor necrosis factor- $\alpha$  (TNF- $\alpha$ ), stimulate inflammatory cells (neutrophils and macrophages), increase vascular permeability, and cause swelling and erythema. IL-8 is a chemokine that plays a key role in the recruitment of inflammatory cells to the targeted inflammatory sites after activation. Activated lymphocytes secrete Interferon- $\gamma$  (IFN- $\gamma$ ) which is a primary activator and recruiter of macrophages to the site of infection (Kany et al., 2019).

NPS can trigger an immune response with the production of cytokines to resolve infection due to their particular physiochemical properties. The measured levels of these triggered cytokines act as biomarkers of nanoparticle immunomodulatory effects. TiO<sub>2</sub> nanoparticles and nanodiamonds stimulate the production of the proinflammatory cytokine, maturation of dendritic cells, and activation of lymphocytes. ZnO nanoparticles play an important role in enhancing the expression of IFN- $\gamma$  in lymphocytes and IL-12 in monocytes (Swartzwelter et al., 2020).

The more understanding we have of cytokine production triggered by nanoparticles, the better we can use the level of cytokines as biomarkers of the immunostimulatory properties of nanoparticles.

#### 8.10.5 Effects of nanoparticles on the cells of innate immunity

The cells of innate immunity are Natural Killers (NK), neutrophils, Macrophages, dendritic cells (DCs), mast cells, eosinophils, basophils, and gamma/delta T cells. We will discuss the effects of nanoparticles on these cells and utilize them for therapeutic purposes. Moreover, we will demonstrate the modulation of eosinophils, basophils, and gamma/delta cells with nanoparticles by reviewing the most recent data, which is still a challenging task.

#### 8.10.6 Augmentation of natural killer cell-based immunotherapy

NK cells are large granular lymphocytes of innate immunity, which do not require thymus for maturation. They play an important role in defending the body against viruses naturally, as they do not require any prior exposure (immunologic memory) to that particular viral antigen, hence named “natural” killer cells (Bagheri et al., 2021).

NK cells regulate macrophages and T cells by interacting and activating them with the production of gamma interferon to kill phagocytosed bacteria. They also kill tumor and virus-infected cells non-specifically by the secretion of cytokines, Fas-Fas ligand-mediated apoptosis, and antibody-dependent cellular cytotoxicity (ADCC). Therefore, NK cells are considered a double-edged sword either to limit or worsen the situation of immune responses. It has been reported that patients with deficient NK cells can predispose to life-threatening infections. Hence, NK cell-based immunotherapy could be proved to be an effective strategy against tumors (Liu et al., 2021).

However, NK cell-based immunotherapy is still facing many challenges in treating cancer patients. The tumor microenvironment (TME) with altered immunogenicity disguise NK cells infiltration to the target (Nayyar et al., 2019). Thus, many strategies have been proposed for the expansion, activation, and infiltration of NK cells to the targeted tumor site (Cerwenka and Lanier, 2016; Fehniger and Cooper, 2016).

Recently, it has been reported that nanoparticles with multifunctional properties play a significant therapeutic role to treat various types of tumors with the augmentation of NK cells (Nam et al., 2019; de Lázaro and Mooney, 2020). The multifunctional properties of nanoparticles such as targeted cytokine delivery, tracking, identification, and advanced treatment of cancer have been proven to overcome challenges related to NK cell-based immunotherapy of cancer (Irvine and Dane, 2020; Phung et al., 2020).

The tracking and identification of cells can be made possible with the quantum dots (QD) imaging technique by labeling NK-92 MI cells with anti-CD56 antibody-coated QD705, a quantum dot that emits light in the near about infrared region. The NK-92MI injections were performed and tracked for 12 days after intra-tumoral injections. A significant reduction was observed in the size of the tumor with minimal toxicity after treatment with NK cells as compared to the control.

Quantum dots are used for imaging technology due to several advantages such as; high photostability, Narrow and symmetric peak of emission spectra, high quantum yield, long shelf life, color availability, and small size.

Some compounds cannot be used therapeutically and diagnostically due to the toxic and non-degradable nature of cadmium cores. So, it is highly needed to develop biodegradable and cadmium-free QDs for safe clinical applications (Shapovalova et al., 2018).

The updated data of this review will provide an alternative clinical treatment approach to cure and remove tumors with minimal toxicity of nanoparticles. It will also suggest innovative diagnostic imaging techniques with advanced infiltration of immunology to the three-dimensional (3D) target site without a surgical incision.

### 8.10.7 Neutrophil-based delivery of nanotherapeutics

Polymorphonuclear neutrophils are considered a key component of innate immunity. They are the first ones from the leukocyte family that transmigrates to the target site during acute inflammation and release several types of proinflammatory mediators such as cytokines and chemokines, which further attract and recruit other PMNs, monocytes, macrophages, and lymphocytes to the site of chronic inflammation. The bactericidal activity of neutrophils depends on cytoplasmic granules containing degradative lysosomal enzymes (Mortaz et al., 2018).

The blood vessel barrier is the main hindrance to the efficient and immediate transmigration of neutrophils to the site of inflammation. Therefore, it is highly needed to design a strategic nanotherapeutic approach to deliver nanoparticles such as; nanovesicles, metallic nanoparticles, protein nanoparticles, and polymer nanoparticles by using neutrophils as a delivery vehicle (Dong et al., 2017).

It has been documented that albumin nanoparticles can be incorporated into neutrophils and labeled with fluorescent dyes or radioactive agents for monitoring and analyzing the site of inflammation across the blood vessel barrier by using imaging techniques. (Chu et al., 2015).

It has also been reported that gold nanoparticles (Au NPs) were observed to be trapped by neutrophils in their extracellular traps (NETs). NETosis was found to be visible 15 min after AuNPs come in contact with neutrophils and trapped more NPs gradually. These NETs play a vital role in alerting the immune

system to the signal of danger by the activation of TLR9, a DNA receptor. This activation starts the recruitment of neutrophils to the targeted site of inflammation (Yang et al., 2019).

This study will contribute with an advanced strategic nanotherapeutic approach to recruit activated neutrophils to the site of infection with maximum clearance and minimum toxicity.

### 8.10.8 Interaction between nanoparticles and phagocytic cells (macrophages, dendritic cells)

Professional antigen-presenting cells (APCs), such as macrophages (Ms) and dendritic cells (DCs) are known as phagocytic cells that act as an interface between natural and acquired immunity. Ms is believed to be an efficient component of the innate immune system. They play role in the ingestion and killing of the pathogen in phagolysosomes by a mechanism called phagocytosis. They highly contribute to the rapid and non-specific removal of pathogens by reactive oxygen and nitrogen intermediates (Klopfleisch, 2016).

Antigen presentation is the main second function performed by Ms after phagocytosis. They process the pathogen after ingestion and present it in the form of antigen on the surface in association with class II MHC proteins along with costimulatory molecules such as CD86 and present it to the CD4 helper T-cells for adaptive immune response (Eiz-Vesper and Schmetzer, 2020).

Macrophages also synthesize and secrete several cytokines like IL-1 and Tumor necrosis factor (TNF), which play role in the training and activation of CD4 helper T-cells for the recognition and destruction of a pathogen to resolve different infections. Ms also secrete IL-8, a potent chemokine that attracts and recruit neutrophils and T-cells to the site of inflammation (Hughes et al., 2021).

The DCs are also regarded as professional APCs with the expression of Class II MHC protein on their surface. After phagocytosis of the pathogen, they process and present antigens in association with class II MHC protein to the helper T-cells for the stimulation of adaptive immunity. They also release several cytokines for the activation of natural killer cell (Yin et al., 2021).

Macrophages and dendritic cells are major phagocytes of the innate immune system with strong phagocytic ability. They capture nanoparticles loaded with therapeutic drugs (Ag) from blood circulation and accumulate them. The unique physiochemical properties of nanoparticles carry and protect Ag from degradative enzymes. These APCs are believed to be an ideal vehicle for the safe targeted delivery of drugs due to their efficient phagocytic ability (Banskota et al., 2017).

Several potential therapeutic strategies have been successfully developed using macrophages to deliver nanoparticles loaded with drugs efficiently (Lee et al., 2019; Xie et al., 2019). Drug-loaded nanoparticles can be prepared by loading chemotherapeutic drugs into nanoparticles for their safe



arrival in the macrophages (Zhang et al., 2018; Hui et al., 2019). Different NPs such as lipid nanoparticles (LNPs), carbon nanotubes (CNTs), gold nanoparticles, and natural and artificially synthesized NPs have been used successfully to carry and deliver a drug to macrophages. Lipid nanoparticles (LNPs) have been used safely as drug delivery vessels (García-Pinel et al., 2019). The drug Patisiran can be delivered to macrophages by LNPs, which was approved by the FDA in 2018 (Hoy, 2018). The encapsulation of drugs by LNPs is a simple strategy, that not only protects macrophages from the side effects of drugs but also keeps them safe from carrier materials (Hou et al., 2021).

Multi-walled CNTs (MWCNTs) have also been reported as carrier nanoparticles of cancer antigens to be captured by DCs. The antigen was processed, released, and presented slowly on the surface of DCs in the association of MHC protein to activate CD helper T-cells and CD8 cytotoxic T-cells continuously for the regression of the tumor (Jia et al., 2018).

### 8.10.9 Priming of mast cells with nanoparticles

Mast cells (MCs) are versatile effector cells of the body's immune system with beneficial and deleterious effects against pathogens (Galli et al., 2020). They are abundantly found at the junctions between the tissues and the external environment such as skin and played a vital role in showing inflammatory response against pathogens by secreting inflammatory mediators after recognition (Marshall et al., 2019).

MCs originate from pluripotent stem cells in the bone marrow and mature with the development of secretory granules after reaching at tissue microenvironment by circulation. The activation and IgE-mediated degranulation of mast cells occur with the secretion of preformed inflammatory mediators such as histamine, heparin, lysosomal enzymes, and prostaglandins. MCs are an important first line of defense against various infectious agents due to the presence of TNF- $\alpha$  which recruit further neutrophils to the targeted site of infection and modulate both natural and acquired immune responses (Paivandy and Pejler, 2021).

Nanoparticles are believed to be novel modulators of mast cells for efficient response. Johnson and Duan have documented that nanoparticles can specifically target mast cells through Fc $\epsilon$ RI activation pathways. AgNPs possess antibacterial activity by stimulating mast cells through cell surface scavenger receptors. This results in the activation of intracellular signaling pathways and degranulation with the release of inflammatory mediators (Johnson et al., 2018). TiO<sub>2</sub> nanoparticles enhanced the secretion of histamine and cytosolic Ca<sup>2+</sup> concentration in mast cells without any prior exposure to an allergen (Duguay et al., 2020). Granules of mast cells have been reported to be a strong stimulator of adaptive immunity when they are degranulated at target sites of infection or vaccination (Jain et al., 2019). These findings may further explore the applications and utilizations of nanoparticles for diagnostic and therapeutic purposes of allergic

diseases with the priming of mast cells, which could be of particular concern to allergic populations as the use of NPs in biomedical products are increasing rapidly.

### 8.10.10 Therapeutic strategy of eosinophils for allergic issues

These leukocytes are characterized by the presence of orange or -red-stained granules in the cytoplasm and account for less than 3% of all leukocytes in human blood. They are originated and derived from CD34<sup>+</sup> stem cells of bone marrow and released into blood circulation after maturation. The cytokines like interleukin (IL)-3, granulocyte-macrophage colony-stimulating factor (GM-CSF), and IL-5 play a key role in the development and final differentiation of eosinophils respectively (Ramirez et al., 2018).

Eosinophils defend the body against parasitic, bacterial, viral, and fungal infections through mediators such as major basic protein (MBP), eosinophil peroxidase (EPO), eosinophil cationic protein (ECP), eosinophil-derived neurotoxin (EDN) in the presence of antibodies and complement (Kanda et al., 2020). The significance of eosinophils in inflammatory diseases of the skin, gastrointestinal and respiratory tract has been reported in the literature. The increased count of eosinophils in the blood or sputum sample of patients suffering from asthma is associated with the severity of the disease (Kanda et al., 2021).

NPS is believed to be a promising tool for the diagnosis and treatment of allergic diseases with the direct effect of NPs on eosinophils. It has been documented recently in the literature that AgNPs and ZnONPs have strong potential for the production of pro-inflammatory cytokine-like IL-8, which plays a significant role in the chemotaxis of neutrophils, basophils, and eosinophils to the target site (Vanhare and Girard, 2020). TiO<sub>2</sub>NPs recruit eosinophils from the blood circulation toward the inflamed area to fight against parasites and participate in immediate hypersensitivity by adhesion of eosinophils onto Endothelial Cells of blood vessels (Murphy-Marion and Girard, 2018).

This review may be helpful for researchers to understand the direct effects of various NPs on the biology and mechanism of action (MAO) of eosinophil cells. It will also be of great importance for better predicting their safer use in the diagnosis and treatment of hypersensitivity reactions.

### 8.10.11 Anti-allergic role of basophils along with NPs inhibitor conjugates

Basophils are granular leukocytes with blue-stained cytoplasmic granules. They are the least abundant circulating granulocytes which account for less than 1% of all leukocytes. They resemble mast cells due to the expression of the high-affinity immunoglobulin E (IgE) receptor (Fc $\epsilon$ RI). Basophils act as gatekeepers to control the intrusion of eosinophils to the target site with the release of Th2-related cytokines like IL-4 and IL-13 after binding of Fc $\epsilon$ RI with IgE due to exposure of allergen. The

activated basophils increase vascular permeability and mucus production due to the secretion of histamine and LTC<sub>4</sub> (Iype and Fux, 2021).

The conjugate of allergen and gold nanoparticles AuNPs effectively and vigorously stimulate basophils and cause degranulation with the secretion of preformed mediators including histamine, prostaglandins, leukotrienes, and proteases to mediate immediate and delayed inflammatory immune response (Radauer-Preiml et al., 2015).

Gold nanoparticles (AuNPs) can successfully be used to target and inhibit the IgE-dependent degranulation of basophils with signal transduction inhibitors such as calcineurin and anti-CD203c. AuNPs are relatively non-toxic anti-inflammatory nanoparticles that can be conjugated with pharmacological agents to stimulate anti-allergic responses (Yasinska et al., 2019). The specific targeting of basophils with gold nanoconjugates and signal transduction inhibitors indicates that this technology could be used as a therapeutic potential treatment for allergic diseases with minimal side effects.

#### 8.10.12 Impact of nanoparticles on the stimulation of adaptive immunity

Adaptive immunity is also known as acquired immunity, a specific second-line long-term defense mediated by B and T cells which enables the host to develop a rapid response upon second exposure to antigen. The cells of adaptive immunity require APCs for the recognition of antigens. APCs phagocytose, process, and present antigens to T-cells in association with MHC protein. Nanoparticles target and interact with circulating APCs for efficient response (Marshall et al., 2018).

##### 8.10.12.1 Consequences of nanoparticles on T cells

Nanotechnological techniques are believed to be a potential therapeutic strategy for the effective treatment of many diseases by specifically targeting the region without any detrimental effects. Drug delivery systems based on nanoparticles can be made highly efficient by considering the different physical and chemical properties of nanoparticles such as; size, shape, charge, stability, etc.

Superparamagnetic iron oxide nanoparticles (SPIONPs) target and accumulate T cells in the specific region of interest with the application of an external magnetic field (EMF). This strategy has been proven beneficial in cancer treatment and vaccine preparation (Day et al., 2021). Poliglusam nanoparticles (Polymeric nanoparticles) possess the potential to reduce the size of tumors, particularly of breast origin safely by activating host immunity. It has been documented that Poliglusam has an intrinsic inclination in increasing the production of IFN- $\gamma$  by activated T lymphocytes in cancer cells. These immunotherapeutic effects could be made more effective along with the use of anti-cancerous medication for the complete removal of breast cancer (Soleimani et al., 2019).

Synthetic Janus nanoparticles have been reported to be used in adoptive cancer immunotherapy. These nanoparticles with clustered ligands on the surface stimulate T cells with an inadequate amount of stimulus (Lee and Yu, 2017). Nanoparticles can also be used successfully in the treatment of brain tumors by crossing the blood-brain barrier (BBB) and enhancing T-cell adoptive therapy. The activation of T-cells highly depends upon the size and high surface-to-volume ratio of carbon nanotubes which plays role in the encapsulation of antigens or cytokines (Balakrishnan and Sweeney, 2021).

The vaccine is a strong and economical approach to defending the body against infections by limiting pathogenesis and spreading of disease with the advanced utilization of nanoparticles. Inorganic carboxylated polystyrene nanoparticles stimulate B-cells, helper T-cells, and cytotoxic T-cells to provoke humoral and cell-mediated responses respectively. Fluorescent nanoparticles can be used to trace the attachment of these nanoparticles with cell subsets specifically by flow cytometry (Wilson et al., 2020). Metal-based nanoparticles have also been documented to stimulate T cells for immune responses. TiO<sub>2</sub> nanoparticles play role in the activation and expansion of T cells with the release of inflammatory cytokines. Gold nanoparticles can polarize Th2 and Th17 cells. The induction of Th1 or Th2 immune response decision is dependent on the size of nanoparticles after the introduction of antigen and Nanoparticle conjugate in the body (Luo et al., 2015). This review will guide and explore new ways to develop vaccines and immunotherapies to treat cancer and combat other viral diseases by activating T-cells using a nanotechnological approach.

## 9 Effects of nanoparticles on B cells

B lymphocytes are another important component of the adaptive immune system which combat bacterial diseases by the production of antibodies. They act as APC and present surface IgM receptors for the recognition and attachment of antigens. They internalize, process, and present antigen on its surface in conjunction with MHC class II protein after exposure. B lymphocytes present this complex of antigen and MHC II to T-cell receptors (TCR) of CD4 cells. The T-cells activate and differentiate these B-cells into Ab-producing plasma cells with the production of various interleukins such as; IL-2, IL-4, and IL-5 (Van Langelaar et al., 2020).

The humoral immune response can be achieved enhanced by the use of a nanotechnological approach. It has been documented that antigens are released slowly from the depot form of nano vaccines at a predetermined rate to provoke B-cells for the production of antibody-mediated responses against infections (Singh, 2021). TiO<sub>2</sub> nanoparticles are believed to have the potential to elicit Ab-mediated response by B-cells due to

TABLE 2 Some important applications of nanotechnology.

Nanoparticle type	Size (nm)	Administration type	Mechanism of action	Target/Disease	References
Liposome	<100	Intravenous	Drug delivery	Parkinson	Saeedi et al. (2019)
Carbon Nanotubes	3.5–7	Intraperitoneal	Endocytosis	Parkinson	Saeedi et al. (2019)
Polymeric NPs	1–100	Oral	Drug delivery	Diabetes Mellites	Simon-Deckers et al. (2009)
Layered Double Galactose	40–300	Directly exposed to cells (in the lab)	Target drug delivery	Hepatocellular Carcinoma	Sadeghi et al. (2020)
Al <sub>2</sub> O <sub>3</sub>	60	Direct on surface (in Lab)	particle penetration	<i>E. coli</i> , <i>B. subtilis</i> , <i>Pseudomonas</i>	Jiang et al. (2009)
Silver	50	Direct on the surface (in the lab)	Membrane disruption, Interferes with replication	<i>E. coli</i>	Pal et al. (2007)
Hydrogels	370–800	3D scaffold	Mimic the function of specific cell layers	Cornea wound healing	Khosravimelal et al. (2021a)
Nano-Ag	5–20	Direct on surface	strong and wide-spectrum antimicrobial	Contaminated Water	Qu et al. (2013)
diatomite	10–200 $\mu$ m	Direct exposure to cells (in the lab)	siRNA delivery	Cancer	Rea et al. (2014)
mesoporous silica	200	Nanocarrier	gene delivery applications	Hela cells and macrophages	Park et al. (2008)

increased levels of IL-4 by activated T-cells with minimal toxicity (Malachowski and Hassel, 2020).

The combination of calcium phosphate nanoparticles (CaPNs) and antigenic moiety stimulate B-cells to increase the level of antibodies with a unique circular shape and smooth surface. They are considered a promising candidate for the development of a novel vaccine to elicit a humoral immune response against *B. melitensis* and *B. abortus* (Sadeghi et al., 2020). Iron oxide nanoparticles (IONPs) are widely used nanoparticles in various medical applications due to unique characteristics like high surface-to-volume ratio and super magnetism. They are particularly important in generating humoral immune responses by B-cells as compared to cell-mediated responses by T-cells (Gaharwar et al., 2020).

This latest review data from the literature may help design advanced theragnostic applications by using different combinations of nanoparticles and antigens.

## Other applications of nanobiotechnology

Some other applications of nanobiotechnology include the preparation of hydrogel biomaterials which show promising regenerative effects for damaged corneal tissues (Khosravimelal et al., 2021a). Moreover, it can also help us prepare fabricated antimicrobial nanofibers. These nanofibers show increased antimicrobial activity and can be used as a wound dressing to decrease infection and enhance healing properties (Khosravimelal et al., 2021b). Additionally, Nanopatterned surfaces have shown promising results in stem cell

differentiation. However, there is a need for more research on this topic (Eftekhari et al., 2021). Apart from their significance in regenerative medicine, antimicrobials, drug delivery, and stem biology, Nanobiomaterials can be used for the treatment of diabetes mellitus 1 by generating supplemental oxygen required by islets until the formation of blood vessels (Gholipourmalekabadi et al., 2016). Electrospinning uses the principles of nanobiotechnology for the preparation of biocompatible scaffolds which mimic collagen nanofibers providing protection and mechanical support at the injury site (Farshi et al., 2022).

## 10 Conclusion and future perspectives

Nanotechnological techniques can be used to develop and design cargo systems for the delivery of vaccines, depot formulations, adjuvants, and drugs in association with various types of nanoparticles to trigger cell-mediated and humoral immunological responses by T-cells and B-cells respectively to combat different viral and bacterial infections. Different types of nanoparticles such as organic, inorganic, metallic, non-metallic, and polymeric NPs are believed potentially strong to be widely used in medical applications, such as diagnostic purposes, therapeutic strategies, and gene and drug delivery to the targeted area of interest.

The interactions of nanoparticles and Ag with the immune system have gained attention due to the strong stimulation of immune cells to mediate cell-mediated and humoral immunity in cancer and viral diseases. Although nanoparticles are becoming a

useful candidates in various advanced theragnostic applications still, we are facing many health issues due to limited explored knowledge of nanoparticles.

Comprehensive studies are highly needed to explore further advanced pharmacodynamics, pharmacokinetics, immunomodulatory, and toxicity effects related to different types of nanoparticles critically affecting the health of human beings. A collaboration between nanotechnology and immunology is an emerging field of interest with a strong potential to design diagnostic and therapeutic applications to control health issues (Table 2) (Taniguchi, 1974; Mansoori and Soelaiman, 2005; Feynman, 2018).

## Author contributions

HM and MS have written the manuscript. AF has helped in the review of literature and data collection. SA supervised the manuscript editing, writing, and all the proceedings. HZ helped in drawing the figures. ZM helped in formatting and referencing.

## References

- Ahmed, M. K., Afifi, M., and Uskoković, V. (2020). Protecting healthcare workers during covid-19 pandemic with nanotechnology: A protocol for a new device from Egypt. *J. Infect. public health* 13 (9), 1243–1246. doi:10.1016/j.jiph.2020.07.015
- Almeida, J. P. M., Figueroa, E. R., and Drezek, R. A. (2014). Gold nanoparticle mediated cancer immunotherapy. *Nanomedicine Nanotechnol. Biol. Med.* 10 (3), 503–514. doi:10.1016/j.nano.2013.09.011
- Almeida, L., Felzenszwalb, I., Marques, M., and Cruz, C. (2020). Nanotechnology activities: Environmental protection regulatory issues data. *Heliyon* 6 (10), e05303. doi:10.1016/j.heliyon.2020.e05303
- Amarante-Mendes, G. P., Adjemian, S., Branco, L. M., Zanetti, L. C., Weinlich, R., and Bortoluci, K. R. (2018). Pattern recognition receptors and the host cell death molecular machinery. *Front. Immunol.* 9, 2379. doi:10.3389/fimmu.2018.02379
- Areteanu, R. N. S., Borodetsky, A., Azhari, H., and Weitz, I. S. (2020). Ultrasound-induced and mri-monitored cuo nanoparticles release from micelle encapsulation. *Nanotechnology* 32 (5), 055705. doi:10.1088/1361-6528/abc1a1
- Asha, A. B., and Narain, R. (2020). “Nanomaterials properties,” in *Polymer science and nanotechnology* (Elsevier), 343–359.
- Ashraf, S. A., Siddiqui, A. J., Abd Elmoneim, O. E., Khan, M. I., Patel, M., Alreshidi, M., et al. (2021). Innovations in nanoscience for the sustainable development of food and agriculture with implications on health and environment. *Sci. Total Environ.* 768, 144990. doi:10.1016/j.scitotenv.2021.144990
- Bagheri, Y., Barati, A., Aghebati-Maleki, A., Aghebati-Maleki, L., and Yousefi, M. (2021). Current progress in cancer immunotherapy based on natural killer cells. *Cell Biol. Int.* 45 (1), 2–17. doi:10.1002/cbin.11465
- Balakrishnan, P. B., and Sweeney, E. E. (2021). Nanoparticles for enhanced adoptive T cell therapies and future perspectives for CNS tumors. *Front. Immunol.* 12, 600659. doi:10.3389/fimmu.2021.600659
- Banin, U., Waiskopf, N., Hammarström, L., Boschloo, G., Freitag, M., Johansson, E. M., et al. (2020). Nanotechnology for catalysis and solar energy conversion. *Nanotechnology* 32 (4), 042003. doi:10.1088/1361-6528/abbc8
- Banskota, S., Yousefpour, P., and Chilkoti, A. (2017). Cell-based biohybrid drug delivery systems: The best of the synthetic and natural worlds. *Macromol. Biosci.* 17 (1), 1600361. doi:10.1002/mabi.201600361
- Baragaño, D., Forján, R., Welte, L., and Gallego, J. L. R. (2020). Nanoremediation of as and metals polluted soils by means of Graphene oxide nanoparticles. *Sci. Rep.* 10 (1), 1–10. doi:10.1038/s41598-020-58852-4

## Acknowledgments

We are very thankful to SA for helping out in all these processes.

## Conflict of interest

The authors declare that the research was conducted in the absence of any commercial or financial relationships that could be construed as a potential conflict of interest.

## Publisher's note

All claims expressed in this article are solely those of the authors and do not necessarily represent those of their affiliated organizations, or those of the publisher, the editors and the reviewers. Any product that may be evaluated in this article, or claim that may be made by its manufacturer, is not guaranteed or endorsed by the publisher.

- Barkalina, N., Charalambous, C., Jones, C., and Coward, K. (2014). Nanotechnology in reproductive medicine: Emerging applications of nanomaterials. *Nanomedicine Nanotechnol. Biol. Med.* 10 (5), e921–e938. doi:10.1016/j.nano.2014.01.001
- Bayda, S., Adeel, M., Tuccinardi, T., Cordani, M., and Rizzolio, F. (2019). The history of nanoscience and nanotechnology: From chemical-physical applications to nanomedicine. *Molecules* 25 (1). doi:10.3390/molecules25010112
- Behari, J. (2010). *Principles of nanoscience: An overview*.
- Bilal, M., and Iqbal, H. M. (2020). New insights on unique features and role of nanostructured materials in cosmetics. *Cosmetics* 7 (2), 24. doi:10.3390/cosmetics7020024
- Boholm, M. (2016). The use and meaning of nano in American English: Towards a systematic description. *Ampersand* 3, 163–173. doi:10.1016/j.amper.2016.10.001
- Boverhof, D. R., Bramante, C. M., Butala, J. H., Clancy, S. F., Lafranconi, M., West, J., et al. (2015). Comparative assessment of nanomaterial definitions and safety evaluation considerations. *Regul. Toxicol. Pharmacol.* 73 (1), 137–150. doi:10.1016/j.yrtph.2015.06.001
- Carmona, F. J., Dal Sasso, G., Ramírez-Rodríguez, G. B., Pii, Y., Delgado-López, J. M., Guagliardi, A., et al. (2021). Urea-functionalized amorphous calcium phosphate nanofertilizers: Optimizing the synthetic strategy towards environmental sustainability and manufacturing costs. *Sci. Rep.* 11 (1), 1–14. doi:10.1038/s41598-021-83048-9
- Cerwenka, A., and Lanier, L. L. (2016). Natural killer cell memory in infection, inflammation and cancer. *Nat. Rev. Immunol.* 16 (2), 112–123. doi:10.1038/nri.2015.9
- Chang, T. M. S. (2019). Artificial cell evolves into nanomedicine, biotherapeutics, blood substitutes, drug delivery, enzyme/gene therapy, cancer therapy, cell/stem cell therapy, nanoparticles, liposomes, bioencapsulation, replicating synthetic cells, cell encapsulation/scaffold, biosorbent/immunosorbent haemoperfusion/plasmapheresis, regenerative medicine, encapsulated microbe, nanobiotechnology, nanotechnology. *Artif. Cells, Nanomedicine, Biotechnol.* 47 (1), 997–1013. doi:10.1080/21691401.2019.1577885
- Chevalier, Y., and Bolzinger, M.-A. (2019). “Micelles and nanoemulsions,” in *Nanocosmetics* (Springer), 47–72.
- Choi, W. I., Lee, J. H., Kim, J.-Y., Heo, S. U., Jeong, Y. Y., Kim, Y. H., et al. (2015). Targeted antitumor efficacy and imaging via multifunctional nano-carrier conjugated with anti-her2 trastuzumab. *Nanomedicine Nanotechnol. Biol. Med.* 11 (2), 359–368. doi:10.1016/j.nano.2014.09.009



- Chu, D., Gao, J., and Wang, Z. (2015). Neutrophil-mediated delivery of therapeutic nanoparticles across blood vessel barrier for treatment of inflammation and infection. *ACS Nano* 9 (12), 11800–11811. doi:10.1021/acsnano.5b05583
- Collier, M. A., Bachelder, E. M., and Ainslie, K. M. (2017). Electrosprayed myocet-like liposomes: An alternative to traditional liposome production. *Pharm. Res.* 34 (2), 419–426. doi:10.1007/s11095-016-2072-4
- Cruz-Adalia, A., Ramirez-Santiago, G., Osuna-Pérez, J., Torres-Torresano, M., Zorita, V., Martínez-Riño, A., et al. (2017). Conventional Cd4+ T cells present bacterial antigens to Induce cytotoxic and memory Cd8+ T cell responses. *Nat. Commun.* 8 (1), 1–11. doi:10.1038/s41467-017-01661-7
- Dacoba, T. G., Olivera, A., Torres, D., Crecente-Campo, J., and Alonso, M. J. (Editors) (2017). *Modulating the immune system through nanotechnology. Seminars in immunology* (Elsevier).
- Day, N. B., Wixson, W. C., and Shields, I. V. C. W. (2021). Magnetic systems for cancer immunotherapy. *Acta Pharm. Sin. B* 11 (8), 2172–2196. doi:10.1016/j.apsb.2021.03.023
- de Lázaro, I., and Mooney, D. J. (2020). A nanoparticle's pathway into tumours. *Nat. Mat.* 19 (5), 486–487. doi:10.1038/s41563-020-0669-9
- De Volder, M. F., Tawfick, S. H., Baughman, R. H., and Hart, A. J. (2013). Carbon nanotubes: Present and future commercial applications. *science* 339 (6119), 535–539. doi:10.1126/science.1222453
- Deng, S., Gigliobianco, M. R., Censi, R., and Di Martino, P. (2020). Polymeric nanocapsules as nanotechnological alternative for drug delivery system: Current status, challenges and opportunities. *Nanomaterials* 10 (5), 847. doi:10.3390/nano10050847
- Dobrovolskaia, M. A., Shurin, M., and Shvedova, A. A. (2016). Current understanding of interactions between nanoparticles and the immune system. *Toxicol. Appl. Pharmacol.* 299, 78–89. doi:10.1016/j.taap.2015.12.022
- Dong, P., Rakesh, K., Manukumar, H., Mohammed, Y. H. E., Karthik, C., Sumathi, S., et al. (2019). Innovative nano-carriers in anticancer drug delivery—a comprehensive review. *Bioorg. Chem.* 85, 325–336. doi:10.1016/j.bioorg.2019.01.019
- Dong, X., Chu, D., and Wang, Z. (2017). Leukocyte-mediated delivery of nanotherapeutics in inflammatory and tumor sites. *Theranostics* 7 (3), 751–763. doi:10.7150/thno.18069
- Duguay, B. A., Lu, L., Arizmendi, N., Unsworth, L. D., and Kulka, M. (2020). The possible uses and challenges of nanomaterials in mast cell research. *J. Immunol.* 204 (8), 2021–2032. doi:10.4049/jimmunol.1800658
- Eftekhari, B. S., Eskandari, M., Janmey, P. A., Samadikuchaksaraei, A., and Gholipourmalekabadi, M. (2021). Conductive chitosan/polyaniline hydrogel with cell-imprinted topography as a potential substrate for neural priming of adipose derived stem cells. *RSC Adv.* 11 (26), 15795–15807. doi:10.1039/d1ra00413a
- Eiz-Vesper, B., and Schmetzer, H. M. (2020). Antigen-presenting cells: Potential of proven and new players in immune therapies. *Transfus. Med. Hemother.* 47 (6), 429–431. doi:10.1159/000512729
- El-Zayat, S. R., Sibaii, H., and Mannaa, F. A. (2019). Toll-like receptors activation, signaling, and targeting: An overview. *Bull. Natl. Res. Cent.* 43 (1), 1–12. doi:10.1186/s42269-019-0227-2
- Farshi, P., Salarian, R., Rabiee, M., Alizadeh, S., Gholipourmalekabadi, M., Ahmadi, S., et al. (2022). Design, preparation, and characterization of silk fibroin/carboxymethyl cellulose wound dressing for skin tissue regeneration applications. *Polym. Eng. Sci.* 2022, 2741–2749. doi:10.1002/pen.26057
- Fehniger, T. A., and Cooper, M. A. (2016). Harnessing nk cell memory for cancer immunotherapy. *Trends Immunol.* 37 (12), 877–888. doi:10.1016/j.it.2016.09.005
- Feynman, R. (2018). There's plenty of room at the bottom. *Feynman and computation*. Boca Raton: CRC Press, 63–76.
- Filipe, J. A., and Ferreira, M. A. M. (2021). *Analysis of nanosciences and nanotechnology and their applications*. arXiv preprint arXiv:211103425.
- Frank, L., Gazzi, R., de Andrade Mello, P., Buffon, A., Pohlmann, A., and Guterres, S. (2019). Imiquimod-loaded nanocapsules improve cytotoxicity in cervical cancer cell line. *Eur. J. Pharm. Biopharm.* 136, 9–17. doi:10.1016/j.ejpb.2019.01.001
- Gaharwar, U. S., Kumar, S., and Rajamani, P. (2020). Iron oxide nanoparticle-induced hematopoietic and immunological response in rats. *RSC Adv.* 10 (59), 35753–35764. doi:10.1039/D0RA05901C
- Galli, S. J., Gaudenzio, N., and Tsai, M. (2020). Mast cells in inflammation and disease: Recent progress and ongoing concerns. *Annu. Rev. Immunol.* 38, 49–77. doi:10.1146/annurev-immunol-071719-094903
- Gao, W., Xiong, Y., Li, Q., and Yang, H. (2017). Inhibition of toll-like receptor signaling as a promising therapy for inflammatory diseases: A journey from molecular to nano therapeutics. *Front. Physiol.* 8, 508. doi:10.3389/fphys.2017.00508
- García-Pinel, B., Porras-Alcalá, C., Ortega-Rodríguez, A., Sarabia, F., Prados, J., Melguizo, C., et al. (2019). Lipid-based nanoparticles: Application and recent advances in cancer treatment. *Nanomaterials* 9 (4), 638. doi:10.3390/nano9040638
- Gaudio, S. J., and Kumar, P. (2019). Cross-talk between antigen presenting cells and T cells impacts intestinal homeostasis, bacterial infections, and tumorigenesis. *Front. Immunol.* 10, 360. doi:10.3389/fimmu.2019.00360
- Gholipourmalekabadi, M., Jajarmi, V., Rezvani, Z., Ghaffari, M., Verma, K. D., Shirinzadeh, H., et al. (2016). "Oxygen-generating nanobiomaterials for the treatment of diabetes: A tissue engineering approach," in *Nanobiomaterials in soft tissue engineering* (Elsevier), 331–353.
- Glenn, J. C. (2006). Nanotechnology: Future military environmental health considerations. *Technol. Forecast. Soc. Change* 73 (2), 128–137. doi:10.1016/j.techfore.2005.06.010
- Gopi, S., Amalraj, A., and Thomas, S. (2016). Effective drug delivery system of biopolymers based on nanomaterials and hydrogels—a review. *Drug Des.* 5 (129), 2169–2138. doi:10.4172/2169-0138.1000129
- Guerra, F. D., Attia, M. F., Whitehead, D. C., and Alexis, F. (2018). Nanotechnology for environmental remediation: Materials and applications. *Molecules* 23 (7), 1760. doi:10.3390/molecules23071760
- Hangarter, C. M., Bangar, M., Mulchandani, A., and Myung, N. V. (2010). Conducting polymer nanowires for chemiresistive and fet-based bio/chemical sensors. *J. Mat. Chem.* 20 (16), 3131–3140. doi:10.1039/B915717D
- Hochella, M. F., Spencer, M. G., and Jones, K. L. (2015). Nanotechnology: Nature's gift or scientists' brainchild? *Environ. Sci. Nano* 2 (2), 114–119. doi:10.1039/C4EN00145A
- Hou, T., Wang, T., Mu, W., Yang, R., Liang, S., Zhang, Z., et al. (2021). Nanoparticle-loaded polarized-macrophages for enhanced tumor targeting and cell-chemotherapy. *Nanomicro. Lett.* 13 (1), 6–20. doi:10.1007/s40820-020-00531-0
- Hoy, S. M. (2018). Patisiran: First global approval. *Drugs* 78 (15), 1625–1631. doi:10.1007/s40265-018-0983-6
- Huang, C., Sun, M., Yang, Y., Wang, F., Ma, X., Li, J., et al. (2017). Titanium dioxide nanoparticles prime a specific activation state of macrophages. *Nanotoxicology* 11 (6), 737–750. doi:10.1080/17435390.2017.1349202
- Hughes, H. K., Mills-Ko, E., Yang, H., Lesh, T. A., Carter, C. S., and Ashwood, P. (2021). Differential macrophage responses in affective versus non-affective first-episode psychosis patients. *Front. Cell. Neurosci.* 15, 583351. doi:10.3389/fncel.2021.583351
- Hui, Y., Yi, X., Hou, F., Wibowo, D., Zhang, F., Zhao, D., et al. (2019). Role of nanoparticle mechanical properties in cancer drug delivery. *ACS Nano* 13 (7), 7410–7424. doi:10.1021/acsnano.9b03924
- Hulla, J., Sahu, S., and Hayes, A. (2015). Nanotechnology: History and future. *Hum. Exp. Toxicol.* 34 (12), 1318–1321. doi:10.1177/0960327115603588
- Iravani, S. (2011). Green synthesis of metal nanoparticles using plants. *Green Chem.* 13 (10), 2638–2650. doi:10.1039/c1gc15386b
- Iravani, S. (2014). Bacteria in nanoparticle synthesis: Current status and future prospects. *Int. Sch. Res. notices* 2014, 1–18. doi:10.1155/2014/359316
- Irvine, D. J., and Dane, E. L. (2020). Enhancing cancer immunotherapy with nanomedicine. *Nat. Rev. Immunol.* 20 (5), 321–334. doi:10.1038/s41577-019-0269-6
- Iype, J., and Fux, M. (2021). Basophils orchestrating eosinophils' chemotaxis and function in allergic inflammation. *Cells* 10 (4), 895. doi:10.3390/cells10040895
- Jain, R., Tikoo, S., and Weninger, W. (2019). Mast cell granules: Modulating adaptive immune response remotely. *J. Allergy Clin. Immunol.* 143 (5), 1731–1733. doi:10.1016/j.jaci.2018.11.029
- Jain, K., Patel, A. S., Pardhi, V. P., and Flora, S. J. S. (2021). Nanotechnology in wastewater management: A new paradigm towards wastewater treatment. *Molecules* 26 (6), 1797. doi:10.3390/molecules26061797
- Jeanbart, L., Kourtis, I. C., Van Der Vlies, A. J., Swartz, M. A., and Hubbell, J. A. (2015). 6-Thioguanine-Loaded polymeric micelles deplete myeloid-derived suppressor cells and enhance the efficacy of T cell immunotherapy in tumor-bearing mice. *Cancer Immunol. Immunother.* 64 (8), 1033–1046. doi:10.1007/s00262-015-1702-8
- Jeevanandam, J., Barhoum, A., Chan, Y. S., Dufresne, A., and Danquah, M. K. (2018). Review on nanoparticles and nanostructured materials: History, sources, toxicity and regulations. *Beilstein J. Nanotechnol.* 9 (1), 1050–1074. doi:10.3762/bjnano.9.98
- Jia, J., Zhang, Y., Xin, Y., Jiang, C., Yan, B., and Zhai, S. (2018). Interactions between nanoparticles and dendritic cells: From the perspective of cancer immunotherapy. *Front. Oncol.* 8, 404. doi:10.3389/fonc.2018.00404

- Jiang, W., Mashayekhi, H., and Xing, B. (2009). Bacterial toxicity Comparison between nano- and micro-scaled oxide particles. *Environ. Pollut.* 157 (5), 1619–1625. doi:10.1016/j.envpol.2008.12.025
- Jibowu, T. (2016). the formation of doxorubicin loaded targeted nanoparticles using nanoprecipitation, double emulsion and single emulsion for cancer treatment. *J. Nanomed. Nanotechnol.* 7 (379), 2. doi:10.4172/2157-7439.1000379
- Johnson, M., Alsaleh, N., Mendoza, R. P., Persaud, I., Bauer, A. K., Saba, L., et al. (2018). Genomic and transcriptomic Comparison of allergen and silver nanoparticle-induced mast cell degranulation reveals novel non-immunoglobulin E mediated mechanisms. *PLoS one* 13 (3), e0193499. doi:10.1371/journal.pone.0193499
- Kanda, A., Yasutaka, Y., Van Bui, D., Suzuki, K., Sawada, S., Kobayashi, Y., et al. (2020). Multiple biological aspects of eosinophils in host defense, eosinophil-associated diseases, immunoregulation, and homeostasis: Is their role beneficial, detrimental, regulator, or bystander? *Biol. Pharm. Bull.* 43 (1), 20–30. doi:10.1248/bpb.b19-00892
- Kanda, A., Yun, Y., Van Bui, D., Nguyen, L. M., Kobayashi, Y., Suzuki, K., et al. (2021). The multiple functions and subpopulations of eosinophils in tissues under steady-state and pathological conditions. *Allergol. Int.* 70 (1), 9–18. doi:10.1016/j.alit.2020.11.001
- Kany, S., Vollrath, J. T., and Relja, B. (2019). Cytokines in inflammatory disease. *Int. J. Mol. Sci.* 20 (23), 6008. doi:10.3390/ijms20236008
- Khalid, K., Tan, X., Mohd Zaid, H. F., Tao, Y., Lye Chew, C., Chu, D.-T., et al. (2020). Advanced in developmental organic and inorganic nanomaterial: A review. *Bioengineered* 11 (1), 328–355. doi:10.1080/21655979.2020.1736240
- Khan, A., Rashid, R., Murtaza, G., and Zahra, A. (2014). Gold nanoparticles: Synthesis and applications in drug delivery. *Trop. J. Pharm. Res.* 13 (7), 1169–1177. doi:10.4314/tjpr.v13i7.23
- Khan, I., Saeed, K., and Khan, I. (2019). Nanoparticles: Properties, applications and toxicities. *Arabian J. Chem.* 12 (7), 908–931. doi:10.1016/j.arabjc.2017.05.011
- Khosravimelal, S., Mobaraki, M., Eftekhari, S., Ahearne, M., Seifalian, A. M., and Gholipourmalekabadi, M. (2021). Hydrogels as emerging materials for Cornea wound healing. *Small* 17 (30), 2006335. doi:10.1002/sml.202006335
- Khosravimelal, S., Chizari, M., Farhadihosseinabadi, B., Moosazadeh Moghaddam, M., and Gholipourmalekabadi, M. (2021). Fabrication and characterization of an antibacterial chitosan/silk fibroin electrospun nanofiber loaded with a cationic peptide for wound-dressing application. *J. Mat. Sci. Mat. Med.* 32 (9), 1–11. doi:10.1007/s10856-021-06542-6
- Kim, H., Niu, L., Larson, P., Kucaba, T. A., Murphy, K. A., James, B. R., et al. (2018). Polymeric nanoparticles encapsulating novel tlr7/8 agonists as immunostimulatory adjuvants for enhanced cancer immunotherapy. *Biomaterials* 164, 38–53. doi:10.1016/j.biomaterials.2018.02.034
- Klopfleisch, R. (2016). Macrophage reaction against biomaterials in the mouse model-phenotypes, functions and markers. *Acta biomater.* 43, 3–13. doi:10.1016/j.actbio.2016.07.003
- Komal, M. S. (2021). The analysis on chemical–physical applications to nanomedicine. *Int. J. Eng. Res.* 1 (1), 1–8.
- Koshy, S. T., Cheung, A. S., Gu, L., Graveline, A. R., and Mooney, D. J. (2017). Liposomal delivery enhances immune activation by sting agonists for cancer immunotherapy. *Adv. Biosyst.* 1 (1–2), 1600013. doi:10.1002/adbi.201600013
- Kovarik, M. L., and Jacobson, S. C. (2009). *Nanofluidics in lab-on-a-chip devices*. Bloomington: ACS Publications. doi:10.1021/ac900614k
- Kuempel, E., Castranova, V., Geraci, C., and Schulte, P. (2012). Development of risk-based nanomaterial groups for occupational exposure control. *J. Nanopart. Res.* 14 (9), 1–15. doi:10.1007/s11051-012-1029-8
- Landvik, N. E., Skaug, V., Mohr, B., Verbeek, J., and Zienolddiny, S. (2018). Criteria for grouping of manufactured nanomaterials to facilitate hazard and risk assessment, a systematic review of expert opinions. *Regul. Toxicol. Pharmacol.* 95, 270–279. doi:10.1016/j.yrtph.2018.03.027
- Lee, K., and Yu, Y. (2017). Janus nanoparticles for T cell activation: Clustering ligands to enhance stimulation. *J. Mat. Chem. B* 5 (23), 4410–4415. doi:10.1039/c7tb00150a
- Lee, J. R., Bagge-Hansen, M., Tunuguntla, R., Kim, K., Bangar, M., Willey, T. M., et al. (2015). Ordering in bio-inorganic hybrid nanomaterials probed by *in situ* scanning transmission X-ray microscopy. *Nanoscale* 7 (21), 9477–9486. doi:10.1039/c5nr00622h
- Lee, N.-Y., Ko, W.-C., and Hsueh, P.-R. (2019). Nanoparticles in the treatment of infections caused by multidrug-resistant organisms. *Front. Pharmacol.* 10, 1153. doi:10.3389/fphar.2019.01153
- Lenders, V., Koutsoumpou, X., Sargsian, A., and Manshian, B. B. (2020). Biomedical nanomaterials for immunological applications: Ongoing research and clinical trials. *Nanoscale Adv.* 2 (11), 5046–5089. doi:10.1039/D0NA00478B
- Li, J., Ma, Y., Zhang, T., Shung, K. K., and Zhu, B. (2022). Recent advancements in ultrasound transducer: From material strategies to biomedical applications. *BME Front.* 2022, 9764501–9764519. doi:10.34133/2022/9764501
- Limongi, T., Canta, M., Racca, L., Ancona, A., Tritta, S., Vighetto, V., et al. (2019). Improving dispersal of therapeutic nanoparticles in the human body. *Nanomedicine* 14 (7), 797–801. doi:10.2217/nmm-2019-0070
- Linak, W. P., Miller, C. A., and Wendt, J. O. (2000). Comparison of particle size distributions and elemental partitioning from the combustion of pulverized coal and residual fuel oil. *J. Air & Waste Manag. Assoc.* 50 (8), 1532–1544. doi:10.1080/10473289.2000.10464171
- Liu, S., Galat, V., Galat, Y., Lee, Y. K. A., Wainwright, D., and Wu, J. (2021). Nk cell-based cancer immunotherapy: From basic biology to clinical development. *J. Hematol. Oncol.* 14 (1), 7–17. doi:10.1186/s13045-020-01014-w
- Luisa, R., and Valentina, C. (2021). Remotely activated nanoparticles for anticancer therapy. *Nanomicro. Lett.* 13 (1), 11. doi:10.1007/s40820-020-00537-8
- Luo, Y.-H., Chang, L. W., and Lin, P. (2015). Metal-based nanoparticles and the immune system: Activation, inflammation, and potential applications. *Biomed. Res. Int.* 2015, 1–12. doi:10.1155/2015/143720
- Malachowski, T., and Hassel, A. (2020). Engineering nanoparticles to overcome immunological barriers for enhanced drug delivery. *Eng. Regen.* 1, 35–50. doi:10.1016/j.engreg.2020.06.001
- Mandal, A., and Ray Banerjee, E. (2020). “Introduction to nanoscience, nanotechnology and nanoparticles,” in *Nanomaterials and biomedicine* (Springer), 1–39.
- Mansha, M., Khan, I., Ullah, N., and Qurashi, A. (2017). Synthesis, characterization and visible-light-driven photoelectrochemical hydrogen evolution reaction of carbazole-containing conjugated polymers. *Int. J. Hydrogen Energy* 42 (16), 10952–10961. doi:10.1016/j.ijhydene.2017.02.053
- Mansoori, G. A., and Soelaiman, T. F. (2005). *Nanotechnology—an introduction for the standards community*. Chicago: ASTM International.
- Marshall, J. S., Warrington, R., Watson, W., and Kim, H. L. (2018). An introduction to immunology and immunopathology. *Allergy Asthma Clin. Immunol.* 14 (2), 49–10. doi:10.1186/s13223-018-0278-1
- Marshall, J. S., Portales-Cervantes, L., and Leong, E. (2019). Mast cell responses to viruses and pathogen products. *Int. J. Mol. Sci.* 20 (17), 4241. doi:10.3390/ijms20174241
- Mauter, M. S., and Elimelech, M. (2008). Environmental applications of carbon-based nanomaterials. *Environ. Sci. Technol.* 42 (16), 5843–5859. doi:10.1021/es8006904
- McRae, M. P., Simmons, G., Wong, J., and McDevitt, J. T. (2016). Programmable bio-nanochip platform: A point-of-care biosensor system with the capacity to learn. *Acc. Chem. Res.* 49 (7), 1359–1368. doi:10.1021/acs.accounts.6b00112
- Mocan, T., Matea, C. T., Pop, T., Mosteanu, O., Buzoianu, A. D., Puia, C., et al. (2017). Development of nanoparticle-based optical sensors for pathogenic bacterial detection. *J. Nanobiotechnology* 15 (1), 25–14. doi:10.1186/s12951-017-0260-y
- Mohamed, E. F. (2017). Nanotechnology: Future of environmental air pollution control. *Environ. Manag. Sustain. Dev.* 6 (2), 429. doi:10.5296/emsd.v6i2.12047
- Mohamed, M., Abu Lila, A. S., Shimizu, T., Alaeldin, E., Hussein, A., Sarhan, H. A., et al. (2019). Pegylated liposomes: Immunological responses. *Sci. Technol. Adv. Mater.* 20 (1), 710–724. doi:10.1080/14686996.2019.1627174
- Moratin, H., Ickrath, P., Scherzad, A., Meyer, T. J., Naczinski, S., Hagen, R., et al. (2021). Investigation of the immune modulatory potential of zinc oxide nanoparticles in human lymphocytes. *Nanomaterials* 11 (3), 629. doi:10.3390/nano11030629
- Mortaz, E., Alipoor, S. D., Adcock, I. M., Mumby, S., and Koenderman, L. (2018). Update on neutrophil function in severe inflammation. *Front. Immunol.* 9, 2171. doi:10.3389/fimmu.2018.02171
- Muhammad, Q., Jang, Y., Kang, S. H., Moon, J., Kim, W. J., and Park, H. (2020). Modulation of immune responses with nanoparticles and reduction of their immunotoxicity. *Biomater. Sci.* 8 (6), 1490–1501. doi:10.1039/c9bm01643k
- Murphy-Marion, M., and Girard, D. (2018). Titanium dioxide nanoparticles Induce human eosinophil adhesion onto endothelial ea. Hy926 cells via activation of phosphoinositide 3-kinase/akt cell signalling pathway. *Immunobiology* 223 (2), 162–170. doi:10.1016/j.imbio.2017.10.030
- Nagamune, T. (2017). Biomolecular engineering for nanobio/bionanotechnology. *Nano Conver.* 4 (1), 9–56. doi:10.1186/s40580-017-0103-4
- Nam, J., Son, S., Park, K. S., Zou, W., Shea, L. D., and Moon, J. J. (2019). Cancer nanomedicine for combination cancer immunotherapy. *Nat. Rev. Mat.* 4 (6), 398–414. doi:10.1038/s41578-019-0108-1
- Nayyar, G., Chu, Y., and Cairo, M. S. (2019). Overcoming resistance to natural killer cell based immunotherapies for solid tumors. *Front. Oncol.* 9, 51. doi:10.3389/fonc.2019.00051



- Nel, I., Bertrand, L., Toubal, A., and Lehuen, A. (2021). Mait cells, guardians of skin and mucosa? *Mucosal Immunol.* 14 (4), 803–814. doi:10.1038/s41385-021-00391-w
- Nickoloff, B. J. (2019). *Dermal immune system*. Indianapolis: CRC Press.
- Özgün, S. (2013). Nanoemulsions in cosmetics. *Anadolu Univ.* 1 (6), 3–11. doi:10.3390/cosmetics5040063
- Paivandy, A., and Pejler, G. (2021). Novel strategies to target mast cells in disease. *J. Innate Immun.* 13 (3), 131–147. doi:10.1159/000513582
- Pal, S., Tak, Y. K., and Song, J. M. (2007). Does the antibacterial activity of silver nanoparticles depend on the shape of the nanoparticle? A study of the gram-negative Bacterium *Escherichia coli*. *Appl. Environ. Microbiol.* 73 (6), 1712–1720. doi:10.1128/AEM.02218-06
- Park, I. Y., Kim, I. Y., Yoo, M. K., Choi, Y. J., Cho, M.-H., and Cho, C. S. (2008). Mannosylated polyethylenimine coupled mesoporous silica nanoparticles for receptor-mediated gene delivery. *Int. J. Pharm.* 359 (1–2), 280–287. doi:10.1016/j.jipharm.2008.04.010
- Patel, K. D., Singh, R. K., and Kim, H.-W. (2019). Carbon-based nanomaterials as an emerging platform for theranostics. *Mat. Horiz.* 6 (3), 434–469. doi:10.1039/C8MH00966j
- Phung, C. D., Tran, T. H., and Kim, J. O. (2020). Engineered nanoparticles to enhance natural killer cell activity towards onco-immunotherapy: A review. *Arch. Pharm. Res.* 43 (1), 32–45. doi:10.1007/s12272-020-01218-1
- Pokropivny, V., and Skorokhod, V. (2007). Classification of nanostructures by dimensionality and concept of surface forms engineering in nanomaterial science. *Mater. Sci. Eng. C* 27 (5–8), 990–993. doi:10.1016/j.msec.2006.09.023
- Pradhan, D., Biswasroy, P., Goyal, A., Ghosh, G., and Rath, G. (2021). Recent advancement in nanotechnology-based drug delivery system against viral infections. *Aaps Pharmscitech* 22 (1), 47–19. doi:10.1208/s12249-020-01908-5
- Qu, X., Alvarez, P. J., and Li, Q. (2013). Applications of nanotechnology in water and wastewater treatment. *Water Res.* 47 (12), 3931–3946. doi:10.1016/j.watres.2012.09.058
- Radauer-Preiml, I., Andosch, A., Hawranek, T., Luetz-Meindl, U., Wiederstein, M., Horejs-Hoeck, J., et al. (2015). Nanoparticle-allergen interactions mediate human allergic responses: Protein corona characterization and cellular responses. *Part. Fibre Toxicol.* 13 (1), 3–15. doi:10.1186/s12989-016-0113-0
- Rai, R., Alwani, S., and Badea, I. (2019). Polymeric nanoparticles in gene therapy: New avenues of design and optimization for delivery applications. *Polymers* 11 (4), 745. doi:10.3390/polym11040745
- Ramesh, S. (2013). *Sol-gel synthesis and characterization of Ag*. doi:10.1557/jmr.2009.0314
- Ramirez, G. A., Yacoub, M.-R., Ripa, M., Mannina, D., Cariddi, A., Saporiti, N., et al. (2018). Eosinophils from physiology to disease: A comprehensive review. *BioMed Res. Int.* 2018, 1–28. doi:10.1155/2018/9095275
- Ramsden, J. J. (2012). Nanotechnology for military applications. *Nanotechnol. Percept.* 30, 99–131. doi:10.4024/n07ra12a.ntp.08.02
- Rea, I., Martucci, N. M., De Stefano, L., Ruggiero, I., Terracciano, M., Dardano, P., et al. (2014). Diatomite biosilica Nanocarriers for Sirna transport inside cancer cells. *Biochimica Biophysica Acta - General Subj.* 1840 (12), 3393–3403. doi:10.1016/j.bbagen.2014.09.009
- Romagnoli, G. G., Zelante, B. B., Toniolo, P. A., Migliori, I. K., and Barbutto, J. A. M. (2015). Dendritic cell-derived exosomes may Be a tool for cancer immunotherapy by converting tumor cells into immunogenic targets. *Front. Immunol.* 5, 692. doi:10.3389/fimmu.2014.00692
- Sadeghi, Z., Fasihi-Ramandi, M., and Bouzari, S. (2020). <p>Nanoparticle-Based vaccines for Brucellosis: Calcium phosphate nanoparticles-adsorbed antigens Induce cross protective response in mice</p>. *Int. J. Nanomedicine* 15, 3877–3886. doi:10.2147/ijn.s249942
- Saeedi, M., Eslamifard, M., Khezri, K., and Dizaj, S. M. (2019). Applications of nanotechnology in drug delivery to the central nervous system. *Biomed. Pharmacother.* 111, 666–675. doi:10.1016/j.biopha.2018.12.133
- Saleem, H., and Zaidi, S. J. (2020). Sustainable use of nanomaterials in textiles and their environmental impact. *Materials* 13 (22), 5134. doi:10.3390/ma13225134
- Shang, Y., Hasan, M. K., Ahammed, G. J., Li, M., Yin, H., and Zhou, J. (2019). Molecules 24 (14), 2558. doi:10.3390/molecules24142558
- Shapovalova, M., Pyper, S. R., Moriarty, B. S., and LeBeau, A. M. (2018). The molecular imaging of natural killer cells. *Mol. Imaging* 17, 153601211879481. doi:10.1177/1536012118794816
- Sharma, V. K., Filip, J., Zboril, R., and Varma, R. S. (2015). Natural inorganic nanoparticles—formation, fate, and toxicity in the environment. *Chem. Soc. Rev.* 44 (23), 8410–8423. doi:10.1039/C5CS00236B
- Sharma, P., Jang, N. Y., Lee, J. W., Park, B. C., Kim, Y. K., and Cho, N. H. (2019). Application of zno-based nanocomposites for vaccines and cancer immunotherapy. *Pharmaceutics* 11 (10), 493. Epub 2019/09/29. doi:10.3390/pharmaceutics11100493
- Simon-Deckers, A., Loo, S., Mayne-L'hermite, M., Herlin-Boime, N., Menguy, N., Reynaud, C., et al. (2009). Size-Composition-and shape-dependent toxicological impact of metal oxide nanoparticles and carbon nanotubes toward bacteria. *Environ. Sci. Technol.* 43 (21), 8423–8429. doi:10.1021/es9016975
- Singh, A. (2021). Eliciting B cell immunity against infectious diseases using nanovaccines. *Nat. Nanotechnol.* 16 (1), 16–24. doi:10.1038/s41565-020-00790-3
- Singh, H., Bhardwaj, N., Arya, S. K., and Khatri, M. (2020). Environmental impacts of oil spills and their remediation by magnetic nanomaterials. *Environ. Nanotechnol. Monit. Manag.* 14, 100305. doi:10.1016/j.enmm.2020.100305
- Singh, P., and Nanda, A. (2012). Nanotechnology in cosmetics: A boon or bane? *Toxicol. Environ. Chem.* 94 (8), 1467–1479. doi:10.1080/02772248.2012.723482
- Soleimani, N., Vaseghi, A., and Loconte, V. (2019). Poliglucan nanoparticles activate T cell response in breast cancer cell: An in vivo and in vitro study. *J. Fluoresc.* 29 (4), 1057–1064. doi:10.1007/s10895-019-02423-y
- Srivastava, A., and Rao, D. (2014). Enhancement of seed germination and plant growth of wheat, maize, peanut and garlic using multiwalled carbon nanotubes. *Eur. Chem. Bull.* 3 (5), 502–504. doi:10.1007/s00344-022-10677-3
- Subramanian, V., and Lee, T. (2012). Nanotechnology-based flexible electronics. *Nanotechnology* 23 (34), 340201. doi:10.1088/0957-4484/23/34/340201
- Suk, J. S., Xu, Q., Kim, N., Hanes, J., and Ensign, L. M. (2016). Pegylation as a strategy for improving nanoparticle-based drug and gene delivery. *Adv. Drug Deliv. Rev.* 99, 28–51. doi:10.1016/j.addr.2015.09.012
- Swartzwelter, B. J., Fux, A. C., Johnson, L., Swart, E., Hofer, S., Hofstätter, N., et al. (2020). The impact of nanoparticles on innate immune activation by live bacteria. *Int. J. Mol. Sci.* 21 (24), 9695. doi:10.3390/ijms21249695
- Taniguchi, N. (1974). *On the basic concept of nanotechnology*. Sapporo: Proceeding of the ICPE. doi:10.4024/n15ra09b.ntp.05.03
- Tanjina Hasnat, G. (2021). Sources and impacts of emerging contaminants in agroecosystems. *Sustain. Agric. Rev.* 50, 3–34. Springer. doi:10.1007/978-3-030-63249-6\_1
- Taylor, D. A. (2002). Dust in the wind. *Environ. Health Perspect.* 110 (2), A80–A87. doi:10.1289/ehp.110-a80
- Tiwari, D. K., Behari, J., and Sen, P. (2008). *Application of Nanoparticles in Waste Water Treatment*, 1. doi:10.28921/jan.2018.02.21
- Tran, S., DeGiovanni, P.-J., Piel, B., and Rai, P. (2017). Cancer nanomedicine: A review of recent success in drug delivery. *Clin. Transl. Med.* 6 (1), 44–21. doi:10.1186/s40169-017-0175-0
- Van Langelaar, J., Rijvers, L., Smolders, J., and Van Lujin, M. M. (2020). B and T Cells driving multiple sclerosis: Identity, mechanisms and potential triggers. *Front. Immunol.* 11, 760. doi:10.3389/fimmu.2020.00760
- Vanharen, M., and Girard, D. (2020). Activation of human eosinophils with nanoparticles: A new area of research. *Inflammation* 43 (1), 8–16. doi:10.1007/s10753-019-01064-4
- Verma, A., Gautam, S. P., Bansal, K. K., Prabhakar, N., and Rosenholm, J. M. (2019). Green nanotechnology: Advancement in phytoformulation research. *Medicines* 6 (1), 39. doi:10.3390/medicines6010039
- Vincenzo, B., Asif, I. J., Nikolaos, P., and Francesco, M. (2015). Adaptive immunity and inflammation. *Int. J. Inflam.* 2015, 1. doi:10.1155/2015/575406
- Wagner, S., Gondikas, A., Neubauer, E., Hofmann, T., and von der Kammer, F. (2014). Spot the difference: Engineered and natural nanoparticles in the environment—release, behavior, and fate. *Angew. Chem. Int. Ed. Engl.* 53 (46), 12398–12419. doi:10.1002/anie.201405050
- Wang, M.-R., Deng, L., Liu, G.-C., Wen, L., Wang, J.-G., Huang, K.-B., et al. (2019). Porous organic polymer-derived Nanopalladium catalysts for chemoselective synthesis of antitumor Benzofuro [2, 3-b] pyrazine from 2-bromophenol and isonitriles. *Org. Lett.* 21 (13), 4929–4932. doi:10.1021/acs.orglett.9b01230
- Weir, A., Westerhoff, P., Fabricius, L., Hristovski, K., and Von Goetz, N. (2012). Titanium dioxide nanoparticles in food and personal care products. *Environ. Sci. Technol.* 46 (4), 2242–2250. doi:10.1021/es204168d
- Wilson, K. L., Powles, L., Tsirikis, P., Xiang, S. D., Selomulya, C., Henderson, E., et al. (2020). Utilising nanoparticles to enhance the vaccine induced T cell immune response. *Am. Assoc. Immunol.* 2020. doi:10.1016/j.vaccine.2012.09.036
- Xie, J., Gong, L., Zhu, S., Yong, Y., Gu, Z., and Zhao, Y. (2019). Emerging strategies of nanomaterial-mediated tumor radiosensitization. *Adv. Mat.* 31 (3), 1802244. doi:10.1002/adma.201802244

- Xue, L., Yamazaki, H., Ren, R., Wanunu, M., Ivanov, A. P., and Edel, J. B. (2020). Solid-state nanopore sensors. *Nat. Rev. Mat.* 5 (12), 931–951. doi:10.1038/s41578-020-0229-6
- Yan, J., Yao, Y., Yan, S., Gao, R., Lu, W., and He, W. (2020). Chiral protein supraparticles for tumor suppression and synergistic immunotherapy: An enabling strategy for bioactive supramolecular chirality construction. *Nano Lett.* 20 (8), 5844–5852. doi:10.1021/acs.nanolett.0c01757
- Yang, H., Marion, T. N., Liu, Y., Zhang, L., Cao, X., Hu, H., et al. (2019). Nanomaterial exposure induced neutrophil extracellular traps: A new target in inflammation and innate immunity. *J. Immunol. Res.* 2019, 1–8. doi:10.1155/2019/3560180
- Yang, Y., Zhu, H., Xu, X., Bao, L., Wang, Y., Lin, H., et al. (2021). Construction of a novel lanthanum carbonate-grafted zsm-5 zeolite for effective highly selective phosphate removal from wastewater. *Microporous Mesoporous Mater.* 324, 111289. doi:10.1016/j.micromeso.2021.111289
- Yasinska, I. M., Calzolari, L., Raap, U., Hussain, R., Siligardi, G., Sumbayev, V. V., et al. (2019). Targeting of basophil and mast cell pro-allergic reactivity using functionalised gold nanoparticles. *Front. Pharmacol.* 10, 333. doi:10.3389/fphar.2019.00333
- Yeh, Y.-C., Creran, B., and Rotello, V. M. (2012). Gold nanoparticles: Preparation, properties, and applications in bionanotechnology. *Nanoscale* 4 (6), 1871–1880. doi:10.1039/C1NR11188D
- Yin, X., Chen, S., and Eisenbarth, S. C. (2021). Dendritic cell regulation of T helper cells. *Annu. Rev. Immunol.* 39, 759–790. doi:10.1146/annurev-immunol-101819-025146
- Youn, Y. S., and Bae, Y. H. (2018). Perspectives on the past, present, and future of cancer nanomedicine. *Adv. Drug Deliv. Rev.* 130, 3–11. doi:10.1016/j.addr.2018.05.008
- Zeng, Q., Bie, B., Guo, Q., Yuan, Y., Han, Q., Han, X., et al. (2020). Hyperpolarized Xe nmr signal advancement by metal-organic framework entrapment in aqueous solution. *Proc. Natl. Acad. Sci. U. S. A.* 117 (30), 17558–17563. doi:10.1073/pnas.2004121117
- Zhang, W., Wang, M., Tang, W., Wen, R., Zhou, S., Lee, C., et al. (2018). Nanoparticle-laden macrophages for tumor-tropic drug delivery. *Adv. Mat.* 30 (50), 1805557. doi:10.1002/adma.201805557
- Zhang, J., Wang, Q., Liu, J., Guo, Z., Yang, J., Li, Q., et al. (2019). Saponin-based near-infrared nanoparticles with aggregation-induced emission behavior: Enhancing cell compatibility and permeability. *ACS Appl. Bio Mat.* 2 (2), 943–951. doi:10.1021/acsabm.8b00812
- Zhang, H., He, F., Li, P., Hardwidge, P. R., Li, N., and Peng, Y. (2021). The role of innate immunity in pulmonary infections. *BioMed Res. Int.* 2021, 1–14. doi:10.1155/2021/6646071



## OPEN ACCESS

EDITED BY  
Sandra Camarero-Espinosa,  
Polymat, Spain

REVIEWED BY  
Gonzalo Riadi,  
University of Talca, Chile  
Angelo Accardo,  
Delft University of Technology,  
Netherlands

\*CORRESPONDENCE  
Carolina Testa,  
✉ carolina.testa@polimi.it  
Manuela T. Raimondi,  
✉ manuela.raimondi@polimi.it

†These authors share senior authorship

SPECIALTY SECTION  
This article was submitted to  
Nanobiotechnology,  
a section of the journal  
Frontiers in Bioengineering  
and Biotechnology

RECEIVED 16 May 2022  
ACCEPTED 15 December 2022  
PUBLISHED 06 January 2023

CITATION  
Testa C, Oliveto S, Jacchetti E,  
Donnalaja F, Martinelli C, Pinoli P,  
Osellame R, Cerullo G, Ceri S, Biffo S and  
Raimondi MT (2023), Whole transcriptomic  
analysis of mesenchymal stem cells  
cultured in Nichoid micro-scaffolds.  
*Front. Bioeng. Biotechnol.* 10:945474.  
doi: 10.3389/fbioe.2022.945474

COPYRIGHT  
© 2023 Testa, Oliveto, Jacchetti,  
Donnalaja, Martinelli, Pinoli, Osellame,  
Cerullo, Ceri, Biffo and Raimondi. This is an  
open-access article distributed under the  
terms of the [Creative Commons  
Attribution License \(CC BY\)](https://creativecommons.org/licenses/by/4.0/). The use,  
distribution or reproduction in other  
forums is permitted, provided the original  
author(s) and the copyright owner(s) are  
credited and that the original publication in  
this journal is cited, in accordance with  
accepted academic practice. No use,  
distribution or reproduction is permitted  
which does not comply with these terms.

# Whole transcriptomic analysis of mesenchymal stem cells cultured in Nichoid micro-scaffolds

Carolina Testa<sup>1,2\*</sup>, Stefania Oliveto<sup>3</sup>, Emanuela Jacchetti<sup>2</sup>,  
Francesca Donnalaja<sup>2</sup>, Chiara Martinelli<sup>2</sup>, Pietro Pinoli<sup>1</sup>,  
Roberto Osellame<sup>4</sup>, Giulio Cerullo<sup>4</sup>, Stefano Ceri<sup>1†</sup>, Stefano Biffo<sup>3†</sup>  
and Manuela T. Raimondi<sup>2\*†</sup>

<sup>1</sup>Department of Electronics, Information and Bioengineering, Politecnico di Milano, Milano, Italy,  
<sup>2</sup>Department of Chemistry, Materials and Chemical Engineering "Giulio Natta", Politecnico di Milano, Milano, Italy,  
<sup>3</sup>Department of Bioscience (DBS), University of Milan, Milano, Italy, <sup>4</sup>Institute of Photonics and Nanotechnology (IFN)-CNR and Department of Physics, Politecnico di Milano, Milano, Italy

Mesenchymal stem cells (MSCs) are known to be ideal candidates for clinical applications where not only regenerative potential but also immunomodulation ability is fundamental. Over the last years, increasing efforts have been put into the design and fabrication of 3D synthetic niches, conceived to emulate the native tissue microenvironment and aiming at efficiently controlling the MSC phenotype *in vitro*. In this panorama, our group patented an engineered microstructured scaffold, called Nichoid. It is fabricated through two-photon polymerization, a technique enabling the creation of 3D structures with control of scaffold geometry at the cell level and spatial resolution beyond the diffraction limit, down to 100 nm. The Nichoid's capacity to maintain higher levels of stemness as compared to 2D substrates, with no need for adding exogenous soluble factors, has already been demonstrated in MSCs, neural precursors, and murine embryonic stem cells. In this work, we evaluated how three-dimensionality can influence the whole gene expression profile in rat MSCs. Our results show that at only 4 days from cell seeding, gene activation is affected in a significant way, since 654 genes appear to be differentially expressed (392 upregulated and 262 downregulated) between cells cultured in 3D Nichoids and in 2D controls. The functional enrichment analysis shows that differentially expressed genes are mainly enriched in pathways related to the actin cytoskeleton, extracellular matrix (ECM), and, in particular, cell adhesion molecules (CAMs), thus confirming the important role of cell morphology and adhesions in determining the MSC phenotype. In conclusion, our results suggest that the Nichoid, thanks to its exclusive architecture and 3D cell adhesion properties, is not only a useful tool for governing cell stemness but could also be a means for controlling immune-related MSC features specifically involved in cell migration.

## KEYWORDS

mechanobiology, mesenchymal stem cells, synthetic, niche, 3D cell culture, transcriptomic analysis, cell adhesion molecules, bioengineering, immunomodulation

## 1 Introduction

Traditionally, the most utilized substrates for cell culture have been treated, polystyrene or glass surfaces (Kapalczyńska et al., 2016), but since the environment provided by these systems is generally flat, cells grow forming monolayers, consequently impairing cell-cell and cell-ECM interactions and also modifying their morphology with respect to their native configuration. In

this way, cells shape their cytoskeleton, sending different messages to the nucleus compared to the physiological state (Von der Mark et al., 1977; Petersen et al., 1992; Debnath and Brugge, 2005; Nelson and Bissell, 2006; Mahmud et al., 2009; Kilian et al., 2010), thus altering gene expression, protein synthesis, and other cell functions (Greiner et al., 2012; Santos et al., 2012). For these reasons, over the last few decades, three-dimensional (3D) systems for *in vitro* cell culture have gained increasing interest in several fields of biological research. It has been largely demonstrated that 3D culture conditions constitute a more realistic model as compared to bidimensional (2D) systems, since they create a more physiological microenvironment and, thus, promote cell responses that are more similar to the *in vivo* ones (Pampaloni et al., 2007; Edmondson et al., 2014; Shamir and Ewald, 2014).

One of the areas of greatest interest for the employment of 3D culture systems is stem cell research for tissue engineering and regenerative medicine, therapeutic approaches based on the use of stem cells to repair and regenerate damaged organs and tissues in place of resorting to allogenic transplantation (Heidary Rouchi and Mahdavi-Mazdeh, 2015). This is possible thanks to the self-renewal capacity of stem cells, the ability to maintain their stemness while dividing, and their ability to differentiate toward specific lineages under precise conditions (Kolios and Moodley, 2012; Dulak et al., 2015). The therapeutic potential of different stem cell types has been investigated, and adult stem cells and mesenchymal stem cells, in particular, have displayed the highest potential (Dulak et al., 2015; Liu, 2017). Mesenchymal stem cells (MSCs) are multipotent adult stem cells that can be easily isolated from the bone marrow (BM), adipose tissue, or umbilical cord and are able to differentiate into adipocytes, chondrocytes, osteoblasts, myocytes, smooth muscle cells, and neuron-like cells (Almalki and Agrawal, 2016; Liu, 2017; McKee and Chaudhry, 2017; Saidova and Vorobjev, 2020). Physiologically, MSCs and adult stem cells, in general, reside in specific “niches” which not only provide an anatomical location but also support self-renewal and stemness maintenance through biochemical and biophysical cues (Morrison and Spradling, 2008; Walker et al., 2008). In the last decade, increasing efforts have been made in designing and fabricating 3D synthetic niches, aiming to efficiently control MSCs’ fate *in vitro* and produce therapeutic cells on a large scale (Joddar and Ito, 2013). These scaffolds are conceived to emulate the native microenvironment by finely tuning the substrate physical properties, such as nanotopography (Dalby et al., 2007; Engel et al., 2009; McMurray et al., 2011), material stiffness (Engel et al., 2006; Khatiwala et al., 2009; Winer et al., 2009), and microgeometry (X. Li et al., 2012; Naito et al., 2011; Nerurkar et al., 2011). In the panorama of 3D cell culture systems for stem cell expansion, an innovative engineered substrate mimicking the native stem cell niche, called Nichoid, has recently been developed. It is based on an elementary and easily reproducible microarchitecture. Indeed, it is composed of a 3D interconnection of grids and columns able to create perfectly defined pores at the micrometric scale (Ricci et al., 2017). The main peculiarity of this scaffold is the use of two-photon polymerization (2PP) as a fabrication method, a technique enabling the creation of 3D structures based on a computer-generated model, with control of scaffold geometry at the cellular level (10  $\mu\text{m}$ ) and spatial resolution beyond the diffraction limit, up to 100 nm (Wu et al., 2006; Malinauskas et al., 2010; Nguyen and Narayan, 2017). It is known from the literature that isotropic cytoskeletal forces promote self-renewal and pluripotency, together with low extracellular loads and low oxygen concentration (McBeath

et al., 2004; Guilak et al., 2009; Gilbert et al., 2010; Wan et al., 2010; Nava et al., 2012). The Nichoid substrate was conceived with a 3D microtopology capable of exerting an isotropic system of adhesion forces on cells while reducing cytoskeletal tension. The pore microgeometry is proven to promote stem cell homing inside the structure (Raimondi et al., 2013). Therefore, the fundamental property reproduced on cells by the Nichoid scaffold is the capability to interact mechanically with cells at the single-cell scale, thanks to the very high spatial resolution of the technique used for its microfabrication. The “niche effect” has been investigated by our group on murine embryonic stem cells (mESCs), human and rat bone marrow MSCs, and murine neural precursor cells (NPCs); all these studies have highlighted the Nichoid’s ability to maintain stemness and pluripotency genes switched on at higher levels compared to traditional flat substrates, with no need for adding exogenous soluble factors or feeder layers (Nava et al., 2016a; Nava et al., 2016b; Bonandrini et al., 2018; Carelli et al., 2020; Remuzzi et al., 2020; Rey et al., 2020). This phenomenon occurs thanks to the forces that the Nichoid provides to cells, thus inducing genetic reprogramming by controlling the cytoskeletal tension (Jacchetti et al., 2021). These results suggest that the Nichoid structure is able to emulate the native stem niche microenvironment in terms of self-renewal and stemness conservation, dictating stem cell fate.

In all the aforementioned studies, proliferation of stem cells inside the polymerized niches was also assessed and compared with that in bidimensional controls, demonstrating the ability of the 3D Nichoid to allow and promote cell expansion.

The aim of this work is to go beyond the examination of mesenchymal stemness, thus interrogating the whole transcriptome of these cells cultured inside the Nichoid, in order to deeper understand gene expression and, thus, better elucidate all MSCs’ physiological functions and therapeutic modes of action (Pittenger et al., 2019). We, thus, performed a complete transcriptome analysis, investigating gene modulation and all the biological functions that are modified by culturing MSCs on 3D Nichoids and comparing them with those of MSCs grown on the recently introduced 2D Nichoid, a substrate consisting of a single layer of polymerized grids that we chose as the bidimensional control since it not only allowed a spreading expansion of cells but also enabled us to evaluate how the pure 3D rearrangement of cells can influence their entire genomic profile.

## 2 Materials and methods

### 2.1 Nichoid fabrication

In this work, we compared Nichoids with two geometries: a single-level pattern (2D Nichoids) and a three-level pattern (3D Nichoids). 2D and 3D micro-patterned substrates were fabricated through 2PP (Raimondi et al., 2012) of a negative hybrid organic–inorganic photoresist named SZ2080 (Ovsianikov et al., 2008) and composed of a 2:8 molar ratio of zirconium propoxide (Sigma-Aldrich, United States) and methacryloxypropyl trimethoxysilane (Sigma-Aldrich, United States) (Raimondi et al., 2012; Danilevičius et al., 2013; Ricci et al., 2017). Then, 1% concentration of Irg photoinitiator (Irgacure 369, 2-benzyl-2-dimethylamino-1-(4-morpholinophenyl)-butanone-1) was added to accelerate photopolymerization (Suzuki et al., 2012). A 20  $\mu\text{L}$  drop of resist was deposited on a 12 mm-diameter round glass coverslip suitable for optical microscopy (Bio



Optica, Italy) and allowed to harden to a semi-solid state; micropatterns were then fabricated directly on the coverslip. The pulsed laser source employed for fabrication is an ytterbium (Yb): KWP system based on a cavity-dumped oscillator in mode-locking with 1 MHz repetition rate, 1,030 nm wavelength (near-infrared, NIR), and 300 fs pulse duration. The laser beam was focused inside the sample through a 100× magnification oil-immersion microscope objective with 1.4 numerical aperture (NA) (plan apochromat, Carl Zeiss, Germany) and displacement along the three axes controlled by software (Automation 3200 CNC Operator Interface, Aerotech, United States). A spatial light modulator (SLM) was introduced in the setup to speed up the fabrication by splitting the beam into multiple parallel foci (Zandrini et al., 2019). The employed laser power was 100 mW, about 17 mW for each focus of the six-foci mask, and the writing speed was 3 mm/s. There was no slicing in the z-direction since it was a single line of 3 μm resolution, while the hatching parameter was 300 nm among two lines of 400 nm, leading to a final resolution of about 1 μm in the xy plane. At the end of the laser writing, the unpolymerized photoresist was removed by leaning the sample in a 50% (v/v) methyl isobutyl ketone and 50% (v/v) isopropyl alcohol solution (Sigma-Aldrich, United States) for 20 min (LaFratta et al., 2007; Malinauskas et al., 2013; Ricci et al., 2017).

The 3D sample had the traditional Nichoid architecture (Ricci et al., 2017): 218 squared blocks made up of 5 × 5 (450 × 450 μm<sup>2</sup>) structures with a spacing of 15 μm (Supplementary Figures S1A, B). Each structure is composed of individual niches, the elementary unit of the structure, with size corresponding to 90 × 90 × 30 μm<sup>3</sup>. Inside, there were three “floors” of interconnected rods, with a graded spacing (10, 20, and 30 μm) in the transverse direction and a uniform spacing of 15 μm in the vertical direction. The 2D Nichoid had the same grid geometry, but since it was made up of only one “floor,” it had an overall thickness of 2 μm, resulting in a partial bi-dimensional scaffold (Supplementary Figures S1C, D) used as a control in all biological experiments.

## 2.2 Substrate preparation and cell seeding

To confine cells inside the surface covered by the polymerized structures and to avoid unwanted cell adhesion outside the Nichoid substrate, different strategies were implemented. First, Costar® 6-well plates with an ultra-low attachment surface (Corning Incorporated, United States) were used as supports for cell seeding both on 3D and 2D Nichoids in order to avoid cell adhesion and proliferation on the surface of the wells. Second, the diameter of the glass sample covered with the Nichoid is 8 mm. To avoid cell adhesion on the glass portion of the coverslip surrounding the patterned portion of the samples, the bottom of the culture wells was drilled to create a small hole, 7 mm in diameter, with respect to the diameter of the Nichoid-covered coverslips. Then, the glass samples covered with the Nichoid were glued to the bottom of the culture wells from below using the biocompatible LOCTITE AA 3321 glue (Henkel, Germany) (Supplementary Figure S2). The glass ring surrounding the Nichoid-covered area of the coverslip corresponded to the glued surface in this assembly. Finally, cells were suspended for seeding in 100 μL of culture medium only, that is, the exact volume needed to guarantee complete covering of the structures only and uniform distribution of cells. This procedure was mainly employed in the case of sample seeded for subsequent RNA extraction in order to limit

the cell sample to cells expanded inside the Nichoid structures. For qualitative experiments, such as immunofluorescence image acquisitions, we only used the drop seeding technique, which nevertheless allowed us to ensure controlled disposition of cells on the polymerized structures.

Before seeding, all fabricated samples were sterilized by washing them twice with sterile deionized water, immersing in 70% ethanol for at least 30 min, washing again with sterile water, and letting them dry under a UV lamp (Raimondi et al., 2014).

Primary rat mesenchymal stem cells (rBMSCs), obtained from the bone marrow of Lewis rat and extracted at the Mario Negri Institute for Pharmacological Research (Milano, Italy) following the protocol presented by Zoja et al. (2012), were maintained in culture with an α-minimum essential medium (α-MEM, Gibco, Thermo Fisher Scientific, United States) supplemented by 20% fetal bovine serum (FBS) (EuroClone, Italy), 1% penicillin-streptomycin (EuroClone, Italy), 1% of L-glutamine 200 mM (EuroClone, Italy), and 100 mM of 1% sodium pyruvate (EuroClone, Italy). To avoid differentiation and stemness loss, cells were kept in culture for two passages only and then were detached by trypsin-EDTA solution 1X (EuroClone, Italy), resuspended in phosphate buffered saline (PBS, EuroClone, Italy), and counted using a cell counter (CytoSMART, Netherlands). A total of  $3 \times 10^4$  cells were seeded on each substrate, and drop-seeded samples were incubated for 1 h to permit proper cell adhesion to the structures; the required volume of medium was then added inside each well.

## 2.3 Viability assay and morphology evaluation

To evaluate viability at the fourth day after seeding, live samples were incubated for 10 min with .5 μM Calcein-AM (Invitrogen, Thermo Fisher Scientific, United States) and .2 μM ethidium homodimer-1 (Invitrogen, Thermo Fisher Scientific, United States) diluted in the fresh culture medium. Calcein-AM distribution was also exploited for a morphological evaluation, and nuclei were stained with 1 μM DRAQ5™ (Thermo Fisher Scientific, United States).

Live fluorescence images were acquired by using the Nikon Ar1+ confocal microscope (Nikon, Japan), equipped with an incubator chamber and four wavelength diode lasers ( $\lambda_{\text{excitation}} = 405/488/561/640$  nm). Stained cells were imaged with a 60× immersion oil objective, with 1.4 NA and .13 working distance (WD). The pinhole was set to 1 Airy unit, and  $1,024 \times 1,024$  pixel images were acquired as z-stack images. Cells grown on glass coverslips and 2D and 3D Nichoids were imaged with a 1 μm step, resulting in an acquisition depth of approximately 10 μm for the first two and a depth of approximately 40 μm for the latter.

After z-stack maximum projections, cellular and nuclear areas were measured through Fiji software v2.3.0/1.53f (Schindelin et al., 2012) by manually drawing cell and nucleus profiles.

## 2.4 RNA data collection

Total RNA was isolated at day 4 using the TRIzol reagent (Total RNA Isolation reagent, Invitrogen, Thermo Fisher Scientific, United States) following the standard protocol (Rio et al., 2010). The extracted RNA was quantified with the Qubit 2.0 Fluorometer (Invitrogen, Thermo Fisher Scientific, United States), and its quality



and integrity were evaluated through the Agilent 2100 Bioanalyzer (Agilent Technology, United States). Complementary DNA (cDNA) libraries were prepared using the Universal Plus mRNA-Seq kit (Tecan Genomics, United States) and sequenced in a single-end 75 base pair mode on the NextSeq 500 platform (Illumina, IGA Technologies Services, Italy).

## 2.5 Raw data processing

The per-base quality of the sequenced reads contained in the fastq files was checked with FastQC v0.11.9 (<http://www.bioinformatics.babraham.ac.uk/projects/fastqc/>). All samples were mapped to the mRatBN7.2 *Rattus norvegicus* reference genome ([https://ftp.ensembl.org/pub/release-108/fasta/rattus\\_norvegicus/dna/](https://ftp.ensembl.org/pub/release-108/fasta/rattus_norvegicus/dna/)), and the BAM files were sorted with STAR v2.7.0a (Dobin et al., 2013). Genes were annotated using standard Ensembl gene annotations, a high-quality annotation system used for vertebrate species that automatically indexes the genomic coordinates of each gene by plotting it onto genome assemblies (Aken et al., 2016). Gene expression levels were assessed by counting aligned reads with HTSeq v2.0.2 (Anders et al., 2015).

## 2.6 Differential expression and functional enrichment analyses

The DESeq2 package of R/Bioconductor (Love et al., 2014) was used to analyze the counts matrix produced by HTSeq and to identify differentially expressed genes (DEGs) between rBMSCs grown inside the 3D and 2D Nichoids. As implemented in the DESeq2 package, size factors are estimated to normalize the read counts. Values of  $|\log_2(\text{FoldChange})| > 1$  and false discovery rate (FDR)-adjusted  $p$  value  $\leq .05$  were employed as primary cutoffs to consider expression differences statistically significant.

A functional enrichment analysis to investigate the biological role of DEGs was conducted with the web-based tool g:Profiler (Raudvere et al., 2019) using the Gene Ontology (GO) database. The list of DEGs was ranked by decreasing  $\log_2(\text{FC})$ , and an ordered enrichment test was executed. g:Profiler performs Fisher's exact test to compute the  $p$  value of the enrichment of a pathway, and multiple-test corrections are applied (Reimand et al., 2019). The cutoff value for significantly enriched pathways was fixed to Benjamini-Hochberg (BH) FDR-adjusted  $p$  value  $\leq .05$ . The maximum term size was settled at 500.

Subsequently, the GSEA desktop application v4.1.0 (Mootha et al., 2003; Subramanian et al., 2005) was employed to perform a gene set permutation test with default parameters. It takes as input a pre-ranked list made up of all the available genes coming from the expression profile, without applying any cutoff, and uses a permutation-based test aiming to determine whether the genes included in a gene set fall at the top or at the bottom of the ranked list, rather than being randomly distributed within the list (Subramanian et al., 2005). The analysis was carried out with the H (hallmark) and the C2 (curated) gene sets of the Molecular Signatures Database (MSigDB) v7.2 (<https://www.gsea-msigdb.org/gsea/msigdb/index.jsp>), retrieved and adapted to the *Rattus norvegicus* species through the msigdbR package of R. The number of permutations

was settled at 1,000, and an FDR  $q$ -value  $< .25$  was chosen as the cutoff for statistical significance.

For a graphical visualization of interactions, a protein-protein interaction network was built with Cytoscape software v3.9.1 (Shannon et al., 2003), and the STRING functional enrichment network plugin was used to generate clusters. As query terms for the network, genes belonging to the most enriched GSEA gene sets were selected.

## 2.7 Quantitative real-time PCR

For validation of selected genes through real-time PCR (RT-PCR), RNA was extracted from 3D and 2D Nichoids as previously described, treated with the DNA-free™ DNA removal kit (Invitrogen, Thermo Fisher Scientific, United States), and reverse transcribed into cDNA using the SuperScript™ IV VILO™ kit (Invitrogen, Thermo Fisher Scientific, United States). Real-time PCR amplification was performed with the StepOnePlus™ Real-Time PCR System (Applied Biosystems, Thermo Fisher Scientific, United States) and the GoTaq® qPCR Master Mix (Promega, United States). The following primers (Thermo Fischer Scientific, United States) were designed with NCBI Primer-BLAST and Primer3Plus web tools and cross-checked with the Ensembl gene database: Vcam1 (forward: CTG TTTGCAGTCTCTCAAGC; reverse: AGTCTCCAATCTGAG CGAGC), Ncam1 (forward: GTATGATGCCAAGAAGCCAA CA; reverse: TGTCTTGAAGTCACTGAGTG), Selplg (forward: GGGGCTGGAAGTCTCTGAGAC; reverse: CCGTGGGTGCTAGCCG), and Efemp1 (forward: GCTCCC CGCAGGTATCTTTT; reverse: ATCGGTGCATTGCGTGTA TG). Gapdh (forward: GGCAAGTTCAACGGCACAG; reverse: CGCCAGTAGACTCCACGAC) was chosen as the housekeeping gene to normalize samples and calculate the gene expression level following the  $\Delta\Delta C_t$  method (Livak and Schmittgen, 2001).

## 2.8 Immunofluorescence assay

For immunofluorescence (IF) staining, samples were washed in PBS (Sigma-Aldrich, United States) and fixed in 10% formalin (Bio Optica, Italy) for 15 min. After three washes in glycine (Sigma-Aldrich, United States) to reduce autofluorescence, cells were permeabilized with PBS-.25% Triton® X-100 (Sigma-Aldrich, United States) for 10 min and blocked in PBS-.1% TWEEN® 20 (Sigma-Aldrich, United States) + 2% FBS (EuroClone, Italy) for 4 h. Primary antibodies to stain YAP (rabbit monoclonal anti-YAP antibody, 1:100, #14074, Cell Signaling Technology, United States) and N-cadherin (mouse anti-cadherin N antibody, 1:200, #94622, Immunological Science, Italy) were introduced and incubated at 4°C overnight. Samples were then washed three times in PBS-.1% TWEEN® 20 and incubated with Alexa Fluor® 647 and Alexa Fluor® 488 (1:750, Abcam, UK) secondary antibodies for 45 min at room temperature. FITC-conjugated phalloidin (Sigma-Aldrich, United States) was added, where needed, to stain the actin cytoskeleton. After three additional washes in PBS-.1% TWEEN® 20, the nuclei were stained with Hoechst 33342 (1:500, Thermo Fisher Scientific, United States) and incubated for

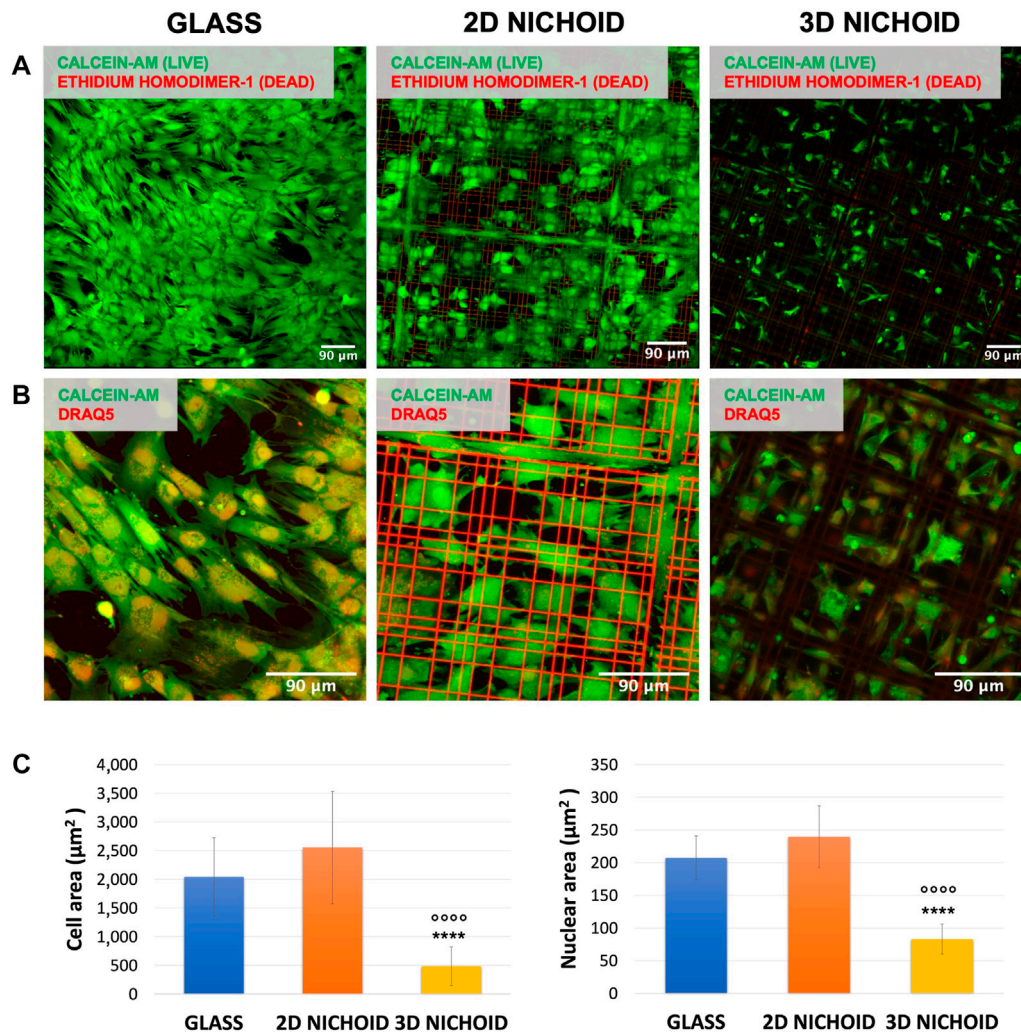


FIGURE 1

(A) Fluorescence images of live (green) and dead (red) rBMSCs cultured on glass coverslips and 2D and 3D Nichoids at day 4. Scale bar = 90 μm. (B) Fluorescence images of the cytoplasm (green) and nuclei (red) of rBMSCs cultured on glass coverslips and 2D and 3D Nichoids at day 4. Scale bar = 90 μm. (C) Quantification of the cellular and nuclear area in the three conditions. \*\*\*\* indicates  $p$  value  $\leq .0001$  for the 3D vs. 2D Nichoid comparison, and oooo indicates  $p$  value  $\leq .0001$  for the 3D vs. glass comparison.

10 min at room temperature. Finally, samples were mounted with Mowiol DABCO® (Sigma-Aldrich, United States) and inspected with a confocal microscope (FLUOVIEW FV10i, Olympus, Italy) equipped with four diode lasers (405, 473, 559, and 635 nm excitation wavelengths). A  $\times 60$  water immersion objective with 1.2 NA was used, and the pinhole was set to 1 Airy unit. Z-stack images of around 35 μm depth for 3D Nichoids and 10 μm depth for 2D Nichoids were acquired with a 1 μm step.

Fiji software v2.3.0/1.53f (Schindelin et al., 2012) was used for channel merge and fluorescence intensity quantification.

## 2.9 Statistical analysis

Data were reported as mean values  $\pm$  standard deviations. The statistical analyses were performed with Student's  $t$ -test, and a  $p$  value  $\leq .05$  was chosen as the cutoff for significance. \*\*\*\* indicates  $p$  values  $\leq .0001$ , \*\* indicates  $p$  values  $\leq .01$ , and \* indicates  $p$  values  $\leq .05$ .

## 3 Results

As a starting point, we carried out a comparison in terms of viability and morphology among cells cultured on traditional glass coverslips and both the 2D and 3D Nichoids.

rBMSC viability was assessed after 4 days of culture, the same time point of RNA extraction used for sequencing analysis. At least three areas per sample were acquired, and a strong predominance (close to 100%) of vital cells (in green) with respect to apoptotic cells (in red) was observed on all the used substrates (Figure 1A).

On the same samples, morphology analyses were performed, and the fluorescent dye DRAQ5 was added to also visualize the cell nucleus. Our observations revealed a variation between the three substrates in terms of cell shape. As visible in Figure 1B, cells cultured on 2D Nichoids were wide and spread, with morphology and dimension more comparable to those grown on glass coverslips, whereas in 3D Nichoids, cells tended to be more retained and confined. The quantification of cellular areas confirmed that cells

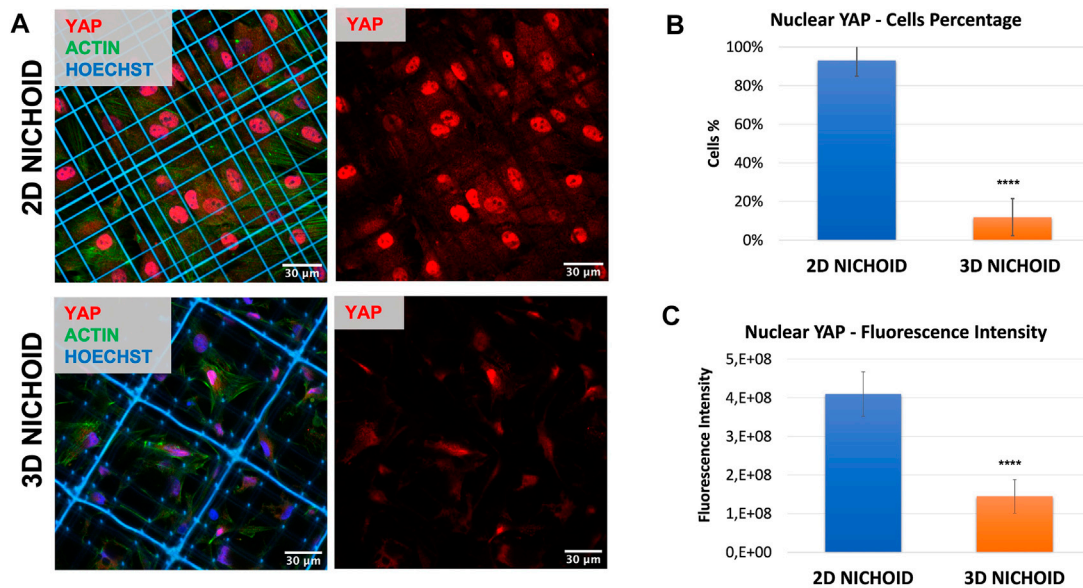


FIGURE 2

(A) Immunofluorescence images of rBMSCs with stained nuclei (blue), actin (green), and YAP (red) in 3D and 2D Nichoids. Scale bar = 30  $\mu$ m. (B) Quantification of the rBMSC percentage of cells with YAP mainly localized in the nucleus; \*\*\*\* indicates  $p$  value  $\leq .0001$  for the 3D vs. 2D Nichoid comparison ( $n = 4$ ). (C) Quantification of rBMSCs' fluorescence intensity of nuclear YAP; \*\*\*\* indicates  $p$  value  $\leq .0001$  for the 3D vs. 2D Nichoid comparison ( $n = 20$ ).

inside the 3D environment are significantly smaller than those in both of the two flat substrates, whereas among the 2D Nichoid and glass coverslips, no discrepancy emerged. In addition, the quantification of nuclear areas highlighted a significant reduction in the dimensions of 3D-grown cells' nuclei with respect to the other conditions (Figure 1C).

Based on these observations, we could state that rBMSCs cultured on 2D Nichoids had a bidimensional and spreading expansion compared to cells growing on glass coverslips. For this reason, we held it reasonable to employ a 2D Nichoid as a flat control in all subsequent experiments.

### 3.1 YAP nuclear/cytoplasmic localization

To corroborate the possibility of using a 2D Nichoid instead of a glass coverslip, we stained the mechano-transducer factor yes-associated protein (YAP) by immunofluorescence to compare its localization in bidimensional and tridimensional culture conditions. Immunofluorescence images (Figure 2A) clearly displayed that, just as it happened on glass coverslips (Remuzzi et al., 2020), in rBMSCs cultured on 2D Nichoids, YAP was almost exclusively localized in the nucleus, while it consistently translocated in the cytoplasm when cells were grown in a 3D environment. Indeed, on average, 93% of cells in 2D Nichoids retained YAP mostly inside the nucleus, whereas in 3D Nichoids, this percentage was around 12% (Figure 2B), and the YAP fluorescence level was significantly higher in the nuclei of cells cultured on bidimensional controls (Figure 2C).

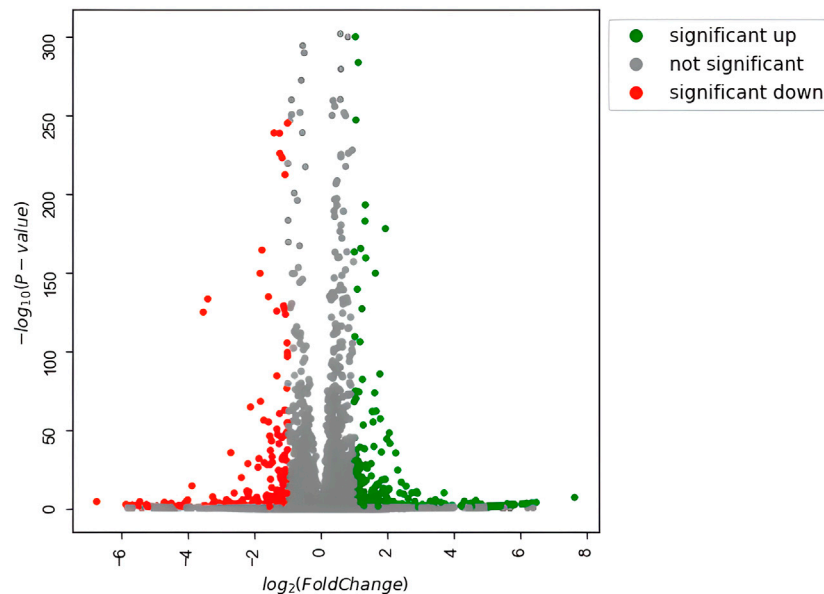
### 3.2 Differentially expressed genes identification and functional enrichment

To investigate how the previously observed morphological differences generated by Nichoid three-dimensionality translate

into variations in terms of rBMSC gene expression, the profiling of the complete transcriptome of Nichoid cultures was performed. All genes resulting from the total RNA-seq are reported in [Supplementary Table S1](#). Results from the bioinformatic pipeline showed that at 4 days from cell seeding, gene deregulation was affected in a significant way, since 654 genes appeared to be differentially expressed (392 upregulated and 262 downregulated) between 3D and 2D Nichoids, which are listed in [Supplementary Table S2](#). All DEGs, defined as those genes that meet both  $|\log_2(\text{FoldChange})| > 1$  and false discovery rate (FDR)-adjusted  $p$  value  $\leq .05$  cutoffs, are depicted in green (upregulated) and red (downregulated) in the volcano plot in Figure 3.

DEGs were successively used as input datasets for a biological enrichment analysis with the GO database to examine in which pathways they are mainly enriched. Interestingly, the highest dysregulated cellular components category has an extracellular matrix (GO:0031012), in particular, collagen-containing extracellular matrix (GO:0062023), apical plasma membrane (GO:0016324), apical part of the cell (GO:0045177), cell-cell junction (GO:0005911), actin cytoskeleton (GO:0015629), cluster of actin-based cell projections (GO:0098862), external side of the plasma membrane (GO:0009897), and cortical cytoskeleton (GO:0030863). The extracellular space appears to be dysregulated also in the biological functions category [extracellular matrix organization (GO:0030198) and extracellular structure organization (GO:0043062)], together with the regulation of cell adhesion (GO:0045785) and a series of pathways related to the muscle (GO:0033002; GO:0048659), bone (GO:0001503), cartilage (GO:0051216), and adipose tissue (GO:0045444) lineages. Moreover, in the molecular functions category, the top deregulated pathways are related to receptor activity (GO:0030546), cytokine activity (GO:0005125), cell adhesion molecule binding (GO:0050839), actin filament binding (GO:0051015), and integrin binding (GO:0005178) (Figure 4).



**FIGURE 3**

Volcano plot of differentially expressed genes. Significantly upregulated genes [adjusted  $p$  value  $\leq .05$  and  $\log_2(\text{FC}) > 1$ ] are in green; significantly downregulated genes [adjusted  $p$  value  $\leq .05$  and  $\log_2(\text{FC}) < -1$ ] are in red.

For a deeper enrichment investigation, we exploited the GSEA approach. This analysis also showed, among all the aforementioned pathways, significant and marked modifications in the expression of genes related to cell adhesion molecules and the extracellular matrix. Indeed, the KEGG\_CELL\_ADHESION\_MOLECULES\_CAMS and BOWIE\_RESPONSE\_TO\_EXTRACELLULAR\_MATRIX gene sets had positive enrichment scores,  $ES = .51$  and  $ES = .77$ , respectively, meaning that they were significantly (FDR  $q$ -value = .24 and FDR  $q$ -value = .17) overrepresented at the top of the ranked list of genes in the expression dataset. This is also graphically visible by the majority of black lines belonging to the gene set moved to the left. Interestingly, other positively and significantly enriched gene sets were REACTOME\_INTERFERON\_GAMMA\_SIGNALING ( $ES = .56$ ; FDR  $q$ -value = .14) and HALLMARK\_INTERFERON\_GAMMA\_RESPONSE ( $ES = .44$ ; FDR  $q$ -value = .002) (Figure 5A).

The set of genes belonging to these four significantly enriched gene sets was used as query terms for network construction to investigate potential connections. The network was divided into several clusters; the main two are shown in Figure 5B and include core genes with the highest rank metric scores of CAMs and IFN- $\gamma$  gene sets. Genes belonging to the response to the ECM gene set are contained in the IFN- $\gamma$  cluster. This graphical visualization highlighted how these pathways are closely interconnected with each other.

### 3.3 Cell adhesion molecules

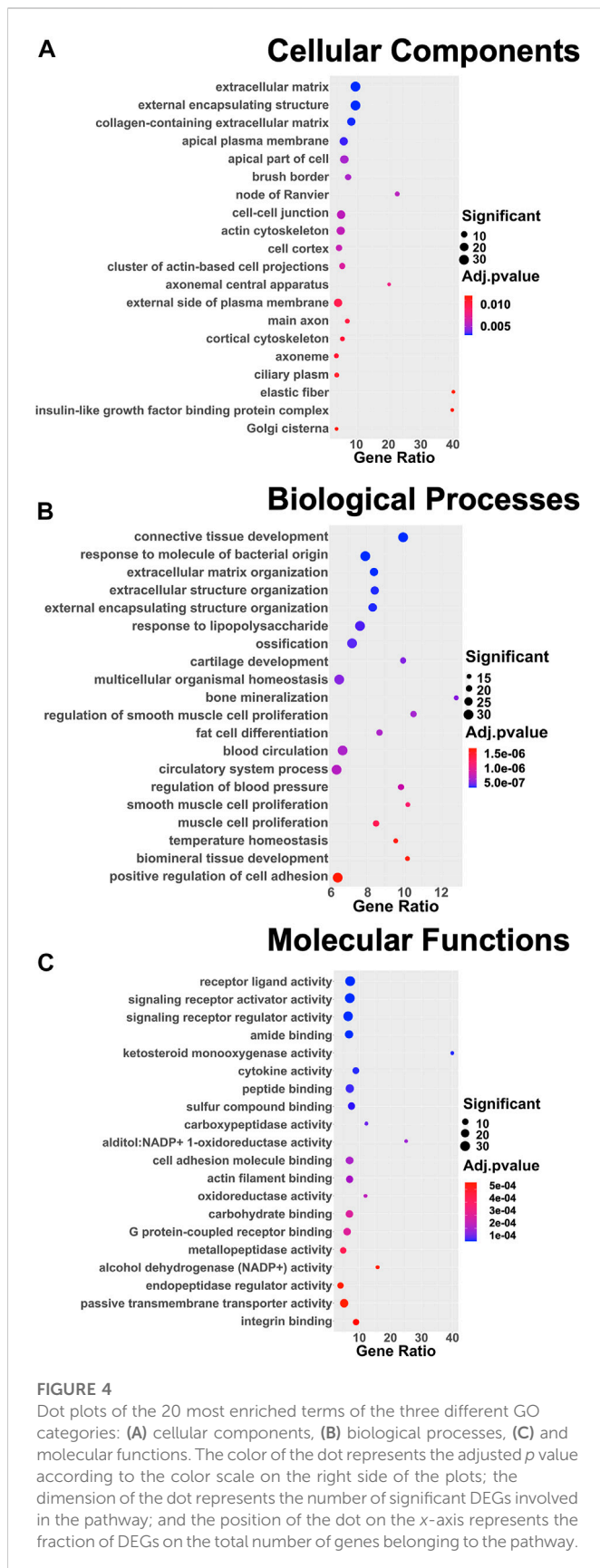
We then focused our attention on adhesion molecules. Therefore, the expression of four upregulated genes belonging to enriched pathways was analyzed through RT-PCR, which confirmed the overexpression of Selpg, Vcam1, Ncam1, and Efemp1 detected

from the sequencing in the 3D Nichoid with respect to the 2D Nichoid (Figure 6A).

To also evaluate homotypic cell–cell adhesions, we stained N-cadherin, a calcium-dependent cell adhesion protein that is predominantly expressed by MSCs (Hatta and Takeichi, 1986; Wuchter et al., 2007). Immunofluorescence images display a slight increase, although not significant, in the synthesis of this protein in rBMSCs grown in 3D Nichoids compared to bidimensional expansion. More interestingly, images showed a different localization of the proteins inside cells: in rBMSCs grown in 2D Nichoids, N-cadherin appears to be homogeneously distributed in the cytoplasm, whereas in 3D Nichoids, it is more localized in spots and distant from the nucleus in areas of cell–cell contacts (Figure 6B).

## 4 Discussion

Mesenchymal stem cells appear to be among the most promising stem cell sources for cell-based regenerative therapies, thanks mainly to their ease of extraction from several tissues and their differentiation potential toward a wide cohort of end-stage lineages (Han et al., 2019). Nevertheless, beyond their potential for differentiation and tissue regeneration, it has been demonstrated that MSCs have immunomodulatory and anti-inflammatory properties exercised through cytokine secretion and trophic activity (Zhao et al., 2016; Weiss and Dahlke, 2019; Song et al., 2020); they express a large number of genes encoding for a variety of regulatory proteins involved not only in mesoderm specification but also in other biological processes including inflammation and immune activation, cell motility, and communication (Phinney et al., 2006; Phinney, 2007; Phinney, 2009; Cruz-Barrera et al., 2020). Furthermore, it has been demonstrated that among the mostly expressed transcripts, there are also those encoding for structural and functional extracellular matrix



(ECM) proteins, which may contribute to MSCs' clinical regenerative potential, immune modulatory effects, and anti-inflammatory effects (J. Ren et al., 2011). These features make MSCs an ideal source for

autologous cell-based treatments since their trophism could be even more significant for their therapeutic potential than their pluripotency (Phinney, 2007; Lukomska et al., 2019).

However, to enable these cells to maintain all their characteristics and properties, it is of fundamental relevance to expand them in an appropriate environment where they can replicate *in vitro* the correct disposition and conformation they possess *in vivo* through the restoration of their physiological shape and the proper interactions with both the ECM and surrounding cells. In order to model a more physiological environment than the one that can be obtained with a simple slide or plate, we employed the Nichoid, a 3D scaffold designed to replicate the architectural microenvironment of the native stem niche. It is fabricated through a two-photon laser polymerization technique, the only one capable of achieving a defined structure at the sub-micrometric level, which is essential to ensure control over MSC responses at the individual cell scale.

Cells cultured on Nichoid samples were first examined to assess morphological and viability differences between three culture conditions. In 2D Nichoids, cells adhered to the underlying glass, and they showed a flattened and spread shape, correlated to an anisotropic tensional state, with an area comparable to that of cells cultured on traditional glass coverslips. On the contrary, in 3D Nichoids, the cytoplasm of cells was distributed in a more confined space, and evidence from several sources in the literature shows that this morphology is linked to reduced cytoskeletal tensions on the nucleus (Jacchetti et al., 2021) and to a greater cell multipotency (Nava et al., 2012; Saei Arezoumand et al., 2017). Despite these morphological differences, the viability assay did not show a significant difference, confirming the biocompatibility of the employed resin and demonstrating that the scaffold material in both 3D and 2D substrates does not impact rBMSC viability. These inspections allowed substituting the standard glass coverslip as the bidimensional control with the 2D Nichoid in all experiments, allowing us to determine the mere architectural effect of the scaffold tridimensionality on rBMSC gene expression and protein localization, separating it from the influence of the material properties relevant to the scaffold. In support of this hypothesis, our immunofluorescence results confirmed the same behavior observed by Remuzzi et al. (2020), where an increased percentage of the cytoplasmic fraction of YAP in rBMSCs cultured in 3D Nichoids was appreciable with respect to rBMSCs grown in monolayers on flat controls. In particular, this occurred despite differences in the number of cells seeded, time points, and, above all, substrate used as the flat control, which, in our case, was the 2D Nichoid in place of glass coverslips.

To investigate the consequent variation in gene expression inside the two different culture substrates, the transcriptome of rBMSCs cultured on Nichoids was sequenced and analyzed, aiming at determining the "niche effect" provided by the engineered cues of the 3D Nichoid architecture on the whole stem cell genetic response. For this purpose, the total RNA extracted from rBMSCs cultured on 2D and 3D Nichoids was profiled for the first time using next-generation sequencing technology, which allows for a more straightforward and affordable analysis of gene regulation compared to microarrays and other sequencing techniques with a higher sensitivity in detecting differentially expressed genes (J. Li et al., 2016; Marguerat and Bähler, 2010).

The measured differential expression confirmed that the morphological differences induced by the two substrates are



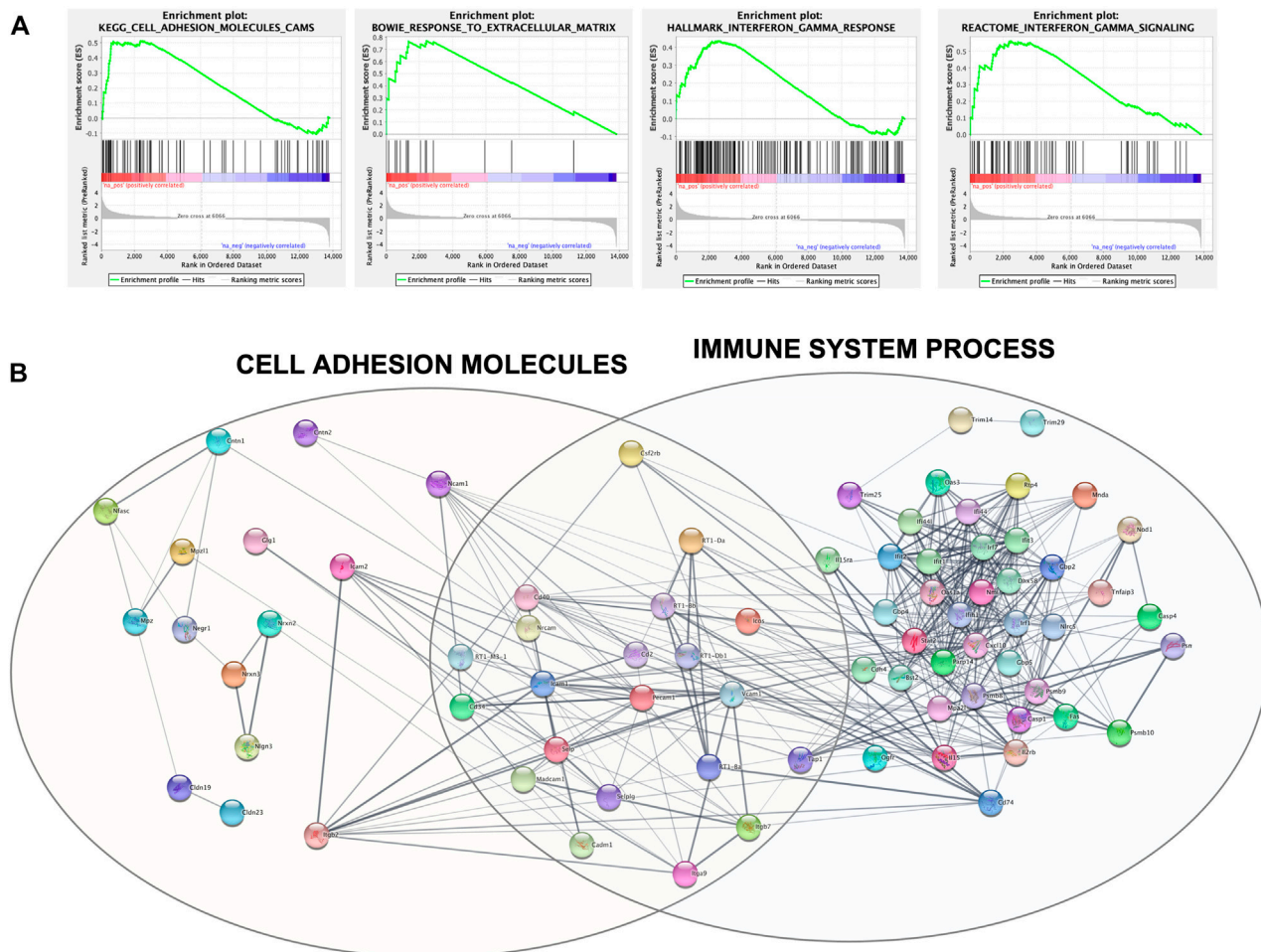


FIGURE 5

(A) GSEA output of the four mainly enriched gene sets. Each vertical black line corresponds to a gene, and its shift to the left indicates its positive enrichment. (B) Protein-protein interaction network built with Cytoscape and clustered with the STRING functional enrichment network plugin.

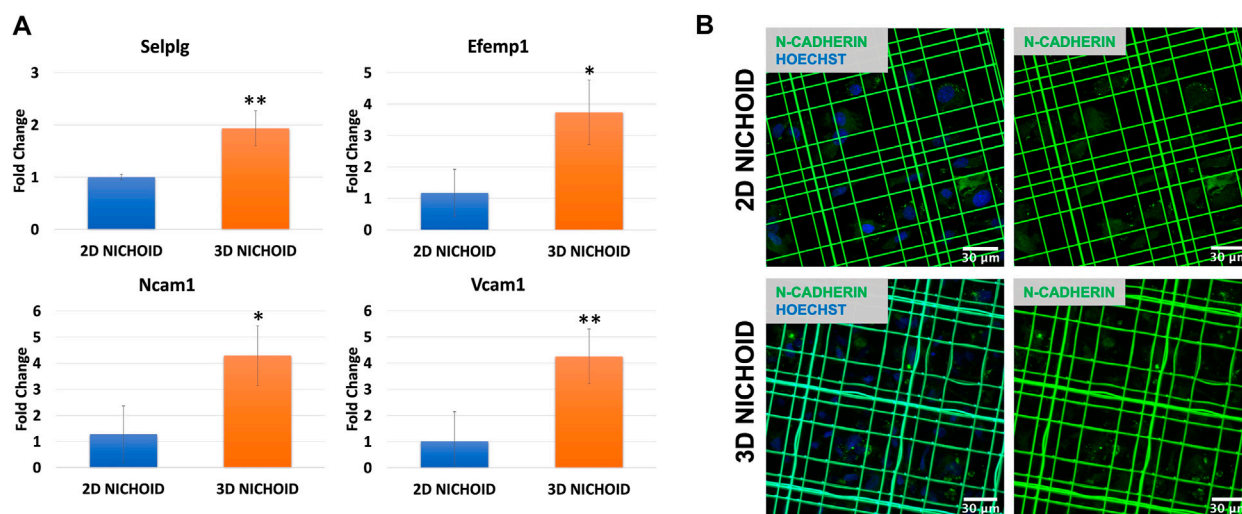


FIGURE 6

(A) Gene expression quantification through real-time PCR of Selp1g ( $n = 3$ ), Efemp1 ( $n = 4$ ), Ncam1 ( $n = 3$ ), and Vcam1 ( $n = 4$ ) in rBMSCs grown in 3D and 2D Nichoids for 4 days. Gapdh was used as the housekeeping gene. Data are represented as mean  $\pm$  SD; \* indicates  $p$  value  $\leq .05$ , and \*\* indicates  $p$  value  $\leq .01$  vs. 2D Nichoid. (B) Immunofluorescence images of nuclei (blue) and N-cadherin (green) in 3D and 2D Nichoids are shown. Scale bar = 30  $\mu$ m.

enough to lead to a significant genetic reprogramming of cellular processes, and the experimental design in use leads to the conclusion that these results are attributable exclusively to the three-dimensionality of the culture substrate.

To understand in which pathways they were mainly involved, the identified DEGs were subsequently subjected to functional enrichment for GO annotation with g:Profiler. The list of the top 20 affected pathways in the three categories seems to suggest that there was a deregulation in the entire mechano-transduction chain, starting from the extracellular matrix, moving through cell adhesions, and, by means of a reorganization of the actin cytoskeleton, reaching the nucleus. The modifications in this chain influenced biological processes and molecular functions of rBMSCs that were different between the 3D and 2D Nichoids, which mainly involved differentiation toward different lineages, receptors, and cytokine activity. The GSEA further underlined the discrepancy between the two culture systems in the expression of genes encoding for cell adhesion molecules and in the response to the ECM. This analysis revealed that two gene sets related to IFN- $\gamma$  also appeared to be upregulated, and interestingly, several connections were identified among the four gene sets by network analysis, reiterating how CAMs and the ECM play a relevant role also in the response of immune-related functions. These pathways are relevant since it is well established that MSCs primed with IFN- $\gamma$  enhance their immunosuppressive capacity (Klinker et al., 2017; Kim et al., 2018). However, several pieces of evidence showed that 3D-disposed MSCs are capable of self-activating their paracrine functions, increasing their pro-angiogenic potential, and intensifying the secretion of factors associated with immune cell modulation and tissue regeneration, even without external inflammatory signals (Ylostalo et al., 2014; Murphy et al., 2017; Xie et al., 2021).

Following the results obtained from the enrichment analyses, we focused our attention on this gene set, confirming the upregulation of Selplg, Vcam1, Ncam1, and Efemp1 in the 3D Nichoid with respect to the 2D Nichoid *via* RT-PCR experiments. Selplg encodes for the P-selectin glycoprotein ligand-1, which is part of the adhesion molecules involved in the regulation of leukocyte migration in response to inflammatory stimuli (Hirata et al., 2000; Hidalgo et al., 2007); interestingly, it has been shown how MSCs expressing this gene can rapidly move to the site of inflammation, exerting a superior anti-inflammatory effect (Levy et al., 2013; Liao et al., 2016). In addition to being an MSC marker, Vcam1 (vascular cell adhesion molecule 1) is recognized to play a critical role in MSC-related immunosuppression, and its expression is induced by the simultaneous presence of IFN- $\gamma$  and inflammatory cytokines (Ren et al., 2010). Moreover, Ncam1 (neural cell adhesion molecule 1) has been found to be expressed in MSCs and involved in cell migration *via* MAPK/ERK signaling activation (Shi et al., 2012). Efemp1, also known as fibulin-3, is a gene that encodes for the EGF-containing fibulin-like extracellular matrix protein 1, which is involved not only in cell adhesion and migration but also in negative regulation of chondrocyte differentiation (GO:0032331). Vukovic et al. (2009) demonstrated that this protein is highly expressed in olfactory ensheathing cells (OECs), which are endowed with a noteworthy self-repair potential and, together with their associated ECM, play an important role in proliferation during regenerative events. These results indicated that one of the effects of the 3D Nichoid is to regulate the adhesion molecules related to the immunomodulatory pathways; therefore, one might reasonably assert that the 3D Nichoid is able to affect the immunomodulatory ability of MSCs.

The upregulation of Vcam1 in 3D Nichoids could also be related to a higher number of cell-cell contacts mediated by N-cadherin that we investigated through immunofluorescence staining. It has been demonstrated that cell-cell adhesion mediated by N-cadherin promotes the expression of Vcam1 by activating the nuclear factor  $\kappa$ B (NF- $\kappa$ B) pathway *via* the platelet-derived growth factor receptor beta (PDGFR $\beta$ ) (Aomatsu et al., 2014; Chosa and Ishisaki, 2018). Our results show that this contact protein was slightly more expressed in 3D Nichoids, but above all, it was more aggregated; this suggests that the 3D structure of the scaffold promoted MSC-homotypic cell-cell adhesion among neighboring cells.

Cell-cell adhesions through N-cadherin also underlay the translocation of the mechano-transduction factor YAP from the nucleus to the cytoplasm. YAP, together with the transcriptional co-activator with a PDZ-binding motif (TAZ), is a key driver of stem cell behavior since it responds to physical stimuli, such as ECM stiffness, cell geometry, or mechanical forces of the cytoskeleton, with specific transcriptional programs (Donnalaja et al., 2020; Y. Li et al., 2021; Piccolo et al., 2014). As a matter of fact, the spatial organization of focal adhesions in cells inside the 3D Nichoid modifies the transmission of forces to the nucleus, determining weaker forces than in spreading cells and, thus, affecting the nuclear import of signaling molecules (Jacchetti et al., 2021). In addition to the effect of focal adhesions, the presence of N-cadherin, which is involved in mechano-transduction, affects the perception of the microenvironment stiffness, reducing the contractile state of the cell and subsequently YAP translocation (Cosgrove et al., 2016; Qin et al., 2020; Zhang et al., 2021).

YAP is a fundamental downstream effector of the Hippo pathway, which plays a role in several mechanisms such as development, stem cell self-renewal and differentiation, regeneration, immune modulation, and cancer (Moya and Halder, 2019; Dey et al., 2020; LeBlanc et al., 2021). Among target genes of activated YAP/TAZ, in our transcriptome analysis, we found both Snai2 (zinc finger protein SNAI2) and Jag1 (protein jagged-1) to be overexpressed in 3D Nichoids. It has been proven that Snai2 is a transcription factor included among the major upregulators for BM-MSC maintenance, fate decision, cell adhesion, and cell structure regulation (Sánchez-Luis et al., 2020; Wei et al., 2020). In turn, Snai2 can bind to Cxcl12 (C-X-C motif chemokine 12) promoters; Cxcl12, which we also found slightly over-expressed, is critical to retain both MSCs and hematopoietic stem cells in the bone marrow niche and also for hematopoietic stem and progenitor cells' quiescent state maintenance (Roson-Burgo et al., 2016). Interestingly, Giri et al. (2020) also demonstrated that BM-MSC-secreted Cxcl12, cooperating with CCL2 (C-C motif chemokine 2), exercised an anti-inflammatory capacity in toxic colitis by upregulating IL10 expression in CCR2<sup>+</sup> macrophages. Furthermore, Jag1, which is part of the Notch pathway, has been shown to be a potent pro-angiogenic regulator (Benedito et al., 2009).

To conclude, our results demonstrated how restoring both the correct morphology of the stem cells and the correct adhesions in an *in vitro* culture system is important to preserve the native cell functionality. It is known that adhesion molecules are the essential initial point of a mechano-transduction chain that starts from the membrane and, through the cytoskeletal organization and tension, reaches the nucleus, conditioning several biological aspects of the cell, such as transcription. In this context, the Nichoid proved to be able to perform these tasks and, thus, demonstrates, thanks to its peculiar

capability to restore 3D cell adhesions, especially those among neighboring cells, to be not only an ideal substrate for MSC expansion and stemness maintenance but also a means for controlling other specific MSC features such as immunomodulation, thus supporting its potential for clinical application in immune-based diseases.

## Data availability statement

The data presented in the study are deposited in the GEO repository, accession number GSE199846: <https://www.ncbi.nlm.nih.gov/query/acc.cgi?acc=GSE199846>.

## Author contributions

CT, SO, and EJ designed the experiments and analyzed and interpreted the data. CT fabricated both the 3D and 2D microstructured substrates. CT and SO performed cell cultures, viability and morphological assays, RNA extraction, and RT-PCR experiments. CT, EJ, CM, and FD performed immunofluorescence experiments and confocal image acquisition. CT and PP performed RNA-seq raw data processing, differential expression, and functional enrichment analyses. RO and GC provided scientific supervision on the 2PP fabrication process. MR, SB, and SC supervised the work, revised the manuscript, and provided financial support. All authors read and approved the final version of the article.

## Funding

Funded by the European Union grant ERC-AdG-2021 project BEACONSANDEGG; G.A. nr 101053122. Views and opinions expressed are however those of the author(s) only and do not

necessarily reflect those of the European Union or the ERC. Neither the European Union nor the granting authority can be held responsible for them. Funded also by an unrestricted grant from “Fondazione Romeo ed Enrica Invernizzi” to Stefano Biffo.

## Acknowledgments

The authors wish to thank Joy Atoe for generating part of the data in the context of her master's thesis.

## Conflict of interest

MTR, RO, and GC are co-founders of a university spin-off company, MOAB srl, and hold shares.

The remaining authors declare that the research was conducted in the absence of any commercial or financial relationships that could be construed as a potential conflict of interest.

## Publisher's note

All claims expressed in this article are solely those of the authors and do not necessarily represent those of their affiliated organizations, or those of the publisher, the editors, and the reviewers. Any product that may be evaluated in this article, or claim that may be made by its manufacturer, is not guaranteed or endorsed by the publisher.

## Supplementary material

The Supplementary Material for this article can be found online at: <https://www.frontiersin.org/articles/10.3389/fbioe.2022.945474/full#supplementary-material>

## References

- Aken, B. L., Ayling, S., Barrell, D., Clarke, L., Curwen, V., Fairley, S., et al. (2016). The Ensembl gene annotation system. *Database J. Biol. Databases Curation* 2016, baw093. doi:10.1093/database/baw093
- Almalki, S. G., and Agrawal, D. K. (2016). Key transcription factors in the differentiation of mesenchymal stem cells. *Differentiation* 92 (1–2), 41–51. doi:10.1016/j.diff.2016.02.005
- Anders, S., Pyl, P. T., and Huber, W. (2015). HTSeq-A Python framework to work with high-throughput sequencing data. *Bioinformatics* 31 (2), 166–169. doi:10.1093/bioinformatics/btu638
- Aomatsu, E., Chosa, N., Nishihira, S., Sugiyama, Y., Miura, H., and Ishisaki, A. (2014). Cell-cell adhesion through N-cadherin enhances VCAM-1 expression via PDGFRβ in a ligand-independent manner in mesenchymal stem cells. *Int. J. Mol. Med.* 33 (3), 565–572. doi:10.3892/ijmm.2013.1607
- Benedito, R., Roca, C., Sørensen, I., Adams, S., Gossler, A., Fruttiger, M., et al. (2009). The Notch ligands Dll4 and Jagged1 have opposing effects on angiogenesis. *Cell* 137 (6), 1124–1135. doi:10.1016/j.cell.2009.03.025
- Bonandrini, B., Figliuzzi, M., Conti, S., Zandrini, T., Osellame, R., Cerullo, G., et al. (2018). Effect of the 3D artificial nichoid on the morphology and mechanobiological response of mesenchymal stem cells cultured *in vitro*. *Cells* 9, 1873–1928. doi:10.3390/cells9081873
- Carelli, S., Giallongo, T., Rey, F., Barzaghi, B., Zandrini, T., Pulcinelli, A., et al. (2020). Neural precursors cells expanded in a 3D micro-engineered niche present enhanced therapeutic efficacy *in vivo*. *Nanotheranostics* 5 (1), 8–26. doi:10.7150/ntno.50633
- Chosa, N., and Ishisaki, A. (2018). Two novel mechanisms for maintenance of stemness in mesenchymal stem cells: SCRG1/BST1 axis and cell-cell adhesion through N-cadherin. *Jpn. Dent. Sci. Rev.* 54 (1), 37–44. doi:10.1016/j.jdsr.2017.10.001
- Cosgrove, B. D., Mui, K. L., Driscoll, T. P., Caliar, S. R., Mehta, K. D., Assoian, R. K., et al. (2016). N-Cadherin adhesive interactions modulate matrix mechanosensing and fate commitment of mesenchymal stem cells. *Nat. Mater.* 15, 1297–1306. doi:10.1038/nmat4725
- Cruz-Barrera, M., Flórez-Zapata, N., Lemus-Díaz, N., Medina, C., Galindo, C. C., González-Acero, L. X., et al. (2020). Integrated analysis of transcriptome and secretome from umbilical cord mesenchymal stromal cells reveal new mechanisms for the modulation of inflammation and immune activation. *Front. Immunol.* 11, 575488–575519. doi:10.3389/fimmu.2020.575488
- Dalby, M. J., Gadegaard, N., Tare, R., Andar, A., Riehle, M. O., Herzyk, P., et al. (2007). The control of human mesenchymal cell differentiation using nanoscale symmetry and disorder. *Nat. Mater.* 6 (12), 997–1003. doi:10.1038/nmat2013
- Danilevičius, P., Rekštyte, S., Balčiunas, E., Kraniuskauskas, A., Širmenis, R., Baltrikiene, D., et al. (2013). Laser 3D micro/nanofabrication of polymers for tissue engineering applications. *Opt. Laser Technol.* 45 (1), 518–524. doi:10.1016/j.optlastec.2012.05.038
- Debnath, J., and Brugge, J. S. (2005). Modelling glandular epithelial cancers in three-dimensional cultures. *Nat. Rev. Cancer* 5 (9), 675–688. doi:10.1038/nrc1695
- Dey, A., Varelas, X., and Guan, K.-L. (2020). Targeting the Hippo pathway in cancer, fibrosis, wound healing and regenerative medicine. *Nat. Rev. Drug Discov.* 19 (7), 480–494. doi:10.1038/s41573-020-0070-z
- Dobin, A., Davis, C. A., Schlesinger, F., Drenkow, J., Zaleski, C., Jha, S., et al. (2013). STAR: Ultrafast universal RNA-seq aligner. *Bioinformatics* 29 (1), 15–21. doi:10.1093/bioinformatics/bts635
- Donnalaja, F., Carnevali, F., Jacchetti, E., and Raimondi, M. T. (2020). Lamin A/C mechanotransduction in laminopathies. *Cells* 9 (5), 1306. doi:10.3390/cells9051306



- Dulak, J., Szade, K., Szade, A., Nowak, W., and Józkowicz, A. (2015). Adult stem cells: Hopes and hypes of regenerative medicine. *Acta Biochim. Pol.* 62 (3), 329–337. doi:10.18388/abp.2015\_1023
- Edmondson, R., Broglie, J. J., Adcock, A. F., and Yang, L. (2014). Three-dimensional cell culture systems and their applications in drug discovery and cell-based biosensors. *Assay Drug Dev. Technol.* 12 (4), 207–218. doi:10.1089/adt.2014.573
- Engel, E., Martínez, E., Mills, C. A., Funes, M., Planell, J. A., and Samitier, J. (2009). Mesenchymal stem cell differentiation on microstructured poly (methyl methacrylate) substrates. *Ann. Anat.* 191 (1), 136–144. doi:10.1016/j.aanat.2008.07.013
- Engler, A. J., Sen, S., Sweeney, H. L., and Discher, D. E. (2006). Matrix elasticity directs stem cell lineage specification. *Cell* 126 (4), 677–689. doi:10.1016/j.cell.2006.06.044
- Gilbert, P. M., Havenstrite, K. L., Magnusson, K. E. G., Sacco, A., Leonardi, N. A., Kraft, P., et al. (2010). Substrate elasticity regulates skeletal muscle stem cell self-renewal in culture. *Science* 329 (5995), 1078–1081. doi:10.1126/science.1191035
- Giri, J., Das, R., Nysten, E., Chinnadurai, R., and Galipeau, J. (2020). CCL2 and CXCL12 derived from mesenchymal stromal cells cooperatively polarize IL-10+ tissue macrophages to mitigate gut injury. *Cell Rep.* 30 (6), 1923–1934. doi:10.1016/j.celrep.2020.01.047
- Greiner, A. M., Richter, B., and Bastmeyer, M. (2012). Micro-engineered 3D scaffolds for cell culture studies. *Macromol. Biosci.* 12 (10), 1301–1314. doi:10.1002/mabi.201200132
- Guilak, F., Cohen, D. M., Estes, B. T., Gimble, J. M., Liedtke, W., and Chen, C. S. (2009). Control of stem cell fate by physical interactions with the extracellular matrix. *Cell Stem Cell* 5 (1), 17–26. doi:10.1016/j.stem.2009.06.016
- Han, Y., Li, X., Zhang, Y., Han, Y., Chang, F., and Ding, J. (2019). Mesenchymal stem cells for regenerative medicine. *Cells* 8 (8), 886. doi:10.3390/cells8080886
- Hatta, K., and Takeichi, M. (1986). Expression of N-cadherin adhesion molecules associated with early morphogenetic events in chick development. *Nature* 324, 447–449. doi:10.1038/320447a0
- Heidary Rouchi, A., and Mahdavi-Mazdeh, M. (2015). Regenerative medicine in organ and tissue transplantation: Shortly and practically achievable? *Int. J. Organ Transplant. Med.* 6 (3), 93–98.
- Hidalgo, A., Peired, A. J., Wild, M., Vestweber, D., and Frenette, P. S. (2007). Complete identification of E-selectin ligands on neutrophils reveals distinct functions of PSGL-1, ESL-1, and CD44. *Immunity* 26 (4), 477–489. doi:10.1016/j.immuni.2007.03.011
- Hirata, T., Merrill-Skoloff, G., Aab, M., Yang, J., Furie, B. C., and Furie, B. (2000). P-selectin glycoprotein ligand 1 (Psgl-1) is a physiological ligand for E-selectin in mediating T helper 1 lymphocyte migration. *J. Exp. Med.* 192 (11), 1669–1676. doi:10.1084/jem.192.11.1669
- Jacchetti, E., Nasehi, R., Boeri, L., Parodi, V., Negro, A., Albani, D., et al. (2021). The nuclear import of the transcription factor MyoD is reduced in mesenchymal stem cells grown in a 3D micro-engineered niche. *Sci. Rep.* 11 (1), 3021–3119. doi:10.1038/s41598-021-81920-2
- Joddar, B., and Ito, Y. (2013). Artificial niche substrates for embryonic and induced pluripotent stem cell cultures. *J. Biotechnol.* 168 (2), 218–228. doi:10.1016/j.jbiotec.2013.04.021
- Kapalczyńska, M., Kolenda, T., Przybyła, W., Zajączkowska, M., Teresiak, A., Filas, V., et al. (2016). 2D and 3D cell cultures – a comparison of different types of cancer cell cultures. *Archives Med. Sci.* 14 (4), 910–919. doi:10.5114/aoms.2016.63743
- Khatiwala, C. B., Kim, P. D., Peyton, S. R., and Putnam, A. J. (2009). ECM compliance regulates osteogenesis by influencing MAPK signaling downstream of RhoA and ROCK. *J. Bone Mineral Res.* 24 (5), 886–898. doi:10.1359/jbmr.081240
- Kilian, K. A., Bugarija, B., Lahn, B. T., and Mrlsich, M. (2010). Geometric cues for directing the differentiation of mesenchymal stem cells. *Proc. Natl. Acad. Sci. U. S. A.* 107 (11), 4872–4877. doi:10.1073/pnas.0903269107
- Kim, D. S., Jang, I. K., Lee, M. W., Ko, Y. J., Lee, D. H., Lee, J. W., et al. (2018). Enhanced immunosuppressive properties of human mesenchymal stem cells primed by interferon- $\gamma$ . *EBioMedicine* 28, 261–273. doi:10.1016/j.ebiom.2018.01.002
- Klinker, M. W., Marklein, R. A., Lo Surdo, J. L., Wei, C. H., and Bauer, S. R. (2017). Morphological features of IFN- $\gamma$ -stimulated mesenchymal stromal cells predict overall immunosuppressive capacity. *Proc. Natl. Acad. Sci. U. S. A.* 114 (13), E2598–E2607. doi:10.1073/pnas.1617933114
- Kolios, G., and Moodley, Y. (2012). Introduction to stem cells and regenerative medicine. *Respiration* 85 (1), 3–10. doi:10.1159/000345615
- LaFratta, C. N., Fourkas, J. T., Baldacchini, T., and Farrer, R. A. (2007). Multiphoton fabrication. *Angew. Chem. - Int. Ed.* 46, 6238–6258. doi:10.1002/anie.200603995
- LeBlanc, L., Ramirez, N., and Kim, J. (2021). Context-dependent roles of YAP/TAZ in stem cell fates and cancer. *Cell. Mol. Life Sci.* 78 (9), 4201–4219. doi:10.1007/s00018-021-03781-2
- Levy, O., Zhao, W., Mortensen, L. J., LeBlanc, S., Tsang, K., Fu, M., et al. (2013). MRNA-engineered mesenchymal stem cells for targeted delivery of interleukin-10 to sites of inflammation. *Blood* 122 (14), e23–e32. doi:10.1182/blood-2013-04-495119
- Li, J., Hou, R., Niu, X., Liu, R., Wang, Q., Wang, C., et al. (2016). Comparison of microarray and RNA-Seq analysis of mRNA expression in dermal mesenchymal stem cells. *Biotechnol. Lett.* 38 (1), 33–41. doi:10.1007/s10529-015-1963-5
- Li, X., Liu, H., Niu, X., Yu, B., Fan, Y., Feng, Q., et al. (2012). The use of carbon nanotubes to induce osteogenic differentiation of human adipose-derived MSCs *in vitro* and ectopic bone formation *in vivo*. *Biomaterials* 33 (19), 4818–4827. doi:10.1016/j.biomaterials.2012.03.045
- Li, Y., Wang, J., and Zhong, W. (2021). Regulation and mechanism of YAP/TAZ in the mechanical microenvironment of stem cells (Review). *Mol. Med. Rep.* 24 (1), 506–511. doi:10.3892/mmr.2021.12145
- Liao, W., Pham, V., Liu, L., Riazifar, M., Pone, E. J., Zhang, S. X., et al. (2016). Mesenchymal stem cells engineered to express selectin ligands and IL-10 exert enhanced therapeutic efficacy in murine experimental autoimmune encephalomyelitis. *Biomaterials* 77, 87–97. doi:10.1016/j.biomaterials.2015.11.005
- Liu, T. M. (2017). Stemness of mesenchymal stem cells. *J. Stem Cell Ther. Transplant.* 1 (1), 071–073. doi:10.29328/journal.jsctt.1001008
- Livak, K. J., and Schmittgen, T. D. (2001). Analysis of relative gene expression data using real-time quantitative PCR and the 2- $\Delta\Delta$ CT method. *Methods* 25 (4), 402–408. doi:10.1006/meth.2001.1262
- Love, M. I., Huber, W., and Anders, S. (2014). Moderated estimation of fold change and dispersion for RNA-seq data with DESeq2. *Genome Biol.* 15 (12), 550–621. doi:10.1186/s13059-014-0550-8
- Lukomska, B., Stanaszek, L., Zuba-Surma, E., Legosz, P., Sarzynska, S., and Drela, K. (2019). Challenges and controversies in human mesenchymal stem cell therapy. *Stem Cells Int.* 2019, 1–10. doi:10.1155/2019/9628536
- Mahmud, G., Campbell, C. J., Bishop, K. J. M., Komarova, Y. A., Chaga, O., Soh, S., et al. (2009). Directing cell motions on micropatterned ratchets. *Nat. Phys.* 5 (8), 606–612. doi:10.1038/nphys1306
- Malinauskas, M., Danilevicius, P., Baltrikien, D., Purlis, V., Paipulas, D., Bukelskien, V., et al. (2010). 3D artificial polymeric scaffolds for stem cell growth fabricated by femtosecond laser. *Lithuanian J. Phys.* 50(1), 75–82. doi:10.3952/lithphys.50121
- Malinauskas, M., Farsari, M., Piskarskas, A., and Juodkazis, S. (2013). Ultrafast laser nanostructuring of photopolymers: A decade of advances. *Phys. Rep.* 533 (1), 1–31. doi:10.1016/j.physrep.2013.07.005
- Marguerat, S., and Bähler, J. (2010). RNA-seq: From technology to biology. *Cell. Mol. Life Sci.* 67 (4), 569–579. doi:10.1007/s00018-009-0180-6
- McBeath, R., Pirone, D. M., Nelson, C. M., Bhadriraju, K., and Chen, C. S. (2004). Cell shape, cytoskeletal tension, and RhoA regulate stem cell lineage commitment. *Dev. Cell* 6 (4), 483–495. doi:10.1016/S1534-5807(04)00075-9
- McKee, C., and Chaudhry, G. R. (2017). Advances and challenges in stem cell culture. *Colloids Surfaces B Biointerfaces* 159, 62–77. doi:10.1016/j.colsurfb.2017.07.051
- McMurray, R. J., Gadegaard, N., Tsimbouri, P. M., Burgess, K. V., McNamara, L. E., Tare, R., et al. (2011). Nanoscale surfaces for the long-term maintenance of mesenchymal stem cell phenotype and multipotency. *Nat. Mater.* 10 (8), 637–644. doi:10.1038/nmat3058
- Mootha, V. K., Lindgren, C. M., Eriksson, K. F., Subramanian, A., Sihag, S., Lehar, J., et al. (2003). PGC-1 $\alpha$ -responsive genes involved in oxidative phosphorylation are coordinately downregulated in human diabetes. *Nat. Genet.* 34 (3), 267–273. doi:10.1038/ng1180
- Morrison, S. J., and Spradling, A. C. (2008). Stem cells and niches: Mechanisms that promote stem cell maintenance throughout life. *Cell* 132 (4), 598–611. doi:10.1016/j.cell.2008.01.038
- Moya, I. M., and Halder, G. (2019). Hippo–YAP/TAZ signalling in organ regeneration and regenerative medicine. *Nat. Rev. Mol. Cell Biol.* 20 (4), 211–226. doi:10.1038/s41580-018-0086-y
- Murphy, K. C., Whitehead, J., Falahee, P. C., Zhou, D., Simon, S. I., and Leach, J. K. (2017). Multifactorial experimental design to optimize the anti-inflammatory and proangiogenic potential of mesenchymal stem cell spheroids. *Stem Cells* 35 (6), 1493–1504. doi:10.1002/stem.2606
- Naito, H., Dohi, Y., Zimmermann, W. H., Tojo, T., Takasawa, S., Eschenhagen, T., et al. (2011). The effect of mesenchymal stem cell osteoblastic differentiation on the mechanical properties of engineered bone-like tissue. *Tissue Eng. - Part A* 17 (17–18), 2321–2329. doi:10.1089/ten.tea.2011.0099
- Nava, M. M., Maggio, N., Di Zandrini, T., Cerullo, G., Osellame, R., Martin, I., et al. (2016a). Synthetic niche substrates engineered via two-photon laser polymerization for the expansion of human mesenchymal stromal cells. *J. Tissue Eng. Regen. Med.* 11, 2836. doi:10.1002/term
- Nava, M. M., Piuma, A., Figliuzzi, M., Cattaneo, I., Bonandrini, B., Zandrini, T., et al. (2016b). Two-photon polymerized “nichoid” substrates maintain function of pluripotent stem cells when expanded under feeder-free conditions. *Stem Cell Res. Ther.* 7, 132. doi:10.1186/s13287-016-0387-z
- Nava, M. M., Raimondi, M. T., and Pietrabissa, R. (2012). Controlling self-renewal and differentiation of stem cells via mechanical cues. *J. Biomed. Biotechnol.* 2012, 1–12. doi:10.1155/2012/797410
- Nelson, C. M., and Bissell, M. J. (2006). Of extracellular matrix, scaffolds, and signaling: Tissue architecture regulates development, homeostasis, and cancer. *Annu. Rev. Cell Dev. Biol.* 22 (1), 287–309. doi:10.1146/annurev.cellbio.22.010305.104315
- Nerurkar, N. L., Han, W., Mauck, R. L., and Elliott, D. M. (2011). Homologous structure-function relationships between native fibrocartilage and tissue engineered from MSC-seeded nanofibrous scaffolds. *Biomaterials* 32 (2), 461–468. doi:10.1016/j.biomaterials.2010.09.015

- Nguyen, A. K., and Narayan, R. J. (2017). Two-photon polymerization for biological applications. *Biochem. Pharmacol.* 20 (6), 314–322. doi:10.1016/j.matmod.2017.06.004
- Ovsianikov, A., Viertl, J., Chichkov, B., Oubaha, M., Maccraith, B., Giakoumaki, A., et al. (2008). Ultra-low shrinkage hybrid photosensitive material for two-photon polymerization microfabrication. *ACS Nano* 2, 2257. doi:10.1021/nn800451w
- Pampaloni, F., Reynaud, E. G., and Stelzer, E. H. K. (2007). The third dimension bridges the gap between cell culture and live tissue. *Nat. Rev. Mol. Cell Biol.* 8 (10), 839–845. doi:10.1038/nrm2236
- Petersen, O. W., Ronnov-Jessen, L., Howlett, A. R., and Bissell, M. J. (1992). Interaction with basement membrane serves to rapidly distinguish growth and differentiation pattern of normal and malignant human breast epithelial cells. *Proc. Natl. Acad. Sci. U. S. A.* 89 (19), 9064–9068. doi:10.1073/pnas.89.19.9064
- Phinney, D. G. (2009). A Sage view of mesenchymal stem cells. *Int. J. Stem Cells* 2 (1), 1–10. doi:10.15283/ijsc.2009.2.1.1
- Phinney, D. G. (2007). Biochemical heterogeneity of mesenchymal stem cell populations: Clues to their therapeutic efficacy. *Cell Cycle* 6 (23), 2884–2889. doi:10.4161/cc.6.23.5095
- Phinney, D. G., Hill, K., Michelson, C., DuTreil, M., Hughes, C., Humphries, S., et al. (2006). Biological activities encoded by the murine mesenchymal stem cell transcriptome provide a basis for their developmental potential and broad therapeutic efficacy. *Stem Cells* 24 (1), 186–198. doi:10.1634/stemcells.2004-0236
- Piccolo, S., Dupont, S., and Cordenonsi, M. (2014). The biology of YAP/TAZ: Hippo signaling and beyond. *Physiol. Rev.* 94 (4), 1287–1312. doi:10.1152/physrev.00005.2014
- Pittenger, M. F., Discher, D. E., Péault, B. M., Phinney, D. G., Hare, J. M., and Caplan, A. I. (2019). Mesenchymal stem cell perspective: cell biology to clinical progress. *Npj Regen. Med.* 4 (1), 22. doi:10.1038/s41536-019-0083-6
- Qin, E. C., Ahmed, S. T., Sehgal, P., Vu, V. H., Kong, H., and Leckband, D. E. (2020). Comparative effects of N-cadherin protein and peptide fragments on mesenchymal stem cell mechanotransduction and paracrine function. *Biomaterials* 239, 119846. doi:10.1016/j.biomaterials.2020.119846
- Raimondi, M. T., Eaton, S. M., Laganà, M., Aprile, V., Nava, M. M., Cerullo, G., et al. (2013). Three-dimensional structural niches engineered via two-photon laser polymerization promote stem cell homing. *Acta Biomater.* 9 (1), 4579–4584. doi:10.1016/j.actbio.2012.08.022
- Raimondi, M. T., Eaton, S. M., Nava, M. M., Laganà, M., Cerullo, G., and Osellame, R. (2012). Two-photon laser polymerization: From fundamentals to biomedical application in tissue engineering and regenerative medicine. *J. Appl. Biomater. Funct. Mater.* 10 (1), 56–66. doi:10.5301/jabfm.2012.9278
- Raimondi, M. T., Nava, M. M., Eaton, S. M., Bernasconi, A., Vishnubhatla, K. C., Cerullo, G., et al. (2014). Optimization of femtosecond laser polymerized structural niches to control mesenchymal stromal cell fate in culture. *Micromachines* 2, 341–358. doi:10.3390/mi5020341
- Raudvere, U., Kolberg, L., Kuzmin, I., Arak, T., Adler, P., Peterson, H., et al. (2019). G:Profiler: A web server for functional enrichment analysis and conversions of gene lists (2019 update). *Nucleic Acids Res.* 47 (W1), W191–W198. doi:10.1093/nar/gkz369
- Reimand, J., Isserlin, R., Voisin, V., Kucera, M., Tannus-Lopes, C., Rostamianfar, A., et al. (2019). Pathway enrichment analysis and visualization of omics data using g:Profiler, GSEA, Cytoscape and EnrichmentMap. *Nat. Protoc.* 14 (2), 482–517. doi:10.1038/s41596-018-0103-9
- Remuzzi, A., Bonandrini, B., Tironi, M., Longaretti, L., Figliuzzi, M., Conti, S., et al. (2020). Effect of the 3D artificial nichoid on the morphology and mechanobiological response of mesenchymal stem cells cultured *in vitro*. *Cells* 9 (8), 1873. doi:10.3390/cells9081873
- Ren, G., Zhao, X., Zhang, L., Zhang, J., L'Huillier, A., Ling, W., et al. (2010). Inflammatory cytokine-induced intercellular adhesion molecule-1 and vascular cell adhesion molecule-1 in mesenchymal stem cells are critical for immunosuppression. *J. Immunol.* 184 (5), 2321–2328. doi:10.4049/jimmunol.0902023
- Ren, J., Jin, P., Sabatino, M., Balakumaran, A., Feng, J., Kuznetsov, S. A., et al. (2011). Global transcriptome analysis of human bone marrow stromal cells (BMSC) reveals proliferative, mobile and interactive cells that produce abundant extracellular matrix proteins, some of which may affect BMSC potency. *Cytotherapy* 13 (6), 661–674. doi:10.3109/14653249.2010.548379
- Rey, F., Pandini, C., Barzaghini, B., Messa, L., Giallongo, T., Pansarasa, O., et al. (2020). Dissecting the effect of a 3D micro scaffold on the transcriptome of neural stem cells with computational approaches: A focus on mechanotransduction. *Int. J. Mol. Sci.* 21 (18), 6775–6837. doi:10.3390/ijms21186775
- Ricci, D., Nava, M. M., Zandri, T., Cerullo, G., Raimondi, M. T., and Osellame, R. (2017). Scaling-up techniques for the nanofabrication of cell culture substrates via two-photon polymerization for industrial-scale expansion of stem cells. *Materials* 10, 66. doi:10.3390/ma10010066
- Rio, D. C., Ares, M., Hannon, G. J., and Nilsen, T. W. (2010). Purification of RNA using TRIzol (TRI reagent). *Cold Spring Harb. Protoc.* 5 (6), pdb.prot5439–4. doi:10.1101/pdb.prot5439
- Roson-Burgo, B., Sanchez-Guijo, F., Del Cañizo, C., and De Las Rivas, J. (2016). Insights into the human mesenchymal stromal/stem cell identity through integrative transcriptomic profiling. *BMC Genomics* 17 (1), 944–1027. doi:10.1186/s12864-016-3230-0
- Saei Arezoumand, K., Alizadeh, E., Pilehvar-Soltanahmadi, Y., Esmaeilou, M., and Zarghami, N. (2017). An overview on different strategies for the stemness maintenance of MSCs. *Artif. Cells, Nanomedicine Biotechnol.* 45 (7), 1255–1271. doi:10.1080/21691401.2016.1246452
- Saidova, A. A., and Vorobjev, I. A. (2020). Lineage commitment, signaling pathways, and the cytoskeleton systems in mesenchymal stem cells. *Tissue Eng. - Part B Rev.* 26 (1), 13–25. doi:10.1089/ten.teb.2019.0250
- Sánchez-Luis, E., Joaquín-García, A., Campos-Laborie, F. J., Sánchez-Guijo, F., and De las Rivas, J. (2020). Deciphering master gene regulators and associated networks of human mesenchymal stromal cells. *Biomolecules* 10 (4), 557–617. doi:10.3390/biom10040557
- Santos, E., Hernández, R. M., Pedraz, J. L., and Orive, G. (2012). Novel advances in the design of three-dimensional bio-scaffolds to control cell fate: Translation from 2D to 3D. *Trends Biotechnol.* 30 (6), 331–341. doi:10.1016/j.tibtech.2012.03.005
- Schindelin, J., Arganda-Carreras, I., Frise, E., Kaynig, V., Longair, M., Pietzsch, T., et al. (2012). Fiji: An open-source platform for biological-image analysis. *Nat. Methods* 9 (7), 676–682. doi:10.1038/nmeth.2019
- Shamir, E. R., and Ewald, A. J. (2014). Three-dimensional organotypic culture: Experimental models of mammalian biology and disease. *Nat. Rev. Mol. Cell Biol.* 15 (10), 647–664. doi:10.1038/nrm3873
- Shannon, P., Markiel, A., Ozier, O., Baliga, N. S., Wang, J. T., Ramage, D., et al. (2003). Cytoscape: A software environment for integrated models of biomolecular interaction networks. *Genome Res.* 13 (2498), 2498–2504. doi:10.1101/gr.1239303
- Shi, Y., Xia, Y. Y., Wang, L., Liu, R., Khoo, K. S., and Feng, Z. W. (2012). Neural cell adhesion molecule modulates mesenchymal stromal cell migration via activation of MAPK/ERK signaling. *Exp. Cell Res.* 318 (17), 2257–2267. doi:10.1016/j.yexcr.2012.05.029
- Song, N., Scholtemeijer, M., and Shah, K. (2020). Mesenchymal stem cell immunomodulation: Mechanisms and therapeutic potential. *Trends Pharmacol. Sci.* 41 (9), 653–664. doi:10.1016/j.tips.2020.06.009
- Subramanian, A., Tamayo, P., Mootha, V. K., Mukherjee, S., Ebert, B. L., Gillette, M. A., et al. (2005). Gene set enrichment analysis: A knowledge-based approach for interpreting genome-wide expression profiles. *Proc. Natl. Acad. Sci. U. S. A.* 102 (43), 15545–15550. doi:10.1073/pnas.0506580102
- Suzuki, T., Morikawa, J., Hashimoto, T., Buividas, R., Gervinskaskas, G., Paipulas, D., et al. (2012). Thermal and optical properties of sol-gel and SU-8 resists. *Proc. SPIE - Int. Soc. Opt. Eng.* 8249, 1–9. doi:10.1117/12.907028
- von der Mark, K., Gauss, V., von der Mark, H., and Müller, P. (1977). Relationship between cell shape and type of collagen synthesised as chondrocytes lose their cartilage phenotype in culture. *Nature* 267, 531. doi:10.1038/267531a0
- Vukovic, J., Ruitenbergh, M. J., Roet, K., Franssen, E., Arulpragasam, A., Sasaki, T., et al. (2009). The glycoprotein fibulin-3 regulates morphology and motility of olfactory ensheathing cells *in vitro*. *Glia* 57 (4), 424–443. doi:10.1002/glia.20771
- Walker, M., Patel, K., and Stappenbeck, T. (2008). The stem cell niche. *J. Pathology*, 231–241. doi:10.1002/path
- Wan, L. Q., Kang, S. M., Eng, G., Grayson, W. L., Lu, X. L., Huo, B., et al. (2010). Geometric control of human stem cell morphology and differentiation. *Integr. Biol.* 2 (7–8), 346–353. doi:10.1039/c0ib00016g
- Weil, Q., Nakahara, F., Asada, N., Zhang, D., Gao, X., Xu, C., et al. (2020). Snai2 maintains bone marrow niche cells by repressing osteopontin expression. *Dev. Cell* 53 (5), 503–513. doi:10.1016/j.devcel.2020.04.012
- Weiss, A. R. R., and Dahlke, M. H. (2019). Immunomodulation by mesenchymal stem cells (MSCs): Mechanisms of action of living, apoptotic, and dead MSCs. *Front. Immunol.* 10, 1191–1210. doi:10.3389/fimmu.2019.01191
- Winer, J. P., Janmey, P. A., McCormick, M. E., and Funaki, M. (2009). Bone marrow-derived human mesenchymal stem cells become quiescent on soft substrates but remain responsive to chemical or mechanical stimuli. *Tissue Eng. - Part A* 15 (1), 147–154. doi:10.1089/ten.tea.2007.0388
- Wu, S., Serbin, J., and Gu, M. (2006). Two-photon polymerisation for three-dimensional micro-fabrication. *J. Photochem. Photobiol. A Chem.* 181 (1), 1–11. doi:10.1016/j.jphotochem.2006.03.004
- Wuchter, P., Boda-Heggemann, J., Straub, B. K., Grund, C., Kuhn, C., Krause, U., et al. (2007). Processus and recessus adhaerentes: Giant adherens cell junction systems connect and attract human mesenchymal stem cells. *Cell Tissue Res.* 328 (3), 499–514. doi:10.1007/s00441-007-0379-5



Xie, A. W., Zacharias, N. A., Binder, B. Y. K., and Murphy, W. L. (2021). Controlled aggregation enhances immunomodulatory potential of mesenchymal stromal cell aggregates. *Stem Cells Transl. Med.* 10 (8), 1184–1201. doi:10.1002/sctm.19-0414

Ylostalo, J. ., Bartsoh, T. ., Toblow, A., and Prockop, D. (2014). Unique characteristics of human mesenchymal stromal/progenitor cells pre-activated in 3-dimensional cultures under different conditions. *Cytotherapy* 16 (11), 1486–1500. doi:10.1016/j.jcyt.2014.07.010

Zandrini, T., Shan, O., Parodi, V., Cerullo, G., Raimondi, M. T., and Osellame, R. (2019). Multi-foci laser microfabrication of 3D polymeric scaffolds for stem cell expansion in regenerative medicine. *Sci. Rep.* 9, 11761–11769. doi:10.1038/s41598-019-48080-w

Zhang, C., Zhu, H., Ren, X., Gao, B., Cheng, B., Liu, S., et al. (2021). Mechanics-driven nuclear localization of YAP can be reversed by N-cadherin ligation in mesenchymal stem cells. *Nat. Commun.* 12 (1), 6229. doi:10.1038/s41467-021-26454-x

Zhao, Q., Ren, H., and Han, Z. (2016). Mesenchymal stem cells: Immunomodulatory capability and clinical potential in immune diseases. *J. Cell. Immunother.* 2 (1), 3–20. doi:10.1016/j.jocit.2014.12.001

Zoja, C., Garcia, P. B., Rota, C., Conti, S., Gagliardini, E., Corna, D., et al. (2012). Mesenchymal stem cell therapy promotes renal repair by limiting glomerular podocyte and progenitor cell dysfunction in adriamycin-induced nephropathy. *Am. J. Physiology - Ren. Physiology* 303 (9), 1370–1381. doi:10.1152/ajprenal.00057.2012



## OPEN ACCESS

EDITED BY  
Gianni Ciofani,  
Italian Institute of Technology (IIT), Italy

REVIEWED BY  
Wei Seong Toh,  
National University of Singapore,  
Singapore  
Muhammad Nawaz,  
University of Gothenburg, Sweden

\*CORRESPONDENCE  
Markus Thomas Rojewski,  
✉ markus.rojewski@uni-ulm.de

SPECIALTY SECTION  
This article was submitted to  
Nanobiotechnology,  
a section of the journal  
Frontiers in Bioengineering and  
Biotechnology

RECEIVED 24 November 2022  
ACCEPTED 09 January 2023  
PUBLISHED 24 January 2023

CITATION  
Jakl V, Ehmele M, Winkelmann M,  
Ehrenberg S, Eiseler T, Friemert B,  
Rojewski MT and Schrezenmeier H (2023),  
A novel approach for large-scale  
manufacturing of small extracellular  
vesicles from bone marrow-derived  
mesenchymal stromal cells using a hollow  
fiber bioreactor.  
*Front. Bioeng. Biotechnol.* 11:1107055.  
doi: 10.3389/fbioe.2023.1107055

COPYRIGHT  
© 2023 Jakl, Ehmele, Winkelmann,  
Ehrenberg, Eiseler, Friemert, Rojewski and  
Schrezenmeier. This is an open-access  
article distributed under the terms of the  
Creative Commons Attribution License  
(CC BY). The use, distribution or  
reproduction in other forums is permitted,  
provided the original author(s) and the  
copyright owner(s) are credited and that  
the original publication in this journal is  
cited, in accordance with accepted  
academic practice. No use, distribution or  
reproduction is permitted which does not  
comply with these terms.

# A novel approach for large-scale manufacturing of small extracellular vesicles from bone marrow-derived mesenchymal stromal cells using a hollow fiber bioreactor

Viktoria Jakl<sup>1</sup>, Melanie Ehmele<sup>2</sup>, Martina Winkelmann<sup>1</sup>,  
Simon Ehrenberg<sup>1</sup>, Tim Eiseler<sup>3</sup>, Benedikt Friemert<sup>4</sup>,  
Markus Thomas Rojewski<sup>1,2\*</sup> and Hubert Schrezenmeier<sup>1,2</sup>

<sup>1</sup>Institute for Transfusion Medicine, University Hospital Ulm, Ulm, Germany, <sup>2</sup>Institute for Clinical Transfusion Medicine and Immunogenetics Ulm, German Red Cross Blood Donation Service Baden-Württemberg—Hessia and University Hospital Ulm, Ulm, Germany, <sup>3</sup>Clinic of Internal Medicine I, University Hospital Ulm, Ulm, Germany, <sup>4</sup>Clinic for Trauma Surgery and Orthopedics, Army Hospital Ulm, Ulm, Germany

Mesenchymal stromal cells (MSCs) are promising therapeutic candidates in a variety of diseases due to having immunomodulatory and pro-regenerative properties. In recent years, MSC-derived small extracellular vesicles (sEVs) have attracted increasing interest as a possible alternative to conventional cell therapy. However, translational processes of sEVs for clinical applications are still impeded by inconsistencies regarding isolation procedures and culture conditions. We systematically compared different methods for sEV isolation from conditioned media of *ex vivo* expanded bone marrow-derived MSCs and demonstrated considerable variability of quantity, purity, and characteristics of sEV preparations obtained by these methods. The combination of cross flow filtration with ultracentrifugation for sEV isolation resulted in sEVs with similar properties as compared to isolation by differential centrifugation combined with ultracentrifugation, the latter is still considered as gold standard for sEV isolation. In contrast, sEV isolation by a combination of precipitation with polyethylene glycol and ultracentrifugation as well as cross flow filtration and size exclusion chromatography resulted in sEVs with different characteristics, as shown by surface antigen expression patterns. The MSC culture requires a growth-promoting supplement, such as platelet lysate, which contains sEVs itself. We demonstrated that MSC culture with EV-depleted platelet lysate does not alter MSC characteristics, and conditioned media of such MSC cultures provide sEV preparations enriched for MSC-derived sEVs. The results from the systematic stepwise evaluation of various aspects were combined with culture of MSCs in a hollow fiber bioreactor. This resulted in a strategy using cross flow filtration with subsequent ultracentrifugation for sEV isolation. In conclusion, this workflow provides a semi-automated, efficient, large-scale-applicable, and good manufacturing practice (GMP)-grade approach for the generation of sEVs for clinical use. The use of EV-depleted platelet lysate is an option to further increase the purity of MSC-derived sEVs.

## KEYWORDS

mesenchymal stromal cells, mesenchymal stem cells, platelet lysate, hollow fiber bioreactor, exosomes, small extracellular vesicles, isolation

## Introduction

Within the last decades, the interest in mesenchymal stromal/stem cells (MSCs) increased continuously due to their regenerative and immunomodulatory potential. MSCs were first identified by Friedenstein et al. in 1976 as fibroblast precursors (Friedenstein et al., 1976). Since then, a lot of research was performed, and in 2006, the International Society for Cellular Therapy (ISCT) proposed minimal criteria for the definition of MSCs (Dominici et al., 2006). These included plastic adherence of MSCs when being cultured under standard culture conditions, expression of surface antigens cluster of differentiation (CD) 73, CD90, and CD105, and lack of expression of common leukocyte and hematopoietic cell markers (e.g., CD45, CD34, CD14, CD11b, CD79a, or CD19 and histocompatibility leukocyte antigen (HLA) DR) and differentiation capacity into cells of the three mesenchymal lineages (adipocytes, chondrocytes, and osteoblasts) (Dominici et al., 2006). MSCs can be found in numerous tissues of the human body such as bone marrow (BM), adipose tissue, umbilical cord, or dental pulp.

The therapeutic potential of BM-derived MSCs has been shown in a variety of clinical applications like in bone regeneration (Soler et al., 2016; Gjerde et al., 2018; Gomez-Barrena et al., 2019; Gomez-Barrena et al., 2020; Gomez-Barrena et al., 2021) or wound healing (Falanga et al., 2007; Lataillade et al., 2007; Yoshikawa et al., 2008; Dash et al., 2009; Lu et al., 2011), and today, more than 1,200 clinical trials investigating MSC therapy are listed at [clinicaltrials.gov](https://clinicaltrials.gov) (for search term “mesenchymal stromal cells” or “mesenchymal stem cells,” retrieved 11/22/2022). The application of MSCs to humans as an advanced therapy medicinal product (ATMP) has been proven to be safe. However, there are concerns regarding genetic stability (Pan et al., 2014; Stultz et al., 2016), replicative senescence (Wagner et al., 2008), and promotion of tumor proliferation (Pavon et al., 2018) when using *ex vivo* expanded MSCs. Therefore, in recent years, MSC-derived factors such as extracellular vesicles (EVs) became increasingly popular as therapeutic effectors. EVs are membrane-surrounded particles that are secreted by various cell types and are important drivers of intercellular communication by exchanging their cargo (e.g., nucleic acids, lipids, and proteins), thereby modulating different molecular events in the recipient cells. EVs can be subdivided into three main groups, apoptotic bodies (which arise from dying cells during apoptosis), microvesicles, and exosomes. While microvesicles directly bud from the plasma membrane and can be up to 1,000 nm in size, exosomes are released into the extracellular space from intracellular multivesicular bodies and range from 40 to 100 nm in diameter (Raposo and Stoorvogel, 2013). As there are no unique markers for discrimination between different subsets of EVs, Théry et al. proposed the term of small extracellular vesicles (sEVs) for EVs with sizes smaller than 200 nm instead of referring them after their origin (e.g., exosomes) (Théry et al., 2018). As compared to classical cell therapy, sEVs show several advantages including their potential to cross biological barriers (e.g., blood–brain barrier) (Banks et al., 2020), ease of sterilization (e.g., by filtration) (Elsharkasy et al., 2020), and their non-viable nature (due to lack of a functional nucleus) (Théry et al., 2018). Studies directly comparing MSCs and MSC-derived mediators showed similar or even improved therapeutic effectiveness for the latter (Bruno et al., 2009; Shao et al., 2017).

Differential centrifugation (DC) with final enrichment of sEVs by ultracentrifugation (UC) still represents the most commonly used procedure for isolation of sEVs (Gardiner et al., 2016). However, being

labor-intensive and time-consuming, centrifugation-based strategies alone were assumed not to be suitable for large-scale purification of sEVs (Lener et al., 2015; Zeringer et al., 2015; Gurunathan et al., 2019; Witwer et al., 2019). Hence, multi-step approaches combining several methods for initial volume reduction and concentration followed by final sEV enrichment became increasingly popular (Gardiner et al., 2016). Ultrafiltration such as cross flow filtration (CFF) through membranes with different pore sizes or polymer-based methods such as precipitation with polyethylene glycol (PEG) can be applied for concentrating the volume of the starting material (Coumans et al., 2017), although precipitation has been shown to result in sEV preparations with reduced purity (Van Deun et al., 2014; Lobb et al., 2015). For final purification of sEVs, size exclusion chromatography (SEC) could be used besides UC. However, small input volumes for SEC columns limit their use for large-scale purification required for clinical applications (Busatto et al., 2018; Paganini et al., 2019).

Contamination with sEVs from sources other than MSCs can occur due to serum-containing cell culture supplements such as platelet lysate (PL) (Witwer et al., 2019; Almeria et al., 2022). Although sEVs from different sources can be discriminated by surface antigen expression such as lacking expression of CD81 on PL-derived sEVs (Koliha et al., 2016; Wiklander et al., 2018), downstream separation of contaminating sEVs would be difficult. Therefore, collecting sEVs during a starvation period with serum-free or EV-depleted cell culture supplements is commonly applied. Since changed sEV profiles appeared as a consequence of switching to serum-free culture media (Li et al., 2015; Haraszti et al., 2019), and PL-derived sEVs were found to be taken up by MSCs (Torreggiani et al., 2014), absence of PL-derived sEVs could impact characteristics of MSC sEVs due to suboptimal cell expansion conditions (Borger et al., 2020), and cellular stress (Wiest and Zubair, 2020; Almeria et al., 2022).

Adlerz et al. assumed conditioned media (CM) of about 500 million cells to be a requisite for sEV numbers necessary for clinical applications (Adlerz et al., 2020). Large amounts of starting material are hard to generate in conventional cell culture, hence, large-scale expansion methods such as hollow fiber bioreactors could help in resolving this problem by allowing large-scale expansion of MSCs (Rojewski et al., 2013) and the production of several liters of CM (Watson et al., 2016). The Quantum® Cell Expansion System from Terumo BCT (Quantum system) comprises a hollow fiber bioreactor attached to several tubings connected with bags for fluidics in- and output. Being a single use unit, the expansion set is loaded into an incubator with pumps, valves, gas inlet, and user interface allowing for semi-automated expansion of cells. The bioreactor itself is composed of approximately 11,000 hollow fibers providing a growth surface of up to 21,000 cm<sup>2</sup> after coating with proteins such as cryoprecipitate (CP) that enable attachment of cells.

The number of pre-clinical studies investigating sEVs as an MSC substitute increases continuously; however, only few of them have gone across experimental animal models toward a clinical application (36 studies listed at [clinicaltrials.gov](https://clinicaltrials.gov) for search term “mesenchymal stromal cells AND exosomes” or “mesenchymal stem cells AND exosomes” or “mesenchymal stromal cells AND extracellular vesicles” or “mesenchymal stem cells AND extracellular vesicles,” retrieved: 11/22/2022). This could be in part explained by a high burden in the translational process from laboratory-scale protocols toward large-scale manufacturing of clinical doses as standardized and

universal procedures have not been established yet. In addition, sEV characteristics change upon alteration of purification (e.g., isolation method) and culture strategies (e.g., growth media and expansion system), respectively (Lener et al., 2015; Doyle and Wang, 2019; Adlerz et al., 2020; Gowen et al., 2020; Wiest and Zubair, 2020). During this study, suitability of several sEV isolation methods were evaluated prior to an implementation of a hollow fiber bioreactor-based expansion process enabling the large-scale manufacturing of sEVs.

Here, we use this established tool box of various sEV isolation methods and perform a head-to-head comparison to gold standard method DC combined with UC using the starting material of same donors in order to exclude variability from MSC lines or their donors as a confounding factor. Furthermore, we combine the MSC expansion and generation of CM in a hollow fiber bioreactor with subsequent steps of sEV isolation in a novel workflow.

## Materials and methods

### Cell culture and collection of CM

#### Harvesting of primary material

Primary MSCs derived from BM aspirates (iliac crest) of healthy volunteer donors were used for the following experiments. Collection of the material has been approved by the Ethical Committee of the University of Ulm (Ulm, Germany) and informed consent was obtained from all donors. Aspiration was performed by following standard operating procedures to obtain a small-volume BM aspirate of approximately 25–35 mL. MSCs of passage 0 (P0) were obtained as previously described in detail (Rojewski et al., 2019). We used MSCs from up to 10 different donors. MSCs from different donors might also differ in the release of sEVs and their properties. Therefore, CM from the same MSC lines have been used for the experiments comparing different sEV isolation methods against gold standard purification by DC combined with UC (except for one of isolation method II) and different expansion systems for sEV generation. Thus, the comparisons reflect the impact of the different isolation methods and are not influenced by the potential variability among MSC donors.

#### Cell expansion for optimization of sEV isolation methods and collection strategies

MSCs were seeded at 2,000–4,000 cells/cm<sup>2</sup> in  $\alpha$ MEM supplemented with 8% PL (IKT Ulm, Ulm, Germany) and 1 i.U. per mL heparin (Ratiopharm GmbH, Ulm, Germany) ( $\alpha$ MEM+8% PL) and expanded for passage 1 (P1) or passage 2 (P2). After 24–96 h, the media was exchanged completely for subsequent collection of sEVs in CM. Collection was performed for 24–48 h using either  $\alpha$ MEM+8% PL or  $\alpha$ MEM+8% EV-depleted PL (EV depl. PL). The cells were harvested using TrypZean™ (Lonza Group Ltd., Basel, Switzerland), and the cell count was determined with a Neubauer chamber (Glaswarenfabrik Karl Hecht GmbH & Co., KG, Sondheim vor der Rhön, Germany). Dead cells were identified by trypan blue staining (Sigma-Aldrich Chemie GmbH, Taufkirchen, Germany), and viability of cells was given by the ratio of living cell count and total cell count. CM was harvested and stored at –80°C until isolation of sEVs.

PL was manufactured as previously described (Fekete et al., 2012a). For the generation of EV depl. PL, PL was ultracentrifuged for 3 h at 120,000  $\times$  g at 4°C (Optima™ LE-80K with SW 28 Ti Swinging-Bucket Aluminum Rotor; Beckman Coulter GmbH, Krefeld,

Germany), and the supernatant was subsequently sterile filtered through Sartolab® RF vacuum filtration units (Sartorius Lab Instruments GmbH & Co., KG, Göttingen, Germany).

#### Cell expansion for the implementation of a hollow fiber bioreactor

The Quantum® Cell Expansion System (Terumo BCT, Inc., Lakewood, United States) was used for large-scale expansion of MSCs. A two-step expansion process was performed, where MSCs were isolated from BM in a first run (resulting in P0 MSCs; data not shown) followed by a second run, where MSCs were expanded for P1 and sEVs were collected at the end of the run. Briefly, harvested P0 MSCs were stored at room temperature (RT) for approximately 6 h until the preparation of the Quantum system for the next run was completed. This included loading of the single use cell expansion set, priming with phosphate-buffered saline (PBS; Lonza Group Ltd.), coating with CP for 4 h and conditioning of media ( $\alpha$ MEM+8% PL) for 1 h. CP was manufactured from fresh frozen plasma (FFP; IKT Ulm) as follows. FFP of 16 different donors (about 300 mL per donor) was thawed at 4°C overnight, pooled, and centrifuged at 4,777  $\times$  g for 10 min at RT. Supernatant was discarded, 0.1 mL PBS was added per mL FFP and carefully mixed. After incubation for 1 h at RT, resulting CP stock solution was divided into 7.5-mL aliquots and stored at –20°C. For preparation of CP as coating solution, one aliquot of CP stock solution was thawed at RT and filled up with PBS to a total volume of 100 mL. MSCs were seeded into the bioreactor at 1,000 cells/cm<sup>2</sup> and were allowed to attach for 24 h. The media was fed continuously, and the flow rate was adapted according to daily measured lactate concentrations in CM ranging from 0.1 mL/min at the beginning of the run to a maximum of 1.6 mL/min. A new waste bag was connected to the Quantum system 16–19 h prior to the end of the run. CM was collected during this time in addition to a complete system flush directly before cell harvest, resulting in total CM volumes of 700–2,000 mL. Duration of Quantum-based cell expansion varied from 6–9 days.

MSCs obtained from the same donor as for the Quantum system were in parallel isolated (P0; data not shown) and expanded for P1 in a conventional cell culture process in CellSTACK® Culture Chambers (CellSTACK; Corning Incorporated, New York, United States) with a surface area of 1,272 cm<sup>2</sup> as previously described (Fekete et al., 2012b; Rojewski et al., 2019). Briefly, the cells were seeded at 4,000 cells/cm<sup>2</sup> in  $\alpha$ MEM+8% PL and grown for 4–6 days. The media was exchanged completely 24–48 h prior to harvesting of cells, and sEVs were collected in CM.

CM was stored at –80°C until isolation of sEVs for both expansion systems, and the cells were harvested using TrypZean™ (Lonza Group Ltd.). Cell count and viability were determined by trypan blue staining using a Neubauer chamber as described previously.

## Characterization of MSCs

### Flow cytometric characterization of MSCs

The surface antigen expression of MSCs was identified by flow cytometry using the following antibodies: CD14 (clone HCD14; BioLegend, San Diego, United States or clone M $\phi$ P9; BD Biosciences, New Jersey, United States), CD34 (clone 8G12 also known as HPCA2), CD45 (clone HI30), CD73 (clone AD2), CD90 (clone 5E10), CD105 (clone 266), and HLA DRDPDQ (clone

Tu39 also known as TŮ39) (all from BD Biosciences). The cells were stained as per manufacturer's instructions (for staining details see [Supplementary Table S1](#)) and fluorescence intensities were measured using the FACSCelesta™ Cell Analyzer with BD FACSDiva™ software (BD Biosciences). Surface antigens were subdivided into identity markers (CD73, CD90, and CD105) and purity markers (CD14, CD34, CD45, and HLA DRDPDQ).

## Differentiation assays

MSCs were differentiated into cells of adipogenic, chondrogenic, and osteogenic lineages by using differentiation assay kits (human mesenchymal stem cell (hMSC), Adipogenic Differentiation Medium BulletKit™ (Lonza Group Ltd.), and StemMACS™ ChondroDiff Media, human and StemMACS™ OsteoDiff Media, human (both from Miltenyi Biotec B.V. & Co., KG, Bergisch Gladbach, Germany)), as per the manufacturer's instructions. Briefly, the cells were seeded at  $4.5\text{--}20 \times 10^6$  cells/cm<sup>2</sup>, and the media were exchanged every 2–3 days until differentiation of cells was completed. For chondrogenic differentiation, three-dimensional (3D) pellet culture was replaced by a two-dimensional (2D) expansion of cells, as previously performed ([Rojewski et al., 2019](#)). The cells grown in  $\alpha$ MEM+20% fetal bovine serum (FBS; Biological Industries, Kibbutz Beit Haemek, Israel) were used as controls. The cells were stained by Oil Red O and hematoxylin (adipogenic differentiation; Sigma-Aldrich Chemie GmbH) and methylene blue (chondrogenic differentiation; Sigma-Aldrich Chemie GmbH), and alkaline phosphatase activity was visualized by the 5-bromo-4-chloro-3-indolylphosphate (BCIP)/nitroblue tetrazolium (NBT) substrate (osteogenic differentiation; Sigma-Aldrich Chemie GmbH), respectively. Microscopic pictures were taken using an inverted phase contrast microscope (BZ-X710; KEYENCE DEUTSCHLAND GmbH, Neu-Isenburg, Germany) with BZ-X Viewer software.

## Proliferation assay

Proliferation of cells was analyzed by using the CyQUANT™ Cell Proliferation Assay Kit (Thermo Fisher Scientific Inc., Waltham, United States) as per manufacturer's instructions. Briefly, 200 cells per well were seeded into a 96-well plate as triplicates ( $n = 3$ ) in  $\alpha$ MEM+8% PL. After 4 days, the media was exchanged to  $\alpha$ MEM without (w/o) additional supplement,  $\alpha$ MEM+8% PL and  $\alpha$ MEM+8% EV depl. PL, respectively, and the cells were grown for 24 h and 48 h. The cells were washed with PBS, and cell pellets were frozen at  $-80^\circ\text{C}$ . DNA of lysed cells was stained by CyQUANT™ GR dye, and fluorescence intensities were measured by a microplate reader POLARstar Omega (BMG LABTECH GmbH, Ortenberg, Germany), with Reader Control and MARS Data Analysis software.

## Isolation, quantification, and characterization of sEVs

### Isolation of sEVs

sEVs were isolated from CM using four different isolation procedures, as summarized in [Figure 1](#). For all isolation methods, CM was thawed at  $4^\circ\text{C}$  overnight. Protocol variant I was based on DC with a final sEV enrichment step by UC ([Leblanc et al., 2017](#)). First, cellular debris and larger particles were removed by centrifugation at  $2,000 \times g$  and  $10,000 \times g$ , respectively. Then, the supernatant was ultracentrifuged at  $100,000 \times g$  and the sEVs in the pellet were

resuspended in PBS and washed by an additional UC step. Protocol variant II was a two-step protocol consisting of initial volume reduction of the starting material by precipitation with PEG followed by final sEV enrichment by UC ([Ludwig et al., 2018](#)). Cellular debris and larger particles were removed by centrifugation at  $4,777 \times g$ . The supernatant was mixed with 75 mM NaCl and 10% PEG6000 (Sigma-Aldrich Chemie GmbH) and incubated overnight. Precipitated sEVs were centrifuged at  $1,500 \times g$  and resuspended in 0.9% NaCl (Fresenius Kabi Deutschland GmbH, Bad Homburg, Germany). The resuspension volume was set to one-sixth of the original volume of the starting material, thereby leading to volume reduction for the final sEV enrichment step by UC at  $110,000 \times g$ . Protocol variant III was modified after [Armacki et al. \(2020\)](#) and included CFF for volume reduction of the starting material and final sEV purification by SEC. Briefly, cellular debris and larger particles were excluded by centrifugation at  $1,500 \times g$  followed by CFF using the Vivaflow 50 filter device (Sartorius Lab Instruments GmbH & Co., KG), with a pore size of  $0.2 \mu\text{m}$ . Then, the suspension was filtered again using the Vivaflow 50 filter device (Sartorius Lab Instruments GmbH & Co., KG), with a pore size of 100,000 molecular weight cut-off (MWCO) in order to remove smaller particles and to reduce the volume for final sEV purification by the Exo-spin Exosome Purification kit (Cell Guidance Systems Ltd., Cambridge, United Kingdom). This procedure included an overnight incubation with Exo-spin™ buffer, centrifugation at  $16,000 \times g$  and SEC with Exo-spin™ columns. Protocol variant IV was a combined approach of protocol variant I and III, whereby CFF was utilized for initial volume reduction and final sEV enrichment was achieved by UC. The isolated sEVs were resuspended in 50–100  $\mu\text{L}$  PBS (protocol variant I, III, and IV) or 0.9% NaCl (protocol variant II), respectively, and stored at  $-80^\circ\text{C}$ .

### Quantification of sEVs

Protein concentration of sEV suspensions was determined by bicinchoninic acid (BCA) assay using the Pierce™ BCA Protein Assay Kit (Thermo Fisher Scientific Inc.), as per manufacturer's instructions. Absorbance at 562 nm was measured using a microplate reader POLARstar Omega (BMG LABTECH GmbH) with Reader Control and MARS Data Analysis software. Nanoparticle tracking analysis (NTA) was performed for the determination of particle concentration and size distribution of sEV suspensions. Analysis was carried out by NANOSIGHT NS300 (Malvern Instruments Limited, Malvern, United Kingdom) with NTA 3.4 Build software. For comparison of sEV isolation efficiency of methods I–IV, measured protein and particle concentrations were normalized to volumes of CM used for isolation. Protein and particle concentrations per cell were obtained by normalization to number of harvested cells. Purity of sEV suspensions was assessed by particles to protein ratio, as suggested by [Webber and Clayton \(2013\)](#).

### Western blotting

The expression of different proteins by sEVs was verified by sodium dodecylsulfate polyacrylamide gel electrophoresis (SDS-PAGE) and western blotting using the Bolt™ Bis-Tris system with 2-(N-morpholino) ethanesulfonic acid (MES) buffer conditions (Thermo Fisher Scientific Inc.). Analyzed proteins were chosen according to Minimal Information for Studies of Extracellular Vesicles (MISEVs) 2018 criteria and included apolipoprotein A1



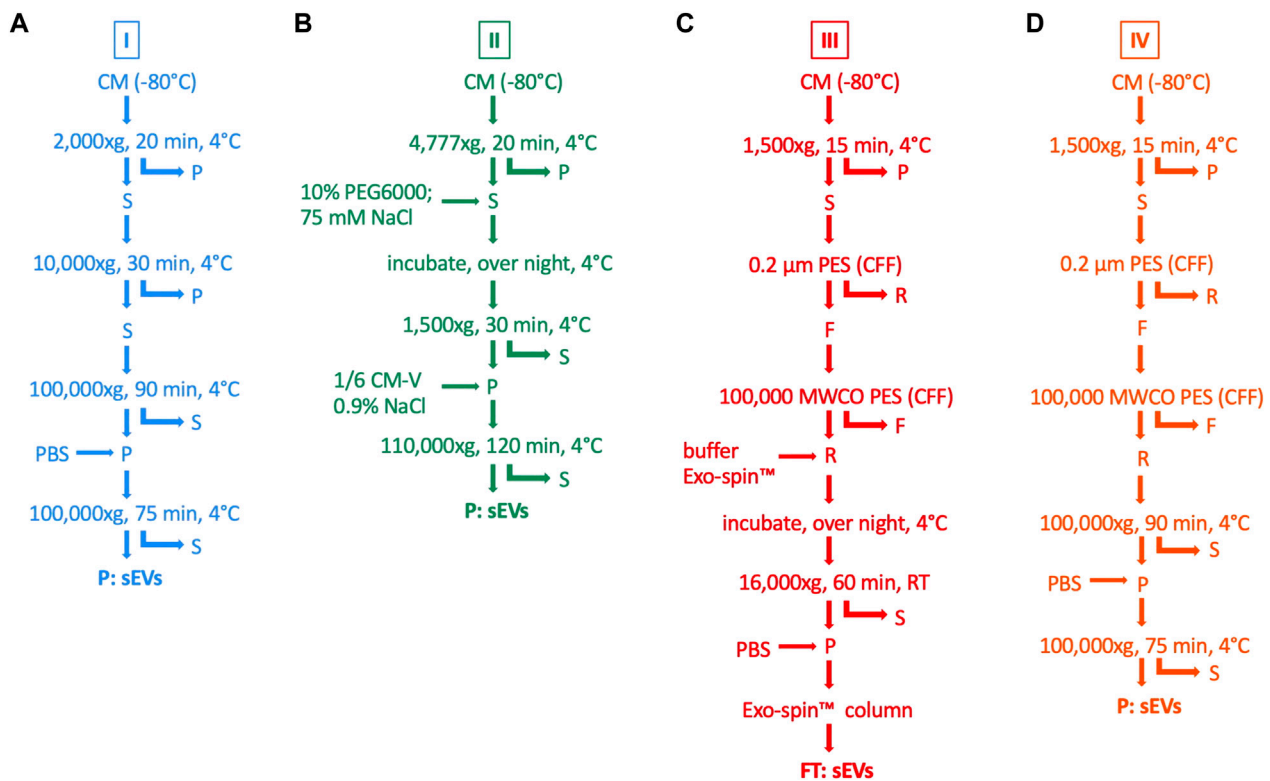


FIGURE 1

Methods for isolation of sEVs from MSC CM. sEVs were isolated from CM by four different isolation protocols (I–IV). **(A)** For protocol variant I (blue), CM was centrifuged at 2,000 × g and the pellet (P) was withdrawn. The supernatant (S) was centrifuged at 10,000 × g and the pellet was withdrawn again. These steps were performed for the removal of cellular debris and larger particles. The supernatant was centrifuged at 100,000 × g, the pellet was washed with PBS and centrifuged again in order to finally purify sEVs. **(B)** For protocol variant II (green), cellular debris and larger particles were removed by centrifugation with 4,777 × g followed by mixing the supernatant with 10% PEG6000 and 75 mM NaCl. After incubation overnight at 4°C, precipitated sEVs were centrifuged at 1,500 × g and resuspended in 0.9% NaCl, whereby the resuspension volume was defined as one-sixth of the initial volume of CM (CM-V). Finally, sEVs were enriched in the pellet after centrifugation with 110,000 × g. **(C)** For protocol variant III (red), centrifugation at 1,500 × g and CFF through a polyether sulfone (PES) filter membrane with a pore size of 0.2 µm was used for the elimination of cellular debris and larger particles in the pellet and retentate (R). Another CFF through a pore size of 100,000 MWCO was performed, thereby removing smaller particles in the filtrate (F) and reducing the volume for final sEV purification. The retentate was mixed with Exo-spin™ buffer, incubated over night at 4°C and centrifuged at 16,000 × g. The pellet was resuspended in PBS, and the sEVs were purified by SEC with Exo-spin™ columns. **(D)** For protocol variant IV (orange), steps for the removal of cellular debris and larger particles and volume reduction were the same as for protocol variant III. Finally, sEVs were enriched by UC at 100,000 × g for two times, including one washing step with PBS, as performed in protocol variant I.

(ApoA1), CD63, CD81, flotillin-1 (Flot-1), and glucose-regulated protein 94 (GRP94) (Thery et al., 2018). β-actin was used as loading control. MSC cell lysate served as positive control for CD63, CD81, Flot-1, and GRP94. EV depl. PL was taken as positive control for ApoA1. PageRuler Plus Prestained Protein Ladder was used as a protein marker (Thermo Fisher Scientific Inc.). All steps were performed at RT unless stated otherwise. Briefly, proteins (5 µg for ApoA1, Flot-1, and GRP94 under reducing conditions; 10 µg for CD63 and CD81 under non-reducing conditions) were separated on a 12% polyacrylamide gel and subsequently blotted on a polyvinylidene fluoride (PVDF) membrane with a pore size of 0.2 µm. Reducing conditions were obtained by the addition of 10X Bolt™ Sample Reducing Agent (Thermo Fisher Scientific Inc.), containing 500 mM dithiothreitol (DTT). Membranes were blocked for 1 h in 5% milk (5% skimmed milk powder (J. M. Gabler-Saliter Milchwerk GmbH & Co., KG, Obergünzburg, Germany) in PBS with 0.1% Tween®20 (Sigma-Aldrich Chemie GmbH) (PBS-T)) and washed four times for 5 min in PBS-T. Primary antibodies were as follows: β-actin (clone AC-15;

Sigma-Aldrich Chemie GmbH), 1:2,000 in 2% bovine serum albumin (BSA) (2% BSA (Sigma-Aldrich Chemie GmbH) in PBS-T), ApoA1 (clone EP1368Y; Abcam, Cambridge, United Kingdom), 1:1,000 or 1:2,000 in 5% milk, CD63 (clone MX-49.129.5; Santa Cruz Biotechnology, Inc., Dallas, United States), 1:1,000 in 5% milk, CD81 (clone JS-81; BD Biosciences), 1:1,000 in 5% BSA; Flot-1 (clone D2V7J; Cell Signaling Technology, Danvers, United States), 1:1,000 in 5% milk; GRP94 (polyclonal; Thermo Fisher Scientific Inc.), 1:1,000 in 5% milk. Incubation with primary antibodies was performed overnight at 4°C. Then, membranes were washed four times for 5 min in PBS-T and incubated with secondary antibodies for 1 h (Peroxidase AffiniPure Goat Anti-Mouse IgG, light chain specific (mouse-LC) for β-actin and CD63; Peroxidase AffiniPure F(ab')<sub>2</sub> Fragment Donkey Anti-Mouse IgG (H + L) (mouse) for β-actin, CD63 and CD81; Peroxidase AffiniPure F(ab')<sub>2</sub> Fragment Donkey Anti-Rabbit IgG (H + L) (rabbit) for ApoA1, Flot-1, and GRP94; all from Jackson ImmunoResearch Europe Ltd., Ely, United Kingdom). The membranes were washed four times for 5 min in PBS-T, and chemiluminescent signals were detected using SuperSignal™ West

Pico PLUS Chemiluminescent Substrate (Thermo Fisher Scientific Inc.) and chemiluminescence detector Fusion FX (Vilber, Collégien, France) with Evolution-Capt software. Signals were quantified using Bio1D software.

### Transmission electron microscopy (TEM)

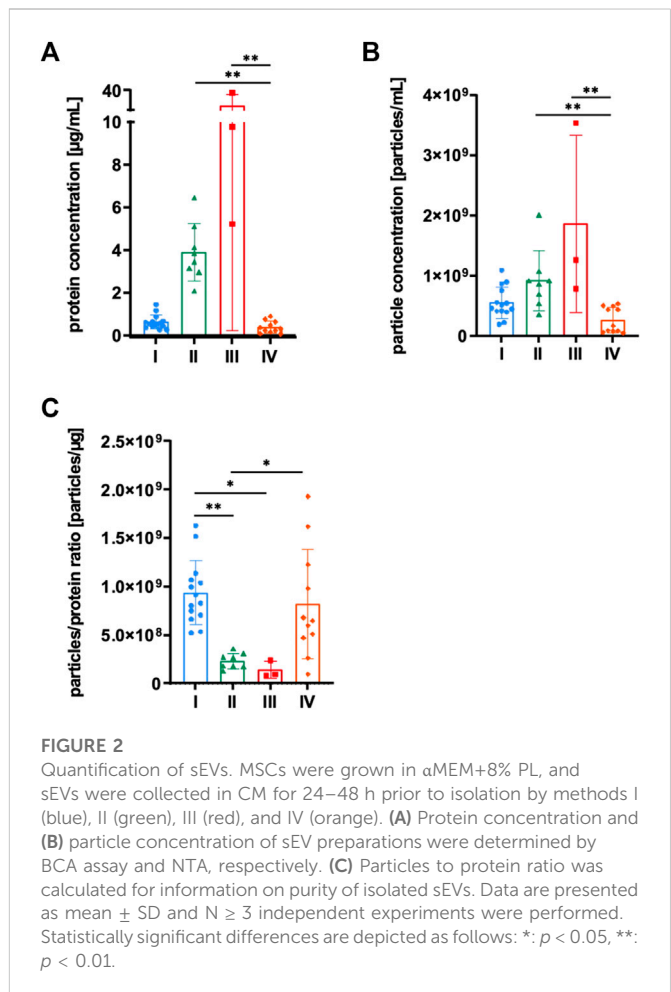
sEVs were visualized by the negative stain technique. Briefly, 10  $\mu$ L of sEV samples diluted with PBS were given on a glow discharged carbon-coated electron microscopy grid (Plano GmbH, Wetzlar, Germany) and incubated for 10 min at RT. Afterward, the grid was washed with three droplets of bi-distilled water prior to the addition of a drop of 2% uranyl acetate in water. Uranyl acetate was blotted with filter paper, and the samples were dried before they were observed in a transmission electron microscope JEM-1400Flash Electron Microscope (JEOL (Germany) GmbH, Freising, Germany) with iTEM software (Olympus Corporation, Tokyo, Japan) at 120 kV accelerating voltage and 60,000 times magnification.

### Magnetic bead-based flow cytometric analysis

Surface antigen expression by sEVs was analyzed using the MACSPlex Exosome Kit, human (Miltenyi Biotec B.V. & Co., KG), as per the manufacturer's instructions. Briefly, 5  $\mu$ g sEVs were incubated with MACSPlex Exosome Capture Beads against 39 different surface antigen epitopes overnight at RT with agitation. Surface antigens included CD9, CD63, CD81, CD105, CD49e, stage-specific embryonic antigen-4 (SSEA-4), melanoma chondroitin sulfate proteoglycan (MCSP), CD146, CD44, CD29, CD62P, CD41b, CD42a, CD40, CD31, HLA ABC, CD45, HLA DPDQDR, CD24, CD69, CD19, CD4, CD3, CD8, CD56, CD2, CD1c, CD25, receptor tyrosine kinase-like orphan receptor 1 (ROR1), CD209, CD11c, CD86, CD326, CD133/1, CD142, CD20, CD14, REA control, and mIgG1 control. Bound sEVs were detected indirectly by allophycocyanin (APC)-coupled MACSPlex Exosome Detection Reagent directed against the tetraspanins CD9, CD63, and CD81 prior to flow cytometric analysis. Gating on single beads, median fluorescence intensity (MFI) of each capture bead population was measured using a FACSCelesta™ Cell Analyzer with BD FACSDiva™ software (BD Biosciences). Expression of each surface antigen was observed by subtracting MFI of the blank (buffer only) from MFI of the respective capture bead population and normalizing on mean MFI of CD9, CD63, and CD81, resulting in tetraspanin-normalized expression. Due to this indirect detection method, no information can be obtained on expression density, rather providing information about general positivity for each surface antigen. Hence, higher tetraspanin-normalized expression values mean more sEVs being positive for this surface antigen at all (Wiklander et al., 2018).

### Statistics

Statistical analysis was performed with GraphPad PRISM software version 9.3.1 (Graphpad Software Inc., San Diego, United States). For all experiments at least three independent experiments ( $N \geq 3$ ) were carried out, and data are presented as mean  $\pm$  standard deviation (SD). Data were tested for normal distribution using the Shapiro–Wilk test and for homogenous variance using the Brown–Forsythe test. Significant differences between groups were investigated as follows. Comparison of two

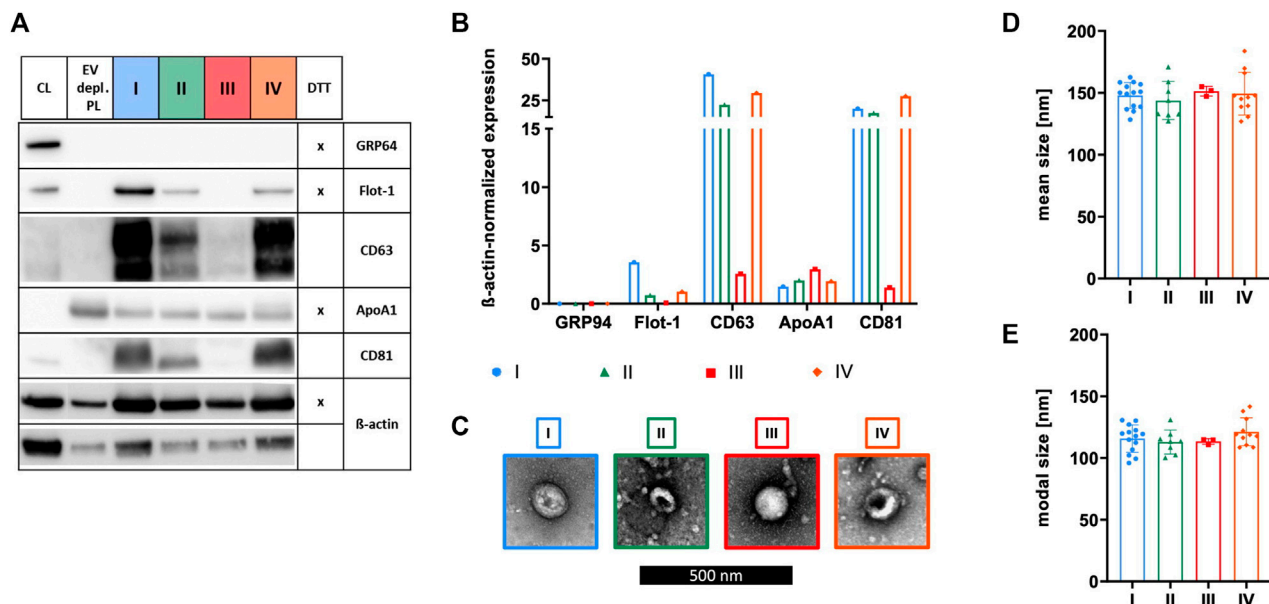


groups was carried out by unpaired t-test or Mann–Whitney test. For data of more than two groups, one-way analysis of variance (ANOVA) or Kruskal–Wallis test was performed. Dunnets and Dunn's correction were applied for multiple testing. Data with inhomogenous variance were tested by one-way ANOVA with Welch correction and Dunnett T3 method for multiple testing. For proliferation assays, significant differences between groups and time points were assessed by two-way ANOVA with Geisser–Greenhouse correction, and Tukey correction was applied for multiple testing.

## Results

### Isolation of sEVs by different methods results in divergent quantity and purity

MSCs were grown in  $\alpha$ MEM+8% PL, and sEVs were collected in CM for 24–48 h prior to isolation by methods I–IV (Figure 1). Then, sEVs were quantified by BCA assay and NTA. Significantly higher protein and particle concentrations were achieved by methods II and III, respectively (Figures 2A, B). However, purity of aforementioned sEV preparations was significantly reduced as indicated by significantly lower particles to protein ratio (Figure 2C). No significant differences were observed between methods I and IV (Figure 2).



## Characteristics of sEVs purified with different isolation methods vary

The identity of sEVs was proven by analyzing the existence of proteins according to the MISEV 2018 recommendation, including the presence of transmembrane/lipid-bound proteins (e.g., CD63 and CD81) or cytosolic proteins recovered in sEVs (e.g., Flot-1), and the absence of proteins of prominent contaminants co-isolated with sEVs (e.g., ApoA1) or proteins of intracellular compartments such as the Golgi apparatus (e.g., GRP94) (Thery et al., 2018). Expressions of Flot-1, CD63, and CD81 in addition to a lack of expression of GRP94 demonstrated isolation of sEVs by methods I, II, and IV. In contrast, method III failed in effectively isolating sEVs due to the absence of Flot-1 and CD81 and only marginal expression of CD63. Presence of co-isolated proteins for all isolation methods was indicated by ApoA1, being the lowest for sEVs isolated by method I (Figures 3A, B). TEM verified the existence of sEVs by microscopic images displaying enclosed particles in size range between approximately 100–200 nm (Figure 3C). More precise size ranges of sEVs were determined by NTA, where no significant differences in size distribution of sEVs isolated by methods I–IV were observed, as shown by similar mean and modal particle sizes (Figures 3D, E).

## Surface antigen expression of sEVs depends on the isolation method

The expression of several surface antigens by sEVs was analyzed using MACSplex technology. While significant differences between

sEVs isolated by methods I and IV were only observed for CD146, numerous significant differences were obtained when sEVs were purified with methods II and III (CD9, CD81, CD105, CD49e, SSEA-4, CD146, CD44, CD41b, CD42a, CD40, CD31, HLA ABC, CD45, HLA DRDPDQ, CD24, and CD69; Figure 4). Tetraspanin-normalized expression of surface markers tended to be the highest in sEVs isolated by protocol I (CD105, CD49e, SSEA-4, CD146, CD44, and CD42a) and protocol IV (CD81, HLA ABC, and HLA DRDPDQ) and the lowest in sEVs isolated by protocol III (CD81, CD105, CD49e, CD146, CD44, CD42a, CD40, CD31, HLA ABC, CD45, HLA DRDPDQ, and CD69). In contrast, the tetraspanin-normalized expressions of CD9 and CD41b were the highest for sEVs purified by method III. Analysis of additional surface antigens analyzed is presented in Supplementary Figure S1.

## Expansion of MSCs in EV-depleted PL does not negatively affect MSC characteristics

Due to the existence of PL-derived sEVs in  $\alpha$ MEM+8% PL, different collection strategies were exerted during MSC expansion in order to enrich for and verify the presence of MSC-derived sEVs. In addition to collecting sEVs during a starvation period in basal media  $\alpha$ MEM ( $\alpha$ MEM w/o) lacking any additional supplement, EV depletion of PL was examined as a suitable strategy for the removal of contaminating sEVs while still containing other growth promoting supplements. As a first step, proliferation of MSC in  $\alpha$ MEM+8% PL,  $\alpha$ MEM+8% EV depl. PL and  $\alpha$ MEM w/o was compared for 24 h and 48 h, respectively, to check for effects on MSC proliferation. Due to a

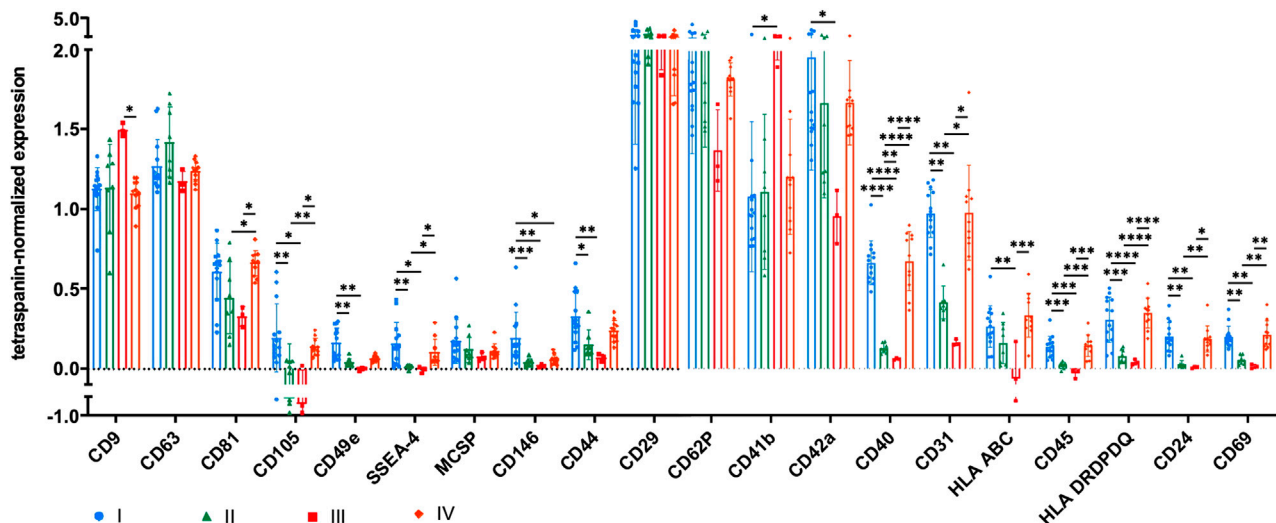


FIGURE 4

Tetraspanin-normalized surface antigen expression by sEVs. Surface antigen expression of sEVs isolated by methods I (blue), II (green), III (red) and IV (orange) was analyzed using MACSPlex technology. sEVs were bound by capture beads with epitopes against each analyzed surface antigen and detected indirectly by an APC-coupled detection reagent directed against the tetraspanins CD9, CD63, and CD81. Due to the indirect detection, fluorescence intensity of each surface antigen was normalized on mean fluorescence intensity of CD9, CD63, and CD81, resulting in tetraspanin-normalized expression. Data are presented as mean  $\pm$  SD, and  $N \geq 3$  independent experiments were performed. Statistically significant differences are depicted as follows: \* $p < 0.05$ , \*\* $p < 0.01$ , \*\*\* $p < 0.001$ , \*\*\*\* $p < 0.0001$ .

highly decreased proliferation rate of MSCs grown in  $\alpha$ MEM w/o, this medium was excluded from further analyses (Figure 5A). No negative impact of expansion in  $\alpha$ MEM+8% EV depl. PL was observed on the expression of identity and purity markers (Figures 5B, C), viability of cells (Figure 5D), and tri-lineage differentiation potential (Figure 5E) as compared to cells grown in  $\alpha$ MEM+8% PL.

## Different collection strategies allow for the generation of varying sEV compositions

In addition to collection media, elongation of collection time could also be beneficial for enriching MSC-derived sEVs. Therefore, collection for 48 h in  $\alpha$ MEM+8% EV depl. PL was investigated as strategy for exclusively generating MSC-derived sEVs. In order to confirm the effectiveness of this strategy, sEVs were isolated from the media  $\alpha$ MEM+8% PL and MSC CM collected for 24 h or 48 h in  $\alpha$ MEM+8% PL (Figure 6). After having tested different sEV isolation procedures during the first part of the study, only method IV was considered as suitable for sEV isolation from MSC CM besides gold standard method I due to consistent characteristics and purity.

## Expansion of MSCs in $\alpha$ MEM+8% EV depl. PL leads to enrichment of MSC-derived sEVs

The identity of sEVs was demonstrated for sEV preparations from the media  $\alpha$ MEM+8% PL and MSC CM collected for 24 h or 48 h in  $\alpha$ MEM+8% PL or  $\alpha$ MEM+8% EV depl. PL, as shown by the protein expression of Flot-1 and CD63 and lack of expression of GRP94. Being absent in sEVs from the media, CD81 increased with collection time and showed the highest expression for sEVs from EV depl. PL

conditions, providing evidence for effective enrichment of MSC-derived sEVs. Similar amounts of co-isolated proteins were found in all sEV preparations indicated by the presence of ApoA1 (Figures 7A, B). TEM further verified sEV identity with microscopic pictures, displaying membrane-surrounded particles for all preparations (Figure 7C). Regarding size distribution of sEVs determined by NTA, the mean and modal particle sizes of sEVs from  $\alpha$ MEM+8% EV depl. PL cultures (groups 4 and 8 in Figures 7D, E) were higher than those of both, sEVs from media (groups 1 and 5 in Figures 7D, E) and sEVs from  $\alpha$ MEM+8% PL cultures (groups 2, 3, 6, and 7 in Figures 7D, E). This provided evidence for differences in size for PL- and MSC-derived sEVs being larger for the latter.

## sEVs collected by different strategies differ in surface antigen expression

Surface antigen expression of sEVs derived from media  $\alpha$ MEM+8% PL and MSC CM collected with different strategies was analyzed. Positivity for several MSC surface antigens was significantly increased for sEVs isolated from CM, and the highest positivity was obtained for those from  $\alpha$ MEM+8% EV depl. PL cultures. These included, e.g., CD81, CD105, SSEA-4, MCSP, CD146, and CD44 (Figures 8A, B). In contrast, significantly less sEVs from  $\alpha$ MEM+8% EV depl. PL cultures were positive for the surface antigens CD63, CD29, CD62P, CD42a, CD40, CD31, HLA DRDPDQ, and CD24 in comparison to those from media (Figures 8A, B). Significant differences were also observed between CM sEVs, both collected for 48 h but with different supplements. In comparison to sEVs from  $\alpha$ MEM+8% EV depl. PL cultures, significantly more sEVs from  $\alpha$ MEM+8% PL cultures were positive for CD62P, CD40, CD31, and CD69 (Figures 8A, B). Analysis of additional surface



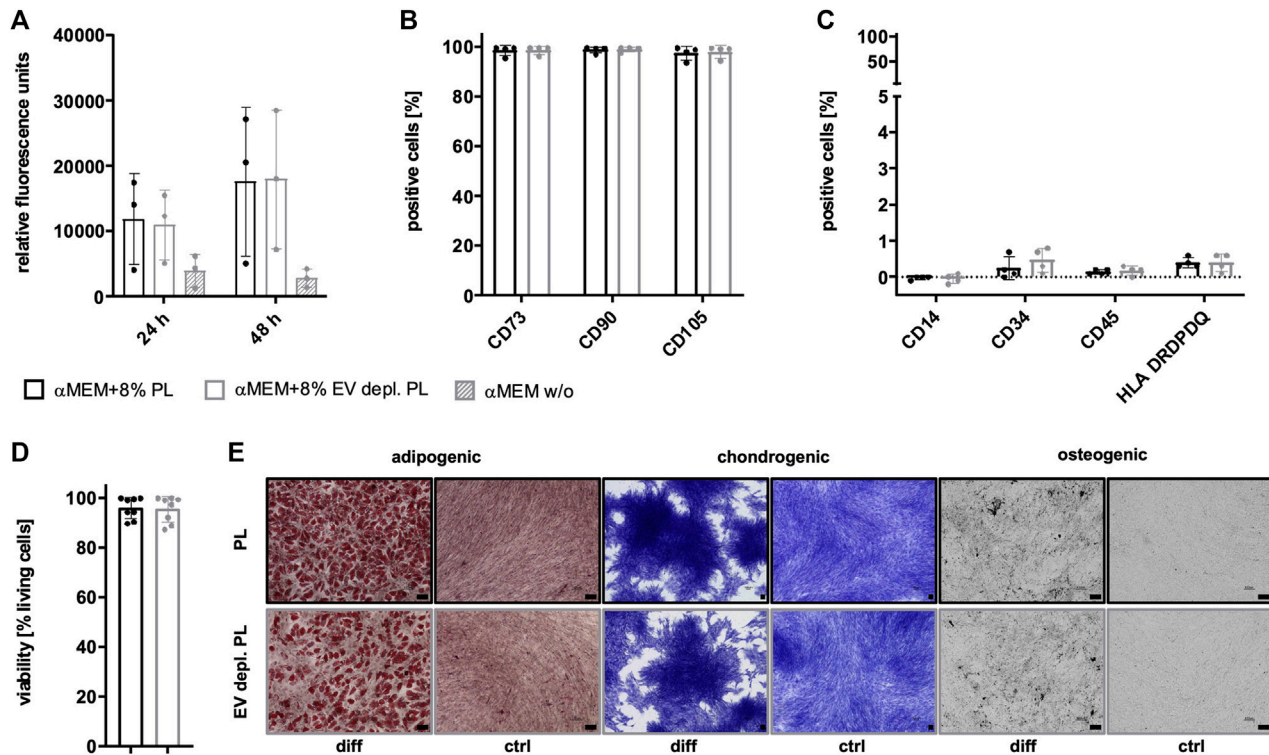


FIGURE 5

Characteristics of MSCs after expansion in different media. (A) MSCs were expanded in αMEM+8% PL (black), αMEM+8% EV depl. PL (gray), and αMEM without supplement (αMEM w/o; gray with stripes) in a 96-well plate (200 cells per well) for 24 h and 48 h, respectively. Triplicates ( $n = 3$ ) were performed for each. The cells were stained with the CyQUANT Cell Proliferation Assays kit and, proliferation of cells was determined by fluorescence intensities. (B–E) MSCs were seeded at 2,000 cells/cm<sup>2</sup> in αMEM+8% PL and αMEM+8% EV depl. PL and expanded for P1 or P2. Expression of identity markers CD73, CD90, and CD105 (B) and lack of expression of purity markers CD14, CD34, CD45, and HLA DRDPDQ (C) was analyzed by flow cytometry. (D) Viability of cells was determined by trypan blue staining. (E) Harvested MSCs of αMEM+8% PL and αMEM+8% EV depl. PL cultures were differentiated into cells of adipogenic, chondrogenic, and osteogenic lineages. For this, the cells were grown in specific differentiation media (diff) or in control media αMEM+20% FBS (ctrl) lacking differentiation-inducing substances. Adipogenic differentiation was verified by Oil Red O and hematoxylin staining, chondrogenic differentiation was demonstrated by methylene blue staining and osteogenic differentiation was proven by activity of alkaline phosphatase using BCIP/NBT substrate. Pictures were taken with 4 times (chondrogenic) and 10 times magnification (adipogenic and osteogenic), respectively. Black scale bars indicate 100 μm. Data are presented as mean ± SD, and  $N \geq 3$  (A–D) or  $N = 2$  (E) independent experiments were performed. Representative images are depicted for differentiation assays.

antigens is presented in [Supplementary Figure S2](#). Diversity in surface antigen expression patterns for sEVs from media and CM was equally indicative for the presence of MSC-derived sEVs, increasing with collection time and EV depl. PL culture condition.

## Hollow fiber bioreactor-based MSC expansion does not negatively affect MSC characteristics

In order to allow large-scale manufacturing of sEVs, a hollow fiber bioreactor-based expansion process was implemented. As a first step, important expansion parameters and cell characteristics were compared for MSCs grown in the CP-coated Quantum system and in conventional CellSTACK-based culture. Significantly, more cells could be harvested for the Quantum system with mean harvested cell numbers of more than 300 million cells showing its potential for large-scale expansion ([Figure 9A](#)), although cells grew significantly slower than that of conventional cell culture ([Figure 9B](#)). Significant differences in surface antigen expression of important identity (CD73, CD90, and CD105; [Figure 9C](#)) and purity markers (CD14, CD34, CD45; [Figure 9D](#)) were not

observed between MSCs of both expansion systems except for significantly lower expression of HLA DRDPDQ for Quantum-derived MSCs ([Figure 9D](#)). Viability of cells was not significantly altered by the bioreactor-based expansion process ([Figure 9E](#)), and the differentiation capacity of MSCs toward cells of the adipogenic, chondrogenic, and osteogenic lineages could be maintained ([Figure 9F](#)).

## Hollow fiber bioreactor allows for the generation of sEVs with consistent properties

sEVs were collected in CM for 16–19 h for the Quantum system and for 24–48 h for CellSTACK-based expansion. As the presence of MSC-derived sEVs in CM could be proven during previous parts of this study, αMEM+8% PL was used as growth media for both expansion systems in order to exclude changes of sEV composition by alteration of culture conditions. Isolation of sEVs by method I was carried out for both expansion systems, whereas method IV was only used for Quantum-derived CM to check its potential for large-scale applicability. No significant differences in quantity were observed between sEVs isolated from the two expansion systems by method I as



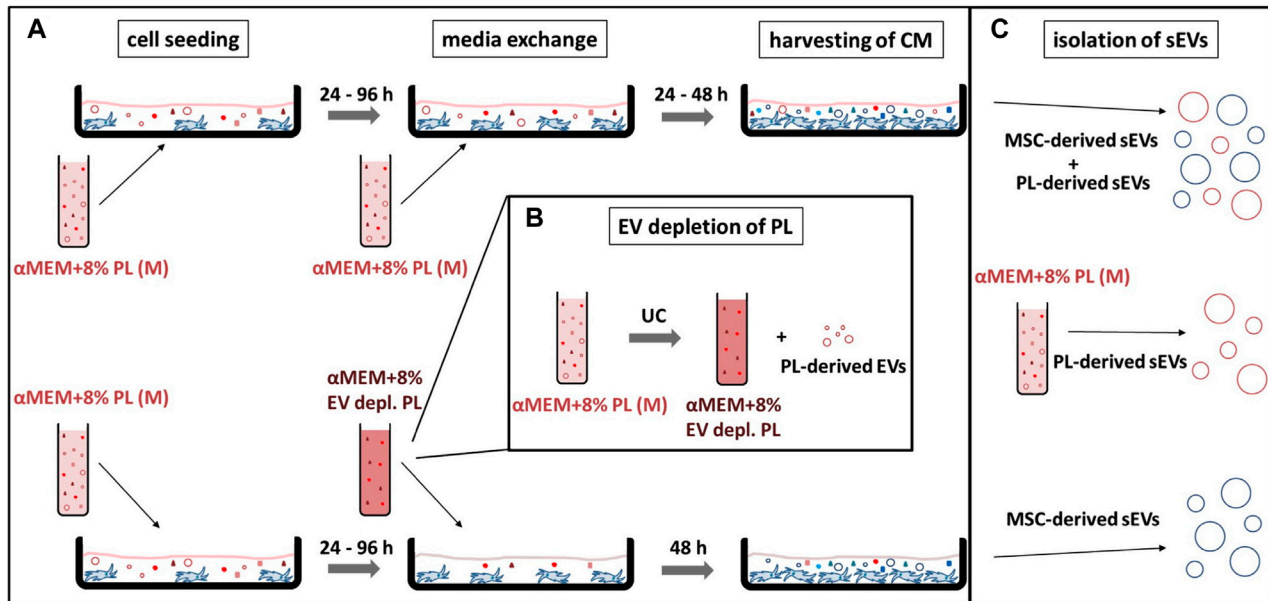


FIGURE 6

Workflow of different sEV collection strategies. **(A)** MSCs were seeded at 2,000–4,000 cells/cm<sup>2</sup> in the media αMEM+8% PL (M) and expanded for P1 or P2. After 24–96 h media was exchanged completely for the collection of sEVs in CM. In addition to αMEM+8% PL, αMEM+8% EV depl. PL was chosen as collection media for enrichment of MSC-derived sEVs. In order to exclude an impact of batch-to-batch variation of PL, the same starting batches of PL (from the same donors) were used for the experiments shown in the upper and lower row, which just differed whether or not EV depletion has been performed. Collection time was set to 24 or 48 h for αMEM+8% PL cultures and to 48 h for αMEM+8% EV depl. PL cultures. CM was harvested and stored at –80°C until isolation of sEVs. **(B)** αMEM+8% EV depl. PL was manufactured by UC of PL for 3 h at 120,000 × g at 4°C, whereby the pellet containing the PL-derived EV was withdrawn. **(C)** sEVs isolated from CM collected with αMEM+8% PL included MSC-derived and PL-derived sEVs, whereas sEVs collected with αMEM+8% EV depl. PL solely included MSC-derived sEVs. PL-derived sEVs were isolated from the media αMEM+8% PL to confirm the hypothesis.

protein and particle concentrations as well as proteins and particles per cell were in similar ranges (Figures 10A, B). Lower protein and particle concentrations were obtained for isolation by method IV (Figures 10A, B); however, elevated particles to protein ratio indicated higher purity of respective sEVs (Figure 10C). sEVs from both expansion systems expressed proteins Flot-1, CD63, and CD81, where the highest levels of tetraspanins CD63 and CD81 were observed for Quantum-derived sEVs isolated by method IV (Figures 10D, E). While GRP94 was absent in all sEV preparations, co-isolated proteins were found at similar levels as indicated by the expression of ApoA1 (Figures 10D, E). Analyses of sEV size showed particles in size range between 100–200 nm with no significant differences between the expansion systems and isolation methods (Figure 10F). TEM confirmed the presence of sEVs in all preparations (Figure 10G). Similar surface antigen expression patterns were observed for all sEV preparations with some markers being more frequently positive for sEVs of CellSTACK-derived expansion (e.g., CD49e, CD29, CD62P, CD41b, CD42a, and CD31; Figure 10H). Analysis of additional surface antigens is presented in Supplementary Figure S3.

## Discussion

Implementation of standardized large-scale applicable procedures for the manufacturing of sEVs is of high relevance in order to overcome barriers currently impeding translation of laboratory-scale protocols toward clinical applications. This not only includes

lacking standardization of culture conditions during sEV production but also of sEV isolation methods. In addition, changing from flask-based expansion processes to a (semi-) automated expansion in bioreactors is still hampered and thus prevents efficient upscaling strategies (Paolini et al., 2022).

For this reason, we investigated possible improvements at various levels: (i) modification of sEV isolation protocols and their impact on efficacy of isolation and the sEV characteristics obtained thereby, (ii) analysis of the impact of culture characteristics (e.g., duration and supplements) on sEV output, and (iii) upscaling of the process toward a bioreactor-based large-scale expansion and generation of CM as a starting material for sEV preparation. Based on our results, we propose a hollow fiber bioreactor-based process for the generation of BM MSC-derived sEVs that, in combination with isolation by CFF and UC, allows for large-scale production of sEVs. Optionally, EV-depleted supplements (e.g., EV depl. PL) could be used in order to enrich for MSC-derived sEVs and to avoid supplement-derived sEVs in the final sEV preparation.

DC with a final enrichment of sEVs by UC is still considered as gold standard for the isolation of sEVs. However, due to its limited applicability for large-scale purification of sEVs from large volumes of starting material, various approaches combining different isolation methods became increasingly popular (Gardiner et al., 2016). CFF or precipitation with PEG can be applied for volume reduction of starting material and, besides UC, SEC can be used for final enrichment of sEVs. In this study, different combinations of isolation methods were evaluated. Only a combination of CFF with UC (method IV) was considered as suitable for the isolation of MSC-derived sEVs in a large-

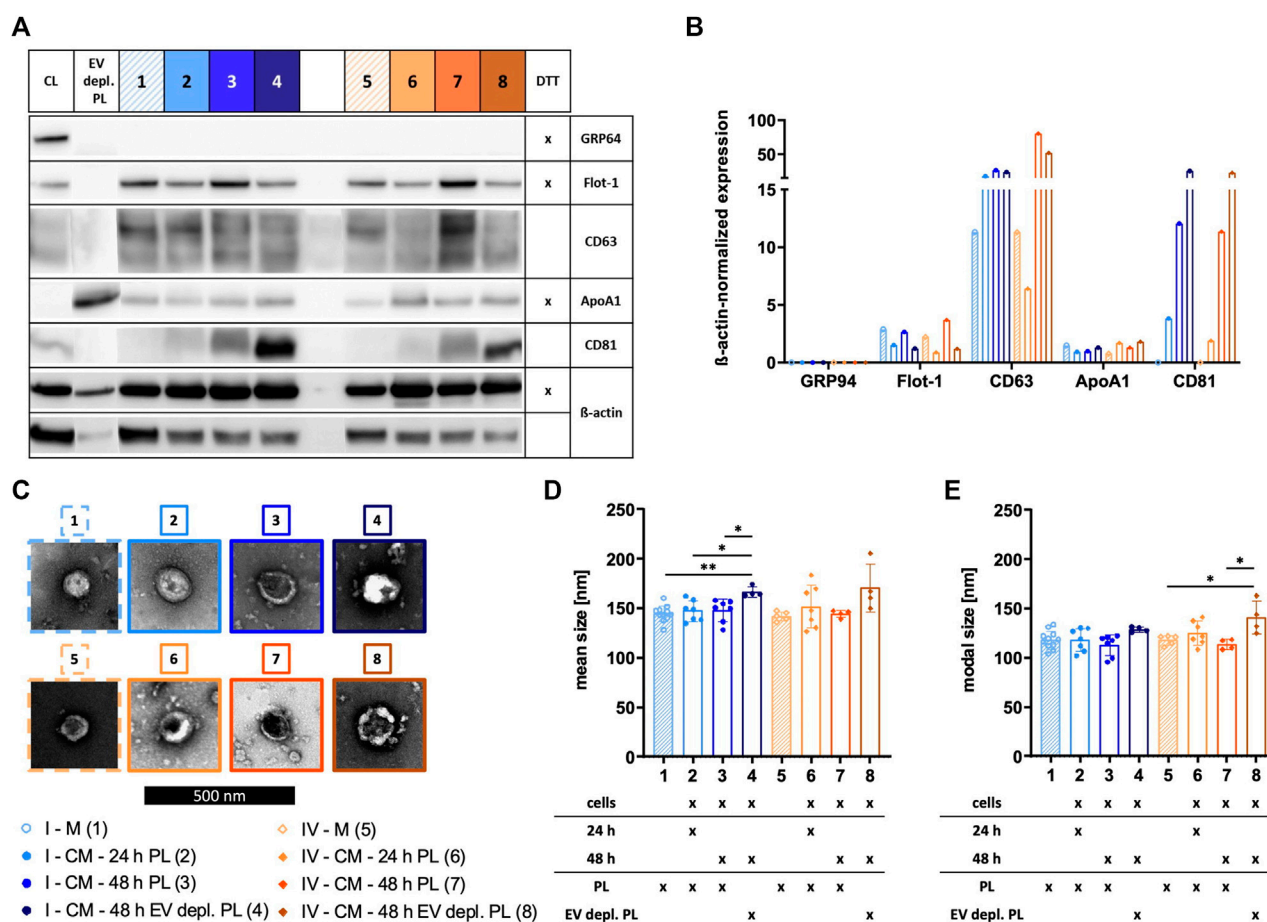


FIGURE 7

Characterization of sEVs collected with different strategies. sEVs were isolated from αMEM+8% PL (M) (1 and 5; with stripes) in order to verify the presence of PL-derived sEVs in the media. MSCs were grown in αMEM+8% PL and αMEM+8% EV depl. PL. sEVs were collected for 24 h (2 and 6) and 48 h (3 and 7) for αMEM+8% PL cultures and for 48 h for αMEM+8% EV depl. PL cultures (4 and 8). Methods I (blue scheme) and IV (orange scheme) were used for sEV isolation from M and CM. (A) Western blotting was performed in order to investigate the expression of proteins GRP94, Flot-1, CD63, ApoA1, and CD81. MSC cell lysate (CL) and EV depl. PL served as controls for primary antibodies, and β-actin was used as loading control. Reducing conditions for indicated proteins were obtained by the addition of dithiothreitol (DTT). (B) Chemiluminescent signal intensities were quantified and normalized on β-actin intensities, resulting in β-actin-normalized expression of proteins. (C) sEVs were visualized by negative contrast staining using TEM with 60,000 times magnification. The black scale bar represents 500 nm. (D) + (E) Mean and modal size of sEVs was determined by NTA. Representative images are depicted for western blotting and TEM. Data are presented as mean ± SD, and N ≥ 4 independent experiments were performed for NTA analyses. Statistically significant differences are depicted as follows: \*;  $p < 0.05$ , \*\*;  $p < 0.01$ .

scale setting. It combines the advantages of CFF-based volume reduction with an efficiency of a UC-derived sEV preparation in the subsequent step. sEVs obtained by this method showed similar characteristics as those purified with the gold standard method DC with UC (method I). This combination was also proposed by Rohde et al. for a good manufacturing practice (GMP)-compliant manufacturing process of MSC-derived sEVs (Rohde et al., 2019) and has been recently implemented for a first-in-human intracochlear application (Warnecke et al., 2021). Both, combination of PEG with UC (method II) and CFF with SEC (method III) resulted in altered sEV characteristics, as shown by different surface antigen expression patterns and in sEV preparations with low purity indicated by a lower particles to protein ratio (Webber and Clayton, 2013). Purity concerns already arose for PEG precipitation-based sEV isolation in other studies (Van Deun et al., 2014; Lobb et al., 2015). In contrast, SEC commonly led to preparations with high purity (Baranyai et al., 2015; Nordin et al., 2015). One possible explanation for the divergent results

could be the intermediate step of incubation with Exo-spin™ buffer prior to final isolation of sEVs by SEC in this study, whereas an intermediate precipitation was not performed by Baranyai et al. and Nordin et al. In accordance with our results, Lobb et al. also found high amount of co-isolated albumin after sEV isolation with the Exo-spin™ system (Lobb et al., 2015). General critical considerations were also made by Witwer et al. in the context of using commercial kits not stating the exact composition of ingredients for GMP-grade sEV production (Witwer et al., 2019).

Since Torreggiani et al. showed the presence of sEVs in PL (Torreggiani et al., 2014), we wanted to prove the co-existence of MSC-derived sEVs in CM and evaluate strategies for enrichment of the latter. For this purpose, sEVs were isolated from the media αMEM+8% PL in addition to CM collected with different strategies. These included collection for 24 h or 48 h and collection during a 48 h period, in which EV depl. PL was used. As the identity of sEVs could be shown for all approaches, the production of MSC-

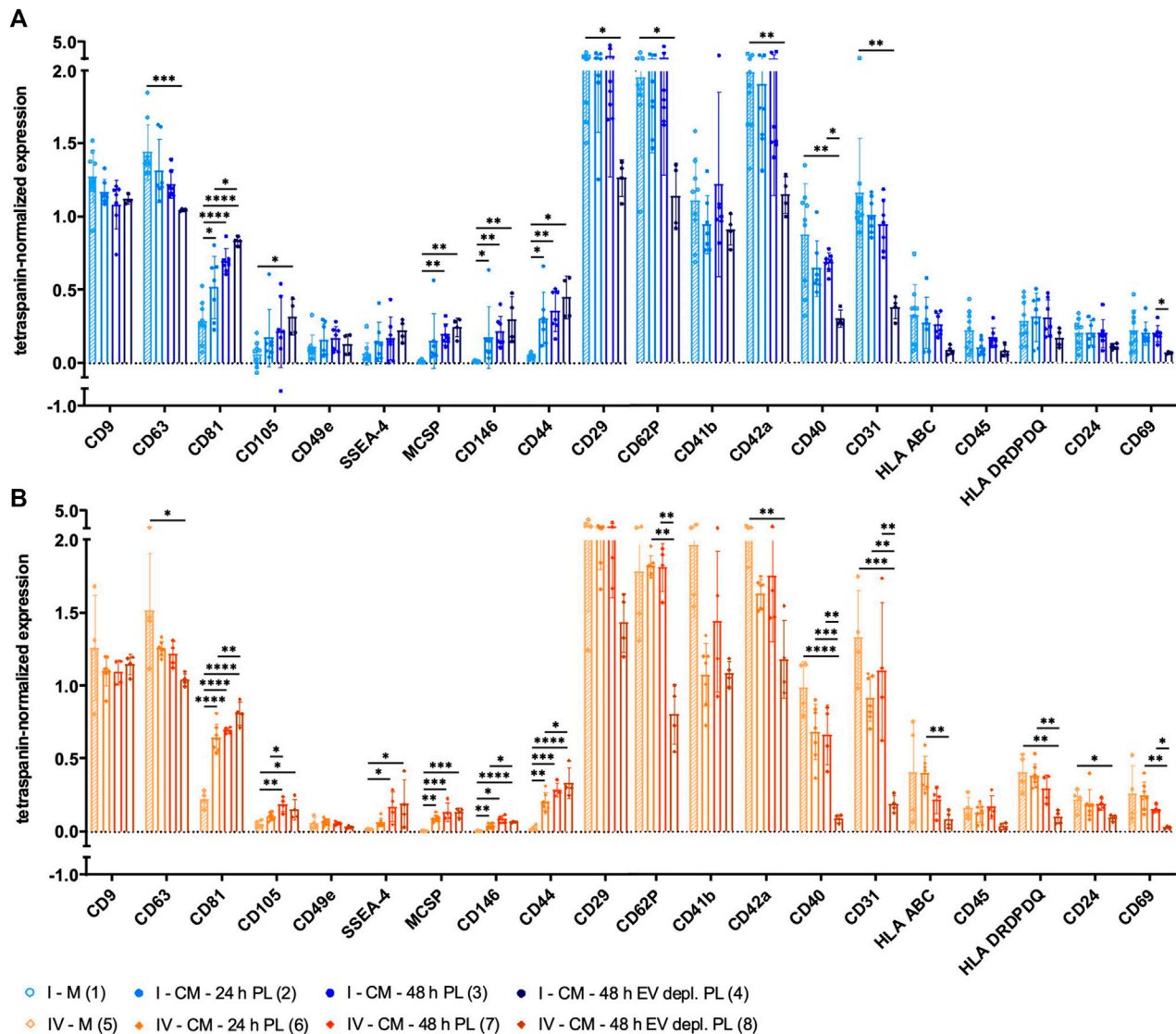


FIGURE 8

Tetraspanin-normalized surface antigen expression by sEVs collected with different strategies. sEVs were isolated from the media  $\alpha$ MEM+8% PL (M) (1 and 5; with stripes) and MSC CM, where sEVs were collected for 24 h (2 and 6) and 48 h (3 and 7) for  $\alpha$ MEM+8% PL cultures and for 48 h for  $\alpha$ MEM+8% EV depl. PL cultures (4 and 8). Methods I (blue scheme) (A) and IV (orange scheme) (B) were used for sEV isolation from M and CM. The expression of several surface antigens by sEVs was analyzed using MACSPlex technology. sEVs were bound by capture beads with epitopes against each analyzed surface antigen and detected indirectly by an APC-coupled detection reagent directed against the tetraspanins CD9, CD63, and CD81. Due to the indirect detection, fluorescence intensity of each surface antigen was normalized on mean fluorescence intensity of CD9, CD63, and CD81, resulting in tetraspanin-normalized expression. Data are presented as mean  $\pm$  SD, and  $N \geq 4$  independent experiments were performed. Statistically significant differences are depicted as follows:

\*:  $p < 0.05$ , \*\*:  $p < 0.01$ , \*\*\*:  $p < 0.001$ , \*\*\*\*:  $p < 0.0001$ .

derived sEVs could especially be verified by the EV depl. PL approach. PL- and MSC-derived sEVs significantly differed in their surface antigen expression pattern with most pronounced disparities for surface antigens CD81, CD105, SSEA-4, MCSP, CD146, CD44 (all more frequently expressed by MSC-derived sEVs), CD63, CD29, CD62P, CD42a, CD40, CD31, HLA DRDPDQ, and CD24 (all more frequently expressed by PL-derived sEVs). In addition, differences between sEVs from  $\alpha$ MEM+8% PL and  $\alpha$ MEM+8% EV depl. PL cultures were observed for surface antigen expression of known platelet markers CD62P, CD40, CD31, and CD69 (Stenberg et al., 1985; Newman et al., 1990; Testi et al., 1990; Inwald et al., 2003). These observations could be partially explained in that sEVs of EV

depl. PL cultures totally lacked PL-derived sEVs, thus including less sEVs positive for typical platelet markers. Although contaminating sEVs might potentiate therapeutic action in some cases, counteraction of proper functionality of MSC-derived sEVs could also be observed (Witwer et al., 2019). EV depletion of cell culture supplements is commonly applied in order to get rid of contaminating sEVs. As alteration of culture conditions has been shown to affect sEV characteristics (Li et al., 2015; Haraszti et al., 2019), critical considerations were made about this strategy. Although EV depl. PL showed no negative impact on important MSC characteristics in this study (e.g., expression of identity and purity markers, tri-lineage differentiation potential, and viability), changes in composition of



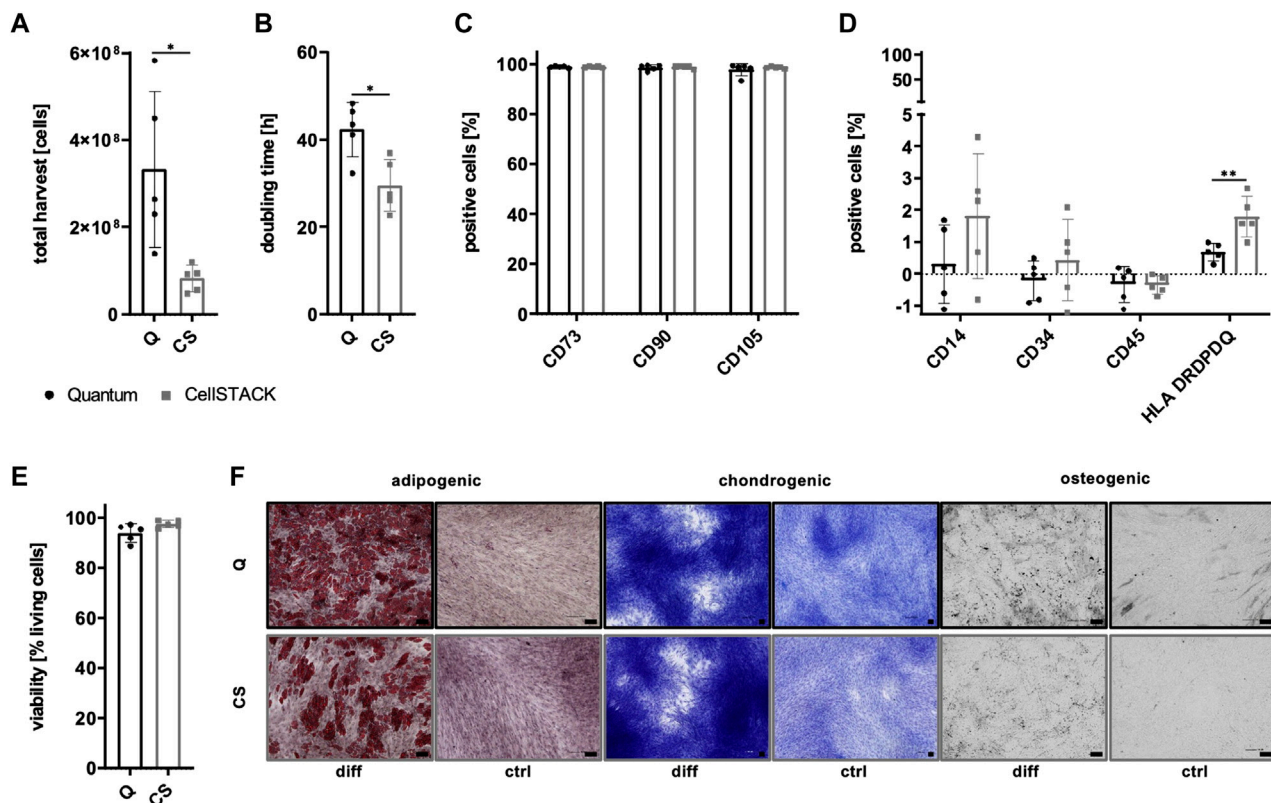


FIGURE 9

Expansion parameters and characteristics of MSCs after Quantum- and CellSTACK-based culture. MSCs were grown in aMEM+8% PL in a CP-coated Quantum hollow fiber bioreactor (Q; black) or in conventional cell culture in a CellSTACK (CS; gray) for P1. The expansion parameters total harvest (A) and doubling time (B) were determined after the harvesting of cells. The expression of identity markers CD73, CD90, and CD105 (C) and purity markers CD14, CD34, CD45, and HLA DRDPDQ (D) were analyzed by flow cytometry. (E) Viability of cells was determined by trypan blue staining. (F) Harvested MSCs were differentiated into cells of adipogenic, chondrogenic, and osteogenic lineages. For this, the cells were grown in specific differentiation media (diff) or in control media aMEM+20% FBS (ctrl) lacking differentiation-inducing substances. Adipogenic differentiation was verified by Oil Red O and hematoxylin staining, chondrogenic differentiation was demonstrated by methylene blue staining and osteogenic differentiation was proven by activity of alkaline phosphatase using BCIP/NBT substrate. Pictures were taken with 4 times (chondrogenic) and 10 times magnification (adipogenic and osteogenic), respectively. The black scale bars indicate 100  $\mu$ m. Data are presented as mean  $\pm$  SD, and  $N \geq 4$  independent experiments were performed. Representative images are depicted for differentiation assays. Statistically significant differences are depicted as follows: \*:  $p < 0.05$ , \*\*:  $p < 0.01$ .

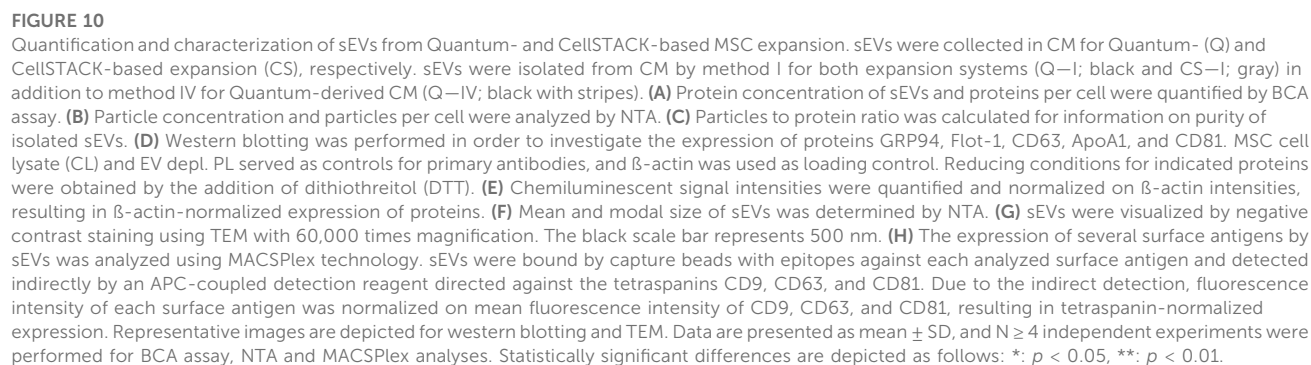
MSC-derived sEVs as a consequence of cellular stress by altered culture conditions cannot be excluded (Wiest and Zubair, 2020; Almeria et al., 2022). Gobin et al. proposed CD40 as an important surface antigen responsible for immunomodulatory capacities of MSC-derived sEVs (Gobin et al., 2021). Since the latter is only marginally expressed by sEVs from aMEM+8% EV depl. PL cultures, this may in general raise questions about the efficacy of sEVs generated with deprivation strategies. Hence, changes of culture conditions always need to be critically evaluated depending on specific purposes. Our preference is the use of PL, which has not been EV depleted. However, if a planned clinical use requires a sEV preparation enriched for MSC-derived sEVs and at the same time avoiding of process-related contamination by platelet-derived sEVs, our study demonstrates that the use of EV depl. PL might be a feasible, alternative approach.

Expansion systems have been shown to influence sEV potency (Cao et al., 2020; Kim et al., 2020; Yan and Wu, 2020). 3D systems such as hollow fiber bioreactors are favorable since they represent a more native microenvironment of cells (Almeria et al., 2022) and allow the collection of several liters of CM for large-scale manufacturing of sEVs. MSC expansion with hollow fiber bioreactors such as the

Quantum system of Terumo BCT has already been implemented for several cell-based applications (Nold et al., 2013; Rojewski et al., 2013; Hanley et al., 2014; Lechanteur et al., 2014; Barchhausen et al., 2016; Haack-Sorensen et al., 2016; Lambrechts et al., 2016; Haack-Sorensen et al., 2018; Mizukami et al., 2018; Frank et al., 2019; Mennan et al., 2019; Lisini et al., 2020; Vymetalova et al., 2020; Cocce et al., 2021; Haberle et al., 2021; Mendt et al., 2021). However, only few studies investigated the use of hollow fiber bioreactor-based systems for the production of MSC-derived sEVs (Mendt et al., 2018; Cao et al., 2020; Yan and Wu, 2020; Gobin et al., 2021; Bellio et al., 2022). In addition, Witwer et al. highlighted the urgent need to investigate the impact of bioreactor-based production processes on sEV characteristics (Witwer et al., 2019).

We showed (to our best knowledge) for the first time a systematic comparison of isolation methods for sEVs generated with the Quantum hollow fiber bioreactor and a CellSTACK-based conventional cell culture system already approved for clinical applications (Gjerde et al., 2018; Gomez-Barrena et al., 2019; Rojewski et al., 2019; Gomez-Barrena et al., 2020; Gomez-Barrena et al., 2021). Surface antigen expression patterns displayed less positive sEVs for known platelet markers such as CD29, CD62P, CD41b,





CD42a, and CD31 (Stenberg et al., 1985; Hynes, 1987; Hickey et al., 1989; Newman et al., 1990; Staatz et al., 1991) for the Quantum system, indicating a lower proportion of PL-derived sEVs. This hypothesis is supported by a lower positivity for these markers for MSC-sEVs from  $\alpha$ MEM+8% EV depl. PL cultures as compared to PL-sEVs from media. Before media is added to the Quantum system, it has to cross a sterile filter barrier (pore size of 0.2  $\mu$ m) during filling of media bags. Thus, PL-derived sEVs could have been partially lost in the filter pores, suggesting the Quantum system being helpful in reducing contaminating PL-sEVs and enriching for MSC-derived sEVs. CD49e, also known as integrin  $\alpha$ -5, is equally expressed by MSC- and PL-derived sEVs, as shown by similar expression levels for sEVs from media and  $\alpha$ MEM+8% EV depl. PL cultures. As part of the fibronectin receptor (Zhang et al., 1993), the differences we observed for Quantum- and CellSTACK-derived sEVs could be the result of divergent adhesion mechanisms for respective MSCs with CP coating of the surface of the Quantum system in contrast to a tissue culture-treated cell culture surface of CellSTACKs.

Although lower protein and particle concentrations were obtained for the isolation of Quantum-derived sEVs by CFF with UC (method IV), as compared to the gold standard method DC with UC (method I), similar expression levels of Flot-1, CD63, and CD81 could provide evidence for equal sEV quantity. This was further reinforced by higher particles to protein ratio indicating higher sEV purity for method IV as proposed by Webber and Clayton (2013). Actual sEV quantity is often overestimated as direct sEV quantification methods are still lacking and quantification by protein and particle concentrations, respectively, is not specific for sEVs (Witwer et al., 2019). Therefore, alternative approaches such as quantification by lipid concentrations (Osteikoetxea et al., 2015; Visnovitz et al., 2019) or fluorescence-based NTA were assumed to be more accurate (Desgeorges et al., 2020).

Other studies described higher sEV quantity for alternative hollow fiber-based expansion systems as compared to 2D culture methods (Cao et al., 2020; Yan and Wu, 2020). Although protein and particle concentrations were comparable to sEVs from CellSTACKs in this study, as shown by similar proteins and particles per cell, respectively, overall sEV yield would be increased for the Quantum system due to higher number of harvested cells. In addition, different parameters could be optimized during collection of sEVs with the Quantum system in order to improve sEV yield. A prolonged sEV collection period could enhance sEV quantity by increasing the amount of CM as a starting material for sEV isolation. Mechanical stimuli such as shear forces have been shown to induce the release of sEVs by leading to elevated intracellular levels of calcium ions important for sEV secretion (Taylor et al., 2020; Kang et al., 2022). Therefore, impact of the media flow rate on sEV yield was investigated by Kang et al. showing best results for a flow rate of 1 mL/min in a flat-plate bioreactor (Kang et al., 2022). In our study, flow rates during sEV collection ranged from 0.4 to 1.6 mL/min demanding further investigation of optimal media flow rates for sEV release. Based on our data, we propose an approach using the Quantum hollow fiber bioreactor as a semi-automated large-scale sEV production system in combination with sEV isolation by CFF with UC for large-scale, GMP-grade sEV generation. Translation of this yet laboratory-scale optimized process toward a GMP-compliant manufacturing for clinical applications could be supported by quality by design (QbD) approaches. Critical process parameters and steps could be identified and different quality controls (e.g., microbial or endotoxin

testing) should be included in the whole manufacturing process (Yu et al., 2014; Paolini et al., 2022).

Finally, the impact of isolation methods and culture conditions on sEV potency and functionality remains to be elucidated. However, given the broad field of therapeutic applications with each potentially requiring specific sEV characteristics and the major challenges in establishing reproducible and robust potency assays, this will be subject of future investigations (Witwer et al., 2019; Gimona et al., 2021).

## Data availability statement

The raw data supporting the conclusions of this article will be made available by the authors, without undue reservation.

## Ethics statement

The studies involving human participants were reviewed and approved by the Ethikkommission der Universität Ulm. The patients/participants provided their written informed consent to participate in this study.

## Author contributions

VJ, MTR, and HS designed the research idea. VJ, ME, and MW performed the experiments. SE, TE, and BF contributed to the research idea. MTR and HS applied for funding. VJ wrote the first version of the manuscript. All co-authors approved the final version of the manuscript.

## Funding

This work was funded by the Sanitätsakademie der Bundeswehr, Projekt E/U2AD/ID018/IF577.

## Acknowledgments

The authors appreciate S. Wespel and S. Kempf for great technical assistance. They thank P. Walther (Central Facility for Electron Microscopy, Ulm University) for help with transmission electron microscopy.

## Conflict of interest

The authors declare that the research was conducted in the absence of any commercial or financial relationships that could be construed as a potential conflict of interest.

## Supplementary material

The Supplementary Material for this article can be found online at: <https://www.frontiersin.org/articles/10.3389/fbioe.2023.1107055/full#supplementary-material>

## References

- Adlerz, K., Patel, D., Rowley, J., Ng, K., and Ahsan, T. (2020). Strategies for scalable manufacturing and translation of MSC-derived extracellular vesicles. *Stem Cell Res.* 48, 101978. doi:10.1016/j.scr.2020.101978
- Almeria, C., Kress, S., Weber, V., Egger, D., and Kasper, C. (2022). Heterogeneity of mesenchymal stem cell-derived extracellular vesicles is highly impacted by the tissue/cell source and culture conditions. *Cell Biosci.* 12 (1), 51. doi:10.1186/s13578-022-00786-7
- Armacki, M., Polaschek, S., Waldenmaier, M., Morawe, M., Ruhland, C., Schmid, R., et al. (2020). Protein kinase D1, reduced in human pancreatic tumors, increases secretion of small extracellular vesicles from cancer cells that promote metastasis to lung in mice. *Gastroenterology* 159 (3), 1019–1035.e22. doi:10.1053/j.gastro.2020.05.052
- Banks, W. A., Sharma, P., Bullock, K. M., Hansen, K. M., Ludwig, N., and Whiteside, T. L. (2020). Transport of extracellular vesicles across the blood-brain barrier: Brain pharmacokinetics and effects of inflammation. *Int. J. Mol. Sci.* 21 (12), 4407. doi:10.3390/ijms21124407
- Baranyai, T., Herczeg, K., Onodi, Z., Voszka, I., Modos, K., Marton, N., et al. (2015). Isolation of exosomes from blood plasma: Qualitative and quantitative comparison of ultracentrifugation and size exclusion chromatography methods. *PLoS One* 10 (12), e0145686. doi:10.1371/journal.pone.0145686
- Barckhausen, C., Rice, B., Baila, S., Sensebe, L., Schrezenmeier, H., Nold, P., et al. (2016). GMP-compliant expansion of clinical-grade human mesenchymal stromal/stem cells using a closed hollow fiber bioreactor. *Methods Mol. Biol.* 1416, 389–412. doi:10.1007/978-1-4939-3584-0\_23
- Bellio, M. A., Kanashiro-Takeuchi, R. M., Takeuchi, L., Kulandavelu, S., Lee, Y. S., Balkan, W., et al. (2022). Systemic delivery of large-scale manufactured Wharton's Jelly mesenchymal stem cell-derived extracellular vesicles improves cardiac function after myocardial infarction. *J. Cardiovasc. Aging* 2, 9. doi:10.20517/jca.2021.21
- Borger, V., Staubach, S., Ditttrich, R., Stambouli, O., and Giebel, B. (2020). Scaled isolation of mesenchymal stem/stromal cell-derived extracellular vesicles. *Curr. Protoc. Stem Cell Biol.* 55 (1), e128. doi:10.1002/cpsc.128
- Bruno, S., Grange, C., Deregius, M. C., Calogero, R. A., Saviozzi, S., Collino, F., et al. (2009). Mesenchymal stem cell-derived microvesicles protect against acute tubular injury. *J. Am. Soc. Nephrol.* 20 (5), 1053–1067. doi:10.1681/ASN.2008070798
- Busatto, S., Vilanilam, G., Ticer, T., Lin, W. L., Dickson, D. W., Shapiro, S., et al. (2018). Tangential flow filtration for highly efficient concentration of extracellular vesicles from large volumes of fluid. *Cells* 7 (12), 273. doi:10.3390/cells7120273
- Cao, J., Wang, B., Tang, T., Lv, L., Ding, Z., Li, Z., et al. (2020). Three-dimensional culture of MSCs produces exosomes with improved yield and enhanced therapeutic efficacy for cisplatin-induced acute kidney injury. *Stem Cell Res. Ther.* 11 (1), 206. doi:10.1186/s13287-020-01719-2
- Cocce, V., La Monica, S., Bonelli, M., Alessandri, G., Alfieri, R., Lagrasta, C. A., et al. (2021). Inhibition of human malignant pleural mesothelioma growth by mesenchymal stromal cells. *Cells* 10 (6), 1427. doi:10.3390/cells10061427
- Coumans, F. A. W., Brisson, A. R., Buzas, E. I., Dignat-George, F., Drees, E. E. E., El-Andaloussi, S., et al. (2017). Methodological guidelines to study extracellular vesicles. *Circ. Res.* 120 (10), 1632–1648. doi:10.1161/CIRCRESAHA.117.309417
- Dash, N. R., Dash, S. N., Routray, P., Mohapatra, S., and Mohapatra, P. C. (2009). Targeting nonhealing ulcers of lower extremity in human through autologous bone marrow-derived mesenchymal stem cells. *Rejuvenation Res.* 12 (5), 359–366. doi:10.1089/rej.2009.0872
- Desgeorges, A., Hollerweger, J., Lassacher, T., Rohde, E., Helmbrecht, C., and Gimona, M. (2020). Differential fluorescence nanoparticle tracking analysis for enumeration of the extracellular vesicle content in mixed particulate solutions. *Methods* 177, 67–73. doi:10.1016/j.ymeth.2020.02.006
- Dominici, M., Le Blanc, K., Mueller, I., Slaper-Cortenbach, I., Marini, F., Krause, D., et al. (2006). Minimal criteria for defining multipotent mesenchymal stromal cells. The International Society for Cellular Therapy position statement. *Cytotherapy* 8 (4), 315–317. doi:10.1080/14653240600855905
- Doyle, L. M., and Wang, M. Z. (2019). Overview of extracellular vesicles, their origin, composition, purpose, and methods for exosome isolation and analysis. *Cells* 8 (7), doi:10.3390/cells8070727
- Elsharkasy, O. M., Nordin, J. Z., Hagey, D. W., de Jong, O. G., Schiffelers, R. M., Andaloussi, S. E., et al. (2020). Extracellular vesicles as drug delivery systems: Why and how? *Adv. Drug Deliv. Rev.* 159, 332–343. doi:10.1016/j.addr.2020.04.004
- Falanga, V., Iwamoto, S., Chartier, M., Yufit, T., Butmarc, J., Kouttab, N., et al. (2007). Autologous bone marrow-derived cultured mesenchymal stem cells delivered in a fibrin spray accelerate healing in murine and human cutaneous wounds. *Tissue Eng.* 13 (6), 1299–1312. doi:10.1089/ten.2006.0278
- Fekete, N., Gadelorge, M., Furst, D., Maurer, C., Dausend, J., Fleury-Cappellesso, S., et al. (2012a). Platelet lysate from whole blood-derived pooled platelet concentrates and apheresis-derived platelet concentrates for the isolation and expansion of human bone marrow mesenchymal stromal cells: Production process, content and identification of active components. *Cytotherapy* 14 (5), 540–554. doi:10.3109/14653249.2012.655420
- Fekete, N., Rojewski, M. T., Furst, D., Kreja, L., Ignatius, A., Dausend, J., et al. (2012b). GMP-compliant isolation and large-scale expansion of bone marrow-derived MSC. *PLoS One* 7 (8), e43255. doi:10.1371/journal.pone.0043255
- Frank, N. D., Jones, M. E., Vang, B., and Coeshott, C. (2019). Evaluation of reagents used to coat the hollow-fiber bioreactor membrane of the Quantum® Cell Expansion System for the culture of human mesenchymal stem cells. *Mater. Sci. Eng. C Mater. Biol. Appl.* 96, 77–85. doi:10.1016/j.msec.2018.10.081
- Friedenstein, A. J., Gorskaja, J. F., and Kulagina, N. N. (1976). Fibroblast precursors in normal and irradiated mouse hematopoietic organs. *Exp. Hematol.* 4 (5), 267–274.
- Gardiner, C., Di Vizio, D., Sahoo, S., Thery, C., Witwer, K. W., Wauben, M., et al. (2016). Techniques used for the isolation and characterization of extracellular vesicles: Results of a worldwide survey. *J. Extracell. Vesicles* 5, 32945. doi:10.3402/jev.v5.32945
- Gimona, M., Brizzi, M. F., Choo, A. B. H., Dominici, M., Davidson, S. M., Grillari, J., et al. (2021). Critical considerations for the development of potency tests for therapeutic applications of mesenchymal stromal cell-derived small extracellular vesicles. *Cytotherapy* 23 (5), 373–380. doi:10.1016/j.jcyt.2021.01.001
- Gjerde, C., Mustafa, K., Hellem, S., Rojewski, M., Gjengedal, H., Yassin, M. A., et al. (2018). Cell therapy induced regeneration of severely atrophied mandibular bone in a clinical trial. *Stem Cell Res. Ther.* 9 (1), 213. doi:10.1186/s13287-018-0951-9
- Gobin, J., Muradia, G., Mehic, J., Westwood, C., Couvrette, L., Stalker, A., et al. (2021). Hollow-fiber bioreactor production of extracellular vesicles from human bone marrow mesenchymal stromal cells yields nanovesicles that mirrors the immuno-modulatory antigenic signature of the producer cell. *Stem Cell Res. Ther.* 12 (1), 127. doi:10.1186/s13287-021-02190-3
- Gomez-Barrena, E., Padilla-Eguiluz, N. G., Rosset, P., Hernigou, P., Baldini, N., Ciapetti, G., et al. (2021). Osteonecrosis of the femoral head safely healed with autologous, expanded, bone marrow-derived mesenchymal stromal cells in a multicentric trial with minimum 5 Years follow-up. *J. Clin. Med.* 10 (3), 508. doi:10.3390/jcm10030508
- Gomez-Barrena, E., Padilla-Eguiluz, N., Rosset, P., Gebhard, F., Hernigou, P., Baldini, N., et al. (2020). Early efficacy evaluation of mesenchymal stromal cells (MSC) combined to biomaterials to treat long bone non-unions. *Injury* 51, S63–S73. doi:10.1016/j.injury.2020.02.070
- Gomez-Barrena, E., Rosset, P., Gebhard, F., Hernigou, P., Baldini, N., Rouard, H., et al. (2019). Feasibility and safety of treating non-unions in tibia, femur and humerus with autologous, expanded, bone marrow-derived mesenchymal stromal cells associated with biphasic calcium phosphate biomaterials in a multicentric, non-comparative trial. *Biomaterials* 196, 100–108. doi:10.1016/j.biomaterials.2018.03.033
- Gowen, A., Shahjin, F., Chand, S., Odegaard, K. E., and Yelamanchili, S. V. (2020). Mesenchymal stem cell-derived extracellular vesicles: Challenges in clinical applications. *Front. Cell Dev. Biol.* 8, 149. doi:10.3389/fcell.2020.00149
- Gurunathan, S., Kang, M. H., Jeyaraj, M., Qasim, M., and Kim, J. H. (2019). Review of the isolation, characterization, biological function, and multifarious therapeutic approaches of exosomes. *Cells* 8 (4), 307. doi:10.3390/cells8040307
- Haack-Sorensen, M., Follin, B., Juhl, M., Brorsen, S. K., Sondergaard, R. H., Kastrup, J., et al. (2016). Culture expansion of adipose derived stromal cells. A closed automated Quantum Cell Expansion System compared with manual flask-based culture. *J. Transl. Med.* 14 (1), 319. doi:10.1186/s12967-016-1080-9
- Haack-Sorensen, M., Juhl, M., Follin, B., Harary Sondergaard, R., Kirchhoff, M., Kastrup, J., et al. (2018). Development of large-scale manufacturing of adipose-derived stromal cells for clinical applications using bioreactors and human platelet lysate. *Scand. J. Clin. Lab. Invest.* 78 (4), 293–300. doi:10.1080/00365513.2018.1462082
- Haberle, H., Magunia, H., Lang, P., Gloeckner, H., Korner, A., Koeppen, M., et al. (2021). Mesenchymal stem cell therapy for severe COVID-19 ARDS. *J. Intensive Care Med.* 36 (6), 681–688. doi:10.1177/0885066621997365
- Hanley, P. J., Mei, Z., Durett, A. G., Cabreira-Hansen Mda, G., Klis, M., Li, W., et al. (2014). Efficient manufacturing of therapeutic mesenchymal stromal cells with the use of the Quantum Cell Expansion System. *Cytotherapy* 16 (8), 1048–1058. doi:10.1016/j.jcyt.2014.01.417
- Haraszti, R. A., Miller, R., Dubuke, M. L., Rockwell, H. E., Coles, A. H., Sapp, E., et al. (2019). Serum deprivation of mesenchymal stem cells improves exosome activity and alters lipid and protein composition. *iScience* 16, 230–241. doi:10.1016/j.isci.2019.05.029
- Hickey, M. J., Williams, S. A., and Roth, G. J. (1989). Human platelet glycoprotein IX: An adhesive prototype of leucine-rich glycoproteins with flank-center-flank structures. *Proc. Natl. Acad. Sci. U. S. A.* 86 (17), 6773–6777. doi:10.1073/pnas.86.17.6773
- Hynes, R. O. (1987). Integrins: A family of cell surface receptors. *Cell* 48 (4), 549–554. doi:10.1016/0092-8674(87)90233-9
- Inwald, D. P., McDowall, A., Peters, M. J., Callard, R. E., and Klein, N. J. (2003). CD40 is constitutively expressed on platelets and provides a novel mechanism for platelet activation. *Circ. Res.* 92 (9), 1041–1048. doi:10.1161/01.RES.0000070111.98158.6C
- Kang, H., Bae, Y. H., Kwon, Y., Kim, S., and Park, J. (2022). Extracellular vesicles generated using bioreactors and their therapeutic effect on the acute kidney injury model. *Adv. Healthc. Mater.* 11 (4), e2101606. doi:10.1002/adhm.202101606
- Kim, H., Lee, M. J., Bae, E. H., Ryu, J. S., Kaur, G., Kim, H. J., et al. (2020). Comprehensive molecular profiles of functionally effective MSC-derived extracellular vesicles in immunomodulation. *Mol. Ther.* 28 (7), 1628–1644. doi:10.1016/j.ymthe.2020.04.020
- Koliha, N., Wiencek, Y., Heider, U., Jungst, C., Kladt, N., Krauthausen, S., et al. (2016). A novel multiplex bead-based platform highlights the diversity of extracellular vesicles. *J. Extracell. Vesicles* 5, 29975. doi:10.3402/jev.v5.29975



- Lambrechts, T., Papanthiou, I., Rice, B., Schrooten, J., Luyten, F. P., and Aerts, J. M. (2016). Large-scale progenitor cell expansion for multiple donors in a monitored hollow fibre bioreactor. *Cytotherapy* 18 (9), 1219–1233. doi:10.1016/j.jcyt.2016.05.013
- Lataillade, J. J., Doucet, C., Bey, E., Carsin, H., Huet, C., Clairand, I., et al. (2007). New approach to radiation burn treatment by dosimetry-guided surgery combined with autologous mesenchymal stem cell therapy. *Regen. Med.* 2 (5), 785–794. doi:10.2217/17460751.2.5.785
- Leblanc, P., Arellano-Anaya, Z. E., Bernard, E., Gallay, L., Provansal, M., Lehmann, S., et al. (2017). Isolation of exosomes and microvesicles from cell culture systems to study prion transmission. *Methods Mol. Biol.* 1545, 153–176. doi:10.1007/978-1-4939-6728-5\_11
- Lechanteur, C., Baila, S., Janssens, M. E., Giet, O., Briquet, A., Baudoux, E., et al. (2014). Large-scale clinical expansion of mesenchymal stem cells in the GMP-compliant, closed automated Quantum<sup>®</sup> cell expansion system: Comparison with expansion in traditional T-flasks. *J. Stem Cell Res. Ther.* 4 (8), doi:10.4172/2157-7633.1000222
- Lener, T., Gimona, M., Aigner, L., Borger, V., Buzas, E., Camussi, G., et al. (2015). Applying extracellular vesicles based therapeutics in clinical trials - an ISEV position paper. *J. Extracell. Vesicles* 4, 30087. doi:10.3402/jev.v4.30087
- Li, J., Lee, Y., Johansson, H. J., Mager, I., Vader, P., Nordin, J. Z., et al. (2015). Serum-free culture alters the quantity and protein composition of neuroblastoma-derived extracellular vesicles. *J. Extracell. Vesicles* 4, 26883. doi:10.3402/jev.v4.26883
- Lisini, D., Nava, S., Frigerio, S., Pogliani, S., Maronati, G., Marcianti, A., et al. (2020). Automated large-scale production of paclitaxel loaded mesenchymal stromal cells for cell therapy applications. *Pharmaceutics* 12 (5), 411. doi:10.3390/pharmaceutics12050411
- Lobb, R. J., Becker, M., Wen, S. W., Wong, C. S., Wiegman, A. P., Leimgruber, A., et al. (2015). Optimized exosome isolation protocol for cell culture supernatant and human plasma. *J. Extracell. Vesicles* 4, 27031. doi:10.3402/jev.v4.27031
- Lu, D., Chen, B., Liang, Z., Deng, W., Jiang, Y., Li, S., et al. (2011). Comparison of bone marrow mesenchymal stem cells with bone marrow-derived mononuclear cells for treatment of diabetic critical limb ischemia and foot ulcer: A double-blind, randomized, controlled trial. *Diabetes Res. Clin. Pract.* 92 (1), 26–36. doi:10.1016/j.diabetes.2010.12.010
- Ludwig, A. K., De Miroshchadi, K., Doepfner, T. R., Borger, V., Ruesing, J., Rebmann, V., et al. (2018). Precipitation with polyethylene glycol followed by washing and pelleting by ultracentrifugation enriches extracellular vesicles from tissue culture supernatants in small and large scales. *J. Extracell. Vesicles* 7 (1), 1528109. doi:10.1080/20013078.2018.1528109
- Mendt, M., Daher, M., Basar, R., Shanley, M., Kumar, B., Wei Inng, F. L., et al. (2021). Metabolic reprogramming of GMP grade cord tissue derived mesenchymal stem cells enhances their suppressive potential in GVHD. *Front. Immunol.* 12, 631353. doi:10.3389/fimmu.2021.631353
- Mendt, M., Kamerkar, S., Sugimoto, H., McAndrews, K. M., Wu, C. C., Gagea, M., et al. (2018). Generation and testing of clinical-grade exosomes for pancreatic cancer. *JCI Insight* 3 (8), e99263. doi:10.1172/jci.insight.99263
- Mennan, C., Garcia, J., Roberts, S., Hulme, C., and Wright, K. (2019). A comprehensive characterisation of large-scale expanded human bone marrow and umbilical cord mesenchymal stem cells. *Stem Cell Res. Ther.* 10 (1), 99. doi:10.1186/s13287-019-1202-4
- Mizukami, A., Pereira-Chilima, T. D., Orellana, M. D., Abreu-Neto, M., Covas, D. T., Farid, S. S., et al. (2018). Technologies for large-scale umbilical cord-derived MSC expansion: Experimental performance and cost of goods analysis. *Biochem. Eng. J.* 135, 36–48. doi:10.1016/j.bej.2018.02.018
- Newman, P. J., Berndt, M. C., Gorski, J., White, G. C., 2nd, Lyman, S., Paddock, C., et al. (1990). PECAM-1 (CD31) cloning and relation to adhesion molecules of the immunoglobulin gene superfamily. *Science* 247 (4947), 1219–1222. doi:10.1126/science.1690453
- Nold, P., Brendel, C., Neubauer, A., Bein, G., and Hackstein, H. (2013). Good manufacturing practice-compliant animal-free expansion of human bone marrow derived mesenchymal stroma cells in a closed hollow-fiber-based bioreactor. *Biochem. Biophys. Res. Commun.* 430 (1), 325–330. doi:10.1016/j.bbrc.2012.11.001
- Nordin, J. Z., Lee, Y., Vader, P., Mager, I., Johansson, H. J., Heusermann, W., et al. (2015). Ultrafiltration with size-exclusion liquid chromatography for high yield isolation of extracellular vesicles preserving intact biophysical and functional properties. *Nanomedicine* 11 (4), 879–883. doi:10.1016/j.nano.2015.01.003
- Osteikoetxea, X., Balogh, A., Szabo-Taylor, K., Nemeth, A., Szabo, T. G., Paloczi, K., et al. (2015). Improved characterization of EV preparations based on protein to lipid ratio and lipid properties. *PLoS One* 10 (3), e0121184. doi:10.1371/journal.pone.0121184
- Paganini, C., Capasso Palmiero, U., Pocsfalvi, G., Touzet, N., Bongiovanni, A., and Arosio, P. (2019). Scalable production and isolation of extracellular vesicles: Available sources and lessons from current industrial bioprocesses. *Biotechnol. J.* 14 (10), e1800528. doi:10.1002/biot.201800528
- Pan, Q., Fouraschen, S. M., de Ruiter, P. E., Dinjens, W. N., Kwekkeboom, J., Tilanus, H. W., et al. (2014). Detection of spontaneous tumorigenic transformation during culture expansion of human mesenchymal stromal cells. *Exp. Biol. Med. (Maywood)* 239 (1), 105–115. doi:10.1177/1535370213506802
- Paolini, L., Monguió-Tortajada, M., Costa, M., Antenucci, F., Barilani, M., Clos-Sansalvador, M., et al. (2022). Large-scale production of extracellular vesicles. *Rep. "massivEVs" ISEV workshop* 1 (10), e63. doi:10.1002/jex.2.63
- Pavon, L. F., Sibov, T. T., de Souza, A. V., da Cruz, E. F., Malheiros, S. M. F., Cabral, F. R., et al. (2018). Tropism of mesenchymal stem cell toward CD133(+) stem cell of glioblastoma *in vitro* and promote tumor proliferation *in vivo*. *Stem Cell Res. Ther.* 9 (1), 310. doi:10.1186/s13287-018-1049-0
- Raposo, G., and Stoorvogel, W. (2013). Extracellular vesicles: Exosomes, microvesicles, and friends. *J. Cell Biol.* 200 (4), 373–383. doi:10.1083/jcb.201211138
- Rohde, E., Pachler, K., and Gimona, M. (2019). Manufacturing and characterization of extracellular vesicles from umbilical cord-derived mesenchymal stromal cells for clinical testing. *Cytotherapy* 21 (6), 581–592. doi:10.1016/j.jcyt.2018.12.006
- Rojewski, M. T., Fekete, N., Baila, S., Nguyen, K., Furst, D., Antwiler, D., et al. (2013). GMP-compliant isolation and expansion of bone marrow-derived MSCs in the closed, automated device quantum cell expansion system. *Cell Transpl.* 22 (11), 1981–2000. doi:10.3727/096368912X657990
- Rojewski, M. T., Lotfi, R., Gjerde, C., Mustafa, K., Veronesi, E., Ahmed, A. B., et al. (2019). Translation of a standardized manufacturing protocol for mesenchymal stromal cells: A systematic comparison of validation and manufacturing data. *Cytotherapy* 21 (4), 468–482. doi:10.1016/j.jcyt.2019.03.001
- Shao, L., Zhang, Y., Lan, B., Wang, J., Zhang, Z., Zhang, L., et al. (2017). MiRNA-Sequence indicates that mesenchymal stem cells and exosomes have similar mechanism to enhance cardiac repair. *Biomed. Res. Int.* 2017, 1–9. doi:10.1155/2017/4150705
- Soler, R., Orozco, L., Munar, A., Huguet, M., Lopez, R., Vives, J., et al. (2016). Final results of a phase I-II trial using *ex vivo* expanded autologous Mesenchymal Stromal Cells for the treatment of osteoarthritis of the knee confirming safety and suggesting cartilage regeneration. *Knee* 23 (4), 647–654. doi:10.1016/j.knee.2015.08.013
- Staat, W. D., Fok, K. F., Zutter, M. M., Adams, S. P., Rodriguez, B. A., and Santoro, S. A. (1991). Identification of a tetrapeptide recognition sequence for the alpha 2 beta 1 integrin in collagen. *J. Biol. Chem.* 266 (12), 7363–7367. doi:10.1016/s0021-9258(20)89455-1
- Stenberg, P. E., McEver, R. P., Shuman, M. A., Jacques, Y. V., and Bainton, D. F. (1985). A platelet alpha-granule membrane protein (GMP-140) is expressed on the plasma membrane after activation. *J. Cell Biol.* 101 (3), 880–886. doi:10.1083/jcb.101.3.880
- Stultz, B. G., McGinnis, K., Thompson, E. E., Lo Surdo, J. L., Bauer, S. R., and Hursh, D. A. (2016). Chromosomal stability of mesenchymal stromal cells during *in vitro* culture. *Cytotherapy* 18 (3), 336–343. doi:10.1016/j.jcyt.2015.11.017
- Taylor, J., Azimi, I., Monteith, G., and Bewaw, M. (2020). Ca(2+) mediates extracellular vesicle biogenesis through alternate pathways in malignancy. *J. Extracell. Vesicles* 9 (1), 1734326. doi:10.1080/20013078.2020.1734326
- Testi, R., Pulcinelli, F., Frati, L., Gazzaniga, P. P., and Santoni, A. (1990). CD69 is expressed on platelets and mediates platelet activation and aggregation. *J. Exp. Med.* 172 (3), 701–707. doi:10.1084/jem.172.3.701
- Thery, C., Witwer, K. W., Aikawa, E., Alcaraz, M. J., Anderson, J. D., Andriantsitohaina, R., et al. (2018). Minimal information for studies of extracellular vesicles 2018 (MISEV2018): A position statement of the international society for extracellular vesicles and update of the MISEV2014 guidelines. *J. Extracell. Vesicles* 7 (1), 1535750. doi:10.1080/20013078.2018.1535750
- Torreggiani, E., Perut, F., Roncuzzi, L., Zini, N., Baglio, S. R., Baldini, N., et al. (2014). Exosomes: Novel effectors of human platelet lysate activity. *Eur. Cell Mater* 28, 137–151. doi:10.22203/ecm.v028a11
- Van Deun, J., Mestdagh, P., Sormunen, R., Cocquyt, V., Vermaelen, K., Vandesompele, J., et al. (2014). The impact of disparate isolation methods for extracellular vesicles on downstream RNA profiling. *J. Extracell. Vesicles* 3, 24858. doi:10.3402/jev.v3.24858
- Visnovitz, T., Osteikoetxea, X., Sodar, B. W., Mihaly, J., Lorincz, P., Vukman, K. V., et al. (2019). An improved 96 well plate format lipid quantification assay for standardisation of experiments with extracellular vesicles. *J. Extracell. Vesicles* 8 (1), 1565263. doi:10.1080/20013078.2019.1565263
- Vymetalova, L., Kucirkova, T., Knopfova, L., Pospisilova, V., Kasko, T., Lejdarova, H., et al. (2020). Large-scale automated hollow-fiber bioreactor expansion of umbilical cord-derived human mesenchymal stromal cells for neurological disorders. *Neurochem. Res.* 45 (1), 204–214. doi:10.1007/s11064-019-02925-y
- Wagner, W., Horn, P., Castoldi, M., Diehlmann, A., Bork, S., Saffrich, R., et al. (2008). Replicative senescence of mesenchymal stem cells: A continuous and organized process. *PLoS One* 3 (5), e2213. doi:10.1371/journal.pone.0002213
- Warnecke, A., Prenzl, N., Harre, J., Kohl, U., Gartner, L., Lenarz, T., et al. (2021). First-in-human intracochlear application of human stromal cell-derived extracellular vesicles. *J. Extracell. Vesicles* 10 (8), e12094. doi:10.1002/jev.2.12094
- Watson, D. C., Bayik, D., Srivatsan, A., Bergamaschi, C., Valentin, A., Niu, G., et al. (2016). Efficient production and enhanced tumor delivery of engineered extracellular vesicles. *Biomaterials* 105, 195–205. doi:10.1016/j.biomaterials.2016.07.003
- Webber, J., and Clayton, A. (2013). How pure are your vesicles? *J. Extracell. Vesicles* 2, 19861. doi:10.3402/jev.v2i0.19861



- Wiest, E. F., and Zubair, A. C. (2020). Challenges of manufacturing mesenchymal stromal cell-derived extracellular vesicles in regenerative medicine. *Cytotherapy* 22 (11), 606–612. doi:10.1016/j.jcyt.2020.04.040
- Wiklander, O. P. B., Bostancioglu, R. B., Welsh, J. A., Zickler, A. M., Murke, F., Corso, G., et al. (2018). Systematic methodological evaluation of a multiplex bead-based flow cytometry assay for detection of extracellular vesicle surface signatures. *Front. Immunol.* 9, 1326. doi:10.3389/fimmu.2018.01326
- Witwer, K. W., Van Balkom, B. W. M., Bruno, S., Choo, A., Dominici, M., Gimona, M., et al. (2019). Defining mesenchymal stromal cell (MSC)-derived small extracellular vesicles for therapeutic applications. *J. Extracell. Vesicles* 8 (1), 1609206. doi:10.1080/20013078.2019.1609206
- Yan, L., and Wu, X. (2020). Exosomes produced from 3D cultures of umbilical cord mesenchymal stem cells in a hollow-fiber bioreactor show improved osteochondral regeneration activity. *Cell Biol. Toxicol.* 36 (2), 165–178. doi:10.1007/s10565-019-09504-5
- Yoshikawa, T., Mitsuno, H., Nonaka, I., Sen, Y., Kawanishi, K., Inada, Y., et al. (2008). Wound therapy by marrow mesenchymal cell transplantation. *Plast. Reconstr. Surg.* 121 (3), 860–877. doi:10.1097/01.prs.0000299922.96006.24
- Yu, L. X., Amidon, G., Khan, M. A., Hoag, S. W., Polli, J., Raju, G. K., et al. (2014). Understanding pharmaceutical quality by design. *AAPS J.* 16 (4), 771–783. doi:10.1208/s12248-014-9598-3
- Zeringer, E., Barta, T., Li, M., and Vlassov, A. V. (2015). Strategies for isolation of exosomes. *Cold Spring Harb. Protoc.* 2015 (4), pdb.top074476–323. doi:10.1101/pdb.top074476
- Zhang, Z., Morla, A. O., Vuori, K., Bauer, J. S., Juliano, R. L., and Ruoslahti, E. (1993). The alpha v beta 1 integrin functions as a fibronectin receptor but does not support fibronectin matrix assembly and cell migration on fibronectin. *J. Cell Biol.* 122 (1), 235–242. doi:10.1083/jcb.122.1.235



## OPEN ACCESS

## EDITED BY

Marco P. Monopoli,  
Royal College of Surgeons in Ireland,  
Ireland

## REVIEWED BY

Anjaneyulu Dirisala,  
Innovation Centre of NanoMedicine  
(iCONM), Japan  
Nazende Günday-Türeli,  
MyBiotech GmbH, Germany

## \*CORRESPONDENCE

Francesco Cellesi,  
✉ francesco.cellesi@polimi.it

RECEIVED 25 April 2023

ACCEPTED 16 May 2023

PUBLISHED 25 May 2023

## CITATION

Porello I and Cellesi F (2023), Intracellular  
delivery of therapeutic proteins. New  
advancements and future directions.  
*Front. Bioeng. Biotechnol.* 11:1211798.  
doi: 10.3389/fbioe.2023.1211798

## COPYRIGHT

© 2023 Porello and Cellesi. This is an  
open-access article distributed under the  
terms of the [Creative Commons  
Attribution License \(CC BY\)](#). The use,  
distribution or reproduction in other  
forums is permitted, provided the original  
author(s) and the copyright owner(s) are  
credited and that the original publication  
in this journal is cited, in accordance with  
accepted academic practice. No use,  
distribution or reproduction is permitted  
which does not comply with these terms.

# Intracellular delivery of therapeutic proteins. New advancements and future directions

Ilaria Porello and Francesco Cellesi\*

Department of Chemistry, Materials and Chemical Engineering "G. Natta", Politecnico di Milano, Milan, Italy

Achieving the full potential of therapeutic proteins to access and target intracellular receptors will have enormous benefits in advancing human health and fighting disease. Existing strategies for intracellular protein delivery, such as chemical modification and nanocarrier-based protein delivery approaches, have shown promise but with limited efficiency and safety concerns. The development of more effective and versatile delivery tools is crucial for the safe and effective use of protein drugs. Nanosystems that can trigger endocytosis and endosomal disruption, or directly deliver proteins into the cytosol, are essential for successful therapeutic effects. This article aims to provide a brief overview of the current methods for intracellular protein delivery to mammalian cells, highlighting current challenges, new developments, and future research opportunities.

## KEYWORDS

intracellular delivery, therapeutic proteins, protein delivery, polymeric nanocarriers, cellpenetrating peptides, protein resurfacing

## 1 Introduction

In the last years, protein-based therapeutics have gained an increasing interest in all areas of medicine (Lv et al., 2019; Zhang S. et al., 2020), attracting the attention of the major pharmaceutical industries (Ren et al., 2022; Pandya and Patravale, 2021), due to their remarkable potentials for treatment, diagnosis, and even prevention (Pakulska et al., 2016; Sá et al., 2021; Tan et al., 2021) of several human pathologies (Liu et al., 2022). Protein therapeutics show notable pharmacological efficacy (Pakulska et al., 2016; Liu X. et al., 2019) combined with high therapeutic potency and selectivity with respect to traditional low molecular weight drugs (Cheng, 2021). Compared to small synthetic molecules (Mitrugotri et al., 2014; Slasnikova et al., 2018), proteins offer the advantage to be active and effective at lower concentration with high substrate specificity, favoring minimal adverse effects (Leader et al., 2008) and reduced risks of off targets (Hou et al., 2016; Gao et al., 2018).

Previous studies show that most attractive targets are typically located inside the cell (Postupalenko et al., 2015; Tan et al., 2022), thus, in order to exploit full potential of protein-based therapeutics, intracellular protein delivery is fundamental to target intracellular biomolecules (Gu et al., 2011; Mitrugotri et al., 2014; Scaletti et al., 2018; Liu X. et al., 2019; Lv et al., 2019). This represent one of the major challenges to overcome since proteins are large and complex biomolecules (Lee et al., 2019; Goswami et al., 2020; Raman et al., 2021; Davis et al., 2022), with markedly hydrophilic features (Lv et al., 2020), resulting in poor cell membrane permeability (Postupalenko et al., 2015; Wang and Yu, 2020). Hence,

**TABLE 1** Examples of therapeutic proteins with intracellular target.

Therapeutic protein		Advantages	Cells/Animal model	References
Clustered regularly interspaced short palindromic repeat-associated nuclease Cas9	CRISPR-Cas9	Gene editing	Human U2OS cells, T-cell	Zuris et al. (2015), Wang et al. (2016), Stadtmayer et al. (2020)
CRISPR-Cas9-single guide RNA complex	CRISPR-Cas9-sgRNA	Gene editing	Human U2OS-EGFP cells, U2OS-EGFP xenograft tumors in nude mice	Sun et al. (2015)
Transcription activator-like effector nuclease	TALEN	Gene editing	HEK 293T cells, human T-cell	Zuris et al. (2015), Stadtmayer et al. (2020)
Antigen from enterovirus 71	VP <sub>1</sub>	Cellular vaccines	BALB/c mice	Qiao et al. (2018)
Protein phosphatase 1B	Ppase 1b	Suppresses tumor necrosis factor- $\alpha$ -induced systemic inflammatory response	HEK 293T cells, mouse model	Yu et al. (2021)
Ribonuclease A	RNase A	Toxic effects in cells	MSC, CD4 <sup>+</sup> T-cell, cancer cells, HeLa cells	Wang et al. (2014), Liew et al. (2020), Barrios et al. (2022)
Saporin	Sap	Blocks the synthesis of proteins in cells	MSC, CD4 <sup>+</sup> T-cell, cancer cells	Wang et al. (2014), Barrios et al. (2022)
Cre recombinase	Cre	Induce site-specific DNA recombination	HEK cells, HeLa cells, MDA-MB-31 cells, RAW 264.7 cells, mammalian cells, HEK 293T cells	Cronican et al. (2010), Kaczmarczyk et al. (2011), Zuris et al. (2015), Goswami et al. (2023)
Caspase-8	CASP8	Apoptosis-inducing protein Susceptible to inactivation during delivery process	HEK 293T cells	Kaczmarczyk et al. (2011)
TRAIL protein	TRAIL	Amplify apoptotic signal	Cancer cells	Sun et al. (2016)
Caspase 3	CASP3	Apoptosis-inducing protein Susceptible to inactivation during delivery process	HeLa cells	Tang et al. (2013), Ventura et al. (2015)
TRAIL Apo2 ligand	TRAIL-Apo2	Cytotoxic protein	C6 glioma cells	Prasetyanto et al. (2016)
Onconase	Onc	Cytotoxic protein	C6 glioma cells	Prasetyanto et al. (2016)

the not spontaneous crossing of the anionic-hydrophobic cell membrane (Mulgrew-Nesbitt et al., 2006) will limit the currently marketed protein drugs to extracellular targets (Marschall et al., 2014; Mitragotri et al., 2014; Slastnikova et al., 2018; Gaston et al., 2019; Qin et al., 2019).

The objective of this concise review is to outline the existing techniques for delivering proteins inside mammalian cells, aiming to highlight the current challenges, recent advancements, and potential research prospects in this field.

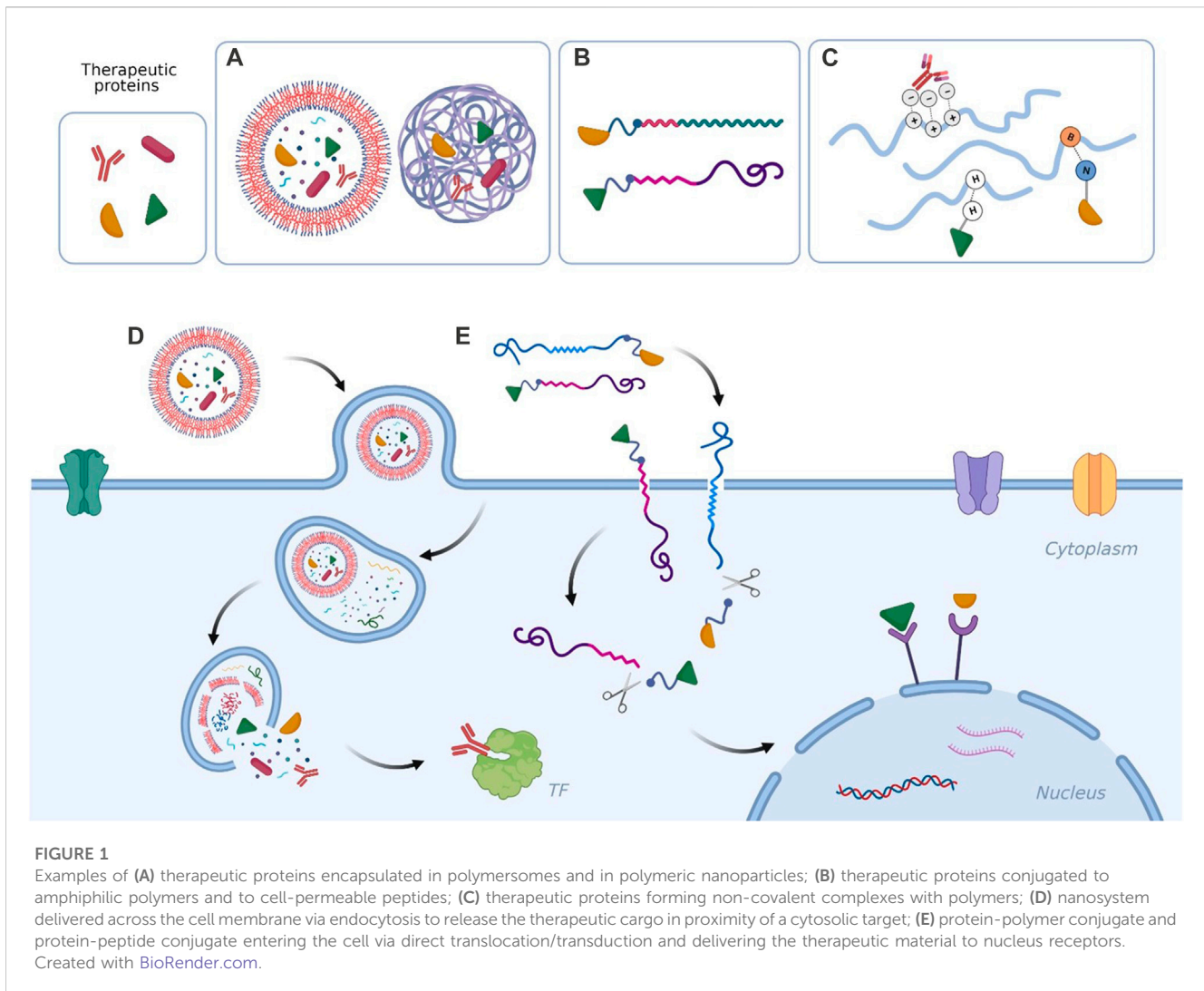
## 2 Developments and challenges in intracellular protein delivery

Different exogenous proteins have been recently explored for intracellular delivery, to modulate cell function and fate, by targeting disease-relevant intracellular receptors. Various strategies for intracellular targeting of antibodies, their fragments, or antibody-like molecules have been extensively reported in other works (Stewart et al., 2016; Slastnikova et al., 2018; Xie et al., 2020). Due to their remarkable specificity and affinity for a target molecule, antibodies are widely used for inhibiting specific activity and for diagnostics, as well as for basic experimental tools, given their role in unveiling cell signaling pathways and

diseases mechanisms. Moreover, other therapeutic proteins have been investigated for targeting intracellular sites, including systems for genome editing, induction of apoptosis or toxicity, and blocking specific protein expression, as summarized in Table 1.

The clinical applications of these protein drugs face several limitations in terms of delivery efficacy, stability, and final intracellular activity. Additional obstacles, such as fast enzymatic degradation in the bloodstream (Yan et al., 2022) and possible immune system response [common to therapeutic proteins for extracellular delivery (Parodi et al., 2017; Moncalvo et al., 2020)], must be considered.

Although delivery vehicles can help transporting proteins across cell membranes (Luther et al., 2020), the limited number of binding sites on protein surface represents a key issue that hinders the efficient transport of the cargo proteins by the appropriate carrier (Lv et al., 2020). In fact, the surface of proteins is notoriously heterogeneous, being covered by cationic, anionic, and hydrophobic groups. For this reason, carriers often rely on covalent conjugation of functional molecules (Loibl and Gianni, 2017), although critical disadvantages of such systems include the limited availability of residues for conjugation, potential effects on protein folding and function (Weiner, 2015) [given their sensitivity to chemical modifications (Zhang et al., 2018)], and complex workflow steps. Moreover, cellular internalization often brings



the nanocarrier to the cytoplasm via endosomes, by means of naturally occurring endocytosis processes, such as clathrin-mediated endocytosis (Kaksonen et al., 2006), caveolae-mediated endocytosis (Nabi and Le, 2003) or micropinocytosis (Kerr and Teasdale, 2009). Endosomes will ultimately be transformed into lysosomes, with a consequent increase of the environment acidity and the secretion of various proteases (Niamsuphap et al., 2020), causing protein degradation. Nonetheless, endosomal discharge is generally an inefficient process, with only ~1% of the total cargo being released intact into the cytoplasm excluding deterioration or expulsion by exocytosis (Stewart et al., 2016). Non-specific clearance by the reticuloendothelial system (RES) after systemic administration of protein-loaded carriers generally causes a significant decrease of the delivery efficiency into the target tissues. To address this issue, strategies as a transient stealth coating of liver reticuloendothelial cells by two-arm-PEG-oligopeptide may be effective in preventing the clearance of nonviral and viral nanovectors by the liver sinusoidal endothelium (Dirisala et al., 2020).

Therefore, the development of efficient and versatile delivery strategies is crucial for an effective use of protein drugs (Feng et al.,

2022). They need to reach cytoplasmic targets safely (Wang and Yu, 2020) by encapsulating the desired cargo into cell-degradable nanocarriers (Tsao et al., 2020; Liu et al., 2022), able to trigger endocytosis and endosomal disruption (Zhang et al., 2018), or capable to directly deliver proteins into the cytosol (Sun et al., 2022).

### 3 Intracellular protein delivery techniques: An overview

During the past decade numerous prominent techniques have been proposed for intracellular delivery of proteins (Fu et al., 2014; Bruce and McNaughton, 2017; Ray et al., 2017; Tian et al., 2022), involving physical methods to cross cell membrane, protein chemical modification and protein transport through carriers (Scaletti et al., 2018; Lee et al., 2019; Goswami et al., 2020) or a combination of the three types. Some examples of the strategies proposed in the next sections are depicted in Figure 1.

In most cases, model proteins have been tested rather than more expensive therapeutic proteins, which are often difficult to track both *in vitro* and *in vivo*. Fluorescent albumin and IgG antibody



(Tian et al., 2013; Sarker et al., 2014; Liew et al., 2020; Barrios et al., 2022; Davis et al., 2022), (enhanced) green fluorescent protein (GFP) (Fuchs and Raines, 2007; Kaczmarczyk et al., 2011; Sarker et al., 2014; Zuris et al., 2015; Kube et al., 2017; Liew et al., 2020; Davis et al., 2022), streptavidin (Shi et al., 2017; Davis et al., 2022), horseradish peroxidase (DePorter and McNaughton, 2014), lysozyme (Tian et al., 2013), and ovalbumin (Goswami et al., 2023) are among the typical model proteins used.

### 3.1 Physical membrane crossing methods

Most of the physical approaches for overcoming cell membrane deal with chemical (Stewart et al., 2018) membrane disruption (Mukherjee et al., 2018) or perforation (Chen N. et al., 2022). Although membrane perforation with electroporation (Mukherjee et al., 2018) and microinjection (Keppeke et al., 2015; Chen N. et al., 2022) or sonoporation (Togtema et al., 2012) is the most straightforward method for cytosolic delivery, these strategies are highly efficient in *in vitro* studies (Tan et al., 2022), but generally toxic, only suitable for introducing a small number of specific proteins into incubated cells and can hardly be used *in vivo*.

### 3.2 Chemical modifications of proteins

Protein modification strategy directly features protein with membrane-permeable ligands, such as cell penetrating peptides (Dixon et al., 2016; Su et al., 2018), chimeric peptides (Yu et al., 2021), cationic peptides or polymers (Su et al., 2018), amphiphilic polymers (Liu X. et al., 2019) and protein transduction domains (Caffrey et al., 2016). Alternatively, the chemical alteration consists in supercharging the protein with cationic groups (Horn and Obermeyer, 2021). The biomodification success depends on the availability of reactive protein handles, located on their surface as free amino acid sides, including amine, hydroxy and thiol groups, or functional moieties present at the protein termini (Stephanopoulos and Francis, 2011). There are many covalent methods available for the modification of protein reactive groups including click chemistry, oxime/hydrazone chemistry (Lutz and Börner, 2008), and strategies such as grafting-to, grafting-from and grafting-through for bioconjugation of proteins with polymers (Stevens et al., 2021).

The amended proteins are capable of entering the cells via cellular membrane transduction and translocation (Horn and Obermeyer, 2021) or through endocytosis, achieving high cytosolic delivery (Posey and Tew, 2018) by increased membrane affinity. Sometime covalent modification of proteins is also applied with anionic species, such as carboxylic acid (Wang and Yu, 2020), boronic acid (Liu X. et al., 2019), anionic peptides and polymers (Zelikin et al., 2016), or nucleic acids (Eltoukhy et al., 2014) to strengthen their negative charge intensity, and thus increase their binding affinity with suitable positively charged carriers that enhance endocytosis (Lv et al., 2020). However, covalent modifications often result in a distribution of products with different degrees of modification, owing to chemically identical active sites distributed on the protein surface (Horn and

Obermeyer, 2021). Protein alteration can be designed to be reversible, via moieties which can be cleaved by intracellular stimuli such as reduction (Qian et al., 2018), reactive oxygen species (ROS) (Liu X. et al., 2019), enzyme (Chang et al., 2019) and endo/lysosomal acidity (Maier and Wagner, 2012), however covalent modifications may alter protein structures and related biofunctions (Zhou et al., 2019; Tan et al., 2022). Moreover, the technique requires complex synthesis and purification procedures which may impede the potential clinical translation (Frokjaer and Otzen, 2005; Stevens et al., 2021). A meaningful example of protein alteration for cytosolic delivery involves charge-conversional modification of cationic lysine surface moieties by cyclic anhydrides (Obermeyer et al., 2016; Zhang M. et al., 2020; Tao et al., 2020), which is pH-reversible at late endosomal pH. For instance, IgG was modified with citraconic anhydride to encapsulate it in pH-sensitive polyion micelles, capable of transferring active IgG to the nuclear envelope (Kim et al., 2016). Esterification of carboxylic acid groups of aspartate and glutamate simultaneously decrease negative charge and increase hydrophobicity, promoting direct protein translocation across the cell membrane (Sangsuwan et al., 2019).

Stable and simultaneously reversible conjugation is critical to translocate proteins across a cellular membrane and release them without losing activity (Dutta et al., 2021). Liu B. et al. (2019) developed a click chemistry approach for generating functional polymer-protein conjugate as nanoassemblies of different sizes and isoelectric points, which release in response to three different stimuli: presence of ROS, reducing environment, and pH variations. Arylboronic acid was employed for lysines modification, given the possibility of inserting a stimuli-responsive linker in the polymer-protein conjugate, required for a residue-free release (Stephanopoulos and Francis, 2011). They successfully delivered ribonuclease A (RNaseA) via endosomal escape, employing hydrogen peroxide (H<sub>2</sub>O<sub>2</sub>) as the stimulus to reverse the bioconjugation. Similarly, Dutta et al. (2021) designed a self-immolative polymer presenting activated carbonate moieties for covalent self-assembly with the lysines displayed on antibodies surface. The reactive side-chain functionalities were responsive to redox stimuli, and the encapsulated antibodies were released preserving their biological activity. However, slow macromolecular reaction kinetics due to the high acid dissociation constant (pKa) of lysine amines (Koniev and Wagner, 2015), incomplete reactivity of activated carbonate groups with lysines (Dutta et al., 2017), and competitive hydrolytic degradation of polymer, are some of the major obstacles for large biomacromolecules conjugation such as antibodies (Dutta et al., 2021). Considerable attention has been given to enhancing the endosomal escape ability of nanocarriers by incorporating pH-buffering (Lee et al., 2021), membrane-disturbing (Han et al., 2021) or fusogenic (Nishimura et al., 2014) materials. pH-responsive polymeric micelles were designed to promote electrostatic and covalent interactions with anti-nuclear pore complex antibodies (Chen P. et al., 2022). This design reached selective delivery into the cytosol and subsequent nucleus targeting was achieved in cancer cells, rather than non-cancerous cells, both *in vitro* and *in vivo*.

### 3.3 Non-covalent assembly of proteins and carriers

Alternatively, proteins could be transported by carriers through physical encapsulation or complexation. The protein cargoes can be loaded into the inner aqueous/hydrophilic cavities or pores (Tang et al., 2017; Wang and Yu, 2020) of synthetic nanocarriers (Qin et al., 2019), such as liposomes (Wang et al., 2016), polymers (Zhou et al., 2019), polymersomes (Jiang et al., 2018), organic or inorganic nanoparticles (Leader et al., 2008; Zelikin et al., 2016; Lee et al., 2019; Zhang S. et al., 2020), and nanogels (Dutta et al., 2017). These nanomaterials allow intracellular delivery of native proteins without any chemical modification, preventing denaturation (Dutta et al., 2017). This approach is generally suitable for *in vivo* applications (Lv et al., 2020), although it often requires complex syntheses and purification processes with low protein loading efficiency (Liu et al., 2022). On the other hand, protein-based nanocomplexes can be formed via non-covalent interactions with polymers, functionalized nanoparticles, peptides, and lipids. Amino acid residues may interact via salt bridge, boronate-nitrogen (Liu X. et al., 2019; Liu et al., 2022) or metal-nitrogen (Ren et al., 2022) coordination interactions, electrostatic forces (Rui et al., 2019), inter-macromolecular ionic, hydrophobic (He et al., 2019), and hydrogen-bond interactions (Lv et al., 2020). Such assemblies should provide stability during cell membrane penetration and protein release (Yu et al., 2018), via reversible binding (Stevens et al., 2021). They are obtained via simple mixing under mild aqueous conditions, avoiding complex purification steps, without altering the proteins native functions (Posey and Tew, 2018; Lv et al., 2019; Lv et al., 2020; Pasut, 2014). While chemical modification is often limited by the vast heterogeneity in composition, structure, and stability of proteins, non-covalent strategies can be applied to a wide variety of protein cargoes (Posey and Tew, 2018).

In the last years, different nanocomplexes formed via simple self-assembly have been developed (Liu X. et al., 2019; Lv et al., 2020; Wang and Yu, 2020). Hyperbranched polymer with phenylboronic acid (PBA) was developed to coordinate with protein cargoes (Liu et al., 2022), and degrade by over-produced  $H_2O_2$  in cancer cells, releasing the proteins (BSA and a monoclonal antibody). Following a similar idea, boronated polymers formed a complex with proteins via nitrogen-boronate coordination and ionic interaction (Yan et al., 2022). Promising cytosolic delivery of cargo proteins and peptides was achieved with maintained bioactivity (Liu X. et al., 2019; Lv et al., 2020). Relying on the same principles, guanidyl groups can strongly bind the residual moieties of protein by a combination of salt bridge and hydrogen bonding interactions. When grafting guanidyl ligands onto nanoparticles or polymers at a high ligand density, the multivalent effect of guanidyl groups allows efficient protein binding (Hatano et al., 2016) and endocytosis (Stanzl et al., 2013; McKinlay et al., 2016). Lv et al. (2020) synthesized guanidyl-grafted polyethylenimine (PEI) to form positively charged nanoparticles with BSA, for an efficient cell membrane penetration. Protein delivery systems poorly performing in serum-containing media were improved by introducing carbamoylated guanidine-containing polymers (Barrios et al., 2022), by chemical modification with fluoros ligands (Zhang et al., 2018) and zwitterionic moieties (Wu et al., 2019), thus decreasing the positive charge density of the nanocomplex (Rui

et al., 2019). A rational guanidine modification approach also enhanced the efficiency of proteins delivery in serum-containing media (Li et al., 2015; Keller et al., 2016; Davis et al., 2022). Tan et al. (2022) proposed boronate-decorated poly-L-lysine (PLL) to efficiently deliver cargo proteins into living cells. Positively charged PLL spontaneously form complexes with negatively charged proteins (Abbas et al., 2017). These nanoparticles can release proteins by intracellular ROS after internalization, with maintained activity and minimal toxicity. Amphipathic poly-b-peptides (Pbps), with designable structures, controllable molecular weights, and proteolysis resistant properties, were also investigated for protein delivery (Ren et al., 2022). Pbps amphipathic and positively charged structures promote non-covalent interactions with proteins and membrane disruption (Tezgel et al., 2017), showing successful delivery of EGFP into osteosarcoma cells.

## 4 Discussion

Significant progress has been made in the field of intracellular delivery in recent years, however the clinical applications of protein drugs are still limited by their real delivery efficacy, stability, and intracellular activity. Therefore, research is moving in various directions with the aim of identifying more appropriate delivery tools. The delivery of proteins into cells is challenging due to two major requirements: efficient uptake and rapid cytosolic delivery without being trapped in the endosomes. Many research efforts have been made regarding protein conjugation with cell-penetrating peptides, and more recently with multifunctional chimeric peptides, which can be designed to accomplish different tasks during cellular uptake and endosomal escape. Other methods for the delivery of purified proteins include protein chemical modification and resurfacing approaches. These methods often need to overcome the limits of toxicity and possible immune activation. Nanocarrier-based protein delivery approaches, such as liposomes, polymer-based nanocarriers, and nanoparticles, are attractive due to the tunable properties of the nanomaterials. It is important to consider additional obstacles such as the rapid enzymatic degradation of therapeutic proteins in the bloodstream and potential immune system responses (Moncalvo et al., 2020). Meanwhile, a significant effort has been dedicated to the design of engineered proteins that can be used to modulate intracellular targets (Miersch and Sidhu, 2016). Co-delivery of protein and nucleic acids has also been examined in the context of targeted genomic editing (Bruce and McNaughton, 2017). Moreover, new intracellular targets within subcellular compartments may be identified for a therapeutic use (Fasciani et al., 2022). Delivery of transcription factors also holds the potential to revolutionize the biomedical field (Ulasov et al., 2018), although the major challenge lies in the delivery process, as it requires proteins transport not only across the cell membrane and the endosome, but also into the nucleus, which represents an additional barrier to overcome.

The field of intracellular protein delivery is still a relatively young area of research and further advancements in this field will require the integration of chemistry, materials science, formulation science, nanomedicine, and biomedical engineering. Enabling therapeutic proteins to access and target intracellular receptors has enormous potential for improving human health and fighting

diseases, as well as for gaining knowledge in this significant area of research.

## Author contributions

All authors listed have made a substantial, direct, and intellectual contribution to the work and approved it for publication.

## Funding

This research was funded by Regione Lombardia (POR FESR 2014–2020) within the framework of the NEWMED project (ID 1175999).

## References

- Abbas, M., Zou, Q., Li, S., and Yan, X. (2017). Self-assembled peptide- and protein-based nanomaterials for antitumor photodynamic and photothermal therapy. *Adv. Mater.* 29, 1605021. doi:10.1002/adma.201605021
- Barrios, A., Estrada, M., and Moon, J. H. (2022). Carbamoylated guanidine-containing polymers for non-covalent functional protein delivery in serum-containing media. *Angew. Chem. - Int. Ed.* 61, e202116722. doi:10.1002/anie.202116722
- Bruce, V. J., and McNaughton, B. R. (2017). Inside job: Methods for delivering proteins to the interior of mammalian cells. *Cell. Chem. Biol.* 24, 924–934. doi:10.1016/j.chembiol.2017.06.014
- Caffrey, L. M., Deronde, B. M., Minter, L. M., and Tew, G. N. (2016). Mapping optimal charge density and length of ROMP-based PTDMs for siRNA internalization. *Biomacromolecules* 17, 3205–3212. doi:10.1021/acs.biomac.6b00900
- Chang, J., Cai, W., Liang, C., Tang, Q., Chen, X., Jiang, Y., et al. (2019). Enzyme-instructed activation of pro-protein therapeutics *in vivo*. *J. Am. Chem. Soc.* 141, 18136–18141. doi:10.1021/jacs.9b08669
- Chen, N., He, Y., Zang, M., Zhang, Y., Lu, H., Zhao, Q., et al. (2022). Approaches and materials for endocytosis-independent intracellular delivery of proteins. *Biomaterials* 286, 121567. doi:10.1016/j.biomaterials.2022.121567
- Chen, P., Yang, W., Hong, T., Miyazaki, T., Dirisala, A., Kataoka, K., et al. (2022). Nanocarriers escaping from hyperacidified endo/lysosomes in cancer cells allow tumor-targeted intracellular delivery of antibodies to therapeutically inhibit c-MYC. *Biomaterials* 288, 121748. doi:10.1016/j.biomaterials.2022.121748
- Cheng, Y. (2021). Design of polymers for intracellular protein and peptide delivery. *Chin. J. Chem.* 39, 1443–1449. doi:10.1002/cjoc.202000655
- Cronican, J. J., Thompson, D. B., Beier, K. T., McNaughton, B. R., Cepko, C. L., and Liu, D. R. (2010). Potent delivery of functional proteins into mammalian cells *in vitro* and *in vivo* using a supercharged protein. *ACS Chem. Biol.* 5, 747–752. doi:10.1021/cb1001153
- Davis, H. C., Posey, N. D., and Tew, G. N. (2022). Protein binding and release by polymeric cell-penetrating peptide mimics. *Biomacromolecules* 23, 57–66. doi:10.1021/acs.biomac.1c00929
- DePorter, S. M., and McNaughton, B. R. (2014). Engineered M13 bacteriophage nanocarriers for intracellular delivery of exogenous proteins to human prostate cancer cells. *Bioconjug Chem.* 25, 1620–1625. doi:10.1021/bc500339k
- Dirisala, A., Uchida, S., Toh, K., Li, J., Osawa, S., Tockary, T. A., et al. (2020). Transient stealth coating of liver sinusoidal wall by anchoring two-armed PEG for retargeting nanomedicines. *Sci. Adv.* 6, eabb8133. doi:10.1126/sciadv.abb8133
- Dixon, J. E., Osman, G., Morris, G. E., Markides, H., Rotherham, M., Bayoussef, Z., et al. (2016). Highly efficient delivery of functional cargoes by the synergistic effect of GAG binding motifs and cell-penetrating peptides. *Proc. Natl. Acad. Sci. U. S. A.* 113, E291–E299. doi:10.1073/pnas.1518634113
- Dutta, K., Hu, D., Zhao, B., Ribbe, A. E., Zhuang, J., and Thayumanavan, S. (2017). Templated self-assembly of a covalent polymer network for intracellular protein delivery and traceless release. *J. Am. Chem. Soc.* 139, 5676–5679. doi:10.1021/jacs.7b01214
- Dutta, K., Kanjilal, P., Das, R., and Thayumanavan, S. (2021). Synergistic interplay of covalent and non-covalent interactions in reactive polymer nanoassembly facilitates intracellular delivery of antibodies. *Angew. Chem. - Int. Ed.* 60, 1821–1830. doi:10.1002/anie.202010412
- Eltoukhy, A. A., Chen, D., Veisoh, O., Pelet, J. M., Yin, H., Dong, Y., et al. (2014). Nucleic acid-mediated intracellular protein delivery by lipid-like nanoparticles. *Biomaterials* 35, 6454–6461. doi:10.1016/j.biomaterials.2014.04.014
- Fasciani, I., Carli, M., Petragliano, F., Colaanni, F., Aloisi, G., Maggio, R., et al. (2022). GPCRs in intracellular compartments: New targets for drug discovery. *Biomolecules* 12, 1343. doi:10.3390/biom12101343
- Feng, Y., Guo, Z., Chen, J., Zhang, S., Wu, J., Tian, H., et al. (2022). Cationic polymer synergizing with a disulfide-containing enhancer achieved efficient nucleic acid and protein delivery. *Biomater. Sci.* 10, 6230–6243. doi:10.1039/d2bm01211a
- Frokjaer, S., and Otzen, D. E. (2005). Protein drug stability: a formulation challenge. *Nat. Rev. Drug Discov.* 4, 298–306. doi:10.1038/nrd1695
- Fu, A., Tang, R., Hardie, J., Farkas, M. E., and Rotello, V. M. (2014). Promises and pitfalls of intracellular delivery of proteins. *Bioconjug Chem.* 25, 1602–1608. doi:10.1021/bc500330j
- Fuchs, S. M., and Raines, R. T. (2007). Arginine grafting to endow cell permeability. *ACS Chem. Biol.* 2, 167–170. doi:10.1021/cb600429k
- Gao, X., Tao, Y., Lamas, V., Huang, M., Yeh, W. H., Pan, B., et al. (2018). Treatment of autosomal dominant hearing loss by *in vivo* delivery of genome editing agents. *Nature* 553, 217–221. doi:10.1038/nature25164
- Gaston, J., Maestrali, N., Lalle, G., Gagnaire, M., Masiero, A., Dumas, B., et al. (2019). Intracellular delivery of therapeutic antibodies into specific cells using antibody-peptide fusions. *Sci. Rep.* 9, 18688. doi:10.1038/s41598-019-55091-0
- Goswami, R., Jeon, T., Nagaraj, H., Zhai, S., and Rotello, V. M. (2020). Accessing intracellular targets through nanocarrier-mediated cytosolic protein delivery. *Trends Pharmacol. Sci.* 41, 743–754. doi:10.1016/j.tips.2020.08.005
- Goswami, R., Lehot, V., Çiçek, Y. A., Nagaraj, H., Jeon, T., Nguyen, T., et al. (2023). Direct cytosolic delivery of citraconylated proteins. *Pharmaceutics* 15, 218. doi:10.3390/pharmaceutics15010218
- Gu, Z., Biswas, A., Zhao, M., and Tang, Y. (2011). Tailoring nanocarriers for intracellular protein delivery. *Chem. Soc. Rev.* 40, 3638–3655. doi:10.1039/c0cs00227e
- Han, X., Zhang, H., Butowska, K., Swingle, K. L., Alameh, M. G., Weissman, D., et al. (2021). An ionizable lipid toolbox for RNA delivery. *Nat. Commun.* 12, 7233. doi:10.1038/s41467-021-27493-0
- Hatano, J., Okuro, K., and Aida, T. (2016). Photoinduced bioorthogonal 1,3-dipolar poly-cycloaddition promoted by oxanionic substrates for spatiotemporal operation of molecular glues. *Angew. Chem.* 128, 201–206. doi:10.1002/ange.201507987
- He, X., Long, Q., Zeng, Z., Yang, L., Tang, Y., and Feng, X. (2019). Simple and efficient targeted intracellular protein delivery with self-assembled nanovehicles for effective cancer therapy. *Adv. Funct. Mater.* 29, 1906187. doi:10.1002/adfm.201906187
- Horn, J. M., and Obermeyer, A. C. (2021). Genetic and covalent protein modification strategies to facilitate intracellular delivery. *Biomacromolecules* 22, 4883–4904. doi:10.1021/acs.biomac.1c00745
- Hou, Y., Yuan, J., Zhou, Y., Yu, J., and Lu, H. (2016). A concise approach to site-specific topological protein-poly(amino acid) conjugates enabled by *in situ*-generated functionalities. *J. Am. Chem. Soc.* 138, 10995–11000. doi:10.1021/jacs.6b05413
- Jiang, Y., Yang, W., Zhang, J., Meng, F., and Zhong, Z. (2018). Protein toxin chaperoned by LRP-1-targeted virus-mimicking vesicles induces high-efficiency glioblastoma therapy *in vivo*. *Adv. Mater.* 30, 1800316. doi:10.1002/adma.201800316
- Kaczmarczyk, S. J., Sitaraman, K., Young, H. A., Hughes, S. H., and Chatterjee, D. K. (2011). Protein delivery using engineered virus-like particles. *Proc. Natl. Acad. Sci. U. S. A.* 108, 16998–17003. doi:10.1073/pnas.1101874108

## Conflict of interest

The authors declare that the research was conducted in the absence of any commercial or financial relationships that could be construed as a potential conflict of interest.

## Publisher's note

All claims expressed in this article are solely those of the authors and do not necessarily represent those of their affiliated organizations, or those of the publisher, the editors and the reviewers. Any product that may be evaluated in this article, or claim that may be made by its manufacturer, is not guaranteed or endorsed by the publisher.



- Kaksonen, M., Toret, C. P., and Drubin, D. G. (2006). Harnessing actin dynamics for clathrin-mediated endocytosis. *Nat. Rev. Mol. Cell. Biol.* 7, 404–414. doi:10.1038/nrm1940
- Keller, M., Kuhn, K. K., Einsiedel, J., Hübner, H., Biselli, S., Mollereau, C., et al. (2016). Mimicking of arginine by functionalized  $\omega$ -carbamoylated arginine as a new broadly applicable approach to labeled bioactive peptides: High affinity angiotensin, neuropeptide Y, neuropeptide FF, and neurotensin receptor ligands as examples. *J. Med. Chem.* 59, 1925–1945. doi:10.1021/acs.jmedchem.5b01495
- Keppeke, G. D., Andrade, L. E. C., Grieshaber, S. S., and Chan, E. K. L. (2015). Microinjection of specific anti-LMPDH2 antibodies induces disassembly of cytoplasmic rods/rings that are primarily stationary and stable structures. *Cell. Biosci.* 5, 1. doi:10.1186/2045-3701-5-1
- Kerr, M. C., and Teasdale, R. D. (2009). Defining macropinocytosis. *Traffic* 10, 364–371. doi:10.1111/j.1600-0854.2009.00878.x
- Kim, A., Miura, Y., Ishii, T., Mutaf, O. F., Nishiyama, N., Cabral, H., et al. (2016). Intracellular delivery of charge-converted monoclonal antibodies by combinatorial design of block/Homo polyion complex micelles. *Biomacromolecules* 17, 446–453. doi:10.1021/acs.biomac.5b01335
- Koniev, O., and Wagner, A. (2015). Developments and recent advancements in the field of endogenous amino acid selective bond forming reactions for bioconjugation. *Chem. Soc. Rev.* 44, 5495–5551. doi:10.1039/c5cs00048c
- Kube, S., Hersch, N., Naumovska, E., Gensch, T., Hendriks, J., Franzen, A., et al. (2017). Fusogenic liposomes as nanocarriers for the delivery of intracellular proteins. *Langmuir* 33, 1051–1059. doi:10.1021/acs.langmuir.6b04304
- Leader, B., Baca, J. Q., and Golan, E. D. (2008). Protein therapeutics: A summary and pharmacological classification. *Nat. Rev. Drug Discov.* 7, 21–39. doi:10.1038/nrd2399
- Lee, J., Sands, I., Zhang, W., Zhou, L., and Chen, Y. (2021). DNA-inspired nanomaterials for enhanced endosomal escape. Available at: <https://www.pnas.org/doi/pdf/10.1073/pnas.2104511118> (Accessed April 14, 2021)
- Lee, Y. W., Luther, D. C., Kretzmann, J. A., Burden, A., Jeon, T., Zhai, S., et al. (2019). Protein delivery into the cell cytosol using non-viral nanocarriers. *Theranostics* 9, 3280–3292. doi:10.7150/thno.34412
- Li, M., Schlesiger, S., Knauer, S. K., and Schmuck, C. (2015). A tailor-made specific anion-binding motif in the side chain transforms a tetrapeptide into an efficient vector for gene delivery. *Angew. Chem. - Int. Ed.* 54, 2941–2944. doi:10.1002/anie.201410429
- Liew, S. S., Zhang, C., Zhang, J., Sun, H., Li, L., and Yao, S. Q. (2020). Intracellular delivery of therapeutic proteins through N-Terminal site-specific modification. *Chem. Commun.* 56, 11473–11476. doi:10.1039/d0cc04728g
- Liu, B., Ianosi-Irimie, M., and Thayumanavan, S. (2019). Reversible click chemistry for ultrafast and quantitative formation of protein-polymer nanoassembly and intracellular protein delivery. *ACS Nano* 13, 9408–9420. doi:10.1021/acs.nano.9b04198
- Liu, X., Wu, F., Ji, Y., and Yin, L. (2019). Recent advances in anti-cancer protein/peptide delivery. *Bioconjug. Chem.* 30, 305–324. doi:10.1021/acs.bioconjug.8b00750
- Liu, X., Zhao, Z., Wu, F., Chen, Y., and Yin, L. (2022). Tailoring hyperbranched poly( $\beta$ -amino ester) as a robust and universal platform for cytosolic protein delivery. *Adv. Mater.* 34, 2108116. doi:10.1002/adma.202108116
- Loibl, S., and Gianni, L. (2017). HER2-positive breast cancer. *Lancet* 389, 2415–2429. doi:10.1016/S0140-6736(16)32417-5
- Luther, D. C., Huang, R., Jeon, T., Zhang, X., Lee, Y. W., Nagaraj, H., et al. (2020). Delivery of drugs, proteins, and nucleic acids using inorganic nanoparticles. *Adv. Drug Deliv. Rev.* 156, 188–213. doi:10.1016/j.addr.2020.06.020
- Lutz, J. F., and Börner, H. G. (2008). Modern trends in polymer bioconjugates design. *Prog. Polym. Sci. Oxf.* 33, 1–39. doi:10.1016/j.progpolymsci.2007.07.005
- Lv, J., Fan, Q., Wang, H., and Cheng, Y. (2019). Polymers for cytosolic protein delivery. *Biomaterials* 218, 119358. doi:10.1016/j.biomaterials.2019.119358
- Lv, J., Tan, E., Wang, Y., Fan, Q., Yu, J., and Cheng, Y. (2020). Tailoring guanidyl-rich polymers for efficient cytosolic protein delivery. *J. Control. Release* 320, 412–420. doi:10.1016/j.jconrel.2020.01.056
- Miersch, S., and Sidhu, S. S. (2016). Intracellular targeting with engineered proteins. *F1000 Fac. Rev.* 10(5), 1947. doi:10.12688/F1000RESEARCH.8915.1
- Maier, K., and Wagner, E. (2012). Acid-labile traceless click linker for protein transduction. *J. Am. Chem. Soc.* 134, 10169–10173. doi:10.1021/ja302705v
- Marschall, A. L. J., Zhang, C., Frenzel, A., Schirrmann, T., Hust, M., Perez, F., et al. (2014). Delivery of antibodies to the cytosol: Debunking the myths. *MABS* 6, 943–956. doi:10.4161/mabs.29268
- McKinlay, C. J., Waymouth, R. M., and Wender, P. A. (2016). Cell-penetrating, guanidinium-rich oligophosphoesters: Effective and versatile molecular transporters for drug and probe delivery. *J. Am. Chem. Soc.* 138, 3510–3517. doi:10.1021/jacs.5b13452
- Mitragotri, S., Burke, P. A., and Langer, R. (2014). Overcoming the challenges in administering biopharmaceuticals: Formulation and delivery strategies. *Nat. Rev. Drug Discov.* 13, 655–672. doi:10.1038/nrd4363
- Moncalvo, F., Martinez Espinoza, M. I., and Cellesi, F. (2020). Nanosized delivery systems for therapeutic proteins: Clinically validated technologies and advanced development strategies. *Front. Bioeng. Biotechnol.* 8, 89. doi:10.3389/fbioe.2020.00089
- Mukherjee, P., Nathamgari, S. S. P., Kessler, J. A., and Espinosa, H. D. (2018). Combined numerical and experimental investigation of localized electroporation-based cell transfection and sampling. *ACS Nano* 12, 12118–12128. doi:10.1021/acsnano.8b05473
- Mulgrew-Nesbitt, A., Diraviyam, K., Wang, J., Singh, S., Murray, P., Li, Z., et al. (2006). The role of electrostatics in protein-membrane interactions. *Biochim. Biophys. Acta Mol. Cell. Biol. Lipids* 1761, 812–826. doi:10.1016/j.bbalip.2006.07.002
- Nabi, I. R., and Le, P. U. (2003). Caveolae/raft-dependent endocytosis. *J. Cell. Biol.* 161, 673–677. doi:10.1083/jcb.200302028
- Niamsuphap, S., Fercher, C., Kumble, S., Huda, P., Mahler, S. M., and Howard, C. B. (2020). Targeting the undruggable: Emerging technologies in antibody delivery against intracellular targets. *Expert Opin. Drug Deliv.* 17, 1189–1211. doi:10.1080/17425247.2020.1781088
- Nishimura, Y., Takeda, K., Ezawa, R., Ishii, J., Ogino, C., and Kondo, A. (2014). A display of pH-sensitive fusogenic GALA peptide facilitates endosomal escape from a Bio-nanocapsule via an endocytic uptake pathway. *J. Nanobiotechnology* 12, 11. doi:10.1186/1477-3155-12-11
- Obermeyer, A. C., Mills, C. E., Dong, X. H., Flores, R. J., and Olsen, B. D. (2016). Complex coacervation of supercharged proteins with polyelectrolytes. *Soft Matter* 12, 3570–3581. doi:10.1039/c6sm00002a
- Pakulski, M. M., Miersch, S., and Shoichet, M. S. (2016). Designer protein delivery: From natural to engineered affinity-controlled release systems. *Science* 351 (6279), aac4750. doi:10.1126/science.aac4750
- Pandya, A. K., and Patravale, V. B. (2021). Computational avenues in oral protein and peptide therapeutics. *Drug Discov. Today* 26 (6), 1510–1520. doi:10.1016/j.drudis.2021.03.003
- Parodi, A., Molinaro, R., Sushnitha, M., Evangelopoulos, M., Martinez, J. O., Arrighetti, N., et al. (2017). Bio-inspired engineering of cell- and virus-like nanoparticles for drug delivery. *Biomaterials* 147, 155–168. doi:10.1016/j.biomaterials.2017.09.020
- Pasut, G. (2014). Polymers for protein conjugation. *Polymers* 6, 160–178. doi:10.3390/polym6010160
- Posey, N. D., and Tew, G. N. (2018). Associative and dissociative processes in non-covalent polymer-mediated intracellular protein delivery. *Chem. Asian J.* 13, 3351–3365. doi:10.1002/asia.201800849
- Postupalenko, V., Desplancq, D., Orlov, I., Arntz, Y., Spohner, D., Mely, Y., et al. (2015). Protein delivery system containing a nickel-immobilized polymer for multimerization of affinity-purified his-tagged proteins enhances cytosolic transfer. *Angew. Chem.* 127, 10729–10732. doi:10.1002/ange.201505437
- Prasetyanto, E. A., Bertucci, A., Septiadi, D., Corradini, R., Castro-Hartmann, P., and De Cola, L. (2016). Breakable hybrid organosilica nanocapsules for protein delivery. *Angew. Chem.* 128, 3384–3388. doi:10.1002/ange.201508288
- Qian, L., Fu, J., Yuan, P., Du, S., Huang, W., Li, L., et al. (2018). Intracellular delivery of native proteins facilitated by cell-penetrating poly(disulfide)s. *Angew. Chem.* 130, 1548–1552. doi:10.1002/ange.201711651
- Qiao, D., Liu, L., Chen, Y., Xue, C., Gao, Q., Mao, H. Q., et al. (2018). Potency of a scalable nanoparticulate subunit vaccine. *Nano Lett.* 18, 3007–3016. doi:10.1021/acs.nanolett.8b00478
- Qin, X., Yu, C., Wei, J., Li, L., Zhang, C., Wu, Q., et al. (2019). Rational design of nanocarriers for intracellular protein delivery. *Adv. Mater.* 31, 1902791. doi:10.1002/adma.201902791
- Raman, V., Van Dessel, N., Hall, C. L., Wetherby, V. E., Whitney, S. A., Kolewe, E. L., et al. (2021). Intracellular delivery of protein drugs with an autonomously lysing bacterial system reduces tumor growth and metastases. *Nat. Commun.* 12, 6116. doi:10.1038/s41467-021-26367-9
- Ray, M., Lee, Y. W., Scaletti, F., Yu, R., and Rotello, V. M. (2017). Intracellular delivery of proteins by nanocarriers. *Nanomedicine* 12, 941–952. doi:10.2217/nnm-2016-0393
- Ren, Q., Chen, Q., Ren, L., Cao, C., Liu, R., and Cheng, Y. (2022). Amphipathic poly- $\beta$ -peptides for intracellular protein delivery. *Chem. Commun.* 58, 4320–4323. doi:10.1039/d2cc00453d
- Rui, Y., Wilson, D. R., Choi, J., Varanasi, M., Sanders, K., Karlsson, J., et al. (2019). Carboxylated branched poly( $\beta$ -amino ester) nanoparticles enable robust cytosolic protein delivery and CRISPR-Cas9 gene editing. *Sci. Adv.* 5, eaay3255. doi:10.1126/sciadv.aay3255
- Sá, J. D. O., Trino, L. D., Oliveira, A. K., Lopes, A. F. B., Granato, D. C., Normando, A. G. C., et al. (2021). Proteomic approaches to assist in diagnosis and prognosis of oral cancer. *Expert Rev. Proteomics* 18, 261–284. doi:10.1080/14789450.2021.1924685
- Sangsuwan, R., Tachachartvanich, P., and Francis, M. B. (2019). Cytosolic delivery of proteins using amphiphilic polymers with 2-pyridinecarboxaldehyde groups for site-selective attachment. *J. Am. Chem. Soc.* 141, 2376–2383. doi:10.1021/jacs.8b10947
- Sarker, S. R., Hokama, R., and Takeoka, S. (2014). Intracellular delivery of universal proteins using a lysine headgroup containing cationic liposomes: Deciphering the uptake mechanism. *Mol. Pharm.* 11, 164–174. doi:10.1021/mp400363z



- Scaletti, F., Hardie, J., Lee, Y. W., Luther, D. C., Ray, M., and Rotello, V. M. (2018). Protein delivery into cells using inorganic nanoparticle-protein supramolecular assemblies. *Chem. Soc. Rev.* 47, 3421–3432. doi:10.1039/c8cs00008e
- Shi, Y., Inoue, H., Wu, J. C., and Yamanaka, S. (2017). Induced pluripotent stem cell technology: A decade of progress. *Nat. Rev. Drug Discov.* 16, 115–130. doi:10.1038/nrd.2016.245
- Slasnikova, T. A., Ulasov, A. V., Rosenkranz, A. A., and Sobolev, A. S. (2018). Targeted intracellular delivery of antibodies: The state of the art. *Front. Pharmacol.* 9, 1208. doi:10.3389/fphar.2018.01208
- Stadtmauer, E. A., Fraietta, J. A., Davis, M. M., Cohen, A. D., Weber, K. L., Lancaster, E., et al. (2020). CRISPR-engineered T cells in patients with refractory cancer. *Science* 367 (6481), eaba7365. doi:10.1126/science.aba7365
- Stanzl, E. G., Trantow, B. M., Vargas, J. R., and Wender, P. A. (2013). Fifteen years of cell-penetrating, guanidinium-rich molecular transporters: Basic science, research tools, and clinical applications. *Acc. Chem. Res.* 46, 2944–2954. doi:10.1021/ar4000554
- Stephanopoulos, N., and Francis, M. B. (2011). Choosing an effective protein bioconjugation strategy. *Nat. Chem. Biol.* 7, 876–884. doi:10.1038/nchembio.720
- Stevens, C. A., Kaur, K., and Klok, H. A. (2021). Self-assembly of protein-polymer conjugates for drug delivery. *Adv. Drug Deliv. Rev.* 174, 447–460. doi:10.1016/j.addr.2021.05.002
- Stewart, M. P., Langer, R., and Jensen, K. F. (2018). Intracellular delivery by membrane disruption: Mechanisms, strategies, and concepts. *Chem. Rev.* 118, 7409–7531. doi:10.1021/acs.chemrev.7b00678
- Stewart, M. P., Sharei, A., Ding, X., Sahay, G., Langer, R., and Jensen, K. F. (2016). *In vitro* and *ex vivo* strategies for intracellular delivery. *Nature* 538, 183–192. doi:10.1038/nature19764
- Su, S., Wang, Y. Y., Du, F. S., Lu, H., and Li, Z. C. (2018). Dynamic covalent bond-assisted programmed and traceless protein release: High loading nanogel for systemic and cytosolic delivery. *Adv. Funct. Mater.* 28, 1805287. doi:10.1002/adfm.201805287
- Sun, W., Ji, W., Hall, J. M., Hu, Q., Wang, C., Beisel, C. L., et al. (2015). Self-assembled DNA nanoclews for the efficient delivery of CRISPR-cas9 for genome editing. *Angew. Chem.* 127, 12197–12201. doi:10.1002/ange.201506030
- Sun, W., Ji, W., Hu, Q., Yu, J., Wang, C., Qian, C., et al. (2016). Transformable DNA nanocarriers for plasma membrane targeted delivery of cytokine. *Biomaterials* 96, 1–10. doi:10.1016/j.biomaterials.2016.04.011
- Sun, Y., Lau, S. Y., Lim, Z. W., Chang, S. C., Ghadessy, F., Partridge, A., et al. (2022). Phase-separating peptides for direct cytosolic delivery and redox-activated release of macromolecular therapeutics. *Nat. Chem.* 14, 274–283. doi:10.1038/s41557-021-00854-4
- Tan, E., Wan, T., Yu, C., Fan, Q., Liu, W., Chang, H., et al. (2022). ROS-responsive polypeptides for intracellular protein delivery and CRISPR/Cas9 gene editing. *Nano Today* 46, 101617. doi:10.1016/j.nantod.2022.101617
- Tan, H. X., Juno, J. A., Lee, W. S., Barber-Axthelm, I., Kelly, H. G., Wragg, K. M., et al. (2021). Immunogenicity of prime-boost protein subunit vaccine strategies against SARS-CoV-2 in mice and macaques. *Nat. Commun.* 12, 1403. doi:10.1038/s41467-021-21665-8
- Tang, R., Kim, C. S., Solfield, D. J., Rana, S., Mout, R., Velázquez-Delgado, E. M., et al. (2013). Direct delivery of functional proteins and enzymes to the cytosol using nanoparticle-stabilized nanocapsules. *ACS Nano* 7, 6667–6673. doi:10.1021/nn402753y
- Tang, R., Wang, M., Ray, M., Jiang, Y., Jiang, Z., Xu, Q., et al. (2017). Active targeting of the nucleus using nonpeptidic boronate tags. *J. Am. Chem. Soc.* 139, 8547–8551. doi:10.1021/jacs.7b02801
- Tao, A., Huang, G., Igarashi, K., Hong, T., Liao, S., Stellacci, F., et al. (2020). Polymeric micelles loading proteins through concurrent ion complexation and pH-cleavable covalent bonding for *in vivo* delivery. *Macromol. Biosci.* 20, 1900161. doi:10.1002/mabi.201900161
- Tezgel, A. Ö., Jacobs, P., Backlund, C. M., Telfer, J. C., and Tew, G. N. (2017). Synthetic protein mimics for functional protein delivery. *Biomacromolecules* 18, 819–825. doi:10.1021/acs.biomac.6b01685
- Tian, L., Kang, H. C., and Bae, Y. H. (2013). Endosomolytic reducible polymeric electrolytes for cytosolic protein delivery. *Biomacromolecules* 14, 2570–2581. doi:10.1021/bm400337f
- Tian, Y., Tirrell, M. V., and LaBelle, J. L. (2022). Harnessing the therapeutic potential of biomacromolecules through intracellular delivery of nucleic acids, peptides, and proteins. *Adv. Healthc. Mater.* 11, 2102600. doi:10.1002/adhm.202102600
- Togtema, M., Pichardo, S., Jackson, R., Lambert, P. F., Curiel, L., and Zehbe, I. (2012). Sonoporation delivery of monoclonal antibodies against human papillomavirus 16 E6 restores p53 expression in transformed cervical keratinocytes. *PLoS One* 7, e50730. doi:10.1371/journal.pone.0050730
- Tsao, C., Yuan, Z., Zhang, P., Liu, E., McMullen, P., Wu, K., et al. (2020). Enhanced pulmonary systemic delivery of protein drugs via zwitterionic polymer conjugation. *J. Control. Release* 322, 170–176. doi:10.1016/j.jconrel.2020.03.019
- Ulasov, A. V., Rosenkranz, A. A., and Sobolev, A. S. (2018). Transcription factors: Time to deliver. *J. Control. Release* 269, 24–35. doi:10.1016/j.jconrel.2017.11.004
- Ventura, J., Eron, S. J., González-Toro, D. C., Raghupathi, K., Wang, F., Hardy, J. A., et al. (2015). Reactive self-assembly of polymers and proteins to reversibly silence a killer protein. *Biomacromolecules* 16, 3161–3171. doi:10.1021/acs.biomac.5b00779
- Wang, M., Alberti, K., Sun, S., Arellano, C. L., and Xu, Q. (2014). Combinatorially designed lipid-like nanoparticles for intracellular delivery of cytotoxic protein for cancer therapy. *Angew. Chem. - Int. Ed.* 53, 2893–2898. doi:10.1002/anie.201311245
- Wang, M., Zuris, J. A., Meng, F., Rees, H., Sun, S., Deng, P., et al. (2016). Efficient delivery of genome-editing proteins using bio-reducible lipid nanoparticles. *Proc. Natl. Acad. Sci. U. S. A.* 113, 2868–2873. doi:10.1073/pnas.1520244113
- Wang, Y., and Yu, C. (2020). Emerging concepts of Nanobiotechnology in mRNA delivery. *Angew. Chem. - Int. Ed.* 59, 23374–23385. doi:10.1002/anie.202003545
- Weiner, G. J. (2015). Building better monoclonal antibody-based therapeutics. *Nat. Rev. Cancer* 15, 361–370. doi:10.1038/nrc3930
- Wu, D., Qin, M., Xu, D., Wang, L., Liu, C., Ren, J., et al. (2019). A bioinspired platform for effective delivery of protein therapeutics to the central nervous system. *Adv. Mater.* 31, 1807557. doi:10.1002/adma.201807557
- Xie, J., Gonzalez-Carter, D., Tockary, T. A., Nakamura, N., Xue, Y., Nakakido, M., et al. (2020). Dual-sensitive nanomicelles enhancing systemic delivery of therapeutically active antibodies specifically into the brain. *ACS Nano* 14, 6729–6742. doi:10.1021/acsnano.9b09991
- Yan, Y., Zhou, L., Sun, Z., Song, D., and Cheng, Y. (2022). Targeted and intracellular delivery of protein therapeutics by a boronated polymer for the treatment of bone tumors. *Bioact. Mater.* 7, 333–340. doi:10.1016/j.bioactmat.2021.05.041
- Yu, C., Tan, E., Xu, Y., Lv, J., and Cheng, Y. (2018). A guanidinium-rich polymer for efficient cytosolic delivery of native proteins. *Bioconjug Chem.* 30, 413–417. doi:10.1021/acs.bioconjugchem.8b00753
- Yu, S., Yang, H., Li, T., Pan, H., Ren, S., Luo, G., et al. (2021). Efficient intracellular delivery of proteins by a multifunctional chimaeric peptide *in vitro* and *in vivo*. *Nat. Commun.* 12, 5131. doi:10.1038/s41467-021-25448-z
- Zelikin, A. N., Ehrhardt, C., and Healy, A. M. (2016). Materials and methods for delivery of biological drugs. *Nat. Chem.* 8, 997–1007. doi:10.1038/nchem.2629
- Zhang, M., Chen, X., Li, C., and Shen, X. (2020). Charge-reversal nanocarriers: An emerging paradigm for smart cancer nanomedicine. *J. Control. Release* 319, 46–62. doi:10.1016/j.jconrel.2019.12.024
- Zhang, S., Shen, J., Li, D., and Cheng, Y. (2020). Strategies in the delivery of Cas9 ribonucleoprotein for CRISPR/Cas9 genome editing. *Theranostics* 11, 614–648. doi:10.7150/thno.47007
- Zhang, Z., Shen, W., Ling, J., Yan, Y., Hu, J., and Cheng, Y. (2018). The fluorination effect of fluoroamphiphiles in cytosolic protein delivery. *Nat. Commun.* 9, 1377. doi:10.1038/s41467-018-03779-8
- Zhou, Z., Yan, Y., Wang, L., Zhang, Q., and Cheng, Y. (2019). Melanin-like nanoparticles decorated with an autophagy-inducing peptide for efficient targeted photothermal therapy. *Biomaterials* 203, 63–72. doi:10.1016/j.biomaterials.2019.02.023
- Zuris, J. A., Thompson, D. B., Shu, Y., Guiling, J. P., Bessen, J. L., Hu, J. H., et al. (2015). Cationic lipid-mediated delivery of proteins enables efficient protein-based genome editing *in vitro* and *in vivo*. *Nat. Biotechnol.* 33, 73–80. doi:10.1038/nbt.3081



## OPEN ACCESS

## EDITED BY

Gianni Ciofani,  
Italian Institute of Technology (IIT), Italy

## REVIEWED BY

Giada Graziana Genchi,  
University of Bari Aldo Moro, Italy  
Elisa De Luca,  
National Research Council (CNR), Italy  
Laura D'Alfonso,  
University of Milano-Bicocca, Italy

## \*CORRESPONDENCE

Ludmila Rudi,  
✉ ludmila.rudi@imb.utm.md

RECEIVED 18 May 2023

ACCEPTED 28 July 2023

PUBLISHED 07 August 2023

## CITATION

Rudi L, Cepoi L, Chiriac T, Mescu V,  
Valuta A and Djur S (2023), Effects of  
citrate-stabilized gold and silver  
nanoparticles on some safety parameters  
of *Porphyridium cruentum* biomass.  
*Front. Bioeng. Biotechnol.* 11:1224945.  
doi: 10.3389/fbioe.2023.1224945

## COPYRIGHT

© 2023 Rudi, Cepoi, Chiriac, Mescu,  
Valuta and Djur. This is an open-access  
article distributed under the terms of the  
[Creative Commons Attribution License  
\(CC BY\)](https://creativecommons.org/licenses/by/4.0/). The use, distribution or  
reproduction in other forums is  
permitted, provided the original author(s)  
and the copyright owner(s) are credited  
and that the original publication in this  
journal is cited, in accordance with  
accepted academic practice. No use,  
distribution or reproduction is permitted  
which does not comply with these terms.

# Effects of citrate-stabilized gold and silver nanoparticles on some safety parameters of *Porphyridium cruentum* biomass

Ludmila Rudi\*, Liliana Cepoi, Tatiana Chiriac, Vera Mescu,  
Ana Valuta and Svetlana Djur

Phycobiotechnology Laboratory, Institute of Microbiology and Biotechnology of Technical University of Moldova, Chisinau, Moldova

**Introduction:** Our research raises the question of how realistic and safe it is to use gold and silver nanoparticles in biotechnologies to grow microalgae, which will later be used to obtain valuable products. To this purpose, it was necessary to assess the influence of 10 and 20 nm Au and Ag nanoparticles stabilized in citrate on the growth of microalga *Porphyridium cruentum* in a closed cultivation system, as well as some safety parameters of biomass quality obtained under experimental conditions.

**Methods:** Two types of experiments were conducted with the addition of nanoparticles on the first day and the fifth day of the cultivation cycle. Changes in productivity, lipid content, malondialdehyde (MDA), as well as antioxidant activity of microalgae biomass have been monitored in dynamics during the life cycle in a closed culture system.

**Results:** The impact of nanoparticles on the growth curve of microalgae culture was marked by delaying the onset of the exponential growth phase. A significant increase in the content of lipids and MDA in biomass was noted. Excessive accumulation of lipid oxidation products within the first 24 h of cultivation resulted in altered antioxidant activity of red algae extracts.

**Discussion:** Citrate-stabilized gold and silver nanoparticles proved to be a stress factor for red microalga *Porphyridium cruentum*, causing significant changes in both biotechnological and biomass safety parameters. Addition of Au and Ag nanoparticles during the exponential growth phase of porphyridium culture led to an enhanced lipid accumulation and reduced MDA values in biomass.

## KEYWORDS

gold, silver, nanoparticles, *Porphyridium cruentum*, biomass, lipids, malondialdehyde, antioxidant activity

## 1 Introduction

Gold and silver nanoparticles are among the most widely studied and applied in practice nanomaterials, being used in optoelectronics, catalysis, environmental protection (as remediation agents or as antimicrobials), food industry (food life extension, food packaging, and releasing of preservatives). These nanomaterials are used in the production of biosensors, targeted drug delivery systems, as well as in diagnostic imaging and cancer therapy (Majdalawieh et al., 2014; Patra et al., 2015; Ismail et al., 2017; Chugh et al., 2018).

The numerous areas in which gold and silver nanoparticles are applied and their increasing availability due to the development of engineering and bioengineering methods of synthesis lead to inevitable environmental pollution with these materials, which raises the question of their toxicity in relation to aquatic organisms, including microalgae (Moreno-Garrido et al., 2015).

Due to their rich and varied content of biologically active compounds, microalgae are considered valuable biotechnological objects. Some species are grown under industrial conditions to obtain nutraceuticals containing proteins, pigments, antioxidants, lipids, and carbohydrates. Nanoparticles display specific characteristics and absorption behavior in the aquatic environment, which can affect the growth and biosynthetic activity of microalgae both in their natural habitat and in bioreactors. For example, under controlled conditions, gold nanoparticles up to 10 nm in size can lead to an almost 2-fold increase in the carotenoid content in green algae biomass (Li et al., 2020). However, depending on the dose of gold nanoparticles to which the microalgae culture was exposed, as well as the surface properties of nanoparticles, the efficiency of photosystem II can either increase or decrease (Kula-Maximenko et al., 2022).

Marine microalga *Porphyridium cruentum* has raised particular interest due to its valuable biomass composition, which includes the following components per dry weight of algae: proteins (30%–35%), sulfated polysaccharides (20%–22%), phycobiliproteins (20%–25%), lipids (6%–8%) and numerous other compounds, present in small quantities (Reboloso Fuentes, 2000). Among bioactive compounds with high commercial value are sulfated polysaccharides, phycobiliproteins and polyunsaturated fatty acids. Sulfated polysaccharides derived from *Porphyridium cruentum* biomass exhibit pronounced immunomodulatory and cytotoxic effects and have been proposed as natural and safe ingredients for nutraceuticals (Casas-Arrojo et al., 2021). Lipids produced by this red microalga are mostly polyunsaturated fatty acids, in particular arachidonic acid (C20:4, n-6) and eicosapentaenoic acid (C20:5, n-3), which can be exploited in various medical applications. *Porphyridium* biomass is also a precious source of natural antioxidants either for direct consumption or for use in food processing (Rodríguez-García and Guil-Guerrero, 2008). This unicellular red alga has been used by several groups of researchers, including the authors of this article, within nanobiotechnological-based research where *Porphyridium cruentum* turned out to be an effective matrix for the synthesis of silver nanoparticles (Bunghez et al., 2010; Cepoi et al., 2021). In addition, some aspects of the interaction of *P. cruentum* culture with silver nanoparticles stabilized in polyethylene glycol and citrate were studied, and the effect of stimulating the accumulation of proteins and carbohydrates in biomass was revealed (Cepoi et al., 2021).

The involved pathway of nanoparticles affecting metabolic processes in microalgae is oxidative stress, and its setting can change the level of synthesis and accumulation of certain components of interest in physiological biomass. However, along with valuable biomass components, induced oxidative stress leads to excessive accumulation of oxidation products of macromolecules, which can compromise the quality of microalgae biomass. In the case of *P. cruentum*, lipids are the first components subjected to stress, and malondialdehyde (MDA) is one of the end products of polyunsaturated fatty acids peroxidation in algal cells (Chen et al., 2008). The degree of oxidative stress caused by nanoparticles depends on the specific characteristics of gold and silver nanoparticles, especially the compounds used to stabilize them.

Moreover, stabilization of noble metal nanoparticles is crucial to maintaining the desired plasmonic behavior, hence various methods have been developed to stabilize nanomaterials, including citrate as a stabilizing layer (Kang et al., 2019). Thus, depending on the properties of nanoparticles and the type of cells that interact with them, numerous beneficial and negative effects can be observed.

The aim of our research was to assess the influence of 10 and 20 nm Au and Ag nanoparticles stabilized in citrate on the growth of *Porphyridium cruentum* culture during the cultivation cycle in a closed system, as well as some safety parameters of the quality of microalgae biomass obtained under experimental conditions.

## 2 Materials and methods

### 2.1 Gold and silver nanoparticles

To implement the design of our experimental studies, we used citrate-stabilized Au and Ag nanoparticles with diameters of 10 and 20 nm (SIGMA-ALDRICH CHEMIE GmbH, Germany). Product No for AuNP 10 nm–741957, and Product No for AuNP 20 nm–741965. Specifications: OD 1 and PDI <0.2. Product No for AgNP 10 nm–730785, and Product No for AgNP 20 nm–730793. Specification: 10 nm and 20 nm particle size (TEM). The characteristics of the nanoparticles are accurate and did not require additional measurements, the error in the size of nanoparticles is  $\pm 0.2$  nm.

### 2.2 *Porphyridium cruentum* strain, nutrient medium, and cultivation conditions

The researches were carried out on *Porphyridium cruentum* CNMN-AR-01 strain (porphyridium), obtained from the National Collection of Nonpathogenic Microorganisms of the Institute of Microbiology and Biotechnology of Technical University of Moldova. Cultivation of *Porphyridium cruentum* CNMN-AR-01 was performed on mineral nutrient medium with the following composition: macroelements (SIGMA-ALDRICH CHEMIE GmbH, Germany): 16.04 g/L KCl; 12.52 g/L NaCl; 1.24 g/L KNO<sub>3</sub>; 2.5 g/L MgSO<sub>4</sub>·7H<sub>2</sub>O; 0.118 g/L CaCl<sub>2</sub>; 0.5 g/L K<sub>2</sub>HPO<sub>4</sub>·3H<sub>2</sub>O; 0.05 g/L KI; 0.05 g/L KBr. The microelements (SIGMA-ALDRICH CHEMIE GmbH, Germany) solution containing 2.86 mg/L H<sub>3</sub>BO<sub>3</sub>; 1.81 mg/L MnCl<sub>2</sub>·4H<sub>2</sub>O; 0.08 mg/L CuSO<sub>4</sub>·5H<sub>2</sub>O; 0.015 mg/L MoO<sub>3</sub>, and the 0.5 mL FeEDTA solution. Microalgae cultivation was performed in 100 mL Erlenmeyer flasks (PYREX, Corning, New York, purchased from MERCK, Germany), with a working volume of 50 mL. The cultivation parameters regulating algal growth under laboratory conditions were strictly maintained: the inoculum size–0.5–0.55 g/L dry biomass; a temperature of 25–28°C, optimum pH in culture medium 6.8–7.2, and continuous illumination of 56  $\mu\text{m photons m}^{-2} \text{s}^{-1}$ . The cultivation cycle lasted 14 days.

### 2.3 Design of experiments

In the experiments involving the addition of gold and silver nanoparticles from the first day of the cultivation cycle of

*Porphyridium cruentum*, Au and Ag nanoparticles, in the selected concentrations, were added to the mineral medium, followed by the inoculation of microalgae. In experimental samples, under the influence of nanoparticles during the exponential phase of porphyridium growth, Au and Ag nanoparticles at selected concentrations as stimulators were introduced into the nutrient medium on the 5th day of the cultivation cycle.

In samples monitoring changes in lipid and MDA content, as well as antioxidant activity, biomass was collected every 24 h.

Biomass collected from all experiments was demineralized [washed from excess salts with a solution of 2.0% ammonium acetate (SIGMA-ALDRICH CHEMIE GmbH, Germany)], standardized to a biomass concentration of 10 mg/mL per sample, and subjected to freezing/thawing procedures.

## 2.4 Determination of the biomass content

The biomass content of *P. cruentum* was determined spectrophotometrically by recording the absorption (Spectrophotometer T80 UV/VIS, PG Instruments, UK) of microalgal suspension at 545 nm and quantitative recalculation (g/L) was performed on the basis of the calibration curve.

## 2.5 Quantification of total lipids

The amount of total lipids was determined in the microalgal biomass spectrophotometrically based on the color reaction between the degradation products of lipids and the components of the phospho-vanillin reagent. To extract lipids from the microalgal biomass, 1.0 mL of chloroform (Merck KGaA (Supleco), Germany)/ethanol (Dita EstFarm SRL, Republic of Moldova) mixture (2v/1v) was added to 10 mg of biomass. The extraction was conducted by stirring (Heidolph Unimax 1010 shaker, Heidolph Instruments GmbH & Co. KG, Germany) at room temperature for 120 min. After the time elapsed, the lipid extract was separated from the other constituents, and 1.0 mL of 0.9% NaCl was added. This mixture was initially stirred and then centrifuged at 13520 g (Hettich centrifuge MIKRO 22R, Andreas Hettich GmbH & Co. KG, Germany). The supernatant was removed. Chloroform evaporated quite easily from the extracts. In the resulting precipitate was added 1.0 mL of concentrated sulfuric acid (Merck KGaA, Germany). For mixing, the samples were placed on a shaker and then transferred to water bath (Gesellschaft für Labortechnik mbH, Germany) at a temperature of 90°C for 20 min. The samples were then cooled under tap water. In dry glass tubes, 0.1 mL lipid extract hydrolysate and 3.0 mL phospho-vanillin reagent (1.2 mg vanillin (Merck KGaA (Supleco), Germany) in 1.0 mL of 68% phosphoric acid (Merck KGaA (Supleco), Germany) were mixed. The mixture of the reactants was kept in darkness at room temperature for 30 min. After incubation in the dark, the absorbance of the samples was recorded at the wavelength of 520 nm with respect to black. The lipid content (% biomass) was calculated on the basis of the calibration curve for pure oleic acid.

## 2.6 Determination of malondialdehyde content

To determine the content of malondialdehyde (MDA), 3.0 mL of 0.76% thiobarbituric acid (SIGMA-ALDRICH CHEMIE GmbH, Germany) in 20% trichloroacetic acid (SIGMA-ALDRICH CHEMIE GmbH, Germany) was added to 10 mg of biomass. The mixture of reactants was incubated on the water bath at 95°C for 40 min. Next, samples were cooled and centrifuged at 13520 g. The absorbance of samples was recorded at 532 nm and 600 nm. The mixture with no biological material was used as a blank sample. Quantitative analysis of malondialdehyde (nM/mL) in the samples was performed using the molar extinction coefficient of MDA-TBA product, which has a maximum absorption peak at 532 nm.

## 2.7 Evaluation of antioxidant activity

Antioxidant activity of freshly collected biomass was determined using the ABTS [2,2'-azinobis (3-ethylbenzothiazoline-6-sulfonic acid)] (SIGMA-ALDRICH CHEMIE GmbH, Germany) in ethanolic extracts derived from microalgal biomass. To prepare the alcoholic extracts, 1.0 mL of biomass with a concentration of 10 mg/mL was centrifuged at 13520 g for 10 min. The supernatant was removed, and 2.0 mL of 55% ethyl alcohol was added to the resulting biomass precipitate. The mixture was stirred at room temperature for 120 min and then centrifuged at 13520 g for 5 min. The obtained extracts were stored at +4°C. ABTS was generated by reacting equal volumes of 7 mM ABTS with 2.45 mM potassium persulfate (SIGMA-ALDRICH CHEMIE GmbH, Germany). The mixture was kept in the dark for 12–16 h, the time required for the formation of ABTS radical. Next, a working solution was prepared with an optical density of  $0.700 \pm 0.02$  at 734 nm. The mixture of reactants consisted of 0.3 mL antioxidant extract and 2.7 mL ABTS. The samples were mixed and after 6 min their optical density was recorded at 734 nm. Antioxidant activity was expressed in % inhibition of ABTS.

## 2.8 Statistical analysis

The results were analyzed using Microsoft Excel, with the Student's t-test and the correlation coefficient calculation. The threshold for statistical significance was  $p < 0.01$ . The investigations were performed in three independent experiments. For each parameter were performed three parallel measurements from each sample. Mean values along with standard deviation (S.D.) and p-values are presented in figures and tables.

# 3 Results

## 3.1 Amount of accumulated biomass

The change in the amount of *P. cruentum* biomass accumulated at the end of the cultivation cycle in the experiments with the application of nanoparticles compared to control is shown in



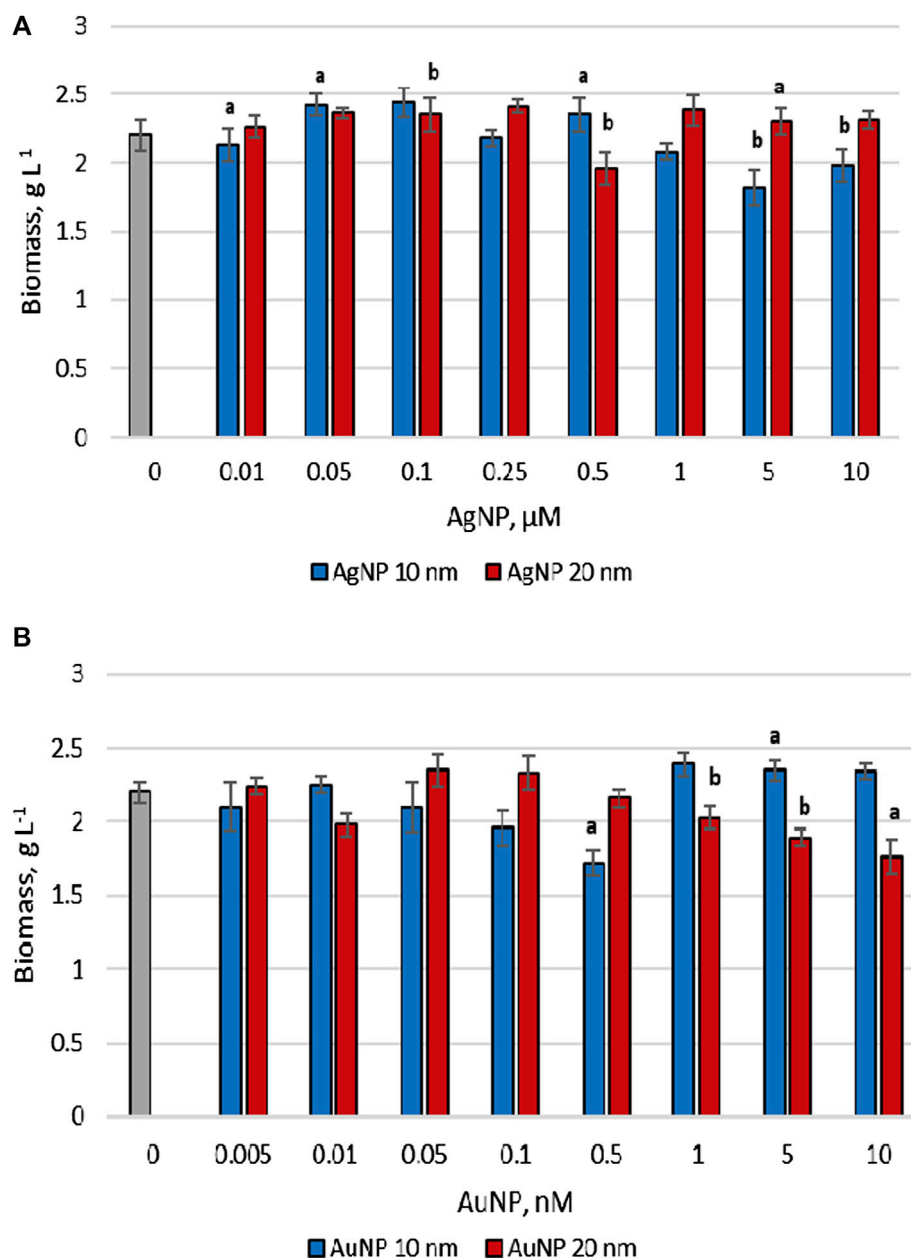


FIGURE 1

The biomass content accumulated by *Porphyridium cruentum* upon exposure to AgNP (A) and AuNP (B) (0–control), a  $-p < 0.01$ ; b  $-p < 0.001$ .

Figure 1. In the case of AgNPs, only those of 10 nm in size at concentrations of 5 and 10  $\mu\text{M}$  reduced the amount of porphyridium biomass accumulated during the growth cycle. In other experiments, their effect was noted as favorable in terms of lipid synthesis or at least neutral (Figure 1A). Addition of 10 nm AuNPs in two of the tested concentrations, namely 0.1 and 0.5 nM, showed a 10.1%–20.2% ( $p < 0.01$ ) reduction in microalgae biomass (Figure 1B). In the other studied cases, the effect of 10 nm gold nanoparticles stabilized in citrate on the amount of porphyridium biomass was neutral. Gold nanoparticles with a diameter of 20 nm at concentrations up to 1 nM did not produce significant changes on monitored parameter, while concentrations of 5 nM and 10 nM led to a decrease in the amount of biomass by 14.1 ( $p < 0.001$ )–20.2% ( $p < 0.01$ ).

### 3.2 The amount of lipids and malondialdehyde at the end of the cultivation cycle

The effects of citrate-stabilized gold and silver nanoparticles on the lipid and malondialdehyde content in *Porphyridium cruentum* biomass at the end of the cultivation cycle can be observed in Figure 2.

The exposure of *Porphyridium cruentum* culture to Ag nanoparticles of both sizes in the concentration range from 0.01 to 0.1  $\mu\text{M}$  resulted in a decrease in the lipid content in biomass (by up to 41.0% compared to control) (Figure 2A). Further, as supplementation with silver nanoparticles increased in the cultivation medium, lipid accumulation in biomass was also

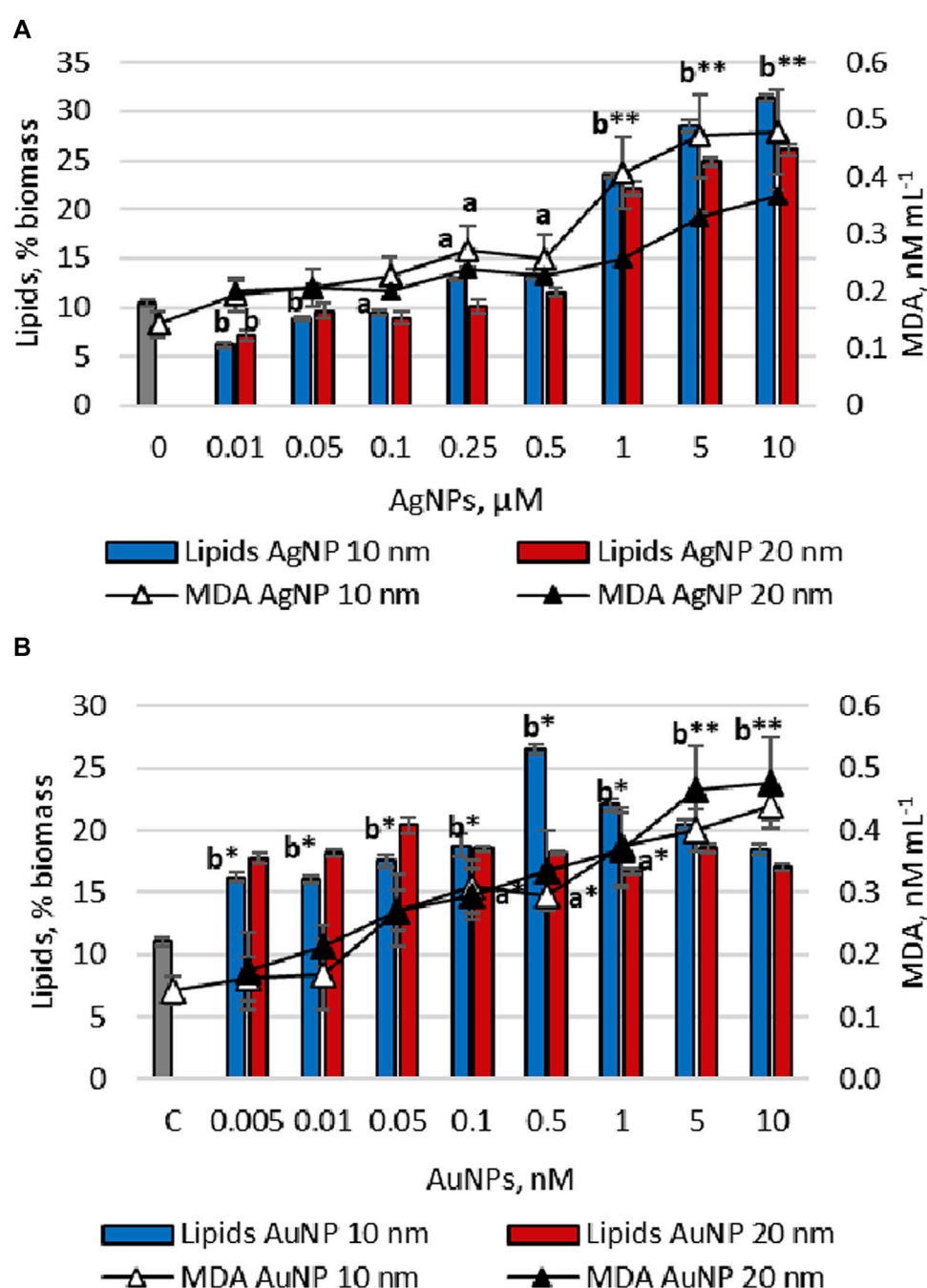


FIGURE 2

Total lipids and MDA content accumulated by *Porphyridium cruentum* upon exposure to AgNP (A) and AuNP (B) (0–control), a -  $p < 0.01$ ; b -  $p < 0.001$ ; a\* -  $p < 0.01$  common for MDA parameter; b\* -  $p < 0.001$  common for lipids parameter; b\*\* -  $p < 0.001$  common for all parameters.

detected. Thus, the addition of 10 nm AgNPs in concentrations of 0.25 and 0.5  $\mu\text{M}$  stimulated lipid synthesis by 23.4%–27.7% ( $p < 0.01$ ) compared to control. Concentrations of 1–10  $\mu\text{M}$  nanoparticles induced an increase in lipid content in microalgal biomass by 2.23–2.99 times ( $p < 0.001$ ). In the case of 20 nm AgNPs, the lipid content increased 2.10–2.48 times ( $p < 0.001$ ).

AgNPs exerted a concentration-dependent effect on the content of MDA in *P. cruentum* biomass and showed an increasing tendency of values with increase in nanoparticle concentration. In the case of

10 nm AgNPs MDA content increased by 36.4%–236% ( $p < 0.001$ ) compared to control, and for nanoparticles of 20 nm in size by 40.8%–159% ( $p < 0.001$ ).

In the case of AuNPs, a significant increase from 45.1 up to 139.9% compared to control in the amount of lipids in biomass was established, depending on the size and concentration of nanoparticles. When using 10 nm AuNPs, the maximum lipid content in biomass was 2.39 times ( $p < 0.001$ ) higher at a concentration of 0.5 nM. Citrate-stabilized 20 nm gold nanoparticles had a weaker stimulatory effect on lipid production

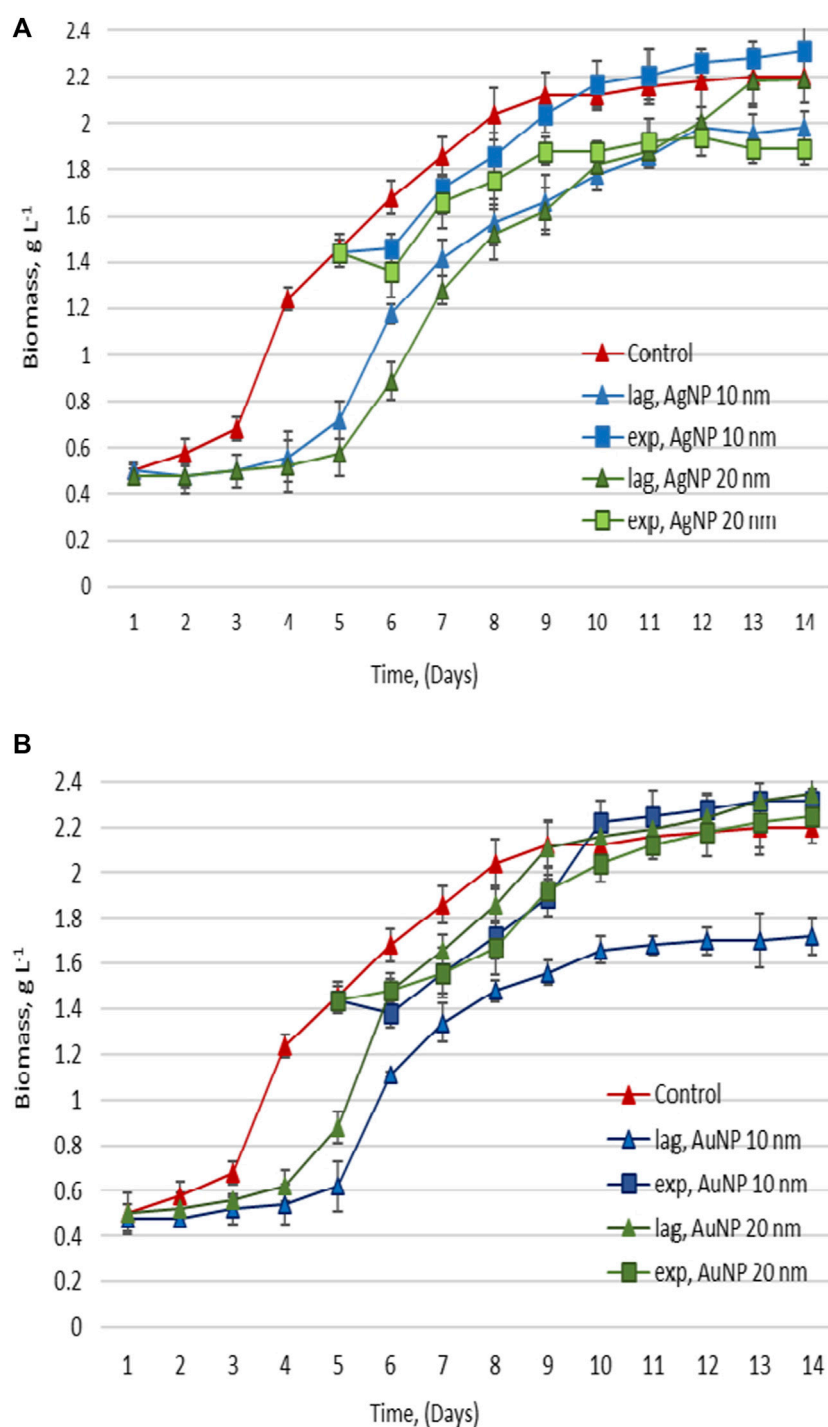


FIGURE 3

Biomass accumulated, upon the exposure of *Porphyridium cruentum* during the lag phase and exponential growth phase to 10  $\mu$ M AgNP 10 nm and 20 nm (A), and 0.5 nM AuNP 10 nm and 0.05 nM AuNP 20 nm (B).

in algae culture than 10 nm nanoparticles (Figure 2B). It was also found that the levels of malondialdehyde were high with increasing concentration of nanoparticles in the nutrient medium. For 10 nm AuNPs, an increase in the amount of MDA in biomass by 13.6 ( $p < 0.01$ )-208.9% ( $p < 0.001$ ) compared to control was determined, while for those of 20 nm in size-by 22.6 ( $p < 0.001$ )-236.1% ( $p < 0.001$ ).

### 3.3 Dynamics of porphyridium biomass accumulation during a cultivation cycle

Concentrations were selected for each type of nanoparticles and the highest lipid content in microalgae biomass was determined. Thus, concentration of 10  $\mu$ M was revealed for AgNPs of 10 nm and

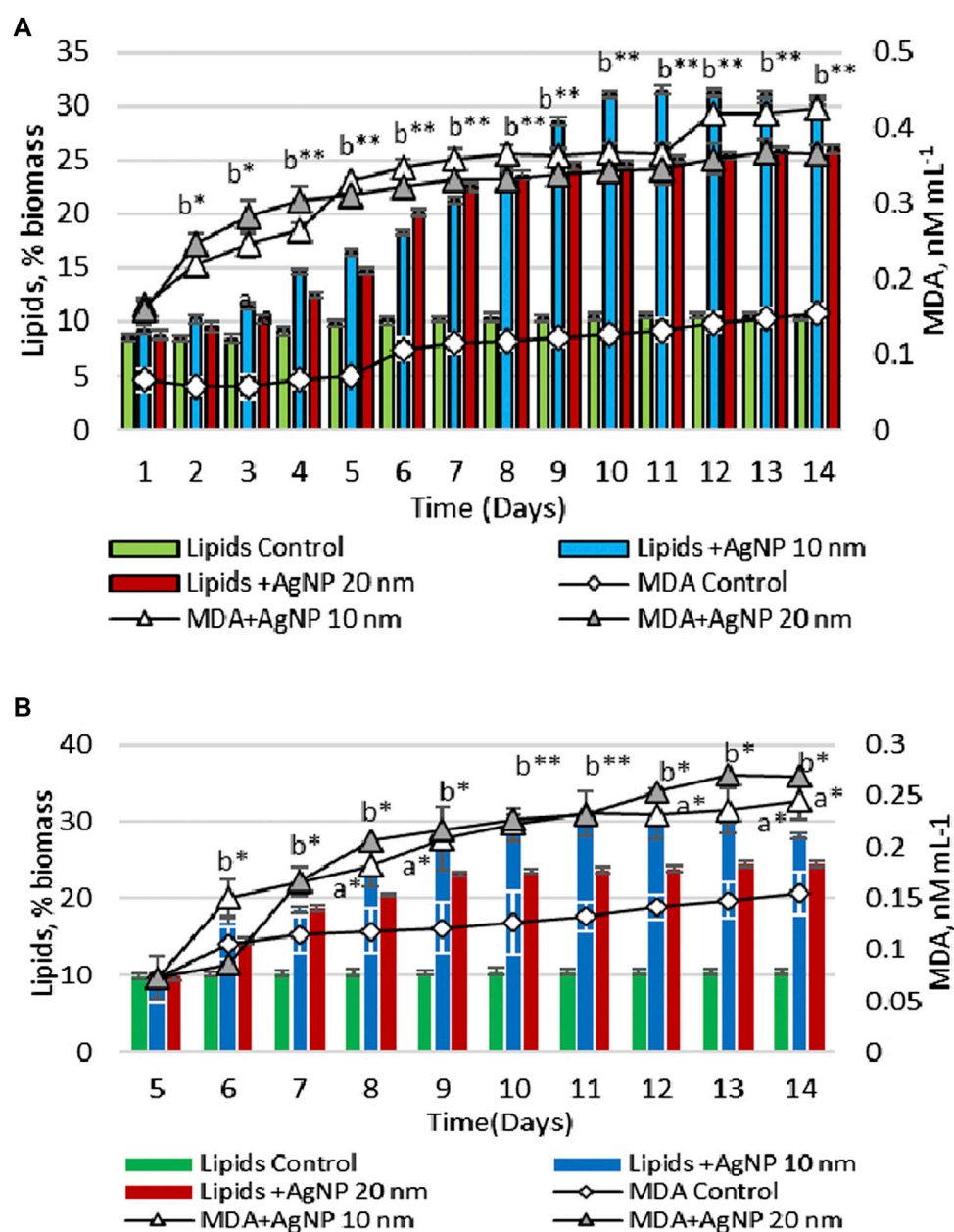


FIGURE 4

Total lipid and MDA contents in the biomass, upon the exposure of *Porphyridium cruentum* during the lag phase (A) and exponential growth phase (B) to 10  $\mu$ M AgNP 10 nm and 10  $\mu$ M AgNP 20 nm; a  $-p < 0.01$ ; b  $-p < 0.001$ ; a\*  $-p < 0.01$  common for two parameters; b\*  $-p < 0.001$  common for two parameters; b\*\*  $-p < 0.001$  common for all parameters.

20 nm in size, while for 10 nm AuNPs–0.5  $\mu$ M, and for 20 nm AuNPs–0.05  $\mu$ M.

Nanoparticles were added to the culture medium on the first day of the cultivation cycle (lag phase of culture growth), and in the other experimental series—on the 5th day, which corresponded to the exponential growth phase. At equal 24-h intervals, samples of *Porphyridium cruentum* culture were taken to determine the amount of biomass, total lipid content and the values of malondialdehyde accumulated in biomass. The results with reference to the amount of produced biomass are shown in Figure 3.

In the case of adding AgNPs to the nutrient medium on the first day of cultivation, lag phase duration increased significantly (Figure 3A). The beginning of the exponential growth phase occurred on the 5th day and was clearly manifested on the 6th day of cultivation (2 days later than in control). In the case of 20 nm AgNPs, biomass amount in the experimental sample was equal to the one in control on the 13th day of cultivation, while in the case of 10 nm AgNPs, it remained significantly lower. When silver nanoparticles of both sizes were added on day 5 of cultivation, delays in the growth phases were avoided, with



**TABLE 1** Lipids and MDA content in *Porphyridium cruentum* under the application of Ag and Au nanoparticles at different periods of the cultivation cycle (1st day–lag phase; 5th day–exponential growth phase).

Days	AgNPs, 10 nm		AgNPs, 20 nm		AuNPs, 10 nm		AuNPs, 20 nm	
	Lipids g/L	MDA, nM/L	Lipids, g/L	MDA, nM/L	Lipids, g/L	MDA, nM/L	Lipids, g/L	MDA, nM/L
Adding NPs on the first day of the cultivation cycle, <sup>a</sup> <i>p</i> < 0.01; <sup>b</sup> <i>p</i> < 0.001								
9	0.47 ± 0.040 <sup>a</sup>	60.42 ± 5.69 <sup>b</sup>	0.39 ± 0.028 <sup>b</sup>	54.76 ± 5.16 <sup>a</sup>	0.28 ± 0.014 <sup>a</sup>	30.57 ± 2.43 <sup>b</sup>	0.35 ± 0.026 <sup>b</sup>	51.06 ± 5.86 <sup>a</sup>
10	0.55 ± 0.028 <sup>a</sup>	65.50 ± 4.53 <sup>b</sup>	0.45 ± 0.028 <sup>b</sup>	62.24 ± 4.74 <sup>a</sup>	0.37 ± 0.019 <sup>a</sup>	35.03 ± 2.18 <sup>a</sup>	0.39 ± 0.020 <sup>b</sup>	55.73 ± 4.66 <sup>a</sup>
11	0.58 ± 0.023 <sup>b</sup>	68.07 ± 4.24 <sup>b</sup>	0.47 ± 0.023 <sup>b</sup>	65.05 ± 6.21 <sup>a</sup>	0.41 ± 0.016 <sup>a</sup>	41.16 ± 1.53 <sup>b</sup>	0.40 ± 0.020 <sup>b</sup>	57.38 ± 4.20 <sup>b</sup>
12	0.62 ± 0.012 <sup>b</sup>	82.76 ± 2.02 <sup>b</sup>	0.51 ± 0.022 <sup>b</sup>	72.16 ± 6.38 <sup>a</sup>	0.43 ± 0.019 <sup>a</sup>	45.22 ± 2.34 <sup>b</sup>	0.45 ± 0.026 <sup>b</sup>	59.58 ± 6.06 <sup>b</sup>
13	0.61 ± 0.030 <sup>b</sup>	81.93 ± 6.28 <sup>b</sup>	0.56 ± 0.036 <sup>b</sup>	80.22 ± 7.75 <sup>a</sup>	0.44 ± 0.038 <sup>b</sup>	48.96 ± 4.79 <sup>a</sup>	0.47 ± 0.026 <sup>b</sup>	61.48 ± 4.87 <sup>b</sup>
14	0.60 ± 0.030 <sup>b</sup>	84.15 ± 5.15 <sup>b</sup>	0.57 ± 0.032 <sup>b</sup>	80.15 ± 6.29 <sup>a</sup>	0.46 ± 0.027 <sup>a</sup>	51.08 ± 4.40 <sup>a</sup>	0.48 ± 0.026 <sup>b</sup>	63.38 ± 6.98 <sup>a</sup>
Adding NPs on the 5th day of the cultivation cycle, <sup>a</sup> <i>p</i> < 0.01; <sup>b</sup> <i>p</i> < 0.001								
9	0.57 ± 0.030 <sup>b</sup>	42.43 ± 5.13 <sup>a</sup>	0.44 ± 0.018 <sup>b</sup>	40.60 ± 5.43 <sup>a</sup>	0.49 ± 0.018 <sup>b</sup>	31.37 ± 4.36 <sup>a</sup>	0.45 ± 0.031 <sup>b</sup>	23.42 ± 4.41
10	0.66 ± 0.039 <sup>b</sup>	48.17 ± 6.78 <sup>a</sup>	0.44 ± 0.017 <sup>b</sup>	42.86 ± 4.10 <sup>a</sup>	0.59 ± 0.020 <sup>b</sup>	40.40 ± 3.76 <sup>a</sup>	0.49 ± 0.024 <sup>b</sup>	27.00 ± 3.52
11	0.68 ± 0.043 <sup>b</sup>	51.49 ± 6.54 <sup>a</sup>	0.45 ± 0.031 <sup>a</sup>	44.54 ± 5.39 <sup>b</sup>	0.64 ± 0.018 <sup>b</sup>	44.10 ± 3.85 <sup>b</sup>	0.53 ± 0.022 <sup>b</sup>	54.00 ± 3.22
12	0.69 ± 0.027 <sup>b</sup>	52.43 ± 8.39 <sup>a</sup>	0.46 ± 0.026 <sup>b</sup>	49.27 ± 6.49 <sup>a</sup>	0.67 ± 0.029 <sup>b</sup>	45.83 ± 5.03 <sup>b</sup>	0.57 ± 0.036 <sup>b</sup>	31.37 ± 5.74
13	0.69 ± 0.026 <sup>b</sup>	53.80 ± 6.67 <sup>b</sup>	0.46 ± 0.021 <sup>b</sup>	51.22 ± 4.65 <sup>b</sup>	0.69 ± 0.036 <sup>b</sup>	47.56 ± 5.73 <sup>a</sup>	0.59 ± 0.034 <sup>b</sup>	35.97 ± 5.52 <sup>a</sup>
14	0.65 ± 0.042 <sup>b</sup>	56.59 ± 8.02 <sup>b</sup>	0.46 ± 0.022 <sup>b</sup>	51.03 ± 4.53 <sup>b</sup>	0.70 ± 0.034 <sup>b</sup>	46.63 ± 5.95 <sup>a</sup>	0.60 ± 0.038 <sup>b</sup>	39.74 ± 5.32 <sup>a</sup>

only a slight decrease in the amount of biomass during the exponential growth phase compared to control (Figure 3B).

If gold nanoparticles of both sizes were added to *P. cruentum* nutrient medium on the first day of vital cycle, lag phase duration also increased by 72 h. In the case of 20 nm AuNPs, the amount of biomass reached the control level on the 9th day of cultivation, and in the case of 10 nm AuNPs, algae biomass was significantly lower than in control sample (Figure 3A). The introduction of AuNPs on the 5th day of cultivation made it possible to avoid delays in the growth phases, and the decrease in the amount of biomass produced on subsequent days was exceeded at the end of the growth cycle (Figure 3B).

### 3.4 Dynamics of lipid and MDA accumulation in *Porphyridium cruentum* biomass during a cultivation cycle

Figure 4 represents the changes in the content of lipids and MDA in biomass during the growth cycle in experiments with the application of nanoparticles in the lag phase and the exponential growth phase. Table 1 shows the lipids and MDA amount calculated in biomass under the application of Au and Ag nanoparticles at different growth phases of cultivation.

Lipid content in the control sample was constant throughout the entire growth cycle and varied within 8.44%–10.56% of dry biomass. The content of MDA was maintained at a stable level during the first 5 days, after which on the 6th day it increased by 60.6% compared to the first day and remained at a higher level until the end of the cultivation cycle.

When AgNPs of both sizes were introduced on the first day, a significant increase in both the amount of lipids and the level of MDA in biomass was found during the vital cycle. On the second day, the amount of lipids and MDA in the biomass resulting from the experiment with nanoparticles was higher than in control sample by 21.5%–197.7% (*p* < 0.001) for lipids and 274.2%–355.5% (*p* < 0.001) for MDA. This difference has been increasing with the advancement of culture in age (Figure 4A).

In the case of adding silver nanoparticles on the 5th day of cultivation, an increase in the content of lipids and MDA was also detected. On day 14, lipid content in algae biomass grown on nutrient medium with 10 nm AgNPs was 2.69 times (*p* < 0.001) higher compared to control. The amount of lipids in microalgae culture was 0.60 g/L (Table 1). However, in this case, the increase of MDA level was less pronounced. On the 6th day of cultivation, MDA level was 42.3% (*p* < 0.001) lower than on the same day, but with the addition of nanoparticles on the first day (Figure 4B). At the end of the cultivation cycle, MDA content was 56.59 nM/L compared to 84.15 nM/L. A similar response pattern was observed for 20 nm AgNPs. The measurement of malondialdehyde content in microalgae culture with the addition of 20 nm AgNPs on the 5th day of cultivation was 51.03 nM/L compared to 80.15 nM/L MDA produced in the case of using nanoparticles on the first day of cultivation. The amount of lipids in microalgae culture was 0.46 g/L (Table 1).

The dynamics of changes in the content of lipids and MDA in *Porphyridium cruentum* biomass during the growth cycle in the presence of gold nanoparticles can be seen in Figure 5.

In porphyridium biomass grown on culture medium with the addition of 10 nm AuNPs on the first day, on the 14th day the lipid content was 2.54 times (*p* < 0.001) higher than the control value and

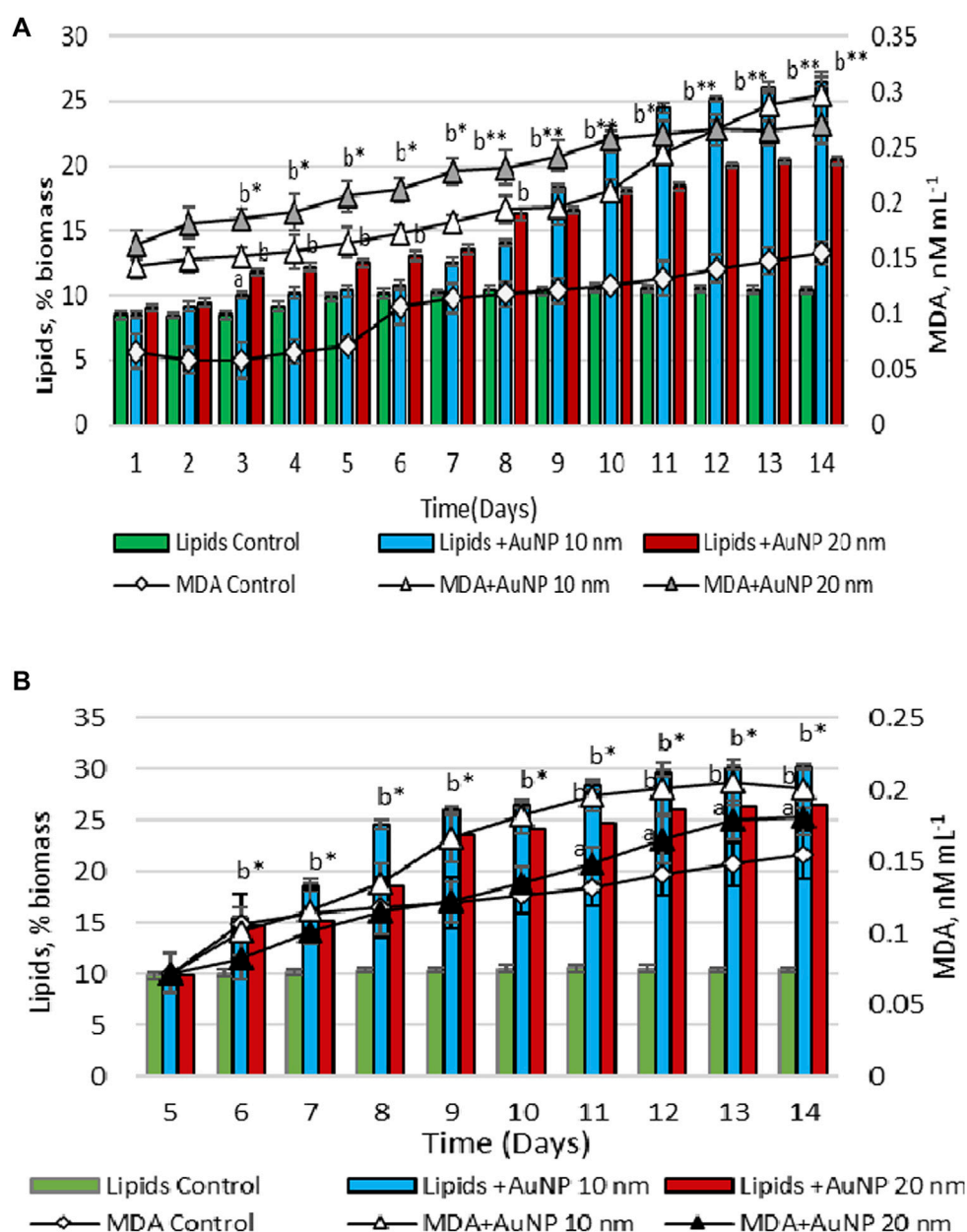


FIGURE 5

Total lipid and MDA contents in the biomass, upon the exposure of *Porphyridium cruentum* during the lag phase (A) and exponential growth phase (B) to 0.5 nM AuNP 10 nm and 0.05 nM AuNP 20 nm; a -  $p < 0.01$ ; b -  $p < 0.001$ ; b\* -  $p < 0.001$  common for two parameters.

amounted to 0.46 g/L (Figure 5A; Table 1). The content of MDA was higher than in control sample throughout the entire cycle of cultivation. AuNPs of 20 nm in size enhanced lipid content by 1.96 times ( $p < 0.001$ ) compared to control (Figure 5A). The amount of lipids in microalgae culture at the end of cultivation was 0.48 g/L. The MDA content during lag phase and the exponential growth phase was higher towards the results obtained in the experiment with 10 nm AuNPs, but at the final harvesting of microalgae culture, the level of this parameter in biomass was the same. The content of MDA in microalgal biomass was 51.08 nM/L for 10 nm AuNPs and 63.38 nM/L for 20 nm AuNPs (Table 1).

Adding Au nanoparticles on the 5th day of the cultivation cycle led to an increase in the lipid content of the biomass compared to their application on the first day and exceeded the control level by 2.9 times ( $p < 0.001$ ) for 10 nm AuNPs and 2.54 times ( $p < 0.001$ ) for 20 nm AuNPs (Figure 5B). Lipid content amounted to 0.70 g/L and 0.60 g/L, respectively (Table 1). On the contrary, MDA content in porphyridium biomass was about 30% lower compared to the values determined in the experiment of using AuNPs on the first day of the cultivation cycle. The MDA content in *P. cruentum* biomass was 46.63 nM/L and 39.74 nM/L, respectively (Table 1).

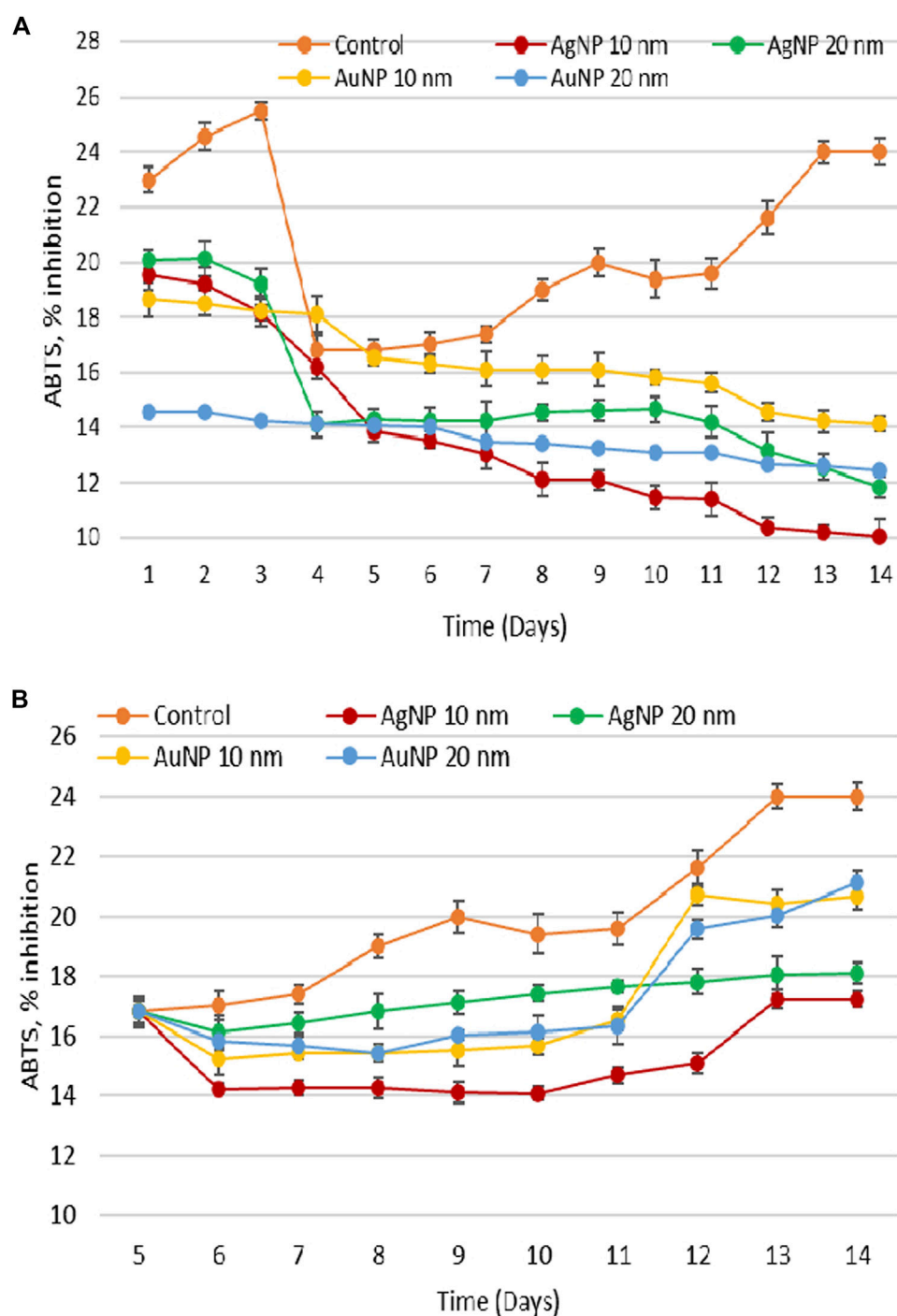


FIGURE 6

Change in antioxidant activity of ethanolic extract from *Porphyridium cruentum* exposed to Ag and Au nanoparticles (10  $\mu$ M AgNP 10 nm; 10  $\mu$ M AgNP 20 nm; 0.5 nM AuNP 10 nm; 0.05 nM AuNP 20 nm) during the lag phase (A) and exponential growth phase (B).

### 3.5 Dynamics of antioxidant activity of hydro-ethanolic extract derived from porphyridium biomass exposed to the action of Au and Ag nanoparticles

Figure 6 shows the change in the antioxidant activity of hydro-ethanolic extract obtained from porphyridium biomass grown on

culture medium with the addition of AgNPs and AuNPs on the first and fifth days of cultivation.

Under optimal laboratory conditions of cultivation, the highest ABTS values were characteristic to lag phase and related to the adaptation of inoculum to fresh nutrient medium. On the fourth day, the ABTS test values decreased significantly, followed by a steady increase until the end of cultivation cycle. The presence of

gold and silver nanoparticles caused a significant decrease in antioxidant activity compared to control that persisted throughout the entire cultivation cycle, especially during the 12th to 14th days. The difference ranged from 20% to 30% in the exponential growth phase and from 40% to 60% in the stationary growth phase.

In the experiment with the addition of nanoparticles on day 5, the antioxidant activity of extracts derived from porphyridium biomass grown on culture medium with nanoparticles was also lower compared to control, but the difference was less obvious than in the experiment with the application of nanoparticles on the first day. At the same time, in this experiment, days 12–14 were characterized by an increase in antioxidant activity towards the values of the exponential growth phase. However, these values were lower compared to control.

## 4 Discussion

*Porphyridium cruentum* is a red microalgae of biotechnological importance, and lipids proved to be valuable components of its biomass. Synthesis and accumulation of large amounts of lipids can be enhanced by applying various biotechnological procedures. A prerequisite for this is biomass quality obtained under these conditions that must be safe for further use, especially for direct human use or as a raw material for the production of various preparations. In parallel with biomass production and lipid content therein, it is necessary to monitor changes in MDA levels, which will be used as a safety parameter within microalgae production schemes.

It is known that the amount of biomass accumulated during a growth cycle of microalgae is one of the main parameters for assessing the toxic effects of nanomaterials on these organisms. Depending on the type of nanomaterials, their concentration, and the organism under study, the effects can be either stimulatory or inhibitory. The size of nanoparticles plays a critical role in their interaction with the cell. In the case of microalgal cell walls, they are equipped with pores with a diameter ranging from 5 to 20 nm, which facilitates the penetration of nanoparticles of the same size (Navarro et al., 2008). Obtaining a stimulatory effect upon nanoparticle action without exhibiting toxicity is extremely important.

Observations regarding the effects of nanoparticles are diverse and contradictory when it comes to the relationship between concentration-dependent effects. There are cases where low concentrations of nanoparticles have shown positive effects, while high concentrations have exerted negative effects (Pádrová et al., 2015; Cepoi et al., 2020). In other cases, however, an inverse relationship has been revealed (Wang et al., 2021). In the context of nanoparticle effects on organisms, the notion of low and high concentrations refers more to the effects produced rather than the quantity. The concentrations of nanoparticles characterized as low have been found to stimulate lipid production (Vargas-Estrada et al., 2020). At the same time, the ranges of nanoparticle concentrations applied to microalgae are highly varied. For example, AgNPs were applied to *Chlamydomonas reinhardtii* culture in the concentration range of 10, 40, 75, 150, and 300  $\mu\text{g/L}$  (Sendra et al., 2017), and in the concentration range of 0.1, 1.0, 10, 100, and 1,000  $\text{mg/L}$  (Pedroso et al., 2013). All these studies aimed to determine the concentration

limits at which a stimulatory effect on biosynthetic processes in microalgae can be established. Similarly, the concentration ranges of AuNPs and AgNPs presented in this research paper were analyzed.

Microalgal cells undergo various biological changes when facing adverse environmental stresses. Lipids are components of microalgae biomass that respond to various xenobiotic substances, including nanoparticles of different types. In this research, citrate-stabilized silver nanoparticles with 10 and 20 nm in diameter exhibited two types of effects on the amount of lipids in *P. cruentum* biomass: inhibitory effect characteristic at low nanoparticle concentrations, and stimulatory effect for high ones. However, within the limits of the applied concentrations of AgNPs, the correlation between their concentration in nutrient medium and lipid content in algae biomass collected on the 14th day of the life cycle was strong, the Pearson correlation coefficient calculated for 10 nm AgNPs was  $r = 0.856$ , and for 20 nm AgNPs  $r = 0.819$ . A similar response was found under the growth conditions of mixotrophic *Chlorella* sp. UJ-3 in the presence of low concentrations of  $\text{Fe}_3\text{O}_4$  nanoparticles in nutrient medium (Wang et al., 2021). In the case of AuNPs of both sizes, lipid content in biomass was significantly higher, but the effect was not concentration-dependent. Thus, within the limits of the used concentrations of AuNPs, it was found a weak negative correlation between the variables. The type of nanoparticles and their concentrations are determinant factors for promoting lipid synthesis in microalgae biomass. Thus, stimulatory effects of some nanoparticles on lipid accumulation have been revealed in other algal cultures treated with different types of nanoparticles: *Oedogonium* sp., *Cladophora* sp., *Ulothrix* sp., and *Spirogyra* sp. using AgNPs (Hasnain et al., 2023); *Scenedesmus obliquus* exposed to  $\text{Fe}_2\text{O}_3$  and  $\text{Fe}_3\text{O}_4$  nanoparticles (He et al., 2017; Wang et al., 2021); *Trachydiscus minutus*, *Desmodesmus subspicatus* and zerovalent iron (ZVI) nanoparticles (Pádrová et al., 2015); *Chlorella vulgaris* upon influence of  $\text{TiO}_2$  nanoparticles and MgNPs (Kang et al., 2014; Sibi et al., 2017).

Lipid production can be induced in microalgae in response to oxidative stress that appears in cells upon their contact with xenobiotics, but lipid oxidation process is also initiated. Malondialdehyde is one of the end products of the peroxidation of polyunsaturated fatty acids in cells and is commonly known as a biomarker of oxidative stress. In this research, there was revealed a strong positive correlation between malondialdehyde levels in *Porphyridium cruentum* biomass and nanoparticle concentrations in the nutrient medium. This was confirmed by correlation coefficients  $r = 0.823$  for AgNPs 10 nm in size, and  $r = 0.899$  for the experiment with 20 nm AgNPs; and in the case of using AuNPs of 10 and 20 nm, the Pearson values were  $r = 0.744$  and  $r = 0.817$ , respectively. Increased MDA levels were determined in other algal cultures treated with different types of nanoparticles, for example in the study of the action of titanium dioxide ( $\text{TiO}_2$ ) nanoparticles on green alga *Chlorella pyrenoidosa* (Middepogu et al., 2018). Another scientific paper noted that AgNPs added to the growth media of microalgae *Chlorella vulgaris* and *Dunaliella tertiolecta* resulted in elevated values of malondialdehyde (Hazani et al., 2013).

The study of the parameters of interest in dynamics during the growth cycle of microalgae *Porphyridium cruentum* showed that gold and silver nanoparticles exerted visible effects on them. The



**TABLE 2** Pearson coefficient calculated for the relationship between MDA values and the antioxidant activity of *Porphyridium cruentum* biomass, depending on the age at which the culture comes into contact with the nanoparticles (lag phase and exponential growth phase) (Duration of the cultivation cycle 14 days).

Growth phase in which the NPs were added	Correlation coefficient value			
	AgNP 10 nm	AgNP 20 nm	AuNP 10 nm	AuNP 20 nm
Lag growth phase	−0.98424	−0.88383	−0.92451	−0.97555
Exponential growth phase	0.845999	0.941365	0.741151	0.874284

most obvious was the change in the duration of culture growth phases with an increase in the length of lag phase and a reduction in the exponential growth phase when nanoparticles were introduced on the first day of cultivation. Except for 10 nm AuNPs, in the second part of the exponential growth phase of microalgae culture, the amount of biomass in the experiment was close to the control values, and accumulated lipid levels were very high. In parallel, a continuous increase was observed in the quantity of MDA and a gradual decrease in the antioxidant activity of porphyridium biomass. Thus, a state of pronounced oxidative stress was detected, which can be diminished by adding nanoparticles later in the growth cycle.

The introduction of nanoparticles on the 5th day of the growth cycle provided the optimal amount of biomass containing high quantities of lipids under conditions of significantly lower levels of MDA (compared to the experiment of adding NPs on the first day) and an adequate level of antioxidant activity of the biomass. The intensity of oxidative degradation processes of macromolecules, including lipids, was influenced by the ability of culture to produce antioxidants capable of scavenging free radicals, thereby breaking oxidation chains and preventing cellular damage. It is known that microalgae responded to different stressors by altering the antioxidant activity, which, depending on the stress intensity, can significantly increase or decrease (Dummermuth et al., 2003; Barone et al., 2021).

The correlation between MDA and ABTS values underlines the essential role of antioxidant components in controlling nanoparticle-induced oxidative stress. Thus, when adding nanoparticles during lag phase, we found a negative correlation, which indicated a low level of components with antioxidant properties. At the same time, when nanoparticles were introduced during the exponential growth phase of life cycle, the correlation between MDA and ABTS values was positive and reflected the involvement of antioxidant compounds in culture protection (Table 2).

According to the data above, it can be concluded that within the described experimental conditions, the most favorable proceedings for obtaining *P. cruentum* biomass with high lipid content are those using 10 nm silver and gold nanoparticles, supplemented during the exponential growth phase. Biomass harvesting should be carried out on the 12th day of the cultivation cycle for estimating its safety in terms of reaching the balance between the main biotechnological parameter - content of lipids of 0.69 g/L for AgNPs and 0.67 g/L for AuNPs, and biomass safety parameter - MDA level of 52.43 nM/L for AgNPs and 45.83 nM/L for AuNPs (Table 1).

## 5 Conclusion

Citrate-stabilized gold and silver nanoparticles 10 and 20 nm in size were a stress factor for red microalgae *P. cruentum*, causing significant changes in both biotechnological and biomass safety parameters. They can be used as factors to stimulate lipid accumulation by microalgae. In the case of using biomass or lipids derived from porphyridium for humans, it is necessary to consider the intensity of lipid oxidation processes so that the end product does not contain increased amounts of oxidative degradation products. From a technological point of view, this balance can be achieved by identifying the type of material used as a stimulator, its concentration, and the phase of the growth cycle at which it is introduced into the biotechnological process.

## Data availability statement

The original contributions presented in the study are included in the article/supplementary material, further inquiries can be directed to the corresponding author.

## Author contributions

The LR, LC, and TC contributed to conception and design of the study. VM organized the database. AV and SD performed the biochemical and statistical analysis. LR and LC wrote the first draft of the manuscript. LR, LC, and TC wrote sections of the manuscript. All authors contributed to the article and approved the submitted version.

## Funding

This research was supported by the Government of the Republic of Moldova-National Agency for Research and Development, project 20.80009.5007.05 “Biofunctionalized metal nanoparticles-obtaining using cyanobacteria and microalgae”.

## Conflict of interest

The authors declare that the research was conducted in the absence of any commercial or financial relationships that could be construed as a potential conflict of interest.

## Publisher's note

All claims expressed in this article are solely those of the authors and do not necessarily represent those of their affiliated

## References

- Barone, M. E., Parkes, R., Herbert, H., McDonnell, A., Conlon, T., Aranyos, A., et al. (2021). Comparative response of marine microalgae to H<sub>2</sub>O<sub>2</sub>-induced oxidative stress. *Appl. Biochem. Biotechnol.* 193 (12), 4052–4067. doi:10.1007/s12010-021-03690-x
- Bunghez, I.-R., Ion, R.-M., Velea, S., Ilie, L., Fierascu, R.-C., Dumitriu, I., et al. (2010). Silver nanoparticles produced by green production method. *Adv. Top. Optoelectron. Microelectron. Nanotechnologies* 5, 78211K. doi:10.1117/12.882053
- Casas-Arrojo, V., Decara, J., De Los Angeles Arrojo-Agudo, M., Pérez-Manríquez, C., and Abdala-Díaz, R. (2021). Immunomodulatory, antioxidant activity and cytotoxic effect of sulfated polysaccharides from *Porphyridium cruentum* (S.F. Gray) Nägeli. *Biomolecules* 11 (4), 488. doi:10.3390/biom11040488
- Cepoi, L., Rudi, L., Zinicovscaia, I., Chiriac, T., Miscu, V., and Rudic, V. (2021). Biochemical changes in microalga *Porphyridium cruentum* associated with silver nanoparticles biosynthesis. *Archives Microbiol.* 203 (4), 1547–1554. doi:10.1007/s00203-020-02143-z
- Cepoi, L., Zinicovscaia, I., Rudi, L., Chiriac, T., Rotari, I., Turchenko, V., et al. (2020). Effects of PEG-coated silver and gold nanoparticles on *Spirulina Platensis* biomass during its growth in a closed system. *Coatings* 10 (8), 717. doi:10.3390/coatings10080717
- Chen, B., Huang, J., Wang, J., and Huang, L. (2008). Ultrasound effects on the antioxidative defense systems of *Porphyridium cruentum*. *Colloids Surfaces B Biointerfaces* 61 (1), 88–92. doi:10.1016/j.colsurfb.2007.07.009
- Chugh, H., Sood, D., Chandra, I., Tomar, V., Dhawan, G., and Chandra, R. (2018). Role of gold and silver nanoparticles in cancer nano-medicine. *Artif. Cells, Nanomedicine, Biotechnol.* 46 (1), 1210–1220. doi:10.1080/21691401.2018.1449118
- Dummermuth, A. L., Karsten, U., Fisch, K. M., König, G. M., and Wiencke, C. (2003). Responses of marine macroalgae to hydrogen-peroxide stress. *J. Exp. Mar. Biol. Ecol.* 289 (1), 103–121. doi:10.1016/S0022-0981(03)00042-X
- Hasnain, M., Munir, N., Abideen, Z., Dias, D. A., Aslam, F., and Mancinelli, R. (2023). Applying silver nanoparticles to enhance metabolite accumulation and biodiesel production in new algal resources. *Agriculture* 13 (1), 73. doi:10.3390/agriculture13010073
- Hazani, A. A., Ibrahim, M. M., Arif, I. A., Shehata, A. I., Ell Gaaly, G., Daoud, M., et al. (2013). Ecotoxicity of Ag-nanoparticles to microalgae. *J. Pure Appl. Microbiol.* 7, 233–241.
- He, M., Yan, Y., Pei, F., Wu, M., Gebreluel, T., Zou, S., et al. (2017). Improvement on lipid production by *Scenedesmus obliquus* triggered by low dose exposure to nanoparticles. *Sci. Rep.* 7 (1), 15526. doi:10.1038/s41598-017-15667-0
- Ismail, R. A., Almashhadani, N. J., and Sadik, R. H. (2017). Preparation and properties of polystyrene incorporated with gold and silver nanoparticles for optoelectronic applications. *Appl. Nanosci.* 7 (3–4), 109–116. doi:10.1007/s13204-017-0550-6
- Kang, H., Buchman, J. T., Rodriguez, R. S., Ring, H. L., He, J., Bantz, K. C., et al. (2019). Stabilization of silver and gold nanoparticles: Preservation and improvement of plasmonic functionalities. *Chem. Rev.* 119 (1), 664–699. doi:10.1021/acs.chemrev.8b00341
- Kang, N. K., Lee, B., Choi, G.-G., Moon, M., Park, M. S., Lim, J. K., et al. (2014). Enhancing lipid productivity of *Chlorella vulgaris* using oxidative stress by TiO<sub>2</sub> nanoparticles. *Korean J. Chem. Eng.* 31 (5), 861–867. doi:10.1007/s11814-013-0258-6
- Kula-Maximenko, M., Gorczyca, A., Pocięcha, E., Gastoł, A., Maciejewska-Prończuk, J., and Oćwieja, M. (2022). Characterization of selected parameters of *Chlorella vulgaris* microalgae after short-term exposure to gold nanoparticles with different surface properties. *J. Environ. Chem. Eng.* 10 (5), 108248. doi:10.1016/j.jece.2022.108248
- Li, X., Sun, H., Mao, X., Lao, Y., and Chen, F. (2020). Enhanced photosynthesis of carotenoids in microalgae driven by light-harvesting gold nanoparticles. *ACS Sustain. Chem. Eng.* 8 (20), 7600–7608. doi:10.1021/acssuschemeng.0c00315
- Majdalawieh, A., Kanan, M. C., El-Kadri, O., and Kanan, S. M. (2014). Recent advances in gold and silver nanoparticles: Synthesis and applications. *J. Nanosci. Nanotechnol.* 14 (7), 4757–4780. doi:10.1166/jnn.2014.9526
- Middepogu, A., Hou, J., Gao, X., and Lin, D. (2018). Effect and mechanism of TiO<sub>2</sub> nanoparticles on the photosynthesis of *Chlorella pyrenoidosa*. *Ecotoxicol. Environ. Saf.* 161, 497–506. doi:10.1016/j.ecoenv.2018.06.027
- Moreno-Garrido, I., Pérez, S., and Blasco, J. (2015). Toxicity of silver and gold nanoparticles on marine microalgae. *Mar. Environ. Res.* 111, 60–73. doi:10.1016/j.marenvres.2015.05.008
- Navarro, E., Baun, A., Behra, R., Hartmann, N. B., Filser, J., Miao, A.-J., et al. (2008). Environmental behavior and ecotoxicity of engineered nanoparticles to algae, plants, and fungi. *Ecotoxicology* 17, 372–386. doi:10.1007/s10646-008-0214-0
- Pádrová, K., Lukavský, J., Nedbalová, L., Čejková, A., Cajthaml, T., Sigler, K., et al. (2015). Trace concentrations of iron nanoparticles cause overproduction of biomass and lipids during cultivation of cyanobacteria and microalgae. *J. Appl. Phycol.* 27 (4), 1443–1451. doi:10.1007/s10811-014-0477-1
- Patra, S., Mukherjee, S., Barui, A. K., Ganguly, A., Sreedhar, B., and Patra, C. R. (2015). Green synthesis, characterization of gold and silver nanoparticles and their potential application for cancer therapeutics. *Mater. Sci. Eng. C* 53, 298–309. doi:10.1016/j.msec.2015.04.048
- Pedroso, S., Helena, R., Costa, R., Popovic, R., and Gerson, W. (2013). Evaluation of toxicity and oxidative stress induced by copper oxide nanoparticles in the green alga *Chlamydomonas reinhardtii*. *Aquat. Toxicol.* 143, 431–440. doi:10.1016/j.aquatox.2013.09.015
- Reboloso Fuentes, M. (2000). Biomass nutrient profiles of the microalga *Porphyridium cruentum*. *Food Chem.* 70 (3), 345–353. doi:10.1016/S0308-8146(00)00101-1
- Rodriguez-Garcia, I., and Guil-Guerrero, J. L. (2008). Evaluation of the antioxidant activity of three microalgal species for use as dietary supplements and in the preservation of foods. *Food Chem.* 108 (3), 1023–1026. doi:10.1016/j.foodchem.2007.11.059
- Sendra, M., Yeste, M. P., Gatica, J. M., Moreno-Garrido, I., and Blasco, J. (2017). Direct and indirect effects of silver nanoparticles on freshwater and marine microalgae (*Chlamydomonas reinhardtii* and *Phaeodactylum tricornutum*). *Chemosphere* 179, 279–289. doi:10.1016/j.chemosphere.2017.03.123
- Sibi, G., D., Kumar, A. T., Gopal, K., Harinath, K., Banupriya, S., and Chaitra, S. (2017). Metal nanoparticle triggered growth and lipid production in *Chlorella vulgaris*. *Int. J. Sci. Res. Environ. Sci. Toxicol.* 2 (1), 1–8.
- Vargas-Estrada, L., Torres-Arellano, S., Longoria, A., Arias, D. M., Okoye, P. U., and Sebastian, P. J. (2020). Role of nanoparticles on microalgal cultivation: A review. *Fuel* 280, 118598. doi:10.1016/j.fuel.2020.118598
- Wang, F., Liu, T., Guan, W., Xu, L., Huo, S., Ma, A., et al. (2021). Development of a strategy for enhancing the biomass growth and lipid accumulation of *Chlorella* Sp. UJ-3 using magnetic Fe<sub>3</sub>O<sub>4</sub> nanoparticles. *Nanomaterials* 11 (11), 2802. doi:10.3390/nano11112802



## OPEN ACCESS

## EDITED BY

Marco P. Monopoli,  
Royal College of Surgeons in Ireland,  
Ireland

## REVIEWED BY

Mehran Alavi,  
Razi University, Iran  
Hiromi Sakai,  
Nara Medical University, Japan

## \*CORRESPONDENCE

Shinji Takeoka,  
✉ takeoka@waseda.jp

RECEIVED 27 May 2023

ACCEPTED 09 August 2023

PUBLISHED 22 August 2023

## CITATION

Ota A, Mochizuki A, Sou K and Takeoka S  
(2023), Evaluation of a static mixer as a  
new microfluidic method for  
liposome formulation.  
*Front. Bioeng. Biotechnol.* 11:1229829.  
doi: 10.3389/fbioe.2023.1229829

## COPYRIGHT

© 2023 Ota, Mochizuki, Sou and Takeoka.  
This is an open-access article distributed  
under the terms of the [Creative  
Commons Attribution License \(CC BY\)](#).  
The use, distribution or reproduction in  
other forums is permitted, provided the  
original author(s) and the copyright  
owner(s) are credited and that the original  
publication in this journal is cited, in  
accordance with accepted academic  
practice. No use, distribution or  
reproduction is permitted which does not  
comply with these terms.

# Evaluation of a static mixer as a new microfluidic method for liposome formulation

Aoba Ota<sup>1</sup>, Ayaka Mochizuki<sup>1</sup>, Keitaro Sou<sup>2</sup> and Shinji Takeoka<sup>1,3\*</sup>

<sup>1</sup>Department of Life Science and Medical Bioscience, Graduate School of Advanced Science and Engineering, Waseda University, Tokyo, Japan, <sup>2</sup>Waseda Research Institute for Science and Engineering, Waseda University, Tokyo, Japan, <sup>3</sup>Institute for Advanced Research of Biosystem Dynamics, Waseda Research Institute for Science and Engineering, Waseda University, Tokyo, Japan

**Introduction:** Microfluidic formulation of liposomes has been extensively studied as a potential replacement for batch methods, which struggle with problems in scalability and difficulty in modulating conditions. Although microfluidic devices are considered to be able to combat these issues, an adequate replacement method has yet to be established.

**Methods:** This paper examines the potential of a static mixer (SM) by comparing the encapsulation efficiency, loading, lamellarity, and user-friendliness with a commonly used microfluidic device, a staggered herringbone micromixer (SHM).

**Results:** In both devices, it was found that as the initial lipid concentration increased, the particle size increased; however, the overall particle size was seen to be significantly larger in the liposomes prepared with SM. PDI remained significantly smaller in SM, however, signifying that better control of the particle size was accomplished in SM. In addition, the encapsulation efficiency was slightly smaller in SM compared to SHM, and in both devices, the values increased as the initial lipid concentration increased. The increase in encapsulation efficiencies was significantly smaller than that of the theoretical encapsulation efficiency, and this was found to be due to the increase in lamellarity as the initial lipid concentration increased.

**Discussion:** In terms of user-friendliness, SM demonstrated significant advantages. The mixing elements could be taken out from the device, allowing for thorough cleaning of the element and device before and after experiments and ensuring experiments are conducted at virgin state in every round. Consequently, it was found that SM not only can produce uniformly distributed liposomes but has the potential to become a more practical method for liposome formulation with modifications in the mixing elements.

## KEYWORDS

liposome, encapsulation, microfluidics, static mixer, staggered herringbone micromixer, nanoparticle

## 1 Introduction

Liposomes are biocompatible spherical nanocapsules formed with phospholipid bilayers, that have recently been extensively researched for their potential in medicine (Filipczak et al., 2020; Guimarães et al., 2021; Tenchov et al., 2021). Their amphipathic nature allows them to encapsulate both hydrophobic and hydrophilic molecules, and with their additional ability to be modified for targeted delivery, they are considered to have a high potential as a drug

delivery system (Kraft et al., 2014; Bulbake et al., 2017; Liu et al., 2022). Much research has been conducted on liposomes which are beneficial in delivering hemoglobin (Takeoka et al., 1996; Sou et al., 2003), genes (Kikuchi et al., 1999; Obata et al., 2008), adenosine 5'-diphosphate (Okamura et al., 2010; Hagsawa et al., 2019), and contrast agents (Saito et al., 2005; Kostevšek et al., 2020). Encapsulation into liposomes has demonstrated benefits in targeting, controlled release (Bibi et al., 2012; Niu et al., 2012), stabilization, and protection from denaturation (Cortesi et al., 1996; Chaize et al., 2004).

Although *in vitro* experimentation of liposomes has shown substantial growth and would suggest great potential *in vivo*, their translation into the medical field and use clinically has not grown as expected. This has been observed to be due to problems in manufacturing, regulations, and the complexity of the technology (Sercombe et al., 2015). Manufacturing remains to be a great issue, with pharmaceutical industries struggling with reproducibility, scalability, and difficulty in adjusting the preparation conditions (Sercombe et al., 2015). The pre-existing methods that allow for successful liposome formulation are commonly batch methods such as ethanol injection method and thin-film hydration method (Šturm and Poklar Ulrih, 2021), and are not considered ideal in scalability, reproducibility, and modulation. Although batch methods are easily accessible to produce liposomes on an experimental scale in the laboratory, these methods only allow for the production of milliliter units, resulting in large amounts of waste when only necessary for *in vitro* experiments. In contrast, the scale would be rather small for preparing liposome samples for animal experiments. Such inefficiency in materials, costs, efforts, and time would be a big obstacle to the progress of liposome technology. On the other hand, in pharmaceutical manufacturing, at least kiloliter units of liposomes are required, so the batch method has to be conducted multiple times for an adequate amount to be manufactured. Additionally, adjusting the scale-up factors of the preparation conditions is complicated and requires proficient experience and skills in batch methods. For clinical uses such as when drugs are encapsulated into liposomes and delivered to tumors, accurate modification of liposome size is essential since it heavily impacts its dynamics (Nagayasu et al., 1999). However, batch methods are incapable of preparing a monodisperse sample of liposomes, and often require multi-step processing such as extrusion to unify and control the size of the liposomes (Šturm and Poklar Ulrih, 2021). Since extrusion requires the liposomes to pass through membrane filters of decreasing pore sizes, clogging of the membrane filters and loss of the lipids and encapsulated molecules have been serious problems in this step.

Microfluidic formulation of liposomes can combat these issues, allowing for a more uniformly distributed size of liposomes to be generated in a continuous flow-synthesis method (Jahn et al., 2008). T- and Y-shaped micromixers allow for two liquids to consecutively be mixed, allowing there to be no limit to how much liposomes are prepared as long as liquids are being passed through; in other words, preparation of minuscule volumes to potentially an endless supply can be made possible without changing the conditions. In addition, in a microfluidic device, by simply altering different parameters such as the total flow rate (TFR, the volume at which the liquids are passed through the device per minute), flow rate ratio (FRR, the ratio at which the organic and aqueous solution are pushed through the device), and the initial lipid concentration of the organic solution (ILC), properties of the resultant sample can be modulated. Thus,

there is no need for subsequent size control steps such as extrusion, minimizing the hassle and loss during liposome preparation.

A staggered herringbone micromixer (SHM) is a microfluidic device that incorporates a series of asymmetric protrusions in a flow channel for rapid mixing. To this day, the SHM device has been evaluated to produce lipid-based nanoparticles including liposomes and lipid nanoparticles (Chen et al., 2012; Cheung and Al-Jamal, 2019). By modulating the preparation conditions, SHM can prepare nanoparticles that have controlled size and can efficiently encapsulate therapeutic agents such as hydrophobic drugs and mRNA (Chen et al., 2012; Kastner et al., 2015). While microfluidic technologies have many advantages, the devices used in the experiments are problematic in that blockages frequently occur, and the devices are extremely fragile to exterior force. Many of these chips have channels that are micrometers in width and thickness, resulting in the devices being clogged with the smallest dust particles finding their way through the channel. Therefore, this method does not seem promising especially if macromolecules or molecules with high aggregation are intended to be encapsulated. Solvent resistance is another limitation of these devices which are fabricated by soft lithography. The performance of devices made of polydimethylsiloxane, which is a commonly used material for conventional microfluidic devices, may change by swelling and deformation when in contact with organic solvents. Furthermore, the low volumetric throughput of the microfluidic device due to the narrow channels is another disadvantage for the translation of laboratory-scale preparation to large-scale production for clinical study and commercial scale.

A static mixer (SM), a device that can mix two liquids in a channel of a few millimeters in diameter with a structure shown in Figure 1, is considered to have the potential for liposome preparation. SMs are motionless mixers that have been applied in the blending of fluids, solids gases, and heat transfer (Thakur et al., 2003). Their structure allows for thorough homogenization and due to mixing being conducted without agitation, they are low in energy consumption and require less maintenance, resulting in their prevalence in the pharmaceutical industry, food engineering, and petrochemical industries (Thakur et al., 2003). SMs typically have a larger channel than a microfluidic device, which allows them to be less prone to blockages and allows for high volumetric throughput.

This work utilized a SM which has a channel of 1 mm diameter, allowing for the observation of blockages with the naked eye. Furthermore, the structure of the device allowed for the elements in the channel to be taken out and washed. This ensured that the device was completely cleansed after each experiment, allowing all experiments to be conducted at virgin state. With the aforementioned user-friendliness being given, this work aims to further understand the potential of using SM in liposome preparation and also evaluate the differences it may hold when compared to the conventional microfluidic device. In this paper, the liposomes produced in SHM are compared to that of SM and evaluated to consider the potential of a static mixer in a liposome preparation.

## 2 Materials and methods

### 2.1 Materials

For lipid components, 1, 2-dipalmitoyl-*sn*-glycerol-3-phosphocholine (DPPC) and cholesterol were purchased from Tokyo Chemical Industry Co. Ltd. (Tokyo, Japan), 1, 5-dihexadecyl-*N*-succinyl-L-glutamate



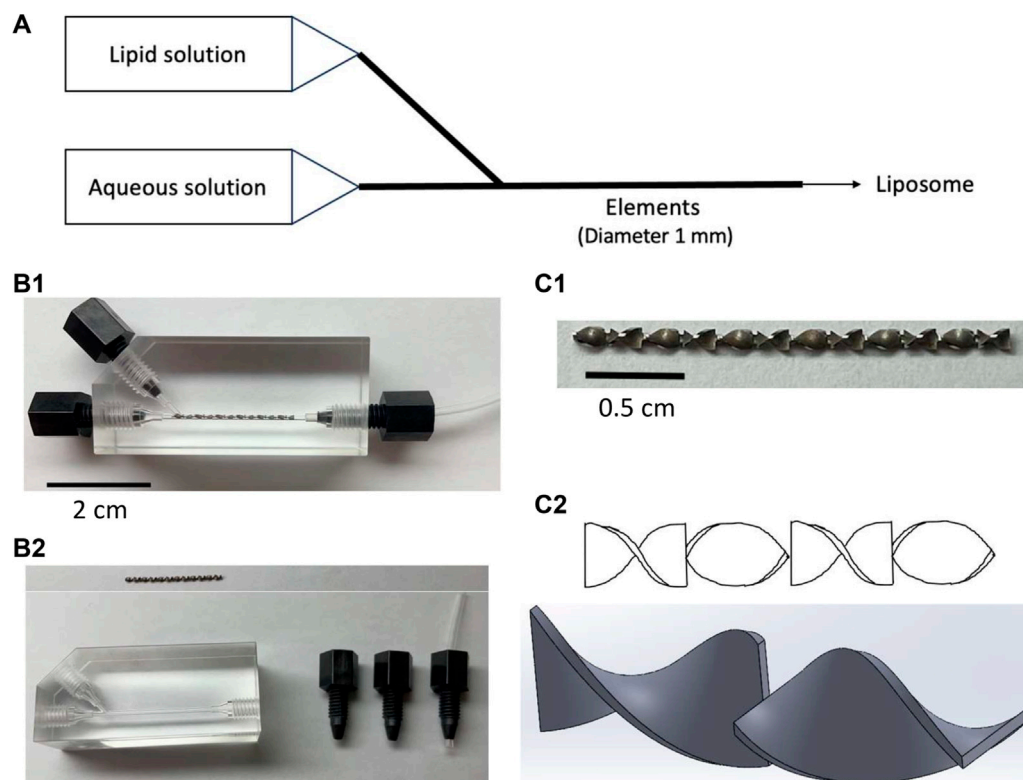


FIGURE 1

Pictures and schemes of the static mixer. (A) Schematic of a microfluidic method for liposome preparation using a static mixer with an element in a channel of 1 mm diameter, (B1) static mixer assembled, (B2) disassembled static mixer with the element removed and placed above the device, (C1) zoomed-up image of the element, and (C2) scheme of the elements viewed from various angles.

(DHSG) was purchased from Nippon Fine Chemical Co. Ltd. (Osaka, Japan), and 1, 2-distearoyl-*sn*-glycero-3-phosphoethanolamine-*N*-[monomethoxy poly (ethylene glycol) (5000)] (PEG-DSPE) was purchased from NOF Co. Ltd. (Tokyo, Japan). For fluorescent dyes, calcein was purchased from Dojindo Laboratories (Kumamoto, Japan), while 1,1'-dioctadecyl-3,3,3',3'-tetramethylindodicarbocyanine, 4-chlorobenzenesulfonate salt (DiD) was purchased from Thermo Fisher Scientific (Waltham, United States).

## 2.2 Liposome formulation with SM and SHM

Liposomes were formulated by using a static mixer (SM) and a staggered herringbone micromixer (SHM) under comparable conditions to understand the potential of SM in liposome formulation when compared to an established microfluidic method such as SHM (Cheung and Al-Jamal, 2019). A modified K-series SM was provided from Noritake (Aichi, Japan) (Figure 1), while SHM (Darwin microfluidics, 2023) was purchased from Darwin Microfluidics (Paris, France) (Supplementary Figure S1). DPPC, cholesterol, DHSG, and PEG-DSPE were dissolved in *t*-butyl alcohol at a molar ratio of 5:5:1:0.066 and DiD was then further added at 0.2 mol% to the total lipid. The mixed solution was freeze-dried to obtain a mixed lipid powder for stock. An aliquot of the freeze-dried powder was dissolved in filtered 99.5% ethanol (Fujifilm Wako Pure Chemical, Japan) at concentrations of 15–90 mg/mL

before each round of the experiment to prepare the lipid solution. Calcein was applied for evaluating the encapsulation efficiency of liposomes. Calcein is widely used as a water-soluble fluorescent marker to evaluate the encapsulation capacity and release properties of liposomes because calcein can be stably encapsulated into liposomes (Grit et al., 1992; Berger et al., 2001). Also, the encapsulation efficiency of calcein into liposomes prepared by a filter extrusion method well agrees with the theoretical value calculated for unilamellar liposomes in the assumption that there is no interaction between the lipid bilayer membrane and encapsulated molecules (Xu et al., 2012). Calcein was dissolved in PBS (Takara Bio, Japan) using NaOH (final concentration 3 mM) to prepare a 1 mM calcein solution as the aqueous solution. The calcein solution was passed through a hydrophilic filter with a pore size of 0.22  $\mu\text{m}$  (Merck Millipore, United States) after it had fully dissolved. Both solutions were filtered to ensure that no blockages would be caused by foreign particles. The mixed lipid ethanol solution and aqueous calcein solution were passed through the devices (SM and SHM) at TFR of 1,500, 2000, and 2,500  $\mu\text{L}/\text{min}$  and aqueous-to-ethanol FRR of 3,4, and 5. The TFR and FRR were adjusted by a syringe pump (Legato 111, KD Scientific, United States). In order to accurately collect liposomes that were generated with the set TFR and FRR, the liposomes produced in the beginning and towards the end of the flows were not collected. The lipid-in-ethanol concentrations were set as 15, 30, 45, 60, and 90 mg/mL, presented as initial lipid concentration (ILC).

## 2.3 Liposome purification

The resultant liposomes were purified by ultrafiltration to remove ethanol and calcein that were not encapsulated into the liposomes. The centrifugal ultrafiltration device Vivaspin® 6, with membrane 100,000 MWCO (Sartorius, Germany) was used, allowing for liposomes to remain in the concentrator while the outer aqueous layer with the unencapsulated calcein and ethanol was dropped into the filtrate container. The sample was centrifuged until the outer aqueous layer was diluted 1,000 times with PBS, and the resultant liquid on the top was collected with a pipette with the liposomes on the membrane being washed down and collected with PBS.

## 2.4 Characterization and encapsulation properties of liposomes

Particle size, polydispersity index (PDI), lipid recovery rate (LRR), encapsulation efficiency (EE), and loading were measured for analysis. Particle size and PDI were measured by Zetasizer Nano (Malvern Panalytical, United Kingdom). LRR, loading, and EE were calculated from equations 1, 2, and 3, respectively. An aliquot of the obtained liposome dispersion (100  $\mu$ L) was mixed with ethanol (900  $\mu$ L) to solubilize the liposomes, and the lipid concentration was calculated from the DiD fluorescence intensity in the ethanol solution ( $\lambda_{ex}$  = 635 nm,  $\lambda_{em}$  = 670 nm). The calcein concentration was calculated from the fluorescence intensity measured after solubilizing the liposomes with octyl glucoside at a final concentration of 45 mM in PBS ( $\lambda_{ex}$  = 480 nm,  $\lambda_{em}$  = 530 nm). All fluorescence intensities were measured using the SynergyH1 fluorescent plate reader (BioTek, United States). In the following equations, mixed solution (MS) refers to the aqueous solution and lipid solution mixed by pipetting in a defined mixing ratio without having passed through any device.

$$LRR [\%] = \frac{\text{Lipid concentration of sample after passing through device} \left( \frac{mg}{mL} \right)}{\text{Lipid concentration of MS} \left( \frac{mg}{mL} \right)} \times 100 \quad (1)$$

$$\text{Loading} = \frac{\text{Calcein concentration of sample after purification} (mM)}{\text{Lipid concentration of sample after purification} \left( \frac{mg}{mL} \right)} \quad (2)$$

$$EE [\%] = \text{Loading} \times \frac{\text{Lipid concentration of sample after passing through device} \left( \frac{mg}{mL} \right)}{\text{Calcein concentration of MS} (mM)} \times 100 \quad (3)$$

The theoretical encapsulation efficiency (TEE) was calculated using a mathematical model created by Xu et al. (Eq. 4), which predicts the encapsulation efficiency in unilamellar liposomes (Xu et al., 2012).

$$TEE [\%] = \frac{\sum_i \left( \frac{4}{3} \pi (r_i - d)^3 \cdot (c \cdot V \cdot N_A) \right) / \sum_i \left( 4 \pi [r_i^2 + (r_i - d)^2] \cdot \frac{P_i}{a} \right) \cdot P_i}{V} \times 100 \quad (4)$$

In the above equation,  $d$ ,  $r_i$ ,  $P_i$ ,  $c$ ,  $a$  and  $V$  refers to the membrane thickness of DPPC bilayer membrane (4.8 nm) (Lewis and Engelman, 1983), the radius of the liposome  $i$ , probability of  $r_i$ , lipid molar concentration, known average molecular area of lipid in monolayer membrane of DPPC and cholesterol at a molar ratio of 1:1 (0.43 nm<sup>2</sup>)

(Kodama et al., 2004), and total sample volume, respectively. The  $c$  and  $V$  were assigned as lipid concentration of a liposome dispersion calculated from FRR and ILC (mM), and the volume of liposome dispersion (mL), respectively.  $N_A$  is Avogadro's number which is equal to  $6.02 \times 10^{23}$ . The variables  $r_i$  and  $P_i$  are the particle size radius measured by the Zetasizer and the probability of the presence of vesicles of the entered size, respectively. To calculate  $P_i$ ,  $r_i$  and size distribution were substituted. However, this model assumes that the liposomes are spherical, have an inner aqueous phase entrapped with a single lipid bilayer separated from the outer aqueous phase, the encapsulated molecule is hydrophilic and has the same concentration as the outer aqueous phase, and the particle size follows a Log-Normal distribution (Xu et al., 2012).

For comparison of the lamellarity of liposomes, a fluorescence probe, 6- $p$ -toluidino-2-naphthalenesulfonic acid (TNS) (Abcam, United Kingdom) was used to compare the total surface area of liposomes, in which the ratio of the surface area at the same lipid concentration represents the number of bilayer membranes (Takeoka et al., 1996). For the liposomes prepared in the SHM and SM, TFR 1500  $\mu$ L/min, FRR 3, and ILC 15, 45, and 90 mg/mL were used (six preparation conditions in total). A liposome sample with the same lipid composition was prepared using a probe-type sonicator (Sonifer 250, Branson), and this was defined as a standard of unilamellar liposomes. The lipid concentration in the liposome samples was determined using a phospholipid assay kit (Fujifilm Wako Pure Chemical, Japan), and the samples were diluted to have the same concentrations. TNS was added to all liposome samples with a five-step gradient in lipid concentration and incubated at ambient temperature for 12 h before fluorescence was measured ( $\lambda_{ex}$  = 321 nm,  $\lambda_{em}$  = 400 nm). After the fluorescence measurement, the relationship between the amount of liposome sample added and the fluorescence intensity was plotted on a graph, and the slopes were calculated. The number of the bilayer membranes of liposomes (lamellarity) was calculated by dividing the slope of the standard unilamellar liposomes by the slope of the liposome samples, with the assumption that the number of the lipids composing each lipid layer is the same as the number of the lipids composing the outermost layer of liposomes.

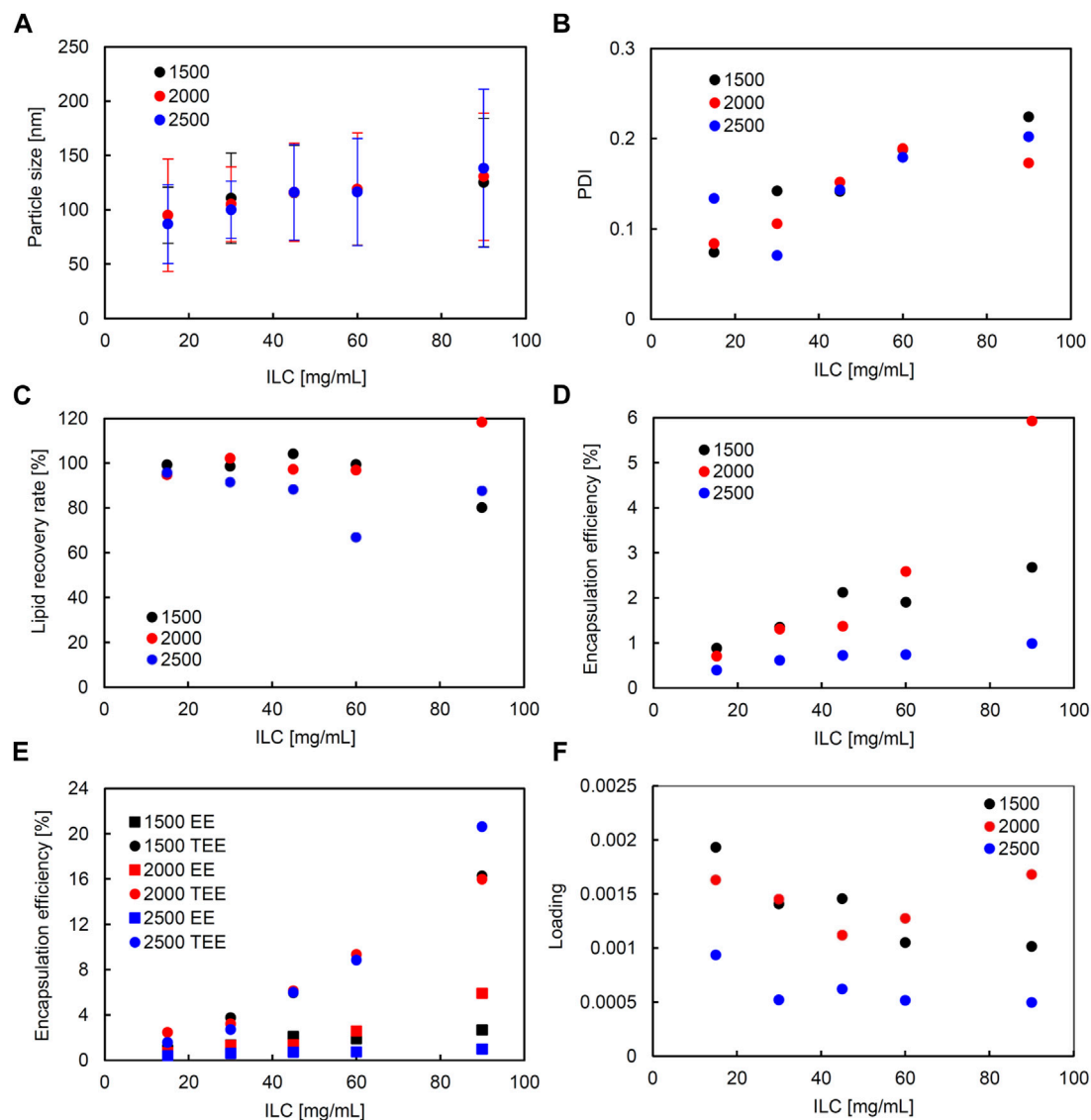
## 2.5 Scatterplot matrix

A scatterplot matrix was performed to examine linear correlations between multiple variables. Scatterplot matrix analysis was conducted using Microsoft Excel for Mac version 16.73. The relationship between the parameters and the characteristics of the liposomes could be visualized by the scatterplot matrix. The  $p$ -value was calculated from the  $t$ -value, which was calculated from the Pearson correlation coefficient and the number of plots using Microsoft Excel for Microsoft 365 MSO version 2307. Statistical significance was considered at  $p < 0.05$ .

## 3 Results

### 3.1 SHM device

In the liposomes formulated in SHM, correlation coefficients of higher than 0.5 were observed between ILC and particle size, ILC



**FIGURE 2**

Comparison of liposome characteristics generated under total flow rate (TFR) of 1,500, 2,000, and 2,500  $\mu\text{L}/\text{min}$  in a staggered herringbone micromixer (SHM) device. The flow rate ratio (FRR) was fixed at 3. (A) Particle size, (B) polydispersity index (PDI), (C) lipid recovery rate (LRR), (D) encapsulation efficiency (EE), (E) theoretical encapsulation efficiency (TEE) and EE, and (F) loading.

and PDI, particle size and PDI, ILC and EE, and particle size and EE (Supplementary Figure S2). Figure 2 shows the characteristics of the lipid particles obtained using SHM when the FRR was fixed at 3 and the TFR was set to 1,500, 2,000, or 2,500  $\mu\text{L}/\text{min}$ . Figure 3 shows the characteristics of the lipid particles when the TFR was fixed at 1,500  $\mu\text{L}/\text{min}$  and the FRR was set to 3, 4, or 5. ILC was varied from 15 to 90 mg/mL at each condition. The mean particle size of the obtained liposomes was between 86–144 nm with a unimodal size distribution (Figures 2A, 3A). The particle size increased as the ILC was increased at any combinations of TFR and FRR, and the average size was seen to range from 91 nm at ILC 15 mg/mL to 131 nm at ILC 90 mg/mL. In addition, as the ILC and particle size increased, the particle size distribution was also seen to increase.

The obtained liposomes exhibit PDI values of 0.071–0.259 (Figures 2B, 3B). The correlation coefficient between the ILC and PDI was 0.64,

with the PDI increasing as the ILC increased (Supplementary Figure S2). This characteristic was seen to be the most evident in Figures 2B, 3B at TFR 1500  $\mu\text{L}/\text{min}$ , FRR 3 where the PDI was 0.074 at ILC 15 mg/mL and 0.224 at 90 mg/mL. The values of calculated LRR were in the range of 60%–118% without a clear correlation with other variables (Figures 2C, 3C; Supplementary Figure S2).

The correlation coefficient was 0.57 between the ILC and EE (Supplementary Figure S2) with the EE increasing as the ILC was increased under any combination of FRR and TFR (Figures 2D, 3D; Supplementary Figure S2). Furthermore, it was also found that EE was higher at lower FRR in all ILCs (Figure 2D). A distinct difference could be observed at ILC 90 mg/mL, where the EE was 2.7%, 1.4%, and 0.8% for FRR 3, 4, and 5, respectively.

The particle size and EE was seen to have a correlation coefficient of 0.50 with the EE increasing as the particle size got larger (Supplementary

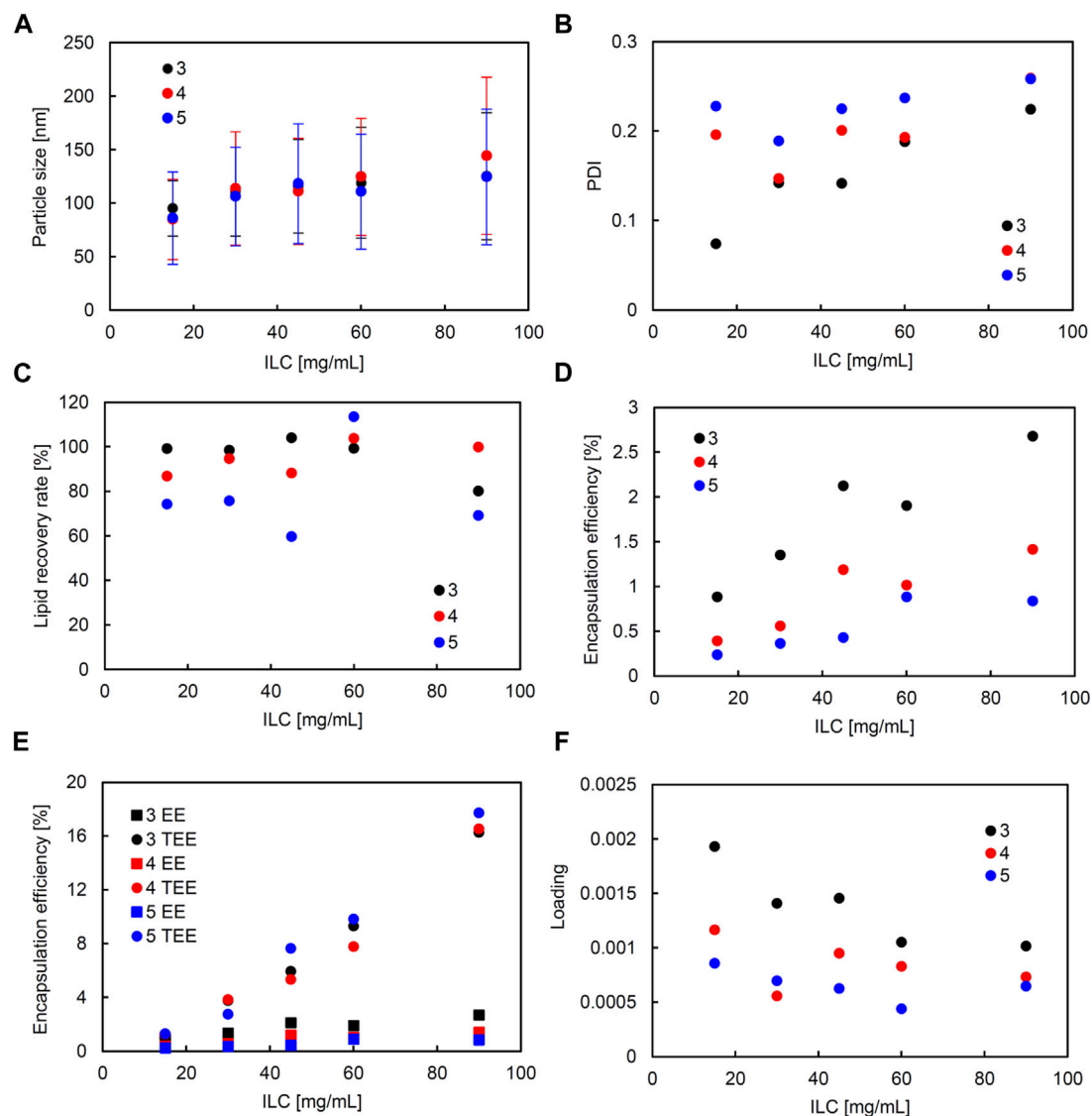


FIGURE 3

Comparison of liposome characteristics generated under flow rate ratio (FRR) of 3, 4, and 5 in a staggered herringbone micromixer (SHM) device. The total flow rate (TFR) was fixed at 1,500  $\mu\text{L}/\text{min}$ . (A) Particle size, (B) polydispersity index (PDI), (C) lipid recovery rate (LRR), (D) encapsulation efficiency (EE), (E) theoretical encapsulation efficiency (TEE) and EE, and (F) loading.

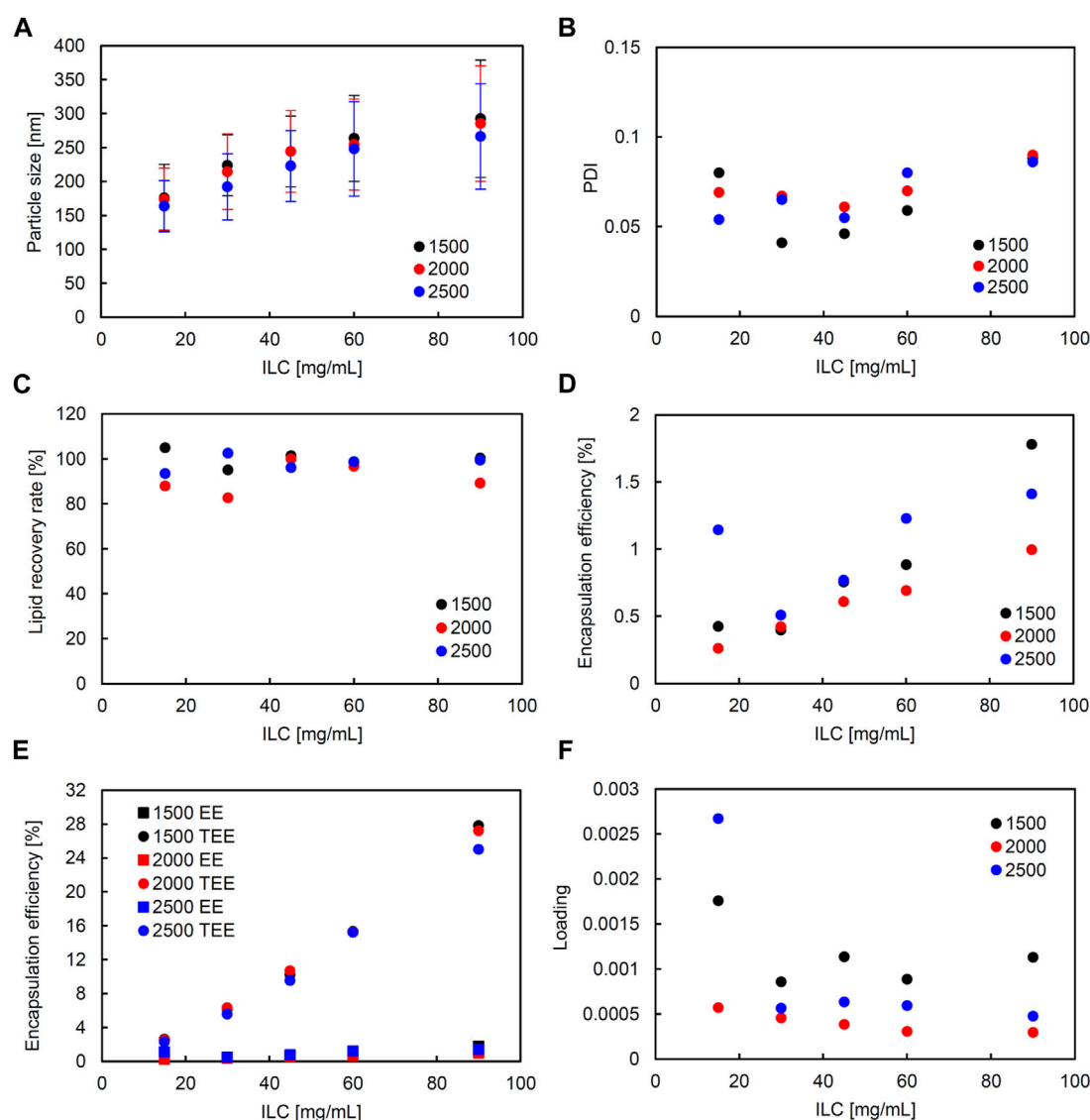
Figure S2). When looking at the data for TFR 2000  $\mu\text{L}/\text{min}$ , it can be seen that at ILC 15 mg/mL when the particle size was 95 nm, the EE was 0.7%; whereas, at ILC 90 mg/mL, when the particle size was 131 nm, the EE was 5.9%, increasing the EE 8-fold with the increase in particle size. In addition, it was found that in all conditions, TEE also increased when ILC increased, with the gap between TEE and EE expanding proportionally to ILC (Figures 2E, 3E; Supplementary Figure S4). The loading varied between 0.000439 and 0.00193, with all values obtained at TFR 2500  $\mu\text{L}/\text{min}$  lower than 0.001 (Figures 2F, 3F).

### 3.2 Static mixer

Similarly, in the SM, correlation coefficients with significance (higher than 0.5 and smaller than  $-0.5$ ) were seen between the

following: ILC and particle size, ILC and EE, and particle size and loading (Supplementary Figure S3). Figure 4 shows the characteristics of the liposomes obtained using SM when the FRR was fixed at 3 and the TFR was set to 1,500, 2000, or 2,500  $\mu\text{L}/\text{min}$ . Figure 5 shows the characteristics of the lipid particles when the TFR was fixed at 1,500  $\mu\text{L}/\text{min}$  and the FRR was set to 3, 4, and 5. ILC was varied from 15 to 90 mg/mL at each condition. The particle size was seen to increase as ILC was increased, with a correlation coefficient of 0.96 (Supplementary Figure S3). This was evident at TFR 2500  $\mu\text{L}/\text{min}$  where the particle size increased from 164 nm at ILC 15 mg/mL to 304 nm at ILC 90 mg/mL. One thing to note was that although the particle size drastically increased, the PDI mostly remained consistently under 0.1 (Figures 4B, 5B). Furthermore, as can be seen in Figure 4A, as TFR was increased, the particle size was seen to decrease. The largest difference was seen at 30 mg/mL where the



**FIGURE 4**

Comparison of liposome characteristics generated under total flow rate (TFR) of 1,500, 2,000, and 2,500  $\mu\text{L}/\text{min}$  in a static mixer. The flow rate ratio (FRR) was fixed at 3. (A) Particle size, (B) polydispersity index (PDI), (C) lipid recovery rate (LRR), (D) encapsulation efficiency (EE), (E) theoretical encapsulation efficiency (TEE) and EE, and (F) loading.

particle size was 224 nm at TFR 1500  $\mu\text{L}/\text{min}$  and 192 nm at TFR 2500  $\mu\text{L}/\text{min}$ . In all conditions, as can be seen in Figures 4C, 5C, the LRR mostly remained within the range of 70%–120%.

A correlation coefficient of 0.58 was seen between ILC and EE (Supplementary Figure S3). In all conditions, as ILC was increased, EE was also seen to increase (Figures 4D, 5D). The most drastic increase was seen in the condition of TFR 1500  $\mu\text{L}/\text{min}$ , FRR 3 where EE was 0.4% at ILC 15 mg/mL and 1.8% at ILC 90 mg/mL, an increase of over 4-fold (Figure 4D).

The particle size and loading had a barely significant correlation of coefficient  $-0.50$ , where, as the size increased, the loading decreased. This is evident in Figures 4A, 5A; Figures 4F, 5F, where the particle size increased and loading decreased as ILC was increased. In addition, as can be found from Figures 4E, 5E,

in all conditions, the gap between the TEE and EE increased as ILC was increased (Supplementary Figure S4).

### 3.3 SHM and SM comparison

When the two devices were compared in the scatterplot matrix, it was found that the difference in device yielded a difference in particle size and PDI with correlation coefficients of 0.89 and  $-0.76$ , respectively (Figure 6). The particle size was significantly smaller in all ILCs for the SHM device when compared to the SM. The average size difference between the liposomes generated using the two devices was 122 nm when compared under the same conditions. The size difference was seen to increase as ILC was increased, with

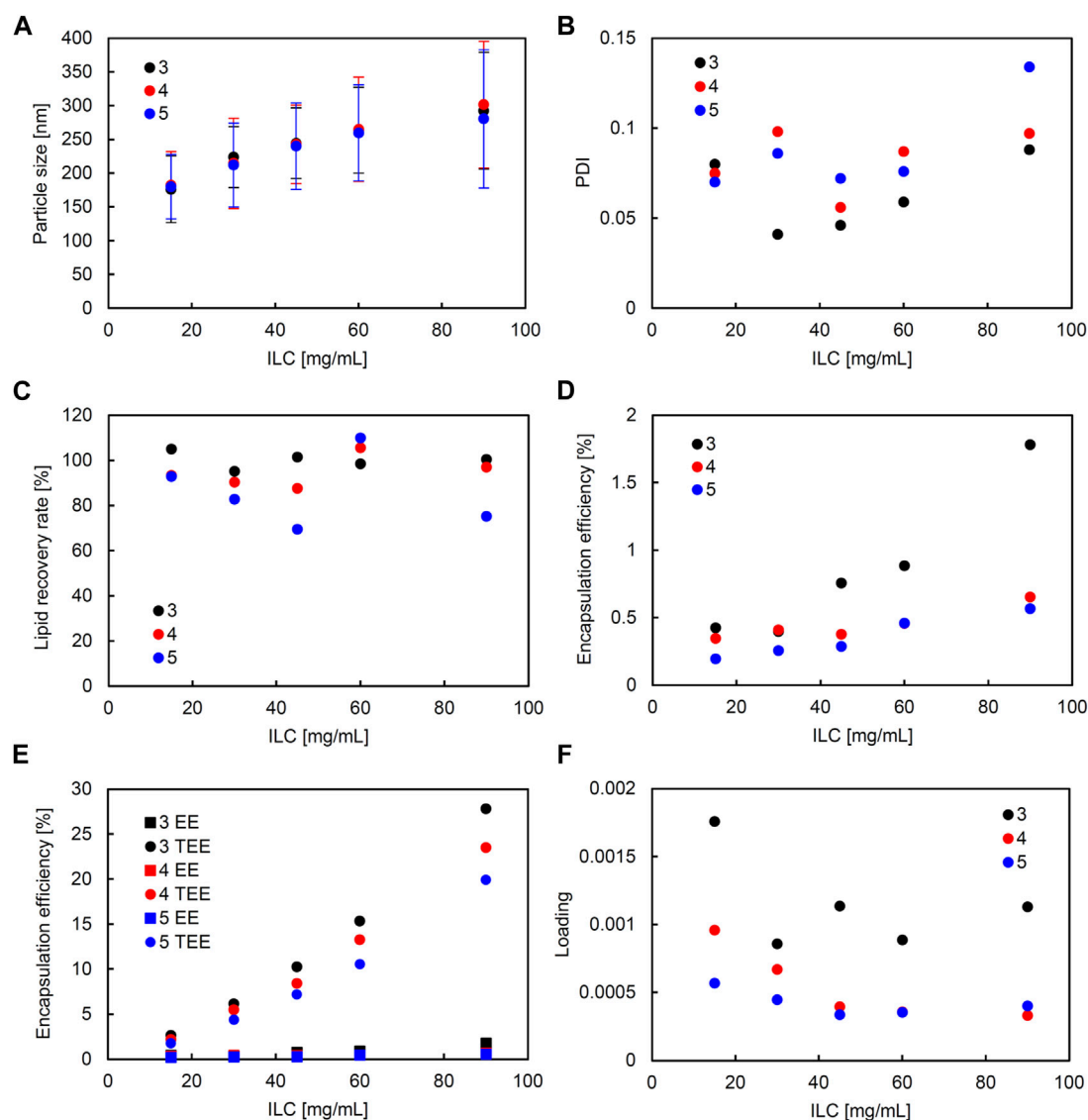


FIGURE 5

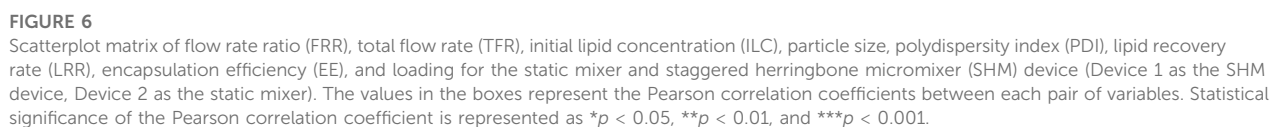
Comparison of liposome characteristics generated under flow rate ratio (FRR) of 3, 4, and 5 in a static mixer. The total flow rate (TFR) was fixed at 1,500  $\mu\text{L}/\text{min}$ . (A) Particle size, (B) polydispersity index (PDI), (C) lipid recovery rate (LRR), (D) encapsulation efficiency (EE), (E) theoretical encapsulation efficiency (TEE) and EE, and (F) loading.

the difference being 85 nm, 106 nm, 124 nm, 141 nm, and 155 nm, for 15, 30, 45, 60, and 90 mg/mL, respectively.

A correlation coefficient of  $-0.76$  was seen between the device and the PDI with SHM having a much larger PDI than SM. The average PDI size for SHM and SM were 0.170 and 0.073, respectively, with the PDI being 2.3 times larger for SHM.

Furthermore, from the scatterplot matrix, it was found that the particle size and PDI had a correlation coefficient of  $-0.60$ . Figure 6 shows a distinct difference between the two particle size ranges and the PDI. The smaller particle sizes are liposomes formulated by SHM and a large range of PDI can be seen; whereas, in the larger particle sizes of liposomes formulated with SM, the PDI remains small. This can also be seen in Figures 2B, 3B; Figures 4B, 5B, where the PDI is seen to range up until approximately 0.26 for SHM, while SM was, excluding one condition, able to maintain the PDI at under 0.1.

TNS fluorescence was measured for six liposome samples formulated at ILC 15, 45, and 90 mg/mL, each with an SHM and SM. For the measurement, the lipid concentration of liposomes was unified, based on the results of a phospholipid assay. The slopes which reflect the relative value of the total surface area of liposomes were found to be 9.3, 7.5, and 6.6 for SHM, and 5.1, 1.7, and 0.73 for SM at ILC 15, 45, 90 mg/mL, respectively (Supplementary Figure S5A). The standard for unilamellar liposomes made through hydration and probe sonication had a slope of 8.6. From this, the lamellarity of the liposomes was calculated to be 0.93, 1.2, and 1.3, for the SHM, and 1.7, 5.1, and 11.9 for SM at ILC 15, 45, and 90 mg/mL, respectively (Supplementary Figure S5B). Thus, it was found that liposomes formed in SM at ILC 45 and 90 mg/mL are more multilamellar or multivesicular, with the lamellarity increasing proportionally to the ILC (Supplementary Figure S5B). When the



In both SHM and SM, the ILC had a great impact on the particle size with a positive correlation. A much greater increase in particle

size was seen for SM, where the particle size at 90 mg/mL was seen to increase an average of 111 nm from 175 nm at 15 mg/mL; whereas, for SHM, the particle size at 90 mg/mL was only seen to increase an average of 41 nm from 91 nm at 15 mg/mL. Moreover, the overall particle size was significantly smaller for SHM compared to SM. However, PDI remained significantly smaller in SM than in SHM, indicating that the liposome samples formulated in SM are more uniformly distributed. While the PDI was seen to be high for SHM as ILC was increased, SM was mostly able to maintain PDI under 0.1. This shows that SM is more able to mix the solutions equally with little unevenness in mixing. Since the accurate manipulation of

particle size is essential in medicinal applications, small PDI in SM is highly promising for future applications.

In addition to the ILC contributing to the particle size, TFR is seen to have an impact on the particle size. As TFR was increased, the particle size was seen to decrease, signifying that the mixing efficiency was increased when more pressure was applied. This can be supported by Zheng *et al.*, where liposome sizes were found to be inversely correlated to TFR at certain FRR and microfluidic devices. They detected that size reduction occurred when the TFR increased, and concluded that this was due to the higher mixing efficiency that can be obtained at higher TFR (Zheng *et al.*, 2022). While the total volumetric flow rate is comparable in this study, the linear flow velocity calculated by dividing the TFR by the cross-sectional area of the flow path is 156 cm/s in SHM and 3 cm/s in SM at TFR 1500  $\mu\text{L}/\text{min}$ . Because linear flow velocity is a critical factor in mixing efficiency and shear stress during flow in a path, the significant difference in the linear flow velocity may be involved in the difference in particle size between liposomes formed in SHM and SM. A higher TFR than 2,500  $\mu\text{L}/\text{min}$  would be considered for SM to increase the linear velocity when the target size of liposomes is smaller than 150 nm. The impact of FRR on particle size was minor in the range of 3–5. Cheung *et al.* reported that increasing the FRR resulted in a decrease in liposome size by using the SHM (Cheung and Al-Jamal, 2019). In their study, the range of FRR that affects particle size was between 1 and 3, and the effect on particle size was minor at FRR 3 or above. Therefore, FRR can be a controlling factor for particle size when the FRR is less than 3. At lower FRR, it takes longer for lipids to diffuse into the aqueous phase, allowing the self-assembled intermediate structure known as bilayered phospholipid fragments (BPFs) to grow larger in size, followed by the formation of larger liposomes (Lasic and Martin, 1990; Gouda *et al.*, 2021).

EE was also seen to increase with ILC in both devices. This is likely due to the increase in particle size and number of liposomes, allowing there to be more space in the particles for calcein to be encapsulated. However, when comparing EE to TEE, it can be seen that EE is lower than TEE in both devices. This may be due to the liposomes formulated by SHM, along with SM, not abiding by the assumptions for the TEE model. The model proposed by Xu *et al.* assumes that the liposomes are single lipid bilayers, that the inner and outer aqueous phases have the same concentration, and that the particle size follows a Log-Normal distribution (Xu *et al.*, 2012). Firstly, the liposome particle size may not have followed the Log-Normal distribution, resulting in variation in the TEE and EE. With the particle size changing with the various conditions and devices that were experimented on, it is difficult to confirm that the particle size conformed with the Log-Normal distribution, resulting in the EE differing from the TEE. In addition, the inner aqueous phase may not have the same calcein concentration as the outer aqueous phase, due to potential ethanol being entrapped. When the rate of liposome formation is more rapid than the mixing rate of the two liquids, the calcein solution is not able to be fully mixed with the lipid ethanol solution before forming liposomes, resulting in the encapsulated calcein solution having a lower concentration. In other words, the potential volume for calcein encapsulation is not fully maximized due to some amount of ethanol being entrapped, decreasing the EE. This point seems to be a common issue in both devices, but the differences between EE and TEE were more distinct in SM than in SHM (Supplementary Figure S4). Similarly, the EE was significantly

lower than the TEE for the batch-type conventional ethanol injection method (Supplementary Tables S1, S2; Supplementary Figure S7). The significant difference between EE and TEE in SM can be attributed to the lamellar structure of the liposomes. Specifically, the increase in the concentration of lipids combined with the larger particle sizes allows for the liposomes to form multiple layers (Supplementary Figure S5), resulting in lowered EE. Due to the liposomes being more multilamellar, the liposomes formulated with SM have a smaller volume for calcein encapsulation. It has been reported that the encapsulation efficiency of water-soluble fluorescent markers and hydrophilic drugs is considerably low with the conventional ethanol injection method when lipid ethanol solution is injected into the aqueous solutions of the water-soluble molecules (Pons *et al.*, 1993). Although increasing the lipid concentration in the mixed solution is expected to enhance the total encapsulation volume, it also results in the formation of multilamellar or multivesicular liposomes. Also, the BPF and liposome formation may be initiated at higher critical ethanol concentrations at higher ILC. The encapsulation efficiency of these liposomes would be significantly lower than the theoretical encapsulation efficiency calculated assuming unilamellar liposomes encapsulating a completely mixed solution. This issue poses a dilemma when applying the methods based on ethanol injection for the passive encapsulation of water-soluble drugs and may necessitate additional processing to improve encapsulation efficiency. On the other hand, the ethanol injection method demonstrates the efficient encapsulation of hydrophobic and amphiphilic drugs (Jaafar-Maalej *et al.*, 2010; Gouda *et al.*, 2021). Also, electrostatic interactions between encapsulation molecules and lipids, such as a combination of anionic nucleic acids and cationic lipids, are effective in improving encapsulation efficiency (Yang *et al.*, 2012).

In our experimental conditions, SHM was superior to formulate size-controlled unilamellar liposomes around 100 nm independent of the ILC. The unilamellar structure is suitable for the encapsulation of water-soluble molecules, but the low encapsulation efficiency was recognized as a technical issue in this study. On the other hand, SM was characterized by the ability to control the size of liposomes with smaller PDI. In addition, the lamellarity of liposomes is controllable depending on the ILC. The multilayer or multivesicular structure of liposomes formulated by SM at high ILCs may be suitable for stably and efficiently encapsulating hydrophobic drugs and mRNA rather than encapsulation of water-soluble molecules. The structure of the micromixers should be a critical factor to control the lamellarity of liposomes as well as their size. The SHM has an optimized structure for rapid mixing with a herringbone groove in a narrow flow path (Chen *et al.*, 2012). The large flow velocity due to the narrow path allows rapid mixing to form small BPFs after the two liquids were contacted. On the other hand, it can be estimated that the interval between the merging of the two liquids and mixing is extended in SM due to the low flow velocity, giving the lipids time to stay and form larger multilamellar or multivesicular liposomes at the junction of the two liquids. This estimation can be supported by the experiments of preparing lipid nanoparticles using SHMs with different distances between the merging point of liquids and the first SHM, in which the size of the generated lipid nanoparticle is increased by increasing the distance between the merging point



and the first SHM (Maeki et al., 2015). The rapid mixing to decrease the ethanol concentration to its critical concentration is crucial to make small-size lipid self-assemblies. They assumed that the formation of BPFs begins at the 80% ethanol condition (mixing rate: 20%) and the BPFs transfer to lipid nanoparticles at the 60% ethanol condition (mixing rate: 40%) (Maeki et al., 2017). The prolonged residence of lipids in a mixing state with 60%–80% ethanol concentrations increases the size of BPFs, which transform into larger lipid nanoparticles when the ethanol concentration drops below 60%. Therefore, control of the residence time of lipids at an ethanol concentration of 60%–80% and the lipid concentration at the critical ethanol concentration can be considered as a key point to control the size of lipid assemblies.

Temperature is also one of the important processing parameters to control the molecular assembling phenomenon because temperature changes the free energy, diffusion coefficient, and viscosity of the systems. In particular, the temperature should be considered as a critical factor when the liposomes exhibit gel-to-liquid crystalline phase transition at a critical temperature. The previous study indicates that liposomes formed at temperatures below the phase transition temperature of the bilayer membranes have larger sizes compared with liposomes prepared around phase transition temperature (Zook and Vreeland, 2010). A further problem in liposome preparation below phase transition temperature is the formation of large aggregates of lipids around the merging zone of liquids, especially at a low flow rate. The formation of lipid aggregates possibly causes the formation of large liposomes with high polydispersity and low reproducibility due to destabilizing the flow. Although the current study was conducted at room temperature, the formation of large aggregates was not observed in either device. This would be due to the addition of an equimolar amount of cholesterol to DPPC, which eliminates the phase transition of the DPPC membrane forming a fluid membrane. Even for liposomes with cholesterol, the heating of the device and fluids increases the diffusion coefficient and decreases the viscosity, resulting in increased mixing efficiency and reduced back pressure. Therefore, microfluidic mixing at higher temperatures allows for rapid mixing to generate smaller liposomes (Cheung and Al-Jamal, 2019).

The element of SM is well-designed for efficient mixing through a process of division, conversion, and inversion (Thakur et al., 2003). The size of multilamellar liposomes can be controlled by the fine mixing process during subsequent passing through the element. Therefore, in addition to the structure of the elements of the static mixer, the design of the channel structure of the micromixer will also be a future issue. The length of the microchannel is one of the considerable parameters in flow mixing. An extension of the microchannel flow path is effective to increase high mixing efficiency to attain a complete mixing state (Natsuhara et al., 2022). However, the back pressure is proportionally increased with increasing the length of the microchannel in pressure-driven flow. Increased back pressure causes breakage of the device. On the other hand, the back pressure is inversely proportional to the square of the channel diameter. In this sense, devices with shorter channels with larger diameters are preferred for safe operation at low back pressure in scale-up processing. SHM has the advantage of being efficiently mixed even in a short channel due to chaotic mixing compared with mixing by hydrodynamic flow focusing through a

plane microchannel. However, it is still difficult to increase volumetric throughput because the mixing efficiency decreases due to a decreased specific surface area in the flow channel in which the herringbone grooves are arranged for chaotic mixing when the cross-sectional area of the channel is increased. As a workaround for this limitation in scale-up, a parallelized device with many microchannels has been proposed for the scalable production of mRNA and siRNA lipid nanoparticles (Shepherd et al., 2021). SM can be expected to overcome the limitation of the conventional microfluidic devices in scale-up because the specification of elements of a static mixer such as shape, size, pitch, and length can be customized depending on the length and diameter of the channels.

In addition to statistically visible differences between the two devices, there is a significant difference in the structure and usability of the devices. SHM is a glass material, with the only access to the interior structure being liquids being pushed in through the entrances. Consequently, washing the interior of the device is extremely troublesome with no guarantee that the inside is completely cleansed. On the other hand, as can be seen in Figure 1, SM can be disassembled, allowing for the washing of the device to be done with ease. In addition, by taking out the elements from the device, the elements can be thoroughly washed and experiments can be conducted at virgin state.

## 5 Conclusion

The present study demonstrated that a static mixer is a powerful device for the continuous generation of size-controlled liposomes in a static flow-mixing manner. SM is interesting as a new fluid dynamic mixing device that bridges microfluidic and macro fluidic scales. Similar to the method using conventional microfluidic devices, particle size, encapsulation efficiency, and lamellarity of liposomes could be tuned by modulating process parameters. The key parameter to control the size of liposomes using SM was ILC, which is the same as the method using SHM. TFR and FRR had no significant impact on the characteristics of the generated liposomes in the range tested in this study. However, considering that the cross-sectional area of the channel in the applied SM is 50 times larger than that in the conventional SHM, the range of TFR applied in this study (1,500–2,500  $\mu\text{L}/\text{min}$ ) might be too low for the SM even if the range of TFR is suitable for SHM in conventional studies (Kastner et al., 2015; Cheung and Al-Jamal, 2019). A much higher TFR range should be targeted to increase the linear flow velocity in the SM. Increased volumetric throughput resulting from an increased TFR is the preferred approach to overcome the limitation of conventional microfluidic devices, which have low volumetric throughput, for scale-up production. SM could be widely applicable not only to preparing liposome formulations but also to preparing nano-formulations based on the formation of molecular assemblies in aqueous media, such as lipid nanoparticles and polymeric nanoparticles. Further research on optimizing manufacturing conditions such as flow rate and temperature to suit the size of the flow path and specifications of SM will enable more precise control of liposome size and structure at various scales.

In the last few decades, liposome technology has played a pioneering role in the development of nanoparticle-based drug

delivery systems. While extensive research has led to clinical applications of several liposomal formulations, the number of approved liposomal drugs is not as large as expected. One of the bottleneck issues is manufacturing, which includes inconsistency of size and structure, lack of reproducibility, low encapsulation efficiency, difficulty in scalability, lack of device and equipment, and complexity of the technology. Although there remains a need to better the mixing efficiency of SM by, for instance, altering the number and curvature of the elements, this research was able to show that a static mixer is indeed capable of preparing liposomes. Furthermore, it depicted great potential in liposome formation due to its user-friendliness and ability to accurately control the particle size of the liposomes. Nowadays, liposome technologies have expanded to a broad range of lipid-based nanoparticles including lipid nanoparticles encapsulating DNA or mRNA. Consequently, the challenges of liposome technology extend beyond drug delivery to gene delivery and vaccine technology. Advances in fluid mixing technology using a static mixer will facilitate reproducible, scalable, and efficient continuous production of advanced lipid-based nanoparticles with controlled size and structure suitable for applications.

## Data availability statement

The original contributions presented in the study are included in the article/[Supplementary Material](#), further inquiries can be directed to the corresponding author.

## Author contributions

AO, AM, and ST conceived and designed the study. AO and AM performed the experiments and analyzed the data. KS was responsible for helping with the experiments and data analysis. AO wrote the draft of the manuscript. AM, KS, and ST contributed to writing and revising the manuscript. All authors contributed to the article and approved the submitted version.

## References

- Berger, N., Sachse, A., Bender, J., Schubert, R., and Brandl, M. (2001). Filter extrusion of liposomes using different devices: comparison of liposome size, encapsulation efficiency, and process characteristics. *Inter. J. Pharm.* 223, 55–68. doi:10.1016/S0378-5173(01)00721-9
- Bibi, S., Lattmann, E., Mohammed, A. R., and Perrie, Y. (2012). Trigger release liposome systems: local and remote controlled delivery? *J. Microencapsul.* 29 (3), 262–276. doi:10.3109/02652048.2011.646330
- Bulbake, U., Doppalapudi, S., Kommineni, S., and Khan, W. (2017). Liposomal formulations in clinical use: an updated review. *Pharmaceutics* 9, 12. doi:10.3390/pharmaceutics9020012
- Chaize, B., Colletier, J. P., Winterhalter, M., and Fournier, D. (2004). Encapsulation of enzymes in liposomes: high encapsulation efficiency and control of substrate permeability. *Artif. Cells Blood Subst. Immobil. Biotechnol.* 32 (1), 67–75. doi:10.1081/bio-120028669
- Chen, D., Love, K. T., Chen, Y., Eltoukhy, A. A., Kastrop, C., Sahay, G., et al. (2012). Rapid discovery of potent siRNA-containing lipid nanoparticles enabled by controlled microfluidic formulation. *J. Am. Chem. Soc.* 134 (16), 6948–6951. doi:10.1021/ja301621z
- Cheung, C. C. L., and Al-Jamal, W. T. (2019). Sterically stabilized liposomes production using staggered herringbone micromixer: effect of lipid composition and PEG-lipid content. *Int. J. Pharm.* 566, 687–696. doi:10.1016/j.ijpharm.2019.06.033
- Cortesi, R., Esposito, E., Manegatti, E., Gambari, R., and Nastruzzi, C. (1996). Effect of cationic liposome composition on *in vitro* cytotoxicity and protective effect on carried DNA. *Int. J. Pharm.* 139 (1–2), 69–78. doi:10.1016/0378-5173(96)04574-7
- Darwin microfluidics (2023). Herringbone mixer - glass chip. Available at: <https://darwin-microfluidics.com/products/herringbone-mixer-glass-chips> (Accessed April 16, 2023).
- Filipczak, N., Pan, J., Yalamarty, S. S. K., and Torchilin, V. P. (2020). Recent advancements in liposome technology. *Adv. Drug Deliv. Rev.* 156, 4–22. doi:10.1016/j.addr.2020.06.022
- Gouda, A., Sakr, O. S., Nasr, M., and Sammour, O. (2021). Ethanol injection technique for liposomes formulation: an insight into development, influencing factors, challenges and applications. *J. Drug Deliv. Sci. Technol.* 61, 102174. doi:10.1016/j.jddst.2020.102174
- Grit, M., Daan, J. A., and Crommelin, D. J. A. (1992). The effect of aging on the physical stability of liposome dispersions. *Chem. Phys. Lipids* 62, 113–122. doi:10.1016/0009-3084(92)90089-8
- Guimarães, D., Cavaco-Paulo, A., and Eugénia Nogueira, E. (2021). Design of liposomes as drug delivery system for therapeutic applications. *Int. J. Pharm.* 601, 120571. doi:10.1016/j.ijpharm.2021.120571
- Hagisawa, K., Kinoshita, M., Takikawa, M., Takeoka, S., Saitoh, D., Seki, S., et al. (2019). Combination therapy using fibrinogen  $\gamma$ -chain peptide-coated, ADP-

## Funding

This work was supported by JSPS KAKENHI Grant Number JP20K12656. This work was the result of using research equipment (SynergyH1: shared equipment ID C4032 in Waseda University) shared in MEXT Project for promoting public utilization of advanced research infrastructure (Program for supporting construction of core facilities) Grant Number JPMXS0440500022.

## Acknowledgments

We thank Noritake Co., Limited for kindly providing a static mixer.

## Conflict of interest

The authors declare that the research was conducted in the absence of any commercial or financial relationships that could be construed as a potential conflict of interest.

## Publisher's note

All claims expressed in this article are solely those of the authors and do not necessarily represent those of their affiliated organizations, or those of the publisher, the editors and the reviewers. Any product that may be evaluated in this article, or claim that may be made by its manufacturer, is not guaranteed or endorsed by the publisher.

## Supplementary material

The Supplementary Material for this article can be found online at: <https://www.frontiersin.org/articles/10.3389/fbioe.2023.1229829/full#supplementary-material>

- encapsulated liposomes and hemoglobin vesicles for trauma-induced massive hemorrhage in thrombocytopenic rabbits. *Transfusion* 59 (10), 3186–3196. doi:10.1111/trf.15427
- Jaafar-Maalej, C., Diab, R., Andrieu, V., Elaissari, A., and Fessi, H. (2010). Ethanol injection method for hydrophilic and lipophilic drug-loaded liposome preparation. *J. Liposome Res.* 20 (3), 228–243. doi:10.3109/08982100903347923
- Jahn, A., Reiner, J. E., Vreeland, W. N., DeVoe, D. L., Locascio, L. E., and Gaitan, M. (2008). Preparation of nanoparticles by continuous-flow microfluidics. *J. Nanopart. Res.* 10, 925–934. doi:10.1007/s11051-007-9340-5
- Kastner, E., Verma, V., Lowry, D., and Perrie, Y. (2015). Microfluidic-controlled manufacture of liposomes for the solubilisation of a poorly water soluble drug. *Int. J. Pharm.* 485 (1–2), 122–130. doi:10.1016/j.ijpharm.2015.02.063
- Kikuchi, H., Suzuki, N., Ebihara, K., Morita, H., Ishii, Y., Kilkuchi, A., et al. (1999). Gene delivery using liposome technology. *J. Control. Release* 62 (1–2), 269–277. doi:10.1016/s0168-3659(99)00047-4
- Kodama, M., Shibata, O., Nakamura, S., Lee, S., and Sugihara, G. (2004). A monolayer study on three binary mixed systems of dipalmitoyl phosphatidyl choline with cholesterol, cholestanol and stigmasterol. *Colloids Surf. B* 33 (3–4), 211–226. doi:10.1016/j.colsurfb.2003.10.008
- Kostevšek, N., Cheung, C. C. L., Serša, I., Kreft, M. E., Monaco, I., Comes, F., et al. (2020). Magneto-liposomes as mri contrast agents: A systematic study of different liposomal formulations. *Nanomaterials* 10 (5), 889. doi:10.3390/nano10050889
- Kraft, J. C., Freeling, J. P., Wang, Z., and Ho, R. J. Y. (2014). Emerging research and clinical development trends of liposome and lipid nanoparticle drug delivery systems. *J. Pharm. Sci.* 103, 29–52. doi:10.1002/jps.23773
- Lasic, D. D., and Martin, F. J. (1990). On the mechanism of vesicle formation. *J. Membr. Sci.* 50, 215–222. doi:10.1016/S0376-7388(00)80317-8
- Lewis, B. A., and Engelman, D. M. (1983). Lipid bilayer thickness varies linearly with acyl chain length in fluid phosphatidylcholine vesicles. *J. Mol. Biol.* 166, 211–217. doi:10.1016/s0022-2836(83)80007-2
- Liu, P., Chen, G., and Zhang, J. (2022). A review of liposomes as a drug delivery system: current status of approved products, regulatory environments, and future perspectives. *Mol. (Basel, Switz.)* 27 (4), 1372. doi:10.3390/molecules27041372
- Maeki, M., Fujishima, Y., Sato, Y., Yasui, T., Kaji, N., Ishida, A., et al. (2017). Understanding the formation mechanism of lipid nanoparticles in microfluidic devices with chaotic micromixers. *PLoS One* 12 (11), e0187962. doi:10.1371/journal.pone.0187962
- Maeki, M., Saito, T., Sato, Y., Yasui, T., Kaji, N., Ishida, A., et al. (2015). A strategy for synthesis of lipid nanoparticles using microfluidic devices with a mixer structure. *RSC Adv.* 5, 46181–46185. doi:10.1039/C5RA04690D
- Nagayasu, A., Uchiyama, K., and Kiwada, H. (1999). The size of liposomes: a factor which affects their targeting efficiency to tumors and therapeutic activity of liposomal antitumor drugs. *Adv. Drug Deliv. Rev.* 40 (1–2), 75–87. doi:10.1016/s0169-409x(99)00041-1
- Natsuhara, D., Saito, R., Okamoto, S., Nagai, M., and Shibata, T. (2022). Mixing performance of a planar asymmetric contraction-and-expansion micromixer. *Micromachine* 13 (9), 1386. doi:10.3390/mi13091386
- Niu, M., Lu, Y., Hovgaard, L., Guan, P., Tan, Y., Lian, R., et al. (2012). Hypoglycemic activity and oral bioavailability of insulin-loaded liposomes containing bile salts in rats: the effect of cholate type, particle size and administered dose. *Eur. J. Pharm. Biopharm.* 81 (2), 265–272. doi:10.1016/j.ejpb.2012.02.009
- Obata, Y., Suzuki, D., and Takeoka, S. (2008). Evaluation of cationic assemblies constructed with amino acid based lipids for plasmid DNA delivery. *Bioconjug. Chem.* 19 (5), 1055–1063. doi:10.1021/bc700416u
- Okamura, Y., Katsuno, S., Suzuki, H., Maruyama, H., Handa, M., Ikeda, Y., et al. (2010). Release abilities of adenosine diphosphate from phospholipid vesicles with different membrane properties and their hemostatic effects as a platelet substitute. *J. Control. Release* 148 (3), 373–379. doi:10.1016/j.jconrel.2010.09.013
- Pons, M., Foradada, M., and Estelrich, J. (1993). Liposomes obtained by the ethanol injection method. *Int. J. Pharm.* 95, 51–56. doi:10.1016/0378-5173(93)90389-W
- Saito, R., Krauze, M. T., Bringas, J. R., Noble, C., McKnight, T. R., Jackson, P., et al. (2005). Gadolinium-loaded liposomes allow for real-time magnetic resonance imaging of convection-enhanced delivery in the primate brain. *Exp. Neurol.* 196 (2), 381–389. doi:10.1016/j.expneurol.2005.08.016
- Sercombe, L., Veerati, T., Moheimani, F., Wu, S. Y., Sood, A. K., and Hua, S. (2015). Advances and challenges of liposome assisted drug delivery. *Front. Pharmacol.* 6, 286. doi:10.3389/fphar.2015.00286
- Shepherd, S. J., Warzecha, C. C., Yadavali, S., El-Mayta, R., Alameh, M. G., Wang, L., et al. (2021). Scalable mRNA and siRNA lipid nanoparticle production using a parallelized microfluidic device. *Nano Lett.* 21 (13), 5671–5680. doi:10.1021/acs.nanolett.1c01353
- Sou, K., Naito, Y., Endo, T., Takeoka, S., and Tsuchida, E. (2003). Effective encapsulation of proteins into size-controlled phospholipid vesicles using freeze-thawing and extrusion. *Biotechnol. Prog.* 19 (5), 1547–1552. doi:10.1021/bp0201004
- Šturm, L., and Poklar Ulrih, N. (2021). Basic methods for preparation of liposomes and studying their interactions with different compounds, with the emphasis on polyphenols. *Int. J. Mol. Sci.* 22 (12), 6547. doi:10.3390/ijms22126547
- Takeoka, S., Ohgushi, T., Terase, K., Ohmori, T., and Tsuchida, E. (1996). Layer-controlled hemoglobin vesicles by interaction of hemoglobin with a phospholipid assembly. *Langmuir* 12 (7), 1755–1759. doi:10.1021/la940936j
- Tenchov, R., Bird, R., Curtze, A. E., and Zhou, Q. (2021). Lipid nanoparticles-from liposomes to mRNA vaccine delivery, a landscape of research diversity and advancement. *ACS Nano* 15 (11), 16982–17015. doi:10.1021/acsnano.1c04996
- Thakur, R. K., Vial, Ch., Nigam, K. D. P., Nauman, E. B., and Djelveh, G. (2003). Static mixers in the process industries—a review. *Chem. Eng. Res. Des.* 81, 787–826. doi:10.1205/026387603322302968
- Xu, X., Khan, M. A., and Burgess, D. J. (2012). Predicting hydrophilic drug encapsulation inside unilamellar liposomes. *Inter. J. Pharm.* 423 (2), 410–418. doi:10.1016/j.ijpharm.2011.12.019
- Yang, S., Chen, J., Zhao, D., Han, D., and Chen, X. (2012). Comparative study on preparative methods of DC-Chol/DOPE liposomes and formulation optimization by determining encapsulation efficiency. *Int. J. Pharm.* 434, 155–160. doi:10.1016/j.ijpharm.2012.05.041
- Zheng, H., Tao, H., Wan, J., Lee, K. Y., Zheng, Z., and Leung, S. S. Y. (2022). Preparation of drug-loaded liposomes with multi-inlet vortex mixers. *Pharmaceutics* 14 (6), 1223. doi:10.3390/pharmaceutics14061223
- Zook, J. M., and Vreeland, W. N. (2010). Effects of temperature, acyl chain length, and flow-rate ratio on liposome formation and size in a microfluidic hydrodynamic focusing device. *Soft Matter* 6, 1352–1360. doi:10.1039/b923299k



## OPEN ACCESS

## EDITED BY

Gianni Ciofani,  
Italian Institute of Technology (IIT), Italy

## REVIEWED BY

Yaron E. Antebi,  
Weizmann Institute of Science, Israel  
Andrea Cascio Timm,  
Johns Hopkins University, United States

## \*CORRESPONDENCE

Jurjen Tel,  
✉ j.tel@tue.nl

RECEIVED 12 June 2023

ACCEPTED 16 August 2023

PUBLISHED 14 September 2023

## CITATION

Yang H and Tel J (2023), Engineering global and local signal generators for probing temporal and spatial cellular signaling dynamics.  
*Front. Bioeng. Biotechnol.* 11:1239026.  
doi: 10.3389/fbioe.2023.1239026

## COPYRIGHT

© 2023 Yang and Tel. This is an open-access article distributed under the terms of the [Creative Commons Attribution License \(CC BY\)](#). The use, distribution or reproduction in other forums is permitted, provided the original author(s) and the copyright owner(s) are credited and that the original publication in this journal is cited, in accordance with accepted academic practice. No use, distribution or reproduction is permitted which does not comply with these terms.

# Engineering global and local signal generators for probing temporal and spatial cellular signaling dynamics

Haowen Yang<sup>1,2</sup> and Jurjen Tel<sup>1,2\*</sup>

<sup>1</sup>Laboratory of Immunoengineering, Department of Biomedical Engineering, Eindhoven University of Technology, Eindhoven, Netherlands, <sup>2</sup>Institute for Complex Molecular Systems, Eindhoven University of Technology, Eindhoven, Netherlands

Cells constantly encounter a wide range of environmental signals and rely on their signaling pathways to initiate reliable responses. Understanding the underlying signaling mechanisms and cellular behaviors requires signal generators capable of providing diverse input signals to deliver to cell systems. Current research efforts are primarily focused on exploring cellular responses to global or local signals, which enable us to understand cellular signaling and behavior in distinct dimensions. This review presents recent advancements in global and local signal generators, highlighting their applications in studying temporal and spatial signaling activity. Global signals can be generated using microfluidic or photochemical approaches. Local signal sources can be created using living or artificial cells in combination with different control methods. We also address the strengths and limitations of each signal generator type, discussing challenges and potential extensions for future research. These approaches are expected to continue to facilitate on-going research to discover novel and intriguing cellular signaling mechanisms.

## KEYWORDS

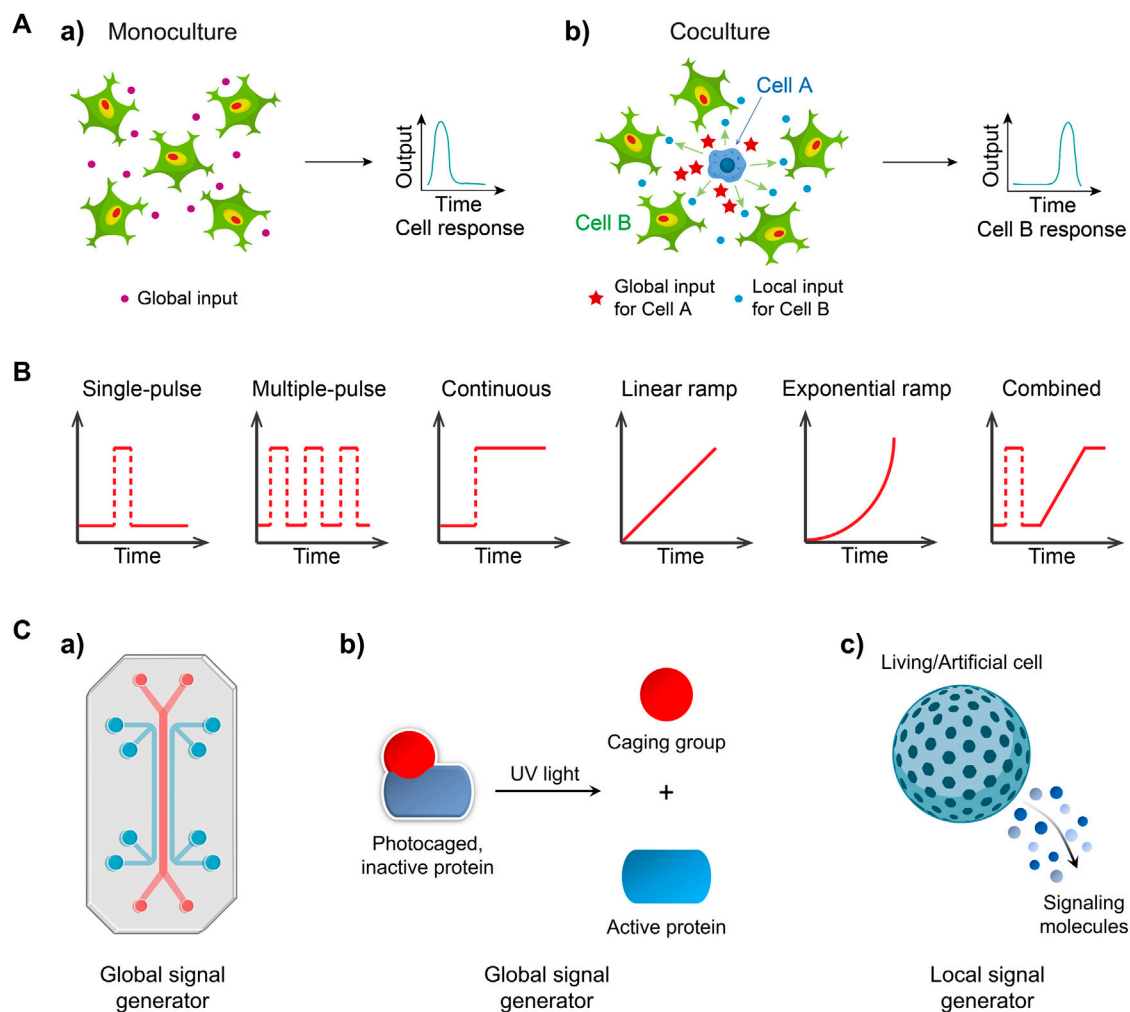
signal generator, microfluidics, signaling dynamics, single cells, cellular communication

## Introduction

Cells possess the remarkable capability to perceive and respond to a wide array of time-varying signals from their environment. This ability stems from a diverse functional repertoire of genes, proteins, and metabolites that interact in response to various external physical cues, such as matrix stiffness (Discher et al., 2005) and fluid shear stress (Chen et al., 2019), as well as biochemical cues, including growth factors (Leof, 2000), cytokines (O'Shea and Murray, 2008), and surface chemistry (Mrksich, 2000). Through intricate signaling networks, individual cells are capable of responding to a wide range of extracellular signals (Osborn and Olefsky, 2012), allowing them to regulate and execute numerous functions in a coordinated manner (Serafini et al., 2015). Cells have evolved sophisticated signaling mechanisms to effectively interpret and translate stimulus-specific information into phenotypic responses, leading to changes in gene and protein expressions (Purvis and Lahav, 2013). These signaling networks often convey diverse signal inputs arising from ligand-receptor interactions, resulting in heterogeneous outputs (Spiller et al., 2010).

The majority of studies in the field of cell signaling can be broadly categorized into two scenarios: 1) homocellular signaling, which involves signal transduction within identical cell types (monoculture), and 2) heterocellular signaling, which describes signal transmission between two distinct cell types (coculture). In the case of homocellular signaling



**FIGURE 1**

Exploring cellular signaling dynamics in response to global and local inputs can involve the use of various signal generators (A) a) Environmental inputs like cytokines are sensed and processed by a group of cells, and then are transformed into an output (e.g., signaling factor activity) b) One cell type (cell A, e.g., macrophage) discerned a global input like bacterial stimuli, and then generated a local input that can be detected by the cocultured neighbors (cell B, e.g., fibroblast) and is thus transformed into a final output Adapted from (Yang et al., 2022) Copyright 2022 CC BY 4.0. (B) Temporal input modes observed in biological systems. Input mode/type refers to how signal molecules are applied to cells. (C) Engineering global signal generators, including a) a microfluidic system and b) photoactivatable signaling molecules and local generators such as c) a living/artificial cell.

(Figure 1Aa), a population of identical cells receives an external input from the environment. This global input signal is then processed and interpreted by activating genetically encoded signaling pathways, such as extracellular signal-regulated kinase (ERK) (Lavoie et al., 2020), nuclear factor-kappa B (NF- $\kappa$ B) (Dorrington and Fraser, 2019) and signal transducer and activator of transcription (STAT) (Villarino et al., 2017), leading to an appropriate response (output) induced by the responding cells. In the context of heterocellular signaling (Figure 1Ab), one subpopulation (cell type A) initiates the first response by converting the original environmental input into a signaling mediator. This mediator is then secreted and released to the extracellular space, serving as a local input. The neighboring heterotypic cells (cell type B) receive and transmit the local input signal through internal signaling pathways, ultimately producing a final output. Understanding these signal flows is crucial for unraveling essential biological processes such as cell growth and

proliferation (Zhu and Thompson, 2019), immune responses (Brubaker et al., 2015), tumor progression (Yuan et al., 2016), and wound healing (Dekoninck and Blanpain, 2019).

Furthermore, the microenvironment within the body is subject to rapidly changes influenced by various signaling processes. The presence of transient gradients of signaling molecules facilitates cellular communication and regulates cellular functions. For instance, gonadotropin-releasing hormone (GnRH) is secreted in short pulses, activating the synthesis and release of pituitary gonadotropin hormones, thereby regulating reproductive functions (Moenter et al., 1992). Pulsatile flow of ERK signaling at different frequencies plays a crucial role in regulating fundamental cellular processes, including proliferation, differentiation, and cell cycle progression (Sun et al., 2015). A pulsed, strong lipopolysaccharide (LPS) signal triggers rapid and uniform nuclear factor- $\kappa$ B (NF- $\kappa$ B) responses in fibroblasts, while a weak, sustained signal results in varied responses (Kellogg et al., 2015). The

**TABLE 1** Summary of microfluidics-based global signal generators for cellular signaling studies.

Cell type	Input molecule	Input type	Application	Reference
NIH3T3 fibroblast	TNF $\alpha$	Pulse, continuous	Nuclear NF- $\kappa$ B dynamics	Tay <i>et al.</i> (2010)
NIH3T3 fibroblast, mouse embryonic fibroblast	platelet-derived growth factor (PDGF)	Pulse	Phosphorylation kinetics of Akt, GSK-3 $\beta$ , p70S6K, S6, Erk1/2, and mTOR	Blazek <i>et al.</i> (2013)
NIH3T3 fibroblast	PDGF, insulin-like growth factor (IGF-1)	Pulse	Phosphorylation kinetics of PDGF and IGF-1 receptors, Akt and GSK-3 $\beta$	Blazek <i>et al.</i> (2015)
NIH3T3 fibroblast	Lipopolysaccharide (LPS)	Pulse, continuous	Nuclear NF- $\kappa$ B dynamics	Kellogg <i>et al.</i> (2015)
PC 12 cell	Epidermal (EGF), nerve (NGF) growth factor	Pulse, continuous	Nuclear ERK dynamics	Ryu <i>et al.</i> (2015)
RAW 264.7 macrophage	LPS	Pulse, continuous	Nuclear NF- $\kappa$ B dynamics, TNF- $\alpha$ secretion dynamics	Junkin <i>et al.</i> (2016)
NIH3T3 fibroblast	TNF $\alpha$	Sine-wave, linear ramping	Nuclear NF- $\kappa$ B dynamics	Piehlér <i>et al.</i> (2017)
HEK293 B <sup>S</sup> , NIH3T3 cell	EGF	Pulse, linear stepwise ramping	Nuclear ERK dynamics	Song <i>et al.</i> (2018)
Murine hematopoietic stem and progenitor cells	Macrophage colony-stimulating factor (M-CSF)	Continuous	Lysozyme M (LysM) gene induction	Dettinger <i>et al.</i> (2018)
PC 12 cell	EGF, NGF, fibroblast GF (FGF2)	Pulse, continuous	Nuclear ERK dynamics	Blum <i>et al.</i> (2019)
HeLa cells	TNF $\alpha$	Continuous, linear ramping	Nuclear NF- $\kappa$ B dynamics	Mokashi <i>et al.</i> (2019)
HeLa cells	IFN $\alpha$	Pulse, continuous	IRF9 dynamics, nuclear STAT1 dynamics	Mudla <i>et al.</i> (2020)
NIH3T3 fibroblast	TNF, interleukin 1 $\beta$ (IL-1 $\beta$ )	Step, linear/exponential stepwise ramping	Nuclear NF- $\kappa$ B dynamics	Son <i>et al.</i> (2021)
K562 cell, NIH3T3 fibroblast	Dimethyl sulfoxide (DMSO), IFN $\gamma$	Pulse, continuous	Caspase 3 dynamics, nuclear STAT1 dynamics	Sinha <i>et al.</i> (2022)
NIH3T3 fibroblast	IFN $\gamma$	Pulse, continuous	Nuclear STAT1/2 dynamics	Yang <i>et al.</i> (2022)

dynamic patterns of signaling molecules encompass pulse, continuous, ramp and combined input signals (Figure 1B).

It is widely recognized that dynamic signal processing are ubiquitous in cellular systems. However, understanding how cells interpret these input signals can be challenging. This challenge arises because population-level measurements often mask the heterogeneous behavior exhibited by individual cells, and conventional methods often lack the ability to generate various types of targeted perturbations other than continuous inputs in signaling pathways, for example, signal molecules simply added in well plates continuously stimulate cells. Moreover, observing cellular events in multiple contexts is essential for multi-dimensional understanding of signaling process, as evident in the distinct cellular responses to global and local inputs (Yang *et al.*, 2022). Consequently, there is a growing demand for the development of specific signal generators that enable precise control over defined input modes, thereby allowing investigations into temporal and spatial dynamics of cellular signaling. In this review, we will highlight various signal generators that have been realized using microfluidic systems (Figure 1Ca), photoactivatable signaling molecules (Figure 1Cb), and living/artificial cells (Figure 1Cc) for global or local input control. Furthermore, we will discuss the advantages and limitations of these signal generators and provide insights for their future development.

## Global signal generators for temporal cellular signaling dynamics

Global signal generators provide uniform inputs that allow for the study of both population-averaged and single-cell responses. Currently, the primary methods employed for generating global inputs include microfluidic molecule delivery and the photodeprotection of caged input molecules. Microfluidic systems can provide a wide range of input modes, such as pulse (Blazek *et al.*, 2015; Ryu *et al.*, 2015), continuous (Dettinger *et al.*, 2018; Mudla *et al.*, 2020), sinusoidal (Piehlér *et al.*, 2017) and ramping (Song *et al.*, 2018; Mokashi *et al.*, 2019). On the other hand, the range of input types is relatively limited when utilizing photochemical methods (Ryu *et al.*, 2014; Mogaki *et al.*, 2019). In this section, we will discuss the principles of these two methods and explore their applications.

## Global input generation with microfluidics

In the past decade, microfluidics has made remarkable advancements in exploring temporal cellular behaviors (Irimia, 2010; Gao *et al.*, 2012; Kim *et al.*, 2014; Sinha *et al.*, 2018). Microfluidic devices can replicate *in vivo* biological environments with great accuracy and enable high-content analysis of cells.

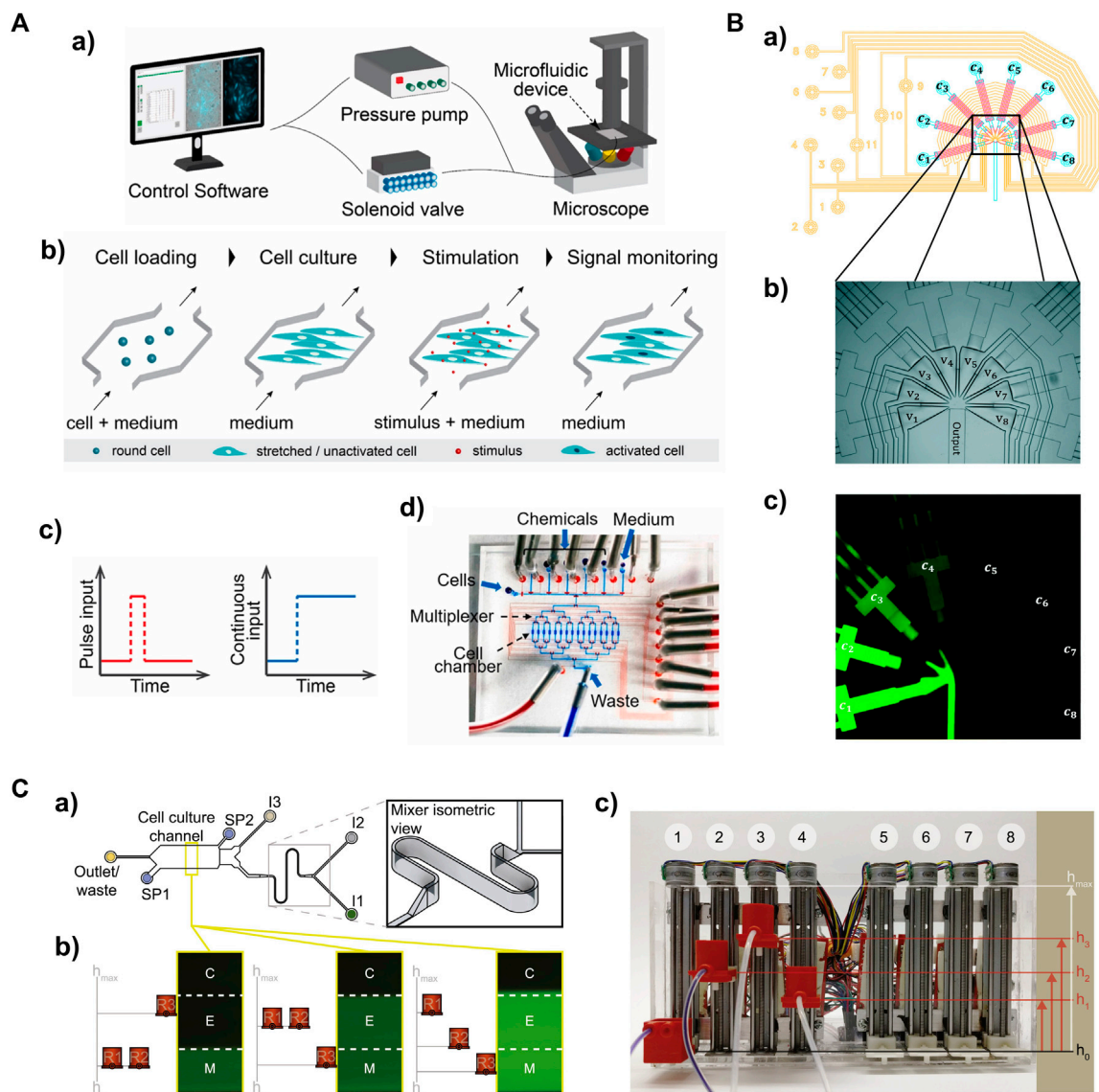


FIGURE 2

Microfluidic-based global signal generators for studying temporal cellular signaling dynamics (A) A microfluidic system capable of producing a pulse or continuous input to cells. a) The entire system. The delivery of defined input types are controlled by a pressure pump and solenoid valves. Outputs are acquired via time-lapse live-cell microscopy. b) The workflow to measure transcription factor activity in adherent cells expressing fluorescence reporters. c) One-pulse and continuous input profiles. d) The multilayer microfluidic device with control layer in red (e.g., microvalves) and flow layer in blue (e.g., cell chambers). Adapted from (Yang et al., 2022) Copyright 2022 CC BY 4.0. (B) A PDMS signal generator capable of producing sinusoidal inputs. a) Design of the signal generator module; control layer in yellow, flow layer in blue and red. b) The injector junction with triangular converging valves v1-v8 in the multilayer microfluidic device. c) The operating signal generator involves mixing fluorescent dye solutions of different concentration (c1-c8). Reproduced with permission from Piehler et al. (2017). Copyright 2017 The Royal Society of Chemistry. (C) A gravity pump-integrated microfluidic system that enables analog control of input strength. a) Top view of the dynamic stimulation device. b) Flow rates through the inlets (I1, I2, and I3) are controlled by hydrostatic pressure differences between corresponding reservoirs (R1, R2, and R3) and the outlet. c) The “gravity pump” comprises eight vertically mounted stepper motors with screw-nut platforms and an Arduino microcontroller to control platform heights. Adapted from (Mokashi et al., 2019) Copyright 2019 CC BY 4.0.

Microfluidics technology offers precise automation and control of analytical functions, enabling high-resolution manipulation of cells and their microenvironments. With these properties, we can modulate cellular signaling pathways to gain insights into mechanisms underlying cell activation, migration, and intercellular communication. Recent studies investigating temporal signaling dynamics using microfluidics-based global input generators are summarized in Table 1.

A typical microfluidic platform for studying cellular signaling consists of a microfluidic device, a custom software control system, a pressure pump, solenoid valves, and a live-cell imaging microscope (Figure 2Aa) (Yang et al., 2022). The low cost and biocompatibility of polydimethylsiloxane (PDMS) make it ideal for rapid fabrication of microfluidic devices using soft lithography, which has led to the development of various microfluidic designs (Sia and Whitesides, 2003). PDMS is permeable to gases, allowing replication of artificial

cellular microenvironments *in vitro*, and its flexibility enables easy integration of membrane valves and pumps to create intricate networks of microchannels (Thorsen et al., 2002). This enables full automation of protocols using programming software (White and Streets, 2018; Kehl et al., 2021). The PDMS microfluidic device consists of a bottom flow layer for sample loading and a top control layer for valve actuation (Figure 2Ad). The membrane valves can be pneumatically/hydraulically actuated using a pressure pump and solenoid valves (Brower et al., 2018; Watson and Senyo, 2019). This precise control allows for cell seeding, medium exchange and input delivery for studying cellular signaling (Figure 2Ab).

Various input profiles can be defined and implemented with high precision (Table 1). Different input types can be achieved by controlling input amplitude and duration through opening and closing the embedded membrane valves (the layer in red in Figure 2Ad). The typical input modes of cytokine interferon  $\gamma$  (IFN $\gamma$ ), such as pulse and continuous (Figure 2Ac), were applied to perturb the activity of transcription factor STAT1 in single fibroblasts or populations (Yang et al., 2022). Distinct STAT1 activation dynamics were observed between one-pulse and continuous IFN $\gamma$  treatment. This indicates that STAT1 activation can be temporally modulated by introducing different temporal stimulation profiles. Another transcription factor, NF- $\kappa$ B, displayed activation and oscillation dynamics when subjected to a continuous cytokine input of tumor necrosis factor  $\alpha$  (TNF $\alpha$ ). Applying a stepwise ramping input of TNF $\alpha$  or interleukine-1 $\beta$  (IL-1 $\beta$ ) to fibroblasts revealed that the activity of the NF- $\kappa$ B signaling pathway correlated with the rate of change in cytokine concentrations rather than the absolute cytokine concentrations. In addition, the implementation of sinusoidal inputs was realized using a multiple-layer PDMS device with eight triangular converging valves (Figure 2B). Fibroblasts stimulated with sinusoidal TNF inputs showed characteristic NF- $\kappa$ B nucleocytoplasmic oscillations with great heterogeneity in single-cell responses (Piehler et al., 2017). While the duration and amplitude of inputs can be readily controlled in membrane valve-embedded PDMS microfluidic devices, implementing ramping analog inputs (Song et al., 2018; Son et al., 2021) in the PDMS devices presents a challenge. Recently, a gravity-driven flow has been achieved in a microfluidic device with high-aspect-ratio channels controlled by a gravity pump (Figure 2C) (Mokashi et al., 2019). This fully analog system is capable of producing arbitrarily complex patterns of input signals. Ramping input of TNF $\alpha$  led to increased NF- $\kappa$ B dynamics in a fraction of cells compared to those showing qualitatively different NF- $\kappa$ B responses to continuous stimulation. These observations demonstrate the ability of microfluidic systems to create various defined input types that can induce distinct cellular responses, which is crucial for discovering underlying mechanisms of temporal cellular signaling.

Microfluidic devices integrated with cell traps have significantly advanced research by providing opportunities to study single cells and gain insights into their signaling dynamics. These devices allow the isolation of individual cells, which is often challenging with other technologies. The designs for single-cell analysis typically utilize unique geometric structures, such as pillar-like (Junkin et al., 2016; Sinha et al., 2022) and V-type (Rho et al., 2016) valves. A microfluidic device with pillar-like traps was developed for quantitative analysis of single-cell immune dynamics (Junkin et al., 2016). With these traps, single macrophages were isolated and exposed to different input types,

including a single-pulse, continuous, and repeated pulses of lipopolysaccharide (LPS), separately. The dynamics of TNF $\alpha$  secretion in single macrophages was found highly heterogeneous and surprisingly uncorrelated with the dynamics of NF- $\kappa$ B, the transcription factor that controls TNF $\alpha$  production. Additionally, simulation analysis revealed that a trap with an optimal geometric structure can achieve single-cell trapping with high precision (Sinha et al., 2022). These global signal generators have facilitated the exploration of temporal signaling dynamics (such as transcription factor dynamics) in single cells encountering defined environmental perturbations, enriching our understanding of how extracellular signal inputs were interpreted by single cells, and how these dynamics affect their downstream signaling events, such as cytokine secretion.

## Global input generation with photoactivation

While microfluidic systems can be used to deliver global input signals to cells, they may result in a delay of seconds for inputs among different locations within cell culture, thereby posing a challenge for investigating fast signaling events. The activity of global input molecules can be suppressed and controllably activated by stimuli, such as light irradiation (Klan et al., 2013). This occurs because every signal is transmitted into cells upon binding of input molecules to specific receptors. Recently, several photoactivation-based methods have been reported (Ryu et al., 2014; Mogaki et al., 2019; Perdue et al., 2020), which allows for spatial control of signal molecules using light. Due to the simplicity and ease of light irradiation, efforts have been made to develop different strategies for small molecules and proteins.

For small molecule inputs, they can be caged by a photocleavable group, such as the 2-nitrobenzyl group, to inhibit their activity. Two small molecules, Imiquimod (R837) and Resiquimod (R848), which are agonists of Toll-like receptor 7 (TLR7) and TLR7/8, respectively, were conjugated with the photo-protecting group carbamate of 2-(2-nitrophenyl)-propyloxycarbonyl (NPPOC) to suppress their spatial activity. Irradiation with 360 nm UV light deprotected these small-molecule agonists, triggering signal transmission and NF- $\kappa$ B pathway activation in cells (Figure 3A) (Ryu et al., 2014). Similarly, a TLR4 agonist, pyrimido [5,4-b]indole, was photocaged at a position critical for receptor binding by protecting the indole nitrogen with 6-nitroveratryloxycarbonyl (NVOC). Upon exposure to UV light, the agonist was uncaged and activated NF- $\kappa$ B (Stutts and Esser-Kahn, 2015). In addition to photocaging methods, photoresponsive conformational switches of small molecule inputs can also reversibly change their activity. A photoswitchable Pam<sub>3</sub>CS<sub>4</sub> derivative-P10 was synthesized to control the activation of the TLR1/2 signaling pathway. The ground-state *trans*-P10 can activate antigen-presenting cells (APCs) by promoting TLR1/2 heterodimerization. In the presence of UV irradiation, *trans*-P10 is converted to *cis*-P10, which reduces the activities of APCs by impeding the TLR1/2 heterodimerization (Hu et al., 2020). These methods offer the potential to regulate immune activation and inflammation.

For macromolecule inputs, such as growth factors and cytokines, it is challenging to directly modify them with photo-protecting



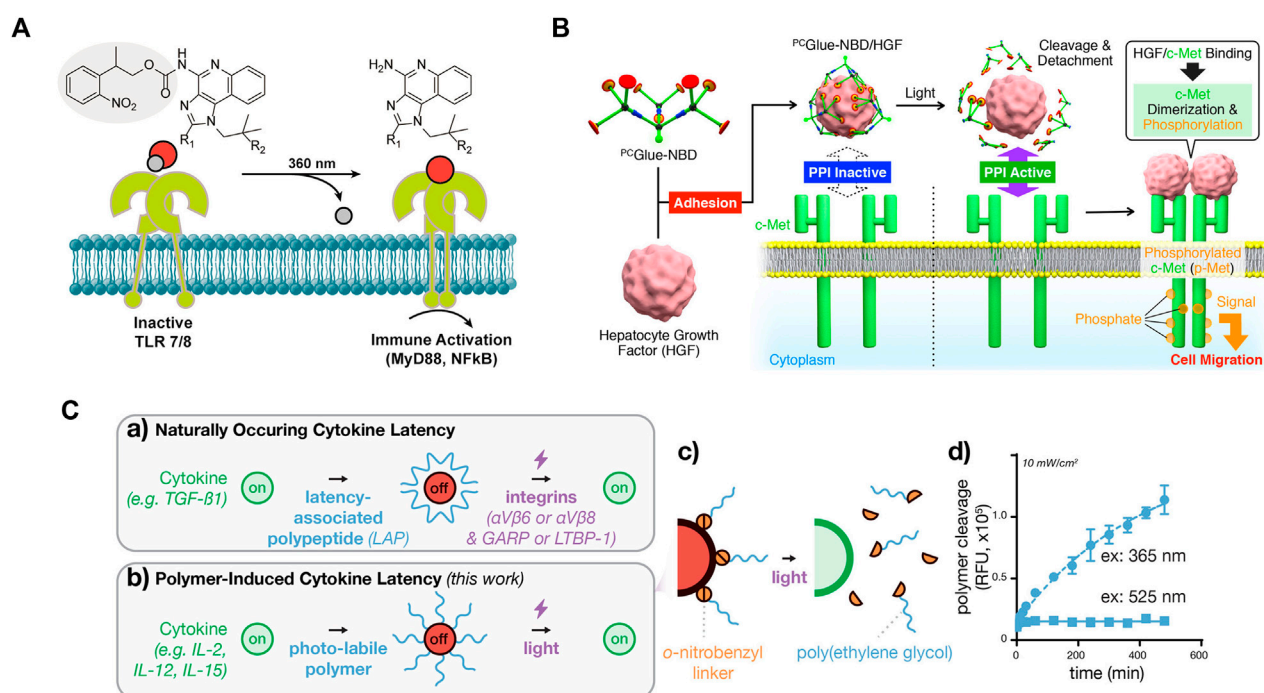


FIGURE 3

Photoactivation of signaling molecules as a global input for cellular signaling study (A) Photodeprotection of caged small-molecule agonist for controlled TLR7/8 activation. Reproduced with permission from (Ryu et al., 2014) Copyright 2014 American Chemical Society. (B) Photodeprotection of dendritic molecular glue-caged hepatocyte growth factor (HGF) induces cell migration. Reproduced with permission from (Mogaki et al., 2019) Copyright 2019 American Chemical Society. (C) Photodeprotection of polymer-caged cytokine for controlled T cell proliferation. The 20 kDa poly(ethylene glycol) polymer chains appended to cytokine lysine residues via o-nitrobenzyl groups, which are rapidly cleaved by blue LED light, as measured by cleavage-induced fluorescence dequenching. Reproduced with permission from (Perdue et al., 2020) Copyright 2020 American Chemical Society.

TABLE 2 Summary of light-controlled global signal generators for cellular signaling studies.

Cell type	Input molecule	Photosensitive moiety	Application	Reference
Bone marrow-derived dendritic cell (BMDC)	TLR7 agonist, Imiquimod (R837), TLR7/8 agonist, Resiquimod (R848)	Carbamate of 2-(2-nitrophenyl)-propyloxycarbonyl (NPPOC)	NF-κB activation, CD40 expression, IL-12, TNF-α and IL-6 secretion	Ryu et al. (2014)
NIH3T3 fibroblast	TLR4 agonist, pyrimido [5,4-b] indole	6-nitroveratryloxycarbonyl (NVOC)	NF-κB activation	Stutts and Esser-Kahn (2015)
Namalwa cell	TLR9 agonist, CpG oligonucleotide	Nitropiperonyloxymethyl (NPOM)	IL-6 expression	Govan et al. (2015)
BMDC	TLR2/6 agonist, Pam <sub>2</sub> CSK <sub>4</sub>	NPPOC	In vivo NF-κB activation, upregulation of nfkb1, cd34, cd28 and ccr7 expression	Ryu et al. (2017)
T lymphocyte	Moth cytochrome c <sub>88-103</sub> (MCC), ovalbumin <sub>257-264</sub> (OVA)	Nitrophenylethyl (NPE)	Diacylglycerol (DAG) accumulation, centrosome reorientation, and Grb2 microcluster formation	Sanchez and Huse (2018)
THP-1 cell and RAW 264.7 macrophage	Pam <sub>3</sub> CSK <sub>4</sub> derivative-P10	The metastable cis-P10 is converted to its thermally stable trans configuration	NF-κB activation, upregulation of CD80, CD86, CD40 expression, and IL-1β, TNF-α, IL-6, IL-12 secretion	Hu et al. (2020)
Human prostate carcinoma DU145 cell	Hepatocyte growth factor (HGF)	Molecular glue PCGlue-NBD, carrying nine Gu <sup>+</sup> pendants and butyrate-substituted NVOC ( <sup>B<sup>A</sup></sup> NVOC) linkages	Cell migration	Mogaki et al. (2019)
CTLL-2 T cell	Human IL-2, mouse scIL-12	Polyethylene glycol (PEG) modified with 2-nitrobenzyl linker derivatives	T cell proliferation, OVA <sub>257-264</sub> antigen-specific T cell activation, and STAT5 activation	Perdue et al. (2020)

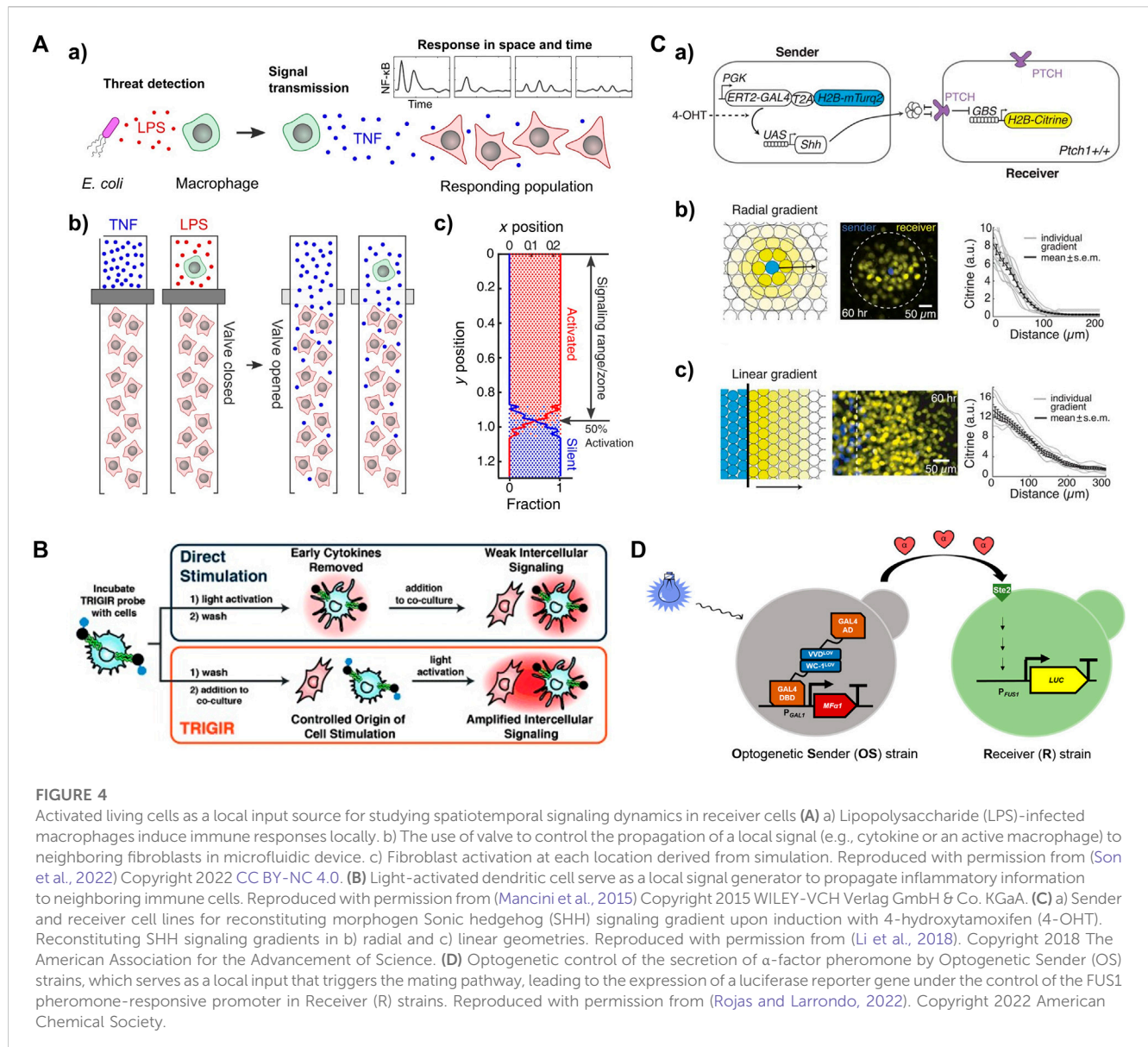


FIGURE 4

Activated living cells as a local input source for studying spatiotemporal signaling dynamics in receiver cells (A) a) Lipopolysaccharide (LPS)-infected macrophages induce immune responses locally. b) The use of valve to control the propagation of a local signal (e.g., cytokine or an active macrophage) to neighboring fibroblasts in microfluidic device. c) Fibroblast activation at each location derived from simulation. Reproduced with permission from (Son et al., 2022) Copyright 2022 CC BY-NC 4.0. (B) Light-activated dendritic cell serve as a local signal generator to propagate inflammatory information to neighboring immune cells. Reproduced with permission from (Mancini et al., 2015) Copyright 2015 WILEY-VCH Verlag GmbH & Co. KGaA. (C) a) Sender and receiver cell lines for reconstituting morphogen Sonic hedgehog (SHH) signaling gradient upon induction with 4-hydroxytamoxifen (4-OHT). Reconstituting SHH signaling gradients in b) radial and c) linear geometries. Reproduced with permission from (Li et al., 2018). Copyright 2018 The American Association for the Advancement of Science. (D) Optogenetic control of the secretion of  $\alpha$ -factor pheromone by Optogenetic Sender (OS) strains, which serves as a local input that triggers the mating pathway, leading to the expression of a luciferase reporter gene under the control of the FUS1 pheromone-responsive promoter in Receiver (R) strains. Reproduced with permission from (Rojas and Larondo, 2022). Copyright 2022 American Chemical Society.

groups. A dendritic molecular glue, <sup>PC</sup>Glue-NBD, carries multiple guanidinium ion (Gu<sup>+</sup>) pendants. This functional molecular glue can strongly adhere to the target protein, hepatocyte growth factor (HGF), and cover the region for protein-protein interactions (PPIs) on their surfaces. The PPIs are inactive, suppressing cellular signaling. Upon irradiation with UV light, <sup>PC</sup>Glue-NBD is photocleaved, reducing the multivalency for the adhesion. Consequently, uncaged HGFs regain its intrinsic PPI affinity toward c-Met, leading to pathway activation and cell migration (Figure 3B) (Mogaki et al., 2019). This study demonstrates a universal strategy for suppressing the activity of macromolecule inputs, holding great promise for controlling protein input-mediated signaling.

Another strategy that can reversibly suppress protein activity is chemical modification with photolabile polymers (Perdue et al., 2020). Cytokines such as human interleukin-2 (IL-2), IL-15, and mouse scIL-12 were caged with polyethylene glycol

(PEG) -conjugated with a 2-nitrobenzyl linker. UV irradiation photocleaved the 2-nitrobenzyl linkers, causing PEG to detach and thus restoring the activity of cytokines (Figure 3C). The magnitude and the duration of cytokine signaling can be tuned on demand, with high spatial resolution. This approach is also applicable to a range of additional cytokine or chemokine proteins. Although the activity of proteins is initially suppressed, cells still initiate a delayed response to the photocaged cytokine proteins. In contrast, the uncaged cytokine proteins induce a significantly faster response. These findings demonstrate the controllability of cytokine signaling latency using light. Although this strategy does not directly control the activation, continuous efforts may lead to improvements for this purpose.

Several recent light-controlled global signal generators are summarized in Table 2. The effectiveness of photoactivation methods relies on the photoresponsive groups or linkers used.

**TABLE 3** Summary of living cell sender-based local signal generators for cellular signaling studies.

Sender/receiver cell type	Method of local input activation	Local input molecule	Application	Reference
T cell/T cell	Pre-stimulation of sender cells with phorbol myristate acetate (PMA) and ionomycin	IL-2	STAT5, FoxP3 activation in receiver cells	Oyler-Yaniv <i>et al.</i> (2017)
RAW 264.7 macrophage/NIH3T3 fibroblast	Microfluidic delivery of LPS to stimulate sender cell	TNF	Nuclear NF- $\kappa$ B dynamics in both sender and receiver cells	Frank and Tay (2015), Son <i>et al.</i> (2022)
RAW 264.7 macrophage/HEK293 cell	Microfluidic delivery of LPS to stimulate sender cell	TNF $\alpha$	Nuclear NF- $\kappa$ B activation in receiver cells	Watson <i>et al.</i> (2022)
HES3 cell/HES3 cell	Microfluidic delivery of bone morphogenetic protein 4 (BMP4) to a colony	BMP4	MIXL1, T, SOX17, CDX2 expression in receiver cells	Manfrin <i>et al.</i> (2019)
Tumor cell/stromal cell	Input molecules secreted in the normal culture in Matrigel-fulfilled microfluidic device	TGF- $\beta$ 1	$\alpha$ -smooth muscle actin ( $\alpha$ -SMA) expression in receiver cells	Fang <i>et al.</i> (2021)
BMDC/RAW Macrophage, HEK293 cell, fibroblast	Light-activated NPPOC-modified TLR2/6 agonist	TNF	NF- $\kappa$ B activation, TNF secretion in receiver cells	Mancini <i>et al.</i> (2015)
Opto-SOS/WT NIH3T3 fibroblast	Light irradiation on sender cells	IL-6	ERK activation in sender cells, STAT3 activation in receiver cells	Toettcher <i>et al.</i> (2013)
NIH3T3 fibroblast/NIH3T3 fibroblast	4-hydroxytamoxifen (4-OHT)-induced production of Sonic hedgehog (SHH) in sender cells	SHH	Reconstitution of SHH signaling gradients for quantitative analysis of spatiotemporal patterning dynamics in receiver cells	Li <i>et al.</i> (2018)

Current methods are based on the use of short-wavelength light, such as UV irradiation. The should be noted that pathways sensitive to UV light may be activated or interfered with (Devary *et al.*, 1993; Li and Karin, 1998; O'Dea *et al.*, 2008). Due to the strong phototoxicity of UV light, cells may not survive prolonged exposures. Exploring alternative photocleavable groups responsive to long wavelengths of light can be a promising direction for controlling cellular signaling (Wegener *et al.*, 2017).

## Local signal generators for spatiotemporal cellular signaling dynamics

While global signal generators can be used to explore temporal signaling dynamics, probing spatial cellular behaviors remains a challenge. *In vivo*, signal sender cells are located within cell populations and transmit signals in either a two-dimensional (2D) or one-dimensional (1D) path (Frank and Tay, 2015). The construction of such signaling patterns requires precise spatial and temporal control over the stimulation of sender cells, referred to as local signal sources, without interfering with receiver cells. Recent methods have focused on leveraging living or artificial cells as local signal generators.

## Local input generation with living cell senders

Living cell senders serve as natural local signal sources due to their ability to secrete signals within the physiological range. A critical step is the activation of sender cells. This section will discuss recent strategies for the controlled activation of living sender cells, including pre-stimulation, microfluidics-assisted stimulation,

photocaged global input, and optogenetic activation. Recent studies on living cell-based local input generators are summarized in Table 3.

To construct a local signaling model, sender cells can be pre-stimulated before cocultured with receiver cells. The activated sender cells become local signal sources, secreting input signals in limited areas. Recently, a diffusion-consumption model has been created using the pre-stimulated T cells as the living senders to produce IL-2, which stimulates surrounding T cell receivers (Oyler-Yaniv *et al.*, 2017). Immunofluorescence staining revealed the generation of microdomains of STAT5-activated T cells around local IL-2 sources. Although this method is operationally simple and can be easily applied to investigate the activation status of cells within local regions, it is challenging to measure the signaling dynamics of receiver cells. The challenge lies in precisely controlling the secretion of cytokine from living sender cells, which makes it difficult to track the origin of signal propagation and transduction in receiver cells.

Valve-integrated microfluidic devices enable the coculture of a single sender cell (e.g., macrophage) and a population of receiver cells (e.g., fibroblasts), as well as the control of signal propagation (Frank and Tay, 2015; Son *et al.*, 2022; Watson *et al.*, 2022). These devices consist of connected channels with a separation valve between macrophages and fibroblasts, (Figure 4Ab), creating a 1D signaling axis (Frank and Tay, 2015; Son *et al.*, 2022). Dynamic LPS inputs can be delivered to single macrophages, initiating NF- $\kappa$ B pathway activation and TNF $\alpha$  secretion, which becomes a local TNF $\alpha$  source. By opening the separation valve, TNF $\alpha$  transmits along the channels in a wave-like propagation, initiating temporal and spatial responses of NF- $\kappa$ B in the cocultured fibroblasts (Figures 4Aa–c). This model enables control of local signal flow by opening and closing the separation valve. A microfluidic device facilitating unidirectional intercellular communication can avoid crosstalk and interference between

sender and receiver cells (Fang et al., 2021). The device consists of two separated half-ellipse-shaped chambers for different cell cultures, which are mixed in Matrigel and loaded into the left and right chambers, respectively. Matrigel and physical barriers restrict the medium flow to form a unidirectional signal flow from sender to receiver cells. Additionally, the device allows the analysis of functional signals secreted by sender cells via a signal-blocking inlet.

Although 1D signaling models have been realized for spatiotemporal signaling studies, the output information is still limited because *in vivo* local signaling patterns are typically 2D or 3D. A 2D model of developmental signaling center has been created in microfluidic device (Manfrin et al., 2019). Localized morphogen signaling sources were generated upon treatment with an input signal of bone morphogenetic protein 4 (BMP4), resulting in the formation of morphogen gradients along human pluripotent stem cell (hPSC) colonies. The hPSCs exhibited spatially differential expression of MIXL1, T, SOX17 and CDX2 genes, demonstrating spatiotemporally controlled morphogen signaling gradients. This study shows the possibility of constructing a 2D signaling model in a microfluidic device, provided that a global signal does not stimulate receiver cells.

Photocaging and photoactivation strategies can also be used to control the activation of sender cells in a 2D signaling model. For example, a light-controlled immunostimulant probe that can photosensitize immune cells was synthesized to control the origin of inflammation (Mancini et al., 2015). This probe, a photocaged TLR agonist modified with a 2-nitrobenzyl linker, can tag and remotely induce a guided immune response (TRIGIR) (Figure 4B). With light irradiation, the TRIGIR probe is uncaged after the photocleavage of the 2-nitrobenzyl linker, functioning as a photoactive immunopotentiator to activate TLR signaling and inflammation pathways. In a coculture environment, the photoactivated TRIGIR probe controllably activates bone marrow-derived dendritic cells (BMDCs) as a global input. The cocultured fibroblasts are further activated upon receiving local input signals from the activated BMDCs, thereby initiating TNF secretion.

Synthetic biology offers powerful tools such as chemogenetic (Keifer et al., 2020; Tsai et al., 2021; Raper and Galvan, 2022) and optogenetic (Tischer and Weiner, 2014; Zhang and Cu, 2015; Leopold et al., 2018; Hongdusit et al., 2020; Farahani et al., 2021; Kramer et al., 2021) techniques to control the activity of signaling proteins in living cells. By leveraging these tools, it is possible to control the activation of living sender cells that have been transfected with chemogenetic or optogenetic response elements. An example involved the production of morphogen Sonic Hedgehog (SHH) by a sender cell line under the control of the chemical 4-hydroxytamoxifen (4-OHT) (Figure 4Ca) (Li et al., 2018). The SHH signaling gradients resulted in radial and linear activation geometries in neighboring receiver cells, as evidenced by the expression of nuclear-localized Histone 2B (H2B)-Citrine fluorescent protein (Figure 4Cb). This finding showcases the ability to achieve localized signal sources through the utilization of synthetic circuits controlled by chemical inputs. The optogenetic approach allows the construction of an intercellular communication model in which local signal generation can be precisely controlled through light irradiation on living sender cells. The design of an opto-SOS system enabled the controlled initiation of signaling protein Ras activation, nuclear translocation of Erk2, and secretion of IL-6 family cytokines (Toettcher et al., 2013). The

observation of STAT3 nuclear translocation in receiver cells confirmed the propagation of IL-6 from the signaling senders. Notably, 2 hours of light irradiation on sender cells led to STAT3 activation in the receivers, whereas two separate 1-h light irradiations with an interval did not produce the same effect. In another study, an optogenetic intercellular system was implemented in the budding yeast *Saccharomyces cerevisiae*. This system involved controlling the production of  $\alpha$ -factor pheromone through blue light irradiation of Optogenetic Sender (OS) strains, subsequently leading to luciferase induction in the Receiver (R) strains (Figure 4D) (Rojas and Larrondo, 2022). These studies demonstrate the versatility of optogenetic tools in the introducing different types of local inputs that lead to distinct fate decisions in receiver cells.

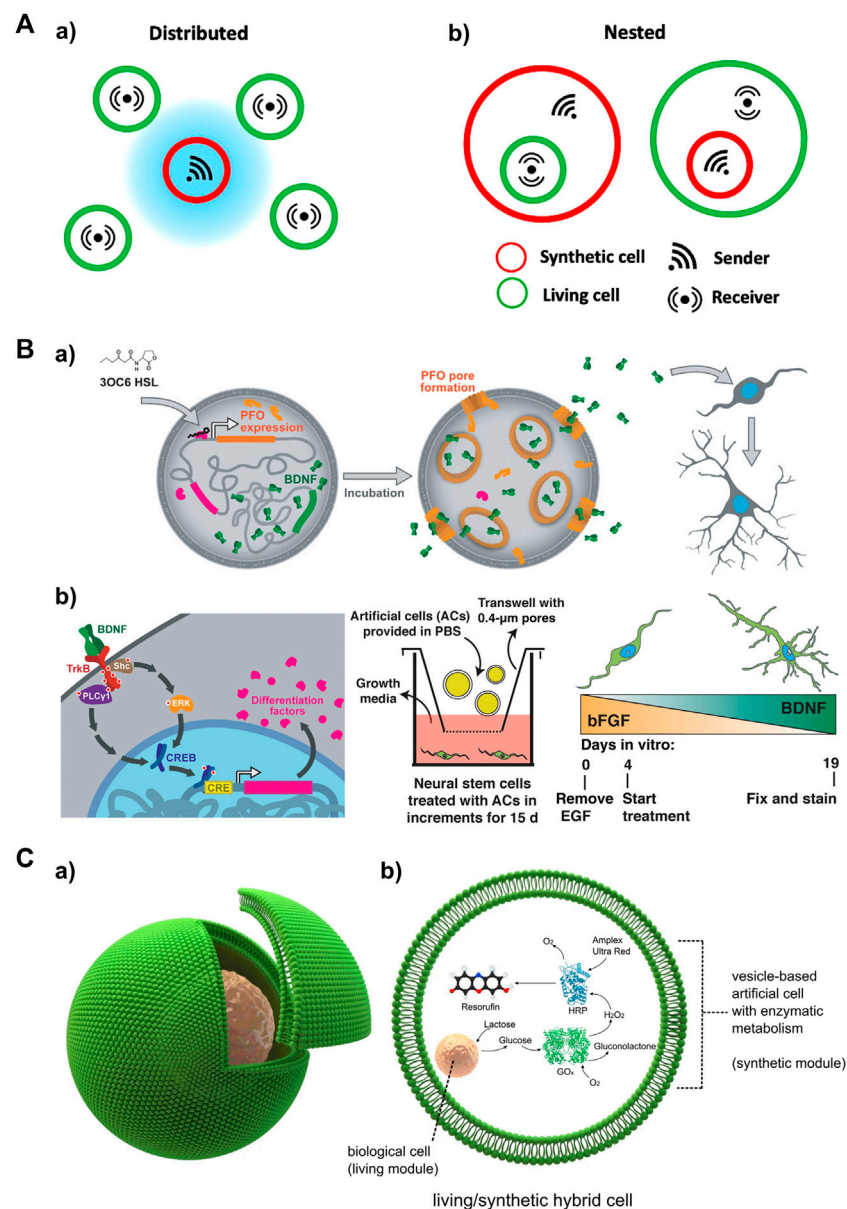
## Local input generation with artificial cell senders

Artificial cells, also known as synthetic protocells, are designed to replicate the structures and functions of living cells. These cell mimics provide a valuable tool for studying intercellular communications with minimal interference from cellular complexity, such as diverse secretion levels and rates of signal molecules. Additionally, artificial cells offer advantages in controlling the release of local input signals compared to living cells, which opens up new possibilities for various applications. In the context of local signal generation, artificial cells can be engineered to replace living cells as local signal sources. While several studies have investigated communication between artificial cells (Niederholtmeyer et al., 2018; Aufinger and Simmel, 2019; Joesaar et al., 2019; Karoui et al., 2022), the interaction between artificial and living cells has received less attention. This section will introduce three types of signaling models, namely, paracrine, contact-dependent, and embedded signaling, in the context of artificial-living cell communities (Figure 5A).

Paracrine signaling involves the transmission of signals over short distances, eliciting diverse responses in receiver cells. Artificial cells with biocompatibility can be cocultured with living cells to deliver local input signals via paracrine signaling. A recent development induces an artificial cell system that integrated a brain-derived neurotrophic factor (BDNF) and perfringolysin O (PFO) gene expression construct (Toparlak et al., 2020). This system allows for the controlled activation of both genes using *N*-3-oxohexanoyl homoserine lactone (3OC6 HSL). In the presence of 3OC6 HSL, both PFO and BDNF are produced, and BDNF is released through formed PFO pores. In a coculture system, the artificial cells responded to 3OC6 HSL, releasing BDNF that subsequently drives the differentiation of mouse embryonic stem cell-derived neural stem (mNS) cells (Figure 5B). Communication between artificial cells and engineered HEK293T cells has also been established through the addition of 3OC6 HSL. The released BDNF induces GFP expression in the HEK293T cells. These results demonstrate the suitability of artificial cells in delivering paracrine signals as substitutes for biological cells.

Nested (or embedded) architectures involving artificial and living cells provide non-native signaling configurations (Figure 5Ab). In this construct, artificial cells are embedded within living cells, allowing for the exploration of signaling events initiated inside the system, such as antiviral innate immune signaling (Seth et al., 2006). Although this approach has been relatively less explored in current studies, it holds



**FIGURE 5**

Activated artificial cells as a local input source for studying spatiotemporal signaling dynamics in receiver cells **(A)** Schematic depicting different types of localized signaling in artificial/living cell consortia, including local signaling among a) distributed and b) nested cell populations. Adapted from (Mukwaya et al., 2021) Copyright 2021 CC BY 4.0. **(B)** Small molecule-triggered signaling in an artificial cell as a local signal source to drive neural differentiation. a) 3OC6 HSL induced PFO expression and pore formation, along with BDNF release, which subsequently leads to the differentiation and maturation of mNS cells. b) Left: Signaling between artificial cells and mNS cells. Middle: Artificial cells were incubated with mNS cells in a transwell. Right: BDNF secretion gradually increased over the course of artificial cell treatment (days 4–19). Reproduced with permission from (Toparlak et al., 2020). Copyright 2020 CC BY 4.0. **(C)** Artificial/Living hybrid cells. a) a biological cell encapsulated inside a vesicle-based artificial cell. b) The encapsulated cell functions similarly to an organelle within the vesicle reactor. It processes chemical elements, which are subsequently metabolized downstream by a co-encapsulated synthetic enzymatic cascade in the vesicle. Reproduced from (Elani et al., 2018). Copyright 2018 CC BY 4.0.

promise for future applications. For example, micron- or submicron-sized artificial cells loaded with viral DNA/RNA can be endocytosed by living cells, mimicking nested communication during viral infection. The viral DNA/RNA can then be released, triggering the retinoic acid-inducible gene I (RIG-I) and melanoma differentiation-associated gene 5 (MDA5) pathways, as well as NF- $\kappa$ B pathway (Brisse and Ly, 2019; Rehwinkel and Gack, 2020; Onomoto et al., 2021). Another possible configuration involves living cells embedded within an artificial cell,

enabling a cellular bionics approach where living cells can function as organelle-like modules. A recent study presented a cellular bionic system consisting of a single host lipid vesicle-based artificial cell encapsulating colon carcinoma cells, and established an embedded glucose oxidase (GOx)/horseradish peroxidase (HRP) enzyme cascade (Figure 5C) (Elani et al., 2018). This localized communication was initiated by the production of glucose (Glc) upon stimulation of the cancer cells with lactose pre-loaded in the artificial cell. This innovative

**TABLE 4 Comparison of different signal generators in terms of their input types, advantages and limitations.**

	Potential input types	Advantages	Limitations
Global Signal Generators			
Microfluidics-based	Pulse, continuous, ramping	Able to implement various input modes	Shear stress might affect quantification of fluorescence-labelled signaling proteins
		Input is native molecule with known concentration	Challenging to deliver input to suspension cells
Photoactivation-based	Continuous	Easy to execute light irradiation	Chemical modification of input molecules may lower down the activity of protein input
			Long time exposure to short wavelength of light may be harmful to cells
Local Signal Generators (Living Cell Senders)			
Pre-stimulation-based	Wave	No need of extra global input delivery or modification	Challenging to control the origin of signal propagation
Microfluidics-based	Wave	Input is native molecule with known concentration	Challenging to deliver input to suspension cells
			2D signaling models require the inputs that are insensitive to receiver cells
Photo-deprotection-based	Wave	Local input is controllable	The receiver cells must be insensitive to the stimuli
			Prolonged exposure to short wavelength of light may be harmful to sender cells
Optogenetics-based	Wave, continuous	Local input is controllable	The specificity of the expression patterns of the optogenetic probes relies on the availability of the appropriate promoter/enhancer sequences
		Photosensitive elements responsive to long wavelength of light can be applied to activate sender cells	
Local Signal Generators (Artificial Cell Senders)			
Artificial cell-based	Wave, continuous	Local input is controllable	Challenging to quantify the input molecules released from the artificial cells
		Exposure with short wavelength of light does not affect non-living sender cells	

approach has the potential to uncover more signaling mechanisms underlying nested communication.

## Advantages and limitations of current global and local signal generators

Global and local signal generators have been utilized in cellular signaling studies to gain insights into the activation of signaling pathways and dynamics of signaling proteins. Each type of generators has its own set of advantages and limitations, which will be discussed in this section (Table 4).

Microfluidic systems have been widely used as global signal generators for investigating temporal signaling dynamics (Tay et al., 2010; Song et al., 2018; Mokashi et al., 2019; Yang et al., 2022). These systems allow for precise delivery of native molecules, including cytokine proteins, to cell cultures. With the ability to control input amplitude and duration, microfluidic systems can implement various input types, such as pulse, continuous and ramping, to capture dynamic information about cellular behaviors and gain insights into signaling mechanisms. However, microfluidic systems also have limitations. The perfusion of input molecules into cell chambers can generate strong shear stress, which may affect cell morphology. Cells sensitive to shear stress may shrink (Yang

et al., 2022), altering the fluorescence intensity of the nucleus, cytoplasm and the entire cell, thus interfering with the quantitation of signaling proteins. To mitigate this influence, optimization of microchannel geometry, size, and pump pressure is necessary. Additionally, flow-based input delivery is primarily suitable for adherent cells, as keeping suspension cells stationary during perfusion in a microfluidic device is challenging.

Another approach of generating global inputs involves light irradiation to induce the photodeprotection of caged input molecules (Ryu et al., 2014; Stutts and Esser-Kahn, 2015; Ryu et al., 2017). This method addresses the limitations of shear stress and the challenge of handling suspension cells in microfluidic devices. Light irradiation allows for cell experiments to be performed in commercialized well plate, eliminating the need for complex microfluidic device fabrication and setup. However, chemical modification of photocaged groups to input molecules relies heavily on organic synthesis, which may inactivate proteins. To overcome this limitation, proteins can be caged with dendritic molecular glue <sup>PC</sup>Glue-NBD (Mogaki et al., 2019) or PEG conjugated with 2-nitrobenzyl linkers (Perdue et al., 2020) and photodeprotected with UV irradiation. Nevertheless, prolonged UV light exposure can be phototoxic to cells. Additionally, this approach primarily supports continuous inputs, as the input molecules are not removed from cell cultures after light irradiation.

Local signal sources can be established using either living or artificial cell senders. Various strategies have been employed to control the activation of sender cells. A simple 2D signaling model can be constructed by coculturing pre-stimulated living sender cells with receiver cells (Oyler-Yaniv et al., 2017). This method allows for the investigation of interesting pathways without the need for additional delivery or chemical modification of global input molecules. However, controlling the origin of the local signal source is challenging since the local input molecules start propagating during the pre-stimulation process. Thus, this method is more suitable for discovering microdomains of signaling cells and studying the spatial spread of local input molecules, such as cytokines and growth factors (Oyler-Yaniv et al., 2017).

Microfluidic cell coculture systems enable controlled local signaling by compartmentalizing sender and receiver cells in closed environments with integrated separation valves. Depending on the sensitivity of receiver cells to global stimuli, sender cells can be either separated from receiver cells (Frank and Tay, 2015; Son et al., 2022; Watson et al., 2022) or confined together with receiver cells in the same chambers (Manfrin et al., 2019; Yang et al., 2022). However, achieving a 2D signaling model in a microfluidic system remains a challenge when global stimuli can also activate receiver cells. The geometric structure required for a 2D signal flow is difficult to achieve when sender and receiver cells are isolated with separation valves. The advantages and limitations of microfluidic systems as global input generators are also applicable to their applications in local signal generators. Native stimuli molecules with known concentrations allow for easy quantification of various types of global input. However, constructing a local signaling model with suspension cells still poses challenges.

The photodeprotection of caged input molecules have also been applied in local signal generation (Mancini et al., 2015). Sender cells can be activated through light irradiation of caged global stimuli. Another photoactivation-based method utilizes optogenetic tools to engineer photosensitive gene promoters in sender cells (Toettcher et al., 2013). Although both approaches are based on light irradiation, photodeprotection of caged stimuli is typically initiated by UV light, while photosensitive elements responsive to longer wavelengths of light can be used in optogenetic designs. The latter addresses the issue of phototoxicity associated with prolonged irradiation. This allows sender cells to continuously propagate local input signals. However, both methods have limitations, such as the restricted availability of photocaged stimuli and photo-responsive promoters.

Artificial cells have gained significant attention as substitutes for living cells (Xu et al., 2016; Buddingh and van Hest, 2017). These cell mimics provide a simplified platform for constructing cellular communities and storing and releasing interesting molecules with high precision. Artificial cells with biocompatibility have been employed as local signal senders (Toparlak et al., 2020). One key advantage is the high controllability of local signal generation. Signals can be released through passive diffusion, chemical induction (Toparlak et al., 2020) or light irradiation (Yang et al., 2020). Chemical induction allows for the generation of local input signals without directly stimulating living receiver cells. Additionally, the phototoxicity associated with light irradiation does not affect artificial cell senders. However, quantifying the

released input molecules from artificial cells remains a challenge. One potential solution is to use fluorescently labeled input molecules. While studies on local signaling using artificial cells have been relatively limited to date, we believe that the unique advantages of artificial cells will facilitate further research in this area.

## Conclusions and future prospects

Global and local signal generators have significantly enhanced our understanding of temporal and spatial cellular signaling activities and cellular behaviors. In particular, microfluidic systems have emerged as powerful tools for investigating temporal activity of signaling pathways in single cells (Junkin et al., 2016; Sinha et al., 2022; Yang et al., 2022) and cell populations (Tay et al., 2010; Song et al., 2018; Mokashi et al., 2019). These systems allow precise delivery of various global inputs, such as pulse (Blazek et al., 2015; Ryu et al., 2015), continuous (Dettinger et al., 2018), and step-wise ramping (Song et al., 2018; Son et al., 2021), and ramping analog inputs (Mokashi et al., 2019), resulting in distinct cellular responses. Through the study of temporal behavior in individual cells, we have gained insights into fundamental biological processes like cell proliferation and differentiation (Zhu and Thompson, 2019), and immune response (Brubaker et al., 2015). For instance, perturbation of ERK activity with pulsatile inputs of EGF/NGF reveal that transient/sustained ERK dynamics induce proliferation/differentiation in PC-12 cells (Ryu et al., 2015). Continuous and pulse TNF $\alpha$  inputs were shown to elicit digital activation but analogue information processing of NF- $\kappa$ B in fibroblasts (Tay et al., 2010). Additionally, the delivery of linear/exponential stepwise ramping inputs of TNF $\alpha$  to fibroblasts demonstrates that NF- $\kappa$ B activity responds to the absolute difference in cytokine concentration rather than the concentration itself (Son et al., 2021). These findings highlight the power of microfluidic approaches in addressing complex biological questions that are challenging to investigate using conventional experiments conducted in well plates, which often allow for treatments with only continuous inputs or very few pulses of input signals (Ashall et al., 2009; Zhang et al., 2017). Despite significant progress, there is still much to uncover regarding the underlying signaling mechanisms and their implications, considering the diverse range of global input signals encountered by cells during biological events. The remarkable controllability of microfluidic systems opens up possibilities for exploring additional global input types, such as sinusoidal and triangle signals, which may provide further insights into temporal signaling responses in future studies.

The development of photocaging and photodeprotection-based global input generators has been a subject of ongoing research for years. This emerging technology has aided our exploration in control of cellular signaling activation. Several small molecule agonists of TLRs conjugated with 2-nitrobenzyl groups have been applied to control the activation of immune signaling pathways (Ryu et al., 2014; Govan et al., 2015; Stutts and Esser-Kahn, 2015). By exploring the signaling of TLRs using photoactivated agonists, we can gain insights into inflammatory responses and the innate immune system's recognition of non-self, potentially leading to advancements in vaccine design. Photochemical techniques have

also been employed for macromolecule inputs such as growth factors and cytokines. Caged dendritic molecular glues (Mogaki et al., 2019) and polymers (Perdue et al., 2020), have been utilized to photo-protect these protein input molecules, enabling their controlled release and activation of downstream signaling pathways. This has opened up possibilities for using photolabile molecular glues or polymers as universal inhibitors to control protein input-triggered signaling activation. By combined these techniques with reporter cells and time-lapse imaging (Yang et al., 2022), we can extend their applications to study temporal signaling dynamics in future. Furthermore, light irradiation can be programmed to create various input profiles, including multiple-wave and continuous stimulation. For example, photolabile molecular glues or polymers can be modified to photo-protect EGF/NGF and TNF $\alpha$ , allowing controlled activation of the ERK and NF- $\kappa$ B pathways, respectively. By applying specific input profiles of light irradiation, we can investigate the temporal dynamics of ERK and NF- $\kappa$ B signaling pathways.

Living cells have been adapted to serve as local signal generators using various approaches, as discussed in this review. These local signal generators can be easily extended to explore other cell types and signaling pathways, offering versatility and flexibility in experimental design. While artificial cells have not been widely applied as local signal generators in observing signaling dynamics in living receiver cells, recent studies have demonstrated their potential in controlled signaling activation in neural and HEK293 cells (Toparlak et al., 2020). The utilization of artificial cells as local signal generators faces challenges in building photo-responsive promoters and gene expression systems within these synthetic constructs. However, alternative strategies can be explored. For example, light-controlled DNA-mediated signaling between artificial cells has recently attracted attention (Yang et al., 2020). These artificial cells with adjustable permeability can store and release different DNA molecules conjugated with photolabile linkers under light irradiation. It raises the question of whether proteins, such as cytokine or growth factors, modified with photolabile linkers, can also be stored in artificial cells and released upon light irradiation.

In conclusion, the development of robust platforms for both global and local signal generation holds significant promise in enhancing our understanding of how cells encode and decode diverse input information across spatial and temporal dimensions.

The impact of these signal generators is evident in their potential to elucidate the underlying signaling mechanisms governing temporal and spatial signaling dynamics, as well as cellular behaviors. We firmly believe that advancing and expanding upon the techniques discussed in this review will further propel the discovery of novel and intriguing signaling mechanisms.

## Author contributions

HY: Conceptualization, Writing—original draft, Writing—review and editing; JT: Supervision, Funding Acquisition, Writing—review and editing. All authors contributed to the article and approved the submitted version.

## Funding

This result is part of a project, ImmunoCode, that has received funding from the European Research Council (ERC) under the European Union's Horizon 2020 research and innovation programme (Grant agreement No. 802791). Furthermore, we acknowledge generous support by the Eindhoven University of Technology.

## Conflict of interest

The authors declare that the research was conducted in the absence of any commercial or financial relationships that could be construed as a potential conflict of interest.

## Publisher's note

All claims expressed in this article are solely those of the authors and do not necessarily represent those of their affiliated organizations, or those of the publisher, the editors and the reviewers. Any product that may be evaluated in this article, or claim that may be made by its manufacturer, is not guaranteed or endorsed by the publisher.

## References

- Ashall, L., Horton, C. A., Nelson, D. E., Paszek, P., Harper, C. V., Sillitoe, K., et al. (2009). Pulsatile stimulation determines timing and specificity of NF- $\kappa$ B-dependent transcription. *Science* 324, 242–246. doi:10.1126/science.1164860
- Aufinger, L., and Simmel, F. C. (2019). Establishing communication between artificial cells. *Chem-Eur J.* 25, 12659–12670. doi:10.1002/chem.201901726
- Blazek, M., Betz, C., Hall, M. N., Reth, M., Zengerle, R., and Meier, M. (2013). Proximity ligation assay for high-content profiling of cell signaling pathways on a microfluidic chip. *Mol. Cell Proteomics* 12, 3898–3907. doi:10.1074/mcp.M113.032821
- Blazek, M., Santisteban, T. S., Zengerle, R., and Meier, M. (2015). Analysis of fast protein phosphorylation kinetics in single cells on a microfluidic chip. *Lab. Chip* 15, 726–734. doi:10.1039/c4lc00797b
- Blum, Y., Mikelson, J., Dobrzynski, M., Ryu, H., Jacques, M. A., Jeon, N. L., et al. (2019). Temporal perturbation of ERK dynamics reveals network architecture of FGF2/MAPK signaling. *Mol. Syst. Biol.* 15, e8947. doi:10.15252/msb.20198947
- Brisse, M., and Ly, H. (2019). Comparative structure and function analysis of the RIG-I-like receptors: RIG-I and MDA5. *Front. Immunol.* 10. doi:10.3389/fimmu.2019.01586
- Brower, K., Puccinelli, R. R., Markin, C. J., Shimko, T. C., Longwell, S. A., Cruz, B., et al. (2018). An open-source, programmable pneumatic setup for operation and automated control of single- and multi-layer microfluidic devices. *HardwareX* 3, 117–134. doi:10.1016/j.ohx.2017.10.001
- Brubaker, S. W., Bonham, K. S., Zandoni, L., and Kagan, J. C. (2015). Innate immune pattern recognition: A cell biological perspective. *Annu. Rev. Immunol.* 33, 257–290. doi:10.1146/annurev-immunol-032414-112240
- Buddingh, B. C., and van Hest, J. C. M. (2017). Artificial cells: synthetic compartments with life-like functionality and adaptivity. *Accounts Chem. Res.* 50, 769–777. doi:10.1021/acs.accounts.6b00512
- Chen, H. Y., Yu, Z. H., Bai, S. W., Lu, H. X., Xu, D., Chen, C., et al. (2019). Microfluidic models of physiological or pathological flow shear stress for cell biology, disease modeling and drug development. *Trac-Trend Anal. Chem.* 117, 186–199. doi:10.1016/j.trac.2019.06.023
- Dekoninck, S., and Blanpain, C. (2019). Stem cell dynamics, migration and plasticity during wound healing. *Nat. Cell Biol.* 21, 18–24. doi:10.1038/s41556-018-0237-6



- Dettinger, P., Frank, T., Etzrodt, M., Ahmed, N., Reimann, A., Trenzinger, C., et al. (2018). Automated microfluidic system for dynamic stimulation and tracking of single cells. *Anal. Chem.* 90, 10695–10700. doi:10.1021/acs.analchem.8b00312
- Devary, Y., Rosette, C., Di Donato, J. A., and Karin, M. (1993). NF- $\kappa$ B activation by ultraviolet light not dependent on a nuclear signal. *Science* 261, 1442–1445. doi:10.1126/science.8367725
- Discher, D. E., Janmey, P., and Wang, Y. L. (2005). Tissue cells feel and respond to the stiffness of their substrate. *Science* 310, 1139–1143. doi:10.1126/science.1116995
- Dorrington, M. G., and Fraser, I. D. C. (2019). NF-Kappa B signaling in macrophages: dynamics, crosstalk, and signal integration. *Front. Immunol.* 10, 705. doi:10.3389/fimmu.2019.00705
- Elani, Y., Trantidou, T., Wylie, D., Dekker, L., Polizzi, K., Law, R. V., et al. (2018). Constructing vesicle-based artificial cells with embedded living cells as organelle-like modules. *Sci. Rep.-Uk* 8, 4564. doi:10.1038/s41598-018-22263-3
- Fang, G. C., Lu, H. X., Es, H. A., Wang, D. J., Liu, Y., Warkiani, M. E., et al. (2021). Unidirectional intercellular communication on a microfluidic chip. *Biosens. Bioelectron.* 175, 112833. doi:10.1016/j.bios.2020.112833
- Farahani, P. E., Reed, E. H., Underhill, E. J., Aoki, K., and Toettcher, J. E. (2021). Signaling, deconstructed: using optogenetics to dissect and direct information flow in biological systems. *Annu. Rev. Biomed. Eng.* 23, 61–87. doi:10.1146/annurev-bioeng-083120-111648
- Frank, T., and Tay, S. (2015). Automated co-culture system for spatiotemporal analysis of cell-to-cell communication. *Lab. Chip* 15, 2192–2200. doi:10.1039/c5lc00182j
- Gao, D., Liu, H. X., Jiang, Y. Y., Lin, J. M., Liu, H., et al. (2012). Recent developments in microfluidic devices for *in vitro* cell culture for cell-biology research. *Trac-Trend Anal. Chem.* 35, 150–164. doi:10.1016/j.trac.2012.02.008
- Govan, J. M., Young, D. D., Lively, M. O., and Deiters, A. (2015). Optically triggered immune response through photocaged oligonucleotides. *Tetrahedron Lett.* 56, 3639–3642. doi:10.1016/j.tetlet.2015.01.165
- Hongdusit, A., Liechty, E. T., and Fox, J. M. (2020). Optogenetic interrogation and control of cell signaling. *Curr. Opin. Biotech.* 66, 195–206. doi:10.1016/j.copbio.2020.07.007
- Hu, H. G., Chen, P. G., Wang, G. Y., Wu, J. J., Zhang, B. D., Li, W. H., et al. (2020). Regulation of immune activation by optical control of TLR1/2 heterodimerization. *Chembiochem* 21, 1150–1154. doi:10.1002/cbic.201900591
- Irimia, D. (2010). Microfluidic technologies for temporal perturbations of chemotaxis. *Annu. Rev. Biomed. Eng.* 12, 259–284. doi:10.1146/annurev-bioeng-070909-105241
- Joesaar, A., Yang, S., Bogels, B., van der Linden, A., Pieters, P., Kumar, B. V. V. S. P., et al. (2019). DNA-based communication in populations of synthetic protocells. *Nat. Nanotechnol.* 14, 369–378. doi:10.1038/s41565-019-0399-9
- Junkin, M., Kaestli, A. J., Cheng, Z., Jordi, C., Albayrak, C., Hoffmann, A., et al. (2016). High-content quantification of single-cell immune dynamics. *Cell Rep.* 15, 411–422. doi:10.1016/j.celrep.2016.03.033
- Karoui, H., Patwal, P. S., Kumar, B. V. V. S. P., and Martin, N. (2022). Chemical communication in artificial cells: basic concepts, design and challenges. *Front. Mol. Biosci.* 9, 880525. doi:10.3389/fmolb.2022.880525
- Kehl, F., Cretu, V. F., and Willis, P. A. (2021). Open-source lab hardware: A versatile microfluidic control and sensor platform. *HardwareX* 10, e00229. doi:10.1016/j.ohx.2021.e00229
- Keifer, O., Kambara, K., Lau, A., Makinson, S., and Bertrand, D. (2020). Chemogenetics a robust approach to pharmacology and gene therapy. *Biochem. Pharmacol.* 175, 113889. doi:10.1016/j.bcp.2020.113889
- Kellogg, R. A., Tian, C. Z., Lipniacki, T., Quake, S. R., and Tay, S. (2015). Digital signaling decouples activation probability and population heterogeneity. *Elife* 4, e08931. doi:10.7554/eLife.08931
- Kim, D., Wu, X. J., Young, A. T., and Haynes, C. L. (2014). Microfluidics-based *in vivo* mimetic systems for the study of cellular biology. *Accounts Chem. Res.* 47, 1165–1173. doi:10.1021/ar4002608
- Klan, P., Solomek, T., Bochet, C. G., Blanc, A., Givens, R., Rubina, M., et al. (2013). Photoremovable protecting groups in chemistry and biology: reaction mechanisms and efficacy. *Chem. Rev.* 113, 119–191. doi:10.1021/cr300177k
- Kramer, M. M., Lataster, L., Weber, W., and Radziwill, G. (2021). Optogenetic approaches for the spatiotemporal control of signal transduction pathways. *Int. J. Mol. Sci.* 22, 5300. doi:10.3390/ijms22105300
- Lavoie, H., Gagnon, J., and Therrien, M. (2020). ERK signalling: A master regulator of cell behaviour, life and fate. *Nat. Rev. Mol. Cell Bio* 21, 607–632. doi:10.1038/s41580-020-0255-7
- Leof, E. B. (2000). Growth factor receptor signalling: location, location, location. *Trends Cell Biol.* 10, 343–348. doi:10.1016/S0962-8924(00)01795-5
- Leopold, A. V., Chernov, K. G., and Verkhusha, V. V. (2018). Optogenetically controlled protein kinases for regulation of cellular signaling. *Chem. Soc. Rev.* 47, 2454–2484. doi:10.1039/c7cs00404d
- Li, N. X., and Karin, M. (1998). Ionizing radiation and short wavelength UV activate NF-kappa B through two distinct mechanisms. *P Natl. Acad. Sci. U. S. A.* 95, 13012–13017. doi:10.1073/pnas.95.22.13012
- Li, P. L., Markson, J. S., Wang, S., Chen, S. H., Vachharajani, V., and Elowitz, M. B. (2018). Morphogen gradient reconstitution reveals Hedgehog pathway design principles. *Science* 360, 543–548. doi:10.1126/science.aao0645
- Mancini, R. J., Stutts, L., Moore, T., and Esser-Kahn, A. P. (2015). Controlling the origins of inflammation with a photoactive lipopeptide immunopotentiator. *Angew. Chem. Int. Ed.* 54, 5962–5965. doi:10.1002/anie.201500416
- Manfrin, A., Tabata, Y., Paquet, E. R., Vuaridel, A. R., Rivest, F. R., Naef, F., et al. (2019). Engineered signaling centers for the spatially controlled patterning of human pluripotent stem cells. *Nat. Methods* 16, 640–648. doi:10.1038/s41592-019-0455-2
- Moenter, S. M., Brand, R. M., Midgley, A. R., and Karsch, F. J. (1992). Dynamics of gonadotropin-releasing-hormone release during a pulse. *Endocrinology* 130, 503–510. doi:10.1210/endo.130.1.1727719
- Mogaki, R., Okuro, K., Ueki, R., Sando, S., and Aida, T. (2019). Molecular glue that spatiotemporally turns on protein-protein interactions. *J. Am. Chem. Soc.* 141, 8035–8040. doi:10.1021/jacs.9b02427
- Mokashi, C. S., Schipper, D. L., Qasimeh, M. A., and Lee, R. E. C. (2019). A system for analog control of cell culture dynamics to reveal capabilities of signaling networks. *Isience* 19, 586–596. doi:10.1016/j.isci.2019.08.010
- Mrksich, M. (2000). A surface chemistry approach to studying cell adhesion. *Chem. Soc. Rev.* 29, 267–273. doi:10.1039/a705397e
- Mudla, A., Jiang, Y. F., Arimoto, K. I., Xu, B. X., Rajesh, A., Ryan, A. P., et al. (2020). Cell-cycle-gated feedback control mediates desensitization to interferon stimulation. *Elife* 9, e58825. doi:10.7554/eLife.58825
- Mukwaya, V., Mann, S., and Dou, H. J. (2021). Chemical communication at the synthetic cell/living cell interface. *Commun. Chem.* 4, 161. doi:10.1038/s42004-021-00597-w
- Niederholtmeyer, H., Chagga, C., and Devaraj, N. K. (2018). Communication and quorum sensing in non-living mimics of eukaryotic cells. *Nat. Commun.* 9, 5027. doi:10.1038/s41467-018-07473-7
- O'Dea, E. L., Kearns, J. D., and Hoffmann, A. (2008). UV as an amplifier rather than inducer of NF-kappa B activity. *Mol. Cell* 30, 632–641. doi:10.1016/j.molcel.2008.03.017
- Onomoto, K., Onoguchi, K., and Yoneyama, M. (2021). Regulation of RIG-I-like receptor-mediated signaling: interaction between host and viral factors. *Cell Mol. Immunol.* 18, 539–555. doi:10.1038/s41423-020-00602-7
- O'Shea, J. J., and Murray, P. J. (2008). Cytokine signaling modules in inflammatory responses. *Immunity* 28, 477–487. doi:10.1016/j.immuni.2008.03.002
- Osborn, O., and Olefsky, J. M. (2012). The cellular and signaling networks linking the immune system and metabolism in disease. *Nat. Med.* 18, 363–374. doi:10.1038/nm.2627
- Oyler-Yaniv, A., Oyler-Yaniv, J., Whitlock, B. M., Liu, Z. D., Germain, R. N., Huse, M., et al. (2017). A tunable diffusion-consumption mechanism of cytokine propagation enables plasticity in cell-to-cell communication in the immune system. *Immunity* 46, 609–620. doi:10.1016/j.immuni.2017.03.011
- Perdue, L. A., Do, P., David, C., Chyong, A., Kellner, A. V., Ruggieri, A., et al. (2020). Optical control of cytokine signaling via bioinspired, polymer-induced latency. *Biomacromolecules* 21, 2635–2644. doi:10.1021/acs.biomac.0c00264
- Piehl, A., Ghorashian, N., Zhang, C., and Tay, S. (2017). Universal signal generator for dynamic cell stimulation. *Lab. Chip* 17, 2218–2224. doi:10.1039/C7LC00531H
- Purvis, J. E., and Lahav, G. (2013). Encoding and decoding cellular information through signaling dynamics. *Cell* 152, 945–956. doi:10.1016/j.cell.2013.02.005
- Raper, J., and Galvan, A. (2022). Applications of chemogenetics in non-human primates. *Curr. Opin. Pharmacol.* 64, 102204. doi:10.1016/j.coph.2022.102204
- Rehwinkel, J., and Gack, M. U. (2020). RIG-I-like receptors: their regulation and roles in RNA sensing. *Nat. Rev. Immunol.* 20, 537–551. doi:10.1038/s41577-020-0288-3
- Rho, H. S., Yang, Y., Hanke, A. T., Ottens, M., Terstappen, L. W. M. M., and Gardeniers, H. (2016). Programmable v-type valve for cell and particle manipulation in microfluidic devices. *Lab. Chip* 16, 305–311. doi:10.1039/c5lc01206f
- Rojas, V., and Larrondo, L. F. (2022). Coupling cell communication and optogenetics: implementation of a light-inducible intercellular system in yeast. *ACS Synth. Biol.* doi:10.1021/acssynbio.2c00338
- Ryu, H., Chung, M., Dobrzynski, M., Fey, D., Blum, Y., Lee, S. S., et al. (2015). Frequency modulation of ERK activation dynamics rewires cell fate. *Mol. Syst. Biol.* 11, 838. doi:10.15252/msb.20156458
- Ryu, K. A., McGonnigal, B., Moore, T., Kargupta, T., Mancini, R. J., and Esser-Kahn, A. P. (2017). Light guided *in-vivo* activation of innate immune cells with photocaged TLR 2/6 agonist. *Sci. Rep.-Uk* 7, 8074. doi:10.1038/s41598-017-08520-x
- Ryu, K. A., Stutts, L., Tom, J. K., Mancini, R. J., and Esser-Kahn, A. P. (2014). Stimulation of innate immune cells by light-activated TLR7/8 agonists. *J. Am. Chem. Soc.* 136, 10823–10825. doi:10.1021/ja412314j
- Sanchez, E., and Huse, M. (2018). Spatial and temporal control of T cell activation using a photoactivatable agonist. *Jove-J. Vis. Exp.*, 56655. doi:10.3791/56655

- Serafini, N., Vossenrich, C. A. J., and Di Santo, J. P. (2015). Transcriptional regulation of innate lymphoid cell fate. *Nat. Rev. Immunol.* 15, 415–428. doi:10.1038/nri3855
- Seth, R. B., Sun, L. J., and Chen, Z. J. J. (2006). Antiviral innate immunity pathways. *Cell Res.* 16, 141–147. doi:10.1038/sj.cr.7310019
- Sia, S. K., and Whitesides, G. M. (2003). Microfluidic devices fabricated in poly(dimethylsiloxane) for biological studies. *Electrophoresis* 24, 3563–3576. doi:10.1002/elps.200305584
- Sinha, N., Subedi, N., and Tel, J. (2018). Integrating immunology and microfluidics for single immune cell analysis. *Front. Immunol.* 9, 2373. doi:10.3389/fimmu.2018.02373
- Sinha, N., Yang, H., Janse, D., Hendriks, L., Rand, U., Hauser, H., et al. (2022). Microfluidic chip for precise trapping of single cells and temporal analysis of signaling dynamics. *Commun. Eng.* 1, 18. doi:10.1038/s44172-022-00019-2
- Son, M., Frank, T., Holst-Hansen, T., Wang, A. G., Junkin, M., Kashaf, S. S., et al. (2022). Spatiotemporal NF-kappa B dynamics encodes the position, amplitude, and duration of local immune inputs. *Sci. Adv.* 8, eabn6240. doi:10.1126/sciadv.abn6240
- Son, M. J., Wang, A. G., Tu, H. L., Metzger, M. O., Patel, P., Husain, K., et al. (2021). NF-kappa B responds to absolute differences in cytokine concentrations. *Sci. Signal* 14, eaaz4382. doi:10.1126/scisignal.aaz4382
- Song, J., Ryu, H., Chung, M., Kim, Y., Blum, Y., Lee, S. S., et al. (2018). Microfluidic platform for single cell analysis under dynamic spatial and temporal stimulation. *Biosens. Bioelectron.* 104, 58–64. doi:10.1016/j.bios.2017.12.038
- Spiller, D. G., Wood, C. D., Rand, D. A., and White, M. R. H. (2010). Measurement of single-cell dynamics. *Nature* 465, 736–745. doi:10.1038/nature09232
- Stutts, L., and Esser-Kahn, A. P. (2015). A light-controlled TLR4 agonist and selectable activation of cell subpopulations. *Chembiochem* 16, 1744–1748. doi:10.1002/cbic.201500164
- Sumit, M., Takayama, S., and Linderman, J. J. (2017). New insights into mammalian signaling pathways using microfluidic pulsatile inputs and mathematical modeling. *Integr. Biol.-Uk* 9, 6–21. doi:10.1039/c6ib00178e
- Sun, Y., Liu, W. Z., Liu, T., Feng, X., Yang, N., and Zhou, H. F. (2015). Signaling pathway of MAPK/ERK in cell proliferation, differentiation, migration, senescence and apoptosis. *J. Recept Sig Transd* 35, 600–604. doi:10.3109/10799893.2015.1030412
- Tay, S., Hughey, J. J., Lee, T. K., Lipniacki, T., Quake, S. R., and Covert, M. W. (2010). Single-cell NF-kappa B dynamics reveal digital activation and analogue information processing. *Nature* 466, 267–271. doi:10.1038/nature09145
- Thorsen, T., Maerkl, S. J., and Quake, S. R. (2002). Microfluidic large-scale integration. *Science* 298, 580–584. doi:10.1126/science.1076996
- Tischer, D., and Weiner, O. D. (2014). Illuminating cell signalling with optogenetic tools. *Nat. Rev. Mol. Cell Bio* 15, 551–558. doi:10.1038/nrm3837
- Toettcher, J. E., Weiner, O. D., and Lim, W. A. (2013). Using optogenetics to interrogate the dynamic control of signal transmission by the ras/erk module. *Cell* 155, 1422–1434. doi:10.1016/j.cell.2013.11.004
- Toparlak, O. D., Zasso, J., Bridi, S., Dalla Serra, M., Macchi, P., Conti, L., et al. (2020). Artificial cells drive neural differentiation. *Sci. Adv.* 6, eabb4920. doi:10.1126/sciadv.abb4920
- Tsai, Y. H., Doura, T., and Kiyonaka, S. (2021). Tethering-based chemogenetic approaches for the modulation of protein function in live cells. *Chem. Soc. Rev.* 50, 7909–7923. doi:10.1039/d1cs00059d
- Villarino, A. V., Kanno, Y., and O'Shea, J. J. (2017). Mechanisms and consequences of Jak-STAT signaling in the immune system. *Nat. Immunol.* 18, 374–384. doi:10.1038/ni.3691
- Watson, C., Liu, C., Ansari, A., Miranda, H. C., Somoza, R. A., and Senyo, S. E. (2022). Multiplexed microfluidic chip for cell co-culture. *Analyst* 147, 5409–5418. doi:10.1039/d2an01344d
- Watson, C., and Senyo, S. (2019). All-in-one automated microfluidics control system. *Hardwarex* 5, e00063. doi:10.1016/j.ohx.2019.e00063
- Wegener, M., Hansen, M. J., Driessen, A. J. M., Szymanski, W., and Feringa, B. (2017). Photocontrol of antibacterial activity: shifting from UV to red light activation. *J. Am. Chem. Soc.* 139, 17979–17986. doi:10.1021/jacs.7b09281
- White, J. A., and Streets, A. M. (2018). Controller for microfluidic large-scale integration. *Hardwarex* 3, 135–145. doi:10.1016/j.ohx.2017.10.002
- Xu, C., Hu, S., and Chen, X. Y. (2016). Artificial cells: from basic science to applications. *Mater Today* 19, 516–532. doi:10.1016/j.mattod.2016.02.020
- Yang, H. W., Sinha, N., Rand, U., Hauser, H., Koster, M., de Greef, T. F. A., et al. (2022). A universal microfluidic approach for integrated analysis of temporal homocellular and heterocellular signaling and migration dynamics. *Biosens. Bioelectron.* 211, 114353. doi:10.1016/j.bios.2022.114353
- Yang, S., Pieters, P. A., Joesaar, A., Bogels, B. W. A., Brouwers, R., Myrgorodska, I., et al. (2020). Light-activated signaling in DNA-encoded sender-receiver architectures. *ACS Nano* 14, 15992–16002. doi:10.1021/acsnano.0c07537
- Yuan, Y., Jiang, Y. C., Sun, C. K., and Chen, Q. M. (2016). Role of the tumor microenvironment in tumor progression and the clinical applications (Review). *Oncol. Rep.* 35, 2499–2515. doi:10.3892/or.2016.4660
- Zhang, K., and Cu, B. X. (2015). Optogenetic control of intracellular signaling pathways. *Trends Biotechnol.* 33, 92–100. doi:10.1016/j.tibtech.2014.11.007
- Zhang, Q. H., Gupta, S., Schipper, D. L., Kowalczyk, G. J., Mancini, A. E., Faeder, J. R., et al. (2017). NF-Kappa B dynamics discriminate between TNF doses in single cells. *Cell Syst.* 5, 638–645. doi:10.1016/j.cels.2017.10.011
- Zhu, J. J., and Thompson, C. B. (2019). Metabolic regulation of cell growth and proliferation. *Nat. Rev. Mol. Cell Bio* 20, 436–450. doi:10.1038/s41580-019-0123-5



## OPEN ACCESS

## EDITED BY

Marco P. Monopoli,  
Royal College of Surgeons in Ireland,  
Ireland

## REVIEWED BY

Fransisca Leonard,  
Houston Methodist Research Institute,  
United States  
Nick Giannoukakis,  
Allegheny Health Network, United States

## \*CORRESPONDENCE

Tianmeng Sun,  
✉ tsun41@jlu.edu.cn  
Yuning Zhang,  
✉ zhangyuning@jlu.edu.cn

RECEIVED 18 June 2023

ACCEPTED 25 September 2023

PUBLISHED 09 October 2023

## CITATION

Lin G, Wang J, Yang Y-G, Zhang Y and  
Sun T (2023), Advances in dendritic cell  
targeting nano-delivery systems for  
induction of immune tolerance.  
*Front. Bioeng. Biotechnol.* 11:1242126.  
doi: 10.3389/fbioe.2023.1242126

## COPYRIGHT

© 2023 Lin, Wang, Yang, Zhang and Sun.  
This is an open-access article distributed  
under the terms of the [Creative  
Commons Attribution License \(CC BY\)](#).  
The use, distribution or reproduction in  
other forums is permitted, provided the  
original author(s) and the copyright  
owner(s) are credited and that the original  
publication in this journal is cited, in  
accordance with accepted academic  
practice. No use, distribution or  
reproduction is permitted which does not  
comply with these terms.

# Advances in dendritic cell targeting nano-delivery systems for induction of immune tolerance

Guojiao Lin<sup>1,2</sup>, Jialiang Wang<sup>1,2</sup>, Yong-Guang Yang<sup>1,2,3</sup>,  
Yuning Zhang<sup>1,2\*</sup> and Tianmeng Sun<sup>1,2,3,4\*</sup>

<sup>1</sup>Key Laboratory of Organ Regeneration and Transplantation of Ministry of Education, Institute of Immunology, The First Hospital, Jilin University, Changchun, China, <sup>2</sup>National-local Joint Engineering Laboratory of Animal Models for Human Diseases, Changchun, China, <sup>3</sup>International Center of Future Science, Jilin University, Changchun, China, <sup>4</sup>State Key Laboratory of Supramolecular Structure and Materials, Jilin University, Changchun, China

Dendritic cells (DCs) are the major specialized antigen-presenting cells (APCs), play a key role in initiating the body's immune response, maintain the balance of immunity. DCs can also induce immune tolerance by rendering effector T cells absent and anergy, and promoting the expansion of regulatory T cells. Induction of tolerogenic DCs has been proved to be a promising strategy for the treatment of autoimmune diseases, organ transplantation, and allergic diseases by various laboratory researches and clinical trials. The development of nano-delivery systems has led to advances *in situ* modulation of the tolerance phenotype of DCs. By changing the material composition, particle size, zeta-potential, and surface modification of nanoparticles, nanoparticles can be used for the therapeutic payloads targeted delivery to DCs, endowing them with great potential in the induction of immune tolerance. This paper reviews how nano-delivery systems can be modulated for targeted delivery to DCs and induce immune tolerance and reviews their potential in the treatment of autoimmune diseases, organ transplantation, and allergic diseases.

## KEYWORDS

dendritic cell, nanoparticles, immune tolerance, autoimmune diseases, transplantation, allergy

## 1 Introduction

DCs were discovered in the early 1970s, since then their biological properties have been extensively studied. To date, they are known as the “gatekeepers of the immune system” due to their ability to maintain immune homeostasis by activating adaptive immunity or promoting tolerance (Steinman and Cohn, 1973; Steinman and Cohn, 1974; Puhr et al., 2015). DCs serve as immune sentinels, specifically responsible for sensing danger signals as well as capturing, processing, and presenting antigenic substances (Banchereau and Steinman, 1998). DCs can exert regulatory effects on T cells, controlling T cell activation, differentiation and expansion. Among the various phenotypes of DCs, tolerogenic DCs (tol-DCs) can induce T-cell tolerance and inhibit abnormal activation of the immune system through a variety of mechanisms (Tang et al., 2022). Animal models and preclinical studies have revealed that inducing immune tolerance using tol-DCs demonstrated therapeutic effects in autoimmune diseases, allergic diseases, and organ transplant-related diseases (Ness et al., 2021).

Tol-DCs can be induced by alterations in the physiological environment, and the development of nanodrug delivery systems provides an efficient and simple solution for the *in situ* induction of tol-DCs *in vivo* (Carey et al., 2023; Rui et al., 2023). Nano-delivery systems, which can deliver therapeutic agents to specific targets and reduce the side effects of drugs, have led to significant advances in the development of new imaging agents, disease therapies and biological tools such as genome editors and nanomachines (Poon et al., 2020). Nanodrug carriers can not only deliver immunosuppressive drugs, but also self-antigen-related peptides and nucleic acids, or in combinations. The engineered nanoparticles enable the targeted delivery of therapeutic cargoes to DCs and induces the generation of DCs with a tolerogenic phenotype to regulate antigen-specific immune responses *in vivo*.

Here, we review how the optimization of the physicochemical properties of DC targeting nano-delivery systems can improve the ability of nanoparticles to induce the tol-DC phenotype, as well as their therapeutic potential towards autoimmune diseases, allergy, and organ transplantation.

## 2 The role of immune tolerance

The most important function of the immune system is to recognize and eliminate invading antigens and malignant cells while maintaining immune tolerance to its own components. However, unrestricted immune system activation can lead to clinical disorders, including autoimmune diseases, solid organ transplantation (SOT), hematopoietic stem cell transplantation (HSCT) and allergic diseases (Choi et al., 2020; Zhuang et al., 2021; Chang et al., 2022). By inducing immune tolerance, that is, by inducing specific tolerances to disease-inducing immune cells, the body can avoid inflammation while retaining its normal immune response to foreign substances (Ezekian et al., 2018).

Immune tolerance arises from the control of self-reactive T cells in the thymus and periphery, known as central immune tolerance and peripheral immune tolerance, respectively (ElTanbouly and Noelle, 2021). During the positive selection of T cell development in thymus, T cells that recognizing own major histocompatibility complex (MHC) molecules are remained; while T cells with a strong affinity for self-peptides are then removed via negative selection. However, some self-reactive T cells may escape the negative selection, and constitute the potential risk of autoimmune reaction. Peripheral immune tolerance is required to limit the response of these self-reactive T cells and avoid abnormal activation of the immune system (Josefowicz et al., 2012; Klein et al., 2014). Control of self-reactive T cells through chronic antigen exposure that inactivates T cell function (T cell incompetence and T cell deficiency and differentiation of regulatory T cells (Tregs)) is required to achieve peripheral T cell tolerance (Singer et al., 2014).

DCs integrate various immune signals of the body during the induction of immune tolerance. They restore immune homeostasis by inducing apoptosis of inflammatory T cells, modulating pro- and anti-inflammatory responses, and inducing immunomodulatory function by expanding Tregs (Li et al., 2022b). Immature and tolerant DCs are able to suppress T cell activation and induce peripheral tolerance to self-antigens (Morante-Palacios et al., 2021; Yin et al., 2021).

For the treatment of diseases arising from abnormal activation, it is essential that prompt interventions are taken to maintain the dynamic balance and function of immune system. Although immunosuppressive drugs have been widely used in the treatment of autoimmune diseases and transplantation, however these drugs generally require lifelong administration and cannot cure the disease. Moreover, long term administration of immunosuppressive drugs can cause neurological, blood, renal, gastrointestinal, and immune system toxicity. Such side effects can also weaken the body's normal immune response and increase the risk of cancer and infection (Feng et al., 2020; Montano et al., 2021). Therefore, researchers are focusing on therapies that induce immune tolerance by targeting immune cells (Ghobadinezhad et al., 2022). Those immunotherapies can establish antigen-specific immune tolerance while the rest of immune functions remains uninfluenced, alleviate symptoms, even completely cure the disease. DC based therapies are ideal immunotherapy strategies, which have shown promising results in clinical trials for diseases such as breast cancer, type 1 diabetes, multiple sclerosis, and post-transplant solid organ rejection (Phillips et al., 2019; van Pul et al., 2019; Zubizarreta et al., 2019; Que et al., 2020).

## 3 Induction of immune tolerance by DCs for disease treatment

DCs are commonly defined as specialized APCs that express major histocompatibility complex molecules and high level co-stimulatory molecules (Kushwah and Hu, 2011; Gardner et al., 2020). The main function of DCs is to capture and process exogenous antigens in peripheral tissues for presentation to T cells after migration to draining lymph nodes. DCs are able to produce great tolerance in response to environmental signals. DCs recognize a large number of pathogen-associated molecular patterns (PAMPs) and damage-associated molecular patterns (DAMPs) through pattern recognition receptors (PRRs) and toll-like receptors (TLRs) (Tiberio et al., 2018). For example, after recognizing relevant molecular patterns on bacterial and viral pathogens, DCs initiate immune response by inducing T cells and natural killer cells to clear infections (Stergioti et al., 2022).

DCs can change phenotypically and functionally in response to environmental stimuli. Based on their phenotype and function, DCs are divided into four main types (Liu, 2005; Guernonprez et al., 2019): conventional DCs (cDCs), including cDCs1 and cDCs2; plasmacytoid DCs (pDCs); monocyte-derived DCs (mo-DCs); and Langerhans cells (LCs). Different subpopulations of DCs can respond differently to environmental triggers and differentiate extensively into immunologically active helper cells, thus providing a critical link between innate and acquired immune responses (Ness et al., 2021; Li et al., 2022b). For example, cDCs1 effectively silence CD8<sup>+</sup> T cells, cDCs2 promote CD4<sup>+</sup> T cell proliferation, mo-DCs produce anti-tumor immunity, and LCs are widely present in skin tissues and can secrete a large number of cytokines to support the development of T cells (Devi and Anandasabapathy, 2017; Zhang et al., 2021b; Zhang et al., 2022).

DCs can also be divided into stimulated DCs (sDCs) and tol-DCs according to the characteristics of the cellular immune



tolerance (Waisman et al., 2017; Passeri et al., 2021). Although there are no specific markers for tol-DCs, tol-DCs usually consist of a population of different types of immature or semi-mature DCs. These DCs are characterized by low expression of co-stimulatory molecules (CD80, CD86, and CD40), upregulation of inhibitory and regulatory receptors, and secreting high levels of anti-inflammatory cytokines and attenuate pro-inflammatory cytokine secretion (Suuring and Moreau, 2021). Presenting an antigen without activating the inflammatory effector T cell response is essential for tol-DCs to induce and maintain self-tolerance.

Exposure of DCs to drugs, such as vitamin A, vitamin D<sub>3</sub>, rapamycin, dexamethasone, growth factors, and cytokines (such as tumor necrosis factor and IL-10), can induce tol-DC production (Boks et al., 2012). Induction of tol-DCs has shown significant promise in alleviating autoimmune disease symptoms, improving allograft survival, and suppressing graft-versus-host disease after stem cell transplantation (Devi and Anandasabapathy, 2017; Que et al., 2020). Purification of patient-derived precursor DCs to tol-DCs for re-infusion back to patients *in vitro* has been shown to be a promising approach in clinical trials for the treatment of autoimmune diseases (Benham et al., 2015; Nikolic et al., 2020). However, the tremendous efforts and extremely high costs of isolation, purification and *in vitro* expansion of tol-DCs, and histocompatibility issues of DCs have limited the broad application of tol-DC based therapies (Chuang et al., 2022). Researchers, therefore, have focused on the *in situ* induction of tol-DCs *in vivo*.

## 4 Optimization of DC-targeted nano-delivery systems

The biomaterial composition and physicochemical properties of DC targeting nano-delivery systems such as shape, surface potential, surface modification, and loaded bioactive molecules, have a great impact on the phenotype and function of the DCs (Tkach et al., 2013; Park et al., 2015; Zhu et al., 2019; Punz et al., 2022; Uzhviyuk et al., 2022).

### 4.1 Material composition

The four major classes of materials suitable for biomedical applications are polymers, lipids, inorganic materials and proteins (Chuang et al., 2022). The constituent materials of nanoparticle carriers should be selected to ensure that they do not have toxic effects on the organism and that they have good biocompatibility and bioavailability (Horvath and Basler, 2023). For example, materials that produce strong immunostimulatory effects, such as saponin-based adjuvants and aluminum salt adjuvants, should not be selected in the face of a range of diseases in which immune system activation is predominant (Huang et al., 2020; Huis In't Veld et al., 2022).

Polymeric nanoparticles are one of the most commonly used nanoparticle carriers for delivering therapeutic goods. Synthetic polymeric materials, such as poly (lactic acid-glycolic ester) (PLGA), poly (glutamic acid) (PGA), and nanoparticles synthesized from natural materials (such as chitosan, gelatin, and

collagen), are widely studied and used in the biomedical field. For example, PLGA has been approved by the U.S. Food and Drug Administration (FDA) and the European Medicines Agency (EMA) for use in humans (Operti et al., 2021). The degradation products of PLGA are lactic and glycolic acids, and the accompanying release of degradation products has a suppressive effect on the local immune microenvironment; it also downregulates MHC-II molecules, creating immune tolerance in humans (Allen et al., 2018; Chuang et al., 2022).

Liposomes are another class of nano-delivery systems commonly used to target DCs. They are composed of phospholipids and cholesterol, also found in cell membranes, and are highly biocompatible *in vivo*. The immunological effects of DCs can be activated or inhibited by altering the surface charge, composition, hardness, and size of the liposomes during nanoparticle fabrication (Bozzuto and Molinari, 2015). For example, by adding cholesterol to lipid bilayers can enhance the stability and improve hepatic targeting of adducted liposomes (Akinc et al., 2010). Kranz et al. introduce an RNA encapsulated lipid nanoparticle (RNA-LPX), which can precisely target DCs *in vivo*. The surface charge of the nanoparticles can be modified by adjusting the amount of cationic lipids in RNA-LPX. Researchers have demonstrated that as the cationic lipid content decreased, it was shown that the site of enrichment site of RNA-LPX with neutral or slightly negatively charge shifted from the lungs to the spleen and selectively expressed in the spleen (Kranz et al., 2016).

In addition to serving as a drug delivery vehicle, nanomaterials are also capable of inducing tolerogenic DCs by altering the DC phenotype. For example, agarose in the agarose gel treatment of DCs, which inhibits DC maturation and polarize T cell responses toward Th1 and Th2 and induce Treg expansion (Figure 1A) (Park et al., 2015). Cellulose nanofibers (CNFs) are able to hinder the maturation and differentiation of mo-DCs and induce human tolerant DCs; they are also able to weaken Th1 and Th17-mediated responses and induce Tregs production (Tomić et al., 2016). Cerium nanoparticles can prevent oxidative stress in DCs by reducing the level of reactive oxygen species (ROS) in DCs and reducing the level of CD86 and MHC-II expression on DCs (Figures 1B,C) (Nguyen et al., 2022). Other materials, such as gold and pSi, have little immunogenicity, do not stimulate DCs, which would otherwise lead to their activation, and are good choices for the loading of various immunosuppressive drugs (Arosio et al., 2014; Stead et al., 2018b).

By making an appropriate choice of materials, researchers can better control the safety profile of nano-delivery systems. However, this is only a single parameter that must be considered in nanoparticle design; nanoparticle size and shape also need to be taken into account.

### 4.2 Size and shape

Size of nanoparticles has a great effect on the cellular uptake of nanoparticles *in vivo*. Nanoparticle size for drug delivery in nano-delivery systems is usually controlled to be in the range of 10–1,000 nm (Sun et al., 2014). Nanoparticles can be effectively taken up by DCs through lectin-mediated endocytosis when their size is less than 100 nm. Particles larger than 200 nm are internalized

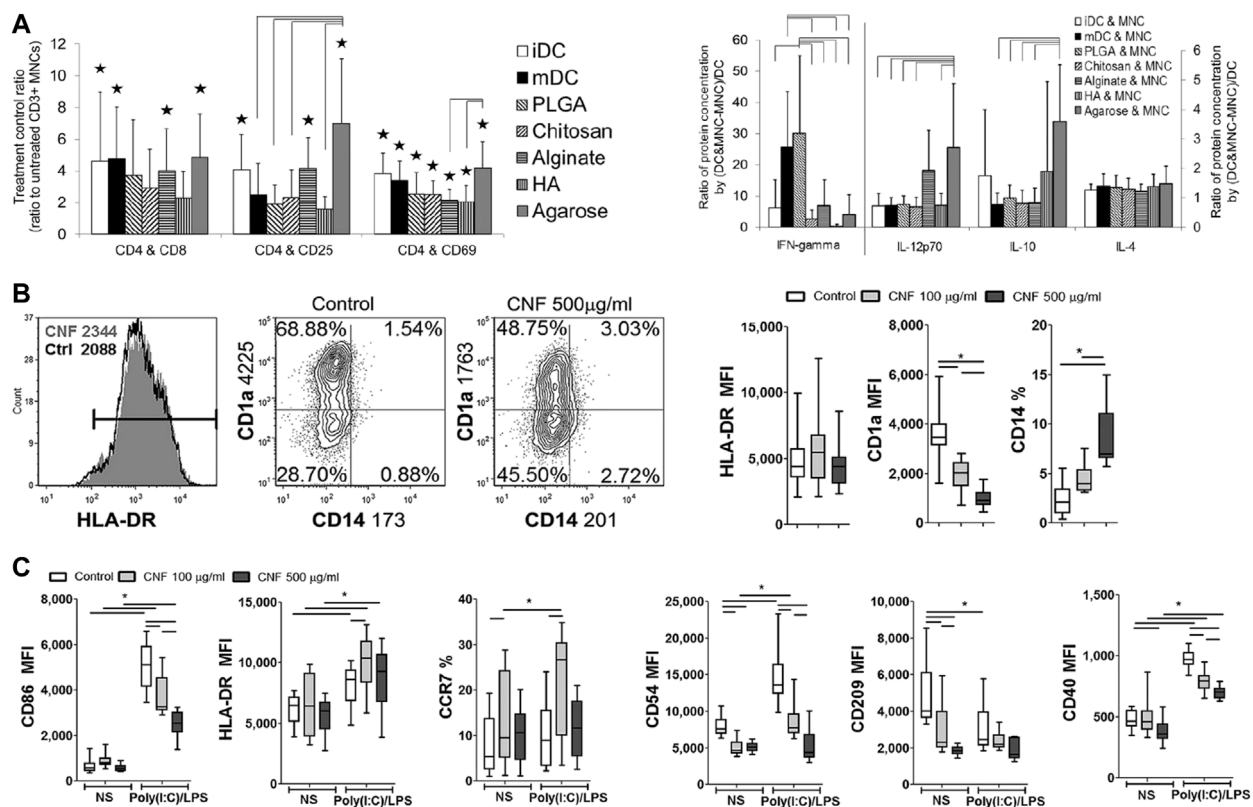


FIGURE 1

The interaction of DCs with different nanomaterials. (A) Multifunctional effects of DCs treated with different biomaterial films on autologous T cell-mediated phenotypes and polarization (Park et al., 2015). (B, C) Effects of CNFs on differentiation (B) and Poly(I:C)/LPS-induced maturation (C) of m-DCs (Nguyen et al., 2022). Reprinted from ref (Park et al., 2015) with the permission from Wiley Periodicals, Inc., copyright 2014; Reprinted from ref (Nguyen et al., 2022) with the permission from Nature Communications, copyright 2022.

by DCs through phagocytosis or by macrophagocytosis (Getts et al., 2015).

Size has an impact on the *in vivo* distribution of nanoparticles. For example, Parker et al. showed that DCs readily endocytose small graphene oxide (SGO) flakes, while the plasma membrane of a macrophage readily absorbs large graphene oxide (LGO) flakes (Parker et al., 2022). Many studies have shown that nanoparticles measuring less than 200 nm can be processed by DCs in lymph nodes after injection, inducing early T-cell action (Manolova et al., 2008; Blank et al., 2013). For example, Galea et al. synthesized liposomes containing calcineurin and PD-L1 in the size range of 105–135 nm. The liposomes could target lymph nodes from the site of administration via passive drainage, causing lymph node DCs to exhibit increased PD-L1 expression (Figures 2A,B) (Galea et al., 2019). In contrast, nanoparticles larger than 200 nm will stay at the injection site or enter the spleen, liver and lymph nodes with migrating DCs after being internalized by DCs (Robinson and Thomas, 2021).

Particle size is not the only determining factor for the uptake and distribution of nanoparticles by cells *in vivo*. Nanoparticle shape is also an important character and can affect the recognize of nanoparticles by DCs, which has a great impact on the phenotype and function of DCs (Niikura et al., 2013). Rod NPs exhibits a lower internalization rate of APCs, whereas spherical NPs trigger increased phagocytosis and are more likely to accumulate in

the liver, lung, and spleen (Champion and Mitragotri, 2006; Mathaes et al., 2014). By varying the shape of phosphatidylserine (PS) on nanoparticles, Roberts et al. found that rod-shaped PS-PLGA nanoparticles were more likely to induce immune tolerance than spherical PS-PLGA nanoparticles for the same particle size (Figures 2C,D) (Roberts et al., 2015).

### 4.3 Zeta-potential

Adjusting the surface charge of NPs is another key factor affecting the internalization ability, distribution, and immunogenicity of DCs. For example, highly charged nanoparticles will be more stable due to electrostatic repulsion, regardless of whether the surface charge is positive or negative in nature (Ma et al., 2011; Zhang et al., 2021a). Positively charged NPs are more strongly internalized by phagocytes rapidly through interaction with negatively charged cell membranes or through the lectin-mediated endocytosis (Li et al., 2022a). For example, modification of PLGA particles with a negative surface potential with positively charged polymers, such as polyethylene glycol (PEI) or chitosan (CS) (Wang et al., 2021), shifts the zeta potential to positive values and promotes the cellular phagocytosis of nanoparticles by interacting with negatively charged cell membranes (Zupancic et al., 2017). In addition, nanoparticles

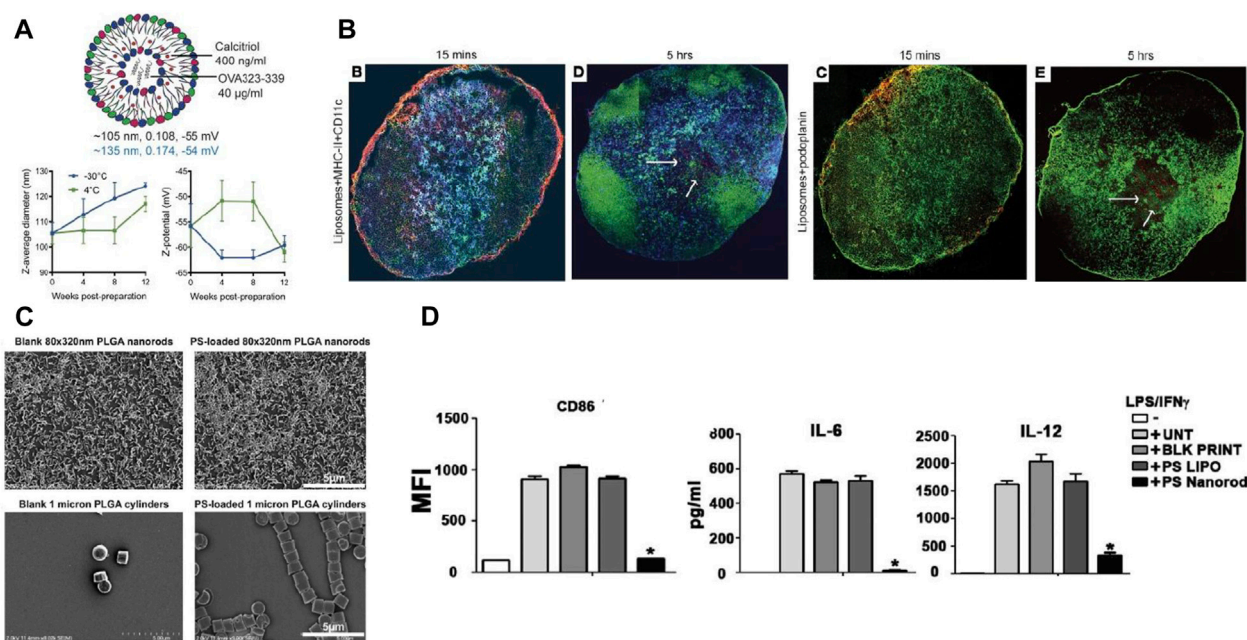


FIGURE 2

Interaction of DCs with nanoparticles of different particle size and morphology. (A) Size, polydispersity (PDI), and surface charge (black: thin film hydration method, blue: microfluidic method) of liposomes encapsulating calcitriol and OVA<sub>323-339</sub>. (B) Calcitriol-antigen liposomes are distributed from the injection site to the draining lymph node (dLN) after administration, subsequently into the dLNs of myeloid DCs and inflammatory mo-DCs (Galea et al., 2019). (C) Changing the geometry of PLGA nanoparticles by geometric manipulation of PS. (D) PS nanorods downregulate inflammatory responses in dendritic cells (Roberts et al., 2015). Reprinted from ref (Galea et al., 2019) with the permission from American Society for Clinical Investigation, copyright 2019; Reprinted from ref (Roberts et al., 2015) with the permission from Elsevier Ltd, copyright 2015.

with cationic surface charge can bind anionic mRNA by electrostatic interaction and improve the transfection efficiency of mRNA to DCs (Yasar et al., 2018).

On the other side, cationic nanoparticles also have disadvantages. It has been shown that cationic liposomes generate highly electrostatic interactions with negatively charged tissues, causing nanoparticles more likely to reside at the site of administration, hindering the transport process of the nanoparticles *in vivo* (Tenchov et al., 2021; Thi et al., 2021). Moreover, cationic nanoparticles exhibit more severe cytotoxic effects compared to anionic nanoparticles. They can disrupt cell membranes, cause hemolysis and platelet deposition, and have a detrimental effect in therapeutic strategies targeting APCs to induce immune tolerance (Patra et al., 2018; Nagy et al., 2021). Studies have shown that cationic liposomes preferentially interact with negatively charged cell membranes of APCs, resulting in the activation of DCs and pro-inflammatory effects, which has negative effects in the treatment of autoimmune diseases and transplant rejection (Dangkoub et al., 2021; Nagy et al., 2021).

Negatively charged particles, although less capable of internalization, are more capable of inducing antigen-specific immune tolerance and ameliorating inflammation (Lau et al., 2022). Certain anionic preparations containing PS or 1,2-distearoylglycerol-3-phosphate glycerol (DSPG) are tolerated in mice after *in vivo* injection of bone marrow-derived DCs (Shi et al., 2007; Wu and Nakanishi, 2011). The results of Nagy et al. showed that, compared with the cationic liposomes DPTAP and DOTAP, neutral or negatively charged liposomes were efficiently

absorbed by human mo-DCs and skin DCs without affecting the immunogenicity of the mo-DCs and skin DCs (Nagy et al., 2022).

## 4.4 Surface functionalization

Nanoparticles as drug delivery vehicles are readily recognized by conditioners when they are injected into the circulation. They are then engulfed by cells in the mononuclear phagocyte system and are rapidly removed from the circulation (Cao et al., 2020). However, in order to deliver sufficient quantity of systemic therapeutic agents to target tissues, these nanoparticles must remain stability and maintain long circulating time in the bloodstream. Functionalized alterations to nanoparticles can help attain this (Punz et al., 2022).

PEGylation of nanoparticles reduces nanoparticle adsorption and aggregation by serum proteins, thus hindering the clearance of nanoparticles by the mononuclear phagocyte system (Van Haute et al., 2018; Toro-Mendoza et al., 2023). PEGylation can improve the stability of liposomes, which has an effect on the cycling time and cell interaction of liposomes (Hald Albertsen et al., 2022). For example, liposome surface modification with PEG chains in a brush conformation improves the *in vivo* stealthy, prolong the circulation time (Moghimi and Szebeni, 2003; Li et al., 2021a).

PEGylation can also improve the targeting of nano-delivery systems. For example, in an LPS-stimulated mouse model of chronic inflammation, PEGylation increases the distribution and retention of nanoparticles at sites of chronic inflammation (O'Mary et al., 2017). Maleimide can react specifically and spontaneously with

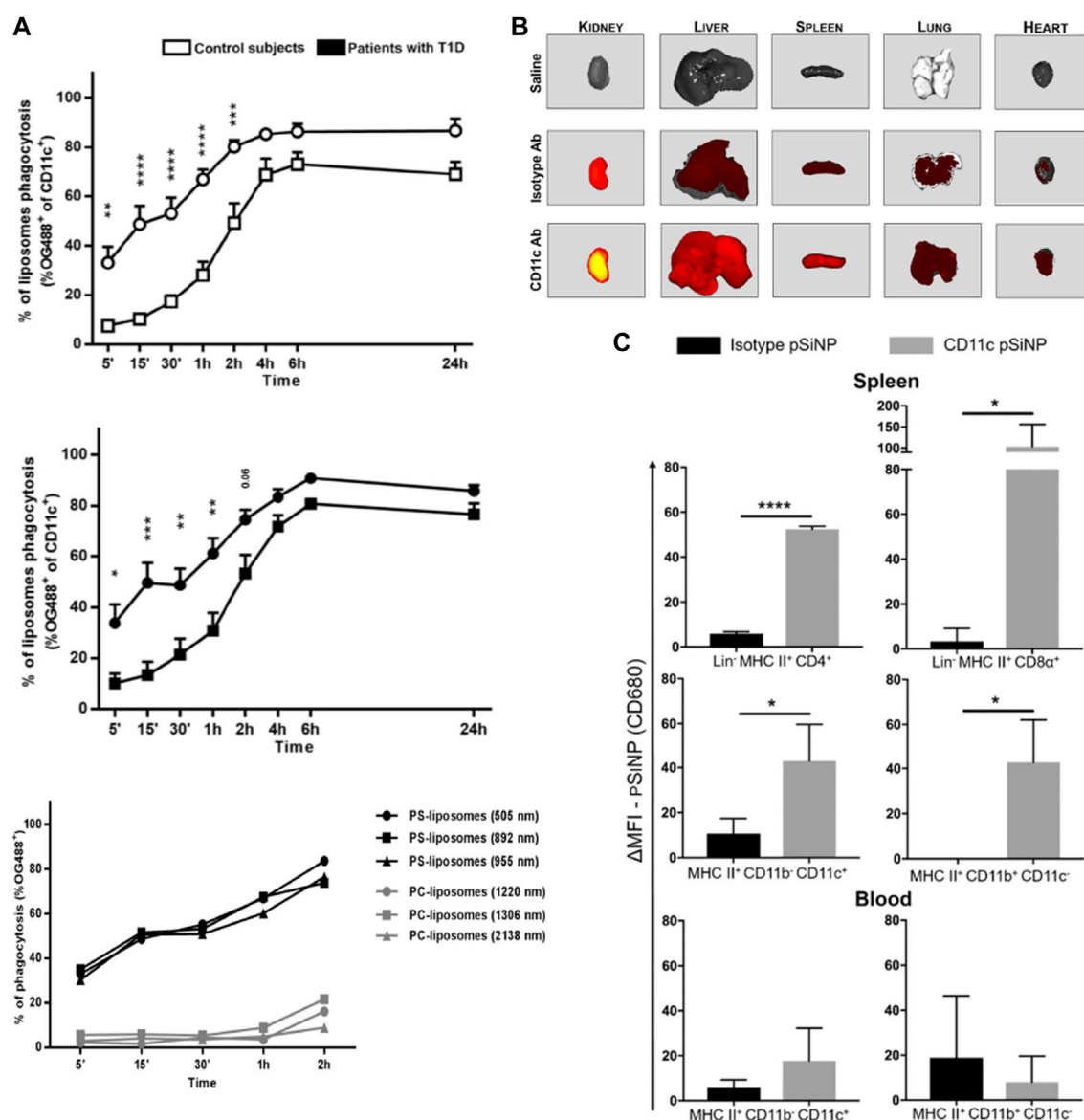


FIGURE 3

Surface modification of nanoparticles affects the interactions between nanoparticles and DCs. (A) The PS component in PS-liposomes is a key factor in accelerating the phagocytosis of liposomes by DCs (Rodriguez-Fernandez et al., 2018). (B) Modification of pSiNP with CD11c antibody enhanced pSiNP accumulation in mouse liver, lung, heart, spleen and kidney. (C) Modification of pSiNP with CD11c antibody increases both CD4<sup>+</sup> and CD8α<sup>+</sup> DC phagocytosis of pSiNP in spleen (Stead et al., 2018a). Reprinted from ref (Rodriguez-Fernandez et al., 2018) with the permission from Frontiers, copyright 2018; Reprinted from ref (Stead et al., 2018a) with the permission from American Chemical Society, copyright 2018.

sulfhydryl groups on cell membranes under physiological pH conditions. This spontaneous reaction can prolong the circulation time of maleimide-functionalized nanoparticles in bloodstream and enhance the internalization of immature DCs (Lee et al., 2020). PLGA nanoparticles usually exhibit negatively charged, but by modifying positively charged materials (e.g., polyethylene glycol (PEG) and chitosan (CS)) on the surface, PLGA nanoparticles can be endowed with positive charge, enhance the phagocytosis of the nanoparticles by immune cells (Horvath and Basler, 2023). Reducing the immunogenicity of nanoparticles can be achieved by covering the nanoparticle surface with a naturally derived cell membrane (Fang et al., 2023; Sun et al., 2023).

Nanoparticle surface functionalization can also reduce the hematotoxicity and cytotoxicity of nanoparticles. For example, dendritic polymers can cause erythrocyte hemolysis, and their modification by PEG can improve the erythrocyte hemolysis response to reduce blood clotting (Santos et al., 2018). Yu et al. introduced a DC targeting nanoparticle modified with peptide antigen OVA24 and adjuvant Pam3CSK4 on the surface, which increased the negative charge on the surface, and significantly reduced the cellular toxicity to DCs (Yu et al., 2022).

Nanoparticles can be used as tolerogenic adjuvants through nanoparticle surface functionalization, inhibiting the maturation and differentiation of DCs. PS is a major component on apoptotic cell membranes, decorating the nanoparticle surface



**TABLE 1 Summary of studies on the induction of immune tolerance by nanoparticles carrying therapeutic cargo and targeting DCs in animal models of disease.**

Animal model	Material	Nanoparticle size (nm)	Zeta potential (mV)	Therapeutic cargo	Route of administration	<i>In vivo</i> results	References
EAE	Mesoporous silica	NA	NA	MOG <sub>35-55</sub>	IV	Disease onset and late chronic phase disease symptom reduction	Nguyen et al. (2022)
EAE	Gold particles with PEG	60	NA	ITE and MOG <sub>35-55</sub>	IV	Significant reduction in clinical scores	Yeste et al. (2012)
EAE	PS-liposomes	861.29 ± 130.49	−36.19 ± 5.32	MOG <sub>40-55</sub>	IV	Slowing down the clinical extent of disease attacks	Pujol-Autonell et al. (2017)
EAE	Liposomes	103.4 ± 28.3	−24.9 ± 9.7	ITE and MOG <sub>35-55</sub>	IV or SC	Significant reduction in clinical scores	Kenison et al. (2020)
EAE	Liposomes	NA	NA	m1Ψ mRNA	IV	Inhibition of disease progression	Krienke et al. (2021)
EAE	PLG	351.3 ± 21.7	14.8 ± 0.89	PLP <sub>139-151</sub>	IT	Significant reduction in clinical scores	Saito et al. (2020)
EAE	PLGA	114–186	NA	PHCCC	SC	Delayed onset and reduced disease severity	Gammon et al. (2015)
EAE	PLGA	582.3 ± 32	8.75	ICAM-1-binding and MOG <sub>35-55</sub>	IV	Prevention of EAE; significant reduction in disease clinical scores	Wang et al. (2022a)
EAE	PLGA	378.4	−34.8	MOG <sub>35-55</sub> conjugated with glucosamine or MOG <sub>35-55</sub> mixed with mannose	IV	Significant reduction in clinical scores	Triantafyllakou et al. (2022)
T1D	RGD- and mannose-modified chitosan	322.5 ± 6.1	34.9 ± 0.5	Heart shock protein 65–6×P277	oral	Prevention of diabetes in NOD mice	Chen et al. (2018)
T1D	Gold particles with PEG	60	NA	B-cell antigen proinsulin and ITE	IP	Stopping the development of T1D	Yeste et al. (2016)
T1D	PEG-PLGA and cationic lipid	138	23	2.5mi peptide, Cas9 mRNA, CD40 gRNA, CD80 gRNA and CD86 gRNA	IV	Suppressed pancreatitis and inflammation and prevented the eventual development of T1D	Luo et al. (2020)
TrpHEL	PLGA and PLA-PEG	100	NA	HEL <sub>46-61</sub> and rapamycin	IV	Improving vitiligo symptoms	Zhang et al. (2021c)
FA	mPEG-PDLLA	175.5 ± 6.5	2.81	R848 and OVA <sub>33-47</sub>	oral	Prevention of allergic reactions	Hong et al. (2019)
AR	mPEG-PDLLA and NGRPEG-PDLLA	17.83 ± 0.28	−6.01 ± 0.96	Xanthatin	nasal administration	Suppression of AR recurrence	Zheng et al. (2020)
murine and NHP model	pSi	<200	NA	Rapamycin and OVA <sub>323-339</sub>	IV	DC-targeted effects in mouse and NHP models; OVA sensitized mice Treg elevation	Stead et al. (2018a)
skin allografts	PEG-PLGA	100	25	CD40 siRNA	IV	Significantly prolonged graft survival time	Wang et al. (2022b)
skin allografts	PEG-PLGA and cationic lipid	100	10	Cas9 mRNA and CD40 gRNA	IV	Relieves graft rejection and prolongs graft survival time	Zhang et al. (2019)
skin allografts	PEG-bl-PPS	39.3 ± 1.5	NA	Rapamycin or tacrolimus	intradermal injection	Extended survival time of grafts	Dane et al. (2011)

with PS can promote the recognition by scavenger receptors and internalization of DCs, while exerting inhibitory effects on the differentiation and maturation of DCs (Figure 3A) (Szondy et al., 2017; Rodriguez-Fernandez et al., 2018).

Modification of nanoparticles with antibodies against specific antigens present on DCs (e.g., CD11c and CD40 antibodies) and targeting agents against c-type lectins on the surfaces of DCs (e.g., mannose receptor and DCs-SIGN) enhance the targeting ability of nanoparticles against DCs and enhance the phagocytosis via receptor-mediated endocytosis (Hlavaty et al., 2015). Stead et al. found that functionalized modification of porous silicon nanoparticles (pSiNP) carrying rapamycin and OVA peptides with anti-CD11c antibodies enhanced pSiNP phagocytosis by DCs in peripheral blood and spleen; it also significantly increased Treg levels in OVA-sensitized mice (Figures 3B,C) (Stead et al., 2018a). He et al. coupled mannose on the surface of nanoparticles (OVA-PLGA NP) and significantly enhancing the OVA-PLGA NP phagocytosis of hMoDCs and promoted hMoDCs to exhibit a tolerogenic phenotype (Wen et al., 2021).

Control of the physical and chemical properties of nanoparticles enhances cargo delivery *in vivo* and the ability of nanoparticles to produce a coordinated enhancement of the therapeutic effect of the cargo in various immune activating or immune tolerant disease settings. Therefore, we next discuss the role of nanoparticles in targeting DC delivery in the context of specific diseases.

## 5 Nanodrug delivery systems targeting DCs to induce immune tolerance for disease treatment

Nanoparticles enhance the immunomodulatory effect of encapsulated cargoes. This provides nano-delivery systems with unique advantages in the delivery of therapeutic cargo to modulate immune cell activity. DC targeting nanoparticles which can induce immune tolerance are divided into four main categories depending on the therapeutic cargo they carry (Kishimoto and Maldonado, 2018; Horwitz et al., 2019): 1) Nanoparticles carrying peptides associated with autoantigens induce antigen-specific T cell production. 2) Nanoparticles carrying immunomodulatory drugs that induce the conversion of immature DCs to tolerant DCs. 3) Nanoparticles carrying nucleic acids or plasmids with gene editing effects that block the co-stimulatory signaling pathway between DCs and T cells. 4) Nanoparticles simultaneously deliver autoantigen-associated peptides, immunomodulatory drugs and nucleic acids. Here we briefly discuss the role of therapeutic cargo-targeted DCs after nano-delivery in the treatment of autoimmune diseases, allergic diseases, and transplant rejection diseases. The aggregated results are shown in Table 1.

### 5.1 Induction of autoantigen-based immune tolerance by DC targeting nanoparticles

Antigen-specific therapeutic strategies have been extensively studied for diseases linked to predominantly activated immune systems. In such therapies, DCs with tolerogenic phenotypes are

utilized for antigen presentation to induce antigen-specific immune tolerance for autoimmune diseases (Pozsgay et al., 2017; Ness et al., 2021). These therapies do not require reducing inflammatory signaling by modulating cellular signaling pathways or preventing cells from overproducing antibodies or migrating to disease sites, disease associated autologous lymphocyte activity can be attenuated by modulating existing cell functions and induce antigen-specific immune tolerance (Castenmiller et al., 2021; Passeri et al., 2021).

Antigen-specific therapies focus on the immune cells and autoantigens involved in the onset of disease symptoms. These therapies were initially used in the prevention and treatment of autoimmune diseases due to the presence of multiple different and recognizable antigens, and have been subsequently applied in the treatment of allergic diseases and transplant rejection. By using nanoparticles carrying peptides derived from their own antigens, the biological instability and poor pharmacokinetics of free peptides or proteins into the body can be modified. Moreover, nanoparticles are capable of improving the delivery efficiency of peptides and avoiding *in vivo* degradation of peptides (Asadirad et al., 2019; Yang et al., 2023). DC targeting nanoparticles carrying autoantigens can induce DCs with tolerance phenotypes. When the antigens are digested by DCs, the antigenic peptide fragments are expressed on the surface of the DCs and presented to T cells via the MHC-TCR pathway (Waeckerle-Men and Groettrup, 2005; Shen et al., 2006).

Apoptotic cell mimicking PS-liposomes can be recognized and phagocytosed by DCs. Pujol-Autonell et al. significantly reduced the expression of CD86, CD40, and MHC class II molecules after co-culturing DCs with PS-liposomes loaded with MOG<sub>40-55</sub>. EAE mice were administered with PSMOG-liposomes, PS-liposomes, and MOG peptide alone separately, but PS-liposomes showed no therapeutic effect. PSMOG-liposomes, however, produced a significant reduction in disease clinical scores and demonstrated better therapeutic effect than MOG peptide alone (Pujol-Autonell et al., 2017). Nanoparticle-encapsulated autoantigen peptides have been applied in the treatment of other autoimmune diseases. By replacing the nanoparticle-encapsulated autoantigens, nanoparticles can be applied to the treatment of other autoimmune diseases. For example, they replaced the MOG peptide encapsulated in PS-liposomes with insulin peptide, this PS-liposomes could promote tolerogenic features on DCs in T1D (Rodriguez-Fernandez et al., 2018).

Mannose-modified nanoparticles are also often used for the targeted delivery of autoantigens to DCs. Chen et al. used chitosan nanoparticles modified with mannose and peptide arginine to carry H6P antigen and prevent the onset of diabetes in NOD mice via oral administration and induced antigen-specific T-cell tolerance (Chen et al., 2018). He et al. used mannose-modified PLGA nanoparticles loaded with OVA (OVA-mann-PLGA NP), co-incubating them with hMoDCs, and found that the hMoDCs showed increased production of pro-inflammatory cytokines IL-10 and TNF- $\alpha$  and decreased production of anti-inflammatory cytokine IL-6. When mice were immunized with OVA-mann-PLGA NP, OVA-sensitized mice exhibited immune tolerance to OVA allergens (Wen et al., 2021).

Delivery of specific peptides using nanoparticles can block signaling pathways on DCs. The NFAT signaling pathway in DCs is responsible for inducing effective T cell activation and graft rejection. Blocking the NFAT signaling pathway on DCs

can inhibit the proliferation of antigen-specific T cells and plays a role in inducing graft tolerance (Otsuka et al., 2021; Colombo et al., 2022). Colombo et al. screened for VIVIT peptides with a high affinity for calcium-regulated neurophosphatase (CN), using them to inhibit the interaction between CN and NFAT to and block the CN/NFAT pathway. Delivery of VIVIT peptides using nanoparticles targeting DCs not only prevents graft rejection during treatment but also induces long-term skin graft tolerance after the end of treatment compared to the immunosuppressant FK-506 in a skin graft model (Colombo et al., 2022).

In the inflammatory setting of disease, although some therapeutic benefit can be achieved by delivering autoantigens, co-delivery with other tolerance agents may achieve better efficiency by ensuring DCs receive all signals while inducing optimal tolerance. For example, co-delivery of therapeutic cargoes via nanoparticles, such as immunosuppressive drugs, adjuvants, cytokines, vitamin D<sub>3</sub>, and RNA with antigens can enhance the ability of nanoparticles to induce tolerance phenotypes in DCs and achieve better therapeutic effect on those diseases (Casey et al., 2018; Hong et al., 2019; Jung et al., 2019; Liu et al., 2022).

## 5.2 Delivery of immunomodulators to induce tol-DCs for disease treatment

Immunomodulators are delivered using nano-delivery systems, which include: 1) Immunosuppressive drugs. 2) Aryl hydrocarbon receptor (AhR) ligand agonists. 3) Glutamate metabotropic receptor-4 agonists. 4) Anti-inflammatory factors (Horwitz et al., 2019; Lamendour et al., 2020). Through the effect of these immunomodulators on DCs it is possible to transform immature DCs into DCs with a tolerogenic phenotype. This therapeutic approach is a promising strategy for establishing permanent specific immune tolerance, it shows significant promise in suppressing autoimmune diseases, in prolonging the survival of allografts, and in the treatment of allergic diseases (Feng et al., 2019; Que et al., 2020). However, many immunosuppressive agents, such as methotrexate, rapamycin, and dexamethasone, have limited biological activity *in vivo*, are randomly and widely distributed in the body, and cause damage to the liver, kidneys, and gastrointestinal tract after systemic administration. The delivery of immunomodulators via nanoparticles not only reduces drug toxicity, but also improves the targeting of drug release. This increases the therapeutic effect and safety of the drug while reducing the drug dose and toxicity (Hong and Dobrovolskaia, 2019; Li et al., 2021b).

Rapamycin is a macrolide antibiotic with immunosuppressive activity and acts as an inhibitor to block the mammalian rapamycin (mTOR) pathway. Rapamycin can reduce the expression of co-stimulatory markers on DC surfaces, prevent complete T cell activation, and promote Tregs expansion (Raich-Regue et al., 2015; Herrero-Sanchez et al., 2016). Delivery of rapamycin using nanoparticles significantly reduces surface co-stimulatory molecule expression and inhibits the maturation of DCs compared to free rapamycin (Haddadi et al., 2008). Co-delivery of rapamycin with disease-associated antigens can induce antigen-specific Treg generation along with the induction of tolerogenic DCs. Kishimoto et al. used rapamycin-loaded PLGA nanoparticles

(SVP-Rapamycin) co-administered with antigen and found that they could greatly reduce the corresponding antibody levels and induce tol-DCs and durable immune tolerance effects (Kishimoto et al., 2016). This was demonstrated by the isolated DCs from animals treated with antigen and SVP-Rapamycin co-administration, which could suppress the proliferation of antigen-associated T cells, while enhance Treg differentiation. The combined delivery of rapamycin and antigen by nanoparticles has also shown therapeutic efficacy in animal disease models. For example, PLGA nanoparticles encapsulated with rapamycin and peptide antigen, which can stimulate the induction of tolerogenic DCs, promote the generation of Tregs, and induce antigen-specific tolerance in models, such as EAE (Maldonado et al., 2015). Zhang et al. found that BMDCs treated with nanoparticles containing rapamycin and NPHEL<sub>46-61</sub> (NPHEL<sub>46-61</sub>/Rapa) could inhibit CD4<sup>+</sup> T cell proliferation while inducing Treg differentiation. Treatment of vitiligo mice with NPHEL<sub>46-61</sub>/Rapa enhanced IL-10 expression and inhibited IFN- $\gamma$  and IL-6 expression in diseased mice (Zhang et al., 2021c).

Drugs with anti-inflammatory and immunosuppressive effects are also often encapsulated in nanoparticles as therapeutic cargoes for the targeting delivery towards DCs. Zheng et al. used polymeric micelles to target CD13 receptors on the surfaces of DCs; the micelles acted as vehicles to deliver Xanthium (NGR-XT-PM) (Zheng et al., 2020). Compared with XT-PM and free XT, NGR-XT-PM considerably reduced the expression of CD80, CD86, and I-A/I-E molecules on the surfaces of DCs. In a mouse model of allergic rhinitis NGR-XT-PM inhibited the recurrence of allergic rhinitis, while relieving nasal symptoms; its therapeutic effect was superior to that of free XT and the commercial product Budesonide. Kim et al. used PLGA nanoparticles to carry both dexamethasone and OVA, and NP [OVA + Dex] treatment caused immature DCs to be converted to tolerant DCs. Moreover, OVA-specific immune tolerance was induced in mice by oral or intravenous administration (Kim et al., 2019b).

The AhR is a ligand-dependent transcription factor receptor and plays an important role in the control of immune responses. Regulation of the function of antigen-presenting cells, such as DCs and macrophages, can be achieved through modulation of AhR signaling, which can impact T-cell differentiation (Gutierrez-Vazquez and Quintana, 2018). ITE is a potent AhR agonist that binds directly to the AhR. Activation of the AhR can lead to the inhibition of co-stimulatory molecule expression and cytokine secretion of DCs, induction of a tolerogenic phenotype in DCs, and inhibit the immune response (Quintana et al., 2010). Yeste et al. delivered both ITE and  $\beta$  cell antigen proinsulin to DCs in nonobese diabetic mice using nanoparticles, preventing the development of type 1 diabetes and inhibiting NF- $\kappa$ B signaling in DCs through a SOCS2-dependent mechanism. This reduced cell surface CD40 and CD86 expression and induced a tolerogenic phenotype in DCs (Yeste et al., 2016). Kenison et al. demonstrated that NLPITE + MOG treatment suppressed EAE onset symptoms and induced long-term immune tolerance in an EAE model while increased the number of MOG-specific IL-10<sup>+</sup> CD4<sup>+</sup> T cells was detected in the central nervous system of NLPITE + MOG-treated EAE mice (Kenison et al., 2020).

The inflammatory status and phenotype of tolerance of DCs can be regulated using metabolic modulators. For example, glutamine is

expressed at high levels during organismal inflammation, and pDCs and cDCs expressed high level of its receptor mGluR4. The release of glutamate from DCs during inflammation facilitates Treg production by activating mGluR4 signaling on DCs (Julio-Pieper et al., 2011). The use of agonists of mGluR4, such as Cinnabarinic acid and PHCCC, can induce Treg production, enhance immune tolerance, and suppress neuroinflammation in the treatment of autoimmune diseases (Fazio et al., 2014; Peferoen et al., 2014). The application of nanoparticles to deliver agonists of mGluR4 has not been well studied. Jewell et al. used PLGA nanocarriers and liposomes to deliver PHCCC, to investigate the effect of controlling immune cell metabolism on immune tolerance in the body and to validate it with autoimmune disease models (Gammon et al., 2015; Gammon et al., 2017). Their results demonstrated that delivery of PHCCC using nanocarriers significantly reduced the toxicity of PHCCC using soluble PHCCC as a comparison. DCs can effectively internalize PHCCC NP, and this internalization has a dose dependence. Co-incubation of PHCCC NP with LPS-stimulated DCs revealed that PHCCC NP significantly reduces CD40, CD80, and CD86 expression on activated DCs, and inhibits T cell proliferation, increases Treg expansion, and decreases IFN- $\gamma$  secretion. In EAE mice treatment experiments, PHCCC NP delayed the onset and reduced the severity of EAE compared to soluble PHCCC.

1,25-Dihydroxyvitamin D3 (aVD3) can exert immunomodulatory and anti-inflammatory effects by controlling different DNA methylation modifications in the metabolic and immune pathways of DCs to induce stable and reproducible tol-DCs (Lamendour et al., 2020; Gallo et al., 2023). Jung et al. synthesized nanoparticles that could deliver both aVD3 and OVA, and NP(OVA + aVD3)-treated DCs exhibited reduced expression of MHC II molecules, CD80, and CD86, and low secretion of pro-inflammatory cytokines IL-1 $\beta$ , IL-6, IL-12, and TNF- $\alpha$ . Tolerogenic DCs induced by NP(OVA + aVD3) can effectively induce Treg differentiation. Oral or intravenous administration of NP(OVA + aVD3) to mice can lead to OVA-specific tolerance (Jung et al., 2019).

### 5.3 Targeting DCs with gene disruption technology for disease treatment

In addition to the induction of tolerance in DCs through the delivery of disease-associated antigens and immunomodulators, and thus the induction of immune tolerance in the body, another promising approach to modulating the immune system is the direct regulation of the expression of co-stimulatory molecules on DCs through the delivery of nucleic acids.

Effective T-cell activation relies on two conditions being met: 1) Antigen-specific TCR binding with MHC molecules on APCs (Zhang and Vignali, 2016). 2) The co-stimulatory effect of the co-stimulatory receptors on T cells and their corresponding ligands on antigen-presenting cells (Bluestone et al., 2015). Simultaneous engagement of costimulatory molecules between T cells and APCs when the co-stimulatory pathway is blocked, T cells lose their effector function and become “incompetent” unable to activate efficiently, either by differentiating into Tregs to induce immune tolerance or by being instructed to undergo apoptosis as a

result of clonal clearance (Bluestone et al., 2015). In view of this, targeted manipulation of co-stimulatory pathways on DCs and T cells can alter the T cell activation status and thus induce immune tolerance. This is a feasible approach to the induction of autoimmune tolerance and transplantation tolerance, as well as to the treatment of allergic diseases (Gu et al., 2006; Suzuki et al., 2010; Zheng et al., 2010).

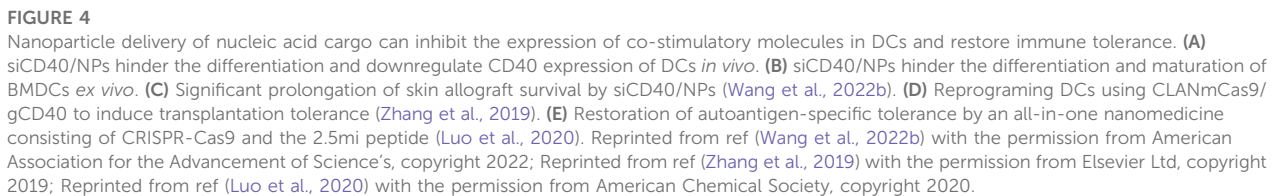
Nucleic acids used to regulate the immune system include plasmid DNA (pDNA), messenger RNA (mRNA), small interfering RNA (siRNA), and microRNA. When nucleic acids administered directly, they are readily degraded by nucleases *in vivo*, and also potentially lead to toxic reactions due to the presence of an anionic phosphate backbones and off-target effects (Janas et al., 2018; Kim et al., 2019a). The challenges inherent to the *in vivo* delivery of nucleic acids, however, can be addressed using carriers composed of lipids, polymers, and inorganic materials. This produces cellular immunity through *in vivo in situ* cell reprogramming (Zhang et al., 2021d; Bogaert et al., 2022; Lam et al., 2023). For example, specific delivery of anti-sense oligonucleotides targeting CD80, CD86, and CD40 to DCs can inhibit the expression of co-stimulatory molecules on DCs and treat autoimmune diseases by inducing Treg (Machen et al., 2004; Phillips et al., 2008; Engman et al., 2015).

Among the nucleic acid-based therapeutic approaches, RNA-based therapies have unique advantages. Unlike DNA has to be delivered into the nucleus of the target cell for proper expression (Fu et al., 2020), RNA can easily be functional in the cytoplasm and exhibits a higher therapy efficiency, therefore is preferred as the therapeutic cargo for nano-delivery. Wang et al. developed a PLGA-based siRNA nanoparticle delivery system (siCD40/NPs), using this system, they successfully delivered CD40 siRNA into hematopoietic stem cells and myeloid progenitor cells of DCs. By down-regulating the expression CD40, siCD40/NPs could inhibit the differentiation and maturation of DCs, suppress alloimmune response, prolong the skin graft survival in mouse allogeneic skin transplantation (Figures 4A–C) (Wang et al., 2022b). Wang et al. introduced a Cas9 mRNA (mCas9) and guide RNA targeting CD40 (gCD40) simultaneous encapsulating PLGA-based cationic lipid-assisted nanoparticles (CLAN). CLANmCas9/gCD40 not only effectively delivered mCas9 and gCD40 to DCs, but also significantly reduced the CD40 expression on the DCs, leading to the expansion of Tregs. CLANmCas9/gCD40 significantly inhibited the graft rejection, and prolonged the skin graft survival in a skin graft rejection model (Figure 4D) (Zhang et al., 2019). Wang et al. also developed an autoimmune associated peptide (2.5mi), CRISPR-Cas9 plasmid (pCas9), gCD40, gCD80, and gCD86 simultaneous encapsulating CLAN (CLANpCas9/gCD80,86,40/2.5mi). CLANpCas9/gCD80,86,40/2.5mi could knocked out the co-stimulatory molecules CD80, CD86 and CD40 on DCs after targeting delivery to DCs, induced the generation of tolerant phenotypes in DCs, triggered the expansion of 2.5mi peptide-specific Tregs, and effectively prevented the development of T1D in mice (Figure 4E) (Luo et al., 2020).

### 5.4 Administration routes of DC targeting nanoparticles

The distribution and immunological effects of nanoparticles *in vivo* are influenced by different drug delivery routes (Casey et al.,





Lymphocytes residing in the spleen, liver, and lymph nodes are commonly employed to induce immune tolerance. Nanoparticles loaded with immunomodulation drugs can be administered intravenously (IV), subcutaneously (SC), and intraperitoneally (Dangkoub et al., 2021). IV administration is the most commonly chosen routes of nanoparticles administration, nanoparticles enter the circulation directly after administration, where they are almost entirely bioavailable in the bloodstream (Ackun-Farmmer and Jewell, 2023). After IV administration, the nanoparticles can distribute and internalized by the APCs in the liver and spleens. However, after IV administration, nanoparticles can also accumulate in non-specific tissues and result in unwanted side effects. The nanoparticles may also be degraded by enzymes and cleared by the liver, which can lead to decreased drug utilization (Li et al., 2022a; Casey et al., 2022). Krienke et al. described a liposome-based antigen encoded mRNA delivery system (mRNA-LPX). After IV administration, mRNA-LPX was able to be internalized by lymphoid tissue resident CD11c<sup>+</sup> APCs throughout the body.

In addition to invasive administration methods, non-invasive administration methods (e.g., oral routes, intranasal routes, endotracheal routes, etc.) have the advantages of reducing the difficulty of administration, improving patient compliance, and reducing the burden on patients. Through the oral route nanoparticles can reach gut-associated lymphoid tissues and encounter DCs in these tissues to induce immune tolerance

(Chen et al., 2018; Li et al., 2023). It should also be noted that after oral administration of nanoparticles, the amount of drug entering the circulation tend to be reduced due to first pass elimination, and the high acid environment in the stomach may result in the degradation of nanoparticles (Abeer et al., 2020; Horvath and Basler, 2023). Studies have demonstrated that less than 10% of the total amount of drug administered could enter the circulation after oral administration of nanoparticles (Ren et al., 2023). Intestinal administration can also deliver nanoparticles into the spleen and achieve targeting of DCs. Yeste et al. developed NPs containing the AhR ligand ITE and MOG<sub>35-55</sub>(NP<sub>ITE+MOG</sub>). After i. p. administration, NP<sub>ITE+MOG</sub> was capable of inducing tolerogenic DCs and expansion of Tregs, reducing Th1 and Th17 cytokine production, suppressing the development of EAE, an experimental model of MS (Yeste et al., 2012). Intratracheal administration is also an effective method of administration for the induction of immune tolerance by nanoparticles. Saito et al. synthesized poly (lactide-co-glycolide) (PLG) nanoparticles carrying myelin proteolipid protein fragment (PLP<sub>139-151</sub>) (Nano-PLP), and compared the therapeutic efficacy of Nano-PLP administrated via intravenous and intratracheal administration in a mouse model of EAE. They interestingly found that compared to IV injection, intratracheal administration significantly improved the utilization of Nano-PLP (Saito et al., 2020).

## 6 Summary and prospects

With the ongoing research into the mechanisms underlying autoimmune diseases, rejection, and allergic diseases, many methods targeting the induction of tol-DCs have been developed and evaluated in preclinical trials. Most clinical trials for tol-DC induction utilize *in vitro* isolation and purification of DCs from the patient's own sources, which are prepared as tol-DC vaccines and then infused back into the patient (Passeri et al., 2021). Although many clinical trials have demonstrated that the induction of tol-DCs is a viable method for the treatment of autoimmune diseases, rejection, and allergic diseases, the difficulty and high cost of operation limits the widespread use of this technology. In addition, after *in vivo* administration of tol-DCs vaccine, exogenous semi-mature DCs may be transformed from a tolerant phenotype to activated DCs with the ability to activate T cells after inflammatory stimuli, and promoting the immune response instead. Therefore, how to maintain the immunomodulatory effects of tol-DCs in an abnormal, inflammatory environment, *in vivo*, is a key challenge.

DC targeting nano-delivery system is a promising strategy for programming *in situ* DCs *in vivo*. Although a large number of fundamental studies have demonstrated the therapeutic effects of DC-targeted nanoparticles in autoimmune diseases, transplantation, and allergic diseases, nanodrugs entered clinical trials to date were

developed for oncology therapy. Clinical researches for the development of DC-targeted nanomedicines focusing on autoimmune diseases and organ transplantation are still limited, and challenges remain for the clinical translation of nanoparticles induced tolerant *in situ* DCs *in vivo*.

Despite the great potential of nanoparticles in the induction of tol-DCs, the DC targeting nanomedicine-based therapy development still face plenty of difficulties: the difference of immune system and genetic environment between animal models and human bodies, optimal targets for the diseases, optimal administration strategies for the nanomedicine, biosafety evaluation of nanoparticles, and *in vivo* monitoring of nanomedicine induced tol-DCs. The solutions for these problems still require a lot of sustained efforts in basic and clinical research.

## Author contributions

GL: Original draft preparation, review and editing. JW: Writing and editing. Y-GY: Supervision and revision. YZ and TS: Review, editing, supervision and funding acquisition. All authors contributed to the article and approved the submitted version.

## Funding

This work was supported by grants from National Key Research and Development Program of China (2021YFA1100700), NSFC (32171379, U22A20156, 91642208, 81422026), Department of Human Resource and Social Security of Jilin Province (2022DJ02), the Bethune Medical Department of Jilin University (2022JBGS01), Interdisciplinary Innovation Project of the First Hospital of Jilin University (JDYYJCHX001), and the Fundamental Research Funds for the Central Universities, JLU.

## Conflict of interest

The authors declare that the research was conducted in the absence of any commercial or financial relationships that could be construed as a potential conflict of interest.

## Publisher's note

All claims expressed in this article are solely those of the authors and do not necessarily represent those of their affiliated organizations, or those of the publisher, the editors and the reviewers. Any product that may be evaluated in this article, or claim that may be made by its manufacturer, is not guaranteed or endorsed by the publisher.

## References

- Abeer, M. M., Rewatkar, P., Qu, Z., Talekar, M., Kleitz, F., Schmid, R., et al. (2020). Silica nanoparticles: A promising platform for enhanced oral delivery of macromolecules. *J. Control Release* 326, 544–555. doi:10.1016/j.jconrel.2020.07.021
- Akun-Farmmer, M. A., and Jewell, C. M. (2023). Delivery route considerations for designing antigen-specific biomaterial strategies to combat autoimmunity. *Adv. Nanobiomed Res.* 3 (3), 2200135. doi:10.1002/anbr.202200135

- Akinc, A., Querbes, W., De, S., Qin, J., Frank-Kamenetsky, M., Jayaprakash, K. N., et al. (2010). Targeted delivery of RNAi therapeutics with endogenous and exogenous ligand-based mechanisms. *Mol. Ther.* 18 (7), 1357–1364. doi:10.1038/mt.2010.85
- Allen, R. P., Bolandparvaz, A., Ma, J. A., Manickam, V. A., and Lewis, J. S. (2018). Latent, immunosuppressive nature of poly(lactic-co-glycolic acid) microparticles. *ACS Biomater. Sci. Eng.* 4 (3), 900–918. doi:10.1021/acsbomaterials.7b00831
- Arosio, D., Chiodo, F., Reina, J. J., Marelli, M., Penades, S., van Kooyk, Y., et al. (2014). Effective targeting of DC-SIGN by alpha-fucosylamide functionalized gold nanoparticles. *Bioconjug Chem.* 25 (12), 2244–2251. doi:10.1021/bc500467u
- Asadiri, A., Hashemi, S. M., Baghaei, K., Ghanbarian, H., Mortaz, E., Zali, M. R., et al. (2019). Phenotypic and functional evaluation of dendritic cells after exosomal delivery of miRNA-155. *Life Sci.* 219, 152–162. doi:10.1016/j.lfs.2019.01.005
- Banchereau, J., and Steinman, R. M. (1998). Dendritic cells and the control of immunity. *Nature* 392 (6673), 245–252. doi:10.1038/32588
- Benham, H., Nel, H. J., Law, S. C., Mehdi, A. M., Street, S., Ramnath, N., et al. (2015). Citrullinated peptide dendritic cell immunotherapy in HLA risk genotype-positive rheumatoid arthritis patients. *Sci. Transl. Med.* 7 (290), 290ra287. doi:10.1126/scitranslmed.aaa9301
- Blank, F., Stumbles, P. A., Seydoux, E., Holt, P. G., Fink, A., Rothen-Rutishauser, B., et al. (2013). Size-dependent uptake of particles by pulmonary antigen-presenting cell populations and trafficking to regional lymph nodes. *Am. J. Respir. Cell. Mol. Biol.* 49 (1), 67–77. doi:10.1165/rcmb.2012-0387OC
- Bluestone, J. A., Bour-Jordan, H., Cheng, M., and Anderson, M. (2015). T cells in the control of organ-specific autoimmunity. *J. Clin. Invest.* 125 (6), 2250–2260. doi:10.1172/JCI78089
- Bogaert, B., Sauvage, F., Guagliardo, R., Muntean, C., Nguyen, V. P., Pottier, E., et al. (2022). A lipid nanoparticle platform for mRNA delivery through repurposing of cationic amphiphilic drugs. *J. Control Release* 350, 256–270. doi:10.1016/j.jconrel.2022.08.009
- Boks, M. A., Kager-Groenland, J. R., Haasjes, M. S., Zwaginga, J. J., van Ham, S. M., and ten Brinke, A. (2012). IL-10-generated tolerogenic dendritic cells are optimal for functional regulatory T cell induction—a comparative study of human clinical-applicable DC. *Clin. Immunol.* 142 (3), 332–342. doi:10.1016/j.clim.2011.11.011
- Bozzuto, G., and Molinari, A. (2015). Liposomes as nanomedical devices. *Int. J. Nanomedicine* 10, 975–999. doi:10.2147/IJN.S68861
- Cao, Z. T., Gan, L. Q., Jiang, W., Wang, J. L., Zhang, H. B., Zhang, Y., et al. (2020). Protein binding affinity of polymeric nanoparticles as a direct indicator of their pharmacokinetics. *ACS Nano* 14 (3), 3563–3575. doi:10.1021/acsnano.9b10015
- Carey, S. T., Bridgeman, C., and Jewell, C. M. (2023). Biomaterial strategies for selective immune tolerance: advances and gaps. *Adv. Sci. (Weinh)* 10 (8), e2205105. doi:10.1002/advs.202205105
- Casey, L. M., Hughes, K. R., Saunders, M. N., Miller, S. D., Pearson, R. M., and Shea, L. D. (2022). Mechanistic contributions of Kupffer cells and liver sinusoidal endothelial cells in nanoparticle-induced antigen-specific immune tolerance. *Biomaterials* 283, 121457. doi:10.1016/j.biomaterials.2022.121457
- Casey, L. M., Pearson, R. M., Hughes, K. R., Liu, J. M. H., Rose, J. A., North, M. G., et al. (2018). Conjugation of transforming growth factor beta to antigen-loaded poly(lactide-co-glycolide) nanoparticles enhances efficiency of antigen-specific tolerance. *Bioconjug Chem.* 29 (3), 813–823. doi:10.1021/acs.bioconjug.7b00624
- Castenmiller, C., Keumathio-Doungtso, B. C., van Ree, R., de Jong, E. C., and van Kooyk, Y. (2021). Tolerogenic immunotherapy: targeting DC surface receptors to induce antigen-specific tolerance. *Front. Immunol.* 12, 643240. doi:10.3389/fimmu.2021.643240
- Champion, J. A., and Mitragotri, S. (2006). Role of target geometry in phagocytosis. *Proc. Natl. Acad. Sci. U. S. A.* 103 (13), 4930–4934. doi:10.1073/pnas.0600997103
- Chang, C. A., Bhagchandani, P., Poyser, J., Velasco, B. J., Zhao, W., Kwon, H. S., et al. (2022). Curative islet and hematopoietic cell transplantation in diabetic mice without toxic bone marrow conditioning. *Cell. Rep.* 41 (6), 111615. doi:10.1016/j.celrep.2022.111615
- Chen, Y., Wu, J., Wang, J., Zhang, W., Xu, B., Xu, X., et al. (2018). Targeted delivery of antigen to intestinal dendritic cells induces oral tolerance and prevents autoimmune diabetes in NOD mice. *Diabetologia* 61 (6), 1384–1396. doi:10.1007/s00125-018-4593-3
- Choi, J. Y., Eskandari, S. K., Cai, S., Sulkaj, I., Assaker, J. P., Allos, H., et al. (2020). Regulatory CD8 T cells that recognize Qa-1 expressed by CD4 T-helper cells inhibit rejection of heart allografts. *Proc. Natl. Acad. Sci. U. S. A.* 117 (11), 6042–6046. doi:10.1073/pnas.1918950117
- Chuang, S. T., Conklin, B., Stein, J. B., Pan, G., and Lee, K. B. (2022). Nanotechnology-enabled immunoeengineering approaches to advance therapeutic applications. *Nano Conver.* 9 (1), 19. doi:10.1186/s40580-022-00310-0
- Colombo, M., Marongiu, L., Mingozzi, F., Marzi, R., Cigni, C., Facchini, F. A., et al. (2022). Specific immunosuppressive role of nanodrugs targeting calcineurin in innate myeloid cells. *iScience* 25 (10), 105042. doi:10.1016/j.isci.2022.105042
- Dane, K. Y., Nembrini, C., Tomei, A. A., Eby, J. K., O'Neil, C. P., Velluto, D., et al. (2011). Nano-sized drug-loaded micelles deliver payload to lymph node immune cells and prolong allograft survival. *J. Control Release* 156 (2), 154–160. doi:10.1016/j.jconrel.2011.08.009
- Dangkoub, F., Sankian, M., Tafaghodi, M., Jaafari, M. R., and Badiee, A. (2021). The impact of nanocarriers in the induction of antigen-specific immunotolerance in autoimmune diseases. *J. Control Release* 339, 274–283. doi:10.1016/j.jconrel.2021.09.037
- Deckers, J., Hammad, H., and Hoste, E. (2018). Langerhans cells: sensing the environment in Health and disease. *Front. Immunol.* 9, 93. doi:10.3389/fimmu.2018.00093
- Devi, K. S., and Anandasabapathy, N. (2017). The origin of DCs and capacity for immunologic tolerance in central and peripheral tissues. *Semin. Immunopathol.* 39 (2), 137–152. doi:10.1007/s00281-016-0602-0
- Dul, M., Nikolic, T., Stefanidou, M., McAteer, M. A., Williams, P., Mous, J., et al. (2019). Conjugation of a peptide autoantigen to gold nanoparticles for intradermally administered antigen specific immunotherapy. *Int. J. Pharm.* 562, 303–312. doi:10.1016/j.jipharm.2019.03.041
- ElTanbouly, M. A., and Noelle, R. J. (2021). Rethinking peripheral T cell tolerance: checkpoints across a T cell's journey. *Nat. Rev. Immunol.* 21 (4), 257–267. doi:10.1038/s41577-020-00454-2
- Engman, C., Wen, Y., Meng, W. S., Bottino, R., Trucco, M., and Giannoukakis, N. (2015). Generation of antigen-specific Foxp3+ regulatory T-cells *in vivo* following administration of diabetes-reversing tolerogenic microspheres does not require provision of antigen in the formulation. *Clin. Immunol.* 160 (1), 103–123. doi:10.1016/j.clim.2015.03.004
- Ezekian, B., Schroder, P. M., Freischlag, K., Yoon, J., Kwun, J., and Knecht, S. J. (2018). Contemporary strategies and barriers to transplantation tolerance. *Transplantation* 102 (8), 1213–1222. doi:10.1097/TP.0000000000002242
- Fang, R. H., Gao, W., and Zhang, L. (2023). Targeting drugs to tumours using cell membrane-coated nanoparticles. *Nat. Rev. Clin. Oncol.* 20 (1), 33–48. doi:10.1038/s41571-022-00699-x
- Fazio, F., Zappulla, C., Notartomaso, S., Busceti, C., Bessedé, A., Scarselli, P., et al. (2014). Cinnabarinic acid, an endogenous agonist of type-4 metabotropic glutamate receptor, suppresses experimental autoimmune encephalomyelitis in mice. *Neuropharmacology* 81, 237–243. doi:10.1016/j.neuropharm.2014.02.011
- Feng, X., Liu, J., Xu, W., Li, G., and Ding, J. (2020). Tackling autoimmunity with nanomedicines. *Nanomedicine (Lond)* 15 (16), 1585–1597. doi:10.2217/nnm-2020-0102
- Feng, X., Xu, W., Li, Z., Song, W., Ding, J., and Chen, X. (2019). Immunomodulatory nanosystems. *Adv. Sci. (Weinh)* 6 (17), 1900101. doi:10.1002/advs.201900101
- Fu, Y., Fang, Y., Lin, Z., Yang, L., Zheng, L., Hu, H., et al. (2020). Inhibition of cGAS-mediated interferon response facilitates transgene expression. *iScience* 23 (4), 101026. doi:10.1016/j.isci.2020.101026
- Galea, R., Nel, H. J., Talekar, M., Liu, X., Ooi, J. D., Huynh, M., et al. (2019). PD-L1 and calcitriol-dependent liposomal antigen-specific regulation of systemic inflammatory autoimmune disease. *JCI Insight* 4 (18), e126025. doi:10.1172/jci.insight.126025
- Gallo, D., Baci, D., Kustrimovic, N., Lanzo, N., Patera, B., Tanda, M. L., et al. (2023). How does vitamin D affect immune cells crosstalk in autoimmune diseases? *Int. J. Mol. Sci.* 24 (5), 4689. doi:10.3390/ijms24054689
- Gammon, J. M., Adapa, A. R., and Jewell, C. M. (2017). Control of autoimmune inflammation using liposomes to deliver positive allosteric modulators of metabotropic glutamate receptors. *J. Biomed. Mater. Res. A* 105 (11), 2977–2985. doi:10.1002/jbma.36151
- Gammon, J. M., Tostanoski, L. H., Adapa, A. R., Chiu, Y. C., and Jewell, C. M. (2015). Controlled delivery of a metabolic modulator promotes regulatory T cells and restrains autoimmunity. *J. Control Release* 210, 169–178. doi:10.1016/j.jconrel.2015.05.277
- Gardner, A., de Mingo Pulido, A., and Ruffell, B. (2020). Dendritic cells and their role in immunotherapy. *Front. Immunol.* 11, 924. doi:10.3389/fimmu.2020.00924
- Getts, D. R., Shea, L. D., Miller, S. D., and King, N. J. (2015). Harnessing nanoparticles for immune modulation. *Trends Immunol.* 36 (7), 419–427. doi:10.1016/j.it.2015.05.007
- Ghobadinezhad, F., Ebrahimi, N., Mozaffari, F., Moradi, N., Beiranvand, S., Pournazari, M., et al. (2022). The emerging role of regulatory cell-based therapy in autoimmune disease. *Front. Immunol.* 13, 1075813. doi:10.3389/fimmu.2022.1075813
- Gu, X., Xiang, J., Yao, Y., and Chen, Z. (2006). Effects of RNA interference on CD80 and CD86 expression in bone marrow-derived murine dendritic cells. *Scand. J. Immunol.* 64 (6), 588–594. doi:10.1111/j.1365-3083.2006.01845.x
- Guermontprez, P., Gerber-Ferder, Y., Vaivode, K., Bourdely, P., and Helft, J. (2019). Origin and development of classical dendritic cells. *Int. Rev. Cell. Mol. Biol.* 349, 1–54. doi:10.1016/bs.ircmb.2019.08.002
- Gutierrez-Vazquez, C., and Quintana, F. J. (2018). Regulation of the immune response by the aryl hydrocarbon receptor. *Immunity* 48 (1), 19–33. doi:10.1016/j.immuni.2017.12.012
- Haddadi, A., Elamanchili, P., Lavasanifar, A., Das, S., Shapiro, J., and Samuel, J. (2008). Delivery of rapamycin by PLGA nanoparticles enhances its suppressive activity on dendritic cells. *J. Biomed. Mater. Res. A* 84 (4), 885–898. doi:10.1002/jbma.a.31373



- Hald Albertsen, C., Kulkarni, J. A., Witzigmann, D., Lind, M., Petersson, K., and Simonsen, J. B. (2022). The role of lipid components in lipid nanoparticles for vaccines and gene therapy. *Adv. Drug Deliv. Rev.* 188, 114416. doi:10.1016/j.addr.2022.114416
- Herrero-Sanchez, M. C., Rodriguez-Serrano, C., Almeida, J., San-Segundo, L., Inoges, S., Santos-Briz, A., et al. (2016). Effect of mTORC1/mTORC2 inhibition on T cell function: potential role in graft-versus-host disease control. *Br. J. Haematol.* 173 (5), 754–768. doi:10.1111/bjh.13984
- Hlavaty, K. A., Luo, X., Shea, L. D., and Miller, S. D. (2015). Cellular and molecular targeting for nanotherapeutics in transplantation tolerance. *Clin. Immunol.* 160 (1), 14–23. doi:10.1016/j.clim.2015.03.013
- Hong, E., and Dobrovolskaia, M. A. (2019). Addressing barriers to effective cancer immunotherapy with nanotechnology: achievements, challenges, and roadmap to the next generation of nanoimmunotherapeutics. *Adv. Drug Deliv. Rev.* 141, 3–22. doi:10.1016/j.addr.2018.01.005
- Hong, J., Xiao, X., Gao, Q., Li, S., Jiang, B., Sun, X., et al. (2019). Co-delivery of allergen epitope fragments and R848 inhibits food allergy by inducing tolerogenic dendritic cells and regulatory T cells. *Int. J. Nanomedicine* 14, 7053–7064. doi:10.2147/ijn.S215415
- Horvath, D., and Basler, M. (2023). PLGA particles in immunotherapy. *Pharmaceutics* 15 (2), 615. doi:10.3390/pharmaceutics15020615
- Horwitz, D. A., Fahmy, T. M., Piccirillo, C. A., and La Cava, A. (2019). Rebalancing immune homeostasis to treat autoimmune diseases. *Trends Immunol.* 40 (10), 888–908. doi:10.1016/j.it.2019.08.003
- Huang, F., Zhao, J., Wei, Y., Wen, Z., Zhang, Y., Wang, X., et al. (2020). Anti-tumor efficacy of an adjuvant built-in nanovaccine based on ubiquitinated proteins from tumor cells. *Int. J. Nanomedicine* 15, 1021–1035. doi:10.2147/IJN.S237578
- Huis In 't Veld, L. G. M., Ho, N. I., Wassink, M., den Brok, M. H., and Adema, G. J. (2022). Saponin-based adjuvant-induced dendritic cell cross-presentation is dependent on PERK activation. *Cell. Mol. Life Sci.* 79 (5), 231. doi:10.1007/s00018-022-04253-x
- Janas, M. M., Schlegel, M. K., Harbison, C. E., Yilmaz, V. O., Jiang, Y., Parmar, R., et al. (2018). Selection of GalNAc-conjugated siRNAs with limited off-target-driven rat hepatotoxicity. *Nat. Commun.* 9 (1), 723. doi:10.1038/s41467-018-02989-4
- Josefowicz, S. Z., Lu, L. F., and Rudensky, A. Y. (2012). Regulatory T cells: mechanisms of differentiation and function. *Annu. Rev. Immunol.* 30, 531–564. doi:10.1146/annurev.immunol.25.022106.141623
- Julio-Pieper, M., Flor, P. J., Dinan, T. G., and Cryan, J. F. (2011). Exciting times beyond the brain: metabotropic glutamate receptors in peripheral and non-neural tissues. *Pharmacol. Rev.* 63 (1), 35–58. doi:10.1124/pr.110.004036
- Jung, H. H., Kim, S. H., Moon, J. H., Jeong, S. U., Jang, S., Park, C. S., et al. (2019). Polymeric nanoparticles containing both antigen and vitamin D(3) induce antigen-specific immune suppression. *Immune Netw.* 19 (3), e19. doi:10.4110/in.2019.19.e19
- Kenison, J. E., Jhaveri, A., Li, Z., Khadse, N., Tjon, E., Tezza, S., et al. (2020). Tolerogenic nanoparticles suppress central nervous system inflammation. *Proc. Natl. Acad. Sci. U. S. A.* 117 (50), 32017–32028. doi:10.1073/pnas.2016451117
- Kim, B., Park, J. H., and Sailor, M. J. (2019a). Rekindling RNAi therapy: materials design requirements for *in vivo* siRNA delivery. *Adv. Mater.* 31 (49), e1903637. doi:10.1002/adma.201903637
- Kim, S. H., Moon, J. H., Jeong, S. U., Jung, H. H., Park, C. S., Hwang, B. Y., et al. (2019b). Induction of antigen-specific immune tolerance using biodegradable nanoparticles containing antigen and dexamethasone. *Int. J. Nanomedicine* 14, 5229–5242. doi:10.2147/ijn.S210546
- Kishimoto, T. K., Ferrari, J. D., LaMothe, R. A., Kolte, P. N., Griset, A. P., O'Neil, C., et al. (2016). Improving the efficacy and safety of biologic drugs with tolerogenic nanoparticles. *Nat. Nanotechnol.* 11 (10), 890–899. doi:10.1038/nnano.2016.135
- Kishimoto, T. K., and Maldonado, R. A. (2018). Nanoparticles for the induction of antigen-specific immunological tolerance. *Front. Immunol.* 9, 230. doi:10.3389/fimmu.2018.00230
- Klein, L., Kyewski, B., Allen, P. M., and Hogquist, K. A. (2014). Positive and negative selection of the T cell repertoire: what thymocytes see (and don't see). *Nat. Rev. Immunol.* 14 (6), 377–391. doi:10.1038/nri3667
- Kranz, L. M., Diken, M., Haas, H., Kreiter, S., Loquai, C., Reuter, K. C., et al. (2016). Systemic RNA delivery to dendritic cells exploits antiviral defence for cancer immunotherapy. *Nature* 534 (7607), 396–401. doi:10.1038/nature18300
- Krienke, C., Kolb, L., Diken, E., Streuber, M., Kirchhoff, S., Bukur, T., et al. (2021). A noninflammatory mRNA vaccine for treatment of experimental autoimmune encephalomyelitis. *Science* 371 (6525), 145–153. doi:10.1126/science.aay3638
- Kushwah, R., and Hu, J. (2011). Complexity of dendritic cell subsets and their function in the host immune system. *Immunology* 133 (4), 409–419. doi:10.1111/j.1365-2567.2011.03457.x
- Lam, K., Schreiner, P., Leung, A., Stainton, P., Reid, S., Yaworski, E., et al. (2023). Optimizing lipid nanoparticles for delivery in primates. *Adv. Mater.* e2211420. doi:10.1002/adma.202211420
- Lamendour, L., Deluce-Kakwata-Nkor, N., Mouline, C., Gouilleux-Gruart, V., and Velge-Roussel, F. (2020). Tethering innate surface receptors on dendritic cells: A new avenue for immune tolerance induction? *Int. J. Mol. Sci.* 21 (15), doi:10.3390/ijms21155259
- Lau, C. Y. J., Benne, N., Lou, B., Braake, D. T., Bosman, E., van Kronenburg, N., et al. (2022). Tuning surface charges of peptide nanofibers for induction of antigen-specific immune tolerance: an introductory study. *J. Pharm. Sci.* 111 (4), 1004–1011. doi:10.1016/j.xphs.2022.01.030
- Lee, J. Y., Lee, H. S., Kang, N. W., Lee, S. Y., Kim, D. H., Kim, S., et al. (2020). Blood component ridable and CD44 receptor targetable nanoparticles based on a maleimide-functionalized chondroitin sulfate derivative. *Carbohydr. Polym.* 230, 115568. doi:10.1016/j.carbpol.2019.115568
- Li, C., Han, Y., Luo, X., Qian, C., Li, Y., Su, H., et al. (2023). Immunomodulatory nano-preparations for rheumatoid arthritis. *Drug Deliv.* 30 (1), 9–19. doi:10.1080/10717544.2022.2152136
- Li, H., Yang, Y. G., and Sun, T. (2022a). Nanoparticle-based drug delivery systems for induction of tolerance and treatment of autoimmune diseases. *Front. Bioeng. Biotechnol.* 10, 889291. doi:10.3389/fbioe.2022.889291
- Li, M., Jiang, S., Simon, J., Passlick, D., Frey, M. L., Wagner, M., et al. (2021a). Brush conformation of polyethylene glycol determines the stealth effect of nanocarriers in the low protein adsorption regime. *Nano Lett.* 21 (4), 1591–1598. doi:10.1021/acs.nanolett.0c03756
- Li, R., Li, H., Yang, X., Hu, H., Liu, P., and Liu, H. (2022b). Crosstalk between dendritic cells and regulatory T cells: protective effect and therapeutic potential in multiple sclerosis. *Front. Immunol.* 13, 970508. doi:10.3389/fimmu.2022.970508
- Li, Z., Liu, Y., Fang, X., and Shu, Z. (2021b). Nanomaterials enhance the immunomodulatory effect of molecular targeted therapy. *Int. J. Nanomedicine* 16, 1631–1661. doi:10.2147/IJN.S290346
- Liu, M., Thijssen, S., Hennink, W. E., Garssen, J., van Nostrum, C. F., and Willemsen, L. E. M. (2022). Oral pretreatment with beta-lactoglobulin derived peptide and CpG co-encapsulated in PLGA nanoparticles prior to sensitizations attenuates cow's milk allergy development in mice. *Front. Immunol.* 13, 1053107. doi:10.3389/fimmu.2022.1053107
- Liu, Y. J. (2005). IPC: professional type 1 interferon-producing cells and plasmacytoid dendritic cell precursors. *Annu. Rev. Immunol.* 23, 275–306. doi:10.1146/annurev.immunol.23.021704.115633
- Luo, Y. L., Liang, L. F., Gan, Y. J., Liu, J., Zhang, Y., Fan, Y. N., et al. (2020). An all-in-one nanomedicine consisting of CRISPR-cas9 and an autoantigen peptide for restoring specific immune tolerance. *ACS Appl. Mater. Interfaces* 12 (43), 48259–48271. doi:10.1021/acsami.0c10885
- Ma, Y., Zhuang, Y., Xie, X., Wang, C., Wang, F., Zhou, D., et al. (2011). The role of surface charge density in cationic liposome-promoted dendritic cell maturation and vaccine-induced immune responses. *Nanoscale* 3 (5), 2307–2314. doi:10.1039/c1nr10166h
- Machen, J., Harnaha, J., Lakomy, R., Styche, A., Trucco, M., and Giannoukakis, N. (2004). Antisense oligonucleotides down-regulating costimulation confer diabetes-preventive properties to nonobese diabetic mouse dendritic cells. *J. Immunol.* 173 (7), 4331–4341. doi:10.4049/jimmunol.173.7.4331
- Maldonado, R. A., LaMothe, R. A., Ferrari, J. D., Zhang, A. H., Rossi, R. J., Kolte, P. N., et al. (2015). Polymeric synthetic nanoparticles for the induction of antigen-specific immunological tolerance. *Proc. Natl. Acad. Sci. U. S. A.* 112 (2), E156–E165. doi:10.1073/pnas.1408686111
- Manolova, V., Flace, A., Bauer, M., Schwarz, K., Saudan, P., and Bachmann, M. F. (2008). Nanoparticles target distinct dendritic cell populations according to their size. *Eur. J. Immunol.* 38 (5), 1404–1413. doi:10.1002/eji.200737984
- Mathaes, R., Winter, G., Besheer, A., and Engert, J. (2014). Influence of particle geometry and PEGylation on phagocytosis of particulate carriers. *Int. J. Pharm.* 465 (1–2), 159–164. doi:10.1016/j.ijpharm.2014.02.037
- Moghim, S. M., and Szebeni, J. (2003). Stealth liposomes and long circulating nanoparticles: critical issues in pharmacokinetics, opsonization and protein-binding properties. *Prog. Lipid Res.* 42 (6), 463–478. doi:10.1016/s0163-7827(03)00033-x
- Montano, J., Garnica, J., and Santamaria, P. (2021). Immunomodulatory and immunoregulatory nanomedicines for autoimmunity. *Semin. Immunol.* 56, 101535. doi:10.1016/j.smim.2021.101535
- Morante-Palacios, O., Fondelli, F., Ballestar, E., and Martinez-Caceres, E. M. (2021). Tolerogenic dendritic cells in autoimmunity and inflammatory diseases. *Trends Immunol.* 42 (1), 59–75. doi:10.1016/j.it.2020.11.001
- Nagy, N. A., Castenmiller, C., Vigario, F. L., Sparrius, R., van Capel, T. M. M., de Haas, A. M., et al. (2022). Uptake kinetics of liposomal formulations of differing charge influences development of *in vivo* dendritic cell immunotherapy. *J. Pharm. Sci.* 111 (4), 1081–1091. doi:10.1016/j.xphs.2022.01.022
- Nagy, N. A., de Haas, A. M., Geijtenbeek, T. B. H., van Ree, R., Tas, S. W., van Kooyk, Y., et al. (2021). Therapeutic liposomal vaccines for dendritic cell activation or tolerance. *Front. Immunol.* 12, 674048. doi:10.3389/fimmu.2021.674048
- Ness, S., Lin, S., and Gordon, J. R. (2021). Regulatory dendritic cells, T cell tolerance, and dendritic cell therapy for immunologic disease. *Front. Immunol.* 12, 633436. doi:10.3389/fimmu.2021.633436
- Nguyen, T. L., Choi, Y., Im, J., Shin, H., Phan, N. M., Kim, M. K., et al. (2022). Immunosuppressive biomaterial-based therapeutic vaccine to treat multiple sclerosis via re-establishing immune tolerance. *Nat. Commun.* 13 (1), 7449. doi:10.1038/s41467-022-35263-9



- Niikura, K., Matsunaga, T., Suzuki, T., Kobayashi, S., Yamaguchi, H., Orba, Y., et al. (2013). Gold nanoparticles as a vaccine platform: influence of size and shape on immunological responses *in vitro* and *in vivo*. *ACS Nano* 7 (5), 3926–3938. doi:10.1021/n3057005
- Nikolic, T., Zwaginga, J. J., Uit Beijerse, B. S., Woittiez, N. J., de Koning, E. J., Aanstoot, H. J., et al. (2020). Safety and feasibility of intradermal injection with tolerogenic dendritic cells pulsed with proinsulin peptide for type 1 diabetes. *Lancet Diabetes Endocrinol.* 8 (6), 470–472. doi:10.1016/S2213-8587(20)30104-2
- O'Mary, H. L., Aldayel, A. M., Valdes, S. A., Naguib, Y. W., Li, X., Salvady, K., et al. (2017). Acid-sensitive sheddable PEGylated, mannose-modified nanoparticles increase the delivery of betamethasone to chronic inflammation sites in a mouse model. *Mol. Pharm.* 14 (6), 1929–1937. doi:10.1021/acs.molpharmaceut.7b00024
- Operti, M. C., Bernhardt, A., Grimm, S., Engel, A., Figdor, C. G., and Tagit, O. (2021). PLGA-based nanomedicines manufacturing: technologies overview and challenges in industrial scale-up. *Int. J. Pharm.* 605, 120807. doi:10.1016/j.ijpharm.2021.120807
- Otsuka, S., Melis, N., Gaida, M. M., Dutta, D., Weigert, R., and Ashwell, J. D. (2021). Calcineurin inhibitors suppress acute graft-versus-host disease via NFAT-independent inhibition of T cell receptor signaling. *J. Clin. Investig.* 131 (11), e147683. doi:10.1172/JCI147683
- Park, J., Gerber, M. H., and Babensee, J. E. (2015). Phenotype and polarization of autologous T cells by biomaterial-treated dendritic cells. *J. Biomed. Mater. Res. A* 103 (1), 170–184. doi:10.1002/jbm.a.35150
- Parker, H., Gravagnuolo, A. M., Vranic, S., Crlica, L. E., Newman, L., Carnell, O., et al. (2022). Graphene oxide modulates dendritic cell ability to promote T cell activation and cytokine production. *Nanoscale* 14 (46), 17297–17314. doi:10.1039/d2nr02169b
- Passeri, L., Marta, F., Bassi, V., and Gregori, S. (2021). Tolerogenic dendritic cell-based approaches in autoimmunity. *Int. J. Mol. Sci.* 22 (16). doi:10.3390/ijms22168415
- Patra, J. K., Das, G., Fraceto, L. F., Campos, E. V. R., Rodriguez-Torres, M. D. P., Acosta-Torres, L. S., et al. (2018). Nano based drug delivery systems: recent developments and future prospects. *J. Nanobiotechnology* 16 (1), 71. doi:10.1186/s12951-018-0392-8
- Peferoen, L., Kipp, M., van der Valk, P., van Noort, J. M., and Amor, S. (2014). Oligodendrocyte-microglia cross-talk in the central nervous system. *Immunology* 141 (3), 302–313. doi:10.1111/imm.12163
- Phillips, B. E., Garciafigueroa, Y., Engman, C., Trucco, M., and Giannoukakis, N. (2019). Tolerogenic dendritic cells and T-regulatory cells at the clinical trials crossroad for the treatment of autoimmune disease; emphasis on type 1 diabetes therapy. *Front. Immunol.* 10, 148. doi:10.3389/fimmu.2019.00148
- Phillips, B., Nylander, K., Harnaha, J., Machen, J., Lakomy, R., Styche, A., et al. (2008). A microsphere-based vaccine prevents and reverses new-onset autoimmune diabetes. *Diabetes* 57 (6), 1544–1555. doi:10.2337/db07-0507
- Poon, W., Kingston, B. R., Ouyang, B., Ngo, W., and Chan, W. C. W. (2020). A framework for designing delivery systems. *Nat. Nanotechnol.* 15 (10), 819–829. doi:10.1038/s41565-020-0759-5
- Pozsgay, J., Szekanecz, Z., and Sármay, G. (2017). Antigen-specific immunotherapies in rheumatic diseases. *Nat. Rev. Rheumatol.* 13 (9), 525–537. doi:10.1038/nrrheum.2017.107
- Puhr, S., Lee, J., Zvezdova, E., Zhou, Y. J., and Liu, K. (2015). Dendritic cell development-History, advances, and open questions. *Semin. Immunol.* 27 (6), 388–396. doi:10.1016/j.smim.2016.03.012
- Pujol-Autonell, I., Mansilla, M. J., Rodriguez-Fernandez, S., Cano-Sarabia, M., Navarro-Barriuso, J., Ampudia, R. M., et al. (2017). Liposome-based immunotherapy against autoimmune diseases: therapeutic effect on multiple sclerosis. *Nanomedicine (Lond)* 12 (11), 1231–1242. doi:10.2217/nmm-2016-0410
- Punz, B., Johnson, L., Geppert, M., Dang, H. H., Horejs-Hoeck, J., Duschl, A., et al. (2022). Surface functionalization of silica nanoparticles: strategies to optimize the immune-activating profile of carrier platforms. *Pharmaceutics* 14 (5), 1103. doi:10.3390/pharmaceutics14051103
- Que, W., Guo, W. Z., and Li, X. K. (2020). Manipulation of regulatory dendritic cells for induction transplantant tolerance. *Front. Immunol.* 11, 582658. doi:10.3389/fimmu.2020.582658
- Quintana, F. J., Murugaiyan, G., Farez, M. F., Mitsdoerffer, M., Tukpah, A. M., Burns, E. J., et al. (2010). An endogenous aryl hydrocarbon receptor ligand acts on dendritic cells and T cells to suppress experimental autoimmune encephalomyelitis. *Proc. Natl. Acad. Sci. U. S. A.* 107 (48), 20768–20773. doi:10.1073/pnas.1009201107
- Raich-Regue, D., Rosborough, B. R., Watson, A. R., McGeachy, M. J., Turnquist, H. R., and Thomson, A. W. (2015). mTORC2 deficiency in myeloid dendritic cells enhances their allogeneic Th1 and Th17 stimulatory ability after TLR4 ligation *in vitro* and *in vivo*. *J. Immunol.* 194 (10), 4767–4776. doi:10.4049/jimmunol.1402551
- Ren, Y., Wu, W., and Zhang, X. (2023). The feasibility of oral targeted drug delivery: gut immune to particulates? *Acta Pharm. Sin. B* 13 (6), 2544–2558. doi:10.1016/j.apsb.2022.10.020
- Roberts, R. A., Eitas, T. K., Byrne, J. D., Johnson, B. M., Short, P. J., McKinnon, K. P., et al. (2015). Towards programming immune tolerance through geometric manipulation of phosphatidylserine. *Biomaterials* 72, 1–10. doi:10.1016/j.biomaterials.2015.08.040
- Robinson, S., and Thomas, R. (2021). Potential for antigen-specific tolerizing immunotherapy in systematic lupus erythematosus. *Front. Immunol.* 12, 654701. doi:10.3389/fimmu.2021.654701
- Rodriguez-Fernandez, S., Pujol-Autonell, I., Brioso, F., Perna-Barrull, D., Cano-Sarabia, M., Garcia-Jimeno, S., et al. (2018). Phosphatidylserine-liposomes promote tolerogenic features on dendritic cells in human type 1 diabetes by apoptotic mimicry. *Front. Immunol.* 9, 253. doi:10.3389/fimmu.2018.00253
- Rui, Y., Eppler, H. B., Yanes, A. A., and Jewell, C. M. (2023). Tissue-targeted drug delivery strategies to promote antigen-specific immune tolerance. *Adv. Healthc. Mater.* 12 (6), e2202238. doi:10.1002/adhm.202202238
- Saito, E., Gurczynski, S. J., Kramer, K. R., Wilke, C. A., Miller, S. D., Moore, B. B., et al. (2020). Modulating lung immune cells by pulmonary delivery of antigen-specific nanoparticles to treat autoimmune disease. *Sci. Adv.* 6 (42), eabc9317. doi:10.1126/sciadv.abc9317
- Santos, S. D., Xavier, M., Leite, D. M., Moreira, D. A., Custodio, B., Torrado, M., et al. (2018). PAMAM dendrimers: blood-brain barrier transport and neuronal uptake after focal brain ischemia. *J. Control Release* 291, 65–79. doi:10.1016/j.jconrel.2018.10.006
- Shen, H., Ackerman, A. L., Cody, V., Giodini, A., Hinson, E. R., Cresswell, P., et al. (2006). Enhanced and prolonged cross-presentation following endosomal escape of exogenous antigens encapsulated in biodegradable nanoparticles. *Immunology* 117 (1), 78–88. doi:10.1111/j.1365-2567.2005.02268.x
- Shi, D., Fu, M., Fan, P., Li, W., Chen, X., Li, C., et al. (2007). Artificial phosphatidylserine liposome mimics apoptotic cells in inhibiting maturation and immunostimulatory function of murine myeloid dendritic cells in response to 1-chloro-2,4-dinitrobenzene *in vitro*. *Arch. Dermatol. Res.* 299 (7), 327–336. doi:10.1007/s00403-007-0770-9
- Singer, B. D., King, L. S., and D'Alessio, F. R. (2014). Regulatory T cells as immunotherapy. *Front. Immunol.* 5, 46. doi:10.3389/fimmu.2014.00046
- Stead, S. O., Kireta, S., McInnes, S. J. P., Kette, F. D., Sivanathan, K. N., Kim, J., et al. (2018a). Murine and non-human primate dendritic cell targeting nanoparticles for *in vivo* generation of regulatory T-cells. *ACS Nano* 12 (7), 6637–6647. doi:10.1021/acsnano.8b01625
- Stead, S. O., McInnes, S. J. P., Kireta, S., Rose, P. D., Jesudason, S., Rojas-Canales, D., et al. (2018b). Manipulating human dendritic cell phenotype and function with targeted porous silicon nanoparticles. *Biomaterials* 155, 92–102. doi:10.1016/j.biomaterials.2017.11.017
- Steinman, R. M., and Cohn, Z. A. (1974). Identification of a novel cell type in peripheral lymphoid organs of mice. II. Functional properties *in vitro*. *J. Exp. Med.* 139 (2), 380–397. doi:10.1084/jem.139.2.380
- Steinman, R. M., and Cohn, Z. A. (1973). Identification of a novel cell type in peripheral lymphoid organs of mice. I. Morphology, quantitation, tissue distribution. *J. Exp. Med.* 137 (5), 1142–1162. doi:10.1084/jem.137.5.1142
- Stergioti, E. M., Manoloukou, T., Boumpas, D. T., and Banos, A. (2022). Antiviral innate immune responses in autoimmunity: receptors, pathways, and therapeutic targeting. *Biomedicines* 10 (11), 2820. doi:10.3390/biomedicines10112820
- Sun, T., Zhang, Y. S., Pang, B., Hyun, D. C., Yang, M., and Xia, Y. (2014). Engineered nanoparticles for drug delivery in cancer therapy. *Angew. Chem. Int. Ed. Engl.* 53 (46), 12320–12364. doi:10.1002/anie.201403036
- Sun, Z., Liu, J., Li, Y., Lin, X., Chu, Y., Wang, W., et al. (2023). Aggregation-induced-emission photosensitizer-loaded nano-superartificial dendritic cells with directly presenting tumor antigens and reversed immunosuppression for photodynamically boosted immunotherapy. *Adv. Mater.* 35 (3), e2208555. doi:10.1002/adma.202208555
- Suuring, M., and Moreau, A. (2021). Regulatory macrophages and tolerogenic dendritic cells in myeloid regulatory cell-based therapies. *Int. J. Mol. Sci.* 22 (15). doi:10.3390/ijms22157970
- Suzuki, M., Zheng, X., Zhang, X., Zhang, Z. X., Ichim, T. E., Sun, H., et al. (2010). A novel allergen-specific therapy for allergy using CD40-silenced dendritic cells. *J. Allergy Clin. Immunol.* 125(3), 737–743. doi:10.1016/j.jaci.2009.11.042
- Szondy, Z., Sarang, Z., Kiss, B., Garabuczi, E., and Koroskenyi, K. (2017). Anti-inflammatory mechanisms triggered by apoptotic cells during their clearance. *Front. Immunol.* 8, 909. doi:10.3389/fimmu.2017.00909
- Tang, R., Acharya, N., Subramanian, A., Purohit, V., Tabaka, M., Hou, Y., et al. (2022). Tim-3 adapter protein Bat3 acts as an endogenous regulator of tolerogenic dendritic cell function. *Sci. Immunol.* 7 (69), eabm0631. doi:10.1126/sciimmunol.abm0631
- Tenchov, R., Bird, R., Curtze, A. E., and Zhou, Q. (2021). Lipid nanoparticles horizontal line from liposomes to mRNA vaccine delivery, a landscape of research diversity and advancement. *ACS Nano* 15 (11), 16982–17015. doi:10.1021/acsnano.1c04996
- Thi, T. T. H., Suys, E. J. A., Lee, J. S., Nguyen, D. H., Park, K. D., and Truong, N. P. (2021). Lipid-based nanoparticles in the clinic and clinical trials: from cancer nanomedicine to COVID-19 vaccines. *Vaccines (Basel)* 9 (4), 359. doi:10.3390/vaccines9040359
- Tiberio, L., Del Prete, A., Schioppa, T., Sozio, F., Bosio, D., and Sozzani, S. (2018). Chemokine and chemotactic signals in dendritic cell migration. *Cell. Mol. Immunol.* 15 (4), 346–352. doi:10.1038/s41423-018-0005-3

- Tkach, A. V., Yanamala, N., Stanley, S., Shurin, M. R., Shurin, G. V., Kisin, E. R., et al. (2013). Graphene oxide, but not fullerenes, targets immunoproteasomes and suppresses antigen presentation by dendritic cells. *Small* 9 (9–10), 1686–1690. doi:10.1002/sml.201201546
- Tomić, S., Kokol, V., Mihajlović, D., Mirčić, A., and Čolić, M. (2016). Native cellulose nanofibrils induce immune tolerance *in vitro* by acting on dendritic cells. *Sci. Rep.* 6, 31618. doi:10.1038/srep31618
- Toro-Mendoza, J., Maio, L., Gallego, M., Otto, F., Schulz, F., Parak, W. J., et al. (2023). Bioinspired polyethylene glycol coatings for reduced nanoparticle-protein interactions. *ACS Nano*. doi:10.1021/acsnano.2c05682
- Triantafyllakou, I., Clemente, N., Khetavat, R. K., Dianzani, U., and Tselios, T. (2022). Development of PLGA nanoparticles with a glycosylated myelin oligodendrocyte glycoprotein epitope (MOG(35–55)) against experimental autoimmune encephalomyelitis (EAE). *Mol. Pharm.* 19 (11), 3795–3805. doi:10.1021/acs.molpharmaceut.2c00277
- Uzhviyuk, S. V., Bochkova, M. S., Timganova, V. P., Khramtsov, P. V., Shardina, K. Y., Kropaneva, M. D., et al. (2022). Interaction of human dendritic cells with graphene oxide nanoparticles *in vitro*. *Bull. Exp. Biol. Med.* 172 (5), 664–670. doi:10.1007/s10517-022-05451-0
- Van Haute, D., Liu, A. T., and Berlin, J. M. (2018). Coating metal nanoparticle surfaces with small organic molecules can reduce nonspecific cell uptake. *ACS Nano* 12 (1), 117–127. doi:10.1021/acsnano.7b03025
- van Pul, K. M., Vuylsteke, R., van de Ven, R., Te Velde, E. A., Rutgers, E. J. T., van den Tol, P. M., et al. (2019). Selectively hampered activation of lymph node-resident dendritic cells precedes profound T cell suppression and metastatic spread in the breast cancer sentinel lymph node. *J. Immunother. Cancer* 7 (1), 133. doi:10.1186/s40425-019-0605-1
- Waeckerle-Men, Y., and Groettrup, M. (2005). PLGA microspheres for improved antigen delivery to dendritic cells as cellular vaccines. *Adv. Drug Deliv. Rev.* 57 (3), 475–482. doi:10.1016/j.addr.2004.09.007
- Waisman, A., Lukas, D., Clausen, B. E., and Yogeve, N. (2017). Dendritic cells as gatekeepers of tolerance. *Semin. Immunopathol.* 39 (2), 153–163. doi:10.1007/s00281-016-0583-z
- Wang, H., Shang, J., He, Z., Zheng, M., Jia, H., Zhang, Y., et al. (2022a). Dual peptide nanoparticle platform for enhanced antigen-specific immune tolerance for the treatment of experimental autoimmune encephalomyelitis. *Biomater. Sci.* 10 (14), 3878–3891. doi:10.1039/d2bm00444e
- Wang, J., Mao, K., Cong, X., Tan, H., Wu, C., Hu, Z., et al. (2022b). Nanoparticle delivery of CD40 siRNA suppresses alloimmune responses by inhibiting activation and differentiation of DCs and macrophages. *Sci. Adv.* 8 (51), eabq3699. doi:10.1126/sciadv.abq3699
- Wang, Q., Sun, X., Huang, X., Huang, J., Hasan, M. W., Yan, R., et al. (2021). Nanoparticles of chitosan/poly(D,L-Lactide-Co-glycolide) enhanced the immune responses of *Haemonchus contortus* HCA59 antigen in model mice. *Int. J. Nanomedicine* 16, 3125–3139. doi:10.2147/IJN.S301851
- Wen, H., Qu, L., Zhang, Y., Xu, B., Ling, S., Liu, X., et al. (2021). A dendritic cells-targeting nano-vaccine by coupling polylactic-Co-glycolic acid-encapsulated allergen with mannan induces regulatory T cells. *Int. Arch. Allergy Immunol.* 182 (9), 777–787. doi:10.1159/000512872
- Wu, Z., and Nakanishi, H. (2011). Phosphatidylserine-containing liposomes: potential pharmacological interventions against inflammatory and immune diseases through the production of prostaglandin E(2) after uptake by myeloid derived phagocytes. *Arch. Immunol. Ther. Exp. Warsz.* 59 (3), 195–201. doi:10.1007/s00005-011-0123-4
- Yang, W., Cao, J., Cheng, H., Chen, L., Yu, M., Chen, Y., et al. (2023). Nanoformulations targeting immune cells for cancer therapy: mRNA therapeutics. *Bioact. Mater* 23, 438–470. doi:10.1016/j.bioactmat.2022.11.014
- Yasar, H., Biehl, A., De Rossi, C., Koch, M., Murgia, X., Loretz, B., et al. (2018). Kinetics of mRNA delivery and protein translation in dendritic cells using lipid-coated PLGA nanoparticles. *J. Nanobiotechnology* 16 (1), 72. doi:10.1186/s12951-018-0401-y
- Yeste, A., Nadeau, M., Burns, E. J., Weiner, H. L., and Quintana, F. J. (2012). Nanoparticle-mediated codelivery of myelin antigen and a tolerogenic small molecule suppresses experimental autoimmune encephalomyelitis. *Proc. Natl. Acad. Sci. U. S. A.* 109 (28), 11270–11275. doi:10.1073/pnas.1120611109
- Yeste, A., Takenaka, M. C., Mascanfroni, I. D., Nadeau, M., Kenison, J. E., Patel, B., et al. (2016). Tolerogenic nanoparticles inhibit T cell-mediated autoimmunity through SOCS2. *Sci. Signal* 9 (433), ra61. doi:10.1126/scisignal.aad0612
- Yin, X., Chen, S., and Eisenbarth, S. C. (2021). Dendritic cell regulation of T helper cells. *Annu. Rev. Immunol.* 39, 759–790. doi:10.1146/annurev-immunol-101819-025146
- Yu, Z., Vepris, O., Eich, C., Feng, Y., Que, I., Camps, M. G. M., et al. (2022). Upconversion nanoparticle platform for efficient dendritic cell antigen delivery and simultaneous tracking. *Mikrochim. Acta* 189 (10), 368. doi:10.1007/s00604-022-05441-z
- Zhang, B., Su, Y., Zhou, J., Zheng, Y., and Zhu, D. (2021a). Toward a better regeneration through implant-mediated immunomodulation: harnessing the immune responses. *Adv. Sci. (Weinh)* 8 (16), e2100446. doi:10.1002/adv.202100446
- Zhang, Q., and Vignali, D. A. (2016). Co-Stimulatory and Co-inhibitory pathways in autoimmunity. *Immunity* 44 (5), 1034–1051. doi:10.1016/j.immuni.2016.04.017
- Zhang, S., Chopin, M., and Nutt, S. L. (2021b). Type 1 conventional dendritic cells: ontogeny, function, and emerging roles in cancer immunotherapy. *Trends Immunol.* 42 (12), 1113–1127. doi:10.1016/j.it.2021.10.004
- Zhang, X., Li, X., Wang, Y., Chen, Y., Hu, Y., Guo, C., et al. (2022). Abnormal lipid metabolism in epidermal Langerhans cells mediates psoriasis-like dermatitis. *JCI Insight* 7 (13), e150223. doi:10.1172/jci.insight.150223
- Zhang, X., Liu, D., He, M., Lin, M., Tu, C., and Zhang, B. (2021c). Polymeric nanoparticles containing rapamycin and autoantigen induce antigen-specific immunological tolerance for preventing vitiligo in mice. *Hum. Vaccin Immunother.* 17 (7), 1923–1929. doi:10.1080/21645515.2021.1872342
- Zhang, Y., Shen, S., Zhao, G., Xu, C. F., Zhang, H. B., Luo, Y. L., et al. (2019). *In situ* repurposing of dendritic cells with CRISPR/Cas9-based nanomedicine to induce transplant tolerance. *Biomaterials* 217, 119302. doi:10.1016/j.biomaterials.2019.119302
- Zhang, Y., Zhang, Z., Li, S., Zhao, L., Li, D., Cao, Z., et al. (2021d). A siRNA-assisted assembly strategy to simultaneously suppress “self” and upregulate “Eat-Me” signals for nanoenabled chemo-immunotherapy. *ACS Nano* 15 (10), 16030–16042. doi:10.1021/acsnano.1c04458
- Zheng, X., Sun, C., Yu, R., Chu, X., Xu, J., Liu, C., et al. (2020). CD13-specific ligand facilitates Xanthin nanomedicine targeting dendritic cells for therapy of refractory allergic rhinitis. *Int. J. Pharm.* 577, 119034. doi:10.1016/j.ijpharm.2020.119034
- Zheng, X., Suzuki, M., Zhang, X., Ichim, T. E., Zhu, F., Ling, H., et al. (2010). RNAi-mediated CD40-CD154 interruption promotes tolerance in autoimmune arthritis. *Arthritis Res. Ther.* 12 (1), R13. doi:10.1186/ar2914
- Zhu, F. J., Tong, Y. L., Sheng, Z. Y., and Yao, Y. M. (2019). Role of dendritic cells in the host response to biomaterials and their signaling pathways. *Acta Biomater.* 94, 132–144. doi:10.1016/j.actbio.2019.05.038
- Zhuang, B., Shang, J., and Yao, Y. (2021). HLA-G: an important mediator of maternal-fetal immune-tolerance. *Front. Immunol.* 12, 744324. doi:10.3389/fimmu.2021.744324
- Zubizarreta, I., Florez-Grau, G., Vila, G., Cabezon, R., Espana, C., Andorra, M., et al. (2019). Immune tolerance in multiple sclerosis and neuromyelitis optica with peptide-loaded tolerogenic dendritic cells in a phase 1b trial. *Proc. Natl. Acad. Sci. U. S. A.* 116 (17), 8463–8470. doi:10.1073/pnas.1820039116
- Zupancic, E., Curato, C., Paisana, M., Rodrigues, C., Porat, Z., Viana, A. S., et al. (2017). Rational design of nanoparticles towards targeting antigen-presenting cells and improved T cell priming. *J. Control Release* 258, 182–195. doi:10.1016/j.jconrel.2017.05.014

# Frontiers in Bioengineering and Biotechnology

Accelerates the development of therapies,  
devices, and technologies to improve our lives

A multidisciplinary journal that accelerates the  
development of biological therapies, devices,  
processes and technologies to improve our lives  
by bridging the gap between discoveries and their  
application.

## Discover the latest Research Topics

[See more →](#)

### Frontiers

Avenue du Tribunal-Fédéral 34  
1005 Lausanne, Switzerland  
[frontiersin.org](https://frontiersin.org)

### Contact us

+41 (0)21 510 17 00  
[frontiersin.org/about/contact](https://frontiersin.org/about/contact)



Frontiers in  
Bioengineering  
and Biotechnology

